

**CHEMICAL CONSTITUENTS FROM THE RHIZOMES
OF *CURCUMA ZEDOARIA* AND *CURCUMA*
PURPURASCENS AND ASSESSMENT OF
THEIR BIOLOGICAL ACTIVITIES**

OMER ABDALLA AHMED HAMD

**FACULTY OF SCIENCE
UNIVERSITY OF MALAYA
KUALA LUMPUR**

2015

**CHEMICAL CONSTITUENTS FROM THE RHIZOMES
OF *CURCUMA ZEDOARIA* AND *CURCUMA*
PURPURASCENS AND ASSESSMENT OF
THEIR BIOLOGICAL ACTIVITIES**

OMER ABDALLA AHMED HAMDI

**THESIS SUBMITTED IN FULFILLMEN OF THE
REQUIREMENTS FOR THE DEGREE OF
DOCTOR OF PHILOSOPHY**

**DEPARTMENT OF CHEMISTRY
FACULTY OF SCIENCE
UNIVERSITY OF MALAYA
KUALA LUMPUR**

2015

UNIVERSITY OF MALAYA
ORIGINAL LITERARY WORK DECLARATION

Name of Candidate: **OMER ABDALLA AHMED HAMDI**

(I.C/Passport No:

Registration/Matric No:

Name of Degree: **DOCTOR OF PHILOSOPHY**

Title of Project Paper/Research Report/Dissertation/Thesis ("this Work"):

"CHEMICAL CONSTITUENTS FROM THE RHIZOMES OF *CURCUMA ZEDOARIA* AND *CURCUMA PURPURASCENS* AND ASSESSMENT OF THEIR BIOLOGICAL ACTIVITIES"

Field of Study☺ **CHEMISTRY (NATURAL PRODUCTS)**

I do solemnly and sincerely declare that:

- (1) I am the sole author/writer of this Work;
- (2) This Work is original;
- (3) Any use of any work in which copyright exists was done by way of fair dealing and for permitted purposes and any excerpt or extract from, or reference to or reproduction of any copyright work has been disclosed expressly and sufficiently and the title of the Work and its authorship have been acknowledged in this Work;
- (4) I do not have any actual knowledge nor do I ought reasonably to know that the making of this work constitutes an infringement of any copyright work;
- (5) I hereby assign all and every rights in the copyright to this Work to the University of Malaya ("UM"), who henceforth shall be owner of the copyright in this Work and that any reproduction or use in any form or by any means whatsoever is prohibited without the written consent of UM having been first had and obtained;
- (6) I am fully aware that if in the course of making this Work I have infringed any copyright whether intentionally or otherwise, I may be subject to legal action or any other action as may be determined by UM.

Candidate's Signature:

Date:

Subscribed and solemnly declared before,

Witness's Signature:

Date:

Name: **PROFESSOR DR KHALIJAH AWANG**

Designation:

Witness's Signature:

Date:

Name: **PROFESSOR DR NOEL FRANCIS THOMAS**

Designation:

ABSTRACT

Curcuma zedoaria (Christm.) Rosc. (local name: *Temu putih*) and *Curcuma purpurascens* are two medicinally important plants of the genus *Curcuma* and grow abundantly in Asian countries including Malaysia and Indonesia. These two plants are extensively used in the traditional medicinal practice of Malaysia and many other countries of the world for the treatment of various ailments. Phytochemical investigation of the rhizomes of *C. zedoaria* and *C. purpurascens* resulted in the isolation of 27 compounds. *C. zedoaria* afforded eighteen sesquiterpenes, including eight germacrane type (dehydrocurdione **19**, curdione **20**, furanodiene **21**, furanodienone **22**, germacrone **23**, germacrone 4,5-epoxide **24**, germacrone 1,10-epoxide **25**, and zederone **26**), four guaiane type (gweicurculactone **41**, curcumenol **42**, curcumenol second monoclinic **150**, isoprocucumenol **43**, and procucumenol **44**), one *seco*-guaiane (curcuzedoalide **62**), one elemene (curzerenone **111**), one humulene (zerumbone epoxide **151**), one cadianene (comosone II **104**), one carabranene (curcumenone **65**), and one spiro lactone type (*curcumanolide* **101**). The work also resulted in the isolation of three labdane diterpenes (labda-8(17), 12 diene-15, 16 dial **127**, calcaractrin A **128**, and zerumin A **129**, which are reported for the first time from *C. zedoaria*. Phytochemical investigation of *C. purpurascens* produced five compounds including one bisabolane (ar-turmerone **74**) and one guaiane (zedoalactone B **60**) sesquiterpene while the rest three are curcuminoids curcumin **138**, bisdemethoxycurcumin **139**, demethoxycurcumin **140**). A total of 34 compounds were identified through the GC and GC-MS spectroscopic analysis of the essential oil obtained by hydrodistillation of *C. purpurascens*. The major compounds were ar-turmerone **74** (9.4%), germacrone **23** (13.2%), and turmerone **80** (13.5 %). Supercritical fluid extraction of *C. purpurascens* rhizomes showed that the optimum parameters for higher yield and selective extraction could be obtained at the temperature of 313 K, with

the pressure 10.34 MPa and the flow rate of liquid CO₂ at 12 ml/min. Open column chromatography on silica gel (CC), thin layer chromatography (TLC), preparative thin layer chromatography (PTLC), high performance liquid chromatography (HPLC), and size exclusion chromatography by Sephadex[®] (LH-20) were used for the detection and isolation of the compounds. Extensive spectroscopic and chromatographic analysis including 1D and 2D NMR (¹H NMR, ¹³C NMR, DEPT, COSY, HMBC, HSQC, and NOESY), IR, UV, GC-MS, LC-MS were used for the structure elucidation of the isolated compounds. X-ray crystallographic analysis was performed on the second monoclinic crystals of curcumenol (**151**) which is new dimer crystals isolated from *C. zedoaria*. Isolated compounds were subjected to cytotoxicity, anti-oxidant and neuroprotective assays. Curcumenol (**42**) and dehydrocurdione (**19**) showed the highest protection (100%) against hydrogen peroxide induced oxidative stress in NG108-15 cells at the concentrations of 4 and 8 μM, respectively. In the oxygen radical antioxidant capacity assay, zerumbone epoxide (**151**) showed the highest level of antioxidant activity with a Trolox equivalent (TE) of 35.41 μM per 100 μg of sample. In the MTT based cytotoxicity assay against four cancer cell lines (CaSki, MCF-7, PC-3 and HT-29) curcumenol (**42**) and curcumenone (**65**) displayed strong antiproliferative activity (IC₅₀ 9.3 and 8.3 μg/ml, respectively). A quantum chemical study was performed to investigate its relationship with cytotoxic activity and revealed that the dipole moment (μ), molecular volume (V), molecular area (A), polarizability (α) and hydrophobicity (log P) are the most important descriptors that influence the cytotoxic activity of the compounds under investigation. The essential oil obtained the hydrodistillation exhibited strong cytotoxicity against HT29 cells but mild cytotoxicity against the non-cancerous human lung fibroblast cell line (MRC5). The two most active compounds; curcumenol (**42**) and curcumenone (**65**), were investigated for their binding to human serum albumin (HSA), a transportation protein of human blood. The spectrofluorometric

analysis, in conjunction with molecular docking study suggested that both curcumenol (**42**) and curcumenone (**65**) could bind to binding sites I and II of HSA with intermediate affinity while site I was the preferred binding site for both molecules.

ABSTRAK

Curcuma zedoaria (Christm.) Rosc. (nama tempatan: Temu putih) dan *Curcuma purpurascens* (nama tempatan: Temu parlimen) merupakan dua tumbuhan ubatan yang penting daripada genus *Curcuma* dan banyak didapati di negara-negara Asian termasuklah Malaysia dan Indonesia.

Kedua-dua tumbuhan ini digunakan secara meluas dalam amalan perubatan tradisional di Malaysia dan negara-negara lain di dunia untuk merawat pelbagai penyakit. Kajian fitokimia terhadap rizom *C. zedoaria* dan *C. purpurascens* berjaya mengasingkan sebanyak 27 sebatian.

C. zedoaria menghasilkan lapan belas seskuiterpena, termasuk lapan jenis germakrana (dehidrokurdiona **19**, kurdiona **20**, furanodiena **21**, furanodienona **22**, germakrona **23**, germakrona 4,5-eposida **24**, germakrona 1,10-epoksida **25**, dan zederona **26**), empat jenis guaiana (gweikurkulaktone **41**, kurkumenol **42**, kukumenol monoklinik kedua **150**, isoprokurkumenol **43**, dan prokurkumenol **44**), satu seko-guaiana (kurkuzedoalida **62**), satu elemena (kurzerenona **111**), satu humulana (zerumbona epoksida **151**), satu kadianena (komosona II **104**), satu karabrana (kurkumenona **65**), dan satu jenis spirolactona (*kurkumanolida* **101**).

Kajian ini juga berjaya mengasingkan tiga diterpena labdana (labda-8(17), 12 diena-15, 16 dial **127**, kalkaraktrin A **128**, and zerumin A **129**), yang mana ini merupakan laporan kali pertama bagi *C. zedoaria*.

Kajian fitokimia bagi *C. purpurascens* menghasilkan lima sebatian termasuk satu bisabolana (ar-turmernona **74**) dan satu guaiana (zedoalaktone B **60**) seskuiterpena sementara tiga lagi adalah kurkuminoid kurkumin **138**, bisdemetoksikurkumin **139**, demetoksikurkumin **140**).

Sejumlah 34 sebatian telah dikenalpasti melalui analisis spektroskopi GC dan GC-MS terhadap minyak pati yang diperolehi daripada penyulinganhidro *C. putpurascens*.

Sebatian major adalah ar-turmerona **74** (9.4%), germacrona **23** (13.2%), dan turmerona **80** (13.5 %). Pengekstrakkan cecair superkritikal daripada rizom *C. purpurascens* menunjukkan parameter optima bagi penghasilan hasil yang lebih banyak dan pengekstrakkan terpilih berlaku pada suhu 313 K, dengan tekanan 10.34 MPa dan kadar aliran cecair CO₂ pada 12 ml/min.

Kromatografi turus menggunakan gel silica (CC), kromatografi kepingan nipis (TLC), kromatografi kepingan nipis persediaan (PTLC), kromatografi cecair berteknologi tinggi (HPLC), dan kromatografi penyisihan saiz menggunakan Sephadex[®] (LH-20) untuk penentuan dan pengasingan sebatian . Analisis spektroskopi dan kromatografi berulang termasuk 1D dan 2D NMR (¹H NMR, ¹³C NMR, DEPT, COSY, HMBC, HSQC, dan NOESY), IR, UV, GC-MS, LC-MS digunakan untuk penentuan struktur sebatian yang telah diasingkan.

Analisis kristalografi X-ray telah dilakukan pada kristal kurkumenol monoklinik kedua (**151**) yang merupakan dimer baru yang dipencilkan daripada *C. zedoaria*.

Sebatian yang diasingkan telah dilakukan essei sitotoksiti, anti-oksidan dan perlindungan neuro.Kurkumenol (**42**) dan dehidrokurdiona (**19**) menunjukkan perlindungan tertinggi (100%) terhadap hidrogen peroksida tekanan oksidatif yang disebabkan oleh sel NG108-15 pada kepekatan 4 dan 8 µM.

Essei kapasiti antioksidan radikal oksigen, zerumbona epoksida (**151**) menunjukkan tahap tertinggi aktiviti antioksidan dengan menggunakan Trolox setara (TE) pada 35.41 µM per 100 µg sampel.

Dalam essei sitotoksiti MTT terhadap empat jujukan sel kanser (CaSki, MCF-7, PC-3 dan HT-29) kurkumenol (**42**) dan kurkumena (**65**) menunjukkan aktiviti antiproliferatif yang kuat (IC₅₀ 9.3 dan 8.3 µg/ml).

Kajian kuantum kimia yang dijalankan untuk mengkaji hubungan antara aktiviti sitotoksiti dan menunjukkan bahawa momen dwikutub (µ), isipadu molekul (V),

kawasan molekul (A), kebolehpayaan kekutuban (α) dan hidrofobisiti (log P) adalah sangat penting bagi menggambarkan kesan aktiviti sitotoksiti sebatian terhadap kajian. Minyak pati yang terhasil daripada penyulingan hidro menunjukkan kesan sitotoksiti yang kuat terhadap sel HT29 tetapi sitotoksiti sederhana terhadap jujukan sel bukan kanser fibroblast paru-paru (MRC5).

Dua sebatian teraktif; kurkumenol (**42**) dan kurkumenona (**65**), telah dikaji untuk perlekatan kepada serum albumin manusia (HSA), iaitu pengangkutan protein di dalam darah manusia. Analisis spektrofotometrik, selari dengan kajian doking molekul mencadangkan kedua-dua kurkumenol (**42**) dan kurkumenona (**65**) boleh melekat pada tapak perlekatan HSA I dan II dengan perantaraan afiniti sementara tapak I dicadangkan tapak perlekatan bagi kedua-dua molekul.

ACKNOWLEDGEMENTS

In the name of Allah, most Gracious, most Merciful. I would like to admit this work cannot be done without the great help and very kind assistance from Allah S.W.T. I am very much thankful to Allah S.W.T.

I would like to express my great appreciation and sincere gratitude to my supervisor Prof. Dr. Khalijah Awang for her patience, guidance throughout my Ph.D study. Also I would like to express my deep thanks to my second supervisor Prof. Thomas Noel for his constant support, and encouragement.

I highly appreciate the constant support of my beloved dearest brother Dr. Abubaker Hamdi.

My special thanks go to Dr. Jamil A. Shilpi who really give me great support. His kindness and brotherhood is very much appreciated.

I am too much thankful to the phytochemistry lab members for their cooperation and kindness.

I would like also to convey many thanks to the staff at the Department of Chemistry. To the generous scientists in charge of the NMR, IR, UV, GC, and GC MS instruments for their great help and easy accessibility to do most of my work.

I highly appreciated the valuable support of my kind brother Dr. Anouar.

I am too much thankful to Prof. Datin Sri Nurestri Abd Malek and Prof. Habsah Abdul Kadir and my thanks extended to their students Syarifah Nur Syed, and Lo Jia Ye.

I wish to forward my greatest appreciation to Prof. Saad Tayab and his student my younger brother Shevin to all support.

TABLE OF CONTENTS

ABSTRACT	I
ABSTRAK	IV
ACKNOWLEDGEMENTS.....	VII
TABLE OF CONTENTS.....	VIII
LIST OF SCHEMES.....	XII
LIST OF FIGURES	XIII
LIST OF TABLES	XX
LIST OF SYMBOLS AND ABBREVIATIONS.....	XXIV
 CHAPTER 1: INTRODUCTION.....	 1
1.1 Introduction.....	1
1.2 Aims and objectives	4
 CHAPTER 2: LITERATURE REVIEW.....	 7
2.1 Introduction	7
2.2 Botanical and chemical aspects.....	7
2.2.1 The family Zingiberaceae	7
2.3 Chemistry of the <i>Curcuma</i> species	13
2.3.1 Monoterpenes	13
2.3.2 Sesquiterpenes.....	15
2.3.3 Diterpenoids:	32
2.3.4 Biosynthesis of monoterpenes, sesquiterpenes and diterpenes	34

2.3.5	Diarylheptanoids	39
2.4	Bioactivity of the compounds previously isolated from the genus <i>Curcuma</i> 43	
2.5	Chemical composition of the essential oils from the <i>Curcuma</i> species.....	44
CHAPTER 3: RESULTS AND DISCUSSION		49
3.1	Phytochemical studies	49
3.1.1	Compounds isolated from <i>C. zedoaria</i>	50
3.1.2	Phytochemical investigation of <i>C. purpurascens</i> rhizomes.....	179
3.2	Cytotoxicity.....	218
3.2.1	Cytotoxic activity of the crude extracts and the pure compounds from the rhizomes of <i>C. zedoaria</i>	218
3.2.2	Cytotoxic activity of crude extracts, essential oil, supercritical fluid extracts, and pure compounds from <i>C. purpurascens</i> rhizomes	222
3.3	QSAR studies	225
3.3.1	Simple linear regression (SLR) analysis	230
3.3.2	Cytotoxicity against PC-3 cells and SLR analysis.....	236
3.3.3	Multiple linear regression (MLR) analysis	236
3.3.4	Principal component analysis (PCA)	244
3.4	Neuroprotective and antioxidant activity	248
3.4.1	Effect of test compounds on H ₂ O ₂ -induced cell death in NG108-15 cells	249
3.4.2	ORAC assay	251
3.4.3	Activity correlations.....	251
3.5	Spectrofluorometric and molecular docking studies on the binding of curcumenol 42 and curcumenone 65 to Human Serum Albumin (HSA)	255
3.5.1	Analysis of the binding data.....	257

3.5.2	Molecular modelling	258
3.5.3	Results of spectrofluorometric analysis	259
3.5.4	Results of molecular docking studies.....	263
CHAPTER 4: MATERIALS AND METHODS.....		269
4.1	Phytochemical analysis	269
4.1.1	Plant Samples	269
4.1.2	Solvents	269
4.1.3	Instrumentation	269
4.1.4	Chromatography.....	270
4.1.5	Visualisation.....	271
4.1.6	Isolation of the pure compounds from <i>C. zedoaria</i>	272
4.1.7	Isolation of the pure compounds from <i>C. purpurascens</i>	275
4.1.8	Isolation of the essential oils from <i>C. purpurascens</i>	277
4.1.9	Supercritical fluid extraction of <i>C. purpurascens</i>	278
4.2	Cytotoxicity assessment	279
4.2.1	Cell Culture	279
4.2.2	MTT based cytotoxicity assay	279
4.3	QSAR studies of cytotoxic compounds	280
4.4	Neuroprotective and antioxidant activity investigation	282
4.4.1	Assessment of neuroprotective activity	283
4.4.2	Antioxidant activity test by ORAC assay	284
4.5	Binding and docking studies	284
4.5.1	Binding studies.....	284
4.5.2	Molecular docking	285
4.6	Physical and spectral data of isolated compounds from <i>C. zedoaria</i>	286

4.6.1	Germacrane type sesquiterpenes	286
4.6.2	Guaiane type sesquiterpenes	289
4.6.3	<i>Seco</i> -guaiane type sesquiterpene.....	290
4.6.4	Elemmane type sesquiterpene	291
4.6.5	Humulane type sesquiterpene	291
4.6.6	Cadinane type sesquiterpene	291
4.6.7	Carabrone-type sesquiterpene	292
4.6.8	Spirolactone type sesquiterpene	292
4.6.9	Labdane type diterpenoids	293
4.7	Physical and spectral data of isolated compounds from <i>C. purpurascens</i>	294
4.7.1	Bisabolane type sesquiterpene	294
4.7.2	Diarylhepatoids	294
4.7.3	Quaiane type sesquiterpene.....	295
CHAPTER 5: CONCLUSIONS		296
REFERENCES.....		300
APPENDICES		316

LIST OF SCHEMES

Scheme 2.1: General biosynthetic pathway of monoterpene, sesquiterpene and diterpene.....	36
Scheme 2.2: Biosynthetic pathway of monoterpenes.....	37
Scheme 2.3 : Biosynthetic pathway of selected sesquiterpenes	38
Scheme 2.4 : Biosynthetic pathway for the formation of curcuminoids	40
Scheme 3.1: QSAR studies framework.....	228
Scheme 4.1: Isolation and purification of the compounds from hexane and DCM crudes of <i>C. zedoaria</i>	274
Scheme 4.2: Isolation and purification of the compounds from hexane and DCM crudes of <i>C. purpurascens</i>	276
Scheme 5.1: The proposed biosynthetic relationships of three sesquiterpenes types isolated from <i>C. zedoaria</i>	299

LIST OF FIGURES



Figure 1.1: Examples of some therapeutic agents from plants	2
Figure 2.1: White turmeric or <i>C. zedoaria</i> rhizomes	9
Figure 2.2: Rhizomes of <i>C. zedoaria</i>	10
Figure 2.3: The aerial parts of <i>C. purpurascens</i> with flowers	12
Figure 2.4: Germacrane-type sesquiterpenes from <i>Curcuma</i> species	18
Figure 2.5: Guaiane type of sesquiterpenes from the <i>Curcuma</i>	22
Figure 2.6: <i>Seco</i> -guaiane type sesquiterpenes from the <i>Curcuma</i>	23
Figure 2.7: Carabrane type sesquiterpenes from the <i>Curcuma</i>	24
Figure 2.8: Bisabolane-type sesquiterpenes from the <i>Curcuma</i> (cont.).....	26
Figure 2.9: Humulane type sesquiterpenes from the <i>Curcuma</i>	28
Figure 2.10: Spirolactone types sesquiterpenes from the <i>Curcuma</i>	28
Figure 2.11: Cadinane type sesquiterpenes from the <i>Curcuma</i>	29
Figure 2.12: Elemene type sesquiterpenes from the <i>Curcuma</i>	31
Figure 2.13: Eudesmane type sesquiterpenes from the <i>Curcuma</i>	32
Figure 2.14: Labdane type diterpenoids from the <i>Curcuma</i>	34
Figure 2.15: Curcuminoids type from the <i>Curcuma</i>	42
Figure 3.1: Selected HMBC Correlations H  C of <i>dehydrocurdione</i> 19	52
Figure 3.2: ¹ H NMR spectrum of <i>dehydrocurdione</i> 19	54
Figure 3.3: ¹³ C NMR and DPET-135 spectra of <i>dehydrocurdione</i> 19	55
Figure 3.4: COSY spectrum of <i>dehydrocurdione</i> 19	56
Figure 3.5: HSQC spectrum of <i>dehydrocurdione</i> 19	57
Figure 3.6: HMBC spectrum of <i>dehydrocurdione</i> 19	58
Figure 3.7: Selected HMBC Correlations H  C of <i>curdione</i> 20	61

Figure 3.8: ^1H NMR spectrum of curdione 20	62
Figure 3.9: ^{13}C NMR and DEPT-135 spectra of curdione 20	63
Figure 3.10: ^1H NMR spectrum of furanodiene 21	66
Figure 3.11: ^{13}C NMR and DEPT 135 spectra of furanodiene 21	67
Figure 3.12: ^1H NMR spectrum of furanodienone 22	70
Figure 3.13: ^{13}C NMR and DEPT -135 spectra of furanodienone 22	71
Figure 3.14: ^1H NMR spectrum of germacrone 23	74
Figure 3.15: ^{13}C NMR and DEPT 135 spectra of germacrone 23	75
Figure 3.16: ^1H NMR spectrum of germacrone-4,5-epoxide 24	78
Figure 3.17: ^{13}C -NMR and DEPT-135 spectra of germacrone 4,5-epoxide 24	79
Figure 3.18: ^1H -NMR spectrum of germacrone-1,10-epoxide 25	82
Figure 3.19: ^{13}C NMR and DEPT -135 spectra of germacrone-1,10-epoxide 25	83
Figure 3.20: Selected HMBC Correlations $\text{H} \xrightarrow{\quad} \text{C}$ of zederone 26	85
Figure 3.21: ^1H NMR spectrum of zederone 26	86
Figure 3.22: ^{13}C - NMR spectrum of zederone 26	87
Figure 3.23: COSY spectrum of zederone 26	88
Figure 3.24: HSQC spectrum of zederone 26	89
Figure 3.25: HMBC spectrum of zederone 26	90
Figure 3.26: Selected HMBC Correlations $\text{H} \xrightarrow{\quad} \text{C}$ of gweicurculactone 41	92
Figure 3.27: ^1H NMR spectrum of gweicurculactone 41	94
Figure 3.28: : ^{13}C NMR and DEP-T135 spectra of gweicurculactone 41	95
Figure 3.29: COSY spectrum of gweicurculactone 41	96
Figure 3.30: HSQC spectrum of gweicurculactone 41	97
Figure 3.31: HMBC spectrum of gweicurculactone 41	98




Figure 3.32: ^1H NMR spectrum of curcumenol 42	101
Figure 3.33: ^{13}C NMR and DEPT-135 spectra of curcumenol 42	102
Figure 3.34: ORTEP (Oak Ridge Thermal Ellipsoid Plot) representation of the crystal structure of curcumenol second monoclinic (molecule I and molecule II).....	103
Figure 3.35: ^1H NMR spectrum of curcumenol second monoclinic.....	105
Figure 3.36: ^1H -NMR spectrum of Isoprocucumenol 43	108
Figure 3.37: ^{13}C -NMR and DEPT -135 spectra of Isoprocucumenol 43	109
Figure 3.38: ^1H -NMR spectrum of procucumenol 44	112
Figure 3.39: ^{13}C NMR and DEPT-135 spectra of procucumenol 44	113
Figure 3.40: Selected HMBC Correlations H  C of curcuzedoalide 62	115
Figure 3.41: ^1H NMR spectrum of curcuzedoalide.....	117
Figure 3.42: ^{13}C -NMR and DEPT-135 spectra of curcuzedoalide 62	118
Figure 3.43: COSY spectrum of curcuzedoalide 62	119
Figure 3.44: HSQC spectrum of curcuzedoalide 62	120
Figure 3.45: HMBC spectrum of curcuzedoalide 62	121
Figure 3.46: Selected HMBC Correlations H  C of curzerenone 111	123
Figure 3.47: ^1H NMR spectrum of curzerenone 111	125
Figure 3.48: ^{13}C -NMR and DEPT-135 spectra of curzerenone 111	126
Figure 3.49: COSY spectrum of curzerenone 111	127
Figure 3.50: HSQC spectrum of curzerenone 111	128
Figure 3.51: HMBC spectrum of curzerenone 111	129
Figure 3.52: Selected HMBC Correlations H  C of zerumbone epoxide 151	131
Figure 3.53: ^1H NMR spectrum of zerumbone epoxide 151	133
Figure 3.54: ^{13}C NMR and DEPT-135 spectra of zerumbone epoxide 151	134





Figure 3.55: COSY spectrum of zerumbone epoxide 151	135
Figure 3.56: HSQC spectrum of zerumbone epoxide 151	136
Figure 3.57: HMBC spectrum of zerumbone epoxide 151	137
Figure 3.58: Selected HMBC Correlations H  C of comosone II 104 ...	139
Figure 3.59: ¹ H NMR spectrum of comosone II 104	141
Figure 3.60: ¹³ C NMR and DEPT 135 spectra of comosone II 104	142
Figure 3.61: COSY spectrum of comosone II 104	143
Figure 3.62: HSQC spectrum of comosone II 104	144
Figure 3.63: HMBC spectrum of comosone II 104	145
Figure 3.64: Selected HMBC Correlations H  C of <i>curcumenone</i> 65	147
Figure 3.65: ¹ H NMR spectrum of <i>curcumenone</i> 65	149
Figure 3.66: ¹³ C NMR and DEPT-135 spectra of <i>curcumenone</i>	150
Figure 3.67: COSY spectrum of <i>curcumenone</i> 65	151
Figure 3.68: HSQC spectrum of <i>curcumenone</i> 65	152
Figure 3.69: : HMBC spectrum of <i>curcumenone</i> (cont.)	153
Figure 3.70: Selected HMBC Correlations H  C of <i>curcumanolide</i> A 101	156
Figure 3.71: ¹ H NMR spectrum of <i>curcumanolide</i> A 101	158
Figure 3.72: ¹³ C NMR and DEPT spectra of <i>curcumanolide</i> A 101	159
Figure 3.73: COSY spectrum of <i>curcumanolide</i> A 101	160
Figure 3.74: HSQC spectrum of <i>curcumanolide</i> A 101	161
Figure 3.75: HMBC spectrum of <i>curcumanolide</i> A 101	162
Figure 3.76: Selected HMBC Correlations H  C of labda-8(17),12 diene-15,16 <i>dial</i> 127	165
Figure 3.77: ¹ H-NMR spectrum of labda-8(17), 12-diene-15, 16-dial 127	166

Figure 3.78: ^{13}C and DEPT-135 spectra of labda-8(17), 12-diene-15, 16-dial 127	167
Figure 3.79: COSY spectrum of labda-8(17), 12-diene-15, 16-dial 127	168
Figure 3.80: HSQC spectrum of labda-8(17), 12-diene-15, 16-dial 127	169
Figure 3.81: HMBC spectrum of labda-8(17), 12-diene-15, 16-dial 127	170
Figure 3.82: ^1H -NMR spectrum of calcaratarin A 128	173
Figure 3.83: ^{13}C NMR and DEPT-135 spectra of calcaratarin A 128	174
Figure 3.84: ^1H -NMR spectrum of zerumin A 129	177
Figure 3.85: ^{13}C NMR and DEPT spectra of zerumin A 129	178
Figure 3.86: Selected HMBC Correlations $\text{H} \xrightarrow{\quad} \text{C}$ of ar-turmerone A 101	181
Figure 3.87: ^1H -NMR spectrum of ar-turmerone 74	182
Figure 3.88: ^{13}C -NMR and DEPT-135 spectra of ar-turmerone 74	183
Figure 3.89: COSY spectrum of ar-turmerone 74	184
Figure 3.90: HSQC spectrum of ar-turmerone 74	185
Figure 3.91: : HMBC spectrum of ar-turmerone 74	186
Figure 3.92: Selected HMBC Correlations $\text{H} \xrightarrow{\quad} \text{C}$ of <i>curcumin</i> 138	189
Figure 3.93: ^1H -NMR spectrum of <i>curcumin</i> 138	190
Figure 3.94: ^{13}C -NMR and DEPT-135 spectra of <i>curcumin</i> 138	191
Figure 3.95: COSY spectrum of <i>curcumin</i> 138	192
Figure 3.96: HSQC spectrum of <i>curcumin</i> 138	193
Figure 3.97: HMBC spectrum of <i>curcumin</i> 138	194
Figure 3.98: ^1H NMR spectrum of bisdemethoxycurcumin 139	197
Figure 3.99: ^{13}C NMR and DEPT spectra of bisdemethoxycurcumin 139	198
Figure 3.100: ^1H NMR spectrum of demethoxycurcumin 140	201
Figure 3.101: ^{13}C NMR and DEPT -135 spectra of demethoxycurcumin 140	202

Figure 3.102: ^1H NMR spectrum of zedoalactone B 60	205
Figure 3.103: ^{13}C NMR and DEPT-135 spectra of zedoalactone B 60	206
Figure 3.104: The GC-FID profile of the essential oil of <i>C.purpurascens</i> rhizomes .	209
Figure 3.105: Gas chromatogram of SFE extract at 313K and 10.34 MPa	212
Figure 3.106: Gas chromatogram of SFE extracted oil at 313 K and 20.68 MPa	213
Figure 3.107: Gas chromatography profile of SFE extracted oil at 313 K and 34.47	213
Figure 3.108: Gas Chromatogram of SFE extracted oil at 333 K and 10.34 MPa	214
Figure 3.109: Gas Chromatogram of SFE extracted oil at 333 K and 20.68 MPa	214
Figure 3.110: Gas chromatography profile of SFE extracted oil at 333 K and 34.47 MPa	215
Figure 3.111: Gas Chromatogram of SFE extracted oil of at 353 K and 10.34 MPa .	216
Figure 3.112: Gas Chromatography profile SFE extracted oil at 353 K and 20.68 MPa	217
Figure 3.113: Gas chromatography profile of SFE extracted oil at 353 K and 34.47 MPa	217
Figure 3.114: Structures of compounds isolated from <i>C. zedoaria</i>	229
Figure 3.115: Simple linear regression correlation (SLR) curves between the cytotoxic activity on MCF-7 cells and each descriptor of test compounds from <i>C. zedoaria</i>	232
Figure 3.116: HOMO and LUMO orbitals of compounds 127 , 19 and 104	235
Figure 3.117: The predicted $\log(\text{IC}_{50})_{\text{Pred.}}$ and residuals to experimental $\log(\text{IC}_{50})_{\text{Obs.}}$ for the active compounds are given in Table 3.43.....	237
Figure 3.118: Multiple linear regression (MLR) correlation for cytotoxicity against MCF-7 of the active compounds with similar skeleton (127-129 , 21 , 24-25) and the most potent descriptors (see eq. 2).	240
Figure 3.119: Multiple linear regression (MLR) correlation for cytotoxicity against Ca Ski of the active compounds and the most potent descriptors (see eq. 3). ..	241
Figure 3.120: Multiple linear regression (MLR) correlation for cytotoxicity against PC3 cells of the active compounds with similar skeleton (127-129 , 21 , 24-25) and the most potent descriptors (see eq. 5).....	242

Figure 3.121: Plot of the score vectors of first principal components for cytotoxicity of compounds from <i>C. zedoaria</i> against MCF-7 cells.....	246
Figure 3.122: Dendrogram obtained with HCA for compounds with cytotoxic activity of compounds from <i>C. zedoaria</i>	247
Figure 3.123: Neuroprotective effect of curcumenol 42 on the viability of NG108-15 cells	250
Figure 3.124: Neuroprotective effect of dehydrocurdione 19 on the viability of NG108-15 cells	250
Figure 3.125: Emission spectra of HSA in the absence and the presence of increasing curcumenol (A) and curcumenone (B) concentrations, obtained in 20 mM sodium phosphate buffer, pH 7.4 upon excitation at 280 nm. [HSA] = 3 μ M, [Ligand] = (1-13): 0, 3, 6, 9, 12, 15, 18, 24, 30, 37.5, 45, 52.5 and 60 μ M. T = 25 $^{\circ}$ C.	260
Figure 3.126: Stern-Volmer plots for the quenching of HSA fluorescence by curcumenol 42 and curcumenone 65	261
Figure 3.127: Double logarithmic plots for the interaction of HSA with curcumenol 42 and curcumenone 65	262
Figure 3.128: Cluster analyses of the AutoDock docking runs of curcumenol 42 in the drug binding site I (A) and site II (B) of HSA (1BM0).	264
Figure 3.129: Cluster analyses of the AutoDock docking runs of curcumenone 65 in the drug binding site I (A) and site II (B) of HSA (1BM0).	264
Figure 3.130: Predicted orientations of the lowest docking energy conformations of 1BM0-ligand complexes. The binding sites were enlarged to show hydrogen bonding (green lines) between amino acid residues and the ligands. Amino acid residues that form hydrogen bonds with the ligands are rendered in ball and stick and coloured yellow. (A) Curcumenol in the binding site I of HSA (1BM0). (B) Curcumenone in the binding site I of HSA (1BM0).	266
Figure 3.131: Predicted orientations of the lowest docking energy conformations of 1BM0-ligand complexes. The binding sites were enlarged to show hydrogen bonding (green lines) between amino acid residues and the ligands. Amino acid residues that form hydrogen bonds with the ligands are rendered in ball and stick and coloured yellow. (A) Curcumenol in the binding site II of HSA (1BM0). (B) Curcumenone in the binding site II of HSA (1BM0).	267

LIST OF TABLES

Table 2.1: Germacrane type sesquiterpenes from the <i>Curcuma</i> (cont).....	17
Table 2.2: Guaiane type sesquiterpenes from the <i>Curcuma</i>	20
Table 2.3: <i>Seco</i> guaiane type sesquiterpenes from the <i>Curcuma</i>	22
Table 2.4: Carabrane type sesquiterpenes from the <i>Curcuma</i>	23
Table 2.5: Bisabolane type sesquiterpenes from the <i>Curcuma</i>	25
Table 2.6: Humulane type sesquiterpenes from the <i>Curcuma</i>	27
Table 2.7: Spirolactone type sesquiterpenes from the <i>Curcuma</i>	28
Table 2.8: Cadinane type sesquiterpenes from the <i>Curcuma</i>	29
Table 2.9: Elemene type sesquiterpenes from the <i>Curcuma</i>	30
Table 2.10: Eudesmane type sesquiterpenes from <i>Curcuma</i>	32
Table 2.11: Labdane-type diterpenoids from the <i>Curcuma</i>	33
Table 2.12: Curcuminoids isolated from the <i>Curcuma</i>	41
Table 2.13: Bioactive compounds from the <i>Curcuma</i>	44
Table 2.14: The major constituents of the essential oils of the <i>C. zedoaria</i> identified by GC/GC-MS analysis	46
Table 2.15: The major constituents of the essential oils of other <i>Curcuma</i> species identified by GC/GC-MS analysis	47
Table 3.1: Compounds isolated from <i>C. zedoaria</i>	50
Table 3.2: ¹ H NMR (400 MHz) and ¹³ C NMR (100 MHz) spectral data of dehydrocurdione 19 in CDCl ₃	53
Table 3.3: ¹ H (400 MHz) NMR and ¹³ C (100 MHz) NMR spectral data of <i>curdione</i> 20 in CDCl ₃	61
Table 3.4: ¹ H NMR (400 MHz), and ¹³ C NMR (100 MHz) spectral data of furanodiene 21	65
Table 3.5: ¹ H NMR (400 MHz) and ¹³ C NMR (100 MHz) spectral data of furanodienone 22	69

Table 3.6: ^1H NMR (400 MHz), and ^{13}C NMR (100 MHz) spectral data (in CDCl_3) of germacrone 23	73
Table 3.7: ^1H NMR (400 MHz), and ^{13}C NMR (100 MHz) spectral of germacrone 4,5-epoxide 24 data in CDCl_3	77
Table 3.8: : ^1H NMR (400 MHz), and ^{13}C NMR (100 MHz) spectral data of germacrone-1, 10-epoxide 25 in CDCl_3	81
Table 3.9: ^1H (400 MHz) NMR and ^{13}C (100 MHz) NMR spectral data of zederone 26	85
Table 3.10: ^1H (400 MHz) NMR and ^{13}C (100 MHz) spectral data of gweicurculactone 41 in CDCl_3	93
Table 3.11: ^1H NMR (400 MHz) and ^{13}C NMR (100 MHz) spectral data of curcumenol 42	100
Table 3.12: ^1H (400 MHz) NMR, and ^{13}C (100 MHz) NMR spectral data of isoprocurcumenol 43 in CDCl_3	107
Table 3.13: ^1H (400 MHz) NMR, and ^{13}C (100 MHz) NMR spectral data of procurcumenol 44	111
Table 3.14: ^1H (400 MHz) NMR, and ^{13}C (100 MHz) NMR spectral data of curcuzedoalide 62 in CDCl_3	116
Table 3.15: ^1H (400 MHz) NMR and ^{13}C (100 MHz) NMR spectral data of curzerenone 111 in CDCl_3	124
Table 3.16: ^1H (400 MHz) NMR and ^{13}C (100 MHz) NMR spectral data of zerumbone epoxide 151 in CDCl_3	132
Table 3.17: : ^1H NMR (400 MHz) and ^{13}C NMR (100 MHz) spectral data in CDCl_3 of comosone II 104	140
Table 3.18: ^1H NMR (400 MHz) and ^{13}C NMR (100 MHz) spectral data in CDCl_3 of curcumenone 65 in CDCl_3	148
Table 3.19: ^1H NMR (400 MHz), and ^{13}C NMR (100 MHz) spectral data of curcumanolide A 101	157
Table 3.20: ^1H NMR (400 MHz) and ^{13}C NMR (100 MHz) spectral data in CDCl_3 of labda-8(17),12 diene-15,16 dial 127	165
Table 3.21: ^1H NMR (400 MHz), and ^{13}C NMR (100 MHz) spectral data (in CDCl_3) of calcaractrin A 128	172

Table 3.22: : ^1H NMR (400 MHz), and ^{13}C NMR (100 MHz) spectral data recorded in CDCl_3 of zerumin A 129	176
Table 3.23: Compounds isolated from <i>C. purpurascens</i>	179
Table 3.24: ^1H NMR (400 MHz) and ^{13}C NMR (100 MHz) spectral data in CDCl_3 , of ar-turmerone 74	181
Table 3.25: ^1H NMR (400 MHz) and ^{13}C NMR (100 MHz) spectral data of curcumin 138 in acetone- D	189
Table 3.26: ^1H NMR (400 MHz), and ^{13}C NMR (400 MHz) spectral data in acetone- d_6 of bisdemethoxycurcumin 139	196
Table 3.27: ^1H NMR (400 MHz) and ^{13}C NMR (400 MHz) spectral data of demethoxycurcumin 140 in acetone- d_6	200
Table 3.28: ^1H NMR (400 MHz), and ^{13}C NMR (100 MHz) spectral data in acetone- d_6 of zedoalactone 60	204
Table 3.29: Chemical composition of the essential oil of <i>C. purpurascens</i> rhizomes	208
Table 3.30: The yields of the extracts obtained from <i>C. purpurascens</i> by SFE using variable temperatures and pressures.....	211
Table 3.31: Major components of SFE oil extracted at 313 K and 10.34 MPa	212
Table 3.32: Major component of SFE oil extracted at 313 K and 20.68 MPa.....	213
Table 3.33: Major components of SFE oil extracted at 313 K and 34.47 MPa	213
Table 3.34: Major components of SFE extracted oil at 333 K and 10.34 MPa	215
Table 3.35: Major components of SFE extracted oil of at 353 K and 10.34 MPa	216
Table 3.36: Major components of SFE extracted oil of at 353 K and 20.68 MPa	217
Table 3.37: Cytotoxic activity of <i>C. zedoaria</i> extracts against human cancer cells and non-cancer cell lines (MRC-5 and HUVEC)	218
Table 3.38: Cytotoxic activity of pure compounds isolated from <i>C. zedoaria</i> against various cell lines	221
Table 3.39: Cytotoxic activity of crude extracts, hydrodistillation oil, and SFE extracts of the rhizomes of <i>C. purpurascens</i>	223
Table 3.40: Cytotoxic activity of compounds isolated from <i>C. purpurascens</i>	224

Table 3.41: Cytotoxicity IC ₅₀ (μM) and molecular descriptors obtained at B3P86/6-311+G (d, p) and B3P86/6-311+G (d, p) level for the compounds under investigation	231
Table 3.42: Correlation coefficients (R^2), adjusted correlation coefficients (R^2_{adj}) and standard deviations (SD) of simple linear regression curves (SLR) between each descriptor and cell lines assays.....	233
Table 3.43: Experimental and predicted log(IC ₅₀) for the active compounds.	238
Table 3.44: Variances (eigenvalues) obtained for the first three principal components	245
Table 3.45: Loading vectors for the first three principal components	245
Table 3.46: Neuroprotective evaluation of compounds against H ₂ O ₂ -induced cell death in NG108-15 cells.....	249
Table 3.47: Antioxidant capacity of the compounds by ORAC method.	251
Table 3.48: Quenching and binding parameters for curcumenol-/ curcumenone-HSA interactions, as obtained in 20 mM sodium phosphate buffer, pH 7.4 at 25°C.	261
Table 3.49: Predicted hydrogen bonds between interacting atoms of the amino acid residues of HSA (1BM0) and the ligands at site I and site II.	267

LIST OF SYMBOLS AND ABBREVIATIONS

1D-NMR	One Dimensional Nuclear magnetic Resonance Spectroscopy
2D-NMR	Two Dimensional Nuclear magnetic Resonance Spectroscopy
Acetone- d_6	Deuterated acetone
α	Alpha
β	Beta
nm	Nanometer
μM	micromolar
$\mu\text{g/ml}$	Microgram per mililitre
Mg/ml	Miligram per mililitre
g	Gram
kg	Kilogram
Hz	Hertz
MHz	Mega Hertz
$^1\text{H-NMR}$	Proton NMR
^{13}C	13-carbon NMR
s	Singlet
d	Doublet
dd	Doublet of doublet
dt	Doublet of triplet
q	Quartet
t	Triple
m	Multiplet
δ	Chemical shift
J	Coupling constant
ppm	Part per million
cm^{-1}	Per centimeter
GC	Gas chromatography
GC-MS	Gas chromatography-mass spectroscopy
MTT	3-(4, 5-dimethylthiazol-2y)-2, 5-diphenyltetrazolium
COSY	Correlation Spectroscopy
CDCl_3	Deuterated chloroform
UV	Ultraviolet light
DEPT	Distortionless Enhancement by Polarisation Transfer

CC	Open Column Chromatography
ESI MS	Electrospray Ionisation Mass Spectroscopy
EtOAc	Ethyl acetate
HRESI-MS	High Resolution Electrospray Ionisation Mass Spectroscopy
MeOH	Methanol
HMBC	Heteronuclear Multiple Bond Coherence
HMQC	Heteronuclear Multiple Quantum Coherence
MeOD	Deuterated methanol
<i>m/z</i>	Mass to charge ratio
NMR	Nuclear Magnetic Resonance
NOESY	Nuclear Overhauser Enhancement Spectroscopy
TLC	Thin layer chromatography
n-hex	n-hexane
DCM	Dichloromethane
MeOH	Methanol

CHAPTER 1: INTRODUCTION

1.1 Introduction

The use of plants in the treatment of diseases is as old as human civilization on the earth. Although it is not clear how the primitive people discovered the phenomenon that plants could be used to cure disease, but probably through the process of trial and error, they mastered the use of proper plants for the treatment of certain disease. Thereby, some of the most well-known traditional medicinal practices e.g. Indian Ayurveda, Chinese Medicine, Galenical Greek, and Egyptian were developed. Such herbal practices still have thrived throughout the centuries to reserve their values to the modern medications and their efficacies are now proven to be efficient by scientific explorations. The utilization of the plant materials is an active area of research that takes advantage of readily available, valuable and renewable resources. Isolation of biologically active compound(s) is a field of ever increasing interest that originates from the basic ideas to systematic research and high-throughput screening of the plant kingdom. Medicinal plants were and are still the reservoir to produce a wide variety of chemicals that can impart various important biological activities (P. Lai et al., 2004). Surprisingly, the use of medicinal plants remained popular and common in almost all communities, while it is the sole source of basic health care needs in the developing countries, even if it is not very common in developed countries. Not only is this but another fascinating fact about traditional medicines that they represent one of the strongest links in the history of the human kind between the man and nature. Despite the modern lifestyle and westernization, scientists are increasingly turning their attention to natural products with a view to develop important new leads against various diseases, and in particular, for the treatment of cancer (Organization, 2013). Hence, natural medicines continue to play a key role as a source of contemporary cancer chemotherapeutic agents (Balunas et al., 2005).

The WHO reported that in some Asian and African countries, up to 80% of the population relies on traditional medicine for their primary health care needs. Therefore, the updated strategy of the WHO for the period 2014-2023 devotes more attention than its predecessor to prioritizing traditional medicine based health services and systems (Organization, 2002)

(Recent drug discovery techniques based on structure-activity relationships, computer aided molecular modelling, combinatorial chemistry, high throughput screening, various chromatographic tools and spectroscopic methods (MS, NMR, X-ray, and IR) have led to the discovery of many natural products and natural product derived drugs.

Natural products in their simple forms based on the above mentioned technological analysis, dominate the current therapeutic practice. While some pure compounds have been isolated successfully and used as single therapeutic agent in the treatment of a particular disease, i.e. artemisinin (1), paclitaxel (2) and its analogue docetaxel (3) as presented in **Figure 1.1**, preparations containing extract of one plant or a number of plants also have been exploited, mainly by traditional healers.

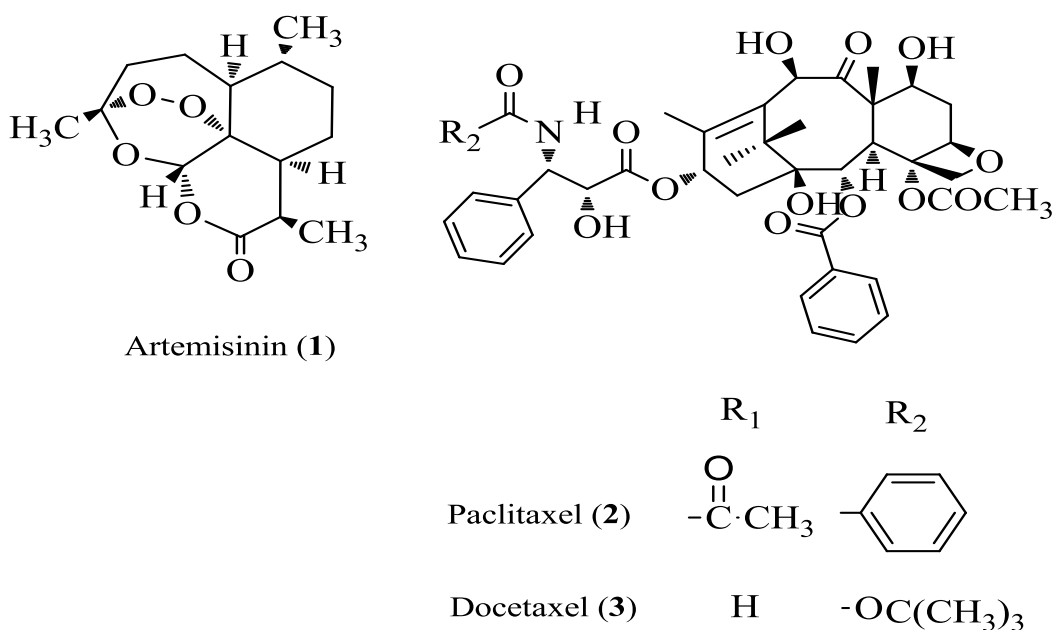


Figure 1.1: Examples of some therapeutic agents from plants

Artemisinin (**1**) for instance is a secondary metabolite of the sesquiterpene lactone type with an unusual endoperoxide bridge produced by *Artemisia annua*, a plant used in Traditional Chinese Medicine (TCM). Artemisinin is the drug of choice for the treatment of malaria and is effective against quinine-resistant strains of *Plasmodium falciparum*. The peroxide bridge is believed to be essential for the drug's antimalarial property (Chaturvedi et al., 2010). *A. annua*, of the family Asteraceae, is native to China and has been used there for over two thousand years to treat fever. In addition to its use in treating malaria, artemisinin has been demonstrated to be effective against a variety of other diseases including hepatitis B, schistosomiasis (Romero et al., 2005), and a wide range of cancers (Singh et al., 2004).

The diterpenoid paclitaxel (taxol) **2**, first isolated from *Taxus brevifolia*, is one of most widely used anti-cancer drugs for the treatment of breast, ovarian and lung cancers (Heinig et al., 2009). Docetaxel (texotere) **3** is a semi-synthetic derivative of paclitaxel, and has potent activity against breast cancer (Ravdin et al., 1995).

Plant derived essential oils also represent an important class of natural products that contributes in various domains of human activities. In nature, essential oils play an important role in the protection of plants. They also attract some insects which in turn disperse pollen and seeds, or repel the undesirable attention of predators (Bakkali et al., 2008; Nerio et al., 2010). Essential oils can be divided into three major classes: oils used for therapeutic purposes; oils used as flavoring agents in foods; used for perfumery, soap and cosmetics perfumery, cosmetics, pharmaceuticals, and aromatherapy. Since the Middle ages, essential oils have been widely used for their antiparasitic, antiviral, bactericidal, fungicidal, insecticidal, and medicinal cosmetic applications broadly nowadays in pharmaceutical, sanitary, cosmetic, agricultural and food industries. For example, the essential oils extracted from the dried lemongrass (*Cymbopogon citratus* or *Andropogon citratus*). The main constituents of the lemongrass derived essential oils

of the lemongrass are citral, citronellal, geranyl acetate, geraniol limonene, myrcene, and nerol. Essential oils also have many beneficial properties e.g. analgesic, antidepressant, anti-pyretic, antifungal and antibacterial (Leite et al., 1986; Sessou et al., 2012; Tzortzakis et al., 2007). The tea tree oil is an essential oil from the leaves of *Melaleuca alternifolia* and has a long history of traditional uses. Australian aborigines use tea tree leaves for healing skin cuts, burns, and infections by crushing the leaves and applying them on the affected area. Tea tree oil contains terpenoids, which have antiseptic and antifungal properties. Tea tree oil is a complex mixture of approximately 100 components, whereas terpinen-4-ol is the most abundant and thought to be the major contributing factor towards the antimicrobial activity of tea tree oil, while 1,8-cineole is a skin irritant (Carson et al., 1995) .

Collectively, natural products shape the modern medical treatment either in the form of a cutting edge pharmaceutical drug, a component of cosmetic preparation, or as simple as a decoction in rural traditional practice.

In view of the importance of natural medicines in the world communities, coupled with the advancement of science and technology to discover the underlying prospects that could be responsible for the manifestation of their biological and pharmacological activities, this work was undertaken to study of two selected Indo-Malay medicinal herbs from the *Curcuma* species used in the Malay archipelago.

1.2 Aims and objectives

C. zedoaria and *C. purpurascens* presents some important uses in traditional practice. However, no scientific evidence has been reported to justify their use. Therefore, it is worth applying modern techniques to support the traditional claims phytochemically and pharmacologically. Results obtained, perhaps, can be used for development therapeutic agents.

The specific aims and objectives of this study are as follows:

Isolation, purification and identification of the chemical constituents from the *n*-hex and DCM extracts of *C. zedoaria* and *C. purpurascens*.

- Extraction of volatile components from *C. purpurascens* using hydrodistillation and supercritical fluid extraction techniques, then analysing by combination of GC/GC-MS spectroscopy.
- Investigation of cytotoxic activity of isolated compounds from *C. zedoaria*:
 - Cytotoxicity test against MCF-7, Ca Ski, HT-29, and PC-3 cell line as well as against non-cancer human fibroblast cell line (MRC-5), and HUVEC cell line using *in vitro* MTT cytotoxicity assay.
 - Elucidation of the structure-cytotoxic activity relationship of twenty-one compounds isolated from *C. zedoaria* using the density functional theory (DFT) method at B3LYP/6-31+G (d,p) level, with a view to calculate electronic and steric molecular descriptors of the compounds under investigation. Statistical methods were applied (SLR, MLR, PCA and HCA) to determine the main descriptors responsible for the cytotoxic activity of the isolated compounds.
- Investigation of cytotoxic activities of the *n*-hex, DCM, MeOH extracts, hydrodistilled essential oil, supercritical fluid extracts, and the isolated pure compounds of *C. purpurascens* using an *in vitro* MTT cytotoxicity assay against various human cancer cell lines.
- Test for neuroprotective activity of selected compounds against H₂O₂-induced oxidative stress in NG108-15 cells.
- Test for antioxidant activity of the compounds tested for neuroprotective activity.
- Investigations on the interaction of human serum albumin (HSA) to the two most active compounds (curcumenol **42** and curcumenone **65**) based on

fluorescence spectroscopic results coupled with molecular docking study.

- Application of molecular docking to investigate the location of interaction of these two compounds at the binding sites (site I and site II) of HSA.

CHAPTER 2: LITERATURE REVIEW

2.1 Introduction

In the present study, the rhizomes of two plants namely, *Curcuma zedoaria* and *Curcuma purpurascens* were chosen for the phytochemical and biological investigations. Thus literature survey on these plants was carried out using some of the most widely accepted abstracting indices including Scifinder Scholar, Pubmed, Web of Knowledge and Scopus. In addition, Google scholar was also used to search for published research work on these two plants that is not available through the above websites. This chapter contains the literature review of the two plants and the topics encompass habitat, traditional uses, previous phytochemical investigation, and biological investigation. This chapter also deals briefly with the classification, biosynthesis of the some of the monoterpenes, sesquiterpenes and diterpenes, found in the genus *Curcuma* and represented as the major class of natural products.

2.2 Botanical and chemical aspects

The family Zingiberaceae and one of its major genera *Curcuma* has drawn the attention of the researchers for their wide use in daily diet, folkloric medicine and rich secondary metabolite content. The use of such plant species in traditional medicine for the treatment of specific disease coupled with their bioactive component holds a good promise towards the development of potential drug leads and nutraceuticals. The following sections deals with the botanical identity of the family Zingiberaceae and the genus *Curcuma* as well as the chemical diversity seen in this genus.

2.2.1 The family Zingiberaceae

The Zingiberaceae is one of the most prolific plant families found in tropical rainforests. Species of the Zingiberaceae are famous for their use and also for their medicinal properties. The family contains approximately 1400 species distributed in 47 genera (Pancharoen et al., 2000). In Peninsular Malaysia, approximately 160 species

belonging to 18 genera are found, mostly growing naturally in damp, shaded parts of the lowland or hill slopes, as scattered plants, or thickets (Larsen et al., 1999). In Asian countries, several species are commonly used as spices, medicines, flavouring agents, as well as the source of certain dyes (Burkill, 1966). Many plants of this family are extensively used in the traditional herbal remedies for treating and preventing diseases particularly in Malaysia, Indian Ayurveda and Chinese medicine (Lakshmi et al., 2011a). All parts of the plants of all members of this family contain essential oils. Leaves, seeds, and rhizomes are usually rich in monoterpenes, sesquiterpenes, aliphatic hydrocarbons, aromatic ketones, which are the characteristic components of volatile oils (Brouk, 1975).

2.2.1.1 The genus *Curcuma*

The genus *Curcuma* (Zingiberaceae) contains various rhizomatous herb and is known as the turmeric genus. The name “*Curcuma*” derived from the Arabic word “Kurkum” meaning “Saffron”, but now refers to turmeric only. The genus *Curcuma* has over 100 species growing in tropical and subtropical areas in Asia. Some of the most famous species of *Curcuma* used in the traditional medicine for thousands of years include *C. aromatic*, *C. longa* , *C. xanthorrhiza*. and *C. zedoaria*.

The orange coloration of the *Curcuma* species is often associated with their curcumin content and other curcumin derivatives, collectively known as curcuminoids. Terpenoids and curcuminoids are the major bioactive compounds of *Curcuma* (Ravindran et al., 2007).

2.2.1.1.1 *Curcuma zedoaria*

C. zedoaria, also known as the white turmeric, is a perennial herb of the family Zingiberaceae and largely found in many Asian tropical countries including Malaysia, Indonesia, India, Japan, and Thailand. In Malaysia, it is locally known as ‘*Temu putih*’

or '*Kunyit putih*' and is widely consumed as a spice, a flavouring agent for native dishes, and is frequently incorporated in food preparations for women in confinement after child birth. It is one of the three most widely used medicinally important plant species from the genus *Curcuma*. Traditionally, the dried rhizomes of *C. zedoaria* are used to make drinks or to be extracted and used as a remedy for various ailments (Larsen et al., 1999).

(a) Morphology of *C. zedoaria*

The leaf blades are 80 cm long, usually with a purple-brown flush running along the midrib on both surfaces of the leaf. In the young plants, the rhizomes of *C. zedoaria* are easily confused with those of *C. aeruginosa* and *C. mangga* since both have almost similar yellow colouration. However, a cross-section of the rhizomes of the mature plants of *C. aeruginosa* is slightly dark purplish, whilst *C. mangga* rhizomes have brighter yellow colour (**Figure 2.1 and 2.2**) (Maciel et al., 2002) .



Figure 2.1: White turmeric or *C. zedoaria* rhizomes



Figure 2.2: Rhizomes of *C. zedoaria*

(b) Traditional uses of *C. zedoaria*

C. zedoaria has been widely used for thousands of years as a healing agent for a variety of illnesses in traditional medicinal practices in many Asian countries. In Malaysia and Indonesia, it is used for the treatment of cancer, dyspepsia, menstrual disorders, stomachic, and vomiting (Lobo et al., 2009). The plant is reported to have antimicrobial, antifungal (Bugno et al., 2007; Ficker et al., 2003; Uechi et al., 2000), antiulcer (P. Gupta et al., 2003), analgesic (Navarro et al., 2002; Pamplona et al., 2006), anti-inflammatory (Tohda et al., 2006), antioxidant (Mau et al., 2003a), hepatoprotective (Hisashi Matsuda et al., 1998b), cytotoxic (Hong et al., 2002; Seo et al., 2005) and antimutagenic (Lee et al., 1988) activities. The rhizomes of this plant have been used as a stimulant, stomachic, carminative, diuretic, anti-diarrheal, anti-inflammatory, anticancer, anti-emetic, antic-pyretic, depurator and also as topical ointment for ulcers, wounds, and other skin disorders (Larsen et al., 1999).

Temu putih is used by the Malaysians and Indonesians in the preparation of traditional medicine-consumed either on their own or in mixtures with other plant

species. *C. zedoaria* is one of the ingredients in “*Jamu*”, a mixture of Indo-Malay traditional herbal medicine, a preparation that came into practice from the experiences of the past, embedded in the culture of the society. *Jamu* is believed to maintain good health and assists in the prevention and treatment of various diseases. The other major herbs used in *Jamu* preparation are *C. aromatica*, *C. domestica*. And *C. xanthorrhiza*. They are also widely consumed as spices, flavours in native dishes and as food preparations in postpartum confinement. *C. zedoaria* commonly referred as *Er-chu* in Chinese is clinically used for the treatment of cervical cancer. In Japan, it is used in the treatment of stomach ailments. In the Ayurvedic medicine, it is used for the treatment of fever (cooling), as mild expectorant, antiseptic, and deodoriser. In Indonesia, *C. zedoaria* is widely consumed in the form of ‘*Jamu*’ for the treatment of breast and cervical cancers.

2.2.1.1.2 *Curcuma purpurascens*

C. purpurascens is another medicinally important plant of the family Zingiberaceae. In Malaysia and Indonesia it is locally known as “*Temu tis*”, and is synonymous to Solo’s (East of Yogyakarta), “*Temu gleneyeh*” or “*Temu belenyeh*” with the scientific name of *Curcuma soloensis* (Koller, 2009) Villagers from the Kediri district located at the base of the Mount Wilis of East Java is one of the major commercial producers of the plant *C. purpurascens* or ‘*Temu tis*’. The rhizomes are dried and ground before selling to the wholesalers as an alternative medicine. *C. purpurascens* is included in the Javanese medicinal plants used in rural communities (Koller, 2009).

(a) Morphology: *C. purpurascens*

C. purpurascens is a herb with the branched rhizomes, outside and inside orange-yellow with whitish tips; leaf blades elliptical (55-70 cm × 19-23 cm), green but purple along the midrib above; inflorescence terminal on a leafy shoot, bracts pale

green, coma bracts white at base and pale green towards the top or almost entirely white, outside pale brown spotted at the top; corolla about 5 cm long, white; labellum about 17 mm × 17 mm, pale creamy yellow with a dark yellow median, other staminodes pale creamy yellow, another with long spurs. *C. purpurascens* grows spontaneously in teak forest (**Figure 2.3**) (Koller, 2009).



Figure 2.3: The aerial parts of *C. purpurascens* with flowers

(b) Traditional uses of *C. purpurascens*

The plant is a Javanese medicinal plant which has been used for numerous indications in rural Javanese communities. Same as other *Curcuma* species, the rhizomes of *C. purpurascens* are extensively used as a spice and also as a folk medicine. Rural communities in Indonesia use this plant for the treatment of boils, cough, fever, itches, scabies, and wounds. Rhizomes are used against tussis, and mixed with *Alyxia stellate* to apply as a poultice after childbirth. The central tuberous root contains extractable starch (Koller, 2009). There are eleven *Curcuma* species used as ingredients of *Jamu* which includes *C. aeruginosa*, *C. aurantiaca*, *C. coloraya*, *C. domestica* (synonym: *C. longa*), *C. euchroma*, *C. manga*, *C. petiolata*, *C. purpurascens*, *C.*

soloensis, *C. xanthorrhiza*, and *C. zedoaria*. These plants are used traditionally as spices and to treat diseases including abdominalgia, anaemia, appendicitis, asthma, diarrhoea, dysentery, hypertension, itch, and rheumatism (Hatcher et al., 2008).

2.3 Chemistry of the *Curcuma* species

Reported *Curcuma* species accounts for over 100. About twenty of these species have undergone extensive phytochemical and biological investigations and resulted in the isolation of various types of compounds presented in Table 2.1-2.9. These compounds can be classified into three major groups: monoterpenoids, sesquiterpenoids, diterpenoids and diarylheptanoids (curcuminoids). The most extensive investigated species are *C. longa*, *C. xanthorrhiza*, and *C. zedoaria*. The highest number of the compounds which have a similar skeleton previously isolated from the genus *Curcuma* documented was a guaiane type sesquiterpenoids. The essential oils from the rhizomes or the leaves of the genus are rich in monoterpenes, but also contain sesquiterpenes. While the essential oils from *C. zedoaria* have been investigated for its content, there is no such report on *C. purpurascens* with respect to its chemical constituents or essential oil composition. The following subchapters will discuss briefly the chemical aspects and biosynthesis of monoterpenes, sesquiterpenes, diterpenes and curcuminoids.

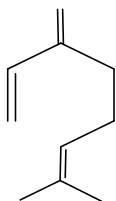
2.3.1 Monoterpenes

Biogenetically, monoterpenes derive from the condensation of two isoprene units (Banthorpe et al., 1972). They are widely distributed in nature as the major components of the plant essential oils. Economically, the important usage of monoterpenes is as perfume and flavor. The *Curcuma* essential oils obtained from various *Curcuma* species are rich in monoterpenes. Among the *Curcuma* species, *C. zedoaria* rhizomes produce monoterpenes in high amounts, with the major monoterpenes found in most of the *Curcuma* species are 1,8-cineole, α -pinene, β -

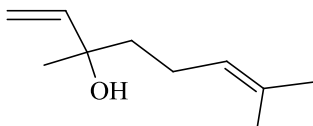
pinene, camphor, and comphene.

Monoterpenes can be divided into three major categories:

- Acyclic (linear) structures such as myrcene **4** and linalool **5**.

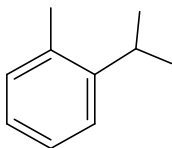


Myrcene **4**

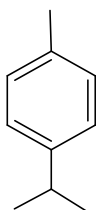


Linalool **5**

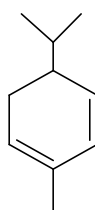
- Monocyclic monoterpenes like *o*-cymene **6**, *p*-cymene **7**, α -phellandrene **8**, and terpinolene **9**.



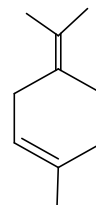
o-Cymene **6**



p-Cymene **7**

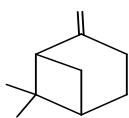


α -Phellandrene **8**

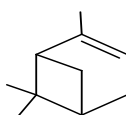


Terpinolene **9**

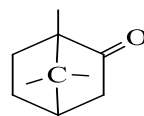
- Bicyclic monoterpenes e.g. β -pinene **11** α -pinene **12**, camphor **13**, and fenchone **16**.



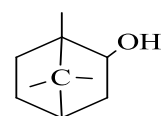
β -Pinene **11**



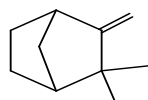
α -Pinene **12**



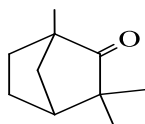
Camphor **13**



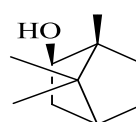
Borneol **14**



Camphene **15**



Fenchone **16**



Isobornyl alcohol **17**



1,8-Cineole **18**

2.3.2 Sesquiterpenes

The sesquiterpenes contain a total of 15 carbon atoms, formed by the assembly of three isoprene units. A large number of sesquiterpenoids (more than 140 compounds) have been isolated from the *Curcuma* species and they can be classified into ten distinctly different structural types; guaiane, germacrane, bisabolane, *seco*-guaiane, carabrane, humulane, spiro lactone, cadinane, elemene, and eudesmane (**Figure 2.6**). However, most of these compounds fall into one of the major categories, guaiane, germacrane, and bisabolane types. Sesquiterpenoids are known to be the key components of many essential oils.

2.3.2.1 Classification of sesquiterpenes based on skeleton type

The plants of the genus *Curcuma* are rich in sesquiterpenoids having a wide range of chemical structures. Different types of sesquiterpenes have been isolated from *Curcuma* which include germacrane, guaiane, *seco*-guaiane, carabrane, bisabolane, humulane, spiro lactone, and cadinane type. These types are presented in Table 2.1-2.10 and **Figure 2.4-2.13**.

2.3.2.1.1 Germacrane type sesquiterpenes

To date, germacrane type sesquiterpenes have been found in ten of the twenty chemically investigated *Curcuma* species. These are *C. zedoaria*, *C. longa*, *C. heyneana*, *C. comosa*, *C. aeruginosa*, *C. malabarica*, *C. aromatica*, *C. sichuanensis*, *C. wenyujin* and *C. amada* (Table 2.1).

The characteristic features of this skeleton are a ten membered ring (C-1 to C-10) ring having two methyls attached to C-4, and C-10 while some compound has isopropyl group attached to C-7. Some of these can undergo cyclisation of the side chain at C-7 (i.e, C-12, C-11, C-13) to form furan ring fused to the ten membered ring.

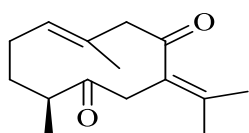
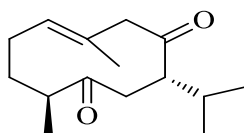
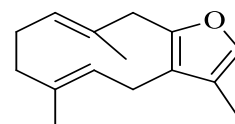
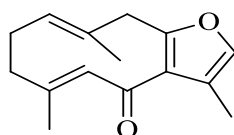
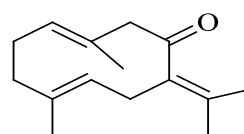
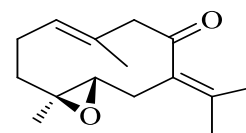
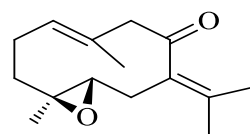
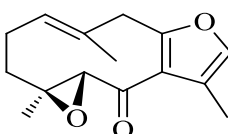
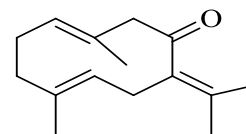
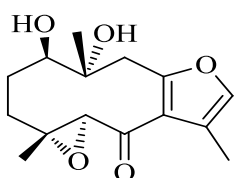
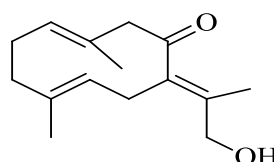
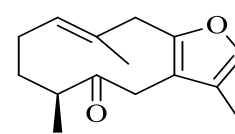
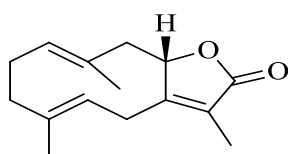
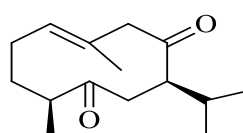
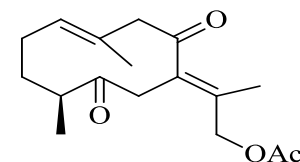
As per the reported data, the number of germacrane type sesquiterpenes isolated is the second highest after guaiane type sesquiterpenes. So far, *C. zedoaria* is the most prolific producer of germacrane sesquiterpenes. This species has been widely studied and samples from India, Indonesia, Malaysia and China have reported the occurrence of 25 different germacrane derivatives such as dehydrocurdione **19**, curdione **20**, furanodiene **22**, furanodienone **22**, germacrone, **23**, and neocurdione **32**. The structure of zederone **19** was first time proposed by Hikino group (Hikino et al., 1968) and was the first germacrane sesquiterpene to have its absolute configuration determined through X-ray crystallography by Prof. Isao Kitagawa et al., 1987. Dehydrocurdione **19** is the most widely distributed germacrane type sesquiterpene in the *Curcuma* species where it has been reported in eight species. Other commonly found germacrane are curdione **20**, furanodiene **21**, furanodienone **22**, germacrone **23**, zederone germacrone-4, 5-epoxide **24**, germacrone-1, 10 epoxide **25**, neocurdione **32** and zederone epoxide **38**. Table 2.1 and **Figure 2.4** represent some of the most common sources of germacrane found in *Curcuma*.

Table 2.1: Germacrane type sesquiterpenes from the *Curcuma* (cont)

Compounds	Source
Dehydrocurdione 19	<i>C. zedoaria</i> (Makabe et al., 2006) <i>C. longa</i> (Ohshiro et al., 1990a) <i>C. heyneana</i> (Firman et al., 1988b) <i>C. comosa</i> (Qu et al., 2009b) <i>C. aeruginosa</i> (Suphrom et al., 2012b) <i>C. malabarica</i> (Wilson et al., 2005) <i>C. aromatica</i> (Choudhury et al., 1996) <i>C. sichuanensis</i>
Curdione 20	<i>C. zedoaria</i> (Hisashi Matsuda, Toshio Morikawa, et al., 2001b) <i>C. wenyujin</i> (Yan et al., 2005) <i>C. aromatica</i> (Choudhury et al., 1996) <i>C. kwangsiensis</i> (Zeng et al., 2009)
Furanodiene 21	<i>C. zedoaria</i> (Makabe et al., 2006) <i>C. wenyujin</i> (Sun et al., 2009) <i>C. aromatica</i> (Giang et al., 2000)
Furanodienone 22	<i>C. zedoaria</i> (Shibuya et al., 1986) <i>C. aromatica</i> (Giang & Son, 2000)
Germacrone 23	<i>C. zedoaria</i> (Makabe et al., 2006) <i>C. wenyujin</i> (Yan et al., 2005) <i>C. aeruginosa</i> (Suphrom et al., 2012a) <i>C. aromatica</i> (Giang & Son, 2000)
Germacrone-4,5-epoxide 24	<i>C. zedoaria</i> (Hisashi Matsuda, Toshio Morikawa, et al., 2001a) <i>C. longa</i> (Ohshiro et al., 1990a) <i>C. aromatica</i> (Choudhury et al., 1996)
Germacrone-1, 10-epoxide 25	<i>C. wenyujin</i> (X.-y. Liu et al., 2007)
Zederone 26	<i>C. zedoaria</i> (Makabe et al., 2006) <i>C. aeruginosa</i> (Suphrom et al., 2012a) <i>C. amada</i> (Faiz Hossain et al.) <i>C. aromatica</i> (Pant et al., 2001)
Germacrone-13-al 27	<i>C. longa</i> (Ohshiro et al., 1990a)
Curcuzederone 28	<i>C. zedoaria</i> (Eun et al., 2010)
13-Hydroxygermacrone 29	<i>C. zedoaria</i> (Hisashi Matsuda, Toshio Morikawa, et al., 2001b)
Isofuranodienone 30	<i>C. zedoaria</i> (Hisashi Matsuda, Toshio Morikawa, et al., 2001a)
Glechomanolide 31	<i>C. zedoaria</i> (Hisashi Matsuda, Toshio Morikawa, et al., 2001b)
Neocurdione 32	<i>C. zedoaria</i> (Makabe et al., 2006) <i>C. aromatica</i> (Choudhury et al., 1996)
(4S)-Acetoxydehydrocurdione 33	<i>C. aromatica</i> (Kuroyanagi et al., 1990b)
4S)-Hydroxydehydrocurdione 34	<i>C. aromatica</i> (Kuroyanagi et al., 1990b)
(4S, 5S)-13-Hydroxygermacrone-4,5-epoxide 35	<i>C. aromatica</i> (Kuroyanagi et al., 1990b)

Table 2.1: Germacrane type sesquiterpenes from the *Curcuma* (cont.)

Compounds	Source
(4S, 5S)-13-Acetoxygermacrone -4,5-epoxide 36	<i>C. aromatic</i> (Kuroyanagi et al., 1990b)
(4S, 5S)-12-Acetoxygermacrone -4,5-epoxide 37	<i>C. aromatica</i> (Kuroyanagi et al., 1990b)
Zederone epoxide 38	<i>Curcuma comosa</i> (Qu et al., 2009b)
Germacrone-1(10), 4 (diepoxide) 39	<i>Curcuma comosa</i> (Qu et al., 2009b)
(2S)-2-Hydroxycurdione 40	<i>Curcuma aromatica</i> (Bamba et al., 2011)

Dehydrocurdione **19**Curdione **20**Furanodiene **21**Furandienone **22**Germacrone **23**Germacrone-4,5-epoxide **24**Germacrone-1,10-epoxide **25**Zederone **26**Germacrone-13-al **27**Curcurzederone **28**13-Hydroxygermacrone **29**Furanogermenone **30**Glechomanolide **31**Neocurdione **32**(4S)-Acetoxydehydrocurdione **33****Figure 2.4:** Germacrane-type sesquiterpenes from *Curcuma* species

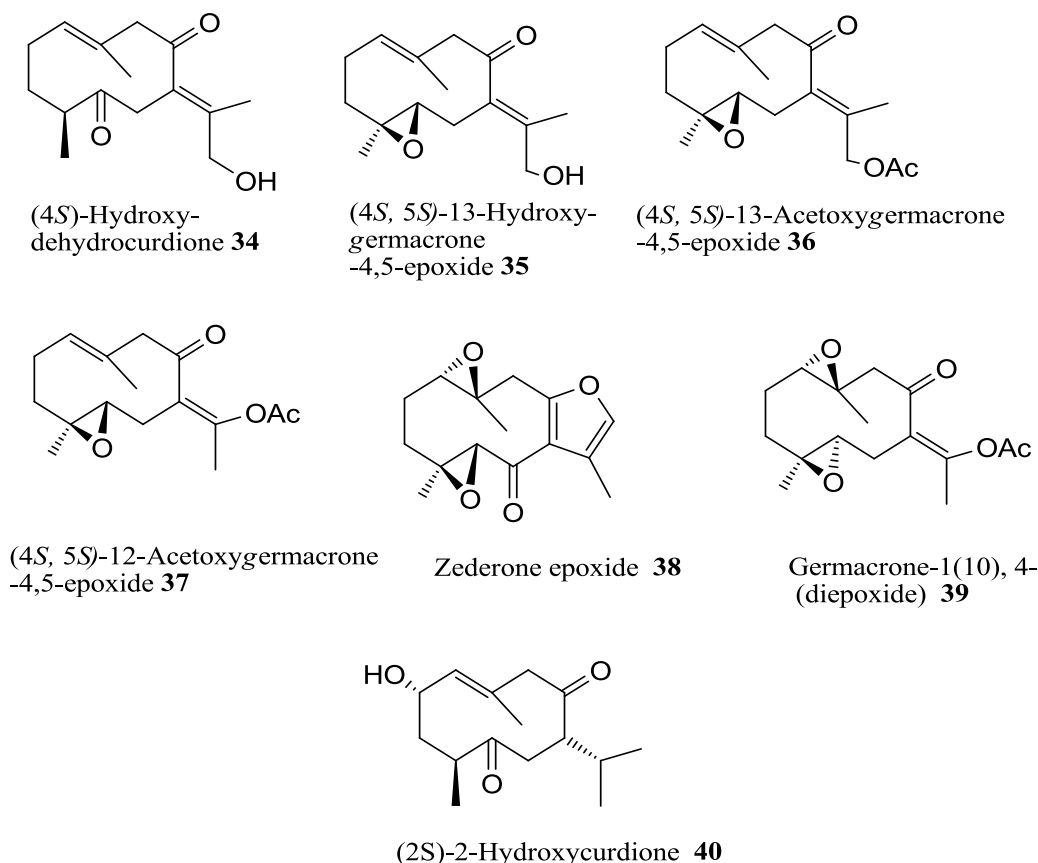


Figure 2.4: Germacrane-type sesquiterpenes from the *Curcuma* (cont.)

2.3.2.1.2 Guaiane type sesquiterpenes

Guaiane type sesquiterpenes represents a major class of sesquiterpenes found in at least 6 species from the genus *Curcuma*. Isocurcumenol **47** being the most abundant compound identified in more than eight species of the genus *Curcuma* such as *C. zedoaria*, *C. aeruginosa*, *C. heyneana*, *C. phaeocaulis*, *C. sichuanensis*, and *C. wenyujin*. Most of the guaiane type sesquiterpenes have been isolated from *C. zedoaria* such as 4-*epi*-curcumenol **45**, neocurcumenol **46**, isocurcumenol **47**, alismoxide **49**, zedoarondiol **51**, zedoarolide A **52**. The characteristic feature of the main skeleton of this type is the presence of a seven membered ring fused onto a five membered ring. Some of the guaiane type sesquiterpenes possess a 5,8-cyclic ether, such as cucumenol **44**, 4-*epi*-curcumenol **45** neocurcumenol **46**, isocurcumenol **47**, zedoarolide B **53**, zedoarol **54**, and isozedoarondiol **55**. Interestingly some guaianes possess a five

membered lactone ring e.g. zedoarolide A **52**, zedoarolide B **53**, and zedoarol **54**. Shiobara (Shiobara et al., 1986), a Japanese group reported first guaiane type sesquiterpene possess a fused furan ring system isolated from *C. zedoaria*. **Table 2.2** lists the guaiane type sesquiterpenes found in *Curcuma* species.

Table 2.2: Guaiane type sesquiterpenes from the *Curcuma*

Compounds	Source
Gweicurculactone 41	<i>C. wenyujin</i> (Yin et al., 2013) <i>C. kwangsiensis</i> (Phan et al., 2014)
Curcumenol 42	<i>C. longa</i> (Ohshiro et al., 1990a) <i>C. aeruginosa</i> (Suphrom et al., 2012a)
Isoprocurcumenol 43	<i>C. longa</i> (Ohshiro et al., 1990a)
Procurcumenol 44	<i>C. longa</i> (Ohshiro et al., 1990a) <i>C. aromatica</i> (Choudhury et al., 1996)
4- <i>epi</i> -Curcumenol 45	<i>C. zedoaria</i> (Hisashi Matsuda, Toshio Morikawa, Iwao Toguchida, et al., 2001)
Neocurcumenol 46	<i>C. zedoaria</i> (Hisashi Matsuda, Toshio Morikawa, Iwao Toguchida, et al., 2001)
Isocurcumenol 47	<i>C. zedoaria</i> (Hisashi Matsuda, Toshio Morikawa, Iwao Toguchida, et al., 2001) <i>C. aeruginosa</i> (Suphrom et al., 2012a) <i>C. heyneana</i> (Firman et al., 1988a) <i>C. phaeocaulis</i> (Chen et al., 2006) <i>C. sichuanensis</i> (Zhou et al., 2007a) <i>C. wenyujin</i> (J. Cao et al., 2006) <i>C. ochrorhiza</i> (Mohd Aspollah Sukari et al., 2010) <i>C. aromatica</i> (Kuroyanagi et al., 1990a)
Curcumol 48	<i>C. wenyujin</i> (Lou et al., 2010)
Alismoxide 49	<i>C. zedoaria</i> (Hisashi Matsuda, Toshio Morikawa, Iwao Toguchida, et al., 2001)
Aerugidol 50	<i>C. zedoaria</i> (Hisashi Matsuda, Toshio Morikawa, Iwao Toguchida, et al., 2001)
Zedoarondiol 51	<i>C. zedoaria</i> (Hisashi Matsuda, Toshio Morikawa, Iwao Toguchida, et al., 2001) <i>C. aromatica</i> (Choudhury et al., 1996) <i>C. aeruginosa</i> (Suphrom et al., 2012a)
Zedoarolide A 52	<i>C. zedoaria</i> (Hisashi Matsuda, Toshio Morikawa, Iwao Toguchida, et al., 2001)
Zedoarolide B 53	<i>C. zedoaria</i> (Hisashi Matsuda, Toshio Morikawa, Iwao Toguchida, et al., 2001)
Zedoarol 54	<i>C. zedoaria</i> (Shiobara et al., 1986)
Isozedoarondiol 55	<i>C. zedoaria</i> (H. Matsuda et al., 2001)
9-Oxo-neoprocurcumenol 56	<i>C. aromatica</i> (Etoh et al., 2003)
Epiprocurcumenol 57	<i>C. longa</i> (Ohshiro et al., 1990a)

Compounds	Source
7 α ,11 α -epoxy-5 β -hydroxy-9-guaiaen-8-one 58	<i>C. zedoaria</i> (Hisashi Matsuda, Toshio Morikawa, et al., 2001a)
Zedoalactone A 59	<i>C. aeruginosa</i> (Takano et al., 1995a)
Zedoalactone B 60	<i>C. aeruginosa</i> (Takano et al., 1995a)
Methylzedoarondiol 61	<i>C. aromatica</i> (Kuroyanagi et al., 1987)

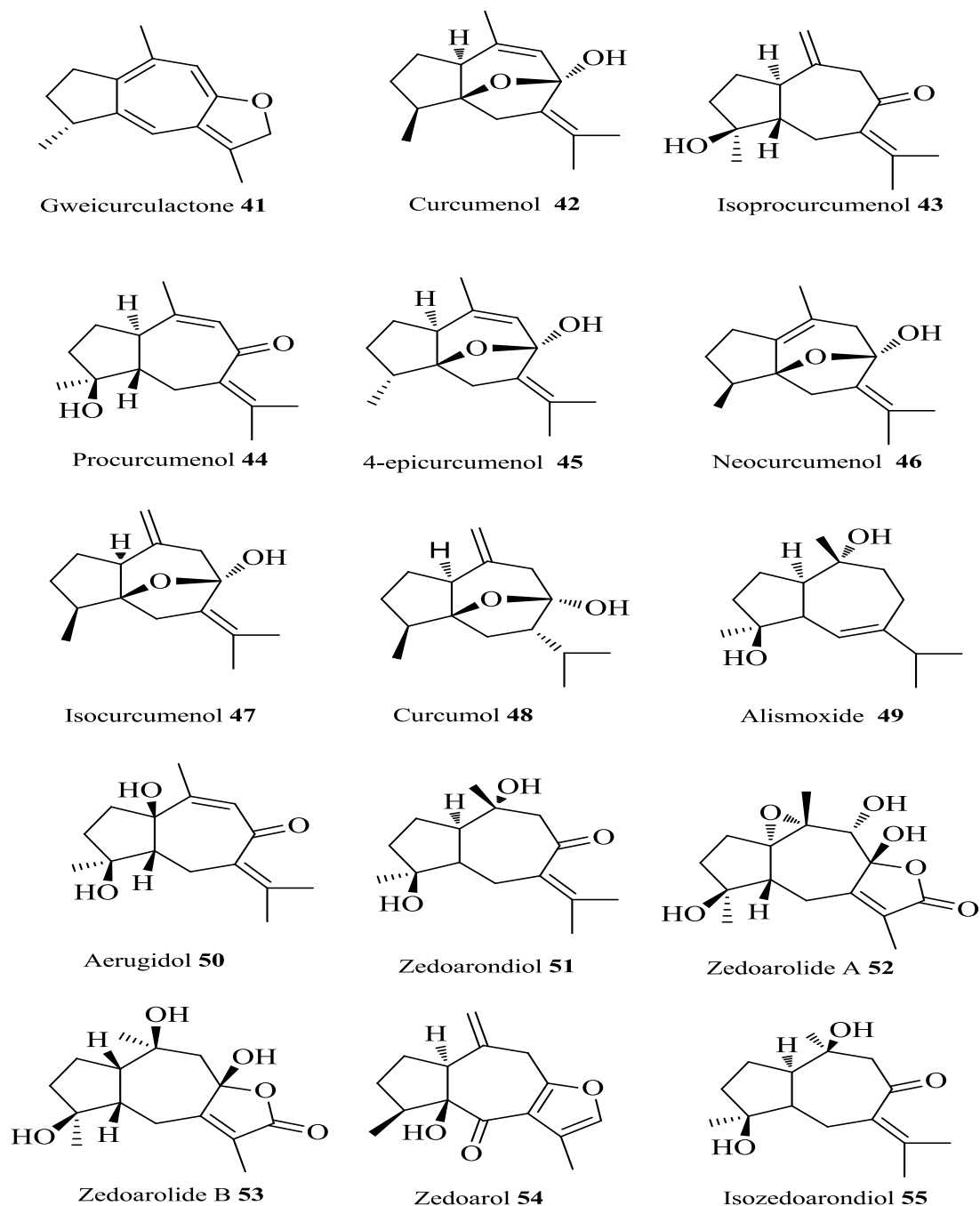


Figure 2.5 Guaiane type sesquiterpenes from the *Curcuma* (cont.)

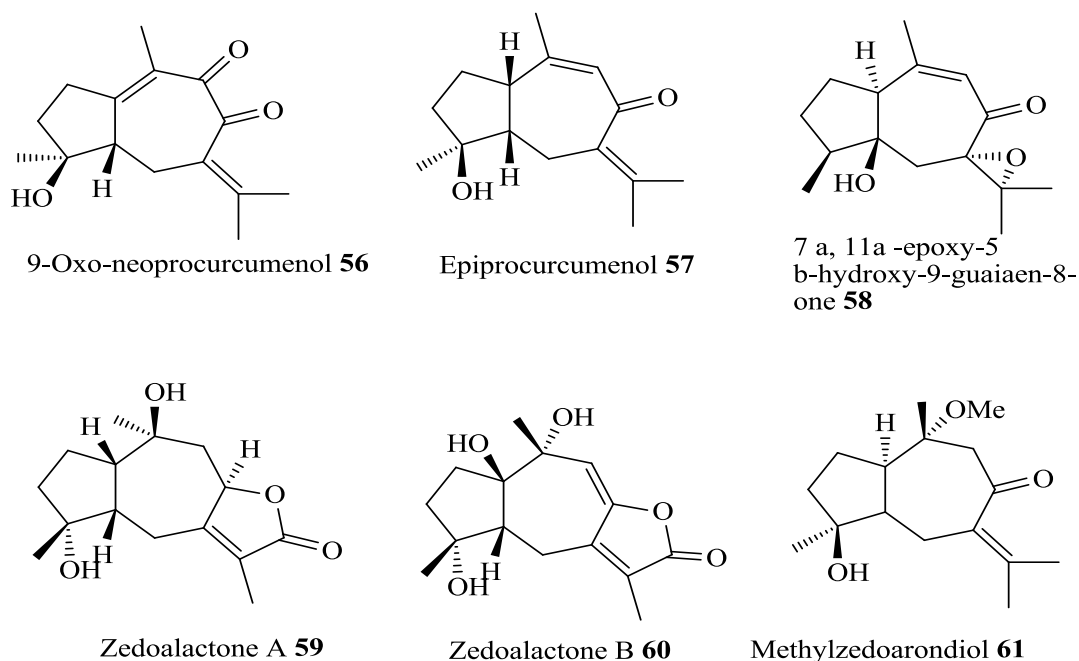


Figure 2.5: Guaiane type of sesquiterpenes from the *Curcuma*

2.3.2.1.3 Seco guaiane type sesquiterpenes

The major source of these sesquiterpenes is *C. zedoaria*. The main features of this skeleton (different from that of guaiane) are the replacement of the seven membered ring by a six-membered ring containing an α,β -unsaturated lactone. Isolated compounds include curcuzedoalide **62**, gajutsulactone A **63**, and gajutsulactone B **64** and are presented in **Table 2.3** **Figure 2.6..**

Table 2.3: Seco guaiane type sesquiterpenes from the *Curcuma*

Compounds	Source
Curcuzedoalide 62	<i>C. zedoaria</i> (Park et al., 2012b)
Gajutsulactone A 63	<i>C. zedoaria</i> (Hisashi Matsuda, Toshio Morikawa, et al., 2001a)
Gajutsulactone B 64	<i>C. zedoaria</i> (Hisashi Matsuda, Toshio Morikawa, et al., 2001a)

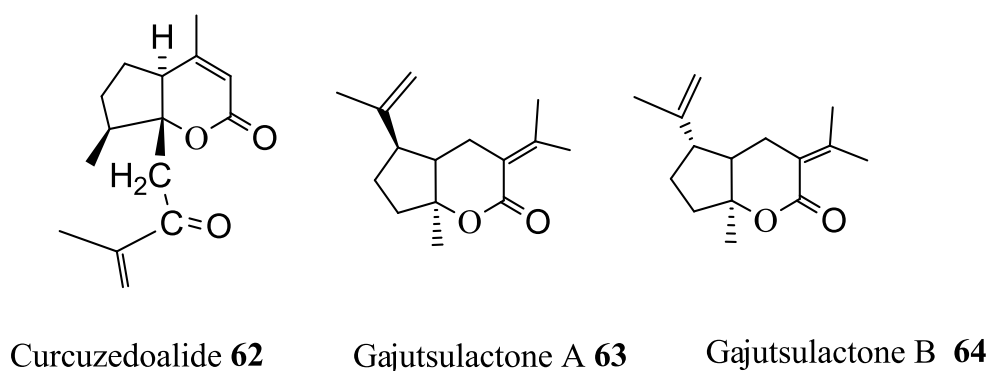


Figure 2.6: *Seco*-guaiane type sesquiterpenes from the *Curcuma*

2.3.2.1.4 Carabrane type sesquiterpenes

Carabrane type sesquiterpenes have a unique skeleton and can be identified by the presence of a cyclohexane ring fused to a cyclopropane ring. The most widespread carabrane sesquiterpene in *Curcuma* species is curcumenone. It is expressed in *C. zedoaria*, *C. longa* and *C. wenyujin*. Some of the carabrane also possess lactone from their basic carabrane skeleton such as curcumenolactone A **69**, curcumenolactone B **70**, and curcumenolactone C **71** (Table 2.4, Figure 2.7). From the reported published data, the major source of these sesquiterpenes was found to be *C. zedoaria*.

Table 2.4: Carabrane type sesquiterpenes from the *Curcuma*

Compounds	Source
Curcumenone 65	<i>C. zedoaria</i> (Shiobara et al., 1985b) <i>C. longa</i> (Ohshiro et al., 1990a) <i>C. wenyujin</i> (Sun et al., 2006)
Curcurabranol A 66	<i>C. zedoaria</i> (Morikawa, 2007)
Curcurabranol B 67	<i>C. zedoaria</i> (Morikawa, 2007)
4S-Dihydrcurcumenone 68	<i>C. zedoaria</i> (Morikawa, 2007)
Curcumenolactone A 69	<i>C. zedoaria</i> (Morikawa, 2007)
Curcumenolactone B 70	<i>C. zedoaria</i> (Morikawa, 2007)
Curcumenolactone C 71	<i>C. zedoaria</i> (Morikawa, 2007)
Dimethoxycurcumenone 72	<i>C. comosa</i> (F. Xu et al., 2008)
Comosone III 73	<i>C. comosa</i> (F. Xu et al., 2008)

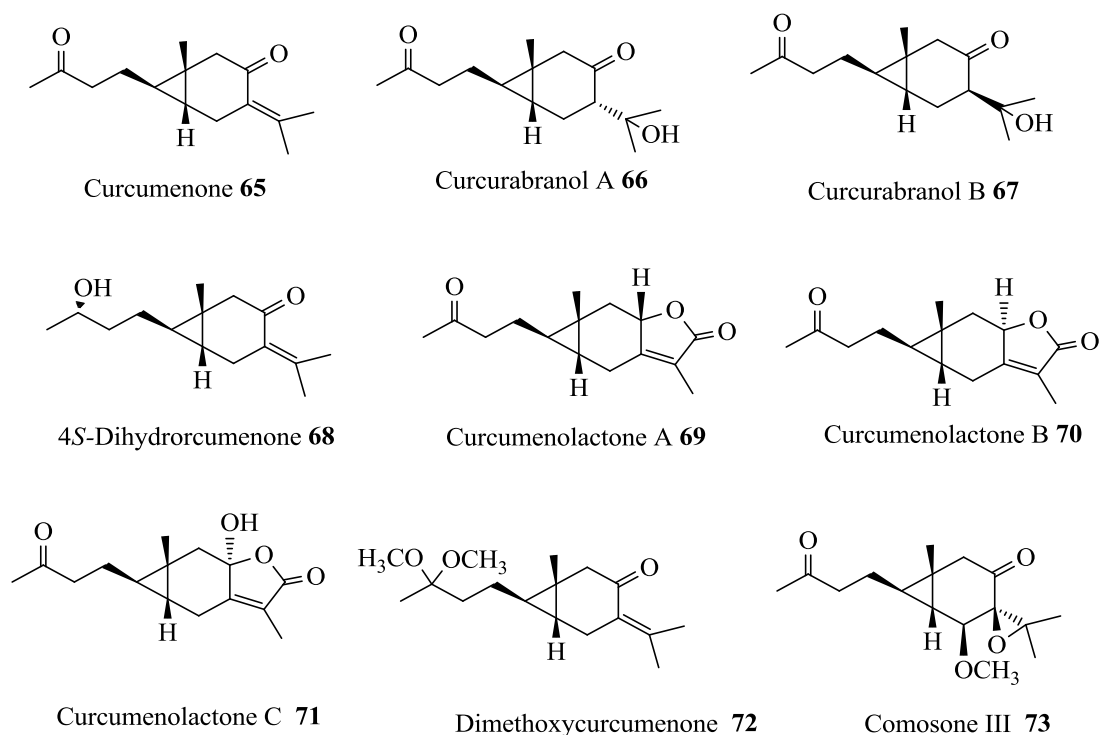


Figure 2.7: Carabrane type sesquiterpenes from the *Curcuma*

2.3.2.1.5 Bisabolane type sesquiterpenes from *Curcuma* species

Bisabolanes are aromatic ring containing sesquiterpenes. It is among the three major classes of sesquiterpenes found in the genus *Curcuma*. The other two types are the guaiane and germacrane sesquiterpenes. The most abundant compound in this genus is ar-turmerone **74**. It is found in *C. longa* and *C. zedoaria*. Sesquiterpenes found in *C. longa*, *C. zedoaria*, *C. xanthorrhiza*, *C. caesia*, and *C. aromatica* and are presented in **Table 2.5** and **Figure 2.8**. Non aromatic bisabolanes like the α , β , γ curcumenes, curlone, and turmerone often occurs in essential oils in *Curcuma* species.

Table 2.5: Bisabolane type sesquiterpenes from the *Curcuma*

Compound	Source
ar-Turmerone 74	<i>C. longa</i> (Tavares et al., 2013) <i>C. zedoaria</i> (Chai Hee Hong et al., 2001) <i>C. xanthorrhiza</i> (TAKEYA, 1985) <i>C. caesia</i> (Pandey et al., 2003) <i>C. aromatica</i> (Bordoloi et al., 1999)
β -Turmerone 75	<i>C. zedoaria</i> (Chai Hee Hong et al., 2001)
α -Turmerone 76	<i>C. xanthorrhiza</i> (S Uehara et al., 1992) <i>C. longa</i> (Ohshiro et al., 1990a)
α -Curcumene 77	<i>C. xanthorrhiza</i> (S Uehara et al., 1992)
β -Curcumene 78	<i>C. xanthorrhiza</i> (S Uehara et al., 1992)
γ -Curcumene 79	<i>C. longa</i> (G Singh et al., 2010)
Turmerone 80	<i>C. longa</i> (Chatterjee et al., 2000)
Bisacumol 81	<i>C. longa</i> (Ohshiro et al., 1990a) <i>C. xanthorrhiza</i> (Shinichi Uehara et al., 1989)
Bisacurone 82	<i>C. longa</i> (Ohshiro et al., 1990a) <i>C. xanthorrhiza</i> (Shinichi Uehara et al., 1989)
4-Hydroxybisabola-2,10-dien-9-one 83	<i>C. longa</i> (Ohshiro et al., 1990a)
Bisabola 3, 10-diene-2-one 84	<i>C. longa</i> (Ohshiro et al., 1990a)
4,5-Dihydroxybisabola-2,10-diene 85	<i>C. longa</i> (Ohshiro et al., 1990a)
Bisacurool B 86	<i>C. domestica</i> (Ishii et al., 2011)
Bisacurool 87	<i>C. domestica</i> (Ishii et al., 2011)
E- α -atlantone 88	<i>C. domestica</i> (Ishii et al., 2011)
Curlone 89	<i>C. domestica</i> (Ishii et al., 2011)
Termernol A 90	<i>C. longa</i> (Khan et al., 2010)
Termernol B 91	<i>C. longa</i> (Khan et al., 2010)
2,3,5,6-Tetrahydroxyarturmerone 92	<i>C. longa</i> (Khan et al., 2010)
Bisacurone A 93	<i>C. xanthorrhiza</i> (Shinichi Uehara et al., 1990)
Bisacurone B 94	<i>C. xanthorrhiza</i> (Shinichi Uehara et al., 1990)
Bisacurone C 95	<i>C. xanthorrhiza</i> (Shinichi Uehara et al., 1990)
Bisacurone epoxide 96	<i>C. xanthorrhiza</i> (Shinichi Uehara et al., 1990)

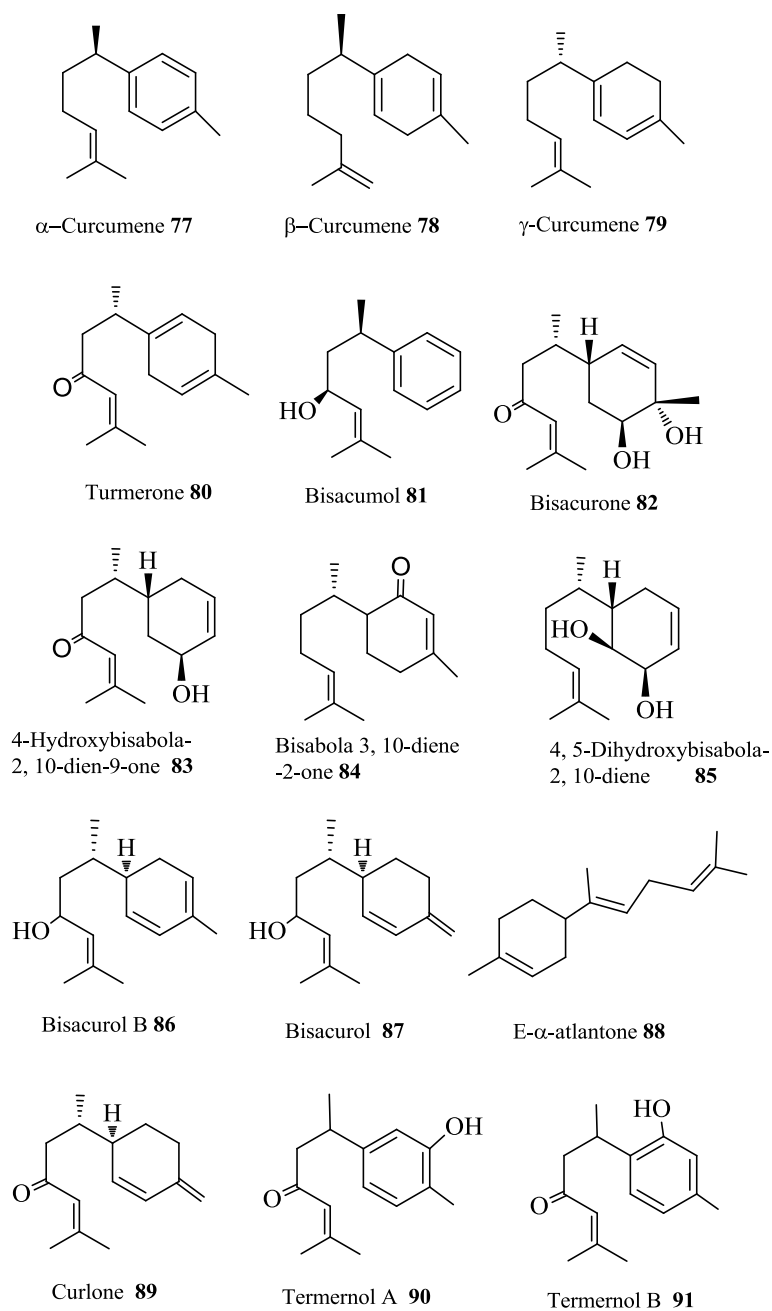


Figure 2.8: Bisabolane-type sesquiterpenes from the *Curcuma* (cont.)

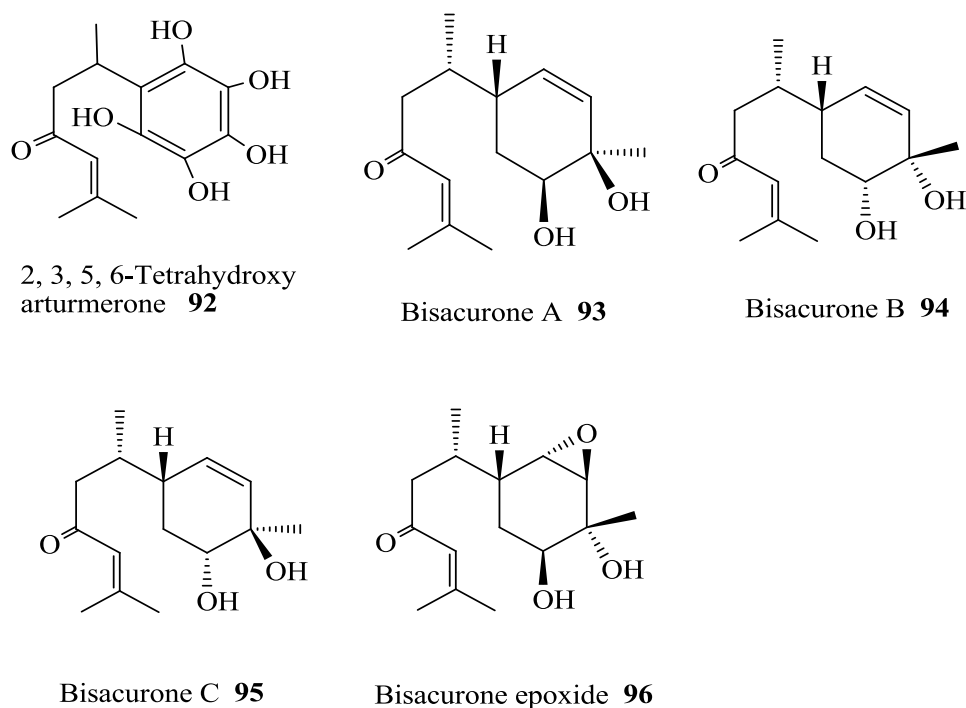


Figure 2.8: Bisabolane-type sesquiterpenoids from the *Curcuma*

2.3.2.1.6 Humulane-type sesquiterpenes from *Curcuma* species

Humulane skeleton consist of only one ten membered ring system with usually 4 methyl substituents. The major sources of these sesquiterpenes are *C. ochrorhiza* and *C. zedoaria*. Zerumbone **97** which is predominant in the *Zingiber* species was also isolated from *C. ochrorhiza*. The compounds α -humulene **98**, β -humulene **99**, and humulene-8-hydroperoxide **100** were isolated from *C. zedoaria*. These sesquiterpenes are presented in **Table 2.6** and **Figure 2.9**.

Table 2.6: Humulane type sesquiterpenes from the *Curcuma*

Compound	Source
Zerumbone 97	<i>C. ochrorhiza</i> (Mohd Aspollah Sukari et al., 2010)
α -Humulene (α -Caryophyllene) 98	<i>C. zedoaria</i> (Mau et al., 2003b)
β -Humulene (β -Caryophyllene) 99	<i>C. zedoaria</i> (Garg et al., 2005)
Humulene-8-hydroperoxide 100	<i>C. zedoaria</i> (Giang, 2003)

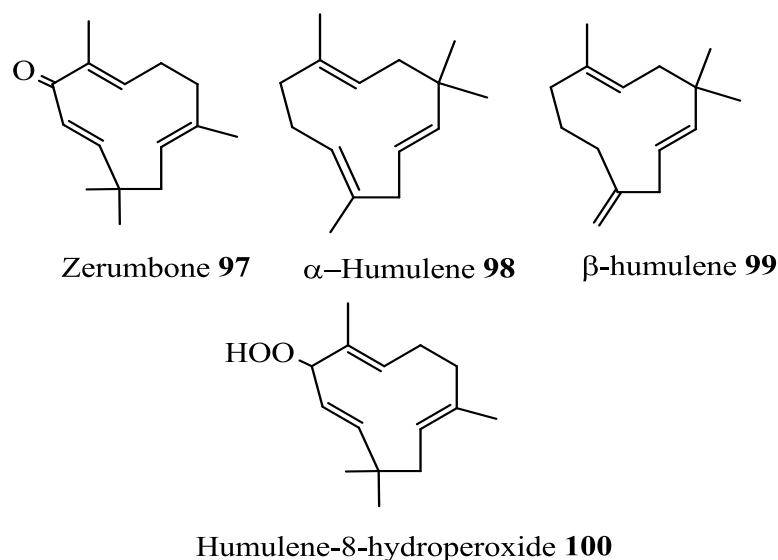


Figure 2.9: Humulane type sesquiterpenes from the *Curcuma*

2.3.2.1.7 Spirolactone-type sesquiterpenes from *Curcuma* species

Spirolactones sesquiterpenes are consisting of two five membered fused at C-5. *Curcumanolide A* **101**, and *curcumanolide B* **102** were isolated from *C. zedoaria* while *curcumanolactone* **103** was reported from *C. wenyujin* (Table 2.7, Figure 2.10). The former two compounds are diastereomers and all the three compounds are also found in essential oils of the *Curcuma* species.

Table 2.7: Spirolactone type sesquiterpenes from the *Curcuma*

Compound	Source
<i>Curcumanolide A</i> 101	<i>C. zedoaria</i> (Shiobara et al., 1985a)
<i>Curcumanolide B</i> 102	<i>C. zedoaria</i> (Shiobara et al., 1985a)
<i>Curcumanolactone</i> 103	<i>C. wenyujin</i> (Harimaya et al., 1991)

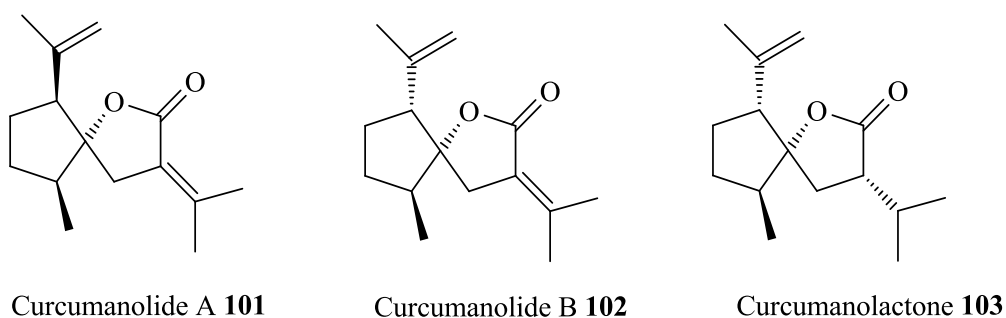


Figure 2.10: Spirolactone types sesquiterpenes from the *Curcuma*

2.3.2.1.8 Cadinane type sesquiterpenes

The main skeleton of this type contains two fused six membered with a side chain attached to C-8. This type is mainly isolated from *C. parviforenes* and *C. comosa* which includes comosone I **104**, comosone II **105**, cadalenequinone **106**, 8-hydroxycadalene **107**, 4 α ,3 α ,4 β -acetoxycadina-2, 9-diene-1,8-dione **108**, 4 α ,3 α ,4 β -acetoxycadina-2, 9-diene-1,8-dione **109** (Table 2.8, Figure 2.11).

Table 2.8: Cadinane type sesquiterpenes from the *Curcuma*

Compound	Source
Comosone I 104	<i>C. comosa</i> (F. Xu et al., 2008)
Comosone II 105	<i>C. comosa</i> (F. Xu et al., 2008)
Cadalenequinone 106	<i>C. parviforenes</i> (Takahashi et al., 2003)
8-hydroxycadalene 107	<i>C. parviforenes</i> (Takahashi et al., 2003)
4 α , 3 α , 4 β -Acetoxycadina-2, 9-diene-1,8-dione 108	<i>C. parviforenes</i> (Sadhu et al., 2009)
1 α , 3 α , 4 β , Trihydroxy-cadinen-8-one 109	<i>C. parviforenes</i> (Sadhu et al., 2009)
6, 8- Cadinatriene-4-one 110	<i>C. wenyujin</i> (Dong et al., 2013)

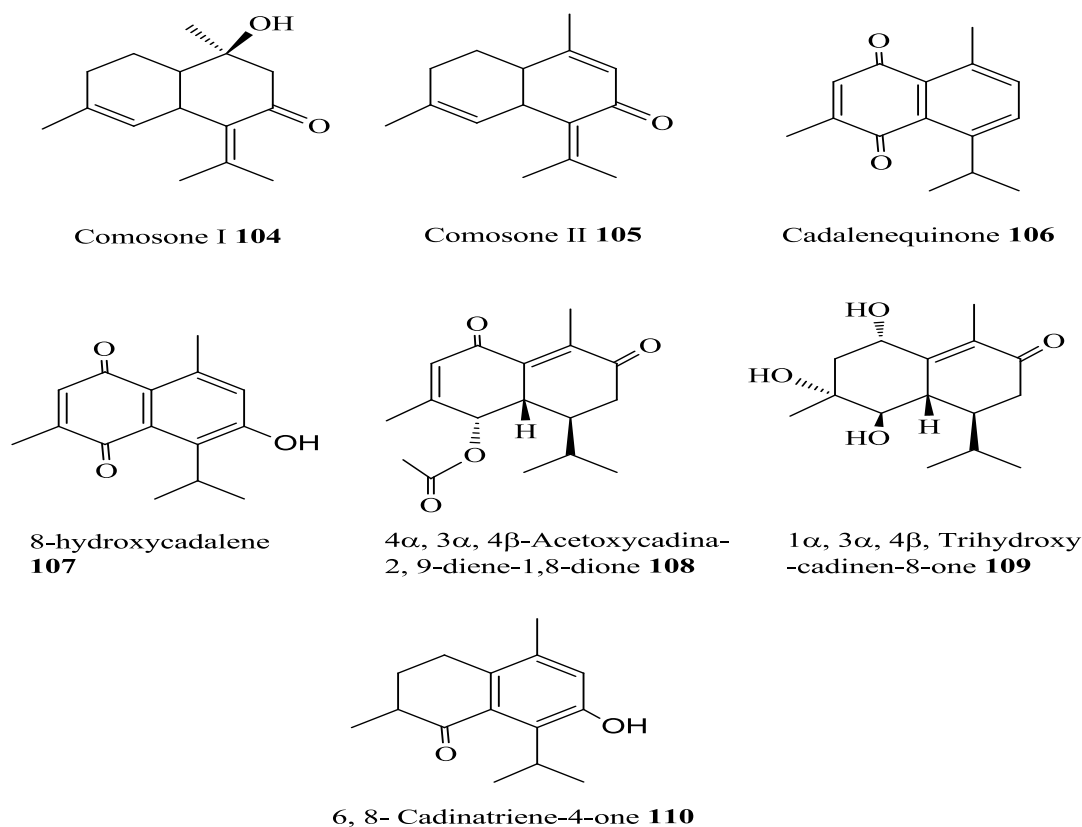


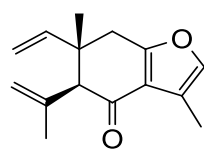
Figure 2.11: Cadinane type sesquiterpenes from the *Curcuma*

2.3.2.1.9 Elemene type sesquiterpenes from *Curcuma*

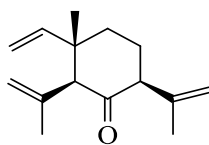
It is well known that germacrone type sesquiterpenes undergo Cope rearrangement to give elemene type sesquiterpenes. Curzerenone **111** is the most widely reported elemene and it occurs in several *Curcuma* species such as *C. caesia*, *C. zedoaria*, *C. comosa* and *C. aromatica* (Table 2.9, Figure 2.12)

Table 2.9: Elemene type sesquiterpenes from the *Curcuma*

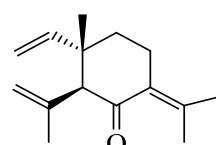
Compound	Source
Curzerenone 111	<i>C. caesia</i> (Vairappan et al., 2013a) <i>C. zedoaria</i> (Hisashi Matsuda, Toshio Morikawa, et al., 2001a) <i>C. comosa</i> (Qu et al., 2009a) <i>C. aromatica</i> (Giang & Son, 2000)
β -Elemene 112	<i>C. zedoaria</i> (Mau et al., 2003b)
γ -Elemene 113	<i>C. zedoaria</i> (Mau et al., 2003b)
Curzerene 114	<i>C. zedoaria</i> (Mau et al., 2003b)
<i>epi</i> -curzerenone 115	<i>C. zedoaria</i> (Mau et al., 2003b)
Elemol 116	<i>C. zedoaria</i> (Mau et al., 2003b)
β -Elemenone 117	<i>C. zedoaria</i> (Mau et al., 2003b)
Elema-1,3,7(11),8-tetraen-8,12-lactam 118	<i>C. wenyujin</i> (Qiu et al., 2013)
Hydroxyisogermafurenolide 119	<i>C. wenyujin</i> (Qiu et al., 2013)
Isogermafurenolide 120	<i>C. wenyujin</i> (Qiu et al., 2013)



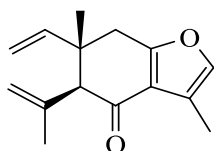
Curzerenone **111**



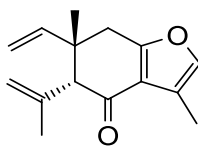
β -Elemene **112**



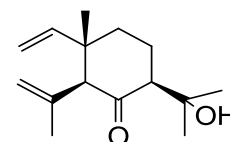
γ -Elemene **113**



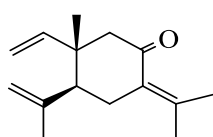
Curzerene **114**



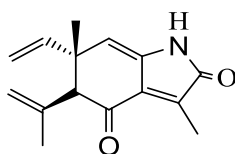
Epi-curzerenone **115**



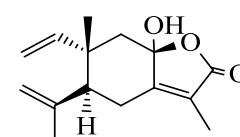
Elemol **116**



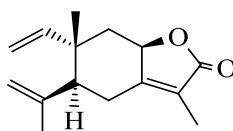
β -Elementone **117**



Elema-1, 3, 7(11), 8-tetraen-8, 12-lactam **118**



Hydroxyisogermafurenolide **119**



Isogermafurenolide **120**

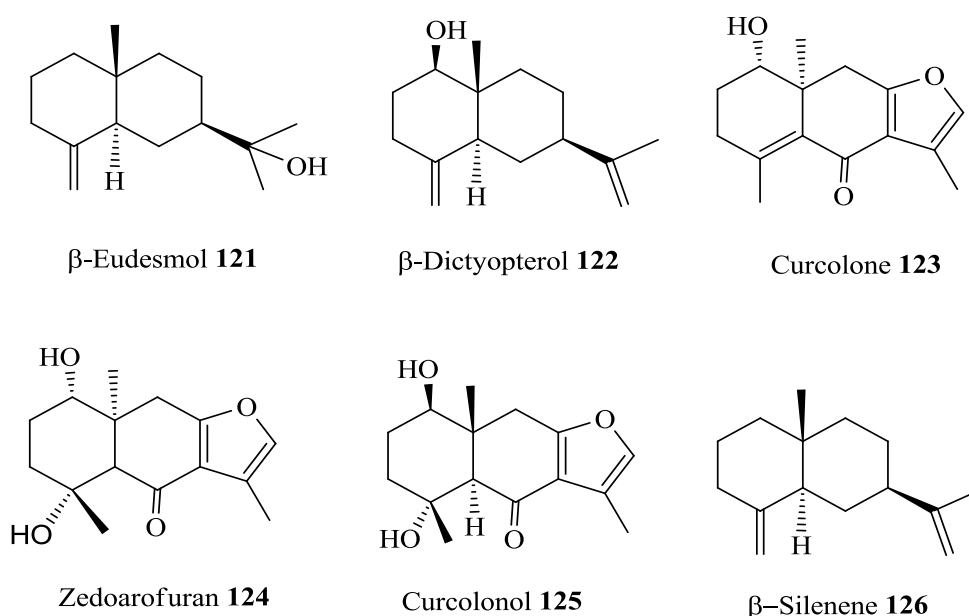
Figure 2.12: Elemene type sesquiterpenes from the *Curcuma*

2.3.2.10 Eudesmane type sesquiterpenes

The main skeleton of this type consists of two fused membered rings with a side chain attached to C-7. *C. zedoaria* and *C. comosa* are the major sources of these sesquiterpenes. Curcolone **123**, a furanoeudesmane type sesquiterpene was isolated from *C. zedoaria* and *C. comosa*. Additionally, zedoarofuran **124**, curcolonol **125** also a furanoeudesmane were isolated from *C. zedoaria* (Table 2.10, Figure 2.13).

Table 2.10: Eudesmane type sesquiterpenes from *Curcuma*

Compound	Source
β -Eudesmol 121	<i>C. zedoaria</i> (Hisashi Matsuda, Toshio Morikawa, et al., 2001a)
β -Dictyopterol 122	<i>C. zedoaria</i> (Hisashi Matsuda, Toshio Morikawa, et al., 2001a)
Curcolone 123	<i>C. comosa</i> (Qu et al., 2009a) <i>C. zedoaria</i> (Morikawa, 2007)
Zedoarofuran 124	<i>C. zedoaria</i> (Morikawa, 2007)
Curcolonol 125	<i>C. zedoaria</i> (Syu et al., 1998)
β -Silenene 126	<i>C. zedoaria</i> (Mau et al., 2003b)
α -Silenene 127	<i>C. zedoaria</i> (Mau et al., 2003b)

**Figure 2.13:** Eudesmane type sesquiterpenes from the *Curcuma*

2.3.3 Diterpenoids:

Diterpenoids are a structurally diverse class of C₂₀ natural compounds, widely distributed in nature and forms by the condensation of four isoprene units through the mevalonate or deoxyxylulose phosphate pathways. Diterpenoids can be classified as linear, bicyclic, tricyclic, tetracyclic, and pentacyclic.

In nature, diterpenoids are commonly found in a polyoxygenated form, containing keto and hydroxyl functions. Such groups can be esterified by small-sized aliphatic or aromatic acids (Dickschat, 2011). Diterpenes have attracted growing

attention because of their interesting biological and pharmacological activities (Lanzotti, 2013). The presence of diterpenoids in *Curcuma* species is less common compared with sesquiterpenes and diaryl heptanoids. Labdanes are the major type of diterpenes known to occur in the Zingiberaceous plants (Abas et al., 2005). The *Curcuma* species reported to contain labdane-type diterpenoid were *C. manga*, *C. heyneana*, *C. kwangsiensis*, and *C. amada* with the most abundant compound was labda-8(17),12 diene-15,16-dial. Labdane compounds from the genus *Curcuma* are presented in **Table 2.11** and **Figure 2.14**.

Table 2.11: Labdane-type diterpenoids from the *Curcuma*

Compound	Source
Labda-8(17),12-diene-15,16-dial 127	<i>C. longa</i> (Roth et al., 1998) <i>C. managga</i> (Y. Liu et al., 2011) <i>C. amada</i> (Alan Sheeja et al., 2012) <i>C. heyneana</i> (Firman et al., 1988a)
Calcaratarin A 128	<i>C. managga</i> (Y. Liu & Nair, 2011)
Zerumin A 129	<i>C. amada</i> (Alan Sheeja & Nair, 2012)
(<i>E</i>)-Labda-8(17),13diene-15,16-olide 130	<i>C. amada</i> (Alan Sheeja & Nair, 2012)
Coronarin B 131	<i>C. amada</i> (Alan Sheeja & Nair, 2012)
Coronarin D 132	<i>C. kwangsiensis</i> (Schramm et al., 2013) <i>C. amada</i> (Alan Sheeja & Nair, 2012)
Zerumin B 133	<i>C. managga</i> (Abas et al., 2005) <i>C. amada</i> (Alan Sheeja & Nair, 2012)
Copallic acid 134	<i>C. managga</i> (Y. Liu & Nair, 2011)
(<i>E</i>)-16-Hydroxylabda-8(17),11,13-trien-15,16-olide 135	<i>C. kwangsiensis</i> (Schramm et al., 2013)
(<i>E</i>)-15-Hydroxylabda-8(17),11,13-trien-15,16-olide 136	<i>C. kwangsiensis</i> (Schramm et al., 2013)
(<i>E</i>)-Labda-8(17),12,14-trien-16-oicacid 137	<i>C. kwangsiensis</i> (Schramm et al., 2013)

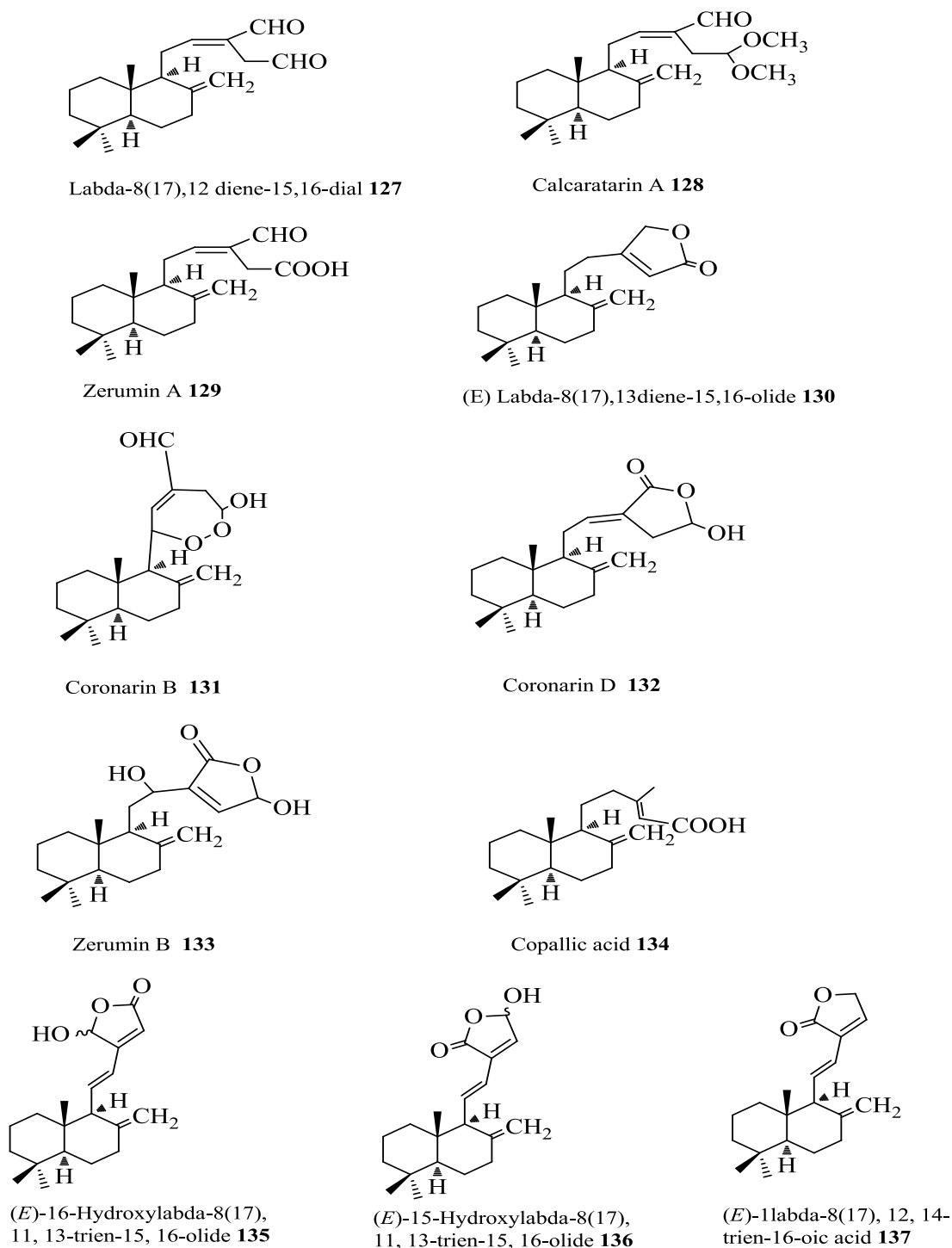


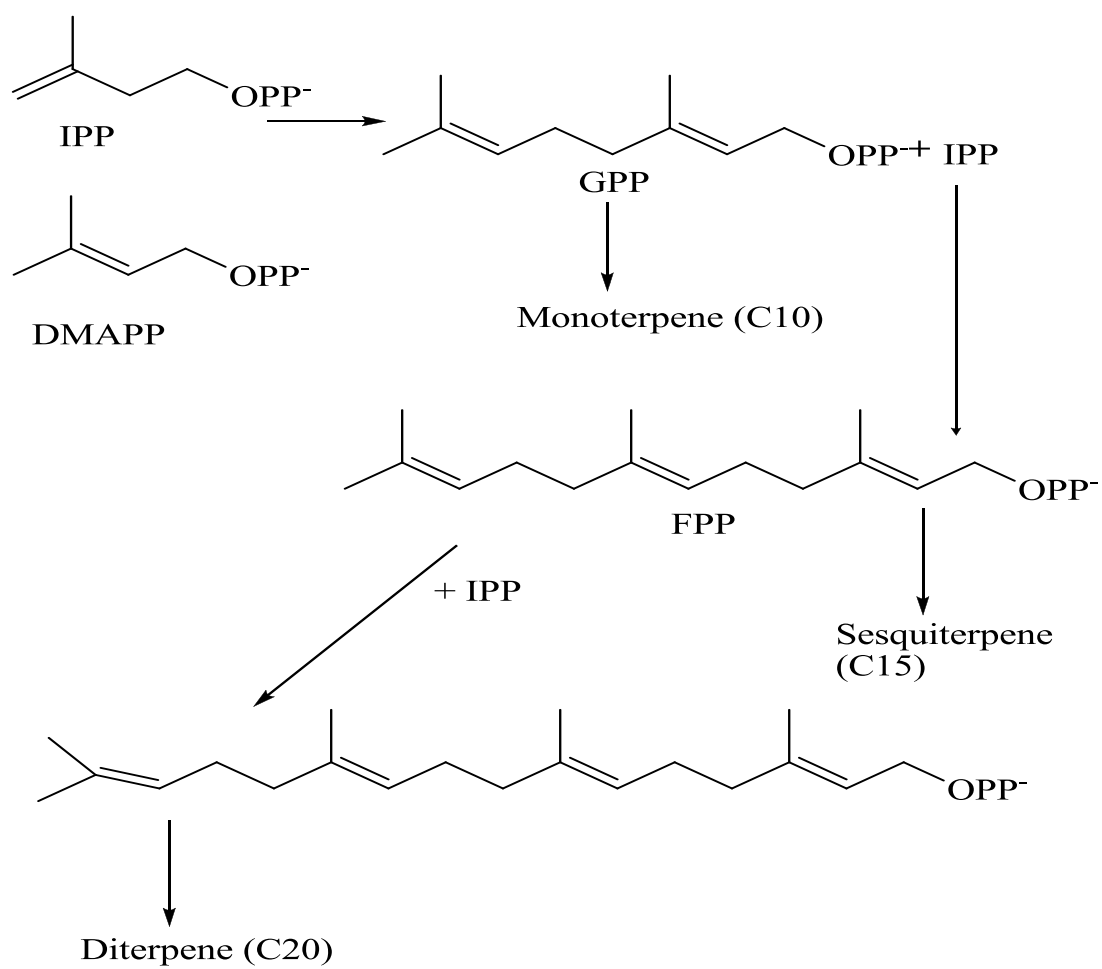
Figure 2.14: Labdane type diterpenoids from the *Curcuma*

2.3.4 Biosynthesis of monoterpenes, sesquiterpenes and diterpenes

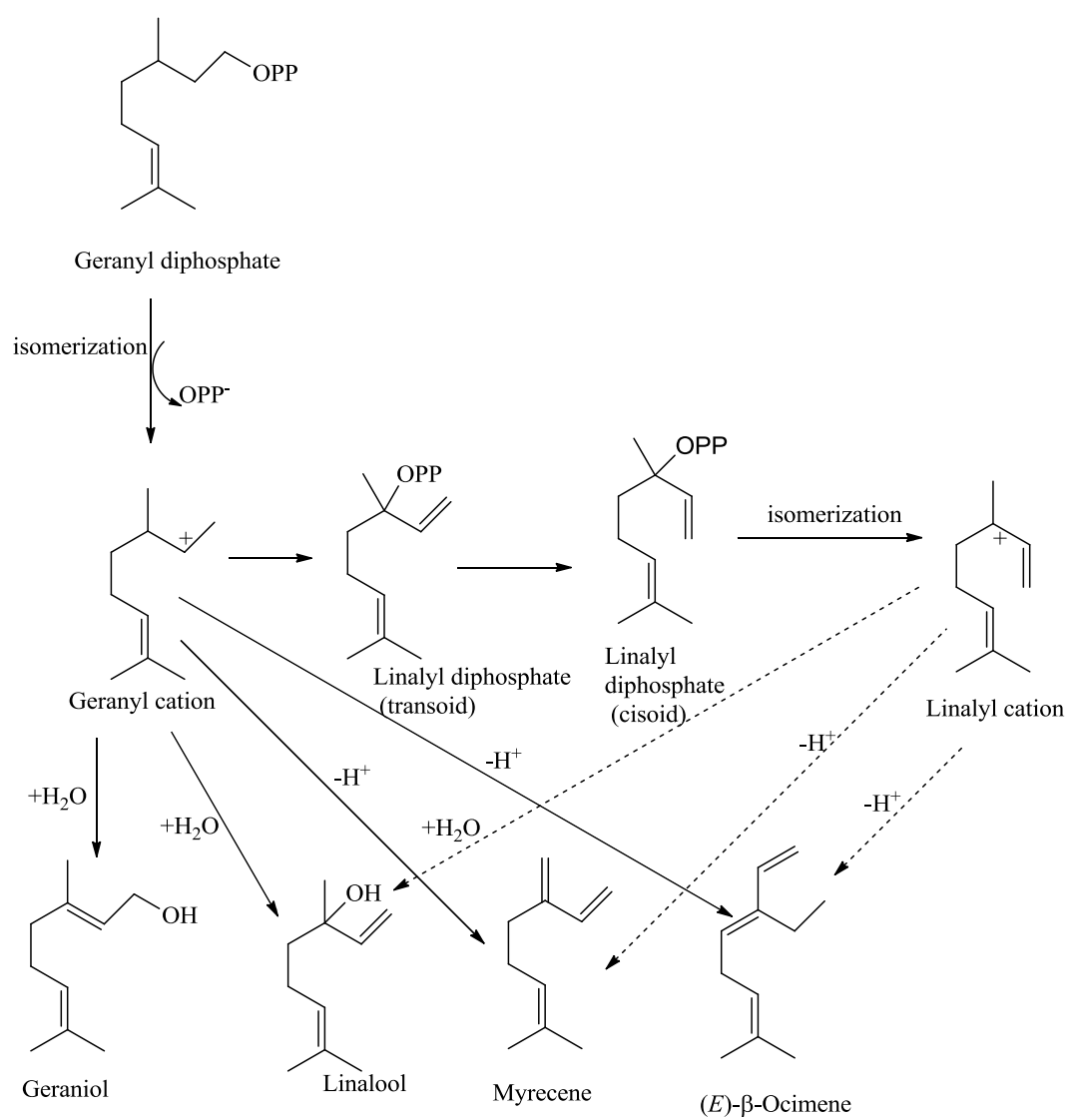
Terpenoids, including monoterpenes, sesquiterpenes and diterpenes are formed from the build-up of isoprene units. In the biological system, the isoprene units are interconvertible into isopentenyl pyrophosphate (IPP) and dimethylallyl pyrophosphate (DMAPP). The first step of terpenoid synthesis is the formation of geranyl

pyrophosphate (GPP) from one IPP and one DMAPP (**Scheme 2.1**). Synthesis of monoterpenes involves the ionisation of GPP to give the carbocationic species which undergoes various steps of cyclisations, hydride shifts or rearrangement reactions and the reaction being terminated through deprotonation or water incorporation. Involvement of a wide range of terpene synthases and the ability of one enzyme to produce more than one product has led to the wide variety of monoterpenes found in abundant in nature (**Scheme 2.3**)

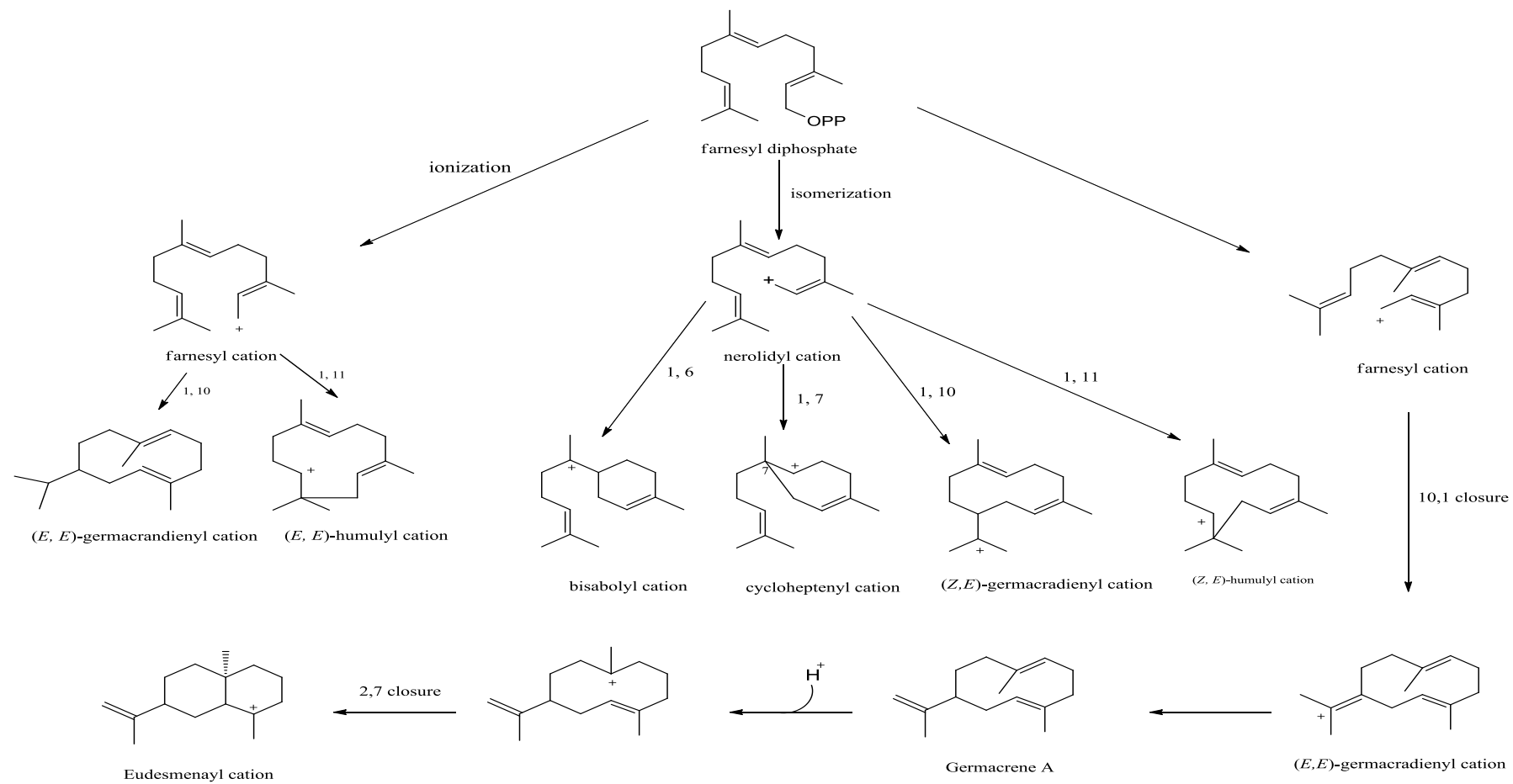
For the synthesis of sesquiterpenes, one GPP reacts with one IPP to form farnesyl diphosphate (**Scheme 2.1**). Removal of the phosphate resulted in an allylic cation, which is prone to electrophilic attack through double bond leading to cyclisation. Depending on whether electrophilic attack occurs on the central or distal double bond, a wide range of structures can be produced (**Scheme 2.2**) (Chern, 2014). These generated various cations such as humulane cation that gives humlane type, eudesmenyl cation that gives eudesmane type, and germacradienyl cation that gives germacrane type. The latter is the precursor of many sesquiterpene skeletons such as cadinane, guaiane and elemene (Bülow et al., 2000).



Scheme 2.1: General biosynthetic pathway of monoterpene, sesquiterpene and diterpene



Scheme 2.2: Biosynthetic pathway of monoterpenes



Scheme 2.3 : Biosynthetic pathway of selected sesquiterpenes

2.3.5 Diarylheptanoids

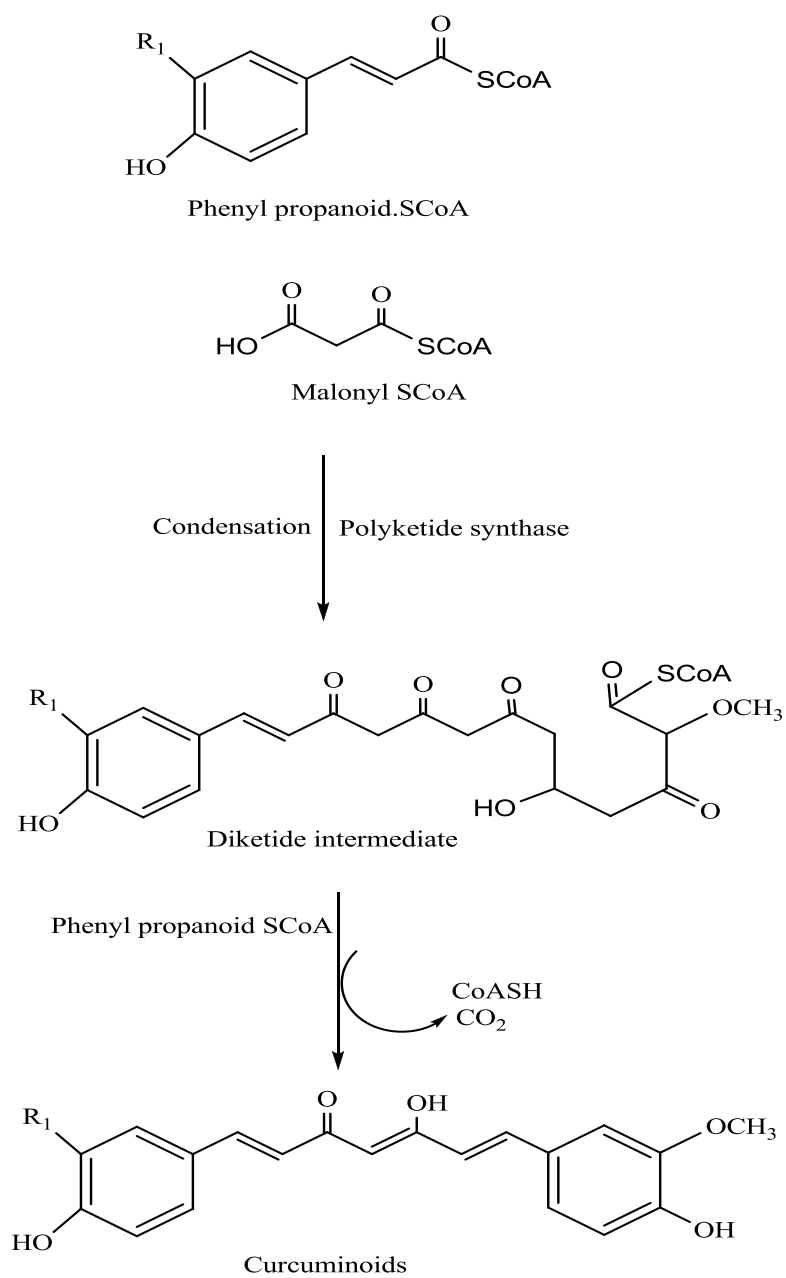
Diarylheptanoids are the most abundant group of the compounds in the genus *Curcuma*, commonly known as curcuminoids. Although over 100 curcuminoids have been identified from *Curcuma* species with varying biological activities, many more have been synthesized to study the structure activity relationships with the view to improve the bioactivities. The main skeleton of curcuminoids have an aryl-C7-aryl skeleton.

Curcumin **138**, desmethoxycurcumin **139** and bisdesmethoxycurcumin **140** are the most widely found compounds in *Curcuma* species. Among the *Cucuma* species, *C. longa* was found to have the highest number of curcuminoids previously isolated. The curcuminoids from *Curcuma* are presented in **Table 2.12** and **Scheme 2.4**

2.3.5.1 Biosynthetic pathway of curcuminoids

(Tomoko et al) have investigated the biosynthesis of curcuminoids in *C. longa* employing ^{13}C -labeled precursors. Analyses of labelled desmethoxycurcumin **140** by ^{13}C -NMR revealed one molecule of acetic acid or malonic acid and two molecules of phenylalanine or phenylpropanoids where incorporated into desmethoxycurcumin **140**. Similarly curcumin **138** incorporation efficiencies of the same precursors and both were in the order malonic acid > *p*-coumaric acid

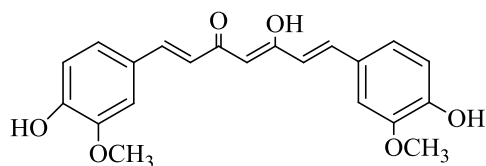
Based on this study the suggested pathway to curcuminoids utilized two cinnamoyl CoAs and one malonyl CoA, and the methoxy and the hydroxyl groups on the aromatic rings were inserted after the formation of the curcumioid skeleton **Scheme 2.4**).



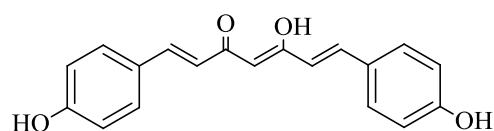
Scheme 2.4 : Biosynthetic pathway for the formation of curcuminoids

Table 2.12: Curcuminoids isolated from the *Curcuma*

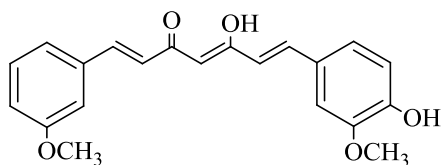
Compounds	Source
Curcumin 138	<i>C. longa</i> (Inoue et al., 2008) <i>C. longa</i> (Kuttan et al., 1985) <i>C. zedoaria</i> (Syu et al., 1998) <i>C. domestica</i> (Masuda et al., 1993) <i>C. amada</i> (A. Gupta et al., 1999)
Bisdesmethoxycurcumin 139	<i>C. longa</i> (Inoue et al., 2008) <i>C. zedoaria</i> (Syu et al., 1998) <i>C. amada</i> (A. Gupta et al., 1999) <i>C. domestica</i> (Masuda et al., 1993)
Desmethoxycurcumin 140	<i>C. longa</i> (Inoue et al., 2008) <i>C. zedoaria</i> (Syu et al., 1998) <i>C. amada</i> (A. Gupta et al., 1999) <i>C. domestica</i> (Masuda et al., 1993)
Tetrahydrocurcumin 141	<i>C. longa</i> (Sandur et al., 2007)
1,5-Dihydroxy-1,7-bis(4-hydroxyphenyl)-4,6-heptadiene-3-one 141	<i>C. longa</i> (Li et al., 2009)
1, 5-Dihydroxy-1-(4-hydroxy-3-methoxyphenyl)-7-(4-hydroxy)-4, 6-heptadiene-3-one 142	<i>C. longa</i> (Li et al., 2009)
1,5-Dihydroxy-1- (4- hydroxyphenyl)-7-(4-hydroxy-3-methoxyphenyl)-4,6-heptadiene-3-one 143	<i>C. longa</i> (Li et al., 2009)
1,5-Dihydroxy-1,7- bis(4-hydroxy-3-methoxyphenyl)-4, 6-heptadiene-3-one 144	<i>C. longa</i> (Li et al., 2009)
3-Hydroxy-1,7-bis-(4-hydroxyphenyl)-6-heptene-1,5-dione 145	<i>C. longa</i> (Li et al., 2009)
5-Hydroxy-1, 7-bis(4-hydroxyphenyl)-4,6-heptadiene-3-one 146	<i>C. longa</i> (Li et al., 2009)
(3 <i>R</i> ', 5 <i>S</i> ')-3, 5-Dihydroxy-1-(4-hydroxy-3-methoxyphenyl)-7-(3,4-dihydroxyphenyl) heptane 148	<i>C. kwangsiensis</i> (ZHU et al., 2009)
2,3,5-Trihydroxy-1-(3-methoxy-4-hydroxyphenyl)-7-(3,5-dimethoxy-4-hydroxyphenyl) heptane 149	<i>C. kwangsiensis</i> (ZHU et al., 2009)



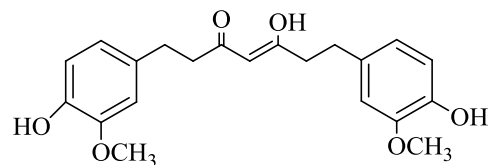
Curcumin **138**



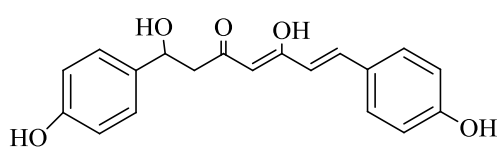
Bisdemethoxycurcumin **139**



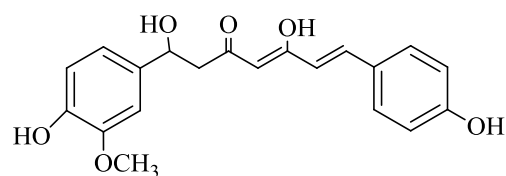
Demethoxycurcumin **140**



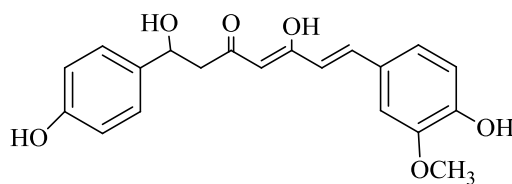
Tetrahydrocurcumin **141**



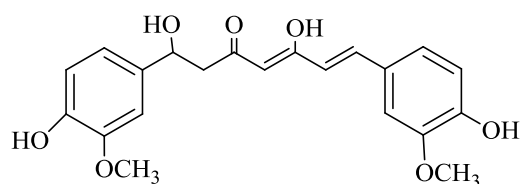
1, 5-Dihydroxy-1, 7-bis(4-hydroxyphenyl)-4, 6-heptadiene-3-one **141**



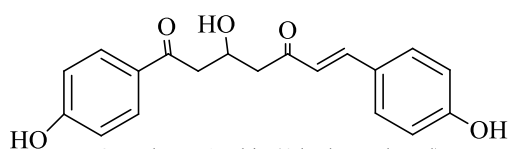
1, 5-Dihydroxy-1-(4-hydroxy-3-methoxyphenyl)-7-(4-hydroxy)-4, 6-heptadiene-3-one **142**



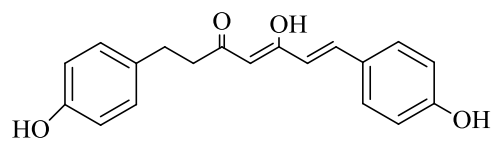
1, 5-Dihydroxy-1-(4-hydroxyphenyl)-7-(4-hydroxy-3-methoxyphenyl)-4, 6-heptadiene-3-one **143**



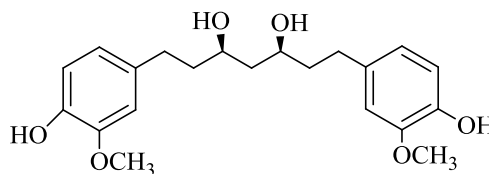
1, 5-Dihydroxy-1,7- bis(4-hydroxy-3-methoxyphenyl)-4, 6-heptadiene-3-one **144**



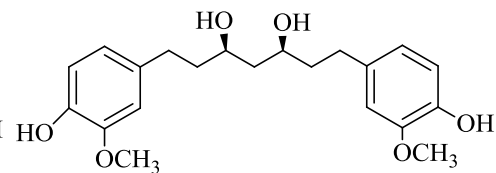
3-Hydroxy-1,7-bis-(4-hydroxyphenyl)-6-heptene-1,5-dione **145**



5-Hydroxy-1, 7-bis(4-hydroxyphenyl)-4,6-heptadiene-3-one **146**



(3R', 5S')-3, 5-Dihydroxy-1-(4-hydroxy-3-methoxyphenyl)-7-(3, 4-dihydroxyphenyl) heptane **148**



2, 3, 5-Trihydroxy-1-(3-methoxy-4-hydroxyphenyl)-7-(3, 5-dimethoxy-4-hydroxyphenyl) heptane **149**

Figure 2.15: Curcuminoids type from the *Curcuma*

2.4 Bioactivity of the compounds previously isolated from the genus *Curcuma*

A good number of compounds with important biological activities have been reported from this genus. The bioactivities of the compounds include cytotoxicity, antibacterial, anti-oxidant, hepatoprotective, analgesic, anti-inflammatory, antiandrogenic, and antiplasmodial activity (Table 2.14). The most studied compound isolated from the genus *Curcuma* which showed multi-biological activities is curcumin **138** (Maheshwari et al., 2006). Curcumin has long history of use as a traditional remedy and food in Asia. Many studies have reported that curcumin has various therapeutic effects for the treatment of several diseases such as anti-cancer, anti-inflammatory, and antioxidant. Extensive research over the last half century has revealed important functions of curcumin **138**. In addition, terpenoids from the genus *Curcuma* have been used in the prevention, inhibition and therapy of many diseases. Curcumenol **42**, a guaiane type sesquiterpene has been reported as analgesic and hepatoprotective (Table 2.14). ar-Turmerone **74**, a bisabolane type sesquiterpene is one of the major active compounds isolated from *C. longa* exhibited potent cytotoxic activity against various cancer cell lines (Ji et al., 2004).

Table 2.13: Bioactive compounds from the *Curcuma*

Compounds	Reported biological activity
Dehydrocurdione 19	Anti-inflammatory (Yoshioka et al., 1998)
Curdione 20	Anti-platelet aggregation and antithrombotic (Xia et al., 2012) Prostaglandin E ₂ inhibitor (Oh et al., 2007)
Germacrone 23	Antiandrogenic potent activity (Suphrom et al., 2012a)
Furanodiene 21	Anti-inflammatory (Makabe et al., 2006) Anti-cancer (Sun et al., 2009)
Zederone 26	Cytotoxic (Mohd Aspollah Sukari et al., 2010)
Furanodienone 22	Anti-inflammatory (Makabe et al., 2006)
Curcumenone 65	Hepatoprotective (Vairappan et al., 2013b)
Curcumenol 42	Analgesic (Pamplona et al., 2006) hepatoprotective (Hisashi Matsuda et al., 1998a)
Isocurcumenol 47	Antitumor (Lakshmi et al., 2011b)
Neocurdione 32	Hepatoprotective (Morikawa et al., 2002)
Curcumin 139	Multi-biological activities (Aggarwal et al., 2003; Maheshwari et al., 2006; Noorafshan et al., 2013)
9-Oxo-neoprocumenol 56	Inhibitor against the Blue Mussel (Etoh et al., 2003)
ar-Turmerone 74	Cytotoxic (Ji et al., 2004)

2.5 Chemical composition of the essential oils from the *Curcuma* species

The major constituents of the essential oils from the *Curcuma* species are monoterpenes and sesquiterpenes, which remain in the form of a complex mixture of low molecular weight compounds, and can be separated by steam distillation or by extraction with organic solvents. Essential oils are prescribed in the traditional medicinal practices and are known to possess various pharmaceutical and biological activities such as anti-inflammatory anti-mutagenic, antidiabetic, antiprotozoal, antiviral, antifungal, and anticancer activity (Raut et al., 2014).

By extensive phytochemical analysis, especially using a combination of GC and GC-MS spectroscopic technique, and the calculation of Kovats indices, major components of the essential oils from different *Curcuma* species were characterized and identified. Table 2.15 lists the major components of the essential oils from some important species of the genus *Curcuma*. The presence of unique compounds in variable

concentrations from 0.25 to 70% in the essential oil can be the key to distinguish *Curcuma* species of different geographic origin. For curzerene and epicurzerenone in *C. zedoaria* from India while camphor is the chemical marker for the species from Indonesia, *curdione* and *xanthorhizol* in *C. aromatica*, α -fenchene in *C. sylvatica*, elemenone in *C. rakthakanta*, curcumenene in *C. malabarica*, and β -eudesmol in *C. aeruginosa* and *C. longa*. The comparison of chemical constituents of *C. zedoaria* essential oils showed that the Indian sources is rich in elemene type sesquiterpenes, e.g., epicurcuzerenone and curzerenone, while the Indonesian one has relatively more monoterpenes with a high content of camphor (**Table 2.15**).

Bisabolane type sesquiterpenes were the major chemical constituents of the essential oils of *C. longa* irrespective of their geographic origin, for example artermenone was found to be the major compound for Indian *C. longa* sample while bisabolene for the Nigerian one (Table 2.16).

In case of *C. aeruginosa* essential oils of Indian origin was found to have guaiane type sesquiterpene as the main constituent i.e., curcumenol **42**. On the other hand, Malaysian sample expressed predominantly elemene type sesquiterpenes and curzerenone **111** as the major constituent. The essential oils of *C. aromatica* from India was found to contain monoterpenes (camphor, 19%), while the Japanese one had the guaiane sesquiterpene curcumol as the major compound (36%) (**Table 2.15**).

Angel et al. (2014) reported recently that some monoterpenes including 1,8-cineole, α -pinene, β -pinene, camphor, and camphene were present in most of the essential oils of the majority of the *Curcuma* species (**Table 2.14, 2.15**).

Table 2.14: The major constituents of the essential oils of the *C. zedoaria* identified by GC/GC-MS analysis

Plant name	Origin	Major constituents	Reference
<i>C. zedoaria</i>	Indonesia	Camphor (49.51%) Isobornyl alcohol (12.66%) borneol (4.23%) Furanodiene (3.61%) Furanodienone (3.49%) 1,8-Cineol (3.42%) Camphene (2.28%) β -Pinene (2.93%)	(Retnowati et al., 2014)
	India	Epicurcuzerenone (19.0%) <i>ar</i> -curcumene (12.1%) Zingiberene (12.0%) β -sesquiphellandrene (9.8%) Curzerene (8.0%) Germacrene B (6.0 %)	(Angel et al., 2014)
	India	Curzerenone (31.6%) Germacrone (10.8%)	(P. Singh et al., 2013)
	India	Curzerenone (22.3%) 1.8-cineole (15.9%) germacrone (9.0%)	(Purkayastha et al., 2006)
	China	Epicurzerenone (46%) Curdione (13.7%) 1,8-Cineole (1.36%) Camphor (1.46%),	(E. Y. Lai et al., 2004).
	India	1,8-Cineol (18.5%) <i>o</i> - and <i>p</i> -Cymene (18.42%) α -Phellandrene (14.93%) Terpinolene (4.11%) α -Pinene (3.28%), β -Turmernote (3.1%), β -Pinene (2.93%)	(G. Singh et al., 2003)

Table 2.15: The major constituents of the essential oils of other *Curcuma* species identified by GC/GC-MS analysis

Plant name	Origin	Major constituents	Reference
<i>C. longa</i>	Bhutan	α -Turmerone (30-2%) ar-Turmerone (17-6%) β -Turmerone (15-18%)	(Sharma et al., 1997).
<i>C. longa</i>	India	ar-Turmerone (51.8%) Ar-Turmerol (11.9%)	(G. Singh et al., 2002)
<i>C. longa</i>	Gorakhpur	ar-Turmerone (24.4%) α -Turmerone (20.5%) β -Turmerone (11.1%)	(G. Singh et al., 2010)
<i>C. longa</i>	North Central Nigeria	Bisabolene (13.9%) Trans-ocimene (9.8%) Myrecene (7.6%) 1,8-cineole (6.9%) Thujene (6.7%) Thymol (6.4%)	(Usman et al., 2009)
<i>C. aeruginosa</i>	India	Curcumenol (38.7%) β -Pinene (27.5%) β -Eudesmol (3.6%)	(Angel et al., 2014)
<i>C. aeruginosa</i>	Malaysia	Curzerenone (24.6%) 1,8-Cineole (11.0%) Camphor (10.6%) Zedoarol (6.3%) Isocurcumenol (5.8%) Curcumenol (5.6%) Furanogermenone (5.5%)	(Sirat et al., 1998).
<i>C. brog</i>	India	1,8-Cineole (28.2%) β -Elemene (8.2%) Camphor (6.9%)	(Angel et al., 2014).
<i>C. aromatica</i>	India	β -Curcumene (31.41%) ar-Curcumene, (23.35%) Germacrone (6.05%) Curzerenone (5.46%) Xanthorrhizol (5.27%)	(Catalan et al., 1989)
<i>C. aromatica</i>	India	Camphor (18.8%) Camphene (10.2%) 1,8-Cineol (10.1%) Borneol (8.2%)	(Angel et al., 2014)
<i>C. aromatica</i>	Japanese	Curcumol (35.77%) 1,8-Cineole (12.22%)	Tsai et al., 2011)
<i>C. aromatica</i>	t India	Camphor (32.3%) Curzerenone (11.0%) α -Turmerone (6.7%) ar-Turmerone (6.3%) 1,8-Cineole (5.5%)	(Bordoloi et al., 1999)
<i>C. sichuanensis</i>	China	δ -Cadinene (13.22%)	(Tsai et al., 2011)
<i>C. sichuanensis</i>	China	epi-Curzerenone (26.9%) Germacrone (12.4%) Isocurcumenol (9.7%) β -Elemene (6.4%) Curzerene (6.2%)	Zhou et al., 2007b).

Table 2.15: The major constituents of the essential oils of other *Curcuma* species identified by GC/GC-MS analysis (Cont.)

Plant name	Origin	Major constituents	Reference
<i>C. heyneana</i>	Indonesia	Curcumanolide (19.6%) Dehydrocurdione (17.2%) Isocurcumenol (16.5%) Curcumenol (13.7%) Curcumenone (6.4%) Germacrone (5.0%)	(Sirat et al., 2009)
<i>C. inodora</i>	Malaysia	Curzerenone (20.8) Germacrone (11.1%) Curdione (7.5%) 1,8-Cineole (5.3%) β -Eudesmol (4.6%)	(S. N. Malek et al., 2006).
<i>C. haritha</i>	India	Camphor (36.0%) 1,8-Cineol (13.9%) Isoborneol (10.6%) Camphene (5.7%) Linalool (4.7%) Curdione (6.9%) Furanogermenone (3.3%) Germacrone (2.8%)	(Raj et al., 2008).
<i>C. rakthakanta</i>	India	1, 8-Cineole (24.6 %) β -Sesquiphellandrene (1.5%) Elemenone (13.6%)	(Angel et al., 2014)
<i>C. caesia</i>	India	1,8-Cineole (40.8%) Camphor (15.2%) ar-Curcumene (18.7%) β -Piene (2.5%)	
<i>C. sylvatica</i>	India	α -Fenchene (70.0%)	(Angel et al., 2014).
<i>C. malabarica</i>	India	1,8-Cineole (40.8%) Curcumenene (18.7%) Camphor (10.2%) β -Pinene (2.5%)	(Angel et al., 2014).
<i>C. amada</i>	India	Myrcene (80.54%) β -Pinene (4.64%)	(G. Singh et al., 2002)

CHAPTER 3: RESULTS AND DISCUSSION

3.1 Phytochemical studies

The phytochemical investigations on the two medicinally important Asian plants; *C. zedoaria* and *C. purpurascens* were performed in the search for bioactive components which resulted in the isolation of a total of 27 compounds. Among these, 22 compounds were isolated from *C. zedoaria* and five compounds were from *C. purpurascens*. The isolation of the pure compounds was accomplished by various chromatographic techniques such as open column chromatography (CC), size exclusion chromatography (Sephadex[®] LH-20), high performance liquid chromatography (HPLC), high performance thin layer chromatography (HPTLC), and preparative thin layer chromatography (PTLC). PTLC was found to be the most efficient technique for the isolation of the pure compounds from the plants under investigation.

Structure elucidation of the pure compounds were established on the basis of extensive spectroscopic analyses; 1D-NMR (¹H-NMR, ¹³C-NMR, and DEPT), 2D-NMR (COSY, HSQC, HMBC, NOESY, *J*-resolved, and H2BC), IR, GC-MS, LC-MS, UV, as well as X-ray crystallography, the latter technique was used for the identification of curcumenol as second monoclinic modification. (O. Ahmed Hamdi et al., 2010).

The structures of the isolated compounds were identified through analysing their spectroscopic data and also by the comparison of their spectral data with those reported in the literature.

Sesquiterpenoids are the major constituents isolated from the rhizomes of *C. zedoaria* (eighteen compounds). However three compounds were labdane-type diterpenoids, whereas ar-turmerone and curcuminoids were the major compounds isolated from *C. purpurascens* rhizomes.

The essential oil obtained by hydrodistillation of *C. purpurascens* rhizomes has resulted in identification of 34 compounds analysed by combination of GC/GC-MS. In

addition, supercritical fluid extraction for the same rhizomes of plant was performed using variable temperatures and pressures.

3.1.1 Compounds isolated from *C. zedoaria*

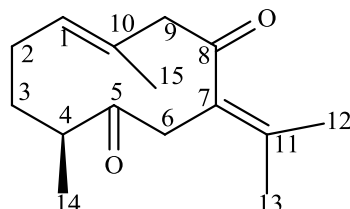
The summary of the compounds isolated from *C. zedoaria* are listed in **Table 3.1**

Table 3.1: Compounds isolated from *C. zedoaria*

No	Compounds	Skeleton
2	Dehydrocurdione 19	Germacrane
1	Curdione 20	Germacrane
3	Furanodiene 21	Germacrane
4	Furanodienone 22	Germacrane
5	Germacrone 23	Germacrane
6	Germacrone-4, 5-epoxide 24	Germacrane
7	Germacrone-1, 10-epoxide 25	Germacrane
8	Zederone 26	Germacrane
11	Gweicurculactone 41	Guaiane
9	Curcumenol 42	Guaiane
10	Curcumenol a second monoclinic modification 150	Guaiane
12	Isoprocurcumenol 43	Guaiane
13	Procurcumenol 44	Guaiane
14	Curcuzedoalide 62	<i>Seco</i> guaiane
15	Curzerenone 111	Elemene
16	Zerumbone epoxide 151	Humulane
17	Comosone II 104	Cadinane
18	Curcumenone 65	Carabrone
19	<i>Curcumanolide</i> A 101	Spirolactone
20	Labda-8(17),12-diene-15,16-dial 127	Labdane-type diterpenoid
22	Calcaractrin A 129	Labdane-type diterpenoid
21	Zerumin A 128	Labdane-type diterpenoid

3.1.1.1 Germacrane type sesquiterpenoids

Dehydrocurdione 19



Dehydrocurdione **19** was isolated as pale yellow oil with $[\alpha]_D^{20} + 280^\circ$ (c 0.3, MeOH). The EI-MS of dehydrocurdione obtained by GC-MS revealed a molecular ion $[M^+]$ peak at m/z 234 corresponding to the molecular formula of $C_{15}H_{22}O_2$. The base peak at m/z 68 was also observed in the EI-MS (Figure 3.7)(Firman et al., 1988a). The UV spectrum showed absorption maxima (λ_{max}) at 207 nm. The IR spectrum exhibited strong absorptions at 1680 and 1742 cm^{-1} implying the presence of conjugated and non conjugated carbonyl groups, respectively.

The 1H NMR (Figure 3.2, Table 3.2) spectrum displayed proton signals typical of germacrane-type sesquiterpenes. These include four methyl signals at δ_H 1.01, 1.63, 1.73, and 1.76 which were assigned as H_3 -14, H_3 -15, H_3 -13, and H_3 -12, respectively. Furthermore, four sets of methylene protons were observed at δ_H 2.09 (H_2 -2), 2.08, 1.64 (H_2 -3), 3.29, 3.32 (H_2 -6) and 3.06, 3.23 (H_2 -9). In addition, there were signals for two methine protons, one was an olefinic proton resonated at δ_H 5.13 (H-1) while the other at δ_H 2.38 (H-4).

The ^{13}C NMR, DEPT-135 and HSQC spectra (Figure 3.3, 3.5, Table 3.2) revealed a total of 15 carbon consisting of four sp^3 methyls at δ_C 16.3 (C-15), 18.4 (C-14), 22.1 (C-13), and 21.0 (C-12), four sp^3 methylenes at δ_C 26.4 (C-2), 34.2 (C-3), 43.4

(C-6) and δ_C 57.0 (C-9), two methines, one of which is sp^2 olefinic carbon at δ_C 133.0 (C-1), while the other is an sp^3 carbon atom at δ_C 46.4 (C-4), five quaternary carbons three of which are sp^2 olefinic carbons resonated at δ_C 129.9 (C-10), 133.0 (C-1) and 137.0 (C-11), and the other two signals are for the carbonyl carbons C-8 (δ_C 207.2), and C-5 (δ_C 211.1).

The 1H - 1H COSY correlations observed were H-4/H₃-14, H-3/H-4, H-2/H-3, H-1/H-2, H-9/H-9', H-6/H-6' coupled with HMBC cross peaks of H-4/ C-5, H-6/C-5, H-1/CH₃-15 H-9/CH₃-15, H-9/C-8, H-6/C-7 confirmed the sequence of C1–C2–C3–C4–C5–C6–C7–C8–C9–C10, or the presence of a ten membered cyclic system of germacrane type sesquiterpene. In addition, the HMBC cross peaks of H₃-12, H₃-13 to C-11 and C-7 confirmed the existence of a dimethyl ethylene group attached to the ring at C-7. COSY and HMBC spectra were able to establish the germacrane skeletal of dehydrocurdione.

From the above spectral data analysis, the identity of the compound was confirmed as dehydrocurdione and were in agreement with the spectral data described in the literature (Makabe et al., 2006).

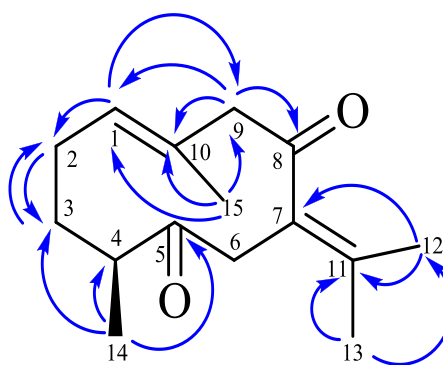


Figure 3.1: Selected HMBC Correlations H \rightarrow C of *dehydrocurdione* **19**

Table 3.2: ^1H NMR (400 MHz) and ^{13}C NMR (100 MHz) spectral data of dehydrocurdione **19** in CDCl_3

Position	δ_{H} (ppm) J in Hz	δ_{C} (ppm)
1	5.13, t (8.24)	133.0
2	2.09, m	26.4
3	2.08, 1.64, m	34.2
4	2.38, <i>m</i>	46.4
5	-	211.1
6	1H-6_{a} , 3.29, d (16.48) 1H-6_{b} , 3.32, d(16.48)	43.4
7	-	129.3
8	-	207.2
9	1H-9_{a} , 3.23, d (11.4) 1H-9_{b} , 3.06, d, (11.44)	57.0
10	-	129.9
11	-	137.0
12	1.76, <i>s</i>	21.0
13	1.73, <i>s</i>	22.1
14	1.01, d (6.88)	18.4
15	1.63, <i>s</i>	16.3

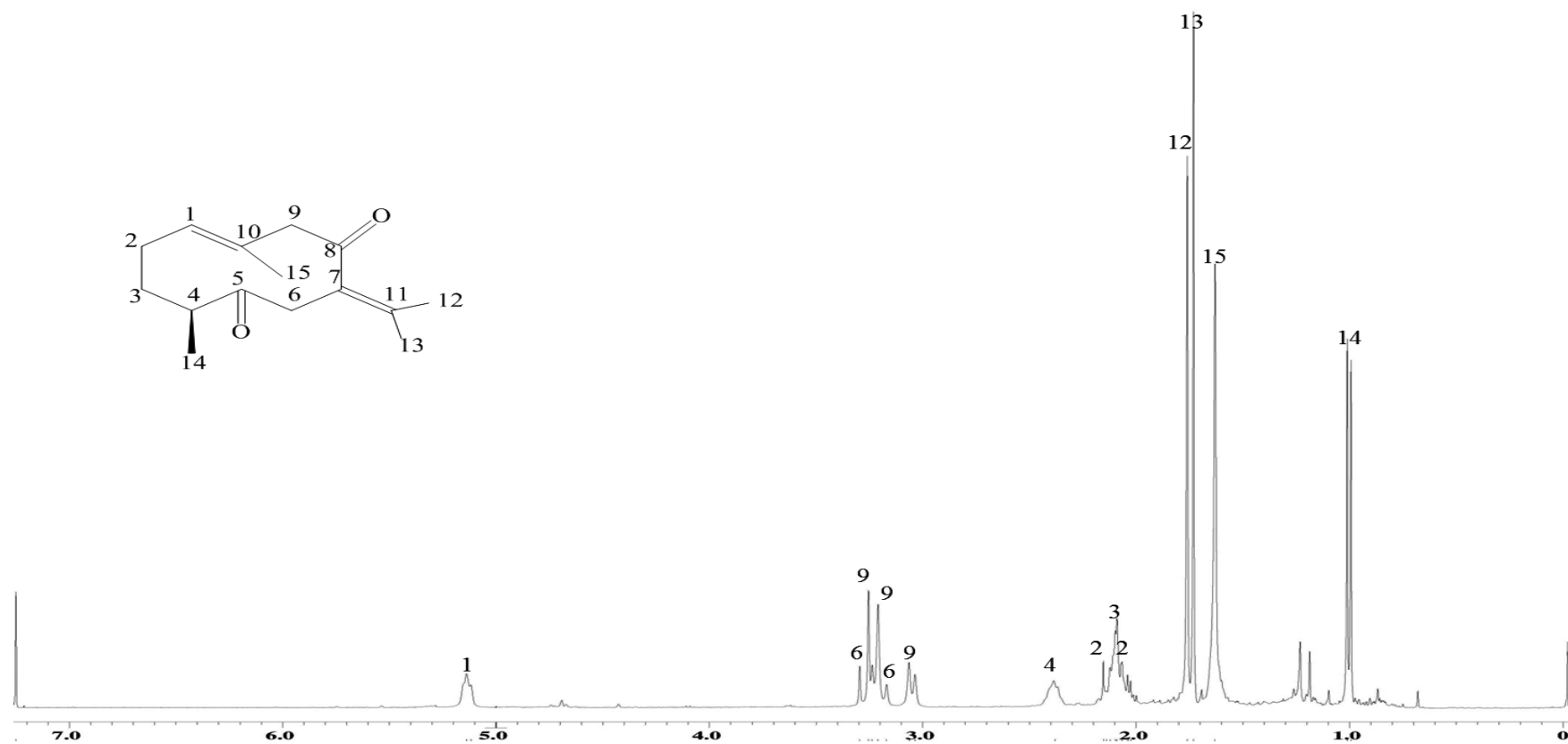


Figure 3.2: ¹H NMR spectrum of dehydrocurdione **19**

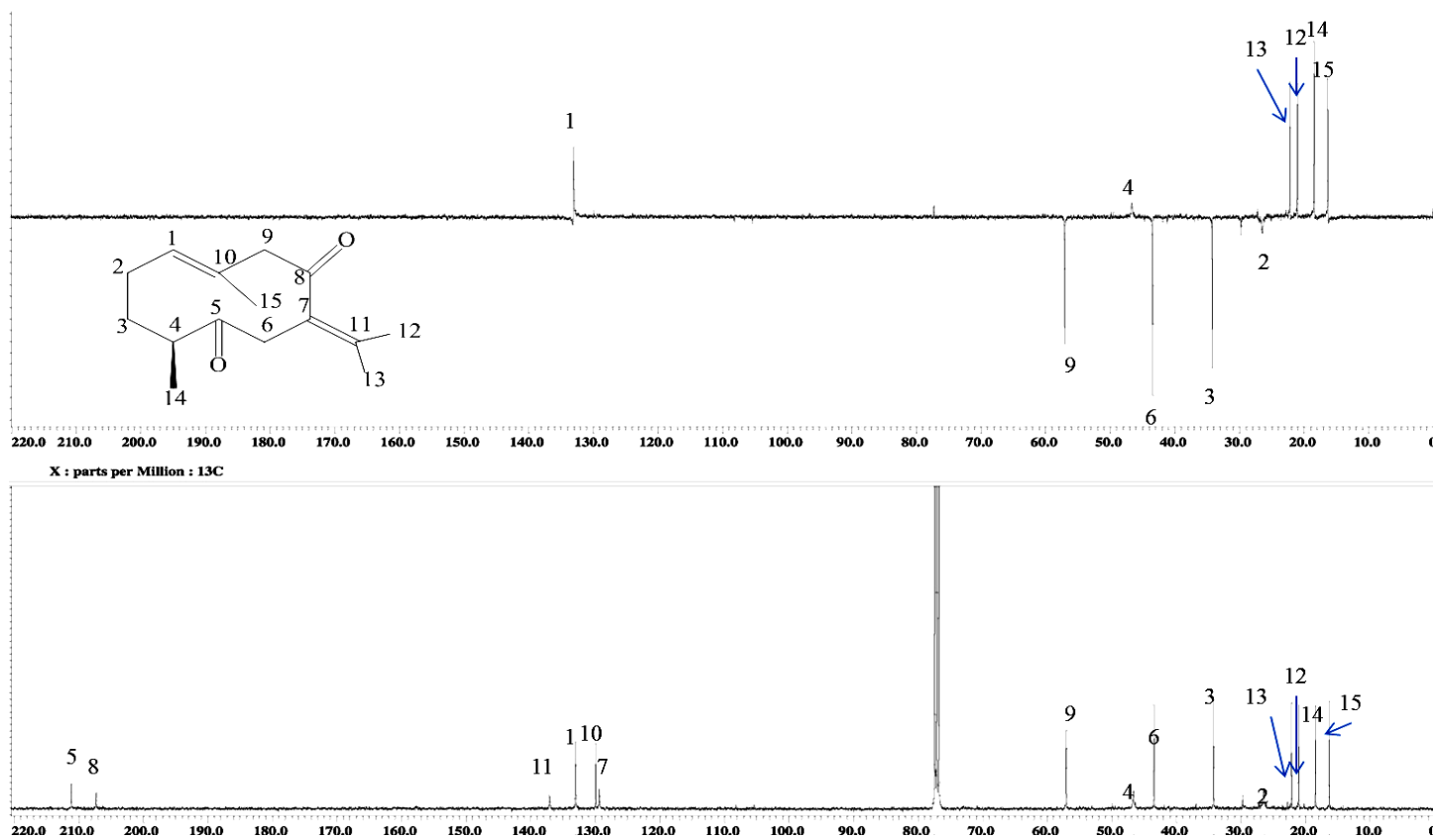


Figure 3.3: ^{13}C NMR and DPET-135 spectra of dehydrocurdione **19**

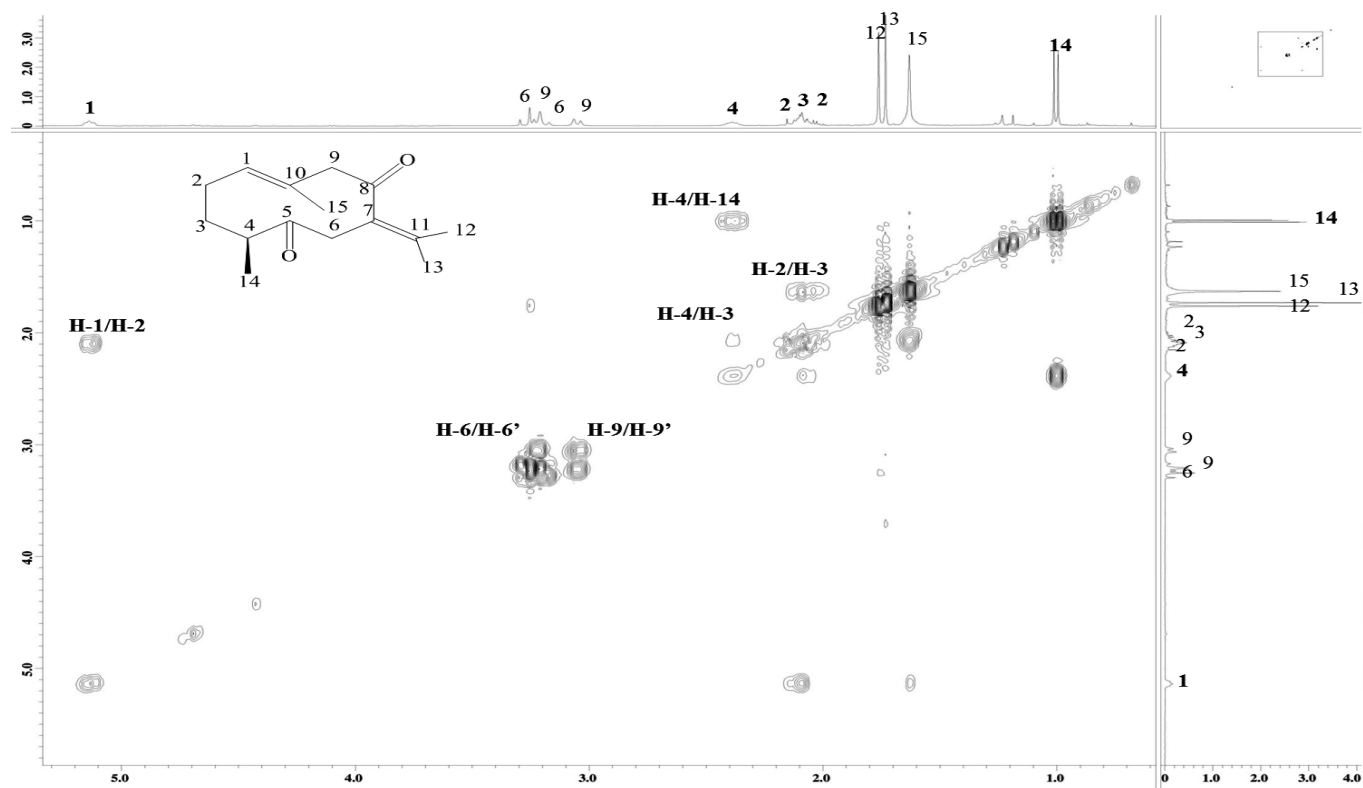


Figure 3.4: COSY spectrum of dehydrocurdione **19**

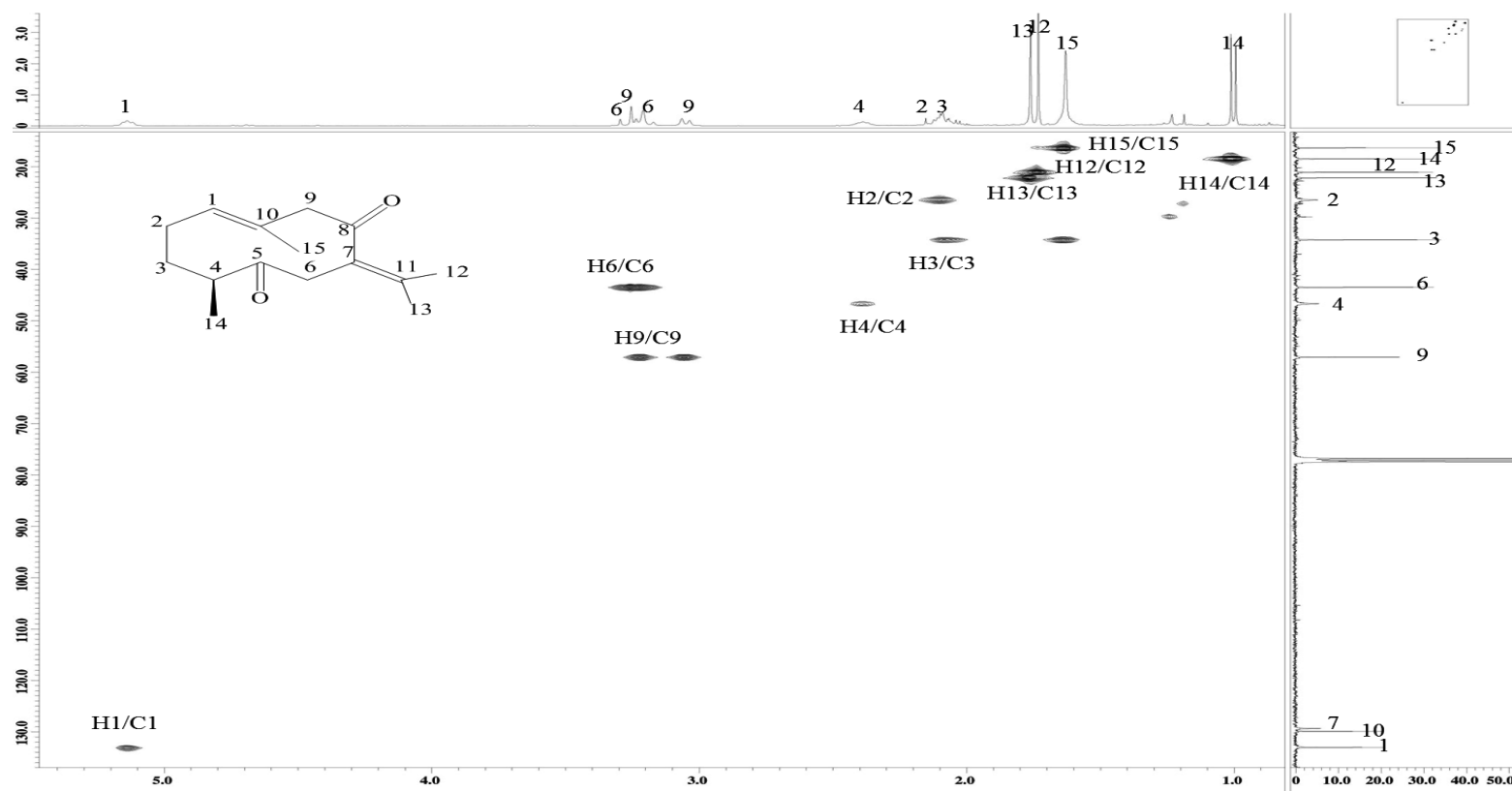


Figure 3.5: HSQC spectrum of dehydrocurdione 19

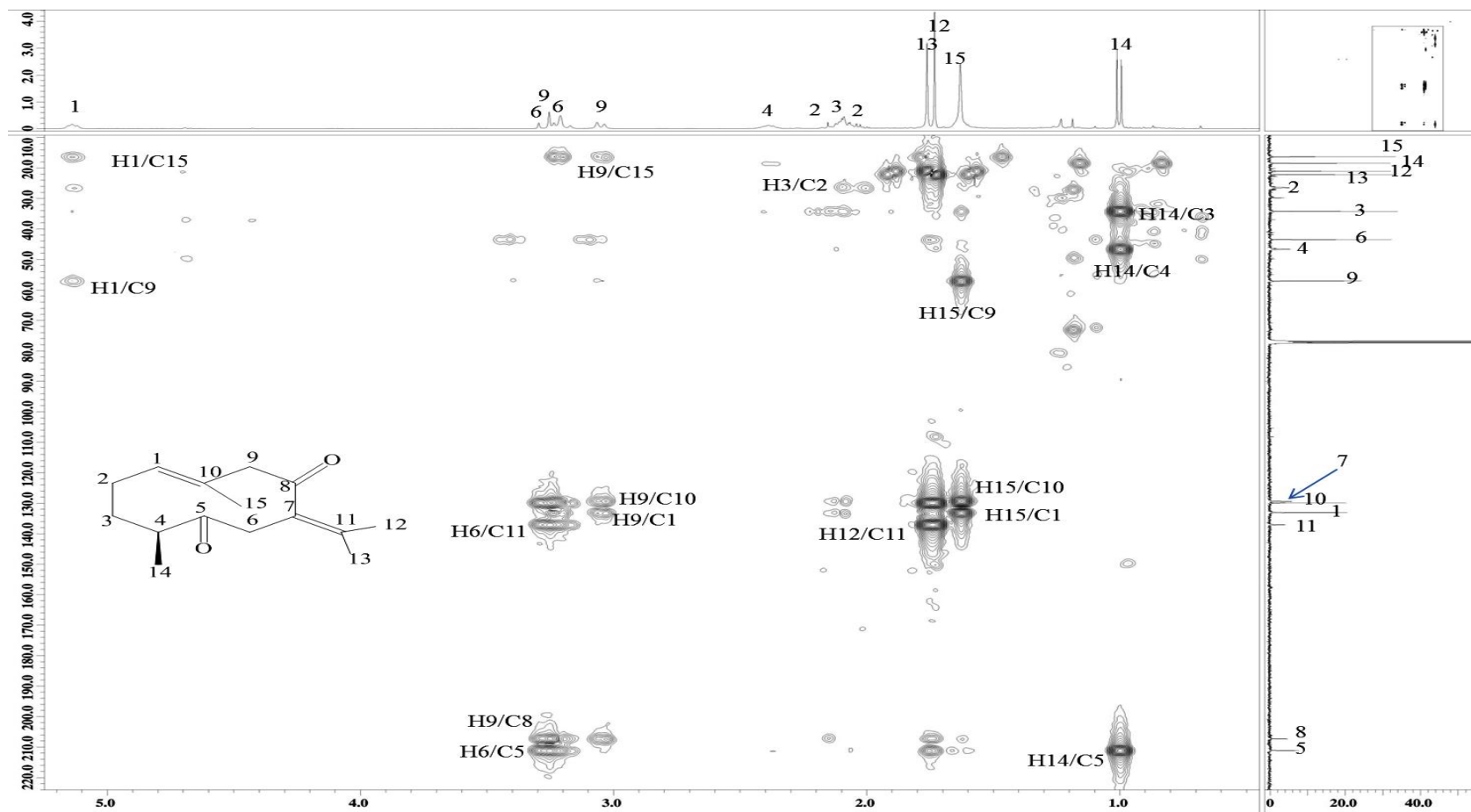
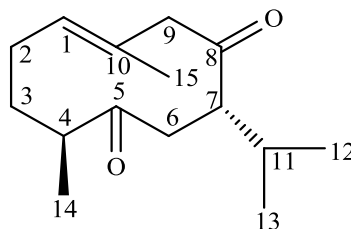


Figure 3.6: HMBC spectrum of dehydrocurdione **19**

Curdione 20



Curdione **20** was afforded as a white amorphous powder with an optical rotation of $[\alpha]_D^{20} + 26^\circ$ ($c=1$ in MeOH). The EI-MS analysis showed the base peak observed at m/z 69 while the molecular ion (M^+) peak at m/z 236 thus corresponding to the molecular formula $C_{15}H_{24}O_2$. The IR spectrum presented strong absorption bands for two carbonyls at 1735 and 1702 cm^{-1} . The UV spectrum displayed one distinct absorption maximum at λ_{max} 204.

The ^1H and ^{13}C NMR spectra (**Figure 3.8, Figure 3.9**) of compound **20** followed same pattern as that of dehydrocurdione **19**, except for the presence of two additional proton signals at δ_{H} 2.81 and 1.84 (H-7, and H-11, respectively). The methyl signals appeared to be shielded as compared to that of dehydrocurdione **19**, further suggesting the saturation of the double bond at $\Delta^{7(11)}$ of dehydrocurdione **19**. The ^{13}C -NMR spectra showed similar chemical shifts for carbons C1 to C-6, while obviously the number of signals in the double bond region reduce from 4 to 2 due to the change of the hybridization of C-7 and C-11 from sp^2 in **19** to sp^3 in **20**.

The ^1H NMR spectrum (**Figure 3.8, Table 3.3**) of compound **20** showed similar evidence for the existence of signals common to a germacrane-skeleton. The proton signals were due to four methyls, one appeared as singlet at δ_{H} 1.67 (H₃-15), whereas the remainder appeared as doublets at 0.96 (d, $J=6.8$ Hz, Me-14), 0.88 (d, $J=6.4$ Hz, Me-13), and δ_{H} 0.93 (d, $J=6.4$ Hz, Me-12). Furthermore, four sets of methylene protons

could be assigned to the signals at δ_{H} 2.08 (H₂-2), 1.63, 2.08 (H₂-3), 2.4 (H₂-6), and δ_{H} 2.91, 3.04 (H₂-9). The proton spectrum also displayed one olefinic proton triplet at δ_{H} 5.10 belonging to H-1 with a coupling constant of 8.24 Hz.

The ^{13}C -NMR and DEPT-135 spectra (**Figure 3.9**, **Table 3.3**) revealed the presence of a total of 15 carbons implying the sesquiterpenic nature of compound **20**. Among them, there were four sp^3 methyls signals resonated at δ_{C} 16.6 (C-15), 18.6 (C-14), 21.2 (C-13), and δ_{C} 19.9 (C-12). Furthermore, four sp^2 methylenes at δ_{C} 26.5 (C-2), 34.1 (C-3), 44.3 (C-6), and δ_{C} 55.9 (C-9), four methines at δ_{C} 131.5 (C-1), 46.8 (C-4), 53.7 (C-7), and 30.1 (C-11) were observed. In addition, three quaternary carbons were apparent including two carbonyls at δ_{C} 211.0 (C-5), and 214.2 (C-8) and one sp^2 quaternary carbon at δ_{C} 129.9 (C-10).

The ^1H - ^1H -COSY correlations observed for compound **20** were reminiscent of the profile of compound **19** but with an additional correlation of the cross peaks between H-7 and H-11. HMBC profile of compound **20** was similar spectral to that of compound **19** but with extra cross peaks presented for the correlations between H-7/C-8, C-6, C-5 and H-11/C-12, C-13, C-9.

The in depth analysis of 2D spectra including COSY, HMQC, and HMBC identified the compound **20** and confirmed its identity as curdione **20** and the spectral data were in agreement with the reported literature data (Hisashi Matsuda, Toshio Morikawa, et al., 2001a).

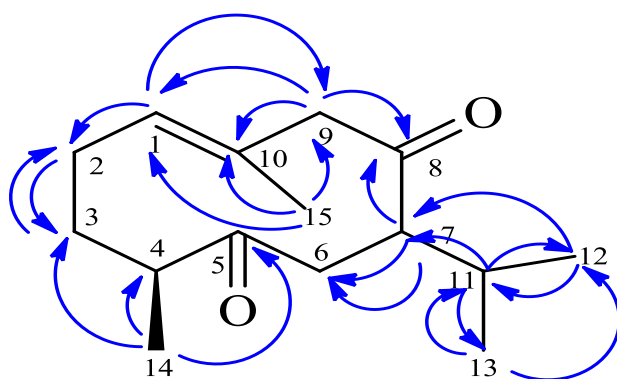


Figure 3.7: Selected HMBC Correlations H $\xrightarrow{\hspace{1cm}}$ C of *curdione 20*

Table 3.3: ^1H (400 MHz) NMR and ^{13}C (100 MHz) NMR spectral data of *curdione 20* in CDCl_3

Position	δ_{H} in ppm, J (Hz)	δ_{C} in ppm
1	5.13, d (8.24)	131.5
2	2.08, m	26.5
3	1.63, 2.08, m	34.1
4	2.36, m	46.8
5	-	211.0
6	2.4, m	44.3
7	2.81, m	53.7
8	-	214.2
9	2.91, 3.04, d (11)	55.9
10	-	129.9
11	1.84, m	30.1
12	0.93, d (6.4)	19.9
13	0.88, d (6.8)	21.2
14	0.96, d (6.8)	18.6
15	1.67, s	16.6

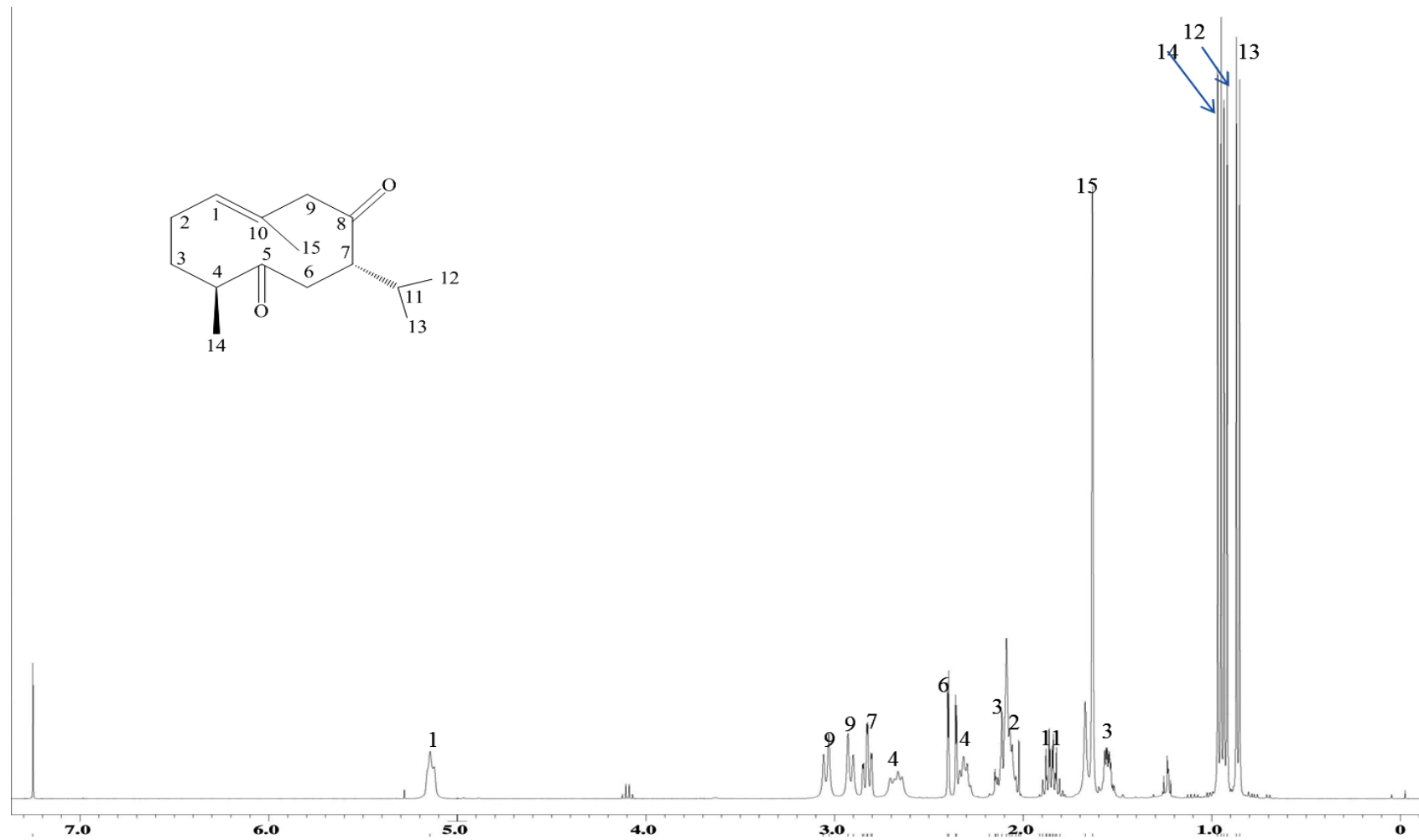


Figure 3.8: ^1H NMR spectrum of curdione 20

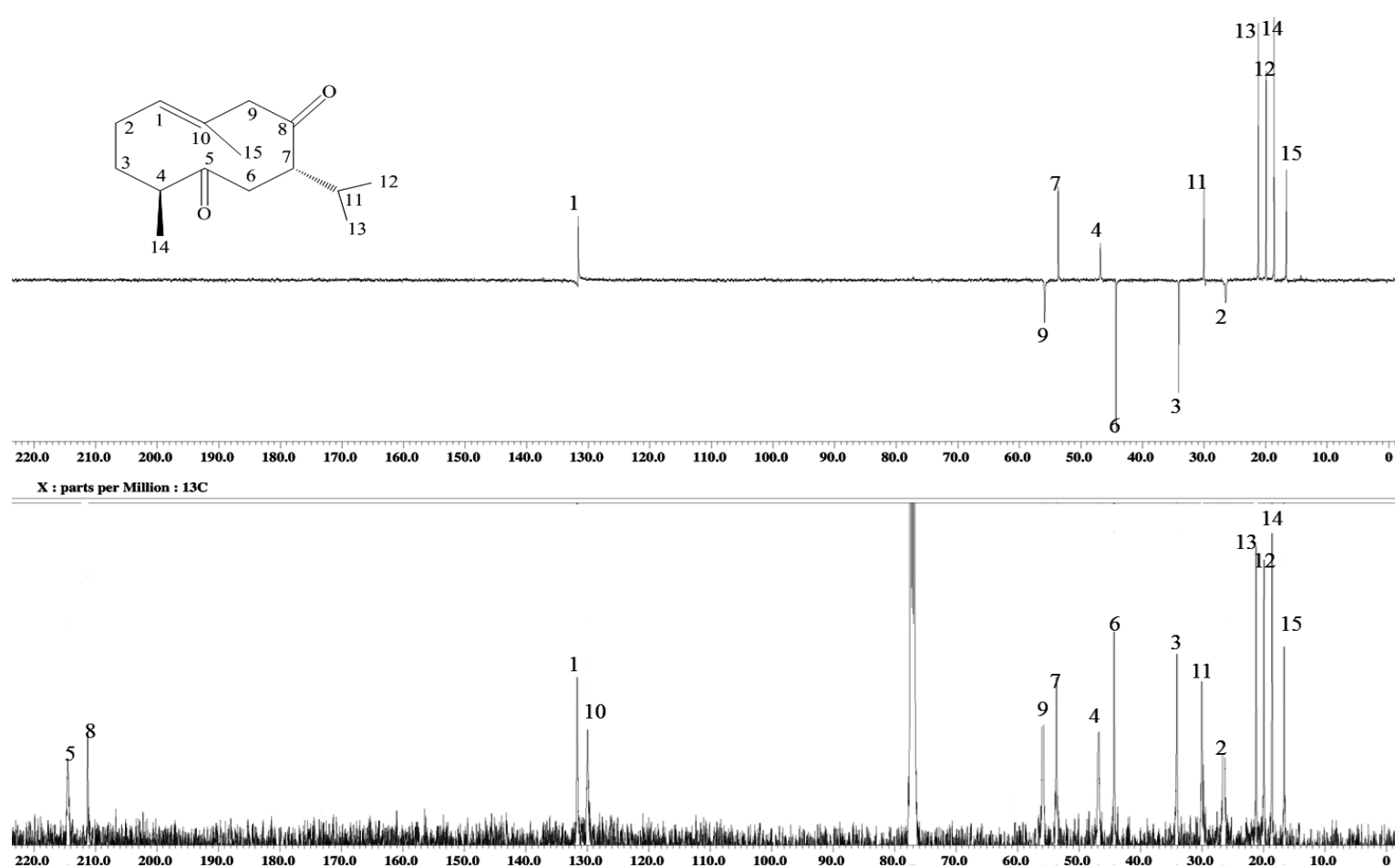
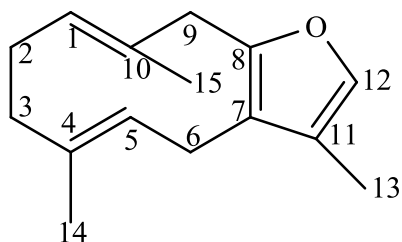


Figure 3.9: ^{13}C NMR and DEPT-135 spectra of curdione 20

Furanodiene **21**



Furanodiene **21** was isolated as white amorphous powder. The GC-MS analysis exhibited the molecular ion peak (M^+) at m/z 216 corresponding to the molecular formula of $C_{15}H_{20}O$. The UV spectrum (MeOH) of **21** showed absorption maximum at λ_{\max} nm (log ϵ): 217 (1.385). The IR spectrum ($CHCl_3$) showed absorptions at ν_{\max} cm^{-1} : 3429, 2928, 1740, 1448.

The 1H NMR spectrum (**Figure 3.10, Table 3.4**) of **21** displayed similar proton signals common to the germacrane skeleton due to the presence of three methyl singlets at δ_H 1.26 (H_3 -15), δ_H 1.59 (H_3 -14), and δ_H 1.92 (H_3 -13), four set of methylenes protons at δ_H 2.11 (H_2 -2), 2.13 (H_2 -3), 2.2, 1.59 (d , $J=7$ Hz, H_2 -6) and δ_H 3.51, 3.72 (d , $J=16$ Hz, H_2 -9). In addition, three olefinic methines appeared at δ_H 4.91 (H -1), 4.73 (t , $J=7$ Hz, H -5), and one proton signal was evident for the presence of furan ring resonated in the downfield region of δ_H 7.07 (1H, s , H -12).

The ^{13}C and DEPT-135 spectra (**Figure 3.11, Table 3.4**) revealed the presence of a total of 15 carbon signals corresponding to three sp^3 methyls at δ_C 16.7 (C-15), 16.3 (C-14), and δ_C 9.0 (C-13), four sp^3 methylenes at δ_C 26.8 (C-2), 39.5 (C-3), 24.4 (C-6), 40.9 (C-9), three sp^2 methines at δ_C 129.0 (C-1), 127.6 (C-5), and δ_C 136.0 (C-12), and five sp^2 quaternary carbons at δ_C 128.9 (C-4), 118.9 (C-7), 149.8 (C-8), 134.4 (C-10), and 121.9 (C-11).

Further, analysis of 2D spectra including COSY, HSQC, HMBC confirmed the identity compound **21** as furanodiene and the structural assignment was supported by the published literature (Makabe et al., 2006).

Table 3.4: ^1H NMR (400 MHz), and ^{13}C NMR (100 MHz) spectral data of furanodiene **21**

Position	δ_{H}, J (Hz)	δ_{C}
1	4.91, m	129.0
2	2.13, m	26.8
3	1.78, 2.25, m	39.5
4	-	128.9
5	4.73, t, (7.32)	127.6
6	3.06, d (7.32)	24.4
7	-	118.9
8	-	149.8
9	3.40, 3.55 (16)	40.9
10	-	134.4
11	-	121.9
12	7.06, brs	136.0
13	1.92, s	9.0
14	1.59, s	16.3
15	1.26, s	16.7

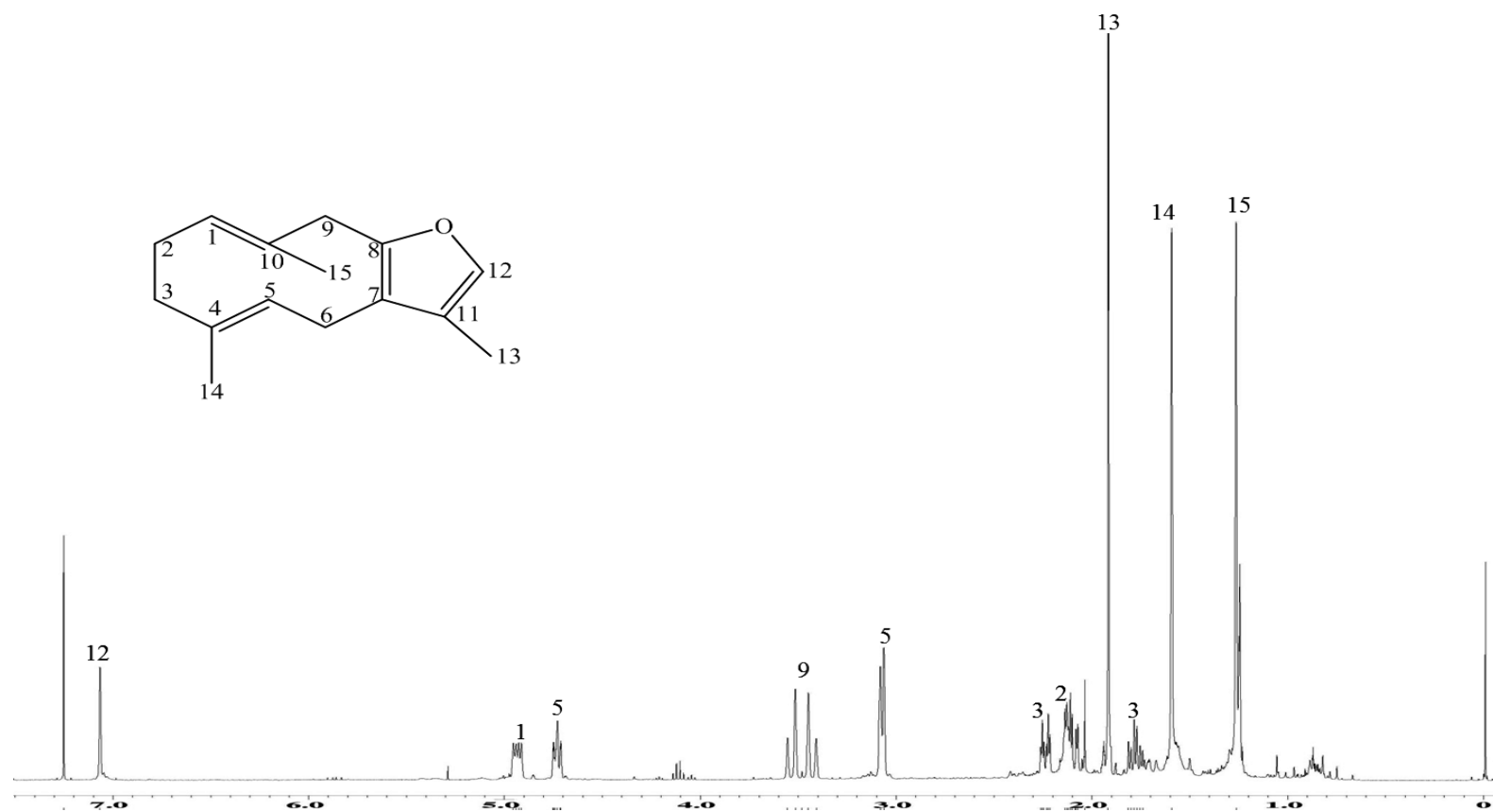


Figure 3.10: ^1H NMR spectrum of furanodiene **21**

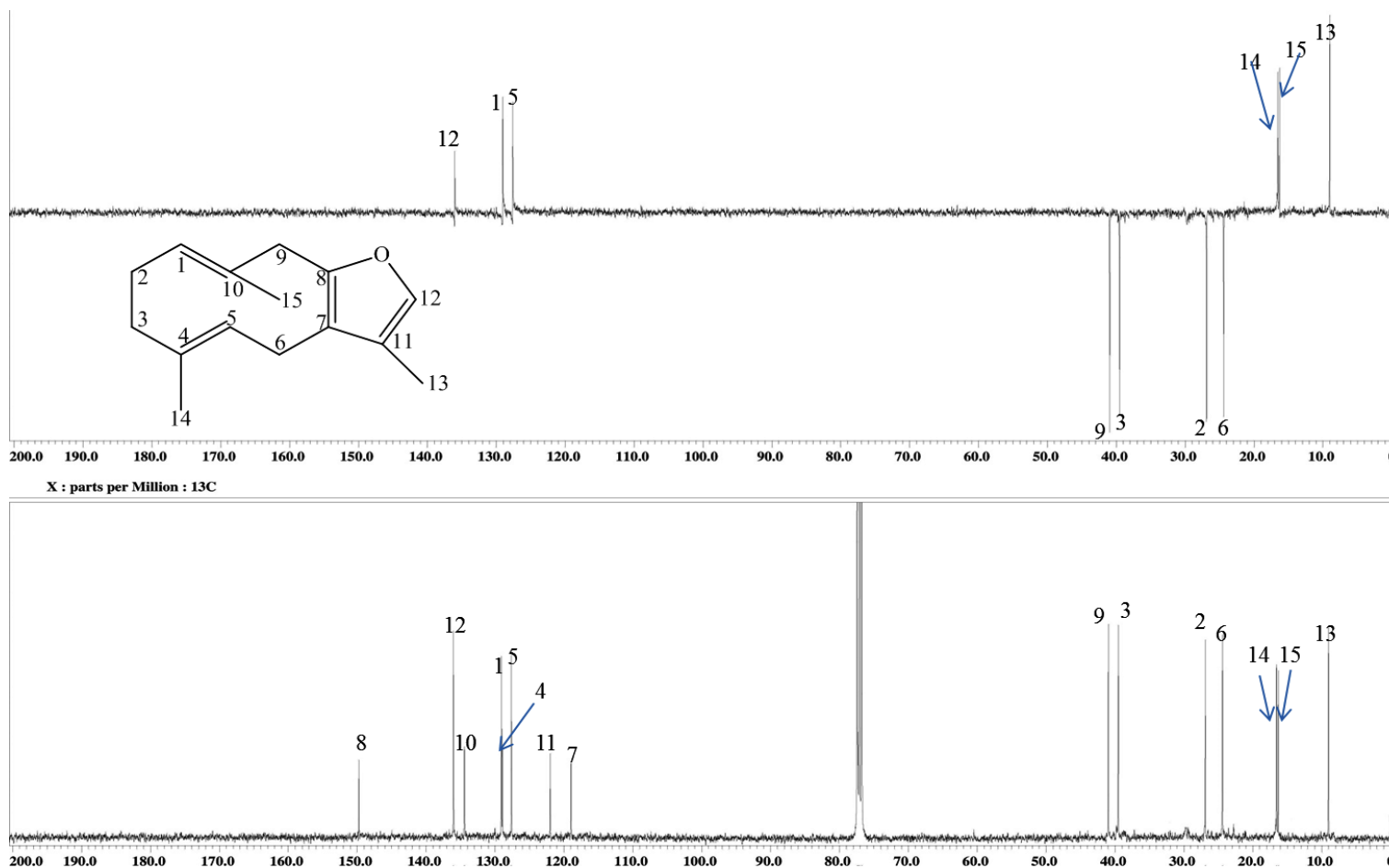
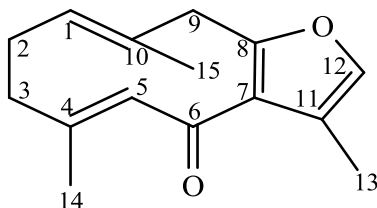


Figure 3.11: ^{13}C NMR and DEPT 135 spectra of furanodiene **21**

Furanodienone 22



Furanodienone **22** was obtained as a colourless crystal (m.p 86-88 °C). The EI-MS displayed the molecular ion peak (M^+) at m/z 230 corresponding to the molecular formula of $C_{15}H_{18}O_2$. The UV spectrum showed absorption band at 217 nm (log ϵ 1.38). The IR spectrum showed strong absorption band at 1653 and 1376 cm^{-1} representing carbonyl group and olefinic carbons, respectively.

The 1H NMR spectrum (**Figure 3.12**, Table 3.5) showed the presence of an olefinic proton characteristic of the furan ring appearing as a singlet at δ 7.06 (H-12). The proton spectrum also displayed two methyl singlets at δ 1.29 (H₃-15), and δ 1.98 (H₃-14), and one methyl appeared as a doublet ($J=1.36$ Hz) at δ 2.12. Three methylenes protons were observed, one appeared as a singlet at δ 3.73 (H₂-9) while the two other methylenes observed as two doublet of triplet at δ 2.17 (H₂-2) and 1.90 (H₂-3). Furthermore, the value of the chemical shift of the olefinic proton (H-5) was shifted to the lower field at δ 5.80 compared to the value normal double is due to the deshielding effect of the carbonyl group. Additionally the doublet of doublet at δ 5.15 was assigned to H-1.

The ^{13}C NMR and DEPT 135 spectra (**Figure 3.13**, Table 3.5) exhibited the presence of a total of 15 carbons including three sp^3 methyls at δ_C 9.6 (C-13), 19.0 (C-14), 15.8 (C-15), three sp^3 methylenes at δ_C 26.5 (C-2), 41.7 (C-3), and δ_C 40.7 (C-9), and three sp^2 methines at δ_C 130.6 (C-1), 132.5 (C-5), and δ_C 138.1 (C-12), and six sp^2 quaternary carbons at δ 145.9 (C-4), 135.5 (C-10), 123.7 (C-11), 122.2 (C-7), 156.6 (C-8), and a carbonyl at δ 189.9 (C-6).

The compound was identified as furanodienone based on the similarity of above spectral data and with those spectral data previously reported (Dekebo et al., 2000).

Table 3.5: ¹H NMR (400 MHz) and ¹³C NMR (100 MHz) spectral data of furanodienone 22

Position	$\delta_{\text{H}}, J \text{ (Hz)}$	δ_{C}
1	5.15, dd (5.04, 11.8)	130.6
2	(1H) 2.17, dt (5.04, 11.8) (1H) 2.31, m	26.5
3	(1H) 1.90 dt (4.12, 11.4) (1H) 2.46, td, (3.64, 11.4)	41.7
4	-	145.9
5	5.80, br s	132.5
6	-	189.9
7	-	122.2
8	-	156.6
9	3.73, br s	40.7
10	-	135.5
11	-	123.7
12	7.06, brs	138.1
13	2.12, d (1.36)	9.6
14	1.98, s	19.0
15	1.29, s	15.8

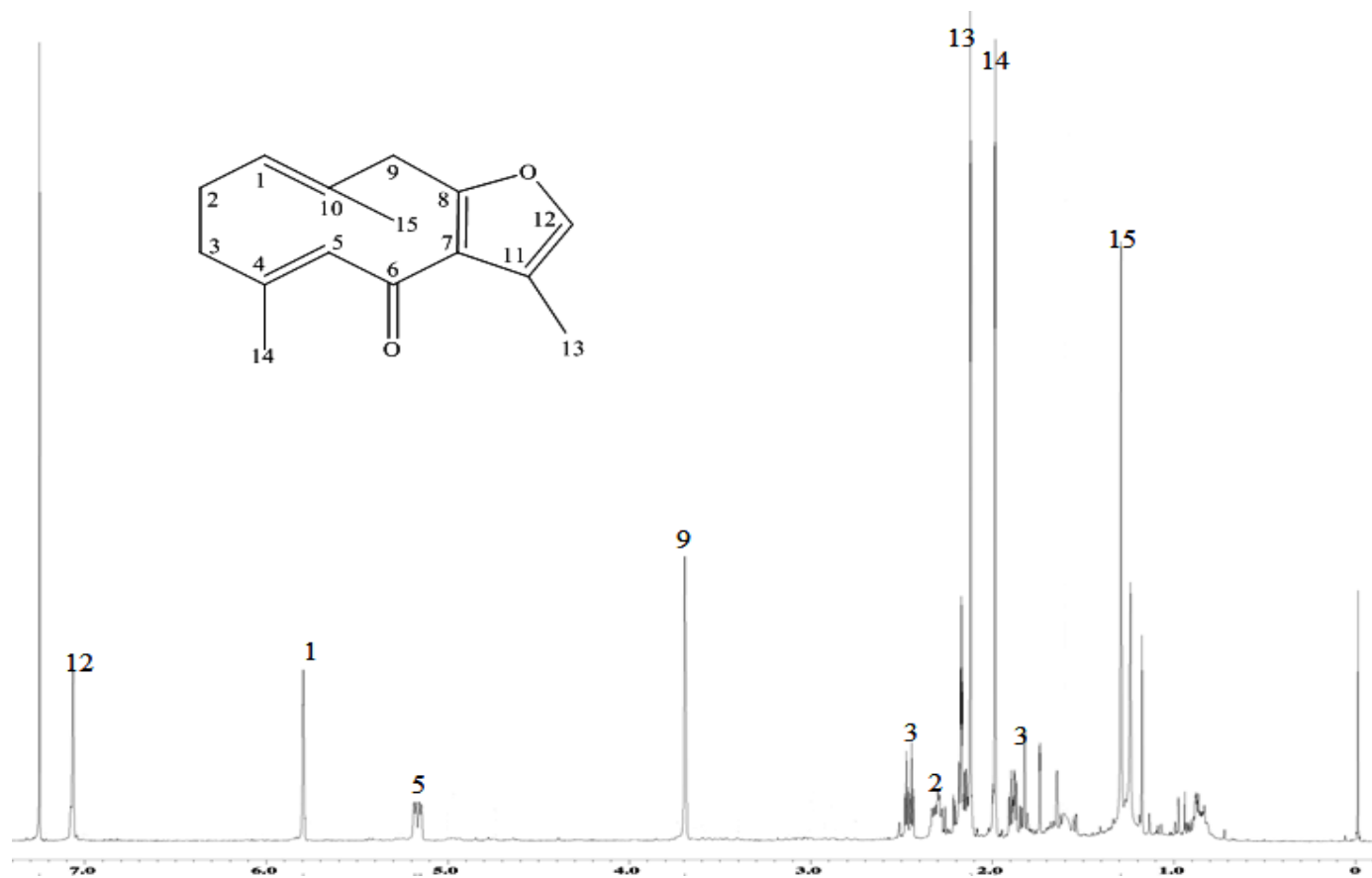


Figure 3.12: ^1H NMR spectrum of furanodienone 22

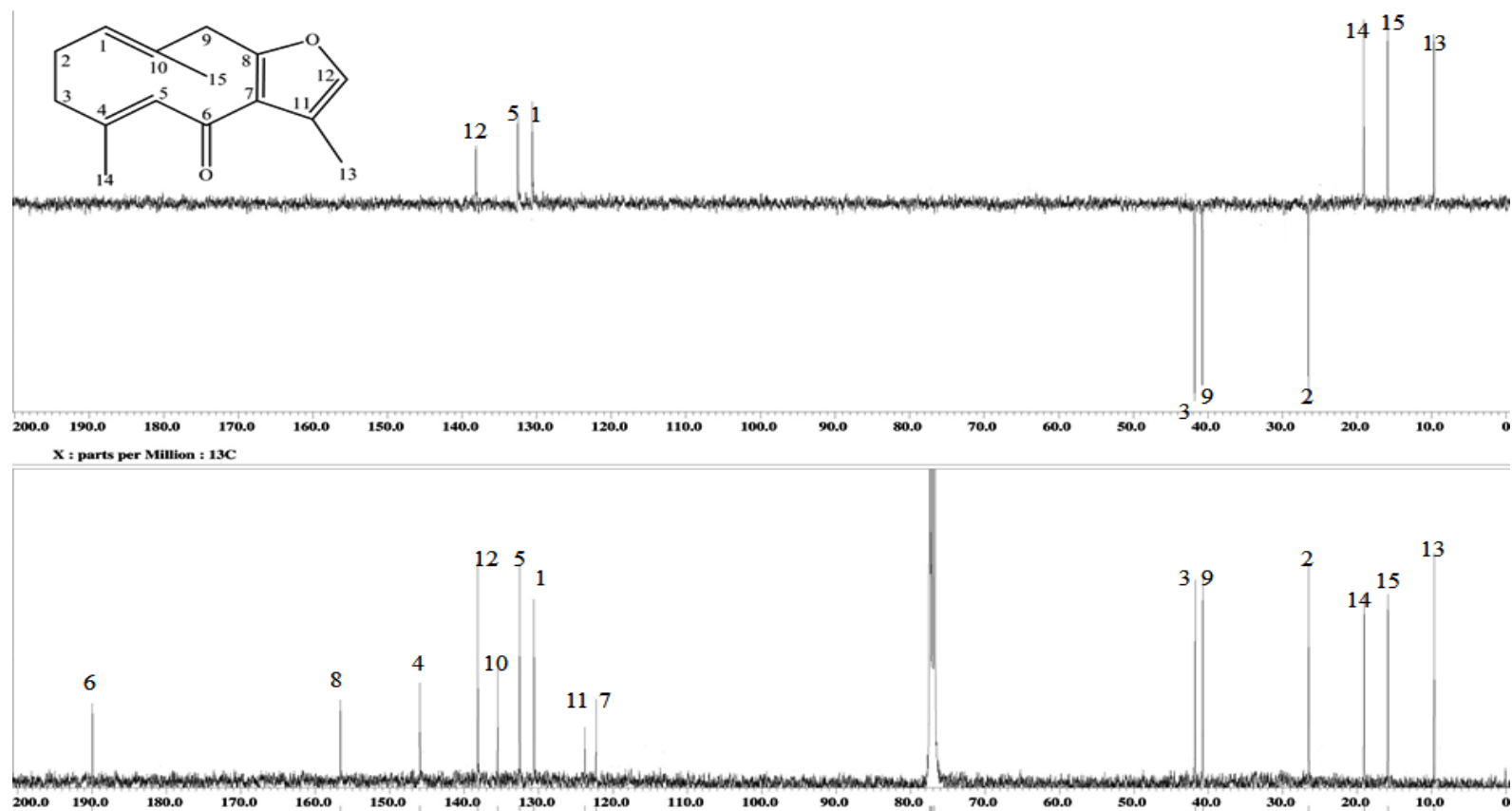
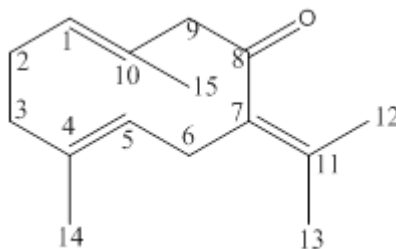


Figure 3.13: ^{13}C NMR and DEPT -135 spectra of furanodienone **22**

Germacrone 23



Germacrone **23** was isolated as white amorphous powder. The EI-MS of germacrone obtained by GC-MS, showed a molecular ion peak (M^+) at m/z 218 corresponding to the molecular formula of $C_{15}H_{22}O$, and also revealed the base peak at m/z 107. The UV spectrum absorption band at 206 nm ($\log \epsilon$ 1.47), while the IR spectrum revealed the absorption at 1677 cm^{-1} indicating the presence of a conjugated carbonyl group.

The ^1H NMR spectral pattern (**Figure 3.14, Table 3.6**) was similar to that of germacrane skeleton with four methyl singlets at δ_{H} 1.62 (H₃-15), 1.43 (H₃-14), 1.76 (H₃-13), and 1.73 (H₃-12). Four pair of methylene protons were observed at δ_{H} 2.08, 2.35 (*m*, H₂-2), 2.15 (*m*, H₂-3), 2.86 (*m*, H₂-6), 3.42, 2.95 (*dd*, *J*=11, 3.68, H₂-9). Moreover, the proton spectrum showed also two olefinic methine protons at δ_{H} 4.94 (1H, *d*, *J*=11.8, H-1) and δ_{H} 4.71 (1H, *d*, *J*=11 Hz, H-5)

The ^{13}C NMR and DEPT-135 spectra (**Figure 3.15**, **Table 3.6**) indicated the presence of a total of 15 carbons; four sp^3 methyls at δ_{C} 16.8 (C-15), 15.6 (C-14), 22.4 (C-13), and 20.0 (C-12), four sp^3 methylenes at δ_{C} 24.0 (C-2), 38.1 (C-3), 29.3 (C-6), and 56.0 (C-9), two sp^2 methines at δ_{C} 132.8 (C-1), 125.4 (C-5), five sp^2 quaternary carbons at δ_{C} 126.0 (C-4), 129.0 (C-7), 135.1 (C-10), and 137.0 (C-11), and a carbonyl at δ_{C} 208.0 (C-8).

Detailed analysis of spectral data including COSY, HSQC, and HMBC confirmed the identity of the compound **23** as germacrone and it is in agreement with those spectral data previously described in the literature (Makabe et al., 2006).

Table 3.6: ^1H NMR (400 MHz), and ^{13}C NMR (100 MHz) spectral data (in CDCl_3) of germacrone **23**

Position	δ_{H}, J (Hz)	δ_{C}
1	4.94, d, (11.8)	132.8
2	2.08, 2.35, m	24.0
3	2.15, m	38.1
4	-	126.0
5	-	125.4
6	2.8, m	29.3
7	-	129.0
8		208.0
9	2.91, 3.04, d (11)	56.0
10	-	135.1
11	3.42, 2.95, dd, (11, 3.68)	137.0
12	1.73, s	20.0
13	1.76, s	22.4
14	1.43, s	15.6
15	1.62, s	16.8

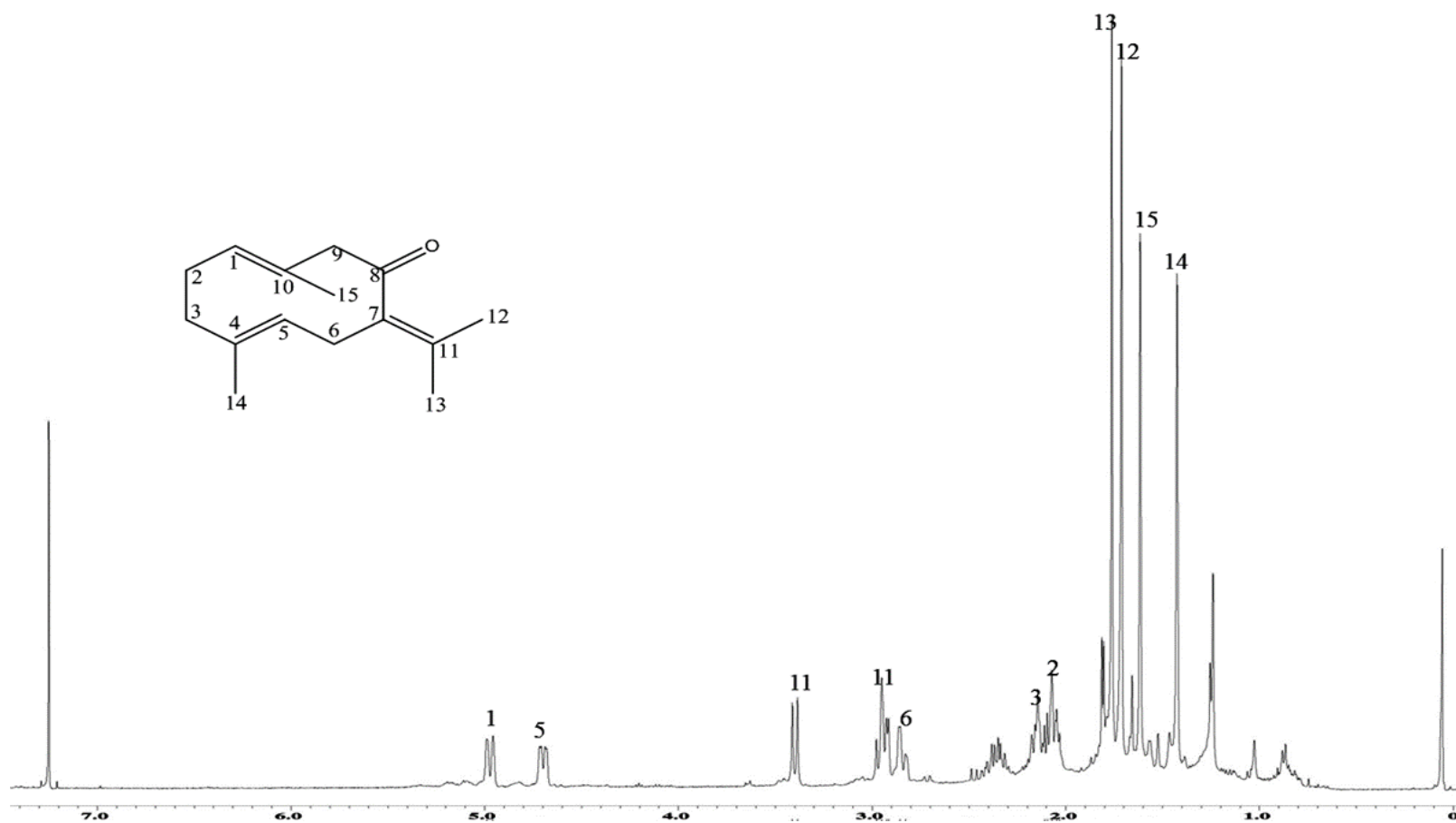


Figure 3.14: ^1H NMR spectrum of germacrone **23**

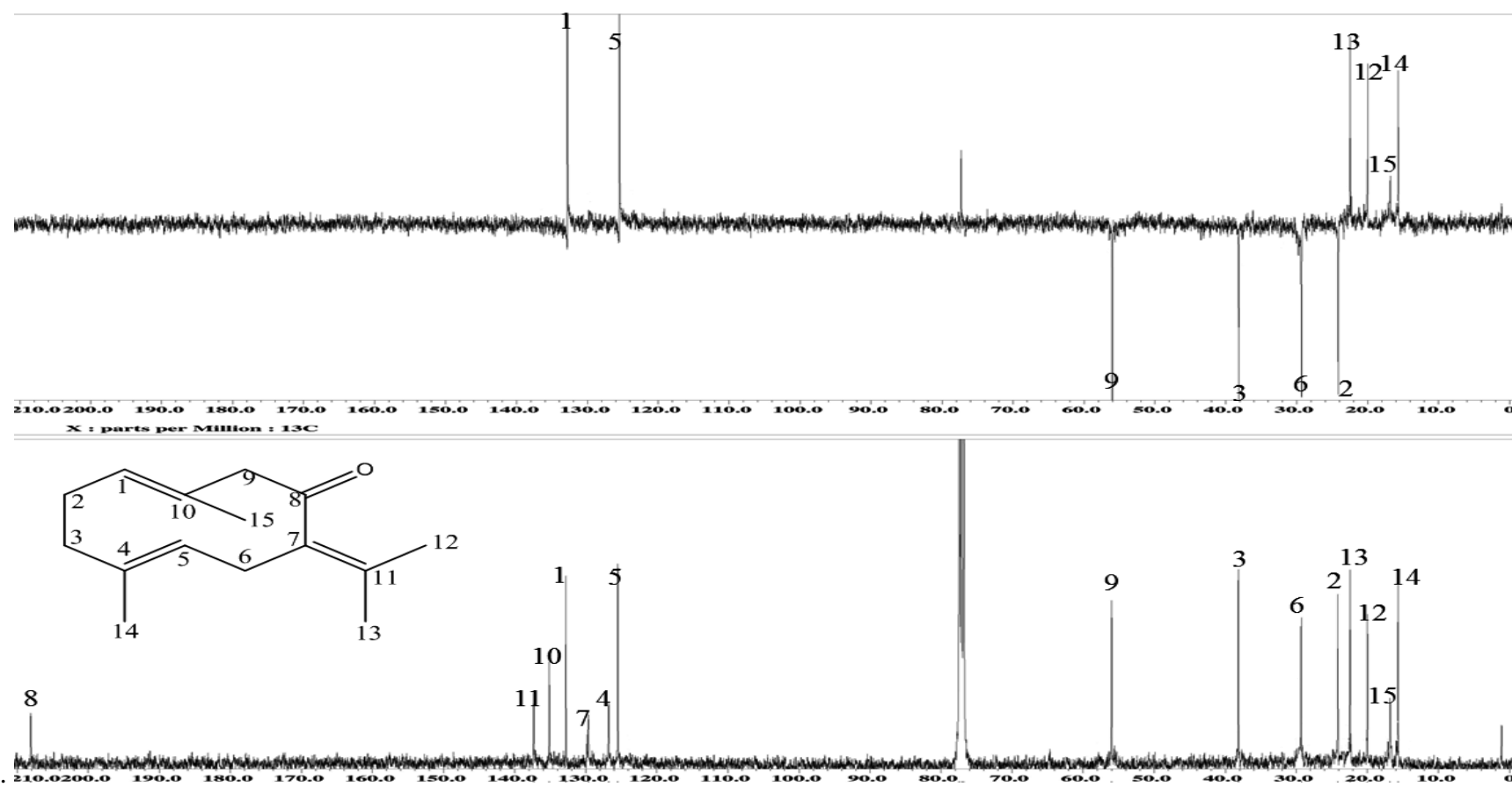
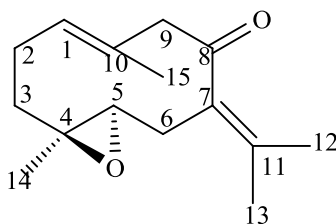


Figure 3.15: ^{13}C NMR and DEPT 135 spectra of germacrone **23**

Germacrone 4,5-epoxide **24**



Germacrone 4,5-epoxide **24** was obtained as a white amorphous solid. The EI-MS analysis showed a molecular ion peak (M^+) at m/z 234 corresponding to the molecular formula of $C_{15}H_{22}O_2$. The UV spectrum showed an absorption maximum at 205 nm ($\log \epsilon$ 1.17). The IR absorption indicated the presence of a carbonyl group at 1702 cm^{-1} .

The ^1H NMR spectrum (**Figure 3.16, Table 3.7**) revealed the presence of four methyl singlets at δ_{H} 1.71 (H_3 -15), 1.02 (H_3 -14), 1.80 (H_3 -13), and δ_{H} 1.81 (H_3 -12), four sets of methylene protons at δ_{H} 2.24 (H_2 -2), 2.13, 2.43 (d , $J=1.84\text{ Hz}$, H_2 -3), 2.88, 2.03 (d , 15.12 Hz , H_2 -6), and δ_{H} 3.43 (br.s, H_2 -9). In addition to two methines at 5.28 (d , $J=9.15\text{ Hz}$, H_1), and δ_{H} 2.40, 2.44 (dd , $1.84, 2.28\text{ Hz}$).

The ^{13}C NMR and DEPT 135 spectra (**Figure 3.17, Table 3.7**) displayed a total of 15 carbons suggesting a possible sesquiterpene structure, four sp^3 methyls at δ_{C} 17.0 (C -15), 15.9 (C -14), 22.8 (C -13), and δ_{C} 20.5 (C -12), four sp^2 methylenes at δ_{C} 24.7 (C -2), 37.7 (C -3), 29.7 (C -6), and δ_{C} 55.6 (C -9), one sp^2 methine at 129.8 (C -1), one sp^3 methine at δ_{C} 64.3 (C -5), three sp^2 quaternary carbons at δ_{C} 126.7 (C -7), 133.7 (C -10), and δ_{C} 133.9 (C -11), one sp^3 quaternary carbon at 60.9 (C -4), and one carbonyl at δ_{C} 204.8 (C -8).

From the spectroscopic data obtained and in comparison with the literature values. The structure of compound **24** was established as germacrone 4, 5-epoxide (Ohshiro et al., 1990a)

Table 3.7: ^1H NMR (400 MHz), and ^{13}C NMR (100 MHz) spectral of germacrone 4,5-epoxide **24** data in CDCl_3

Position	δ_{H}, J (Hz)	δ_{C}
1	5.18, d (8.24)	129.8
2	2.24, m	24.7
3	2.12, m	37.7
4	-	60.9
5	2.40, 2.44, dd (1.84, 2.28)	64.3
6	2.87 m, 2.03, d (13.8)	29.7
7	-	126.7
8	-	204.8
9	2.99, 3.43, brs	55.6
10	-	133.7
11	-	133.9
12	1.81, s	20.5
13	1.80, s	22.8
14	1.02, s	15.9
15	1.71, s	17.0

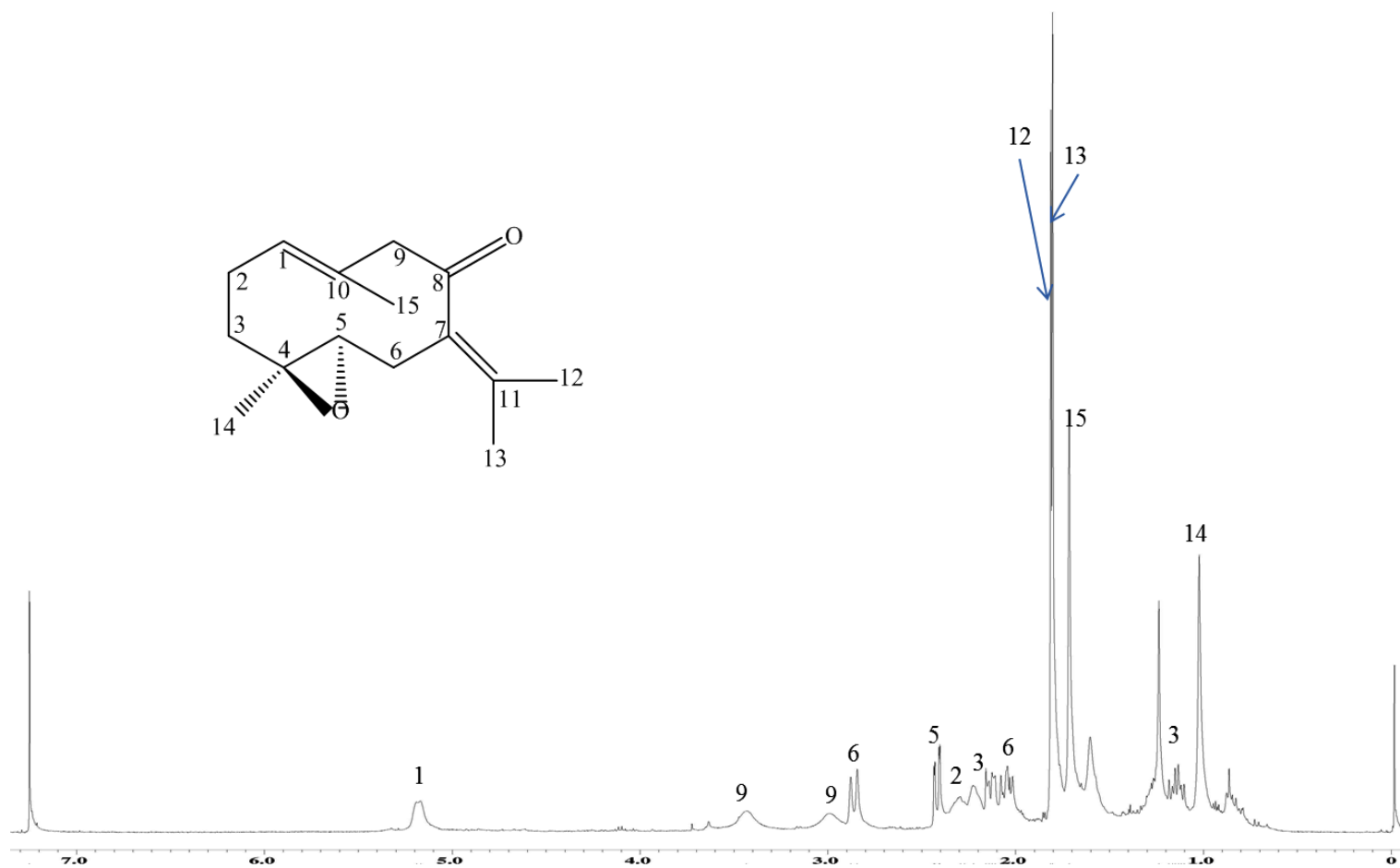


Figure 3.16: ^1H NMR spectrum of germacrone-4,5-epoxide **24**

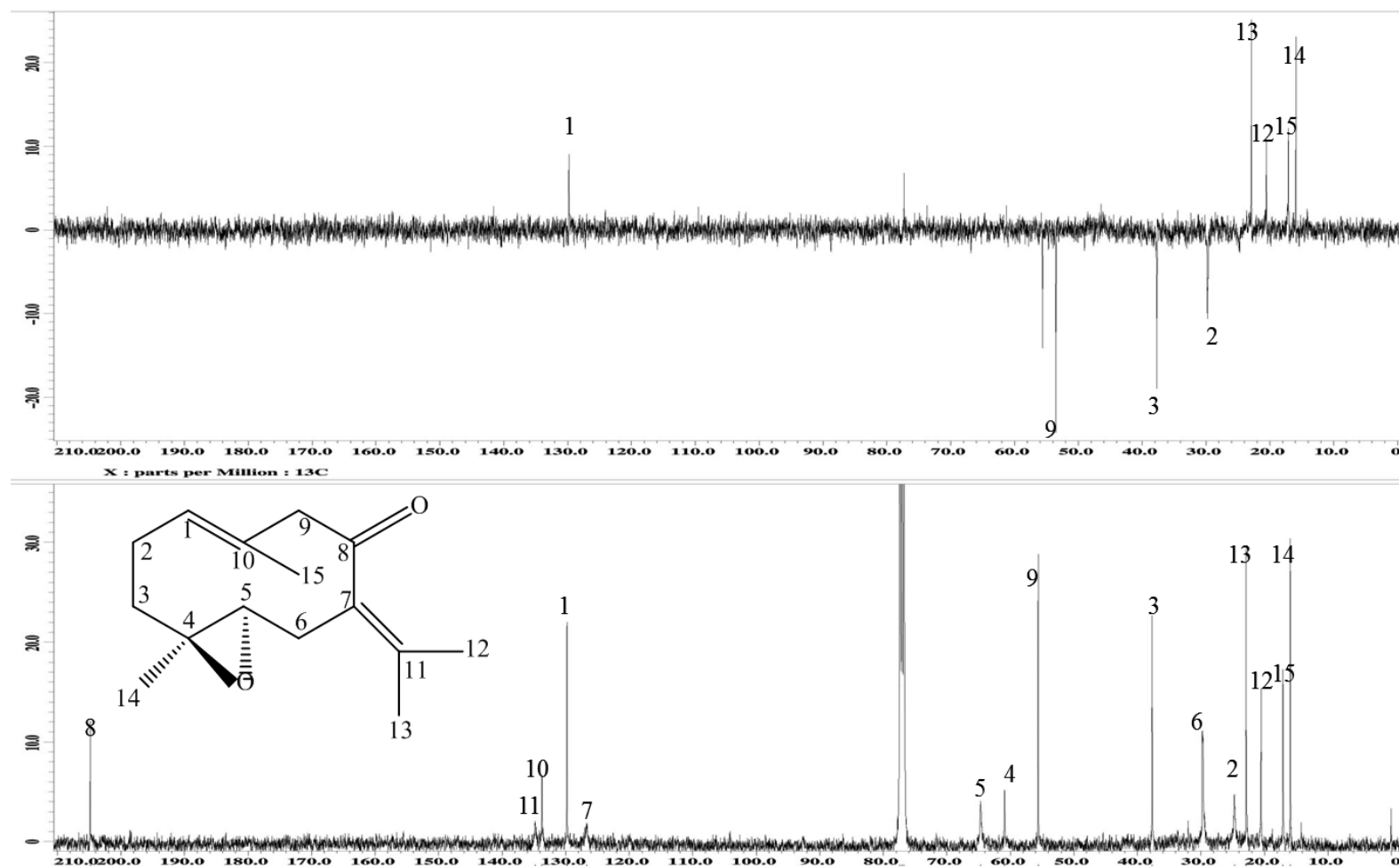
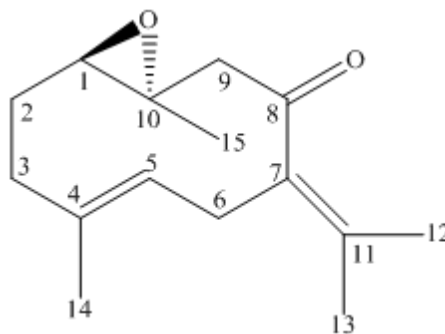


Figure 3.17: ^{13}C -NMR and DEPT-135 spectra of germacrone 4,5-epoxide **24**

Germacrone 1, 10-epoxide 25



Germacrone 1,10-epoxide **25** was obtained as a white solid, the molecular formula was calculated $C_{15}H_{22}O_2$ on the basis on the GS-MS analysis (M^+ , m/z 234). The UV spectrum showed an absorption maximum at 218 nm. The IR absorption at 1710 cm^{-1} presented for carbonyl group.

The ^1H NMR spectrum (**Figure 3.18, Table 3.8**) revealed four methyl singlets at δ_{H} 1.51 ($\text{H}_3\text{-15}$), 1.24 ($\text{H}_3\text{-14}$), 1.75 ($\text{H}_3\text{-13}$), and 1.64 ($\text{H}_3\text{-12}$), four methylenes at δ_{H} 2.85, 3.05 (d t, $J=12.36\text{ Hz}$, H-2), 1.40, 2.00 (H-3), 2.17 (d, $J=4.12\text{ Hz}$, H-6), and δ_{H} 2.46, 2.95 (d, $J=11\text{ Hz}$, H-9), two methines at δ_{H} 2.70 (d, $J=11\text{ Hz}$, H-1), and δ_{H} 5.01 (H-5),

The ^{13}C NMR and DEPT -135 spectra (**Figure 3.19, Table 3.8**) revealed a total of 15 carbons, including four sp^3 methyls at δ_{C} 15.5 (C-15), 17.4 (C-14), 20.0 (C-13), and δ_{C} 22.3 (C-12), four sp^3 methylenes at δ_{C} 29.7 (C-2), 23.3 (C-3), 36.1 (C-6), and δ_{C} 55.3 (C-9), one sp^2 methine at δ_{C} 123.7 (C-5), one sp^3 methine at δ_{C} 64.6 (C-1), four quaternary carbons, three among them sp^2 appearing at δ_{C} 134.0 (C-4), 130.7 (C-7), and δ_{C} 138.1 (C-11), whereas one was sp^3 carbon resonating at δ_{C} 57.8 (C-10). Additionally one carbonyl signal was observed at δ_{C} 209.5 (C-8).

Complete ^1H and ^{13}C -NMR assignments (**Table 3.8**) were established by thorough analysis of COSY, HSQC and HMBC. From the analysis of the spectroscopic data observed and comparison with the literature values, the identity of germacrone-1, 10 epoxide **25** was ensured (Sakui et al., 1992).

Table 3.8: : ^1H NMR (400 MHz), and ^{13}C NMR (100 MHz) spectral data of germacrone-1, 10-epoxide **25** in CDCl_3

Position	$\delta_{\text{H}}, J \text{ (Hz)}$	δ_{C}
1	2.70, d, 11	64.6
2	2.85, 3.05, dt (12.36)	29.7
3	1.40, 2.00, m	23.3
4	-	134.0
5	5.01, m	123.7
6	2.17, d (4.12)	36.1
7	-	130.7
8	-	209.5
9	2.46, 2.95, d (11)	55.3
10	-	57.8
11	-	138.1
12	1.64, s	22.3
13	1.75, s	20.0
14	1.24, s	17.4
15	1.51, s	15.5

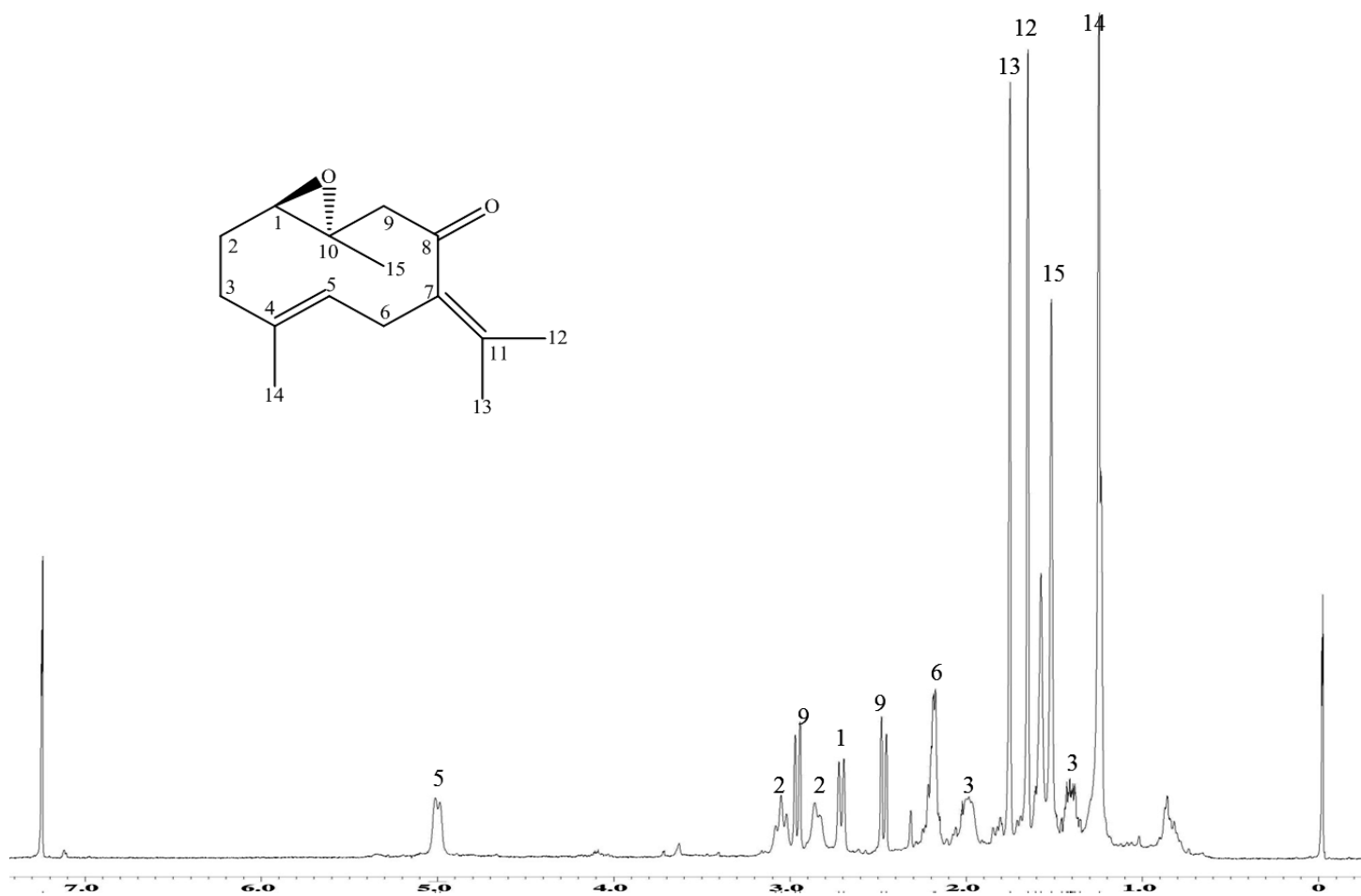


Figure 3.18: ^1H -NMR spectrum of germacrone-1,10-epoxide **25**

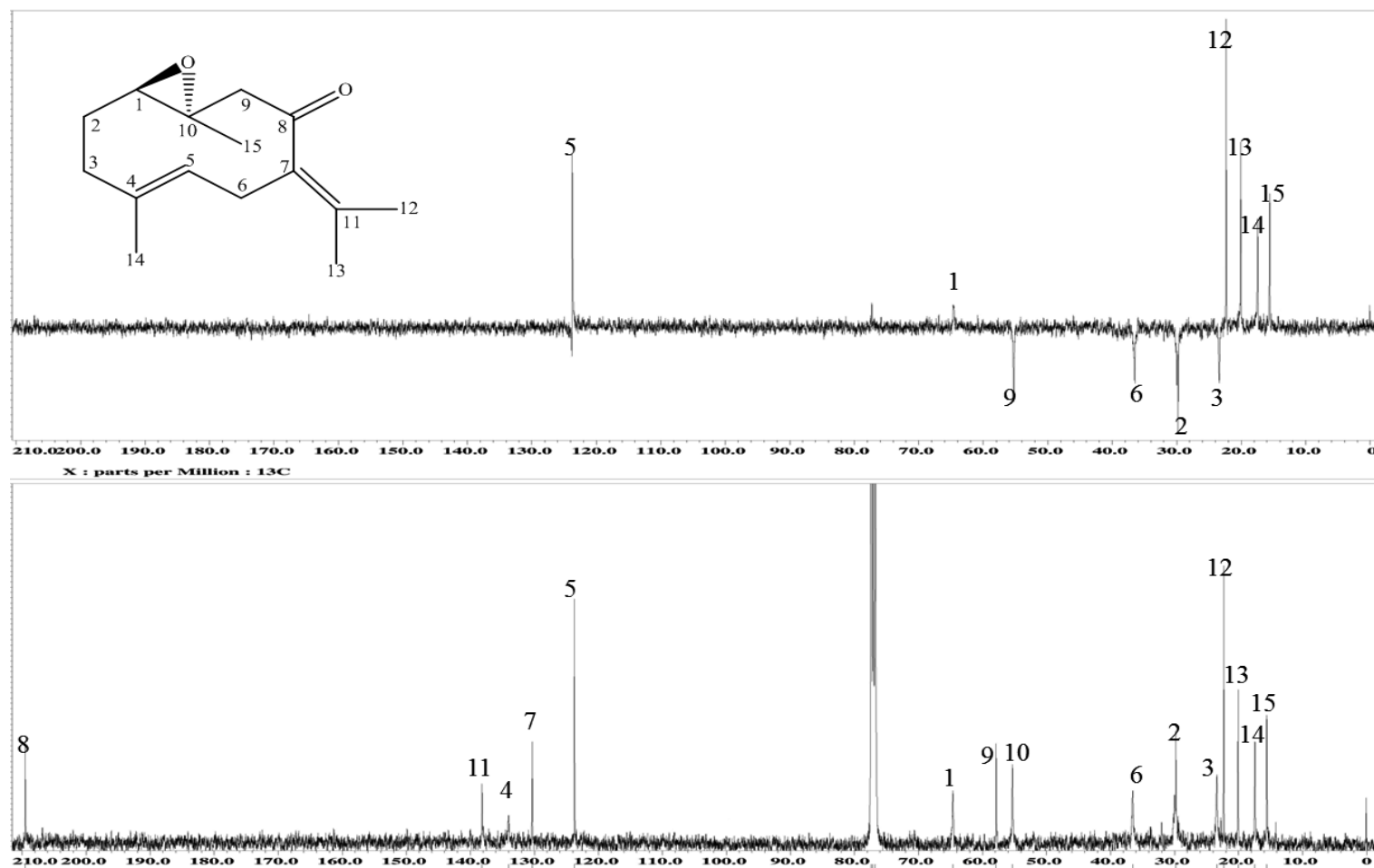
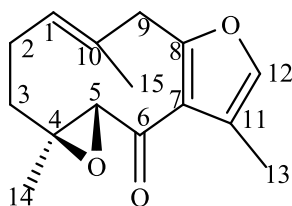


Figure 3.19: ^{13}C NMR and DEPT -135 spectra of germacrone-1,10-epoxide **25**

Zederone 26



Zederone **26** was obtained as a colourless crystal (m.p.152-154°C) with an optical rotation of $[\alpha]_D^{20} + 260^\circ$ (c 0.5, MeOH). The GC-MS analysis showed the base peak (M^+) at m/z 175 and the molecular ion peak M^+ at m/z 246 analysed for $C_{15}H_{18}O_3$. The IR absorptions at 1654, 1404, 1266 cm^{-1} indicated the presence of carbonyl group and double bonds.

The 1H NMR spectrum (**Figure 3.21**, Table 3.9) showed the proton signals characteristic for the germacrane-type of sesquiterpene. Three methyl singlets were observed at δ_H 2.07, 1.30, and 1.56 for the protons H_3 -13, H_3 -14, and H_3 -15, respectively, and also three pair of methylenes protons at δ_H 2.24, 2.46 (H_2 -2), 1.24, 2.27 (H_2 -3), and δ_H 3.68 (H_2 -9). The proton spectrum also suggested the presence of a furan ring due to the downfield olefinic proton singlet at δ_H 7.06 (H -12). Additionally, one olefinic proton signal at δ_H 5.46 (H -1) appeared as a doublet.

The ^{13}C NMR, DEPT 135 and HSQC (**Figure 3.22, 3.24**, Table 3.9) spectra revealed a total of 15 carbons corresponding to three sp^3 methyls at δ_C 15.8 (C-15), 15.2 (C-14), and δ_C 10.3 (C-13), three methylenes at δ_C 24.7 (C-2), 38.0 (C-3), and δ_C 41.9 (C-9), three methines comprising two olefinic sp^2 carbons at δ_C 131.2 (C-1), 138.1 (C-12), and one sp^3 at δ_C 66.6 (C-5). The downfield carbonyl signal was observed at δ_C 192.2.

In the COSY spectrum (**Figure 3.23**) cross peaks were observed between H -1/ H -2 and H -2/ H -3, thus indicating that they are vicinal to each other. The HMBC correlations; H_3 -

15/C-10, H₃-13/C-11 and H₃-14/C-4 established that the methyl groups are attached to C-10, C-11, and C-4, respectively. The nature of the 10 membered ring fused to a furan ring system was deduced from the analysis of COSY, HSQC, and HMBC spectra (**Figure 3.23-3.25**).

Thorough spectral data analysis of the above compound and by using 2D-NMR spectra the structure of compound **26** was elucidated as zederone also by comparison with spectral data reported in literature (Makabe et al., 2006).

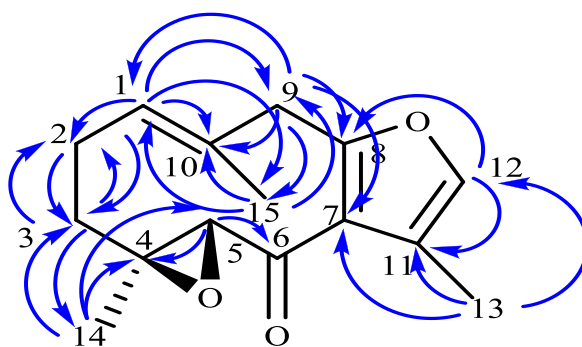


Figure 3.20: Selected HMBC Correlations H $\xrightarrow{\quad}$ C of zederone **26**

Table 3.9: ¹H (400 MHz) NMR and ¹³C (100 MHz) NMR spectral data of zederone 26

Position	δ_{H}, J (Hz)	δ_{C}
1	5.46, d (11.8)	131.2
2	2.24, 2.46, m	24.7
3	1.24, 2.27, m	38.0
4	-	64.0
5	3.77, s	66.6
6	-	192.2
7	-	123.2
8	-	157.2
9	3.68, m	41.9
10	-	131.1
11	-	122.2
12	7.04, brs	138.1
13	2.07, s	10.3
14	1.30, s	15.2
15	1.56, s	15.8

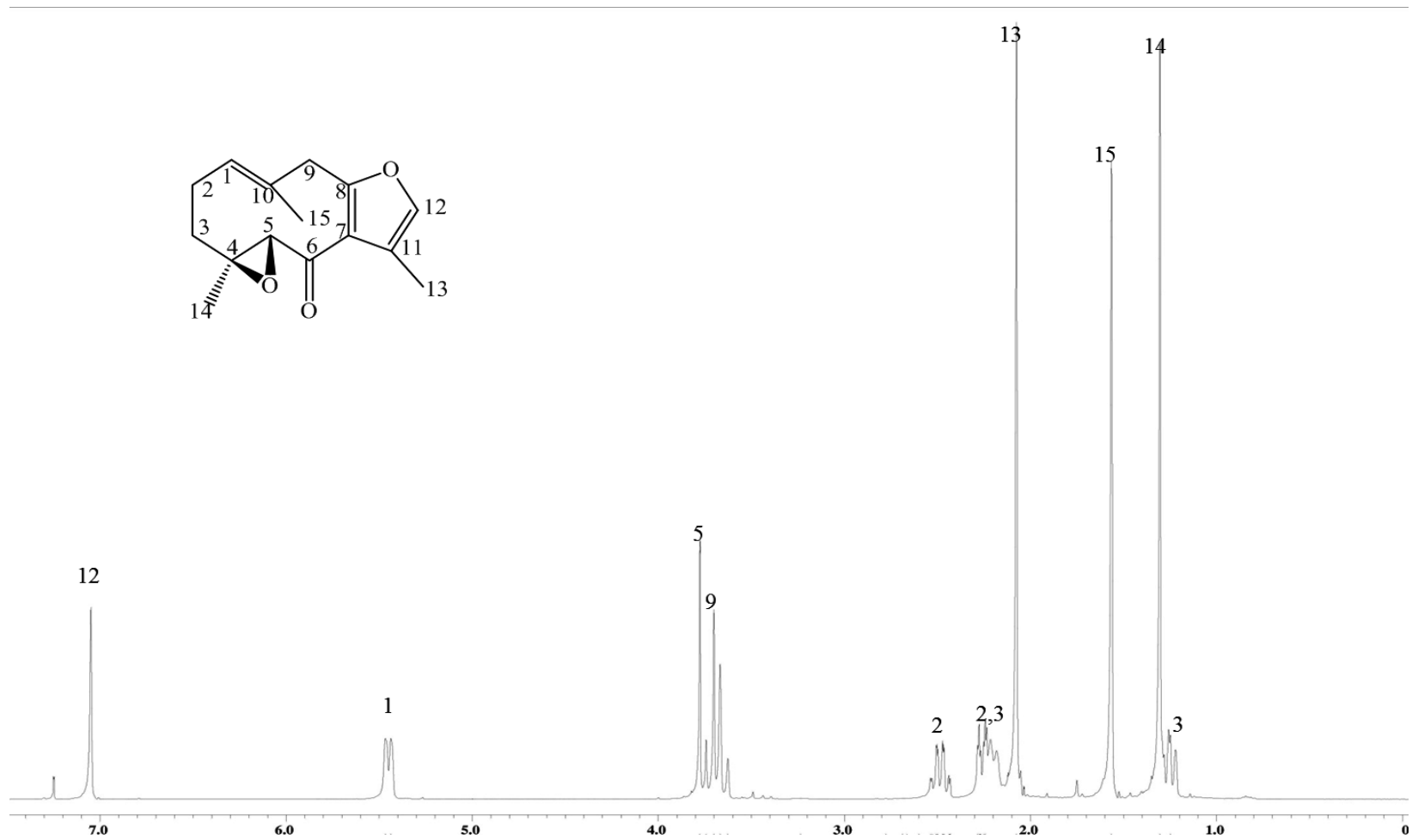


Figure 3.21: ^1H NMR spectrum of zederone **26**

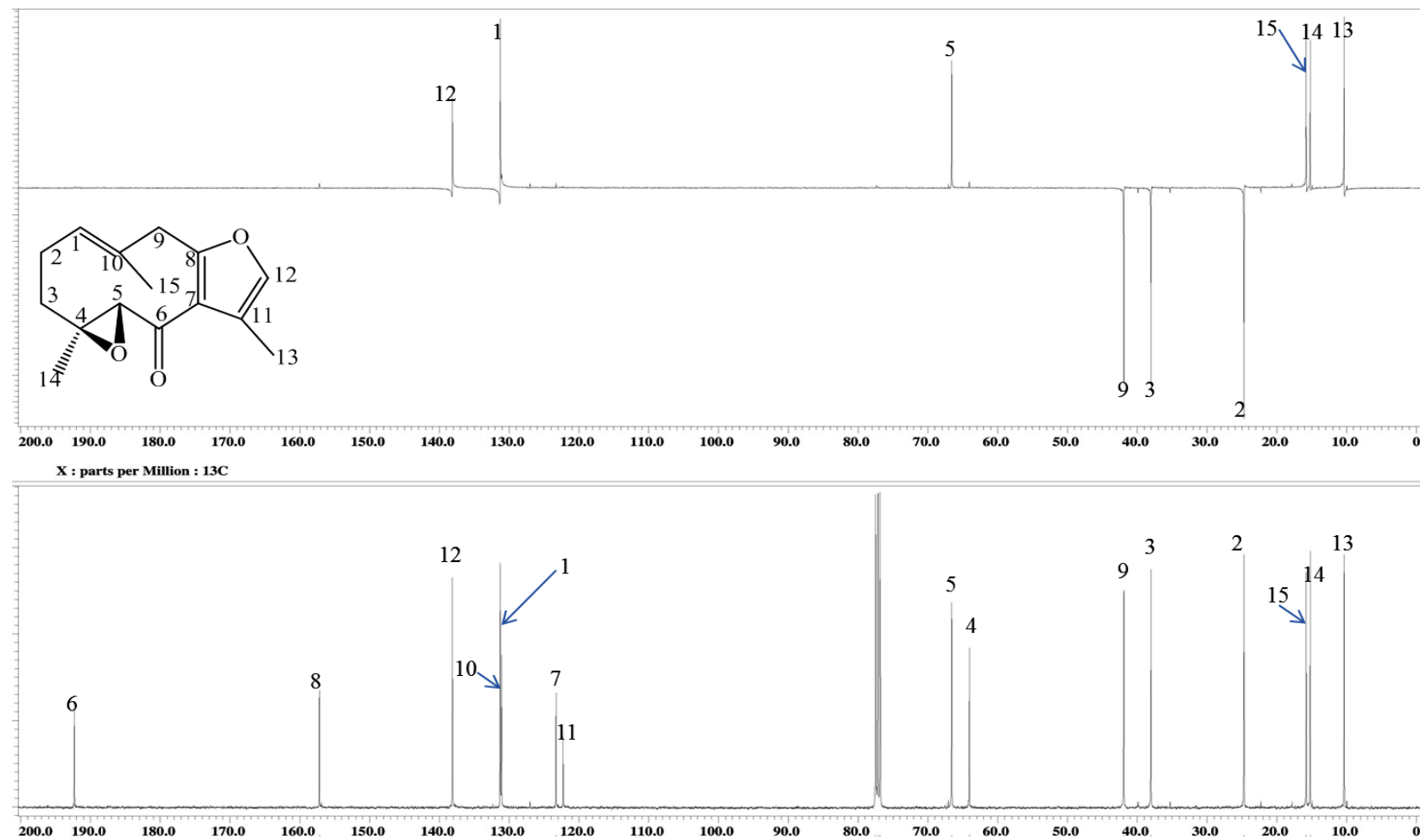


Figure 3.22: ^{13}C - NMR spectrum of zederone 26

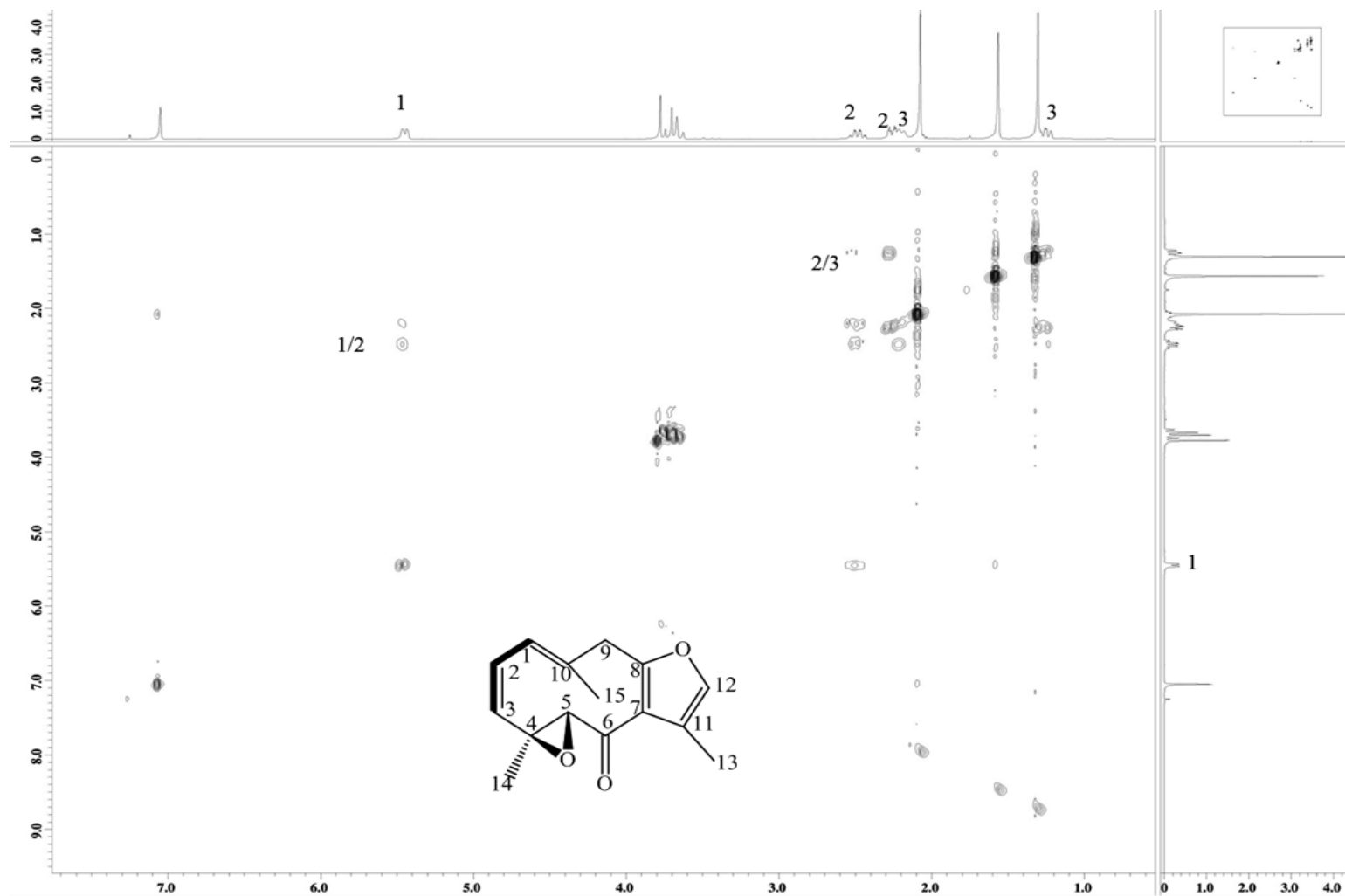


Figure 3.23: COSY spectrum of zederone **26**

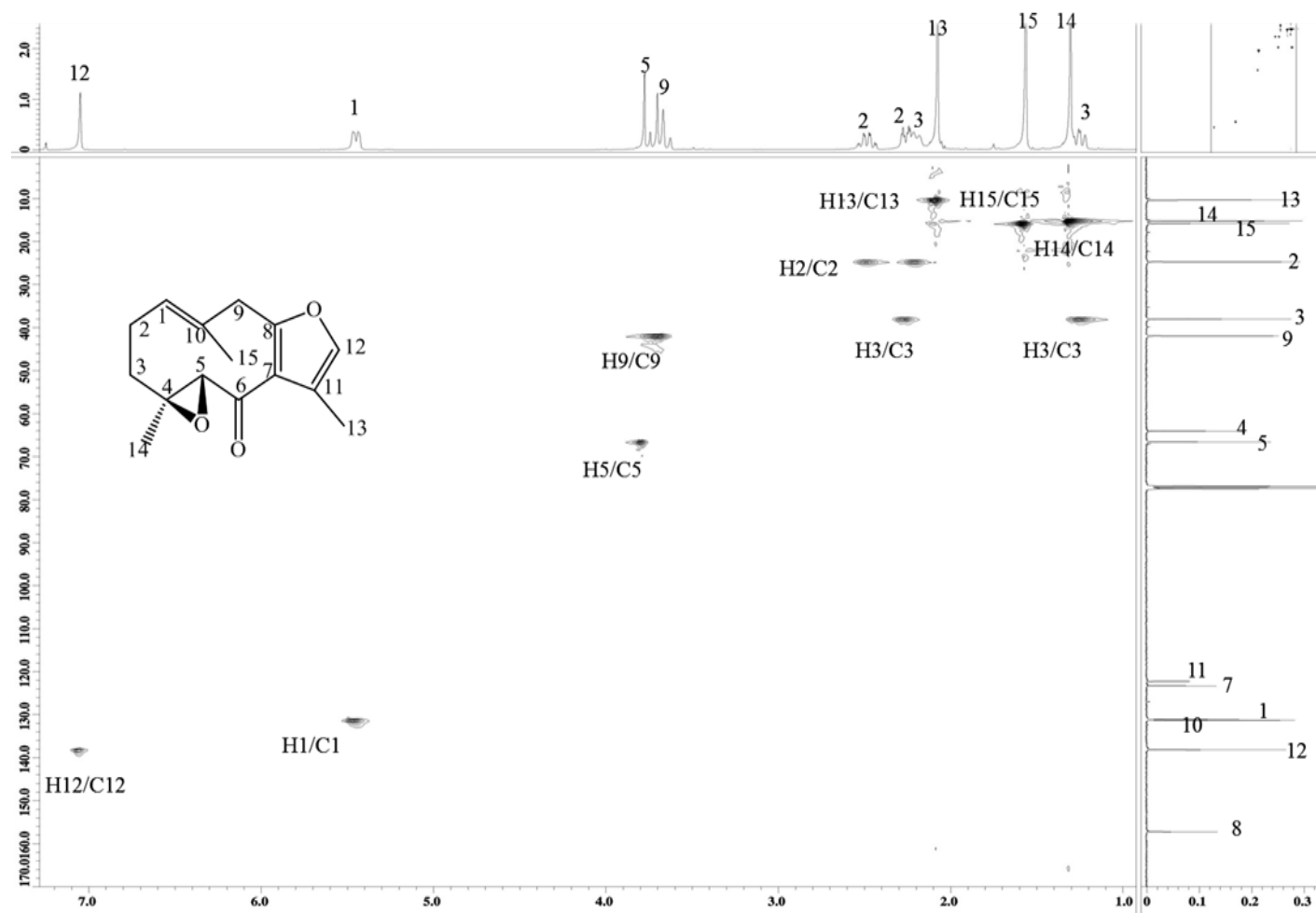


Figure 3.24: HSQC spectrum of zederone **26**

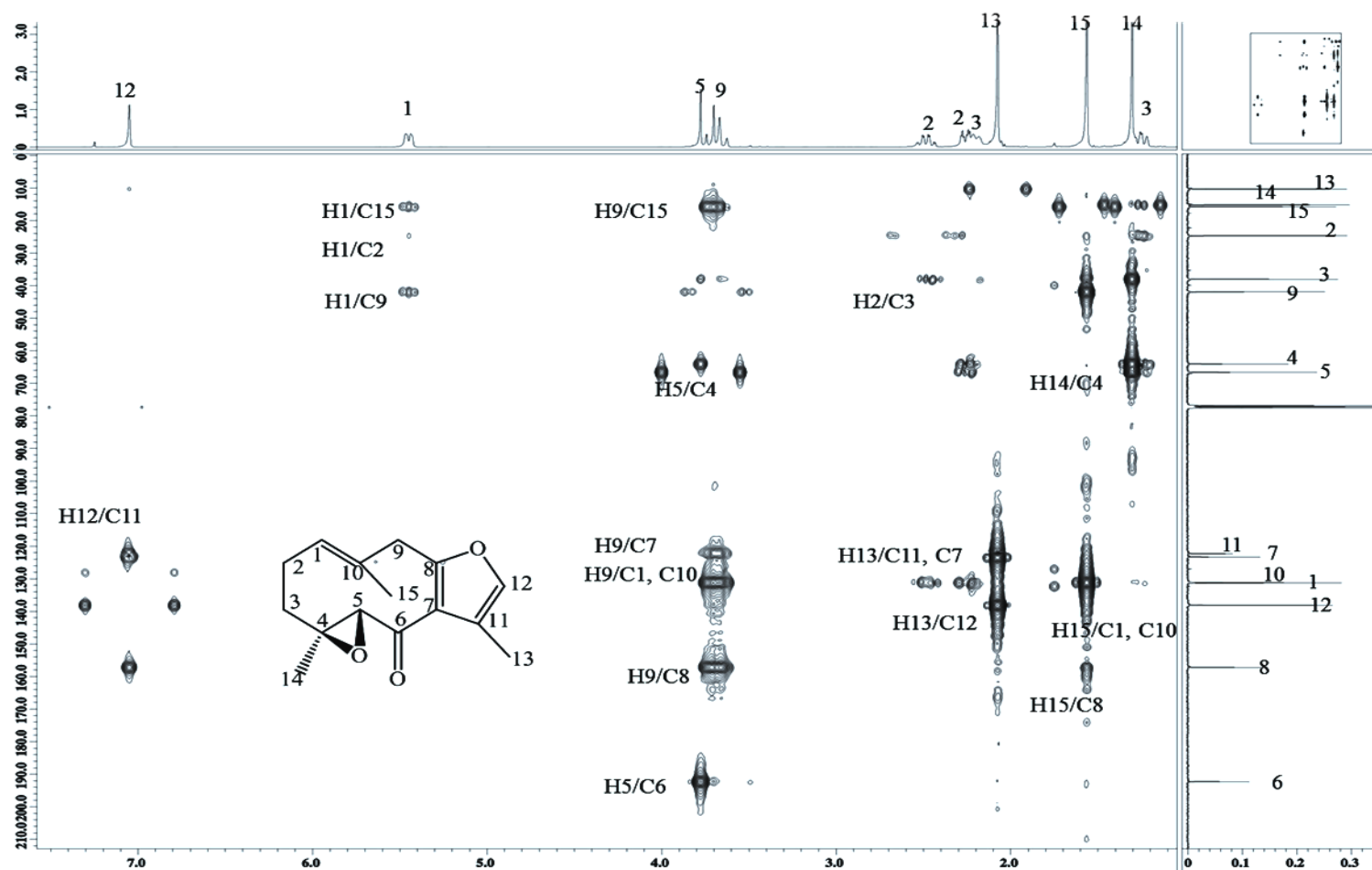
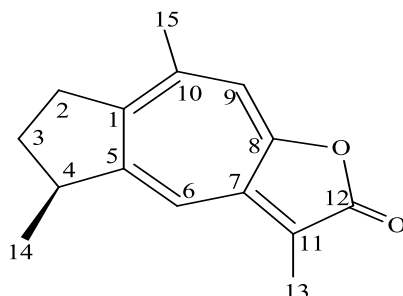


Figure 3.25: HMBC spectrum of zederone 26

3.1.1.2 Guaiane type sesquiterpenes

Gweicurculactone 41



Gweicurculactone **41** was obtained as a reddish crystal (m.p 166-168 °C) with $[\alpha]_D^{25} + 15.2$ (c 0.1, MeOH). The EI-mass spectrum exhibited a molecular ion peak (M^+) at m/z 228 which was consistent with the molecular formula of $C_{15}H_{16}O_2$. The UV spectrum showed maximum absorption at λ_{max} 218 nm indicating the presence of an α , β -unsaturated γ -lactone of conjugated double bonds. The IR absorption at 1726 cm^{-1} indicated the presence of a α , β -unsaturated γ -lactone.

The ^1H NMR spectrum (**Figure 3.27**, **Table 3.10**) had proton signals similar to those observed for guaiane-type sesquiterpenes. The spectrum showed signals corresponding to two methyl singlets which appeared at δ_H 2.24 (H_3 -15), and 1.98 (H_3 -13). Furthermore, one methyl signal was observed as a doublet at δ_H 1.30 (3H, d, $J=6.84\text{ Hz}$, H-14). In addition, two sets of methylene protons multiplets were observed at δ_H 1.53 (H_2 -2) and δ_H 2.81, 2.67 (H_2 -3). Moreover, three methine protons signals were observed, two of these protons signals were olefinic proton singlets at δ 6.88 (H-6), and δ_H 6.73 (H-9) while the other resonated as quarted ($J=14.2\text{ Hz}$) at δ_H 3.08 (H-4)

The ^{13}C NMR and DEPT-135 spectra (**Figure 3.28**, **Table 3.10**) of **41** revealed a total of 15 carbons suggested its sesquiterpene nature. Three sp^3 methyls were

observed at δ_C 24.8 (C-15), 20.1 (C-14), and 7.7 (C-13). Furthermore, two sp^2 methylenes at 31.9 (C-2), and 33.3 (C-3). In addition, two sp^2 methines at δ_C 117.9 (C-6), and 116.4 (C-9) were observed, while one sp^3 methine signal was at δ_C 43.9 (C-4). The ^{13}C NMR spectrum also showed six sp^2 quaternary carbons at δ_C 144.2 (C-1), 156.6 (C-5), 146.2 (C-7), 154.8 (C-8), 136.5 (C-10), and 103 (C-11) with an additional carbonyl resonated at δ_C 170.7 (C-12).

The 1H - 1H COSY correlations between H-2/H-3, H-3/H-4, H-4/H₃-14, together with HMBC correlations observed between H-2/C-1, H-2/C-5, H-4/C-5, H₃-15/C-1, H-6/C-1, and H-6/C-5 suggested a five membered ring fused to a seven membered ring system indicating a guaiane type sesquiterpene skeleton with unsaturations at $\Delta^{1(10)}$, Δ^5 , and Δ^8 . Further investigation of the HMBC correlations of H₃-13 to C-7, C-12 and C-11 suggested an α,β -unsaturated lactone ring attached to the 7-membered ring system through C-7 and C-8. The spectral data of **41** ascertained the identity of the compound as gweicurculactone and were in agreement with the published literature(Phan et al., 2014).

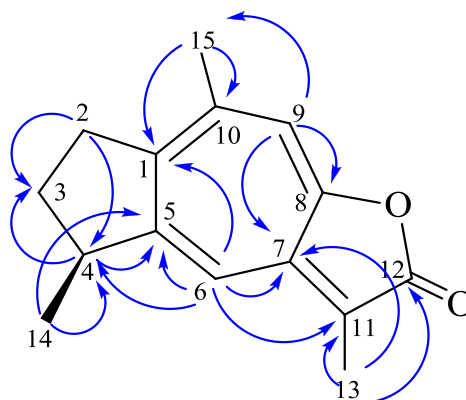


Figure 3.26: Selected HMBC Correlations H $\xrightarrow{\hspace{1cm}}$ C of gweicurculactone **41**

Table 3.10: ^1H (400 MHz) NMR and ^{13}C (100 MHz) spectral data of gweicurculactone **41** in CDCl_3

Position	$\delta_{\text{H}}, J \text{ (Hz)}$	δ_{C}
1	2.12, m	144.2
2	1.53, m	31.9
3	2.81, 2.67, m	33.3
4	3.08, q (14.2)	43.9
5	-	156.6
6	6.88, s	117.9
7	-	146.2
8	-	154.8
9	6.73, s	116.4
10	-	136.5
11	-	103
12	-	170.7
13	1.98, s	7.7
14	1.30, d (6.84)	20.1
15	2.24, s	24.8

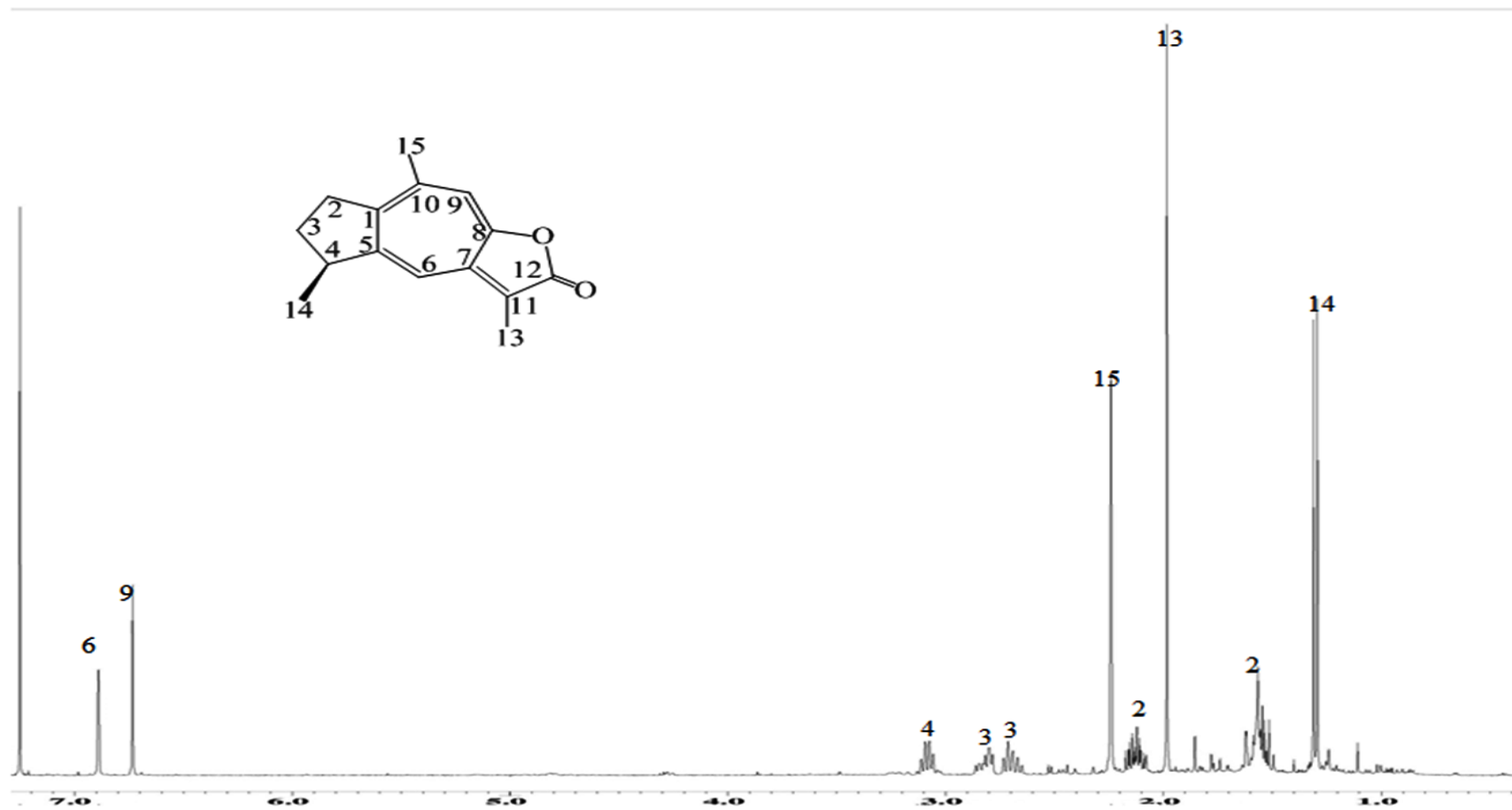


Figure 3.27: ^1H NMR spectrum of gweicurculactone **41**

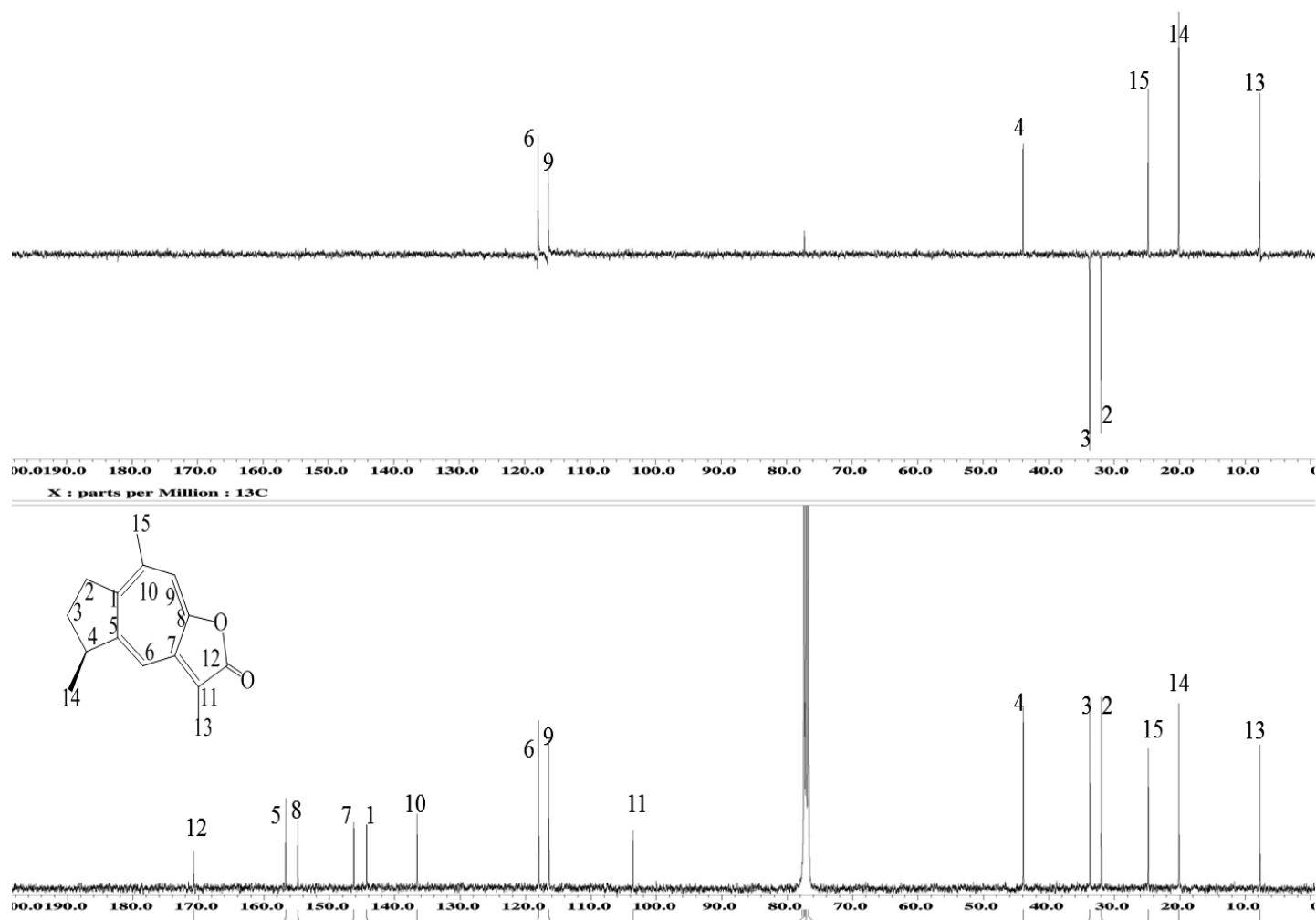


Figure 3.28: ^{13}C NMR and DEPT-135 spectra of gweicurculactone **41**

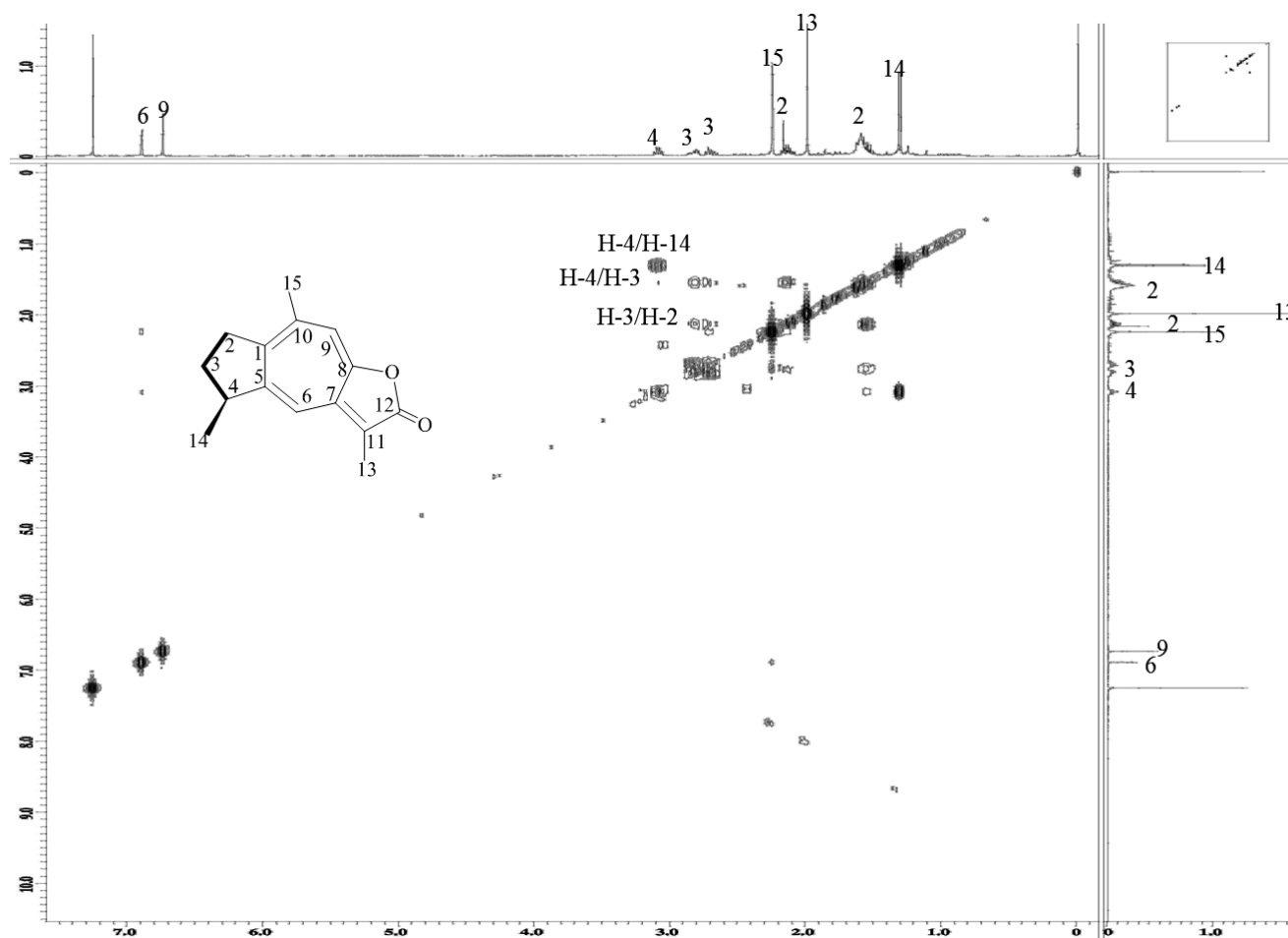


Figure 3.29: COSY spectrum of gweicurculactone 41

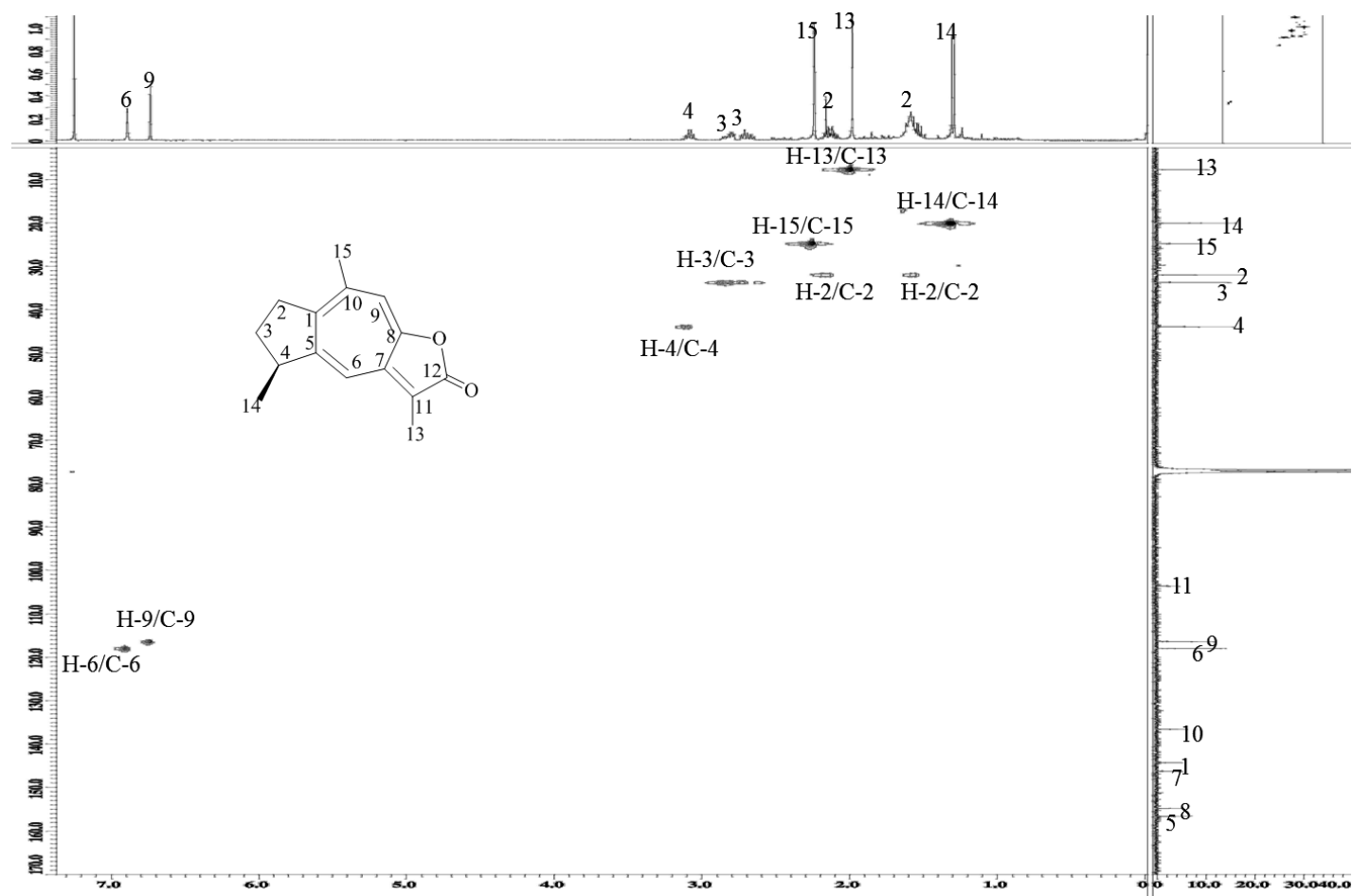


Figure 3.30: HSQC spectrum of gweicurculactone **41**

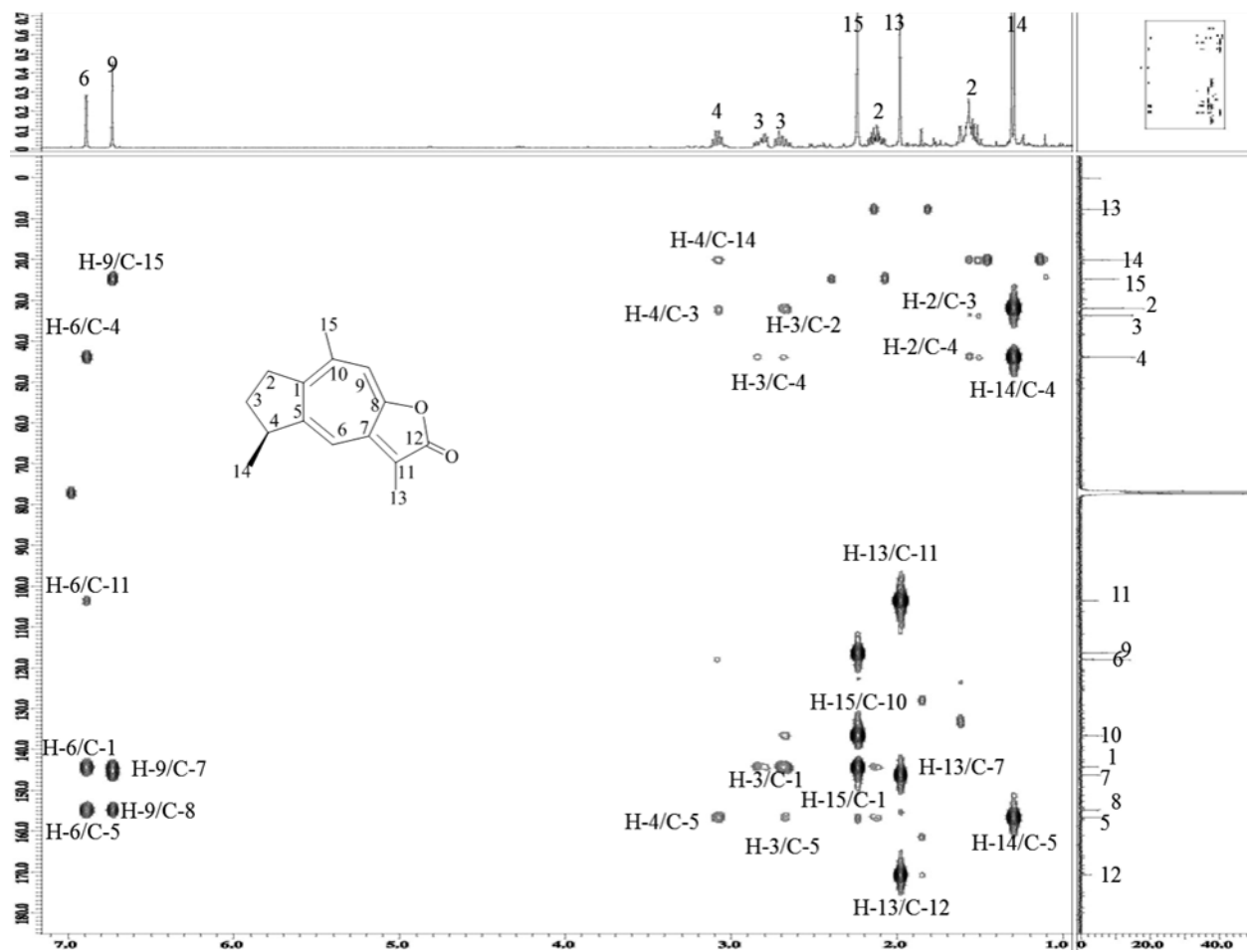
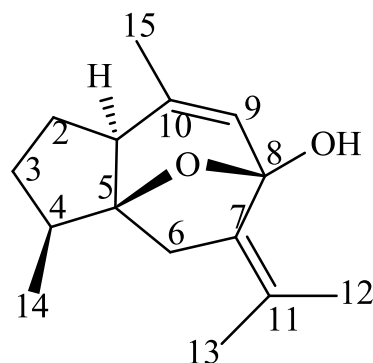


Figure 3.31: HMBC spectrum of gweicurculactone **41**

Curcumenol **42**



Curcumenol **42** was obtained as a colourless oil. The GC-MS analysis revealed the molecular formula of $C_{15}H_{22}O_2$ (m/z 234). The IR spectrum showed absorptions at 3432, 2934, and 1457 cm^{-1} , indicating the presence of hydroxy and olefinic carbons, and C-O bond, respectively. The UV spectrum (MeOH) showed an absorption band at 224 nm ($\log \epsilon$ 3.047).

The ^1H NMR spectrum (**Figure 3.32**, **Table 3.11**) showed the presence of three methyl singlets at δ_{H} 1.79 (H_3 -15), 1.61 (H_3 -13), and 1.54 (H_3 -12). One methyl proton appeared as a doublet at δ_{H} 1.01 ($J=6.4\text{ Hz}$, H-14). three methylenes at δ_{H} 1.9 (H-2, 3), and δ_{H} 2.11, 2.66 (2H, d , $J=15.4\text{ Hz}$, H-6), and three methine at δ_{H} 2.07 (1H, d , $J=15.6\text{ Hz}$, H-1), 1.9 (H-4), and δ_{H} 5.74 (H-9).

The ^{13}C NMR and DEPT-135 spectra (**Figure 3.33**, **Table 3.11**) exhibited 15 carbons, including five quaternary carbons at δ_{C} 85.8 (C-5), 139.2 (C-7), 101.6 (C-8), 137.2 (C-10), δ_{C} 122.3 (C-11), three methylenes at δ_{C} 27.6 (C-2), 31.2 (C-3), and δ_{C} 37.2 (C-6), three methines at δ_{C} 51.3 (C-1), 40.4 (C-4), and δ_{C} 125.7 (C-9), four methyls at δ_{C} 21.0 (C-15), 11.9 (C-14), 18.9 (C-13), and δ_{C} 22.4 (C-12). This compound is different from procurcumenol by the lack of the carbonyl group and the presence of an

ether linkage between C-5 and C-8. This is evidenced by the presence of two deshielded signals of two oxygenated methines.

In depth inspection of all spectral data and comparison with the literature values established the identity of this compound as curcumenol (Ohshiro et al., 1990b).

Table 3.11: ^1H NMR (400 MHz) and ^{13}C NMR (100 MHz) spectral data of curcumenol **42**

Position	$\delta_{\text{H}}, J \text{ (Hz)}$	δ_{C}
1	2.07, d, (15.6)	51.3
2	1.9, m	27.6
3	1.9, m	31.2
4	1.9, m	40.4
5	-	85.8
6	2.11, 2.66, d (15.4)	37.2
7	-	139.2
8	-	101.6
9	5.74, br.s	125.7
10	-	137.2
11	-	122.3
12	1.54, s	22.4
13	1.61, s	18.9
14	1.01, d, (6.4)	11.9
15	1.79, s	21.0

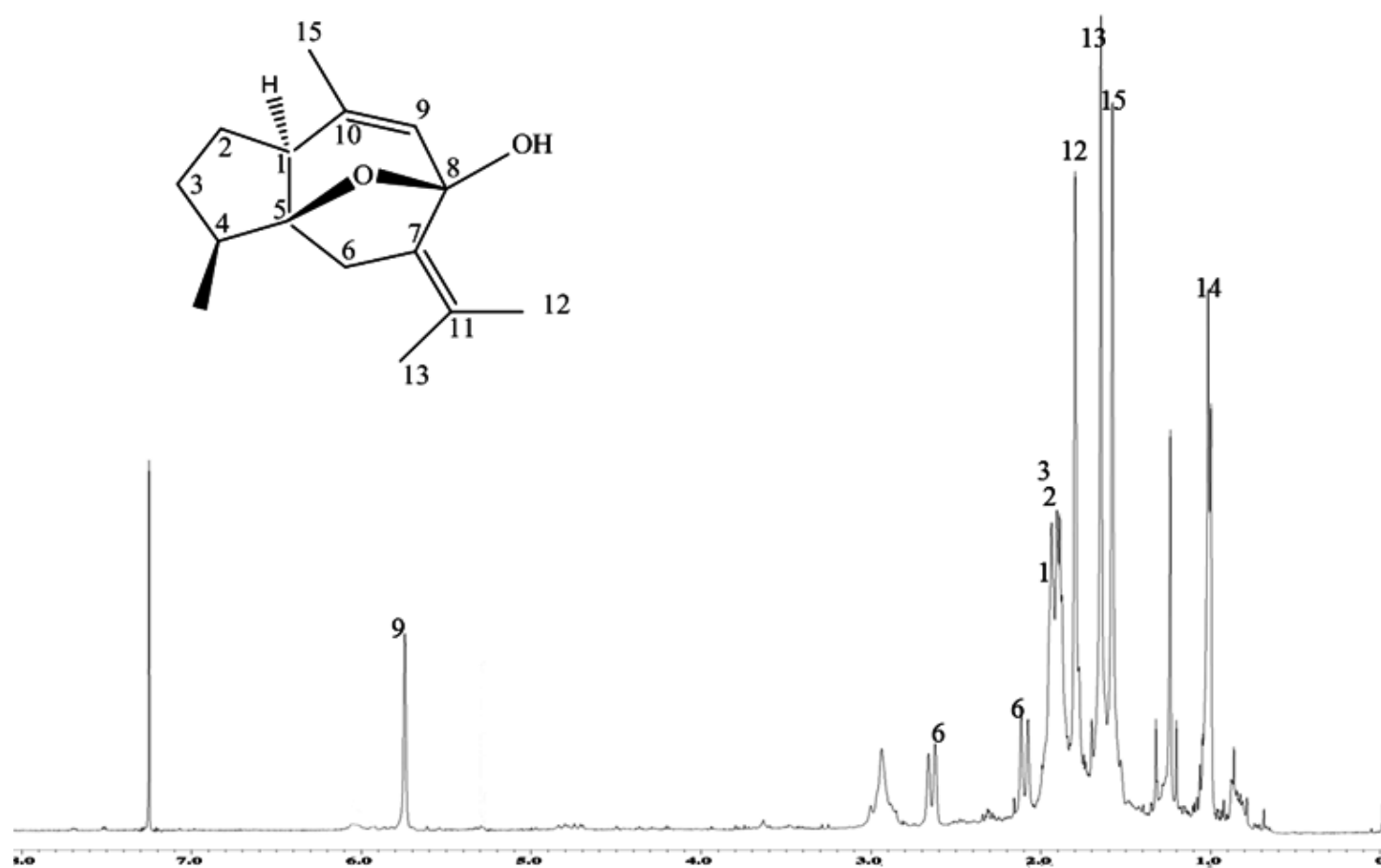


Figure 3.32: ^1H NMR spectrum of curcumenol 42

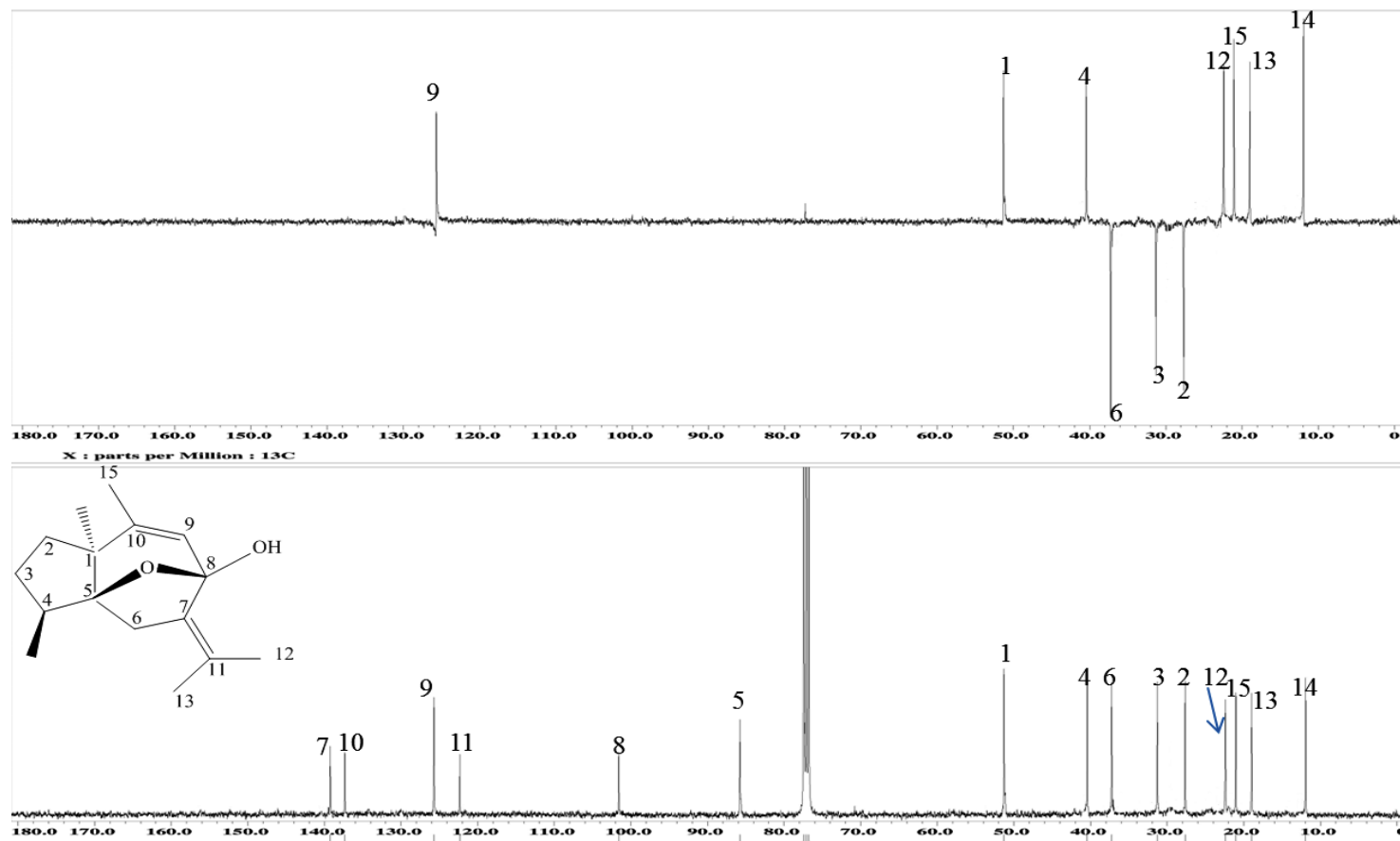
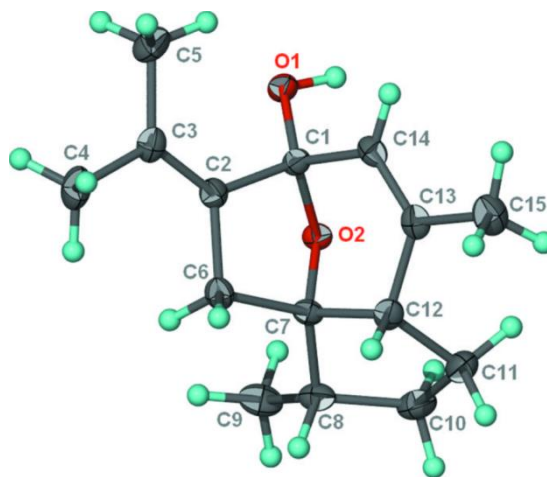
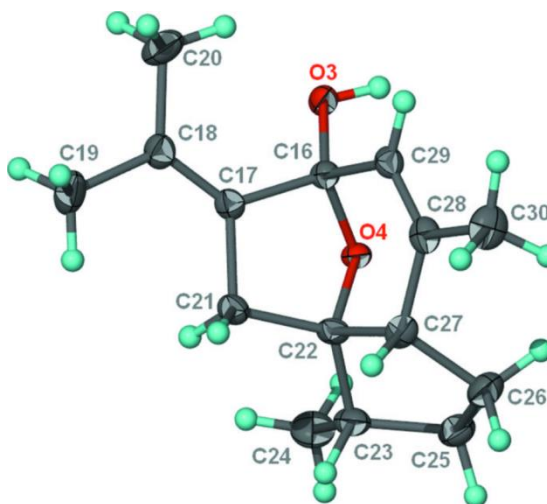


Figure 3.33: ^{13}C NMR and DEPT-135 spectra of curcumenol 42

Curcumenol a second monoclinic modification 150



molecule I



molecule II

Figure 3.34: ORTEP (Oak Ridge Thermal Ellipsoid Plot) representation of the crystal structure of curcumenol second monoclinic (molecule I and molecule II)

The structure of the title compound was established by a single crystal X-ray crystallographic analysis, also known as curcumenol a second monoclinic modification ($C_{15}H_{22}O_2$) was obtained as colorless prisms crystals from fraction 10 of hexane extract by using silica gel column chromatography (CC) followed by HPTLC. The compound was crystallized with two molecules of similar conformation in an asymmetric unit, featuring three fused rings, two of which are five membered and the rest is a six membered ring. Of the two five-membered rings, the one with an oxygen atom has a

distinct envelop shape (with the O atom representing the flap). The six-membered ring is also envelop-shaped as it shares a common O atom with the five-membered ring. In the crystal, the two independent molecules are linked by a pair of O-H...O hydrogen bonds, generating a dimer crystal; O₁-H₁---O₄, and O₃-H₃---O₂. The ORTEP structures are presented in **Figure 3.34**.

The crystals of this compound belong to the monoclinic space group P2, with $a = 9.3495 (7) \text{ \AA}$, $b = 12.535 (1) \text{ \AA}$, $c = 11.7727 (9) \text{ \AA}$, $\beta = 96.532 (1)^\circ$, $V = 1370.76$

$(18) \text{ \AA}^3$, $Z=4$. The data were collected at Bruker SMART APEX diffractometer, 13257 measured reflections.

The ¹H-NMR spectrum (**Figure 3.35**) of the isolated crystal “curcumenol second monoclinic” showed similar pattern to the curcumenol previously discussed. All the proton signals of the dimer were overlapped, except for the methyls CH₃-14 at δ_H 1.09 (d , 4.12 Hz) and CH₃-14' at δ_H 1.01(d , 6.4 Hz). CH₃-14 refers to the molecule with ethereal oxygen in the endo position while CH₃-14' possess an exo ethereal oxygen linkage. The close proximity of the oxygen to CH₃-14' in the exo-isomer could explain its downfield shift, while their opposite orientation in the endo-isomer shifted H₃-14 methyl upfield. (Hamdi et al., 2010).

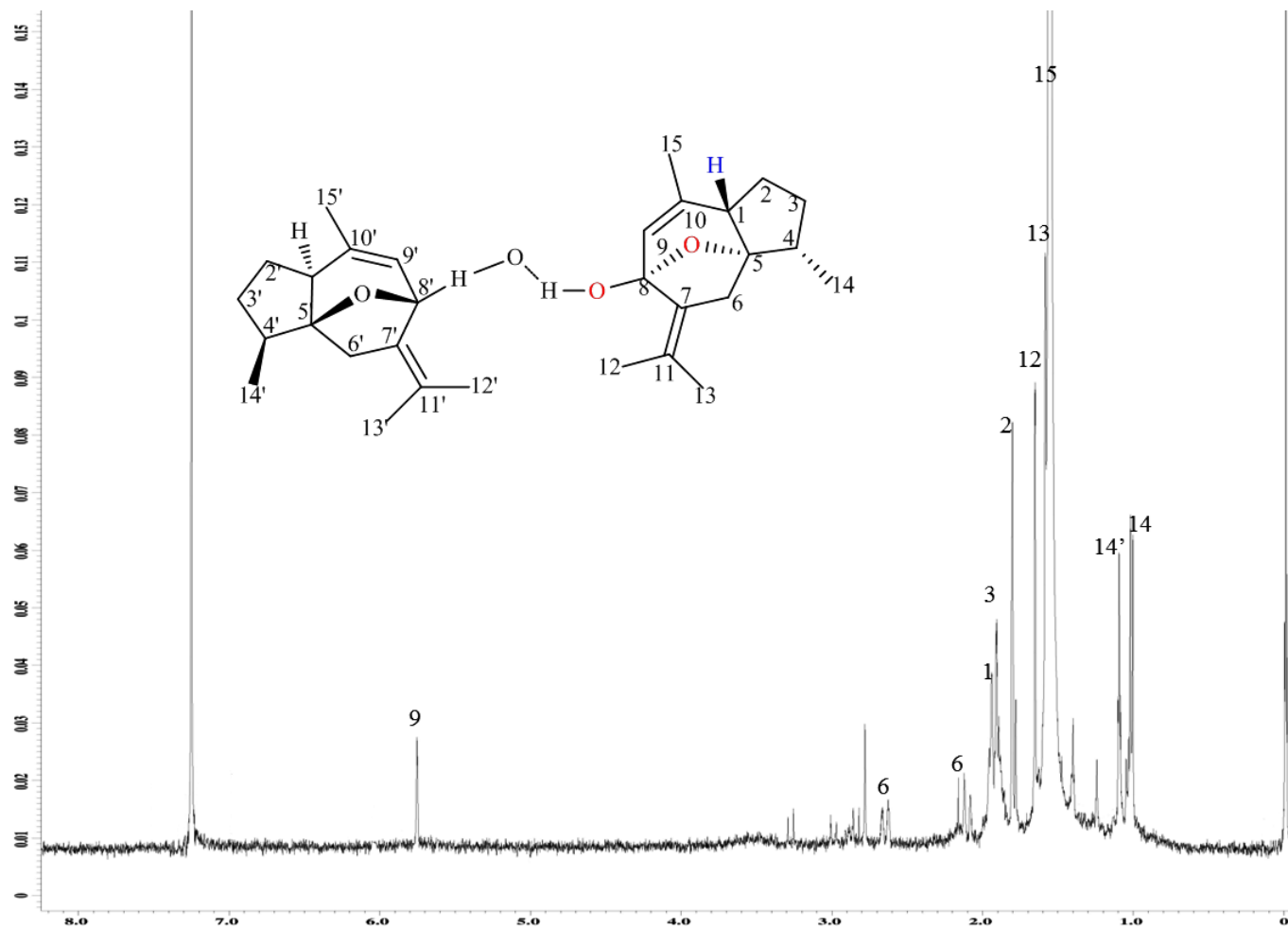
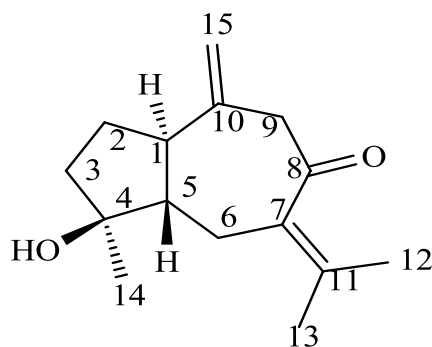


Figure 3.35: ^1H NMR spectrum of curcumenol second monoclinic

Isoprocucumenol **43**



Isoprocucumenol **43** was obtained as colourless oil, the compound revealed the molecular formula of $C_{15}H_{22}O_2$ as analysed by GC-MS spectrum (m/z 234). The UV spectrum showed maximum band at 205 (log ϵ , 1.83). IR absorptions at 3450 and 1674 cm^{-1} were ascribed to hydroxyl and ketone functional groups, respectively. The ketonic function is the difference of this compound compared to gweicurculactone **41**

The 1H NMR spectrum (**Figure 3.36**, **Table 3.12**) revealed the presence of three methyl singlets at δ_H 1.24 (H_3 -14), 1.82 (H_3 -13), 1.92 (H_3 -12), five methylenes at δ_H 1.21 (H_2 -2), 1.39 (H_2 -3), 2.81 (2H, d, $J=14.2$ Hz, H-6), 2.16 (H_2 -9), 4.90 (2H, d, $J=6.88$ Hz, H-15), and two methines at δ_H 3.22 (1H, q, $J=14.68$ Hz, H-1), and 1.40 (H-5).

The ^{13}C NMR and DEPT-135 spectra (**Figure 3.37**, **Table 3.12**) disclosed the presence of 15 carbons with three sp^3 methyls at δ_C 24.4 (C-14), 22.8 (C-13), and 21.9 (C-12), five methylenes, four of the five are sp^3 resonated at δ_C 24.7 (C-2), 28.2 (C-3), 39.8 (C-6), and 53.8 (C-9), while one is sp^2 exomethylene at δ_C 111.6 (C-15). Furthermore, three sp^2 quaternary carbon atoms at δ_C 134.5 (C-7), 141.3 (C-10), and 143.9 (C-11), in addition one is sp^3 quaternary carbon atom at δ_C 77.4 (C-4), and two sp^3 methine carbon atoms at δ_C 51.2 (C-1) and δ_C 58.9 (C-5). Additionally, a carbonyl group resonated at δ_C 203 (C-8) indicating a ketone functionality (Ohshiro et al.,

1990b). Thorough analysis of the spectral data of the above compound indicated that it is very similar in structure with gweicurculactone **41** except that the former has the ketone function as a part of the seven membered ring skeleton, whereas the latter has a lactone function attached to the main skeleton. Indeed after comparison of spectral data with literature values (Kuroyanagi et al., 1990a), the identity of this compound confirmed as the known isoprocurcumenol **43**.

Table 3.12: ^1H (400 MHz) NMR, and ^{13}C (100 MHz) NMR spectral data of isoprocurcumenol **43** in CDCl_3

Position	$\delta_{\text{H}}, J \text{ (Hz)}$	δ_{C}
1	3.22, q (14.68)	51.2
2	1.21, m	24.7
3	1.39, m	28.2
4	-	77.4
5	1.40, m	58.9
6	2.81, d (14.2)	39.8
7	-	134.5
8	-	203(Kuroyanagi et al., 1990a)
9	2.16, s	53.8
10	-	141.3
11	1.90, brs	143.9
12	1.92, s	21.9
13	1.82, s	22.8
14	1.24, s	24.4
15	4.90, d (6.88)	111.6

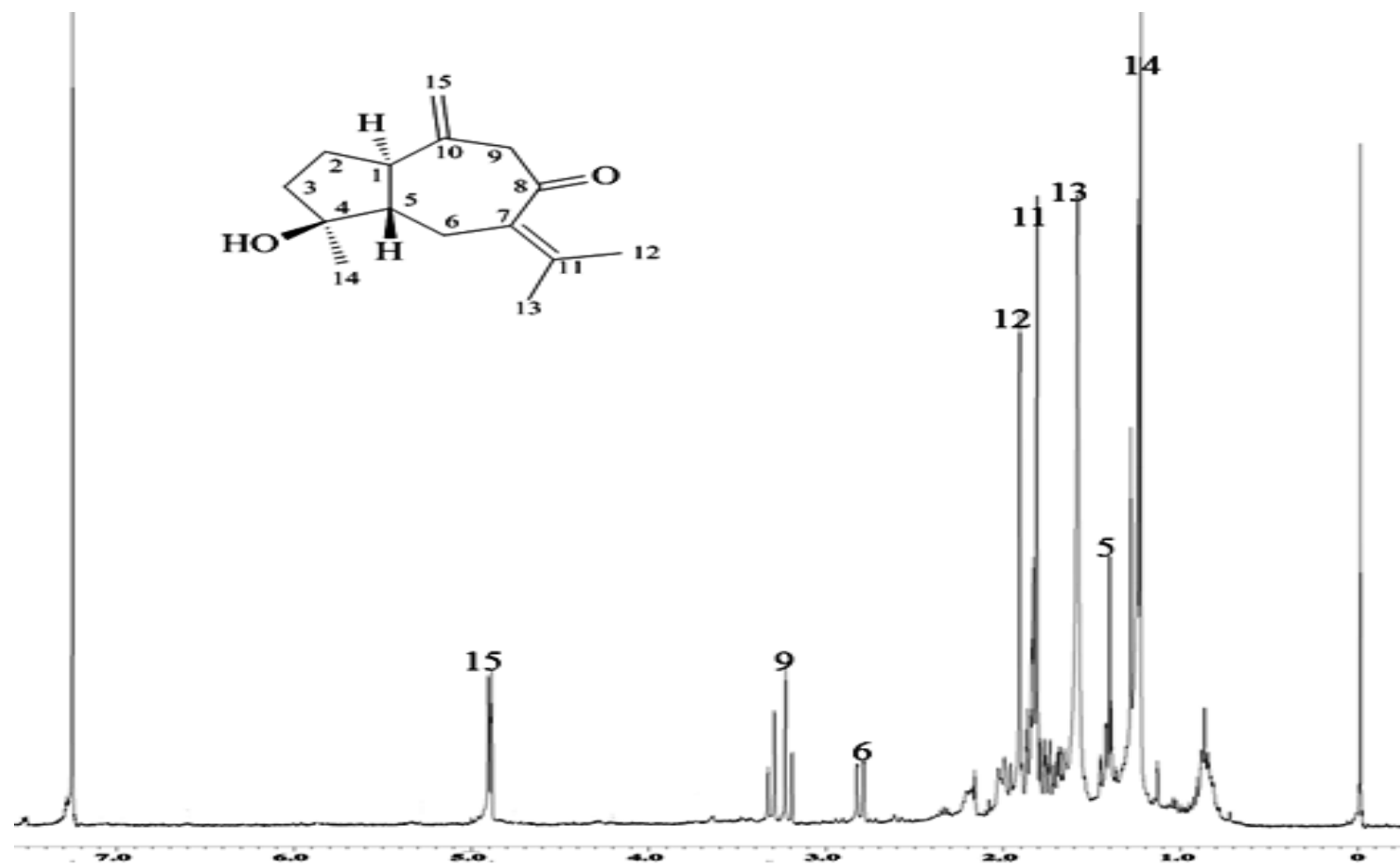


Figure 3.36: ^1H -NMR spectrum of Isoprocucumenol 43

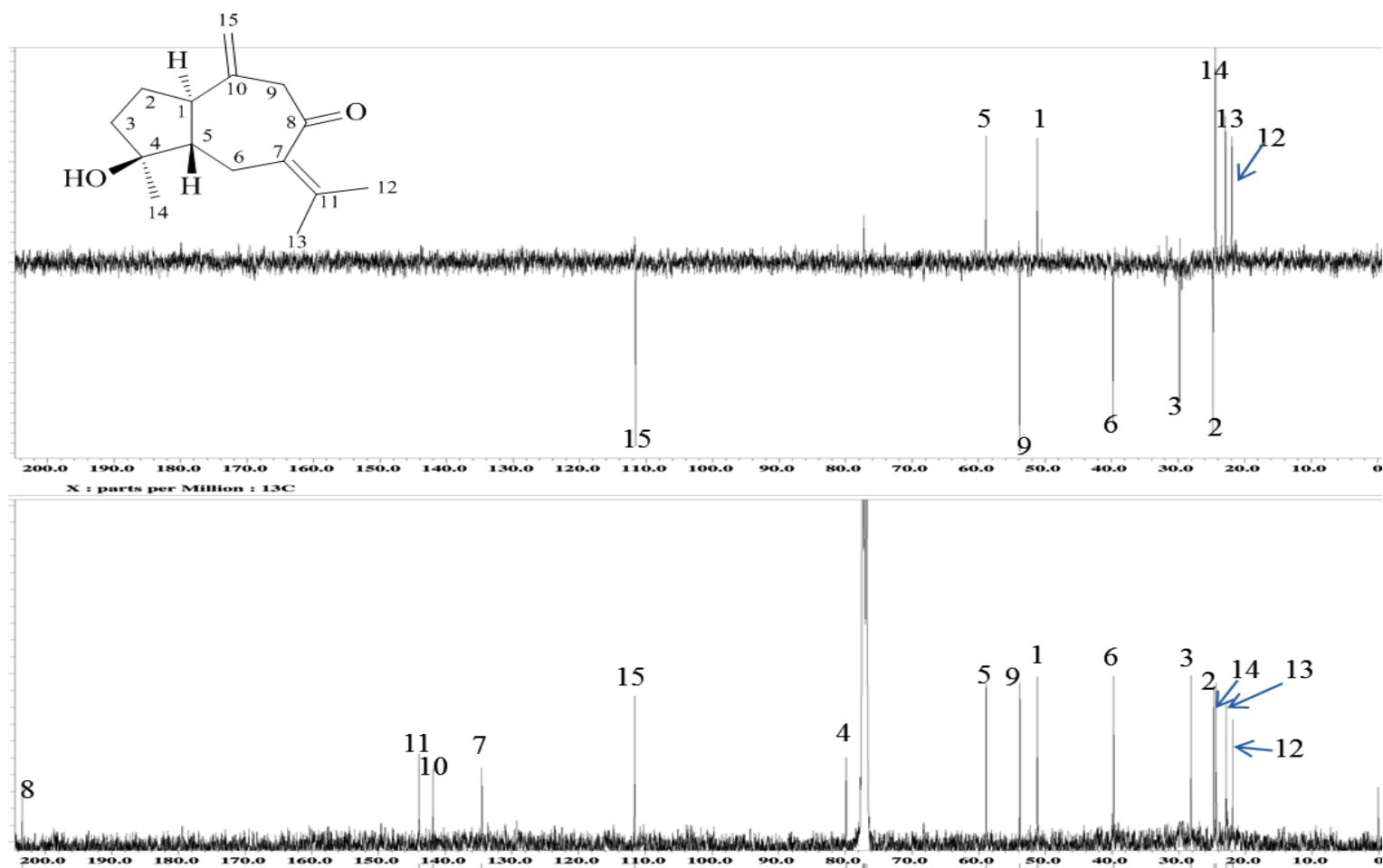
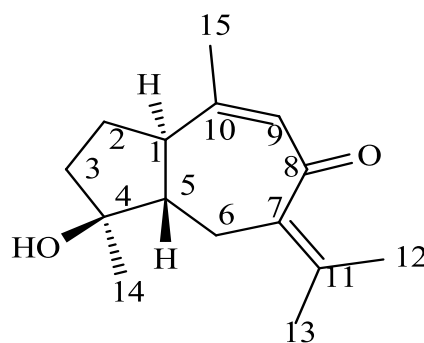


Figure 3.37: ^{13}C -NMR and DEPT-135 spectra of Isoprocurcumenol 43

Procurcumenol **44**



Procurcumenol **44** was isolated as a colourless oil. The UV spectrum showed the absorption maximum at 204 nm ($\log \epsilon$ 1.16). The IR spectrum showed absorption peaks of hydroxyl (3409 cm^{-1}) and carbonyl group (1712 cm^{-1}). By the analysis of GC-MS, the molecular formula of procurcumenol was determined to be $\text{C}_{15}\text{H}_{22}\text{O}_2$ (m/z 234).

The ^1H NMR spectrum (**Figure 3.38**, **Table 3.13**) revealed the presence of four methyl singlets at δ_{H} 1.22 (H-15), 1.86 (H-14), 1.76 (H-13), and 1.73 (H-12), three methylene protons at δ_{H} 1.66, 1.94 (H-2), 1.88 (H-3), and 2.16 δ_{H} (1H, *dd*, $J=13.2$, 15.6 Hz, $\text{H}_{\text{a}}-6$), 2.57(1H, *d*, $J=15.6$ Hz, $\text{H}_{\text{b}}-6$), three methine protons at δ_{H} 2.34 (*dd*, $J=8.7$, 9.6 Hz, H-1), δ_{H} 1.91(H-5), and δ_{H} 5.85 (1H, *d*, $J=1.4$, H-9). This compound **42** has similar spectral pattern to the compound **44** except the presence of methyl protons at H_3-15 compared to an exomethylene protons at H_2-15 in **44**.

The ^{13}C NMR and DEPT 135 spectra (**Figure 3.39**, **Table 3.13**) revealed the existence of a total of 15 carbons, four sp^3 methyls at δ_{C} 24.3 (C-15), 23.4 (C-14), 22.4 (C-13), 21.3 (C-12), three sp^2 methylenes at δ_{C} 26.9 (C-2), 39.9 (C-3), and 28.6 (C-6), three methines, two of which were sp^2 resonanced at δ_{C} 50.5(C-1), and δ_{C} 53.9 (C-5), whereas one was sp^2 methine carbon at δ_{C} 129.2 (C-9), four quaternary carbons, three were sp^2 at δ_{C} 136.9 (C-7), 155.1 (C-10), and δ_{C} 136.3(C-11), and one carbon was sp^3 at

δ_C 80.3 (C-4). Similarly C-15 is a methyl group compared to the compound **43** was an exomethylene resonated at δ_C 112 (C-15).

Extensive spectral data analysis of the above compounds confirmed the identity of compound **44** as procurcumenol **44** and in agreement with the literature values. (Ohshiro et al., 1990b).

Table 3.13: ^1H (400 MHz) NMR, and ^{13}C (100 MHz) NMR spectral data of procurcumenol **44**

Position	δ_H, J (Hz)	δ_C
1	2.34, dd (8.7, 9.6)	50.5
2	1.66, 1.94, m	26.9
3	1.88, m	39.9
4	-	80.3
5	1.91, m	53.9
6	2.16, dd (13.2, 15.6) 2.57, d (15.6)	28.6
7	-	136.9
8	-	199.2
9	5.85, d (1.4)	129.2
10	-	155.1
11	-	136.3
12	1.73, s	21.3
13	1.76, s	22.4
14	1.86, s	23.4
15	1.22, s	24.3

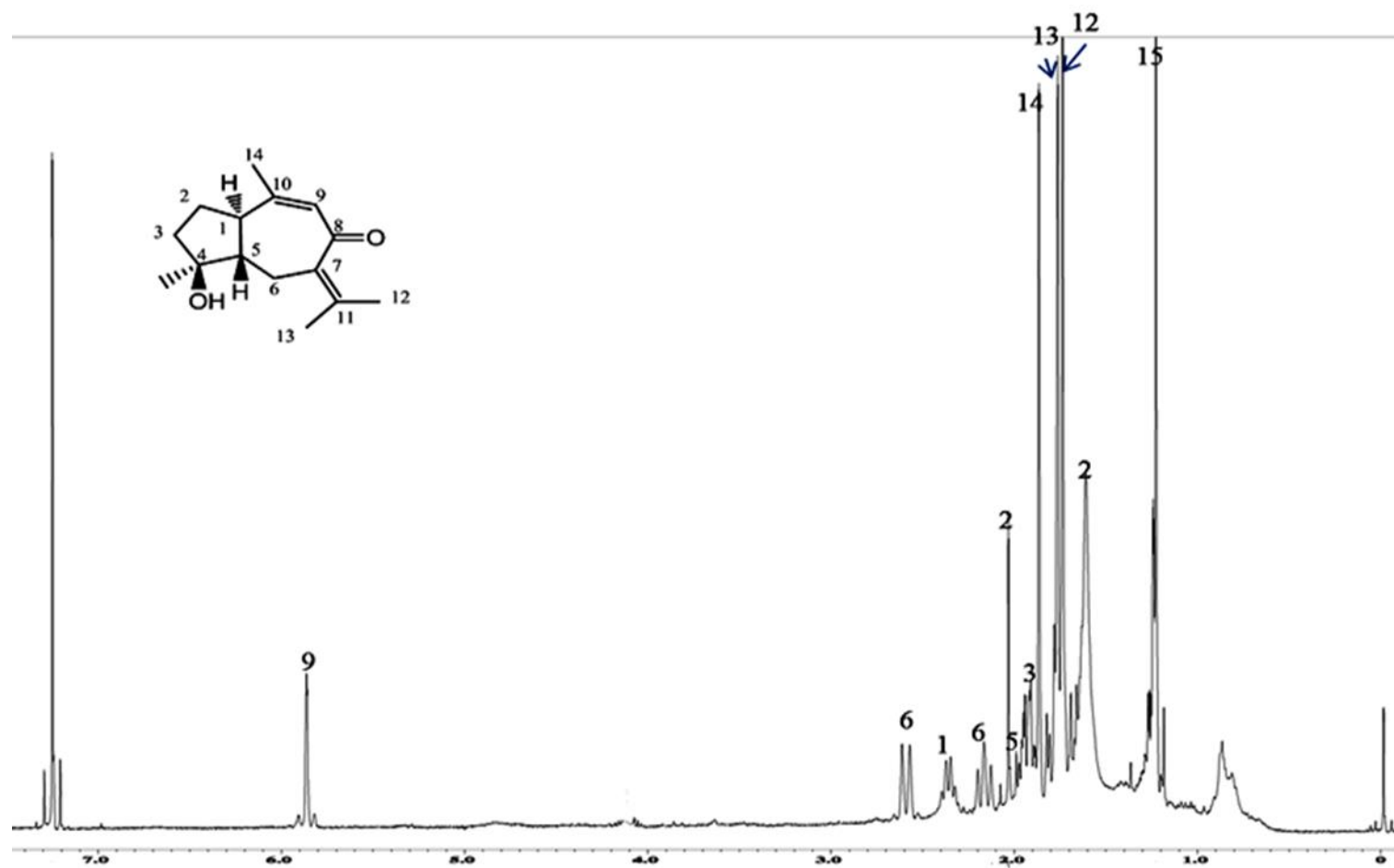


Figure 3.38: ^1H -NMR spectrum of procurcumenol 44

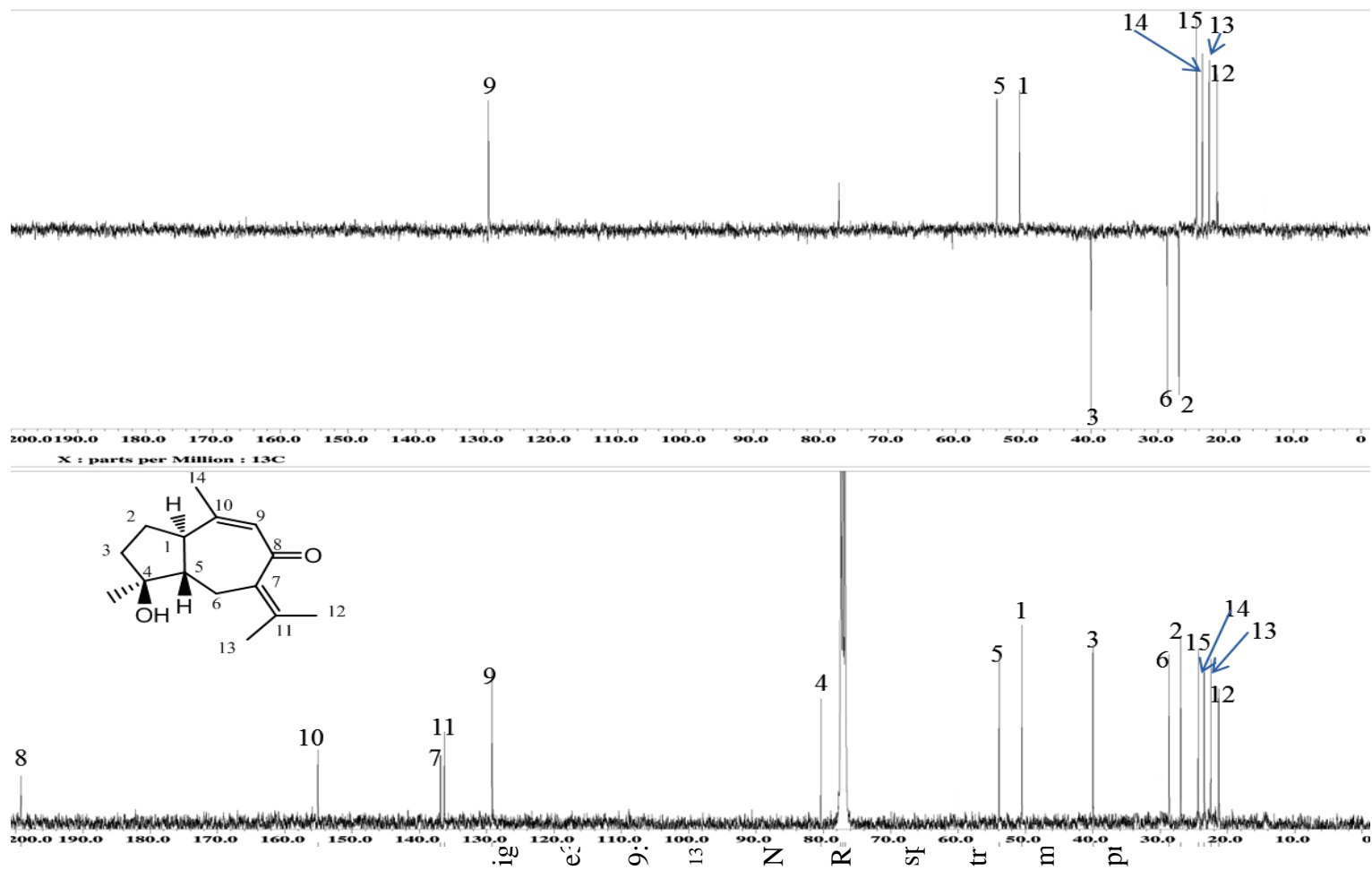
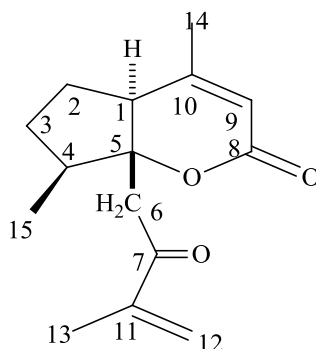


Figure 3.39: ^{13}C NMR and DEPT-135 spectra of procurcumenol 44

3.1.1.3 *Seco-guaiane* type sesquiterpenes

Curcuzedoalide 62



Curcuzedoalide **62** was obtained as a white amorphous powder, GC-MS analysis exhibited the molecular formula of $C_{15}H_{20}O_3$ determined from the molecular ion peak at m/z 248 (M^+) in EI MS, whereas the IR absorption at 1717 cm^{-1} corresponding α,β conjugated carbonyl. The UV (MeOH) λ_{max} nm (log ϵ): 226 (2.37) confirming the conjugation.

The ^1H NMR spectrum (**Figure 3.41, Table 3.14**) displayed the signals of three methyls, two of which were singlets at δ 1.91 (H_3 -14) and 1.81 (H_3 -15). While the other proton signals appeared as doublet δ 1.09 with $J=6.6$. Furthermore, four methylenes were observed at δ 2.17 (H_2 -2), 1.25, 1.91 (H_2 -3), δ 3.26 (1H, d, $J=14.0$, H -6a) and δ 2.83 (1H, d, $J=14.0$, H -6b). In addition to exomethylene was resonated at δ 6.03 (1H, s, H -12_a) and δ 5.88 (1H, d, $J=1.2$, H -12_b). Additionally three methines appeared at 2.87 (1H, *dd*, $J=7.2, 10.0$, H -1), at δ 2.11 (1H, m, H -4), and δ 5.62 (1H, *d*, $J=1.2$ Hz, H -9).

The ^{13}C NMR and DEPT-135 spectra (**Figure 3.42, Table 3.14**) revealed a total of 15 carbons including three sp^3 methyls at δ_{C} : 11.8 (C-15), 22.7 (C-14), and 17.4 (C-

13), in addition to three sp^3 methylenes at δ_C 30.0 (C-2), 31.0 (C-3), and 41.3 (C-6). Furthermore, one sp^2 methylene at δ_C 127.1, and two quaternary sp^2 were observed at δ_C 161.0 (C-10), δ_C 144.9 (C-11). Additionally, one sp^3 quaternary at δ_C 90.9 (C-5), and two carbonyls at δ_C 199.6 (C-7), and δ_C 164.4 (C-8).

The 1H - 1H COSY correlations observed for **62** were H-1/H-2, H-2/H-3, H-3/H-4 and H-4/H-15 while in the HBMBC spectrum, H-2 and H-4 showed correlations to C-1, C-5; H₃-14 showed correlations to C-1, C-8, C-9 and C-10 indicating a five membered ring fused to a six membered α,β -unsaturated lactone ring system. In addition, correlations between H₂-6 to C-5, C-7, and C-11 indicated that the 3-isopentenone moiety is attached to the main skeleton at the ring junction C-5. Thus the spectral analysis of **62** established it to be a *Seco*-guaiane type sesquiterpenoid, namely curcuzedoalide and the data were similar to those published (Park et al., 2012a).

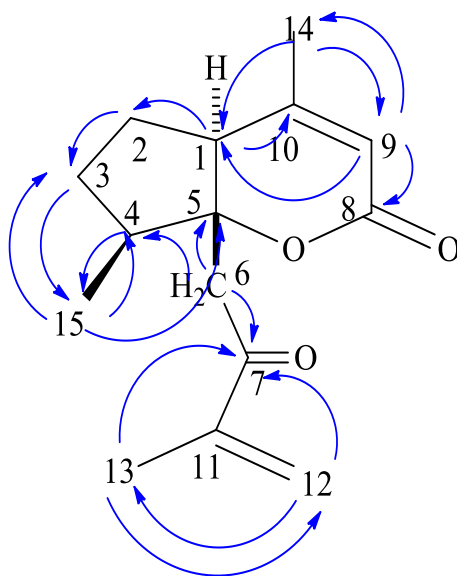


Figure 3.40: Selected HMBC Correlations H \rightarrow C of curcuzedoalide **62**

Table 3.14: ^1H (400 MHz) NMR, and ^{13}C (100 MHz) NMR spectral data of curcuzedoalide **62** in CDCl_3

Position	δ_{H}, J (Hz)	δ_{C}
1	2.87, dd (7.2, 10.0)	44.6
2	1.79, 2.17, m	30.0
3	1.25, 1.91, m	31.0
4	2.11, m	44.1
5	-	90.9
6	H _a -6, 3.26, d (14.0) H _b -6, 2.83, d (14.0)	41.3
7	-	199.6
8	-	164.4
9	5.62, d (1.2)	113.7
10	-	161.0
11	-	144.9
12	H _a -12, 6.03, s H _b -12, 5.88, d	127.1
13	1.81, s	17.4
14	1.91, s	22.7
15	1.09, d (6..6)	11.8

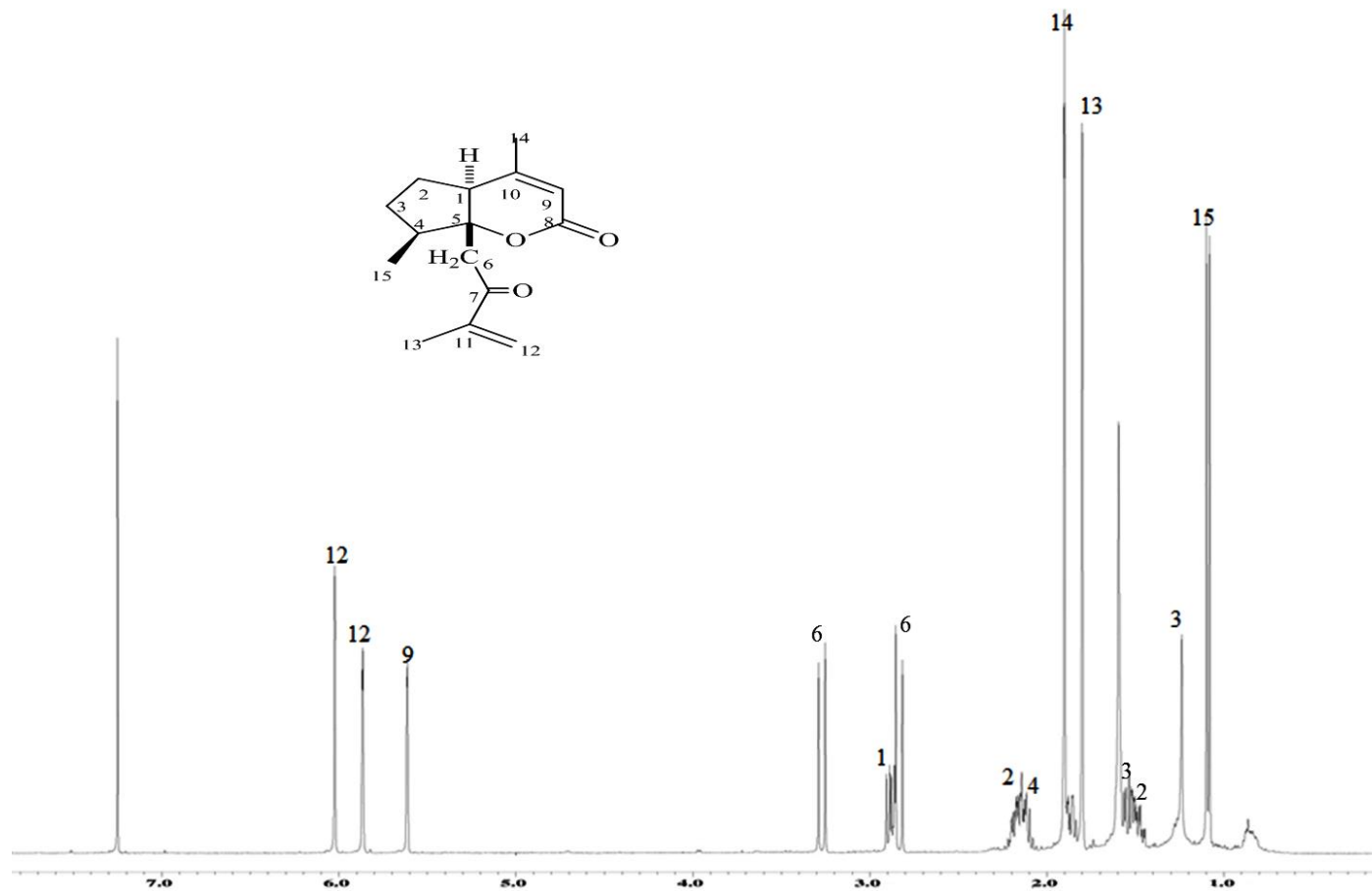


Figure 3.41: ^1H NMR spectrum of curcuzedoalide

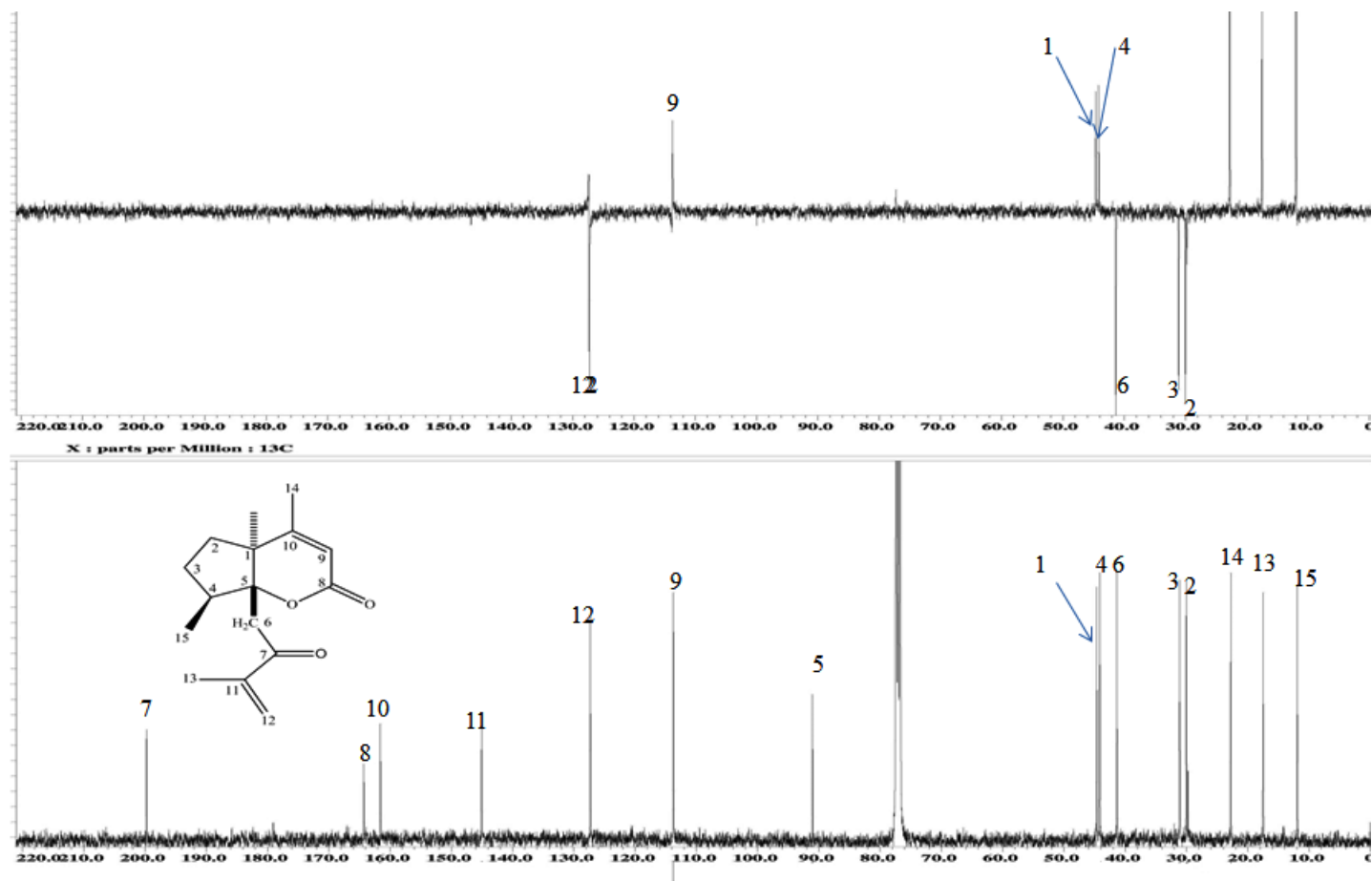


Figure 3.42: ^{13}C -NMR and DEPT-135 spectra of curcuzedoalide **62**

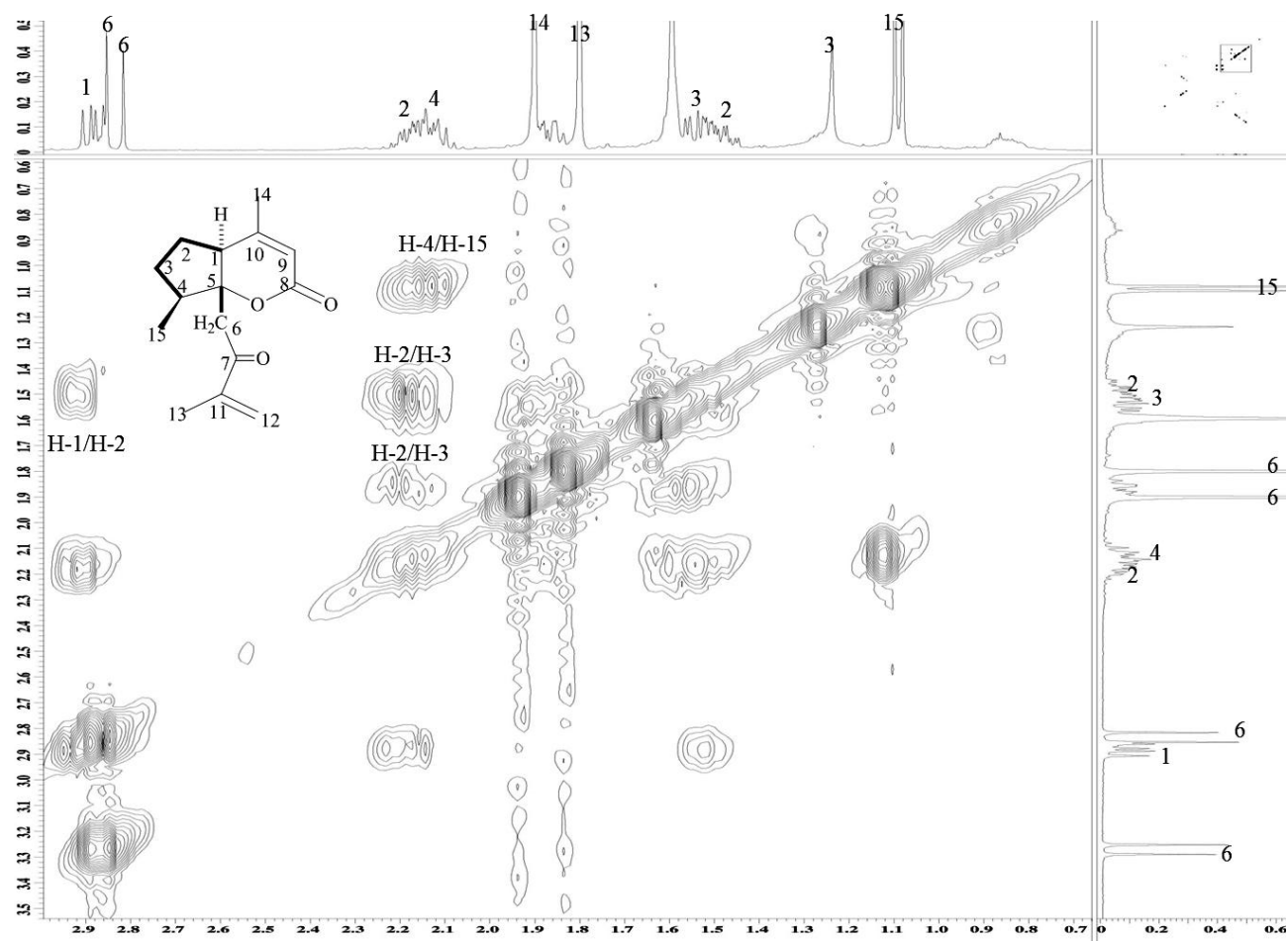


Figure 3.43: COSY spectrum of curcuzedoalide **62**

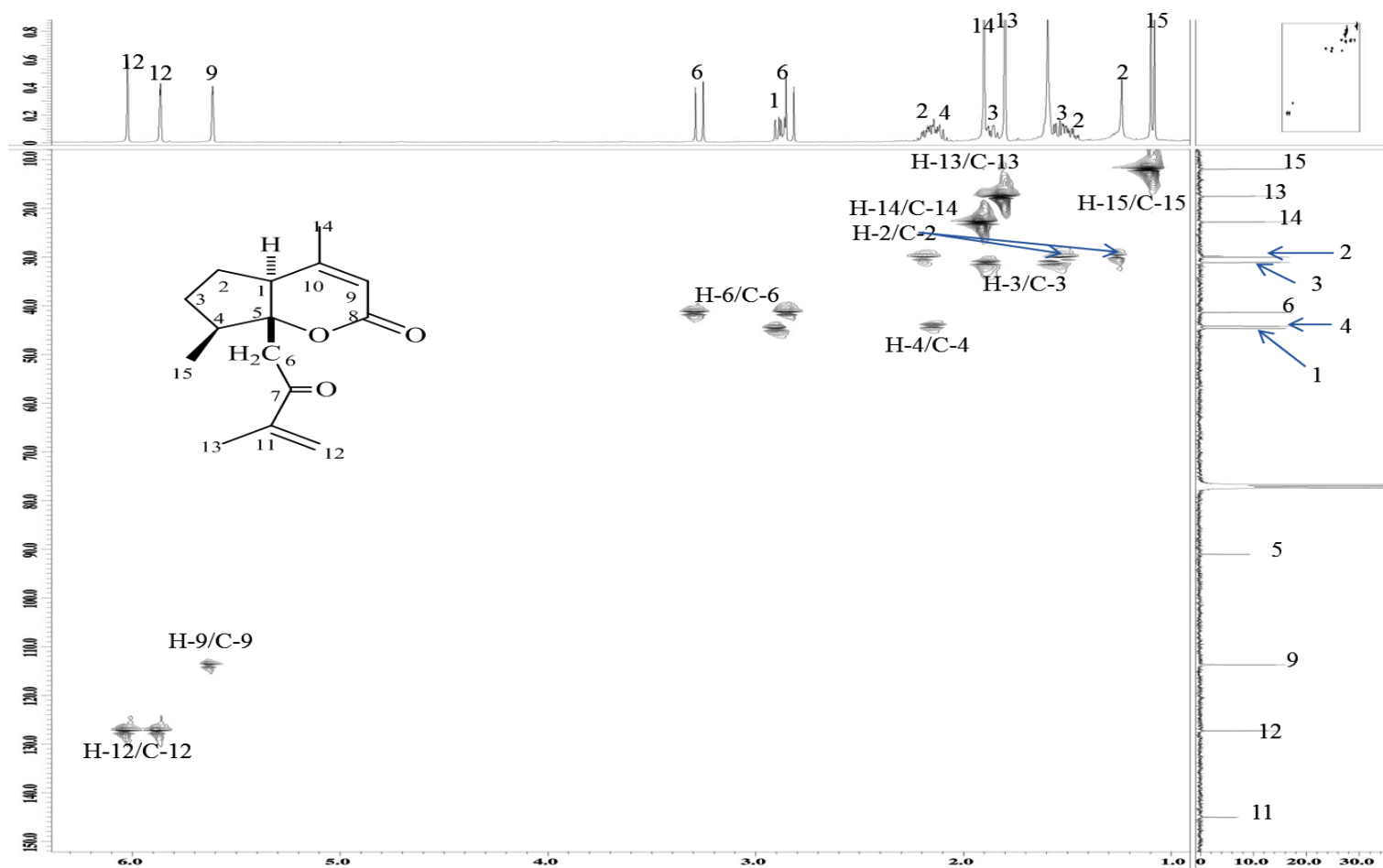


Figure 3.44: HSQC spectrum of curcuzedoalide **62**

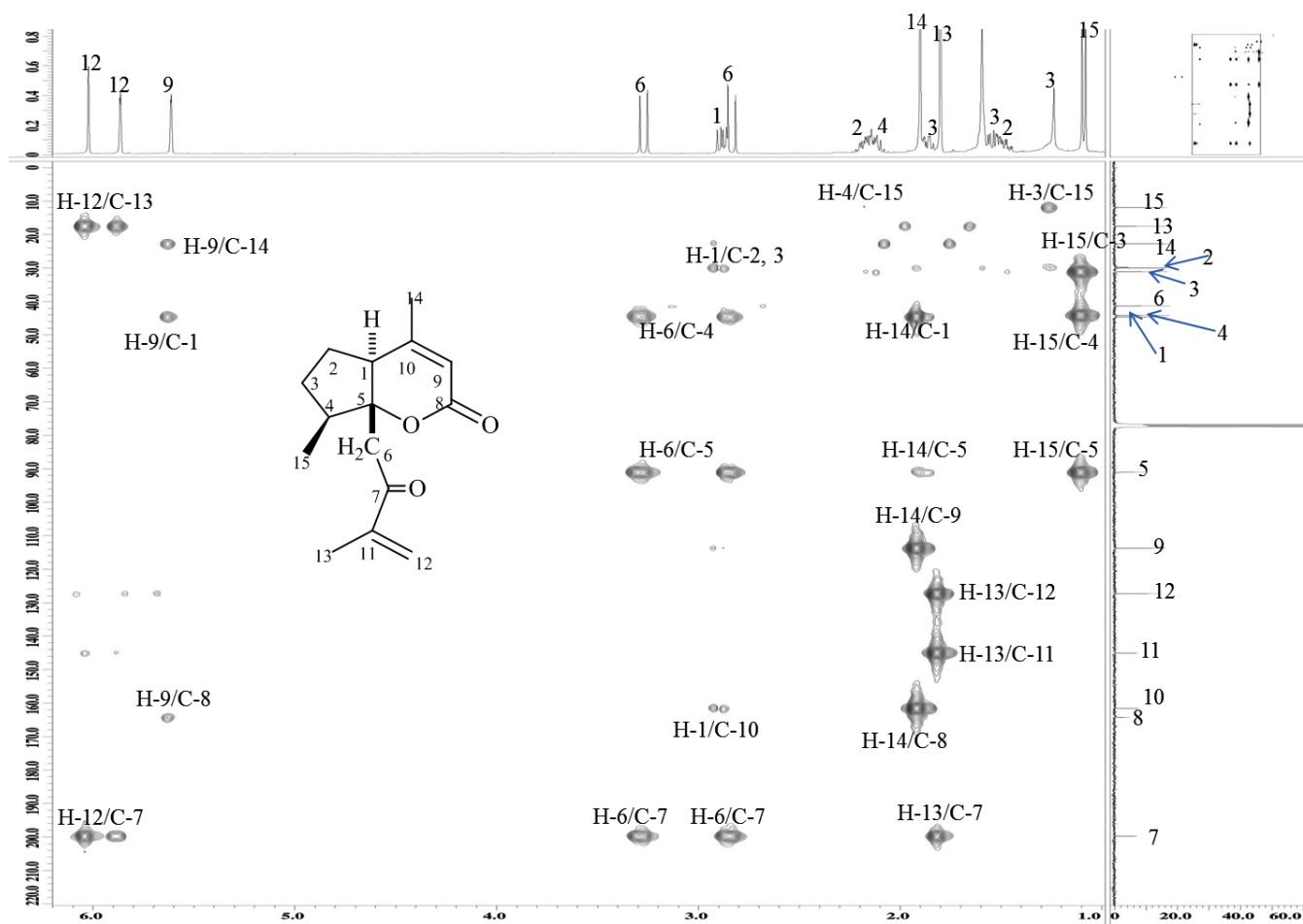
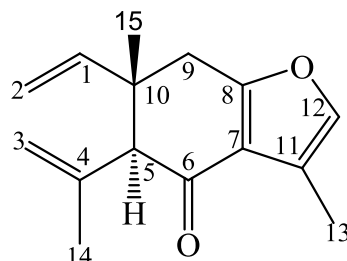


Figure 3.45: HMBC spectrum of curcuzedoalide **62**

3.1.1.4 Elemene type sesquiterpene

Curzerenone 111



Curzerenone **111** was afforded as a colourless oil. the IR spectrum showed an absorption peak at 1712 cm^{-1} . The GC-MS analysis revealed a base peak m/z at 122 while the molecular ion peak (M^+) at m/z 230 implying the molecular formula of $C_{15}H_{18}O_2$.

The ^1H NMR spectrum (**Figure 3.47**, **Table 3.15**) showed the presence of proton signals due to three methyl groups as singlets at δ_{H} 1.18 ($\text{H}_3\text{-15}$), 1.76 ($\text{H}_3\text{-14}$), and 2.20 ($\text{H}_3\text{-13}$). In addition, three methylenes, two of which were exomethylenes at δ_{H} 4.93 ($\text{H}_2\text{-2}$), and 4.84 ($\text{H}_2\text{-3}$) and the other protons as doublets with $J=17.2\text{ Hz}$ at 2.94, 2.74 ($\text{H}_2\text{-9}$). Furthermore, the proton spectrum also showed three methines, two of which were olefinic protons at δ_{H} 5.77 (dd, $J=10.8, 17\text{ Hz}$, H-1), and δ 7.01 (H-12). and the other resonated at 2.94 (H-5).

The ^{13}C NMR and DEPT-135 spectra (**Figure 3.48**, **Table 3.15**) revealed the signals of a total of 15 carbons. Three methyls at δ_{C} 24.8 (C-15), 24.9 (C-14), and 8.9 (C-13). Two sp^2 methylenes were observed at δ_{C} 112.9 (C-2), and δ 115.6 (C-3). In addition, one sp^3 methylene appeared at δ_{C} 33.6 (C-9). Furthermore, two sp^2 methines at δ_{C} 145.5 (C-1),

and 139.5 (C-12), while sp^3 methine at δ_C 64.1 (C-5). Additionally a carbonyl signal was observed at δ_C 194.8 (C-6).

1H - 1H COSY correlation between H-1/H-2 together to HMBC correlations of cross peaks of H-15 to C-5, C-8, C-9, C-10, in addition to H-9 to C-1, C-5, C-8, and C-10, and also H-14 to C-3 and C-5 confirmed the presence of elemene type sesquiterpene with additional furan ring showed by the correlation of H-12 to C-7, C-8, and C-12 indicated that the furan ring fused with a six membered ring at C-8 and C-7.

The spectral data for **111** showed good agreement with the literature. The identity of the compound was thus confirmed as curzerenone (Yang et al., 2011).

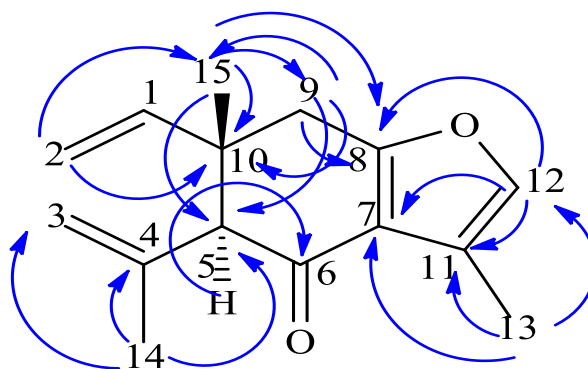


Figure 3.46: Selected HMBC Correlations H $\xrightarrow{\hspace{1cm}}$ C of *curzerenone* **111**

Table 3.15: ^1H (400 MHz) NMR and ^{13}C (100 MHz) NMR spectral data of *curzerenone* **111** in CDCl_3

Position	δ_{H}, J (Hz)	δ_{C}
1	5.77, dd (10.8, 17)	145.5
2	4.93, dd (17, 4.2)	112.9
3	4.84, s	115.6
4	-	141.0
5	2.94, s	64.1
6	-	194.8
7	-	120.1
8	-	165.4
9	2.94, 2.74, d (17.2)	33.6
10	-	42.8
11		119.2
12	7.01, s	139.5
13	2.20, s	8.9
14	1.76, s	24.9
15	1.18, s	24.8

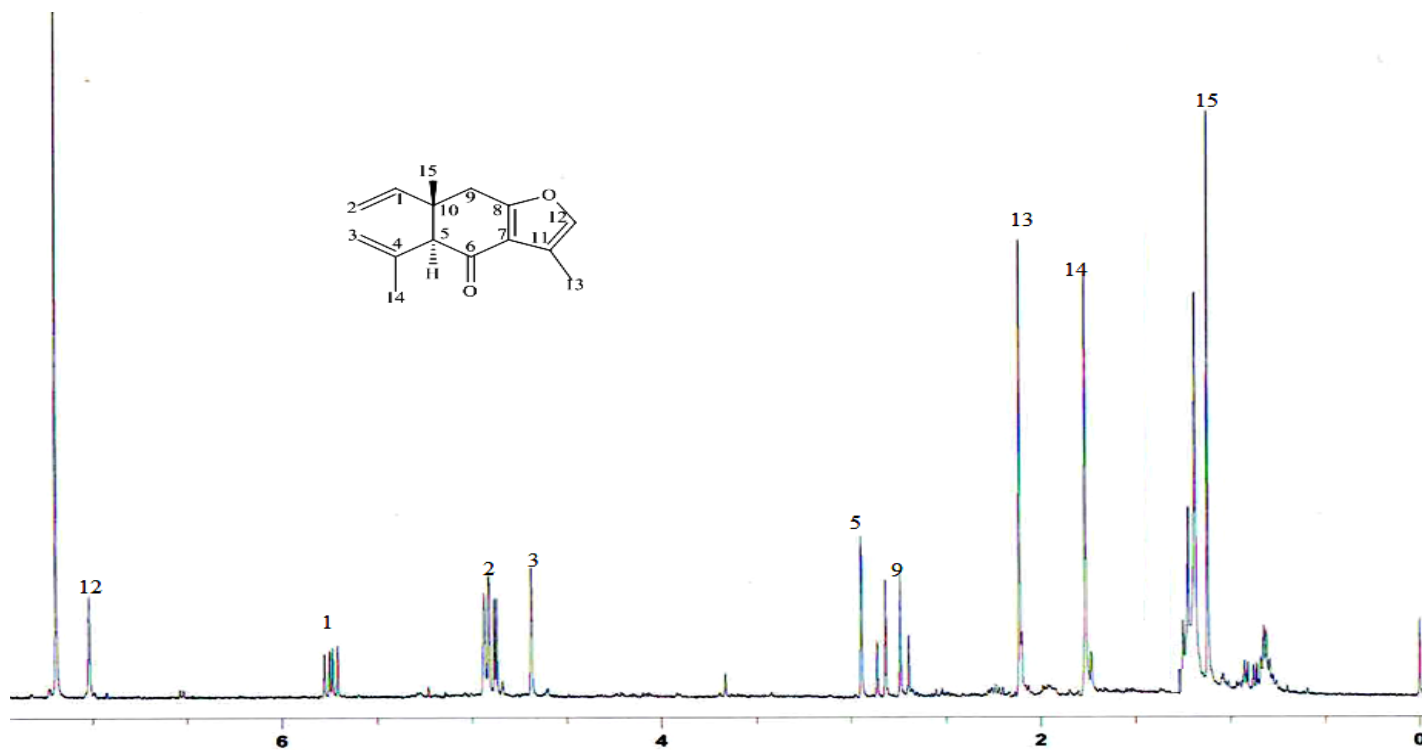


Figure 3.47: ^1H NMR spectrum of curzerenone **111**

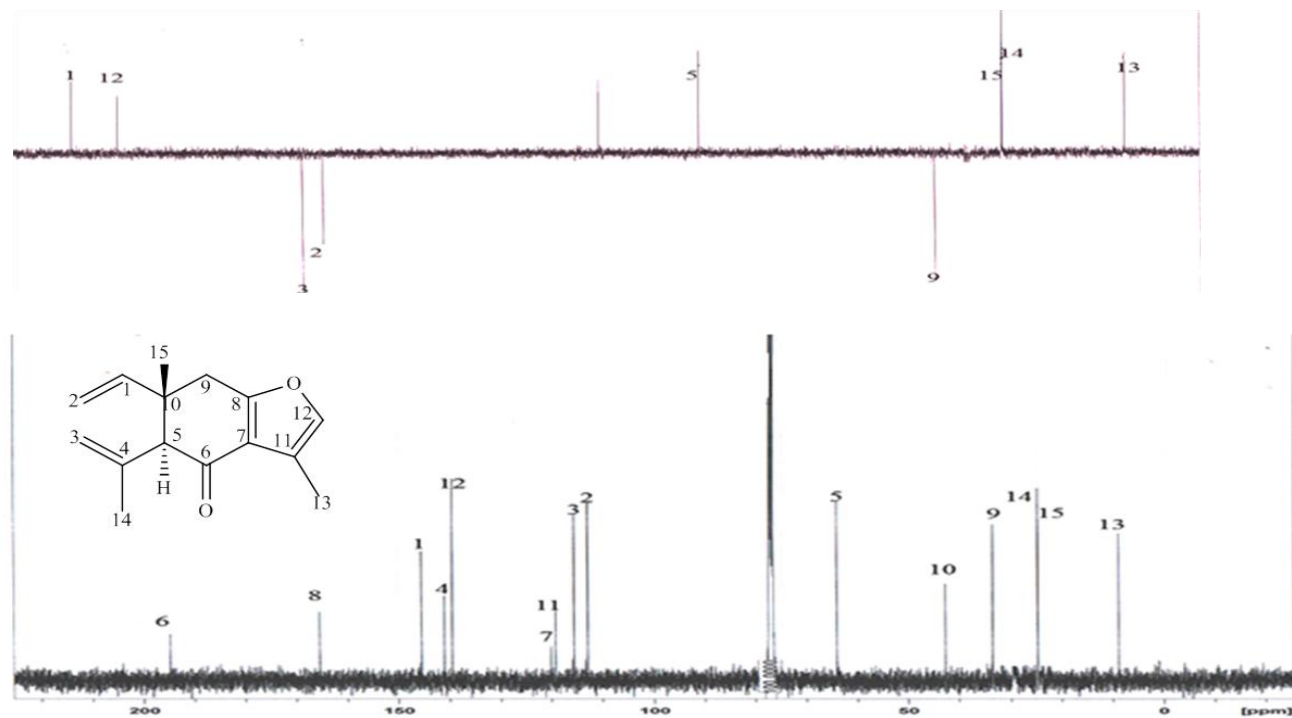


Figure 3.48: ^{13}C -NMR and DEPT-135 spectra of curzerenone **111**

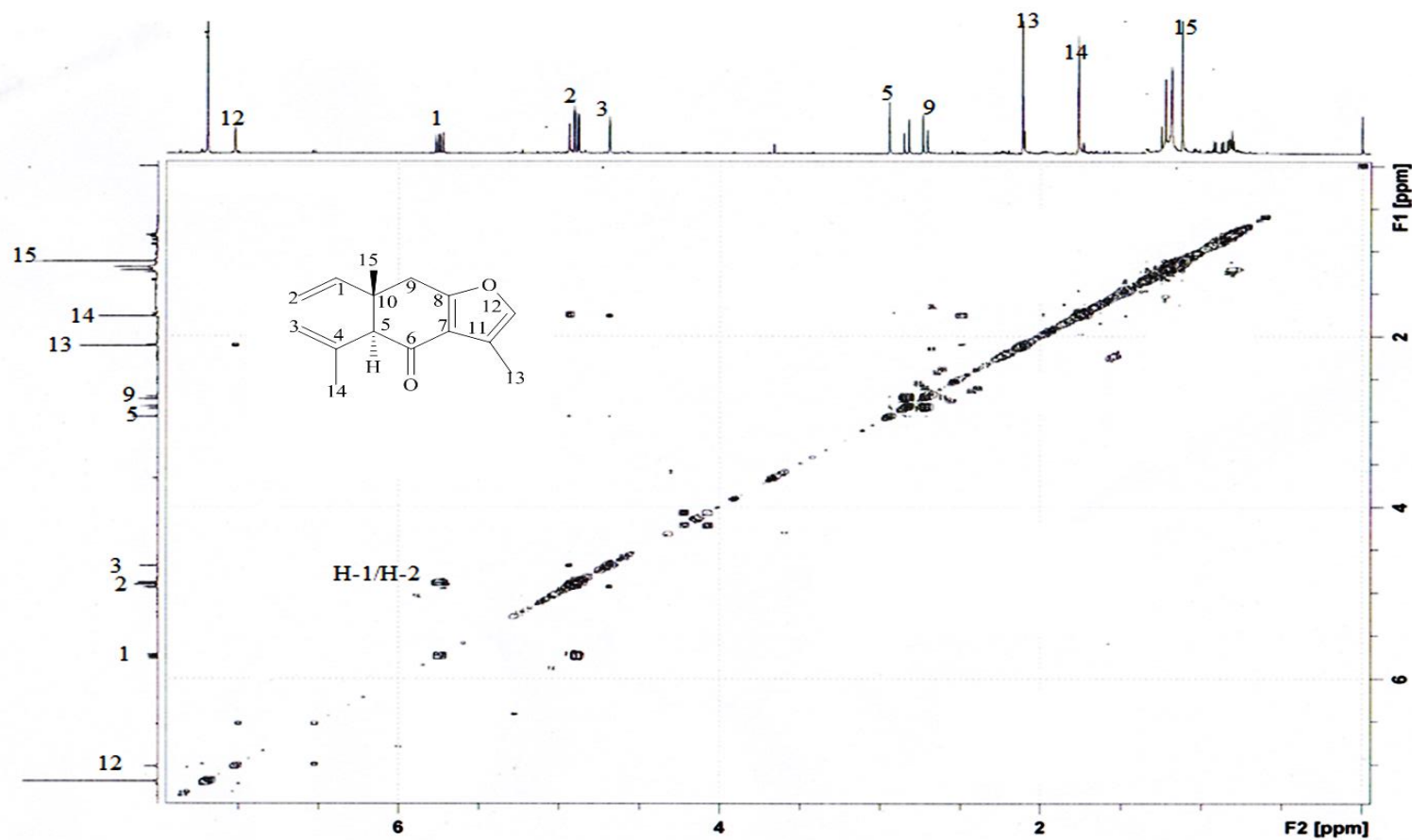


Figure 3.49: COSY spectrum of curzerenone **111**

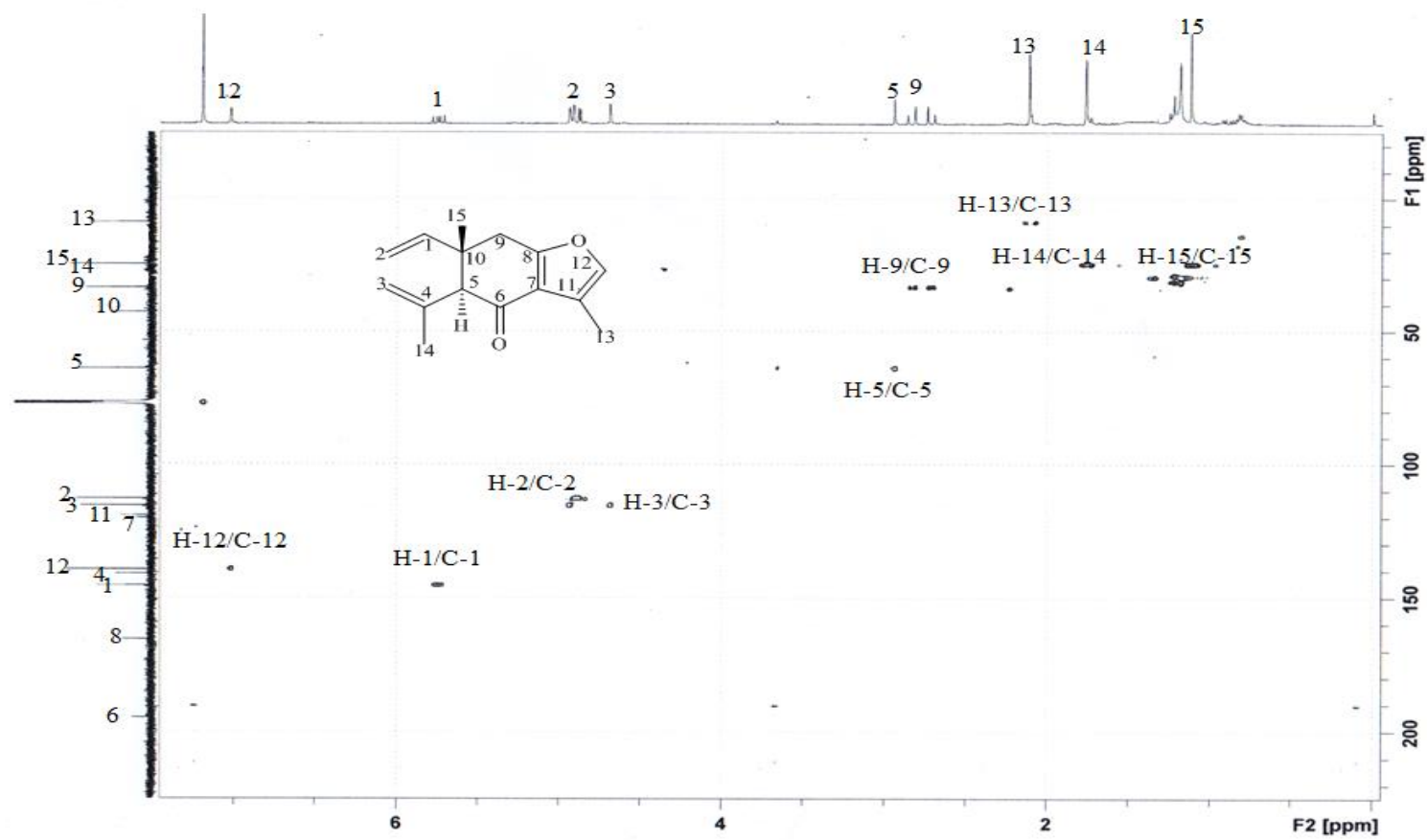


Figure 3.50: HSQC spectrum of curzerenone 111

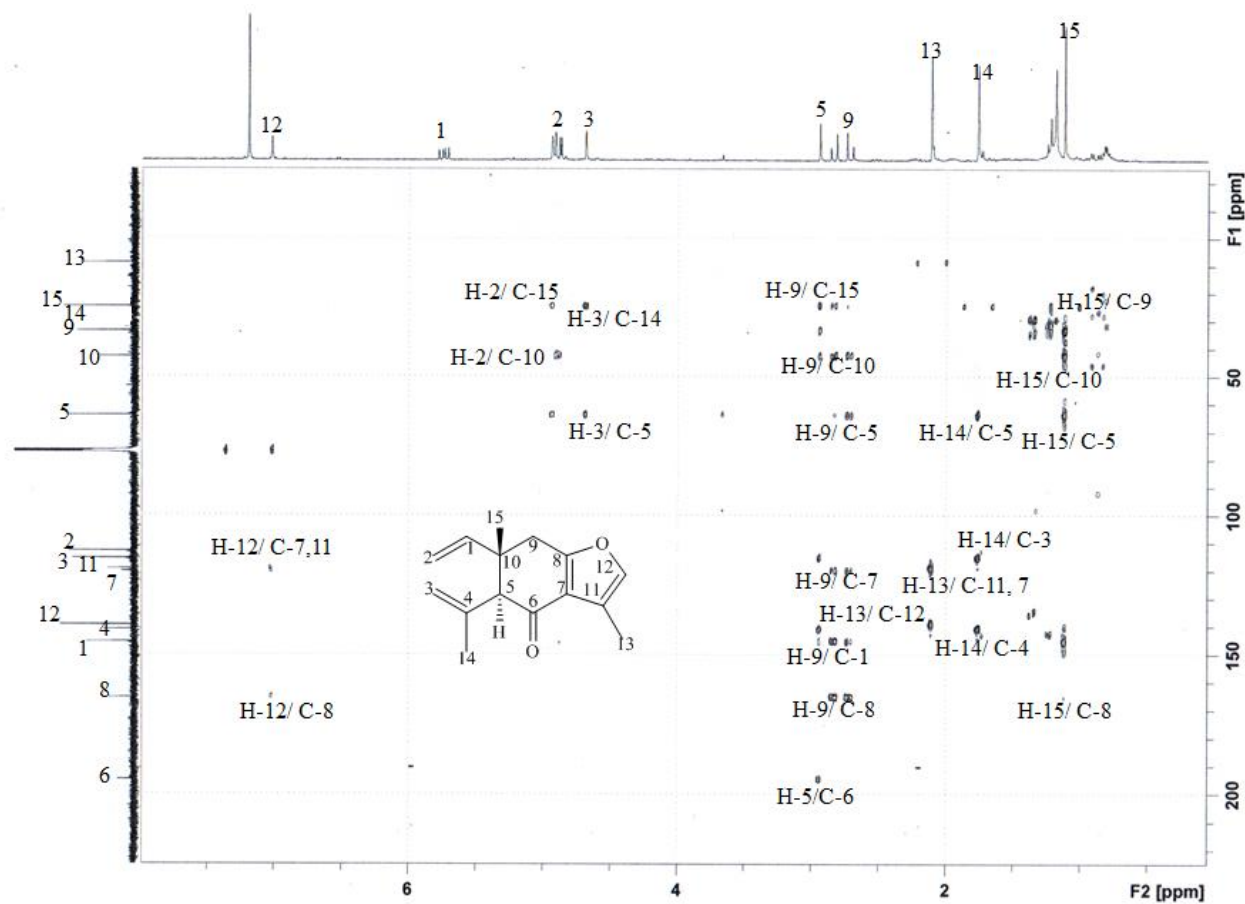
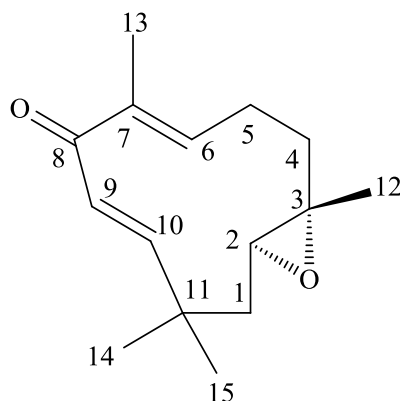


Figure 3.51: HMBC spectrum of curzerenone **111**

3.1.1.5 Humulane type sesquiterpenes

Zerumbone epoxide 151



Zerumbone epoxide **151** was isolated as a pale yellow. The MS of **151** exhibited a molecular ion (M^+) signal at m/z 234 associated with the molecular formula of $C_{15}H_{22}O_2$. The IR absorption at 1712 cm^{-1} indicated the presence of a carbonyl group. The UV spectrum (MeOH) showed a λ_{max} nm (log ϵ) at 216 (2.6).

The ^1H NMR spectrum (**Figure 3.53**, Table **Table 3.16**) displayed the presence of four methyl singlets at δ_{H} 1.07 (H-15), 1.28 (H-14), 1.84 (H-13), and 1.20 (H-12). Three methylene signals were observed at δ_{H} 1.44 (2H, dd, $J=2.7, 11.4\text{ Hz}$), 1.34, 2.22 (2H, m, H-4), 1.94 (1H, d, $J=13\text{ Hz}$, H-5). Furthermore, four methines at δ_{H} 2.74 (1H, d, $J=11$, H-2), 6.1 (1H, d, $J=12.3\text{ Hz}$, H-6), 6.10 (2H, d, $J=1.36\text{ Hz}$, H-9), 6.09 (1H, d, $J=1.36\text{ Hz}$, H-10).

The ^{13}C NMR and DEPT-135 spectra (**Figure 3.54**, Table **Table 3.16**) indicated the presence of 15 carbons. Four methyls at δ_{C} 29.8 (C-15), 24.0 (C-14), 12.1 (C-13), and 15.7 (C-12). Three sp^3 methylenes carbons were observed at 42.7 (C-1), 38.2 (C-4), and 24.7 (C-5). In addition, three sp^2 methines at δ_{C} 147.8 (C-6), 128.3 (C-9), and 159.5 (C-10). Furthermore, one sp^3 methine appeared at δ_{C} 24.0 (C-14). Additionally, three

quaternary carbons, two of which are sp^3 at δ_C 61.9 (C-3), and 36.0 (C-11), while the other is sp^2 at δ_C 139.5 (C-7). One carbonyl carbon was observed at δ_C 203.0 (C-8).

The 1H - 1H COSY correlation observed were H-4/H-5, H-5/H-6, H-1/H-2 together with HMBC correlations of H-1 to C-2, 3, 11. In addition H-15 correlated to C-11, 10, while H-10 correlated to C-9 and H-9 correlated to C-8. Moreover H-13 correlated to C-8, H-4 correlated to C-3, C-6, and H-2 correlated to C-3. These HMBC correlations observations indicated the humulane skeleton.

In view of spectral data analysis observed for the above compound and comparsion with literature led to the conclusion that compound **151** was zerumbone epoxide(Matthes et al., 1980, 1982).

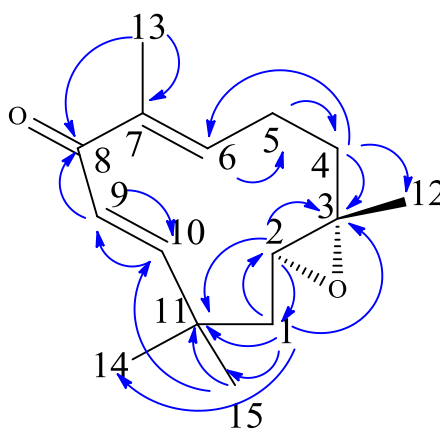


Figure 3.52: Selected HMBC Correlations H $\xrightarrow{\hspace{1cm}}$ C of zerumbone epoxide **151**

Table 3.16: ^1H (400 MHz) NMR and ^{13}C (100 MHz) NMR spectral data of zerumbone epoxide **151** in CDCl_3

Position	$\delta_{\text{H}}, J \text{ (Hz)}$	δ_{C}
1	1.44, d (11.8)	42.7
2	2.74, d (11)	62.5
3	-	61.9
4	1.34, 2.22, m	38.2
5	1.94, d (13.7)	24.7
6	6.1, d (12.3)	147.8
7	-	139.5
8	-	203.0
9	6.10, d (1.36)	128.3
10	6.09, d (1.36)	159.5
11	-	36.0
12	1.20, s	15.7
13	1.84, s	12.1
14	1.28, s	24.0
15	1.07, s	29.8

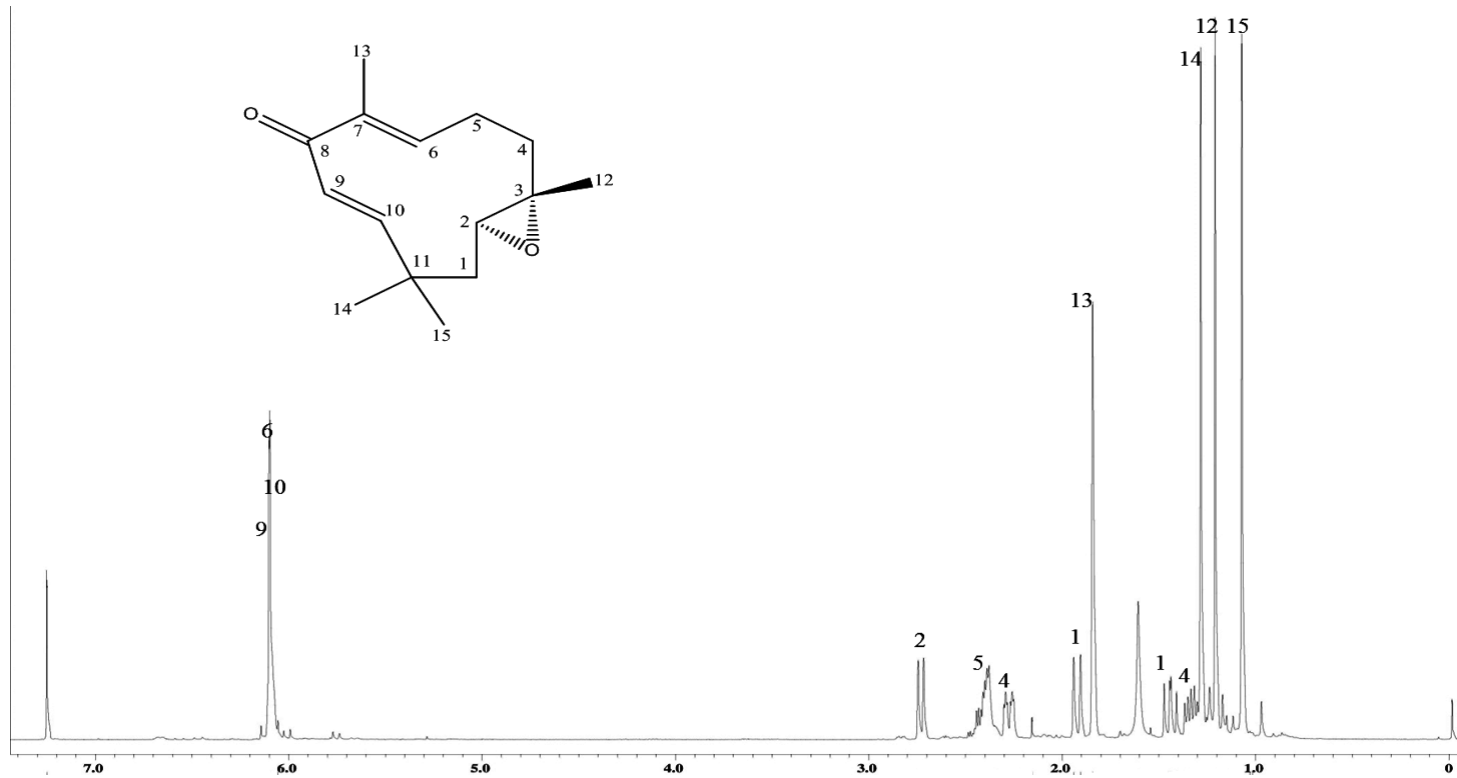


Figure 3.53: ^1H NMR spectrum of zerumbone epoxide **151**

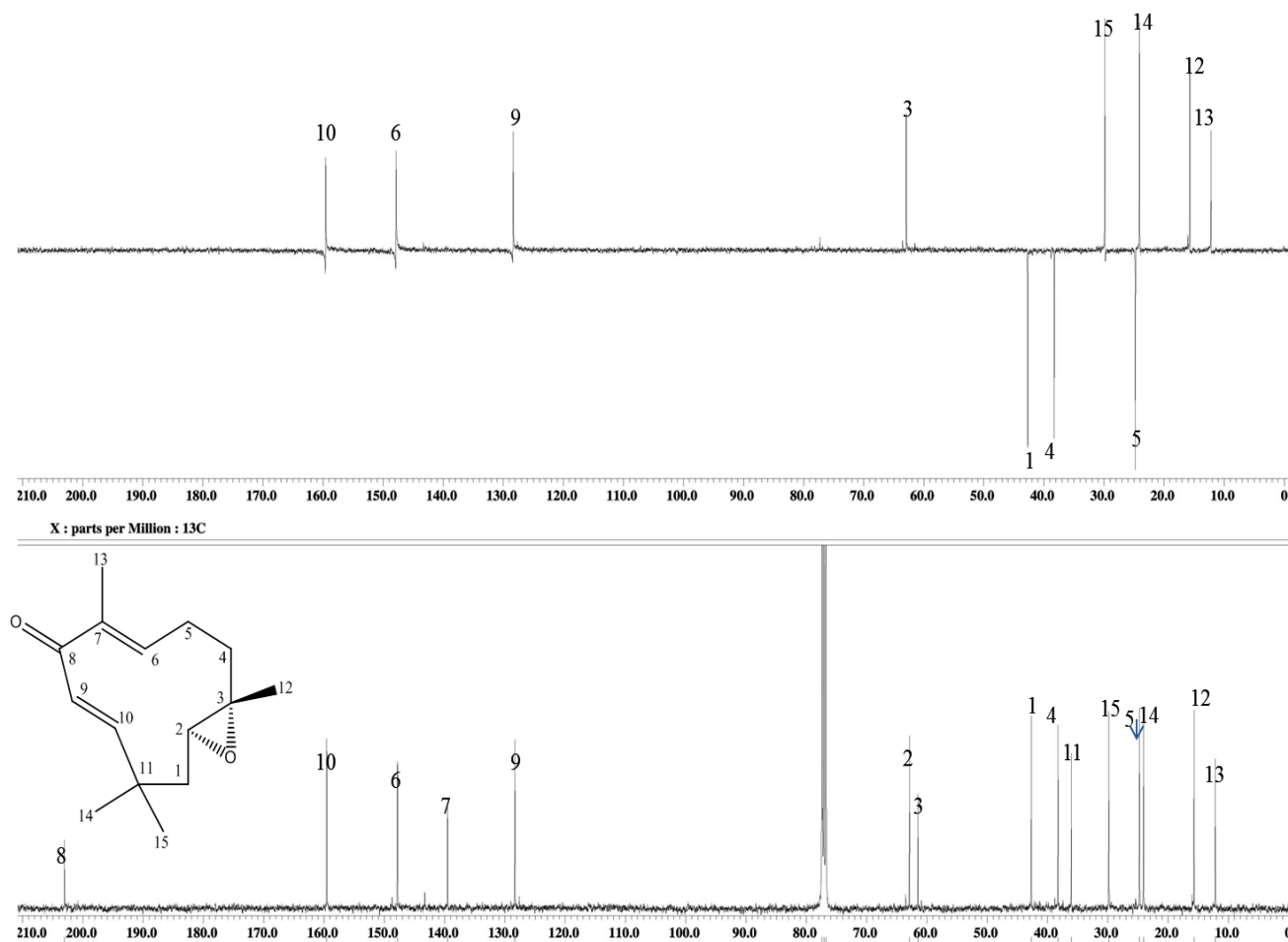


Figure 3.54: ^{13}C NMR and DEPT-135 spectra of zerumbone epoxide **151**

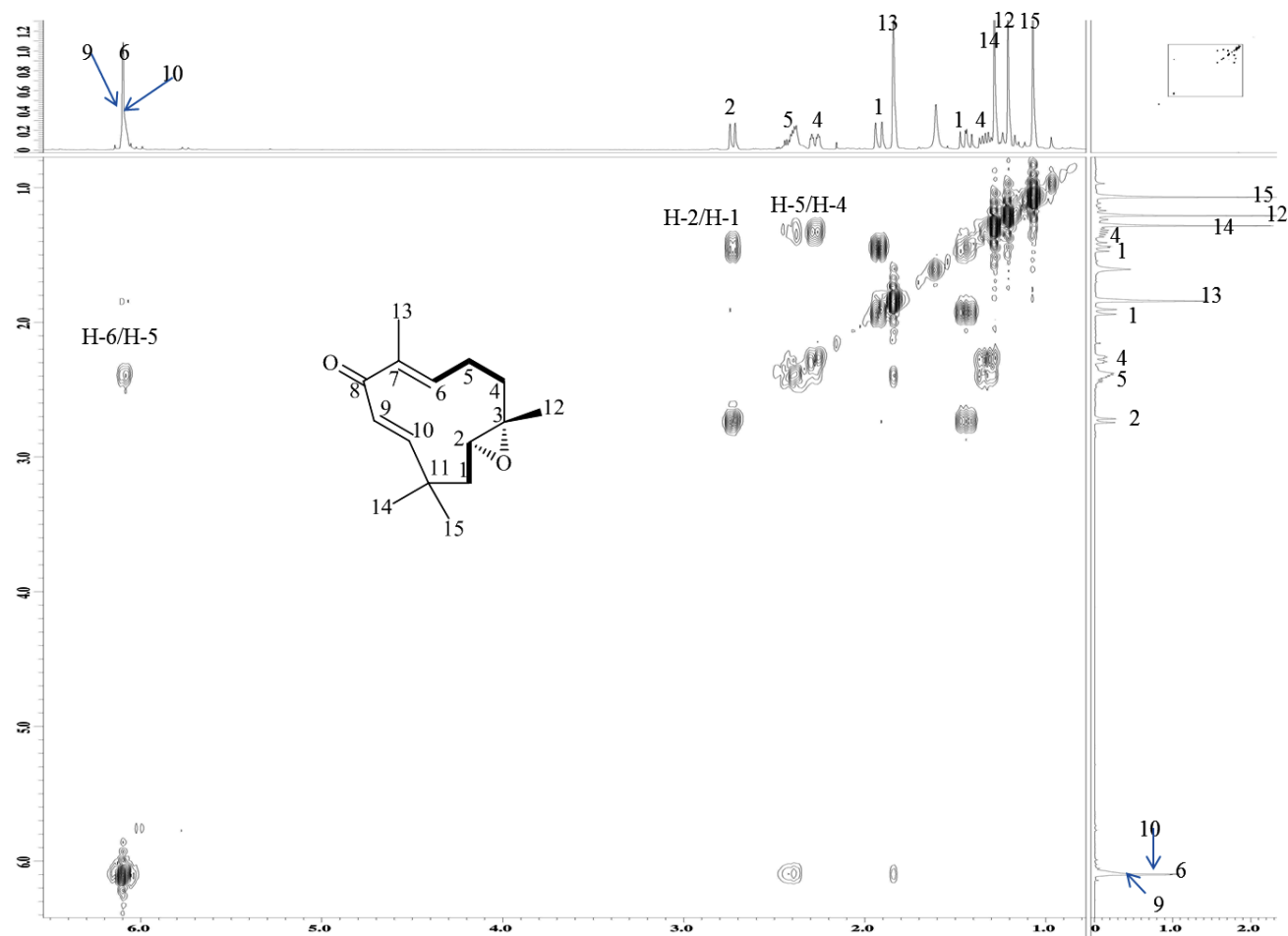


Figure 3.55: COSY spectrum of zerumbone epoxide **151**

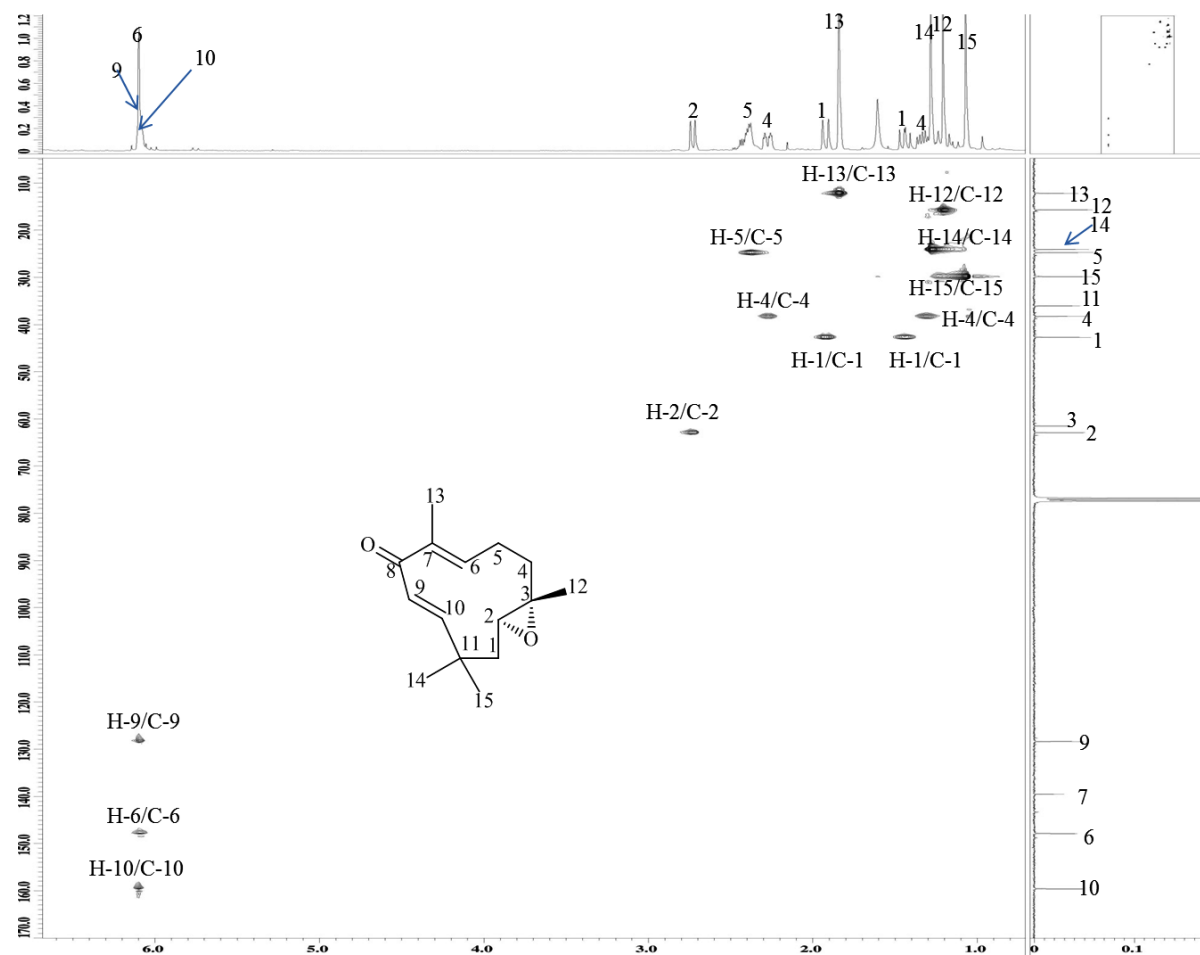


Figure 3.56: HSQC spectrum of zerumbone epoxide **151**

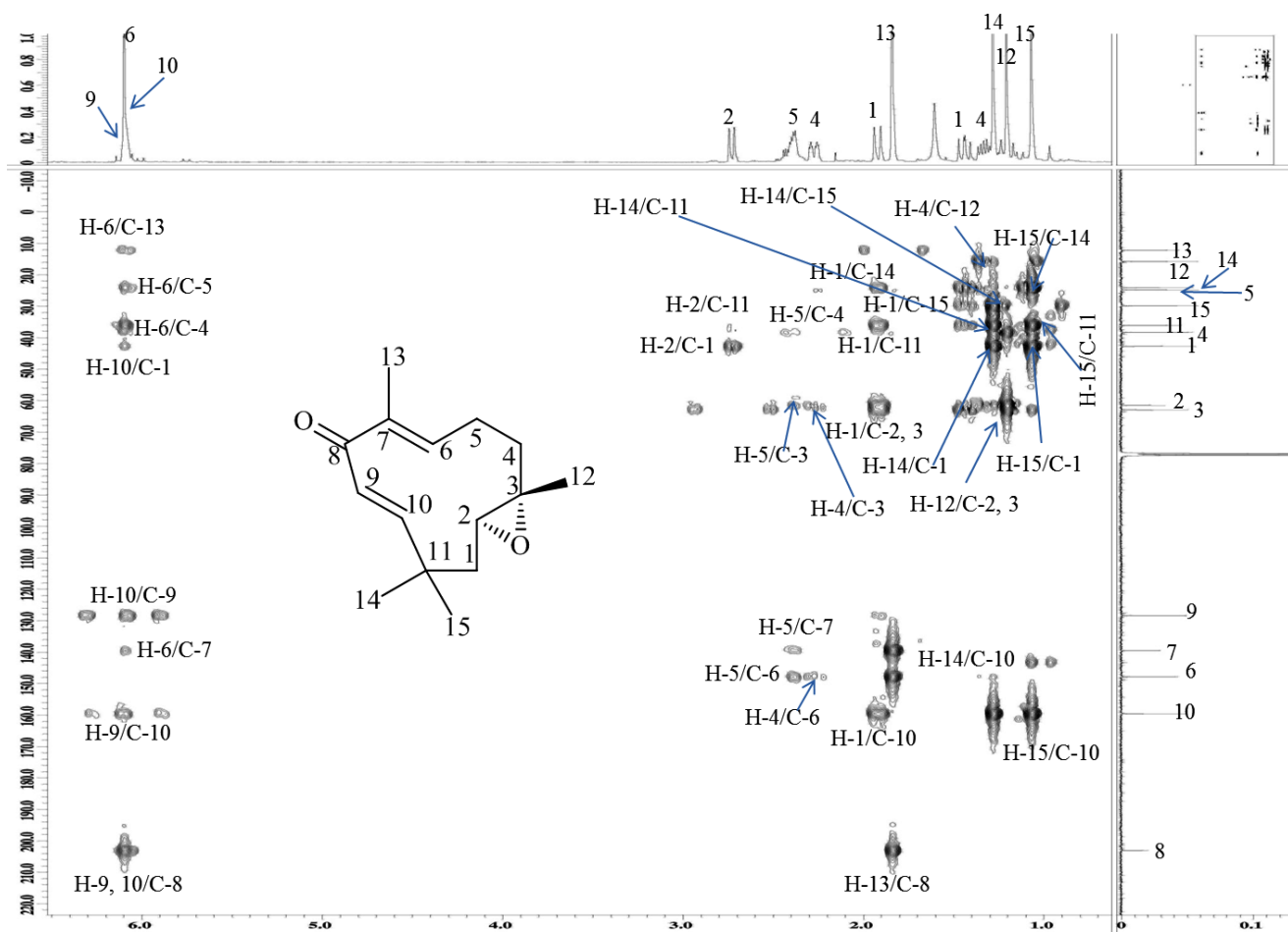
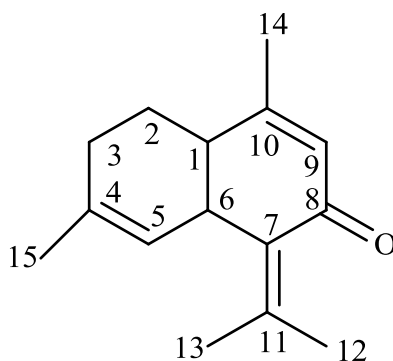


Figure 3.57: HMBC spectrum of zerumbone epoxide **151**

3.1.1.6 . Cadinane type sesquiterpenes

Comosone II **104**



Comosone II **104** was obtained as a colorless oil, with an $[\alpha]_{\text{D}}^{20} + 10.1^{\circ}$ (c, MeOH). The EI-MS revealed a molecular ion (M^{+}) peak m/z 216 indicating the molecular formula of $\text{C}_{15}\text{H}_{20}\text{O}$. The IR spectrum showed strong absorption band at 1653 cm^{-1} implying the presence of an α,β -unsaturated carbonyl group which was further supported by the UV spectrum (MeOH) in which it showed absorption band maximum at 220 nm.

The ^1H NMR spectrum (**Figure 3.59, Table 3.17**) showed the presence of four vinyl methyl singlets at δ_{H} 1.56 ($\text{H}_3\text{-15}$), 1.91 ($\text{H}_3\text{-14}$), 1.85 ($\text{H}_3\text{-13}$), 2.04 ($\text{H}_3\text{-12}$), two methylenes at δ_{H} 1.82, 2.17 ($\text{H}_2\text{-2}$) and δ_{H} 1.81 ($\text{H}_2\text{-15}$), four methines at δ_{H} 2.73 (H-1), 3.74 (H-6), 4.90 (H-5), and 5.88 (H-9),

The ^{13}C NMR, DEPT-135, HSQC spectra (**Figure 3.60, 3.62, Table 3.17**) displayed one carbonyl (δ_{C} 191.9), and six olefinic carbons at δ_{C} 135.1 (C-4), 122.0 (C-5), 133.6 (C-7), 141.7 (C-11), 130.8 (C-9), and 158.5 (C-10). In addition, four methyl groups resonated at δ_{C} 23.5 (C-15), 20.9 (C-14), 21.9 (C-13), and 23.1 (C-12), two

methylenes at δ_C 25.3 (C-2), 26.0 (C-3), and four methines at δ_C 38.3 (C-1), 39.8 (C-6), 122.1 (C-5), 130.8 (C-9).

The ^1H - ^1H -COSY correlations observed were H-1/H-2, H-1/H-6, H-2/H-3, and H-5/H-6 coupled with the HMBC correlations: H-14/C-1, C-9, H-1/C-14, H-2/C-1, H-15/C-3, C-4, C-5, H-9/C-7, H-1/C-7 established the presence of two six membered rings fused together, while other HMBC correlations observed between H-12, H-13 to C-7 and C-7 indicated the dimethylethylene group attached the ring system through C-7. Thus, COSY and HMBC spectra were able to establish the cadinane skeletal of comosone II.

Analysis of the above information in combination with other 2D spectra, including HMBC, HSQC, NOESY confirmed the structure as comosone II and was in agreement with those published previously (Xu et al., 2008).

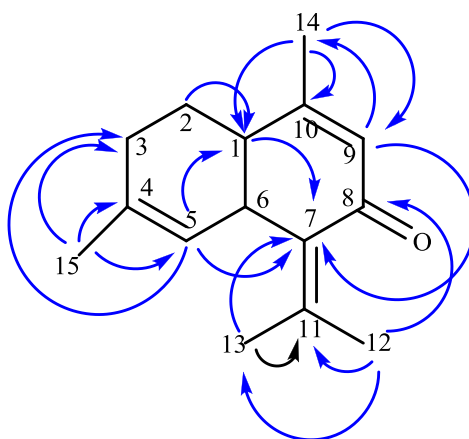



Figure 3.58: Selected HMBC Correlations H  C of comosone II **104**

Table 3.17: : ^1H NMR (400 MHz) and ^{13}C NMR (100 MHz) spectral data in CDCl_3 of comosone II **104**

Position	$\delta_{\text{H}}, J \text{ (Hz)}$	δ_{C}
1	2.73, s	38.3
2	1.82, m 2.17, m	25.3
3	1.81, m	26.0
4	-	135.1
5	4.90, s	122.0
6	3.74, s	39.8
7	-	133.6
8	-	191.9
9	5.90, s	130.8
10	-	158.5
11	-	141.7
12	2.04, s	23.1
13	1.85, s	21.9
14	1.91, s	20.9
15	1.56, s	23.5

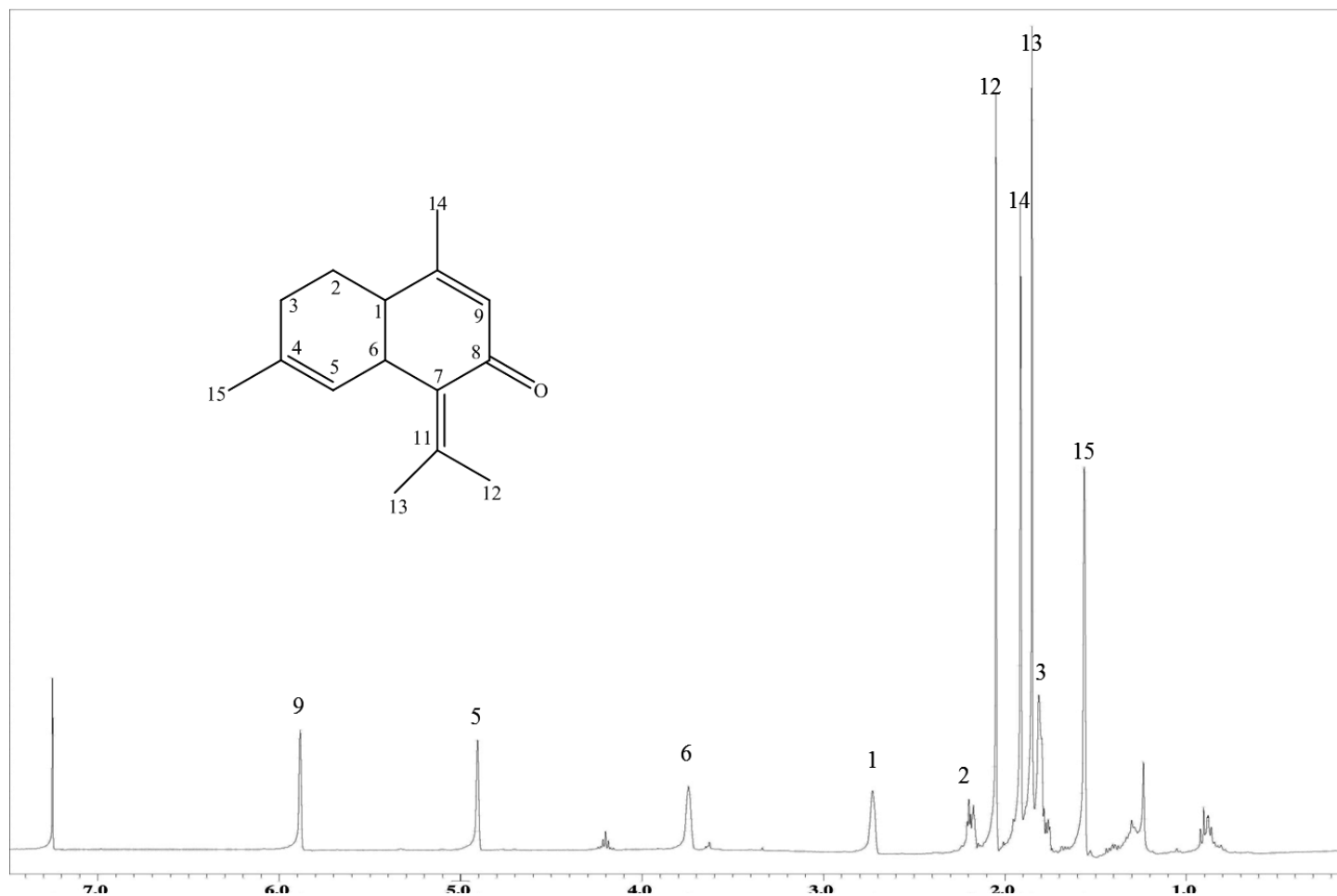


Figure 3.59: ^1H NMR spectrum of comosone II 104

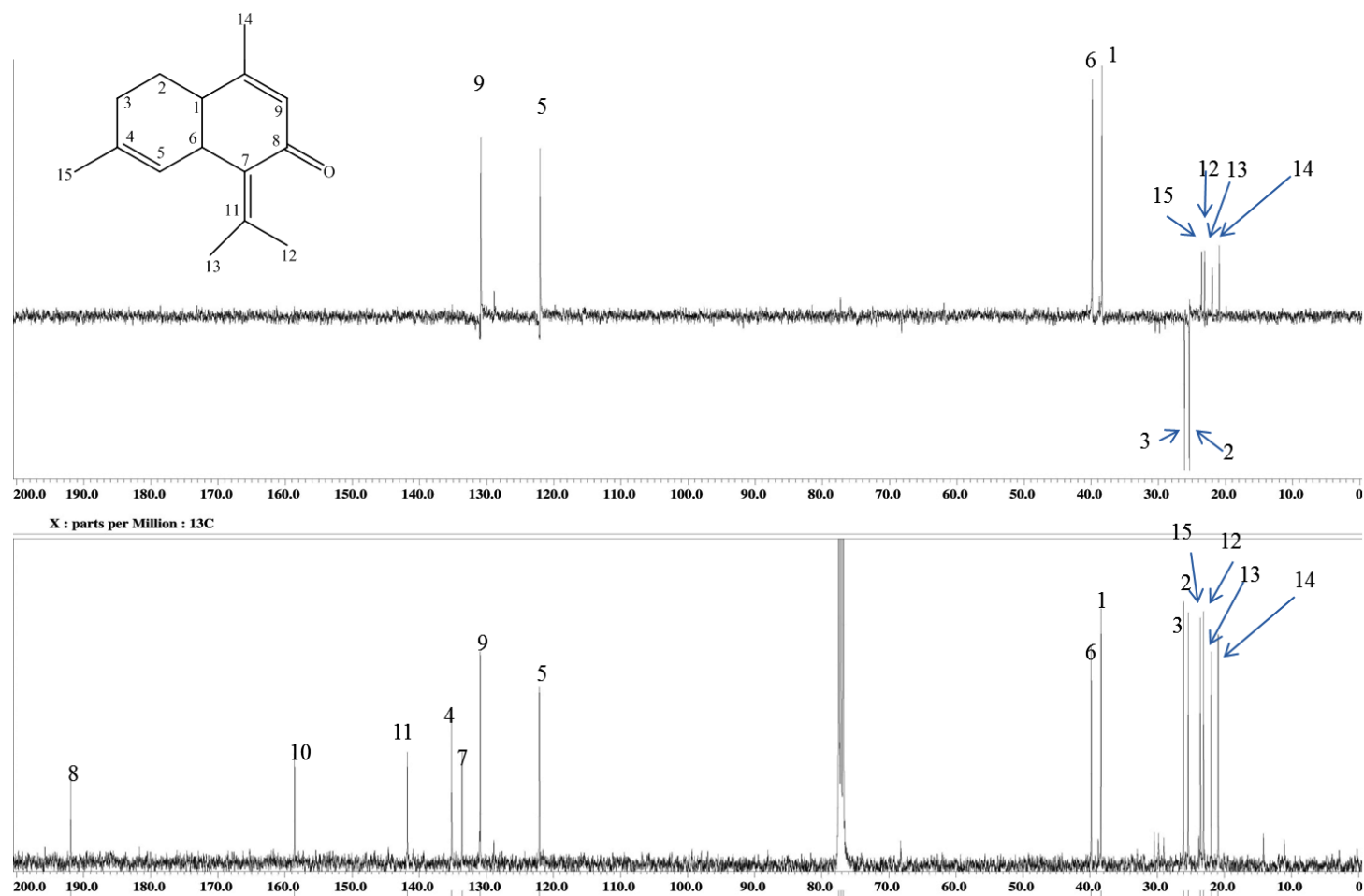


Figure 3.60: ^{13}C NMR and DEPT 135 spectra of comosone II 104

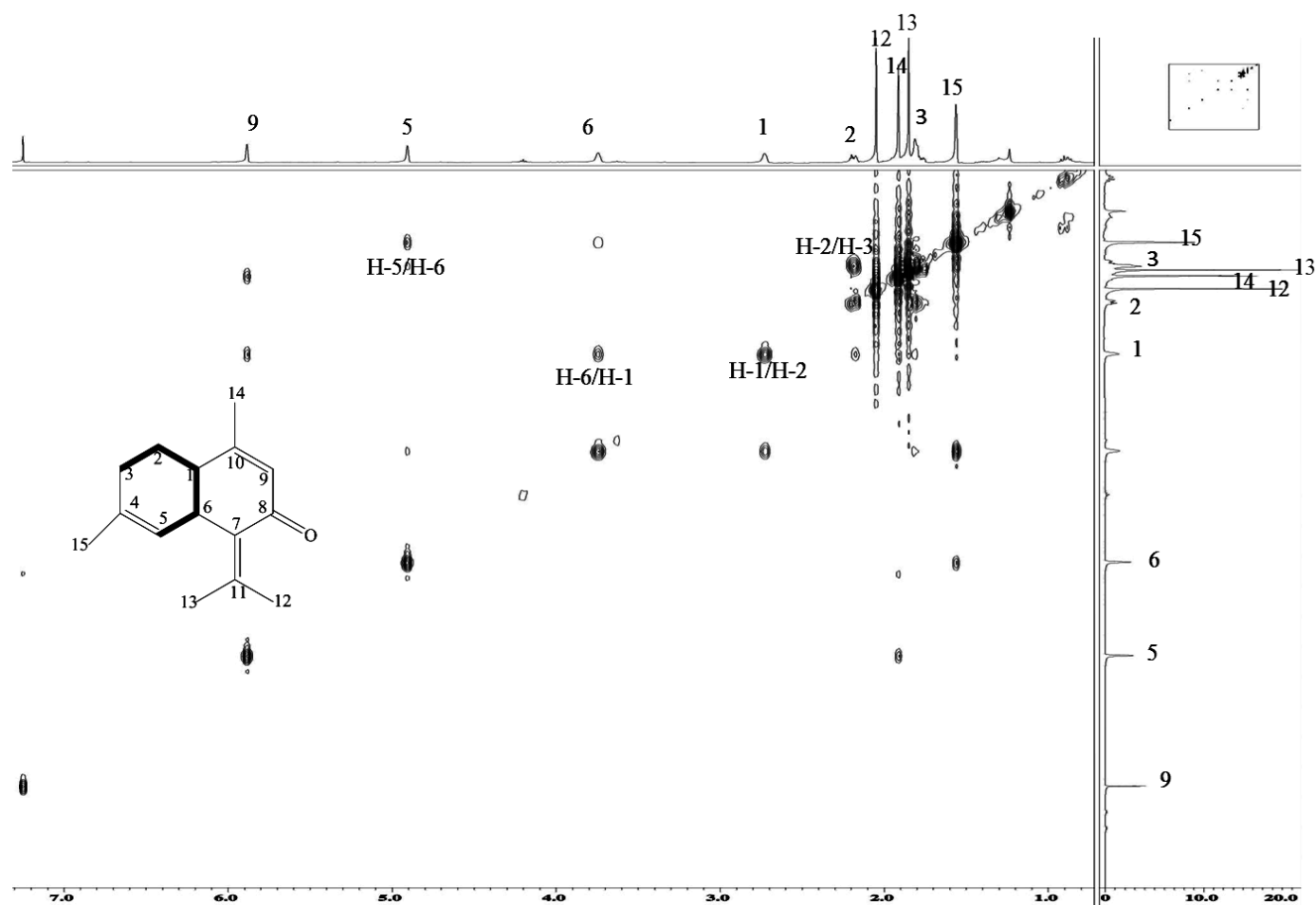


Figure 3.61: COSY spectrum of comosone II 104

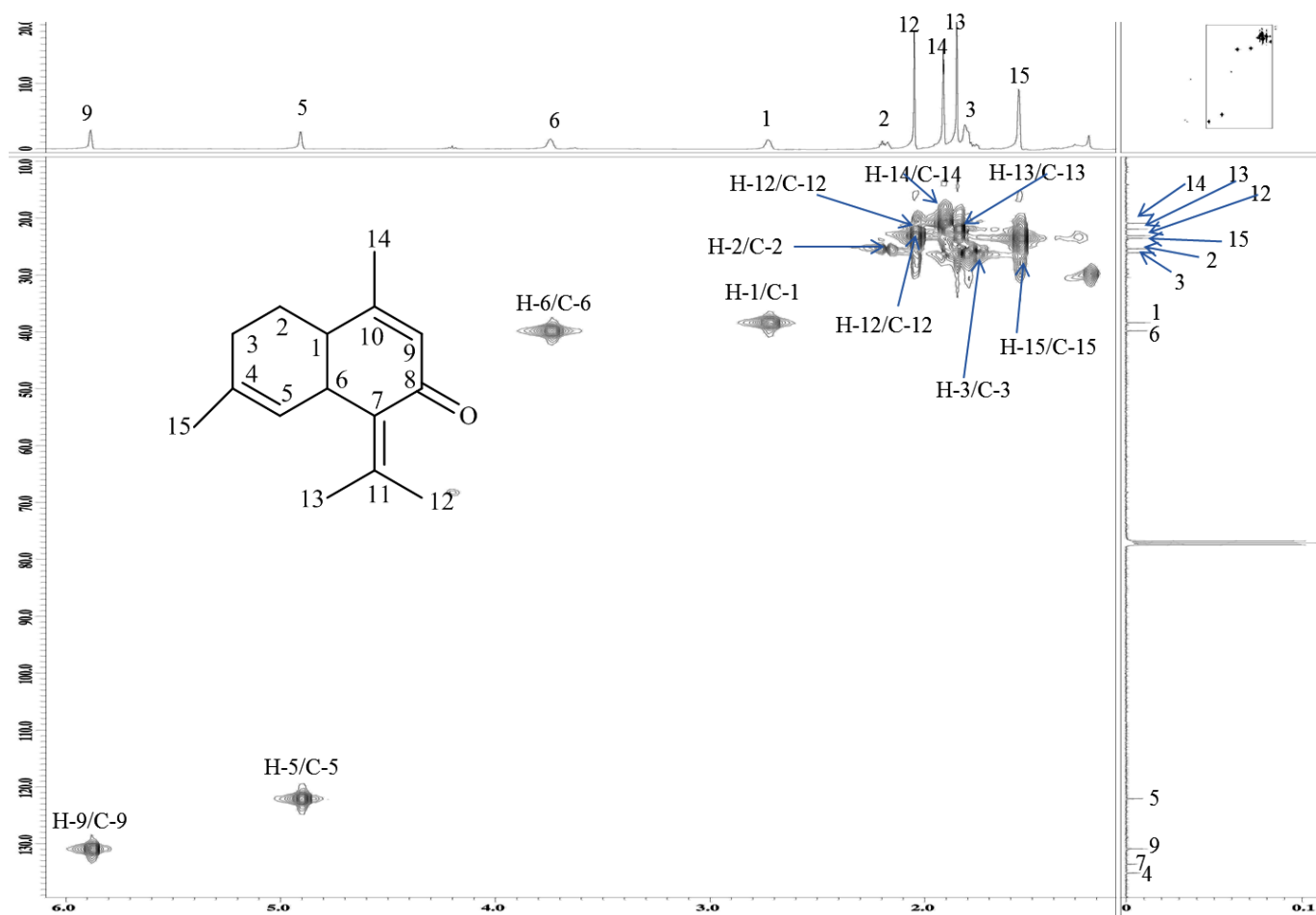


Figure 3.62: HSQC spectrum of comosone II 104

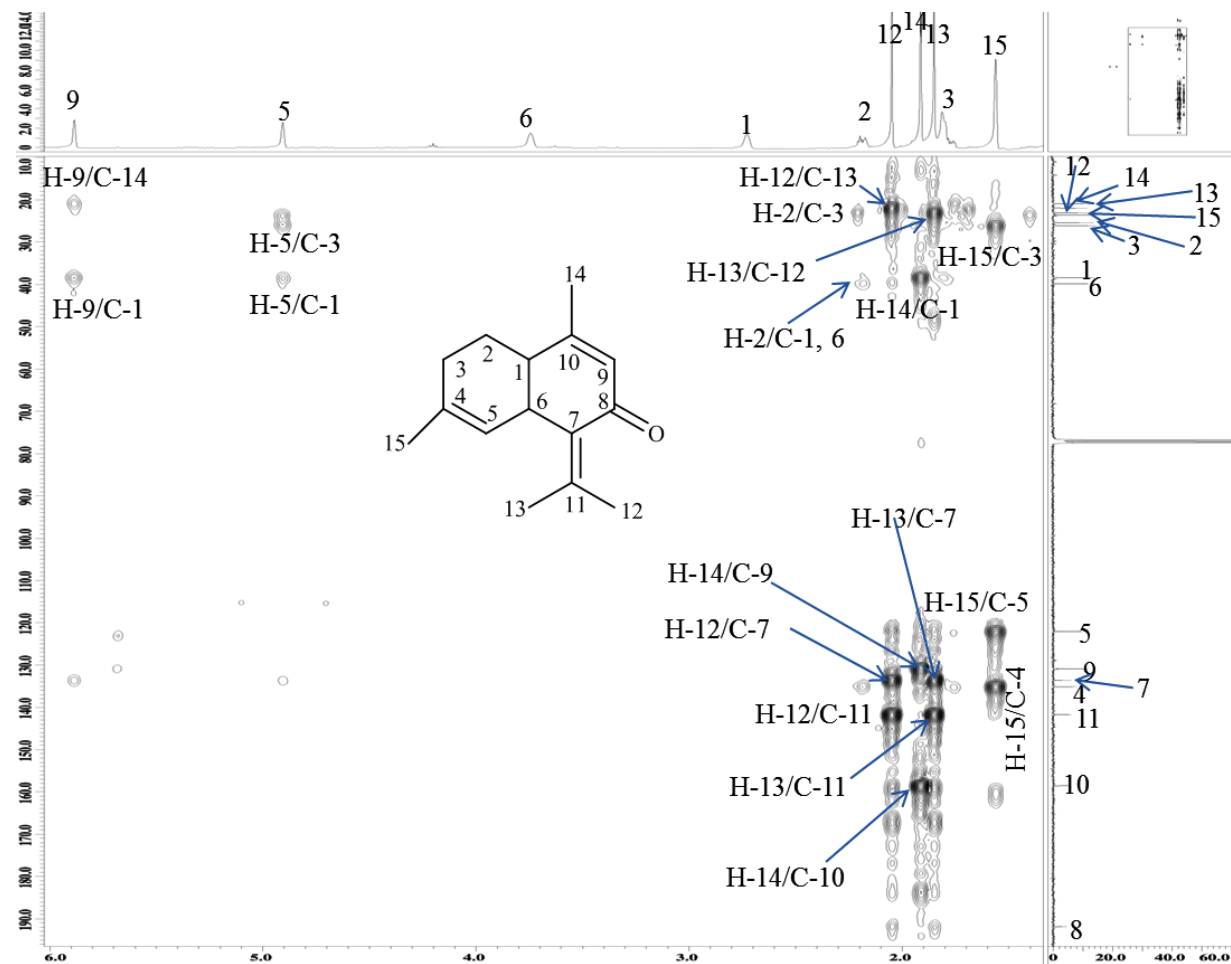
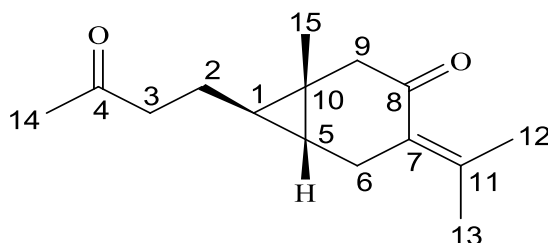


Figure 3.63: HMBC spectrum of comosone II 104

3.1.1.7 Carabrane-type sesquiterpenes

Curcumenone 65



Curcumenone **65** was isolated as a colourless oil ($[\alpha]_D^{20}$ -12.7°, c 1.0, CHCl_3). The GC-MS analysis revealed a molecular ion (M^+) peak at m/z 234 analysed for $\text{C}_{15}\text{H}_{22}\text{O}_2$. The UV (MeOH) spectrum displayed absorpotion maximum band at λ_{max} nm (log ϵ): 205 (1.28). The IR absorptions bands at 1715 cm^{-1} and 1679 cm^{-1} indicating the presence of conjugated and non-conjugated carbonyl groups, respectively.

The ^1H NMR spectrum (**Figure 3.65**, **Table 3.18**) revealed the presnce of four methyl singlets protons signals at two protons δ_{H} 2.07 (H_3 -12), 1.77 (H_3 -13), 2.12 (H-14), and 1.10 (H-15). Furthermore, four sets of methylene protons at δ_{H} 1.64 (H_2 -2), 2.47 (H_2 -3), 2.8 (H_2 -6), and 2.52 (H_2 -9). In addition, two methine protons at δ_{H} 0.43 (H-1) and 0.67 (H-5) were characteristic for a cyclopropane ring.

The ^{13}C NMR, DEPT-135, and HSQC spectra (**Figure 3.66**, **3.68**, **Table 3.18**) showed a total of 15 carbons signals corresponding to four methyls, four sp^2 methylenes, two sp^3 methines, two sp^2 quaternary carbon and two carbonyls. The four methyls signals were observed at δ_{C} 23.53 (C-12), 23.58 (C-13), 30.17 (C-14), and 19.13 (C-15). Further, four methylenes resonated at δ_{C} 23.4 (C-2), 44.0 (C-3), 28.2 (C-6), and 49.0 (C-

9), while two methines appeared at δ 24.1 (C-1), 24.2 (C-5). In addition, two sp^2 quaternary carbons at δ 128.2 (C-7), 147.4 (C-11), while one quaternary carbon sp^3 at δ 20.2. Moreover, two carbonyls at δ 209 (C-4), 201.9 (C-8).

The 1H - 1H COSY spectrum showed the correlations H-1/H-2, H-1/H-5, H-2/H-3, H-6/H-5.

In the HMBC the correlations H-1 to C-1, and C-5 indicated the presence of cyclopropane ring. Also the correlation between H-9/C-8, C-10, H-5/C-6, C-10, and H-6/C-7, C-8 confirmed the cyclohexane ring.

The 2D spectral data including COSY, HSQC and HMBC showed the skeleton having a cyclohexane ring fused to a cyclopropane ring, which is the characteristic of carborane type sesquiterpenes. Based on the above spectral data, the structure of the above compound was confirmed as curcumenone. The results were compared with the reported data for curcumenone and it was in agreement (Shiobara et al., 1985a).

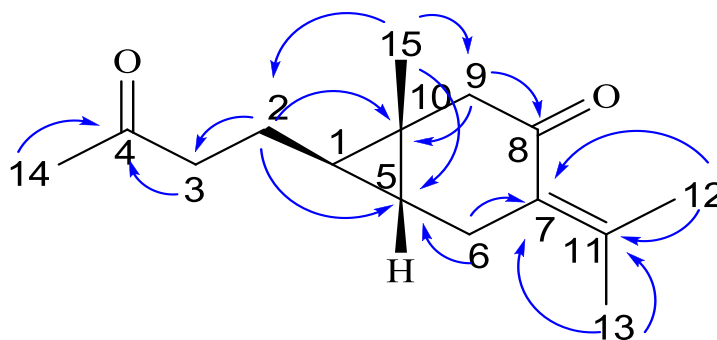


Figure 3.64: Selected HMBC Correlations H $\xrightarrow{\hspace{1cm}}$ C of *curcumenone* **65**

Table 3.18: ^1H NMR (400 MHz) and ^{13}C NMR (100 MHz) spectral data in CDCl_3 of *curcumenone* **65** in CDCl_3

Posit ion	δ_{H}, J (Hz)	δ_{C}
1	0.43, dt (4.56, 7.32)	24.1
2	1.64, q (7.32)	23.4
3	2.47, t (7.36)	44.0
4	-	209
5	0.67, q (4.56)	24.2
6	2.8, m	28.2
7	-	128.1
8	-	201.9
9	2.52, d (15.6)	49.0
10	-	20.2
11	-	147.6
12	2.07, s	23.5
13	1.77, s	23.5
14	2.12, s	30.1
15	1.10, s	19.1

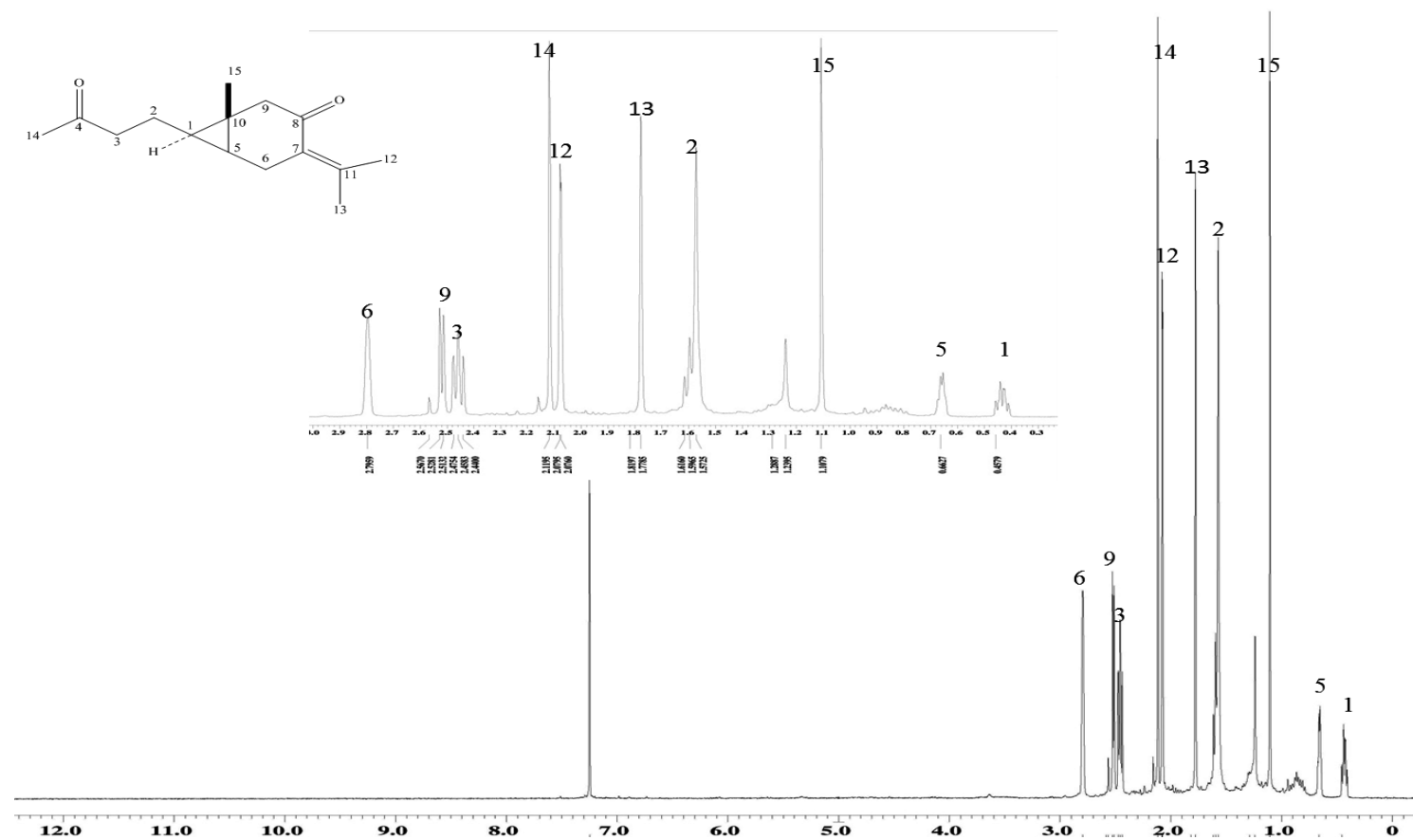


Figure 3.65: ^1H NMR spectrum of *curcumenone* **65**

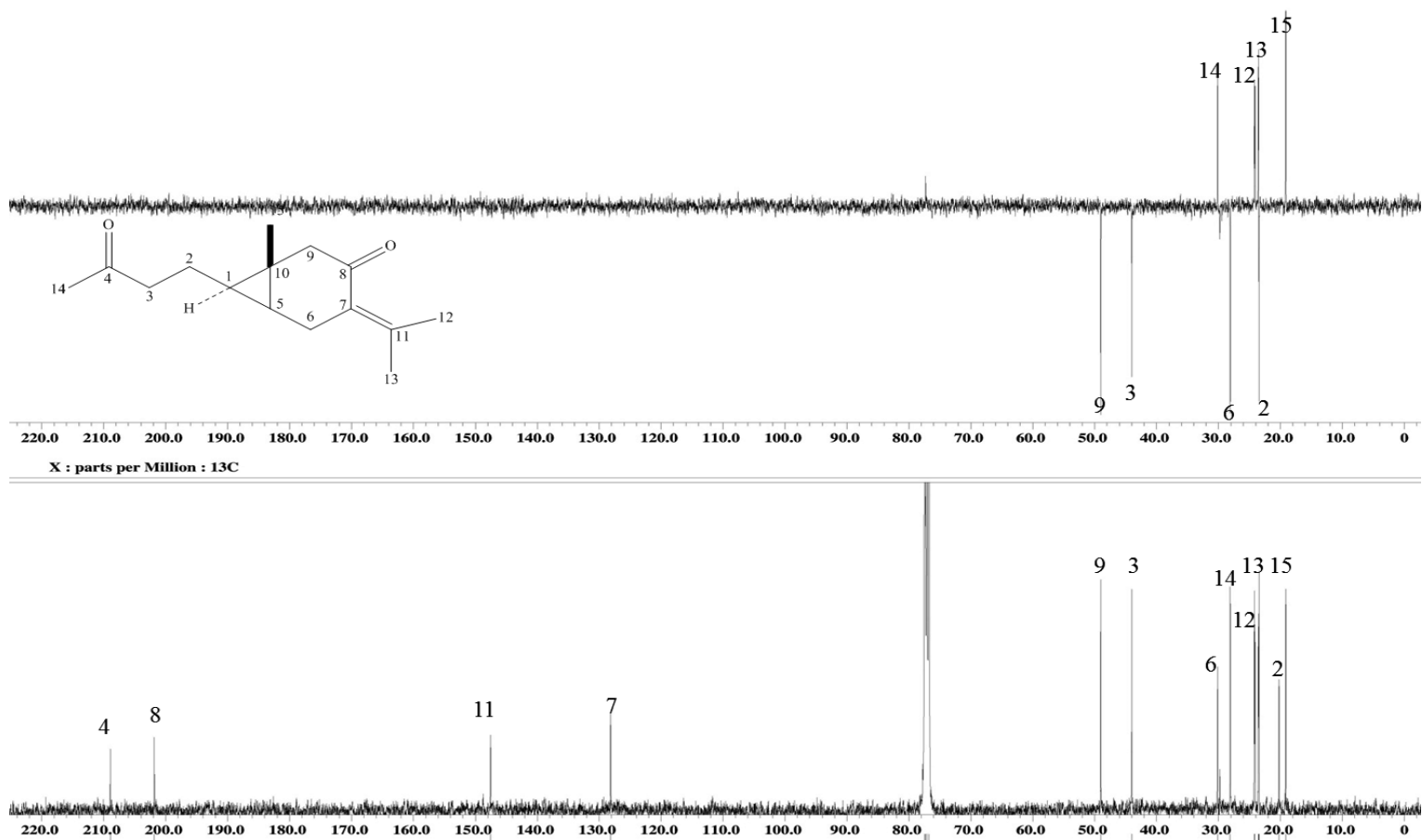


Figure 3.66: ^{13}C NMR and DEPT-135 spectra of curcumenone

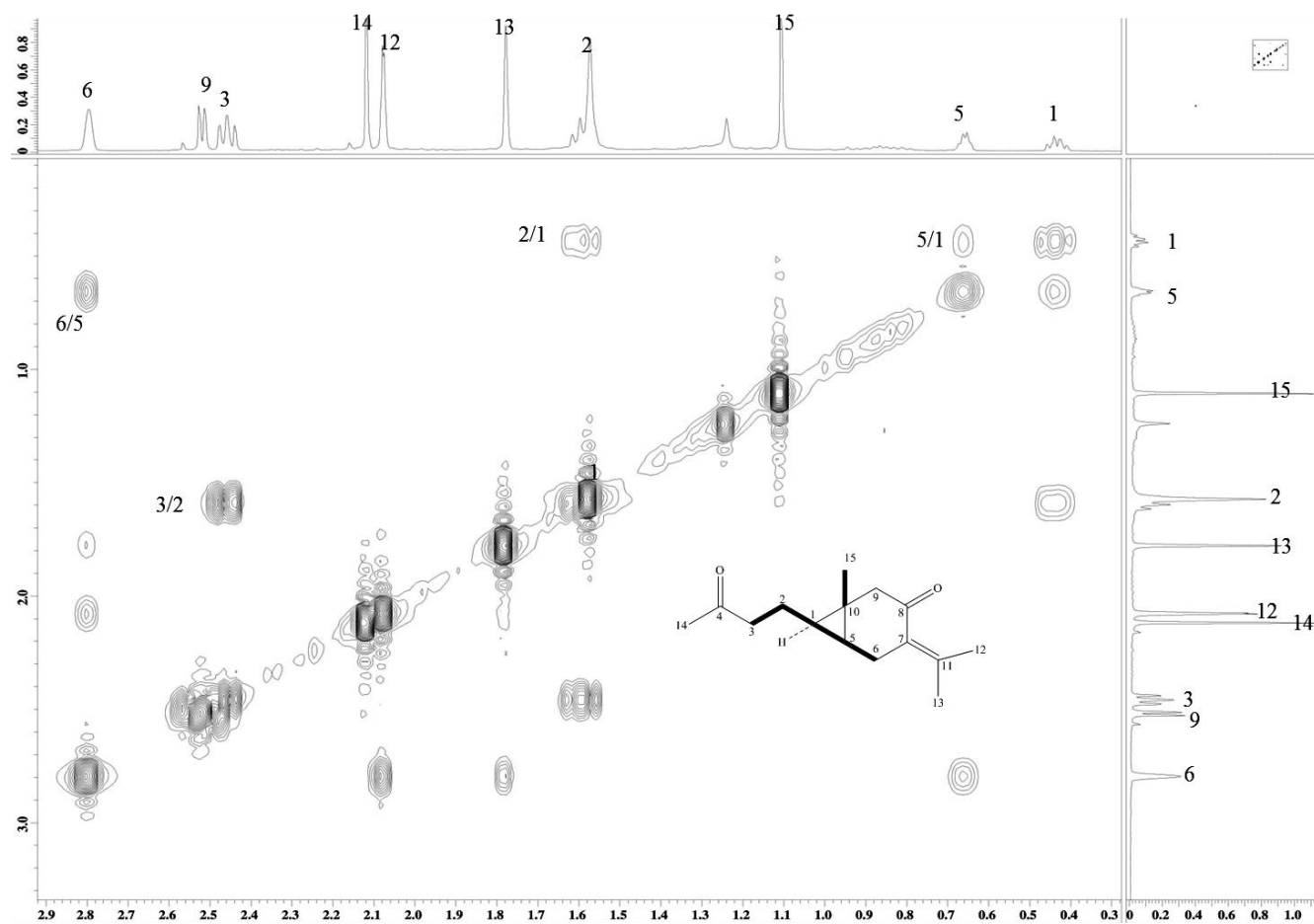


Figure 3.67: COSY spectrum of curcumenone **65**

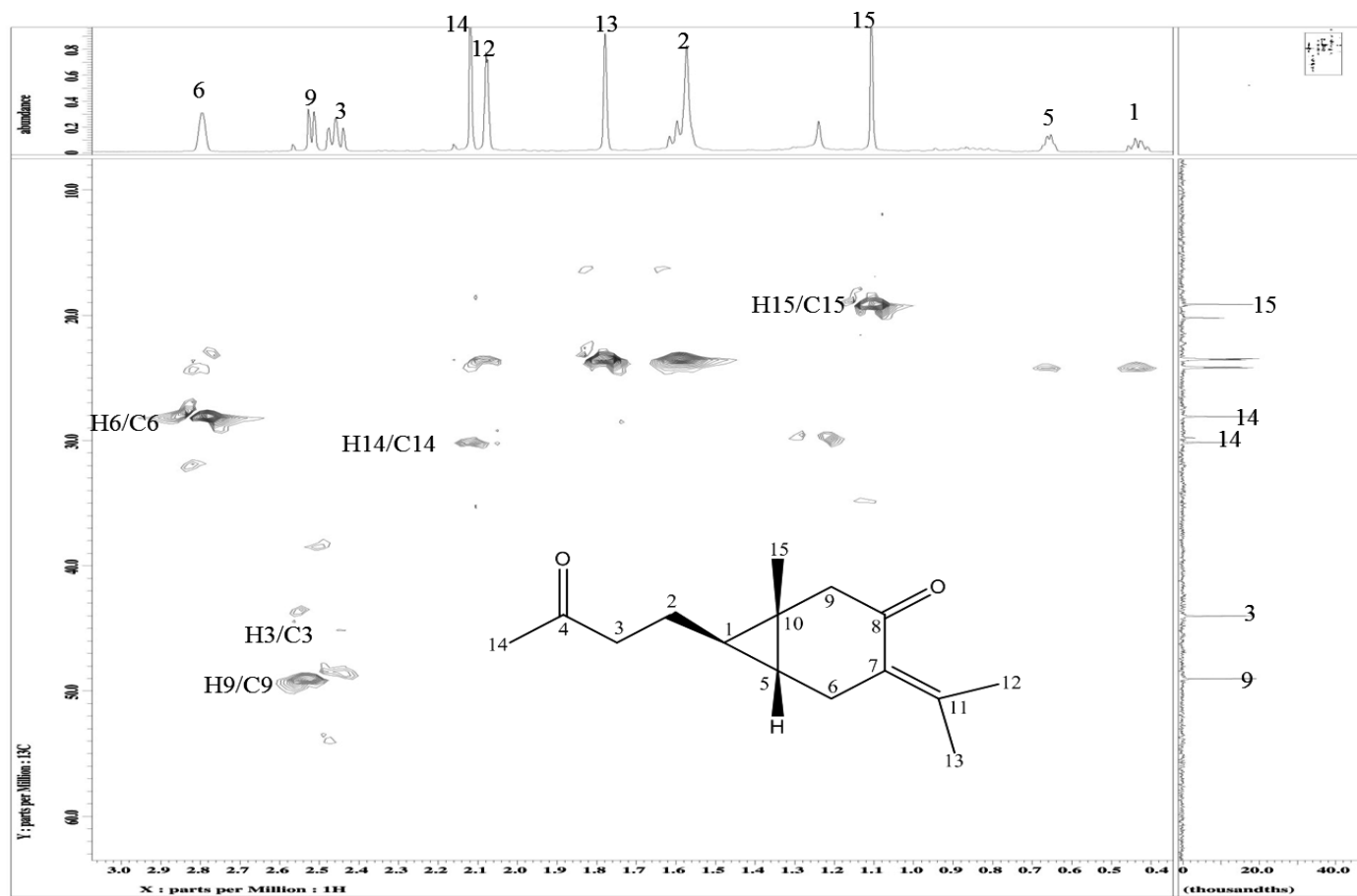


Figure 3.68: HSQC spectrum of curcumenone **65**

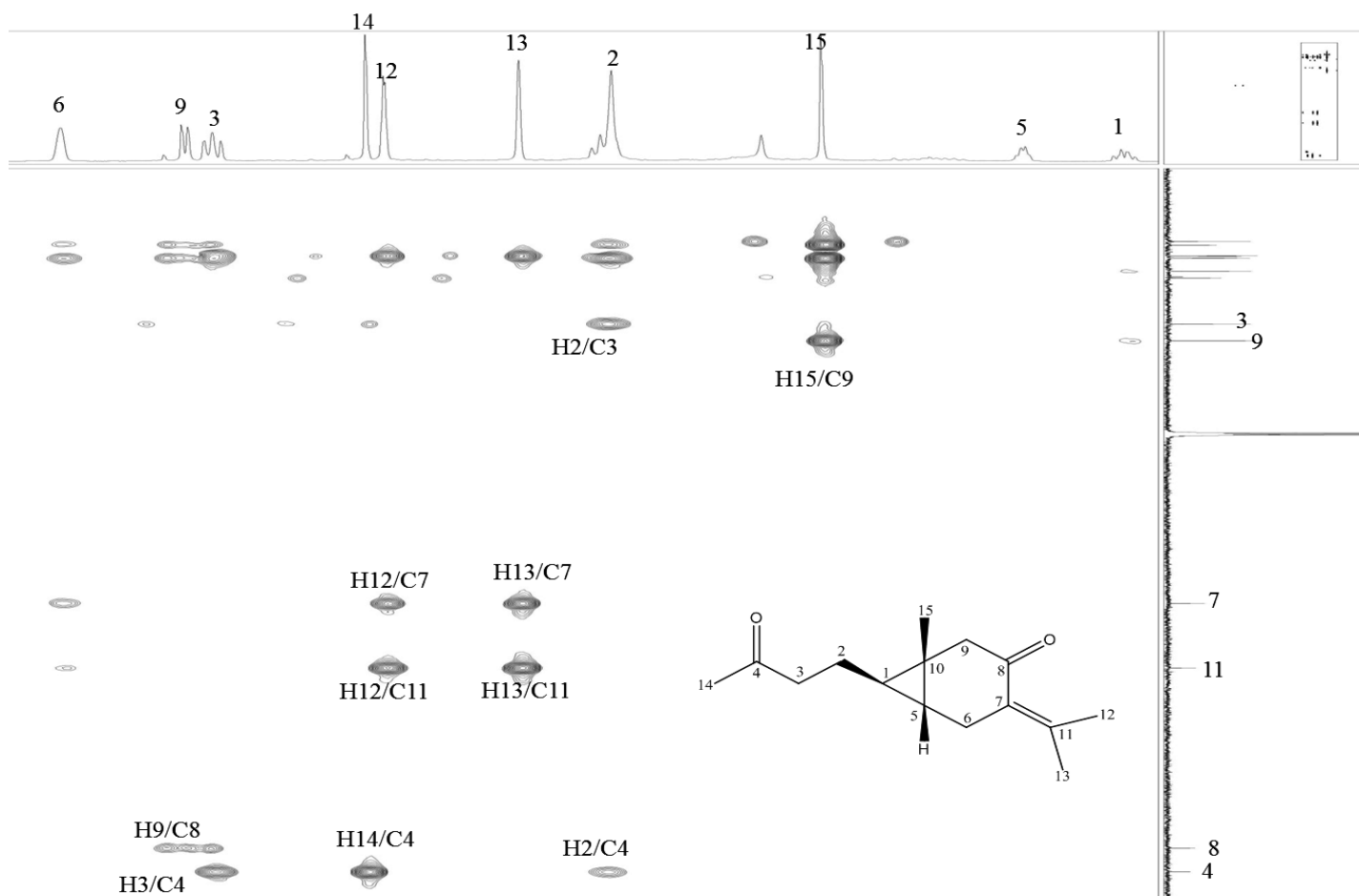


Figure 3.69: : HMBC spectrum of curcumenone (cont.)

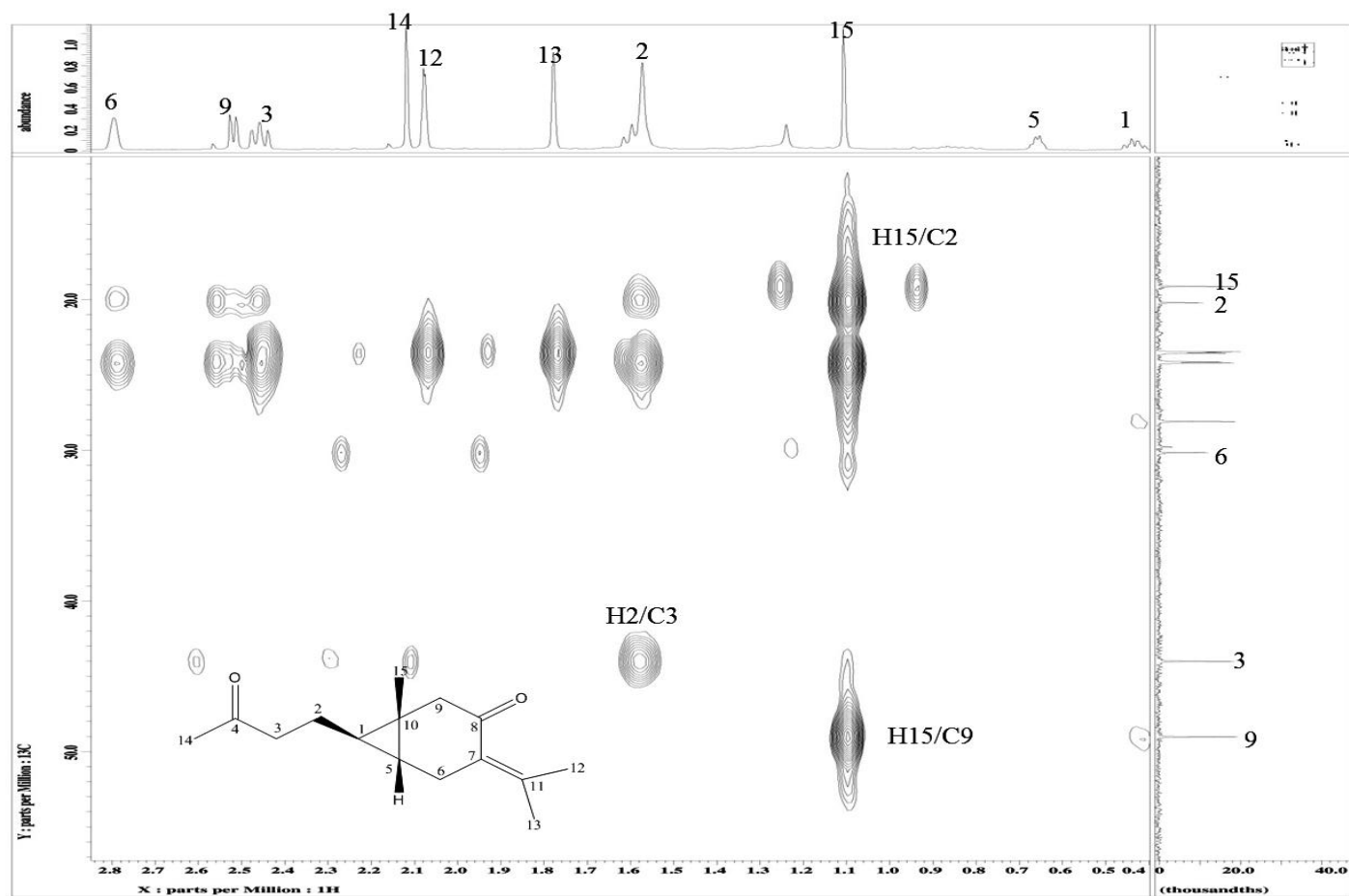
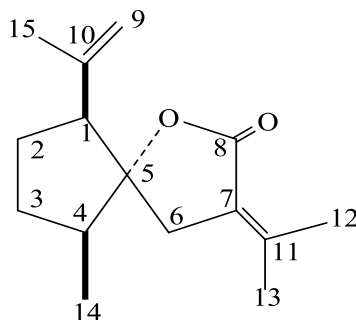


Figure 3.69: HMBC spectrum of curcumenone

3.1.1.8 Spirolactone type sesquiterpenes

Curcumanolide 101



Curcumanolide A 101 was obtained as a colourless oil ($[\alpha]_D^{20}$ -23° , c 1.0, CHCl_3). The GC-MS analysis revealed the molecular formula of $\text{C}_{15}\text{H}_{22}\text{O}_2$ worked out from molecular ion peak (M^+) at m/z 234. The IR absorption at 1717 cm^{-1} indicated the presence of a carbonyl group. The UV spectrum showed absorption at 218 nm suggested for a conjugated system.

The ^1H NMR spectrum (**Figure 3.71, Table 3.19**) displayed four methyl proton singlets at δ_{H} 1.82 (H_3 -15), 0.86 (H_3 -14), 1.83 (H_3 -13), and 2.22 (H_3 -12). Four methylenes were observed at δ_{H} 1.65, 1.82 (H_2 -2), 1.83, 2.22 (H_2 -3), 2.44 (H_2 -6), and 4.74, 4.93 (H_2 -9). In addition to two methines were detected at δ_{H} 2.83 (H_1) and 2.32 (H_4).

The ^{13}C NMR, DEPT-135, and HSQC spectra (**Figure 3.72, 3.74, Table 3.19**) revealed a total of 15 carbons corresponding to four sp^3 methyls at δ_{C} : 19.9 (C-15), 13.1 (C-14), 23.9 (C-13), and 24.4 (C-12), three sp^3 methylenes at δ_{C} 26.5 (C-2), 23.22 (C-3), 27.6 (C-6). In addition to one sp^2 exo-methylene signal appeared at δ_{C} 112 (C-9) and two sp^3 methine carbons observed at δ_{C} 52.3 (C-1) and 42.8 (C-4).

The ^1H - ^1H COSY correlations observed H-1/H-2, H-2/H-3, H-3/H-4, H-4/H-14 coupled with HMBC correlations of the cross peaks of H-14 to C-4, H-4/C-5, H-1/C-5 indicated that the five membered ring linked to the other ring through the connection C-5. In addition, H-12 and H-13 were correlated to C-11 and C-7. These observations indicated that dimethyl ethylene connected to C-7 to the other ring, further H-6 showed correlation to C-9 and 8. Therefore, all these evidence supported the presence of spirolactone skeleton. From the analysis of the spectral data observed of compound **101** together with the literature data values, the identity of **101** was established as *curcumanolide A* (Shiobara et al., 1985a).

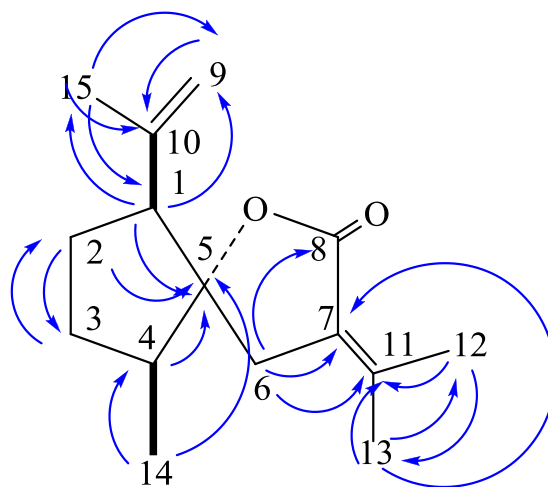


Figure 3.70: Selected HMBC Correlations H \rightarrow C of *curcumanolide A* **101**

Table 3.19: ^1H NMR (400 MHz), and ^{13}C NMR (100 MHz) spectral data of *curcumanolide* A **101**

Position	δ_{H}, J (Hz)	δ_{C}
1	2.83,dd (11.5, 8.7)	52.3
2	1.65, 1.82, m	26.5
3	1.83, 2.22, m	23.2
4	2.32, m	42.8
5	-	89.7
6	2.44, brs	27.6
7	-	120.8
8	-	169.9
9	4.74, 4.93, s	112.7
10	-	149.4
11	-	143.8
12	2.22, brs	24.4
13	1.83, s	23.9
14	0.86, s	13.1
15	1.82, s	19.9

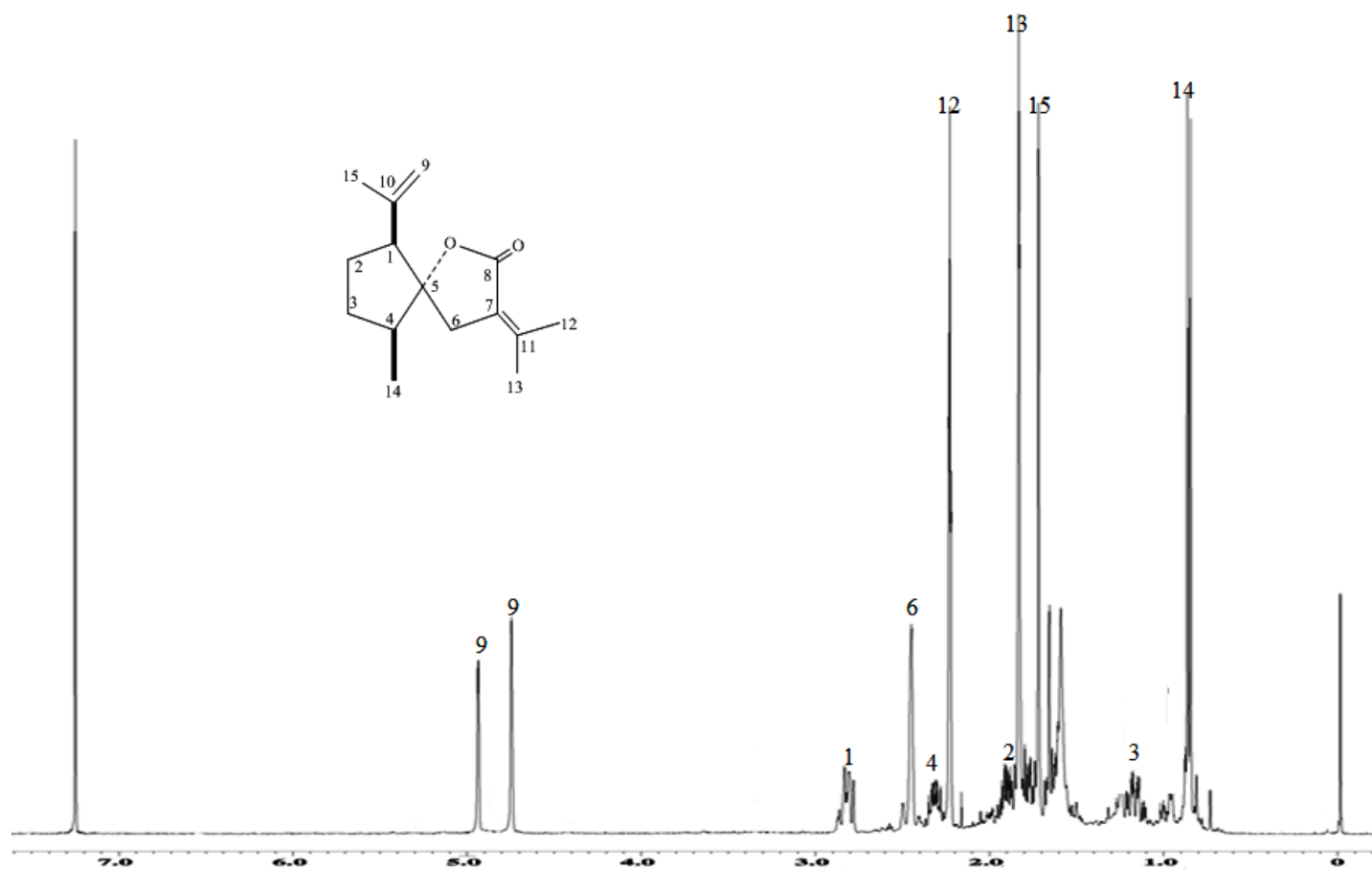


Figure 3.71: ^1H NMR spectrum of curcumenolide A 101

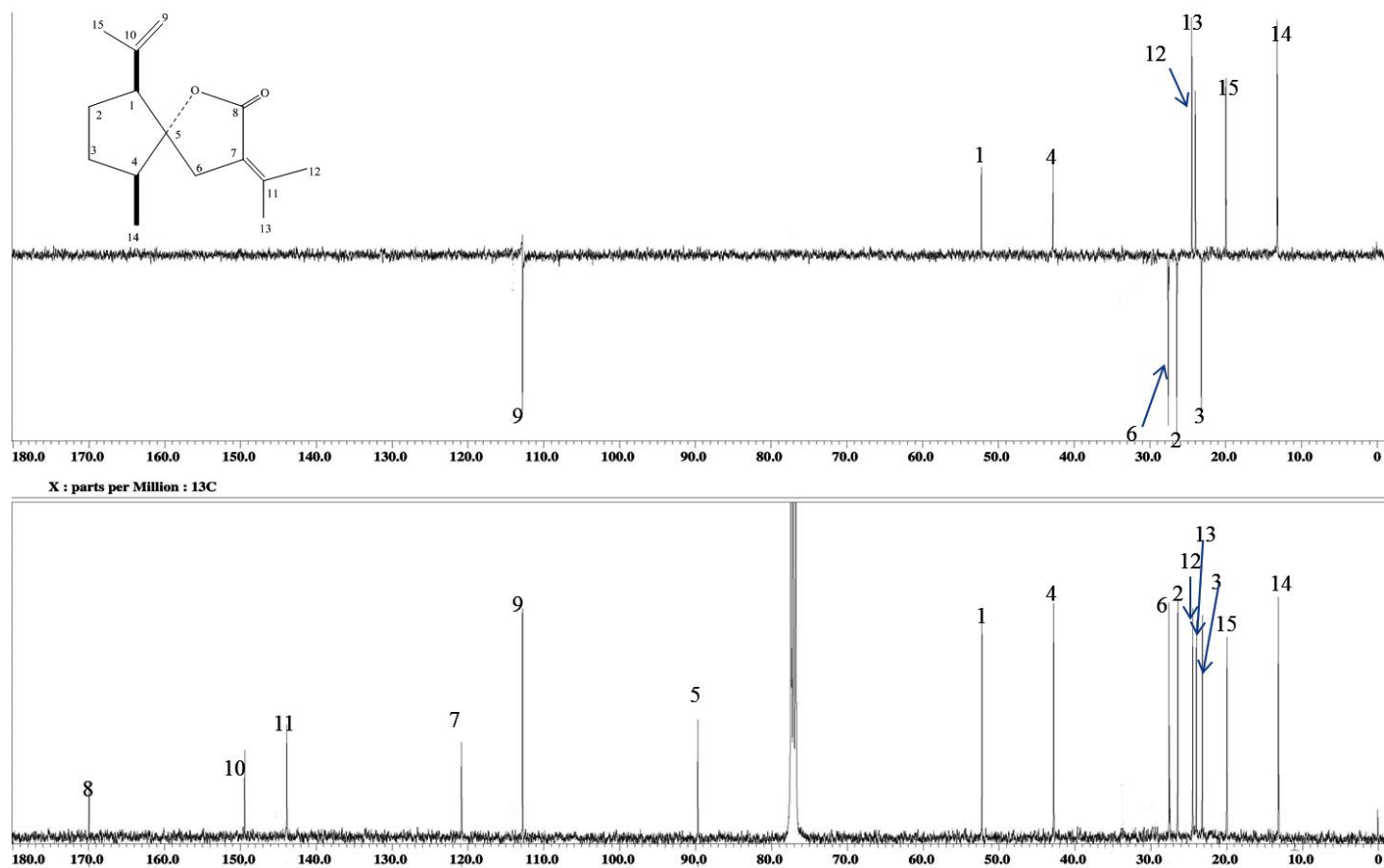


Figure 3.72: ^{13}C NMR and DEPT spectra of curcumenolide A 101

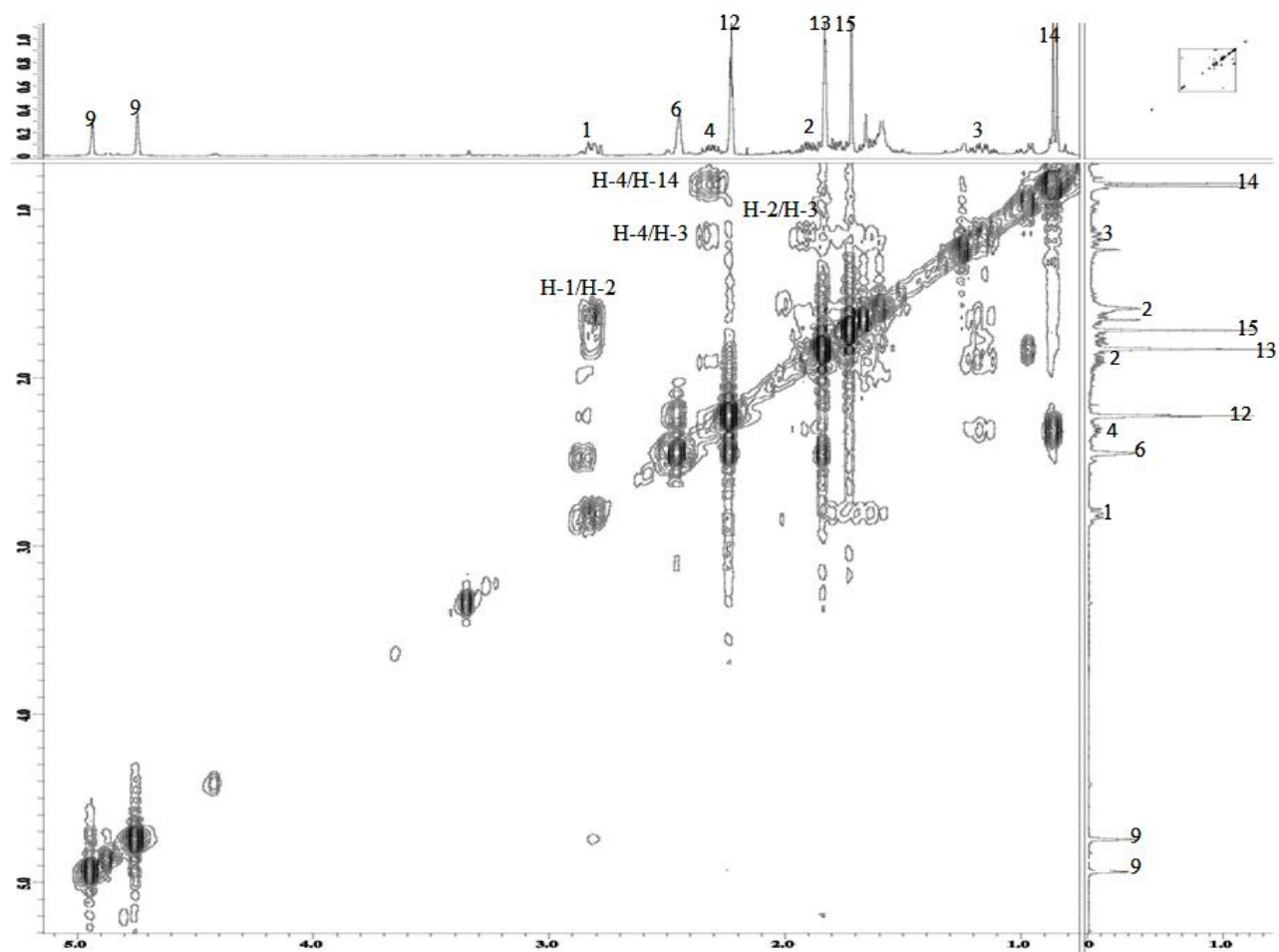


Figure 3.73: COSY spectrum of curcumenolide A 101

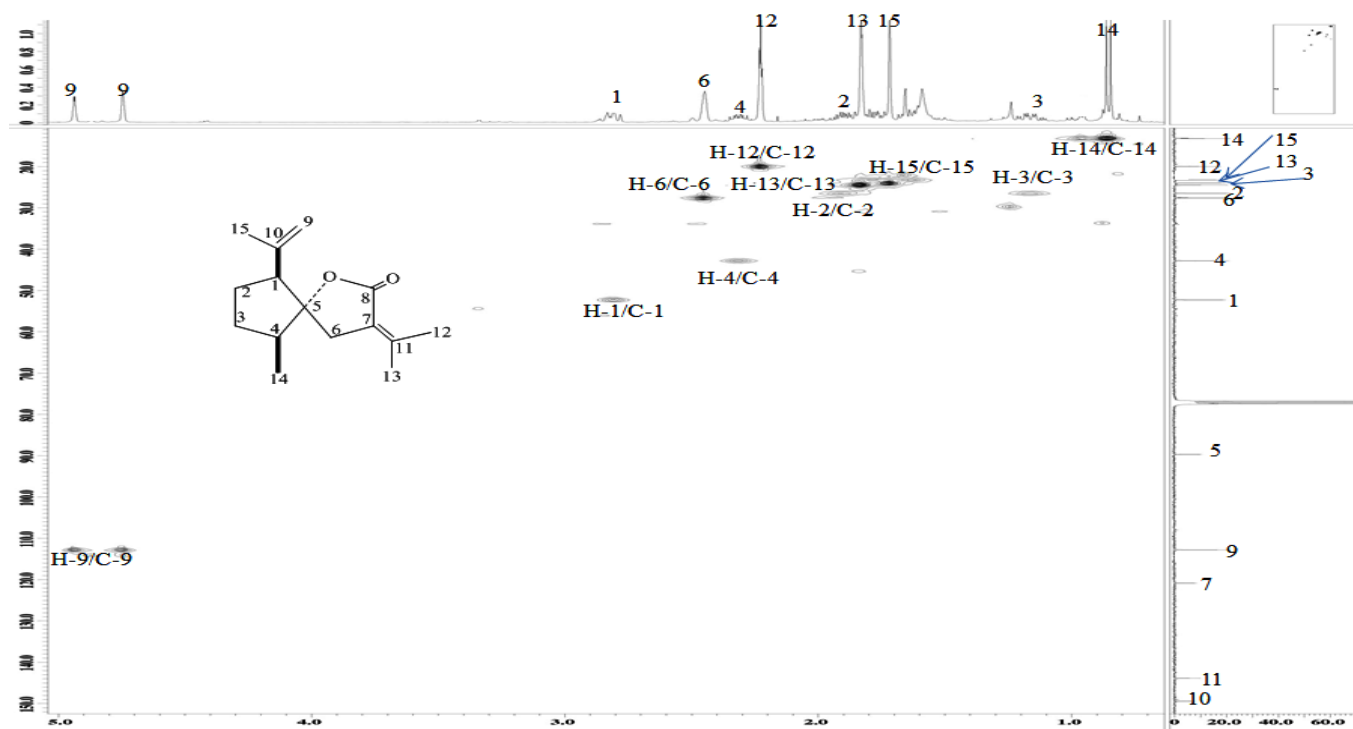


Figure 3.74: HSQC spectrum of curcumenolide A 101

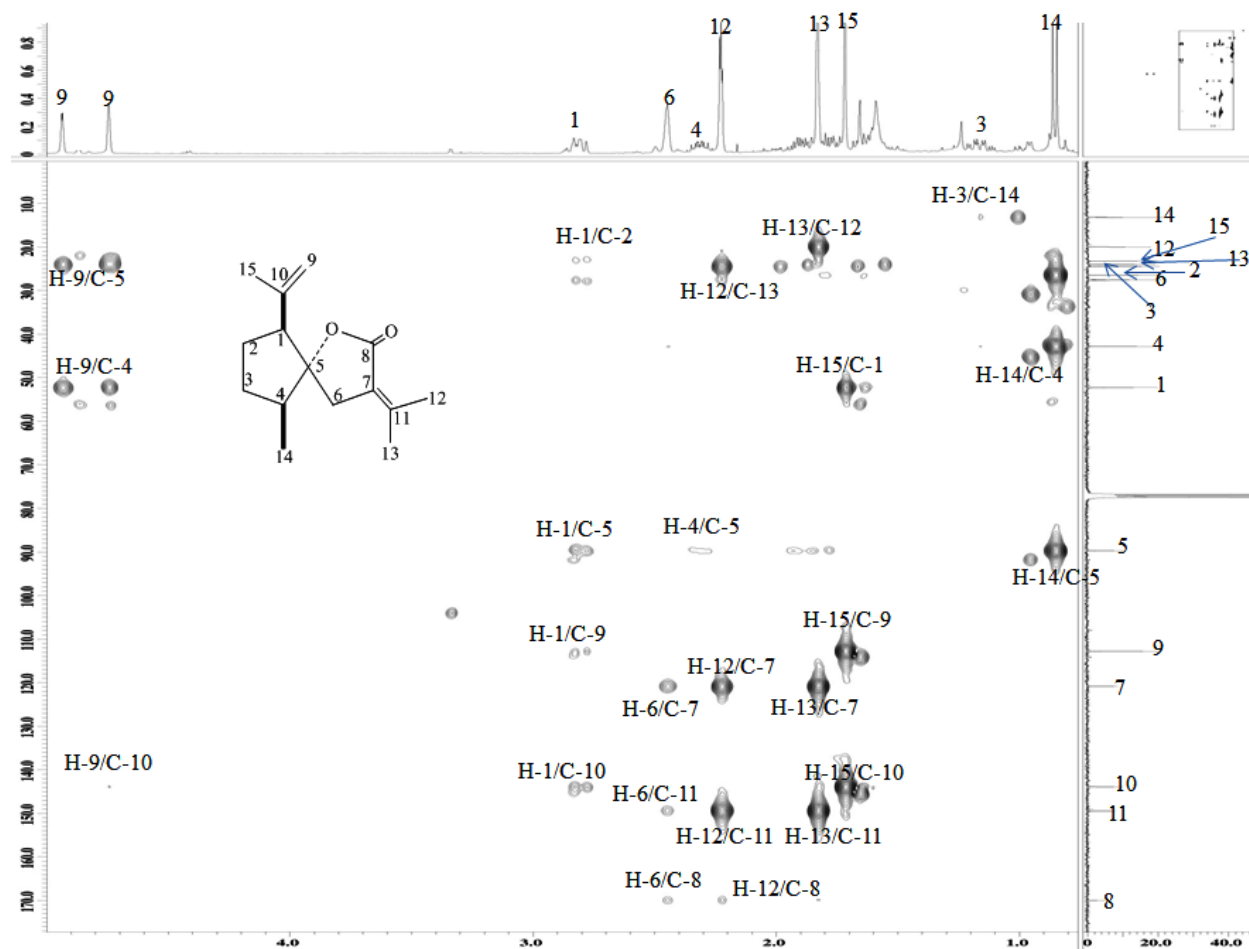
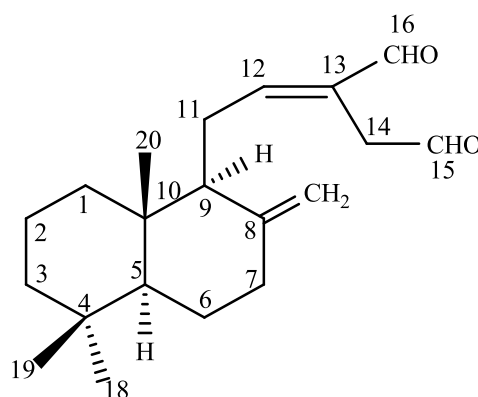


Figure 3.75: HMBC spectrum of curcumenolide A 101

3.1.1.9 Labdane type diterpenoids isolated from *C. zedoaria* rhizomes

Three labdane type diterpenoids were isolated for the first time from *C. zedoaria*. Two of them were obtained from the hexane extract, namely labda-8(17),12-diene-15,16-dial **127**, labda-8(17),12-diene-15,15-dimethoxy-16-al, also known as calcaratarin A **128**, and zerumin A **129**.

Labda-8(17), 12 diene-15, 16 dial **127**



Labda-8(17),12 diene-15,16 dial **127** was obtained as colourless oil. The GC-MS analysis showed a molecular ion peak at m/z 302 (M^+) corresponding to a molecular formula of $C_{20}H_{30}O_2$. The UV spectrum (MeOH) showed absorption bands at λ_{max} 226 and 208 nm ($\log \epsilon$ 1.969 and 2.77, respectively). The IR absorptions at 1683 cm^{-1} (carbonyl) and 889 cm^{-1} (exomethylene).

The ^1H NMR spectrum (**Figure 3.77**, **Table 3.20**) showed some proton signals common to labdane type diterpenoids with three methyl singlets at δ_H 0.71, 0.80 and 0.87 assignable for H_3 -20, H_3 -19, and H_3 -18, respectively. In addition, a pair of broad singlets assignable to the exomethylene protons were observed at δ_H 4.37 (H -17_a) and 4.84 (H -17_b) which is another characteristic feature of bicyclic labdane diterpenoids. The proton signals at δ_H 9.62 (*s*), 9.38 (*s*) indicated the presence of two aldehyde protons and were assigned for H -16 and H -15, respectively. Six sets of methylene protons resonated as multiplets at δ_H 1.07, 1.72 (H_2 -1), 1.52, 1.58 (H_2 -2), 1.22, 1.42 (H_2 -

3), 1.34, 1.76 (H₂-6), 2.03, 2.42 (H₂-7), 2.34, 2.50 (H₂-11), while the methylene protons H₂-14 appeared as a pair of doublets dd at δ_H 3.39 with $J=16$. The methine signal at δ_H 6.75 resonated as a triplet with $J=6.4$ Hz was assigned to H-12. In addition, a doublet with $J=11.4$ Hz at δ_H 1.92 can be attributed to H-9 and while the other methine proton H-5, resonated as dd ($J=2.8, 12.8$) at δ_H 1.3.

The ¹³C NMR, DEPT-135 and HSQC spectra (**Figure 3.78, 3.80, Table 3.20**) displayed a total of 20 carbons; three sp³ methyls at δ_C 14.4 (C-20), 21.8 (C-19), and 33.6 (C-18), seven sp² methylenes at δ_C 39.3 (C-1), 19.3 (C-2), 42.0 (C-3), 24.1 (C-6), 37.9 (C-7), 24.7 (C-11), and δ_C 39.4 (C-14), one sp² methylene at δ_C 107.9 (C-17), two sp³ methine at δ_C 55.4 (C-5), and 56.5 (C-9), one sp² methine at δ_C 160.1 (C-12). The value of C-12 was shifted downfield due to the influence of the nearby carbonyl group. Two sp³ quaternary carbons were observed at δ_C 33.6 (C-4), and 39.6 (C-10), two sp² quaternary carbons at δ_C 148.1 (C-8), and 134.9 (C-13), and two carbonyls at δ_C 193.6 (C-16), and 197.4 (C-15). The presence of the three methyls C-18, C-19, C-20, a methylene C-17, and an sp² quaternary carbon C-8 further evidenced the nature of a labdane type diterpenoid.

The ¹H-¹H COSY correlations observed; H-11/H-12, H₂-14/H-15 (aldehydic proton) coupled with HMBC correlations observed cross peaks between H-12 to C-14, and C-16, aldehydic proton H-16 to C-13, and H₂-14 to C-13, C-15, C-16 established the substructure of the side chain; -CH₂-CH=C(CHO)-CH₂-CHO. The HMBC correlation of C-9 and H-12 together with the 1H-1H COSY crosspeak H-9/H-11, indicated that the side chain is connected to the main labdane skeleton through C-9.

Extensive inspection of the spectral data (HMBC, HSQC, COSY) concluded the structure of the compound as labda-8(17),12 diene-15,16 dial **127**. The spectral data complied with the published literature data (Roth et al., 1998).

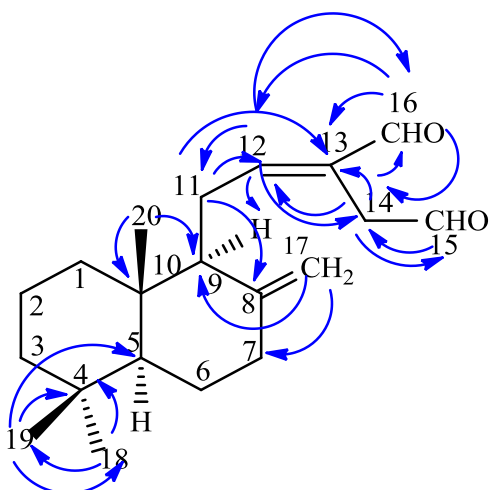


Figure 3.76: Selected HMBC Correlations H \rightarrow C of labda-8(17),12 diene-15,16 dial **127**

Table 3.20: ^1H NMR (400 MHz) and ^{13}C NMR (100 MHz) spectral data in CDCl_3 of labda-8(17),12 diene-15,16 dial **127**

Position	$\delta_{\text{H}}, J \text{ (Hz)}$	δ_{C}
1	1.07, 1.72, m	39.3
2	1.52, 1.58, m	19.3
3	1.22, 1.42, m	42.0
4	-	33.6
5	1.3, dd (2.8, 12.8)	55.4
6	1.34, 1.76, m	24.1
7	2.0.3, m, 2.42,	37.9
8	-	148.1
9	1.92, d (11)	56.5
10	-	39.6
11	2.34, 250, m	24.7
12	6.75, t (6.4)	159.5
13	-	160.1
14	3.39, d (16.4)	39.4
15	9.62, s	197.4
16	9.38, s	193.6
17	4.35, 4.85, br.s	107.9
18	0.87, s	33.6
19	0.80, s	21.8
20	0.71, s	14.4

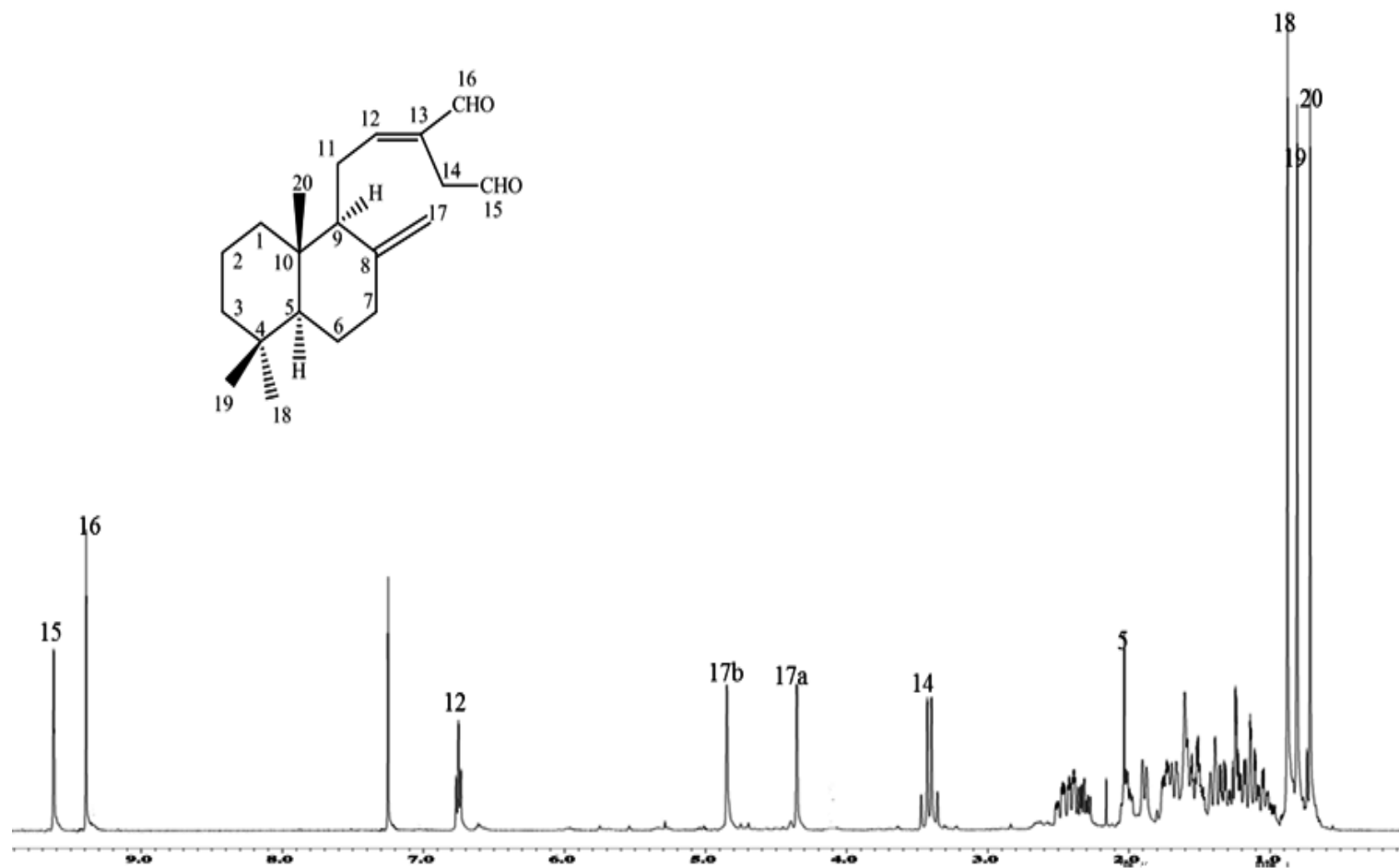


Figure 3.77: ^1H -NMR spectrum of labda-8(17), 12-diene-15, 16-dial **127**

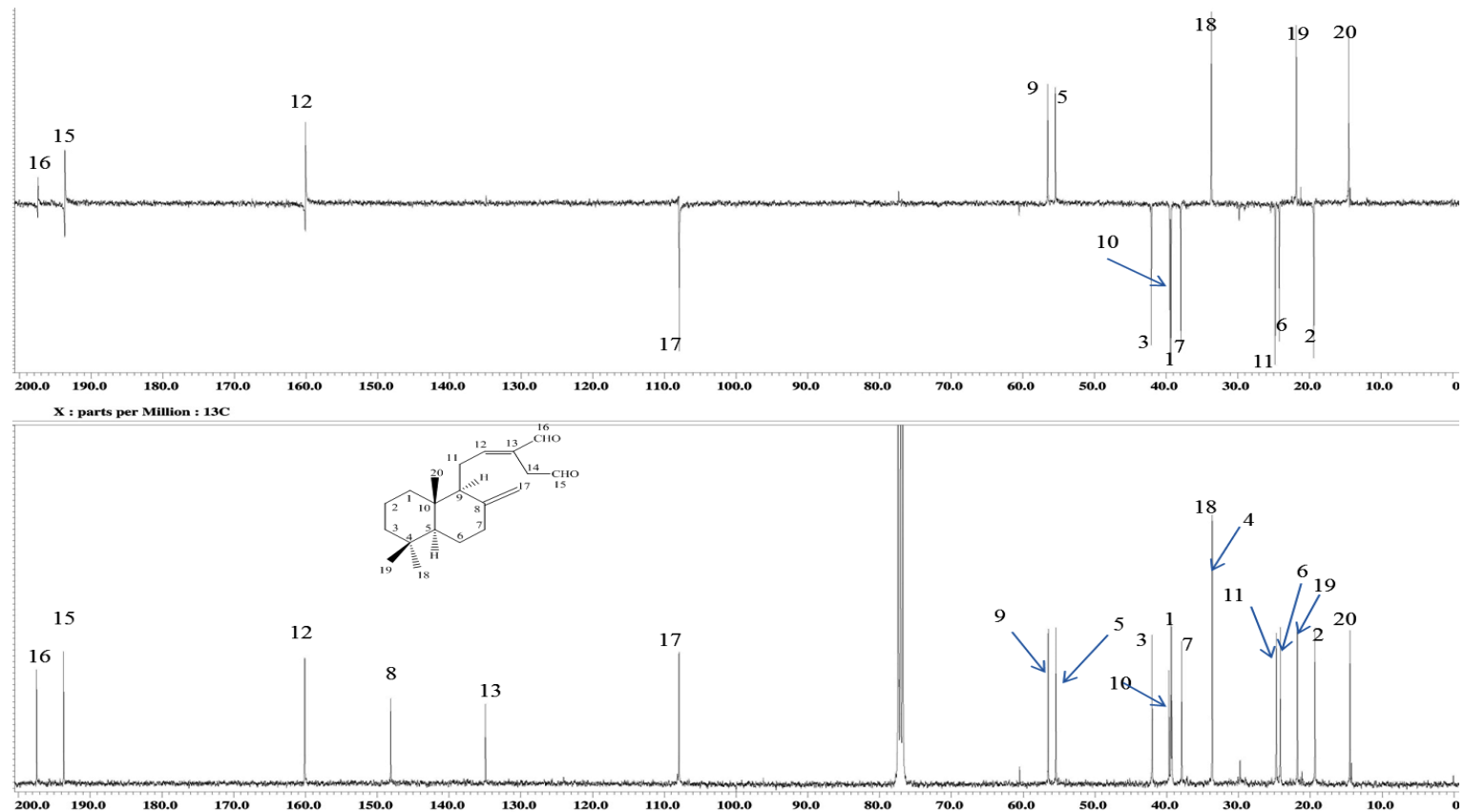


Figure 3.78: ^{13}C and DEPT-135 spectra of labda-8(17), 12-diene-15, 16-dial **127**

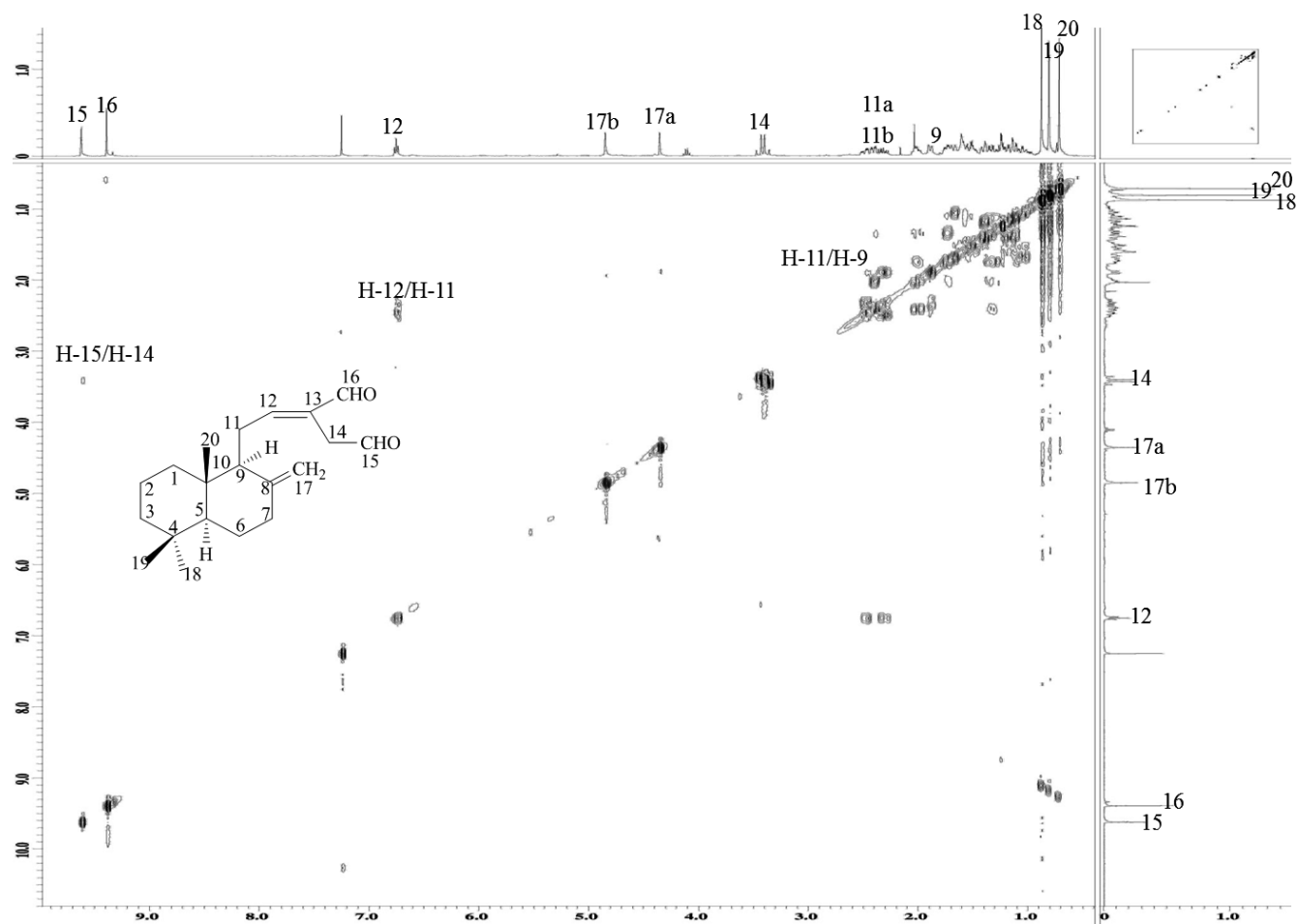


Figure 3.79: COSY spectrum of labda-8(17), 12-diene-15, 16-dial **127**

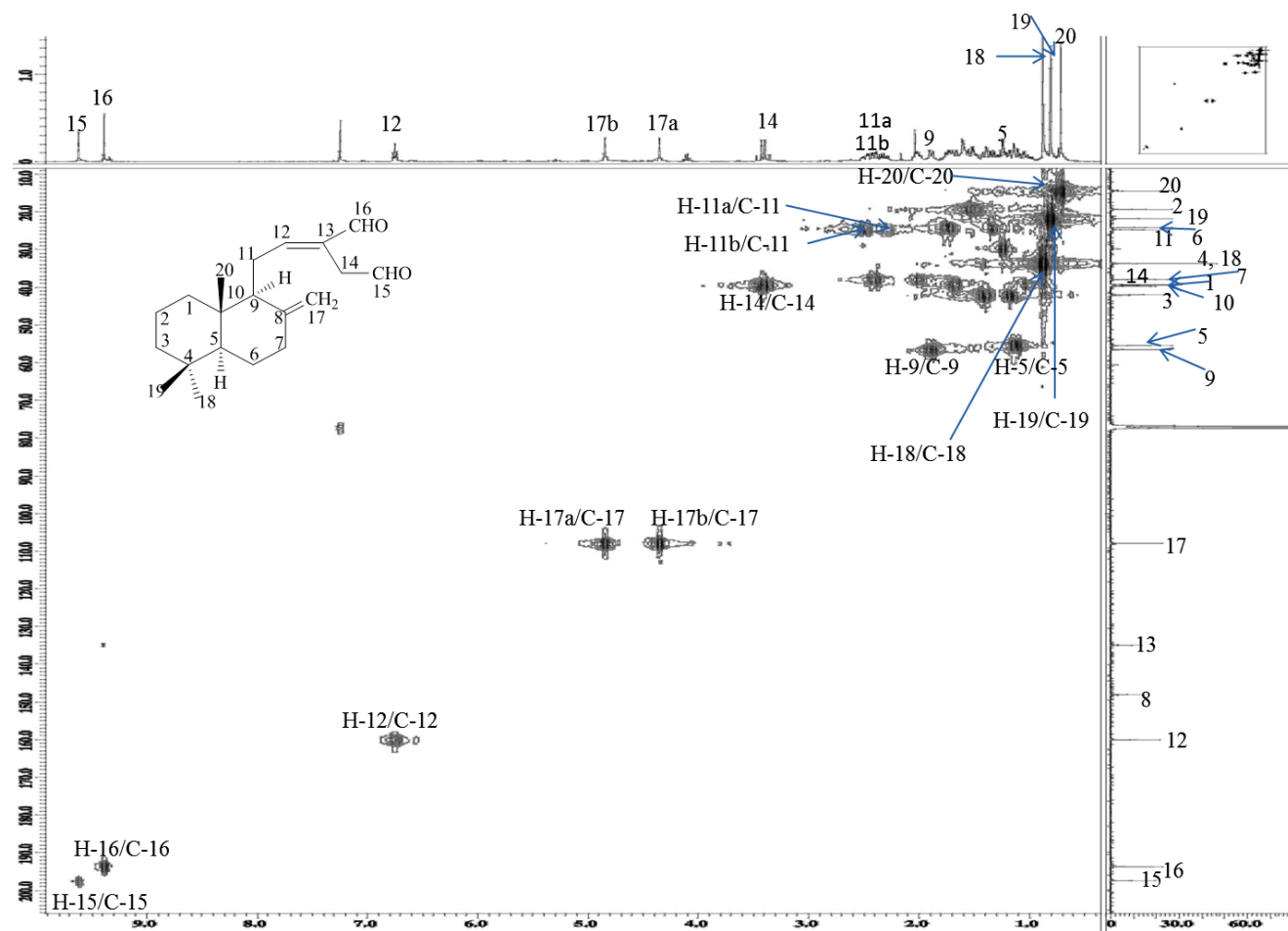


Figure 3.80: HSQC spectrum of labda-8(17), 12-diene-15, 16-dial **127**

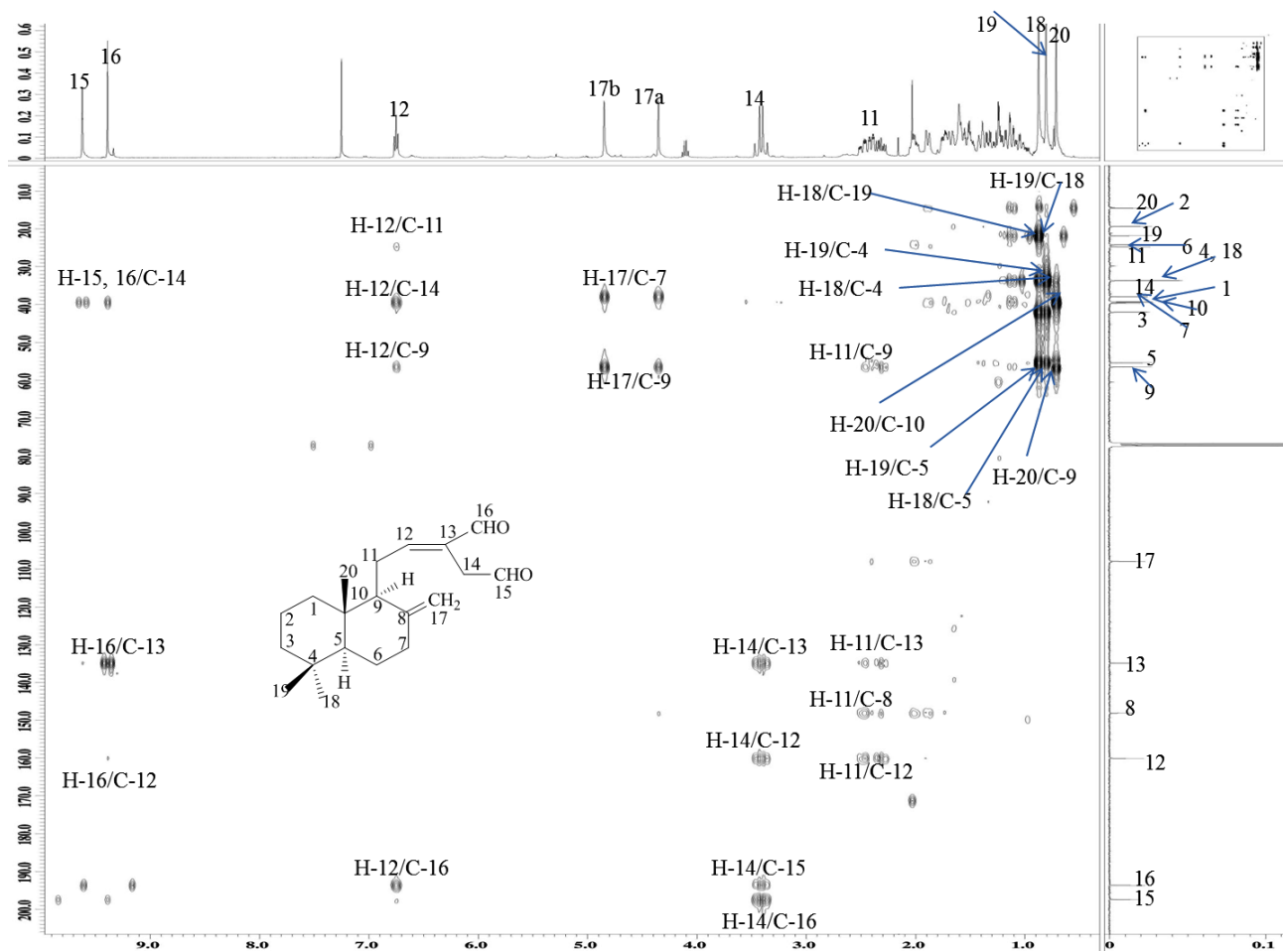
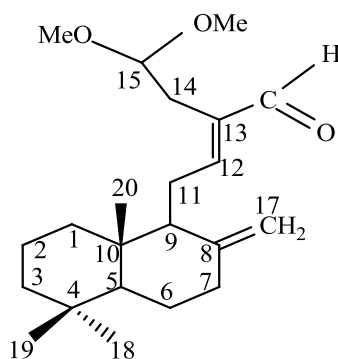


Figure 3.81: HMBC spectrum of labda-8(17), 12-diene-15, 16-dial **127**

Calcaractrin A **128**



Calcaractrin A **128** was obtained as a colourless oil. The UV spectrum showed absorption maximum at 200 nm. The IR spectrum showed absorption bands at 2929, 1708, 1688 cm^{-1} . The GC-MS displayed the M^+ at m/z 318 corresponding to the molecular formula of $\text{C}_{22}\text{H}_{44}\text{O}_3$.

The ^1H NMR spectrum (**Figure 3.82, Table 3.21**: ^1H NMR (400 MHz), and ^{13}C NMR (100 MHz) spectral data (in CDCl_3) of calcaractrin A **128**) showed similar evidence for the presence of labdane type diterpenoid due to the presence of three distinct methyl singlets at δ_{H} 0.87, 0.81, and 0.73 for H-18, H-19, and H-20, respectively. In addition, two exomethylene protons at δ_{H} 4.41, 4.82 (2H, *dd*, $J=1.4, 0.48$ Hz, H-17) was further proof for the characteristic of a bicyclic labdane type diterpenoid. Two clear methoxy groups obviously observed at δ_{H} 3.33, while eight set of methylene protons at δ_{H} 1.74 (H_2 -1), 1.47, 1.56 (H_2 -2), 1.03 (1H, *brs*, H-3), 1.2 (1H, *d*, $J=1.36$ Hz, H-3), 1.32, 1.72 (*m*, H_2 -6), 2.0, 2.38 (*m*, H_2 -7), 2.42, 2.62 (*m*, H_2 -11), 2.56 (*m*, H_2 -14). The proton spectrum showed also four methine protons signals observable at δ_{H} 1.12 (*dd*, $J=2.7, 12.8$ Hz, H-5), 1.92 (*d*, $J=11$ Hz, H-9), 6.53 (*t*, $J=5.9$ Hz, H-12), and 4.41 (*t*, $J=5.4$, H-15).

The ^{13}C NMR and DEPT-135 spectra (**Figure 3.83, Table 3.21**) displayed the presence of a total of 22 carbons comprising of three methyls, eight methylenes, four

methines, four quaternary carbons, two methoxy group, one carbonyl. Two observed signals were obviously assigned to the two methoxy groups at δ_C 54.4 (C-21, 22), three methyls at 14.5 (C-20), 21.8 (C-19), 33.7 (C-18), eight signals observed indicated the presence of eight methylenes at 39.2 (C-1), 19.4 (C-2), 42.1 (C-3), 24.2 (C-6), 37.9 (C-7), 24.6 (C-11), 29.1 (C-14), and 107.9 (C-17). Four methines signals were detected at 55.5 (C-5), 56.6 (C-9), 160.1 (C-12), and 103.9 (C-15). Four quaternary carbons were also observed at δ_C 33.6 (C-4), 148.3 (C-8), 39.6 (C-10), and 138.2 (C-13) while one carbonyl at 195.1 (C-16).

From the spectroscopic data obtained (**Table 3.21**) and comparison with the literature values, the identity of the compound was established as calcaractrin A **128** (Abas et al., 2005).

Table 3.21: ^1H NMR (400 MHz), and ^{13}C NMR (100 MHz) spectral data (in CDCl_3) of calcaractrin A **128**

Position	δ_H, J (Hz)	δ_C
1	1.07, 1.71, m	39.2
2	1.47, 1.56, m	19.4
3	1.17, 1.42, m	42.1
4	-	33.6
5	1.11, dd (2.7, 12.8)	55.5
6	1.32, 1.72, m	24.2
7	2.01, 2.38, m	37.9
8	-	148.3
9	1.92, d (11)	56.6
10	-	39.6
11	2.42, 2.62, m	24.6
12	6.53, t (5.9)	160.1
13	-	138.2
14	2.56, dd (5.4, 9.6)	29.1
15	4.41, t (5.4)	103.9
16	9.32, s	195.1
17	4.41, 4.82, dd (1.4, 0.48)	107.9
18	0.87, s	33.7
19	0.81, s	21.8
20	0.73, s	14.5
21	3.33 (OMe)	54.4
22	3.33(OMe)	54.4

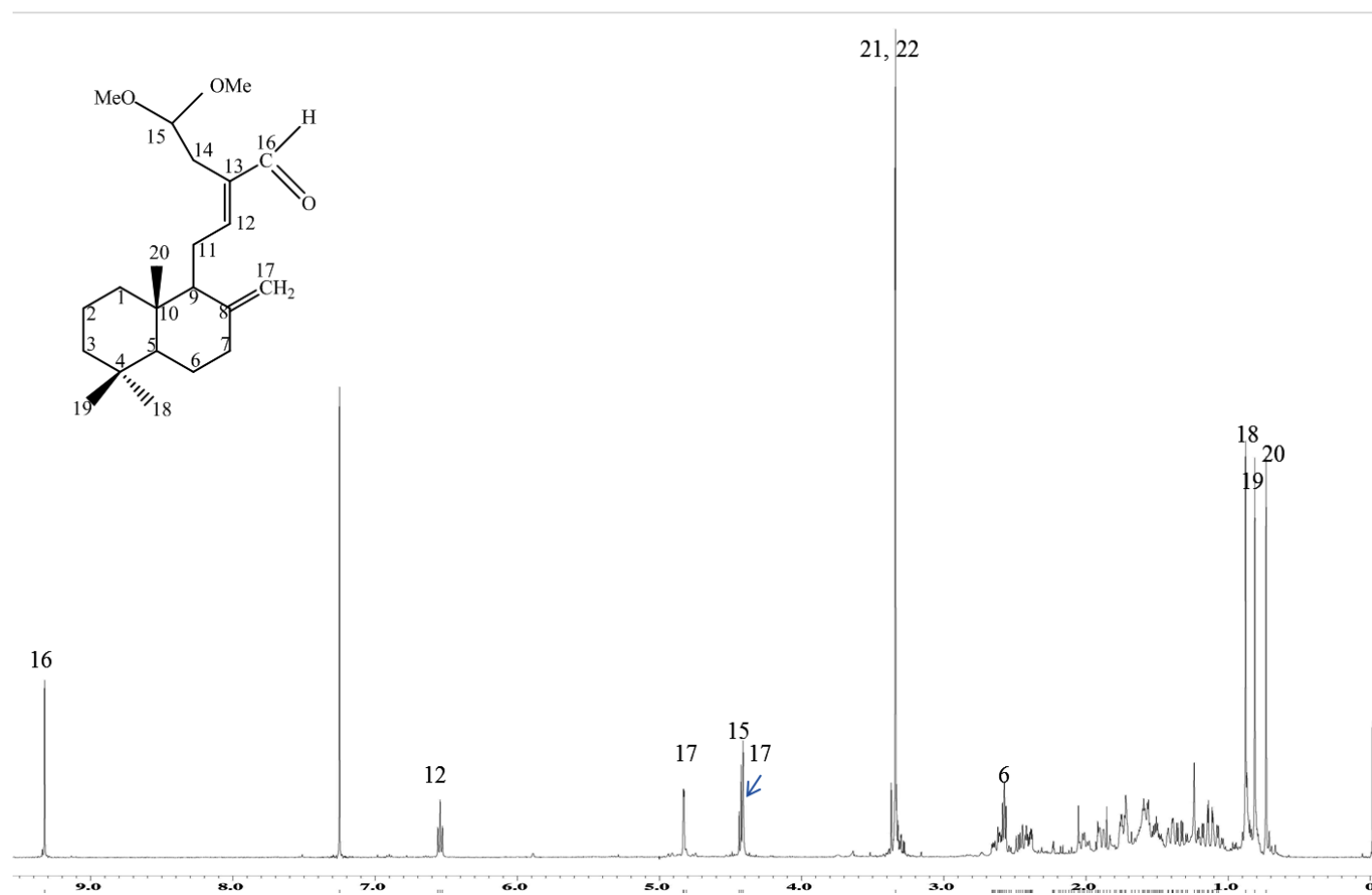


Figure 3.82: ^1H -NMR spectrum of calcaratarin A 128

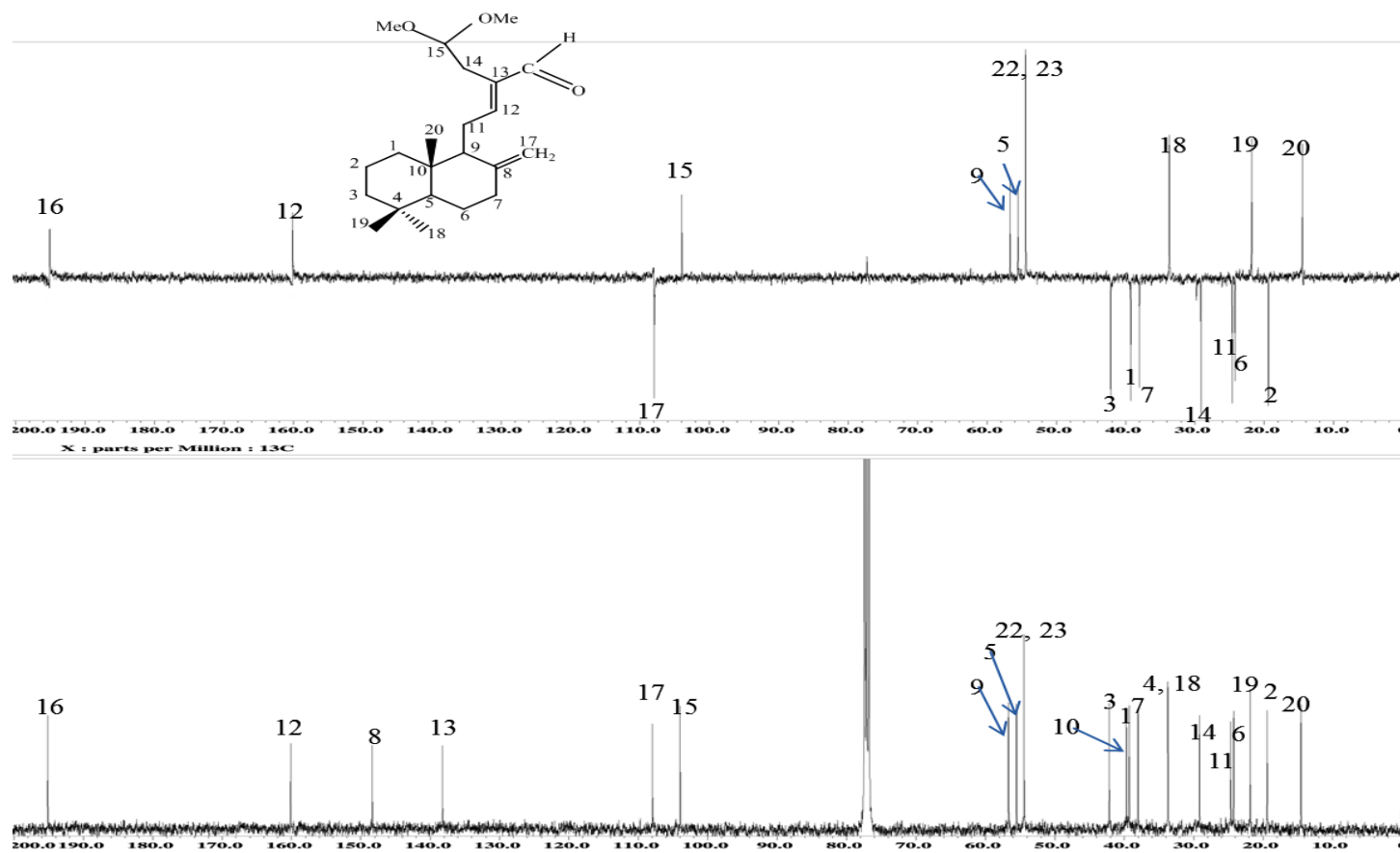
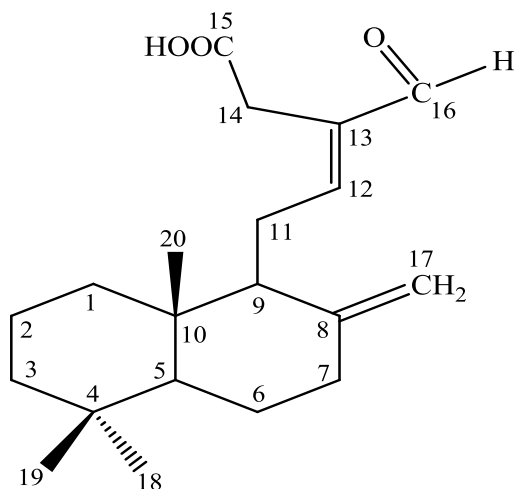


Figure 3.83: ^{13}C NMR and DEPT-135 spectra of calcaratarin A 128

Zerumin A **129**



Zerumin A **129** was obtained as pale yellow oil. The UV spectrum showed maximum absorption band at 210 nm. The compound was assigned with the molecular formula $C_{20}H_{30}O_2$ on the basis of EI-MS analysis ($M^+ m/z=302$).

The 1H NMR spectrum (**Figure 3.84, Table 3.22**) showed common signals similarly to those signals observed in the labdane type diterpenoids due to the presence of two exomethylene protons singlets at δ_H 4.37, 4.84 and the existence of three methyl singlets at δ_H 0.73, 0.81, and 0.87 which were assigned to the three methyl protons for H-20, H-19, and H-18, respectively.

The ^{13}C NMR and DEPT-135 spectra (**Figure 3.85, Table 3.22**) displayed a total of 20 carbon signals due to three methyls, eight methylenes, three methines, four quaternary carbons, two carbonyls. Further evidence that **129** was a labdane type diterpenoid was the existence of three signals for three methyls at δ_C 14.1 (C-20), 21.8 (C-19), and 33.6 (C-18). In addition to an exomethylene carbon at 107.9 (C-17), and a quaternary carbon at δ_C 148.1 (C-8). The presence of two carbonyls clearly observed at δ_C 193.8 (C-16), and 174.3 (C-15). Seven sp^2 methylenes were resonated at 39.2 (C-1),

19.3 (C-2), 42.0 (C-3), 24.1 (C-6), 37.9 (C-7), 24.6 (C-11), and 29.7 (C-14). Two sp^3 methines were observed at 55.4 (C-5), and 56.4 (C-9). In addition to one sp^2 methine at 159.5 (C-12). Four quaternary carbons, including two sp^2 , and 135.7 (C-13), and 148.1(C-8), two sp^3 at δ_{C} 33.6 (C-4), and 39.6 (C-10) were also observed in the ^{13}C spectrum.

Based on the spectral data obtained (Table 3.21) and comparison with literature values, the structure of **129** was established as zerumin A (Xu et al., 1996).

Table 3.22: : ^1H NMR (400 MHz), and ^{13}C NMR (100 MHz) spectral data recorded in CDCl_3 of zerumin A **129**

Position	δ_{H}, J (Hz)	δ_{C}
1	1.07, 1.72, m	39.2
2	1.52, 1.59, m	19.3
3	1.21, 1.42, m	42.0
4	-	33.6
5	1.13, dd (2.7, 12.8)	55.4
6	1.36, 1.75, m	24.1
7	2.41, m,	37.9
	2.02, dd (5.0,13.2)	
8	-	148.1
9	1.92, d (11)	56.4
10	-	39.6
11	2.55, ddd (2.7, 3.2, 6.3)	24.6
12	6.68, (6.4)	159.5
13	-	135.7
14	3.36, d (16.4)	29.7
15	-	174.3
16	9.37, s	193.8
17	4.37, 4.84, brs	107.9
18	0.87, s	33.6
19	0.81, s	21.8
20	0.73, s	14.1

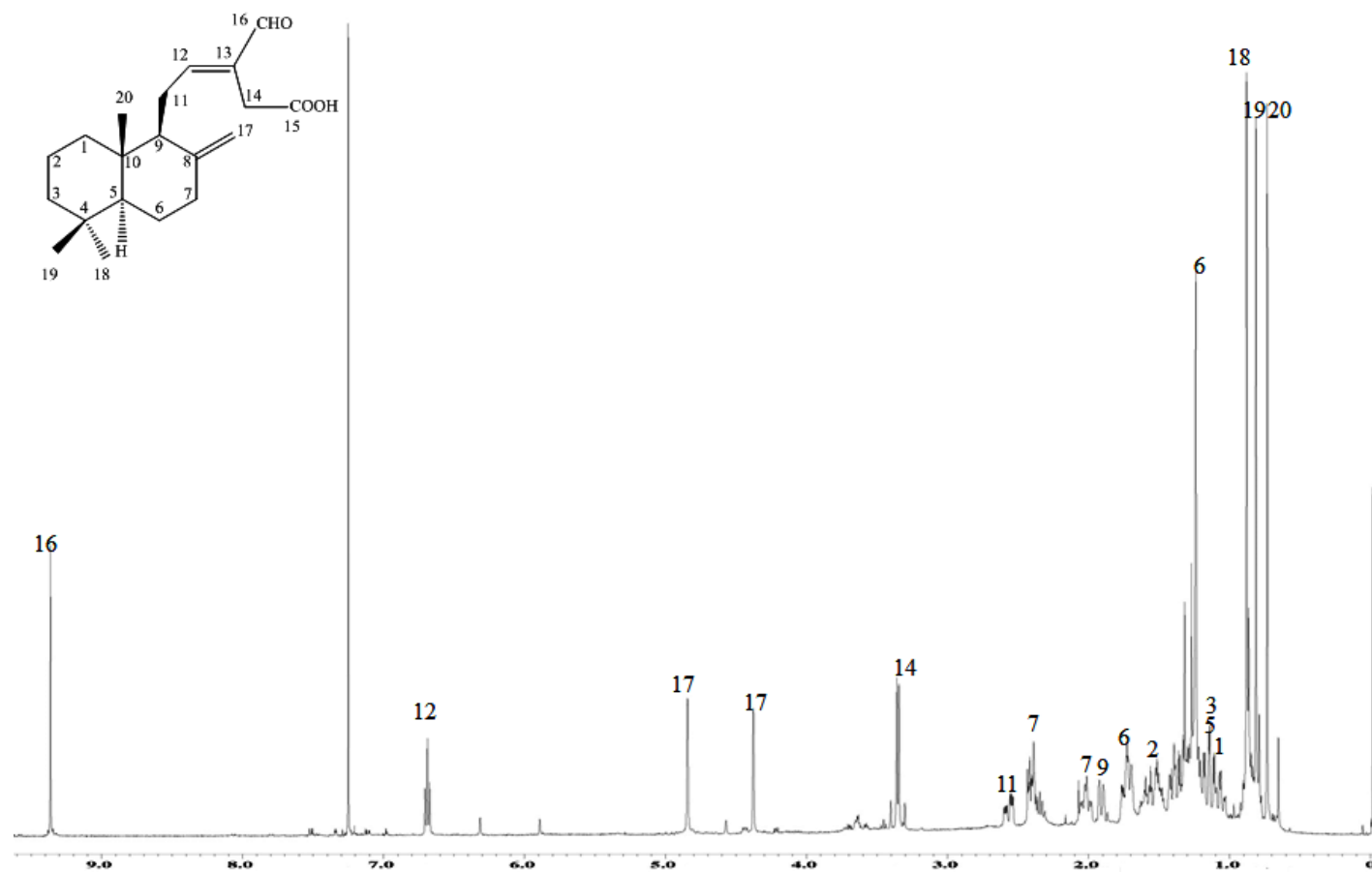


Figure 3.84: ^1H -NMR spectrum of zerumin A 129

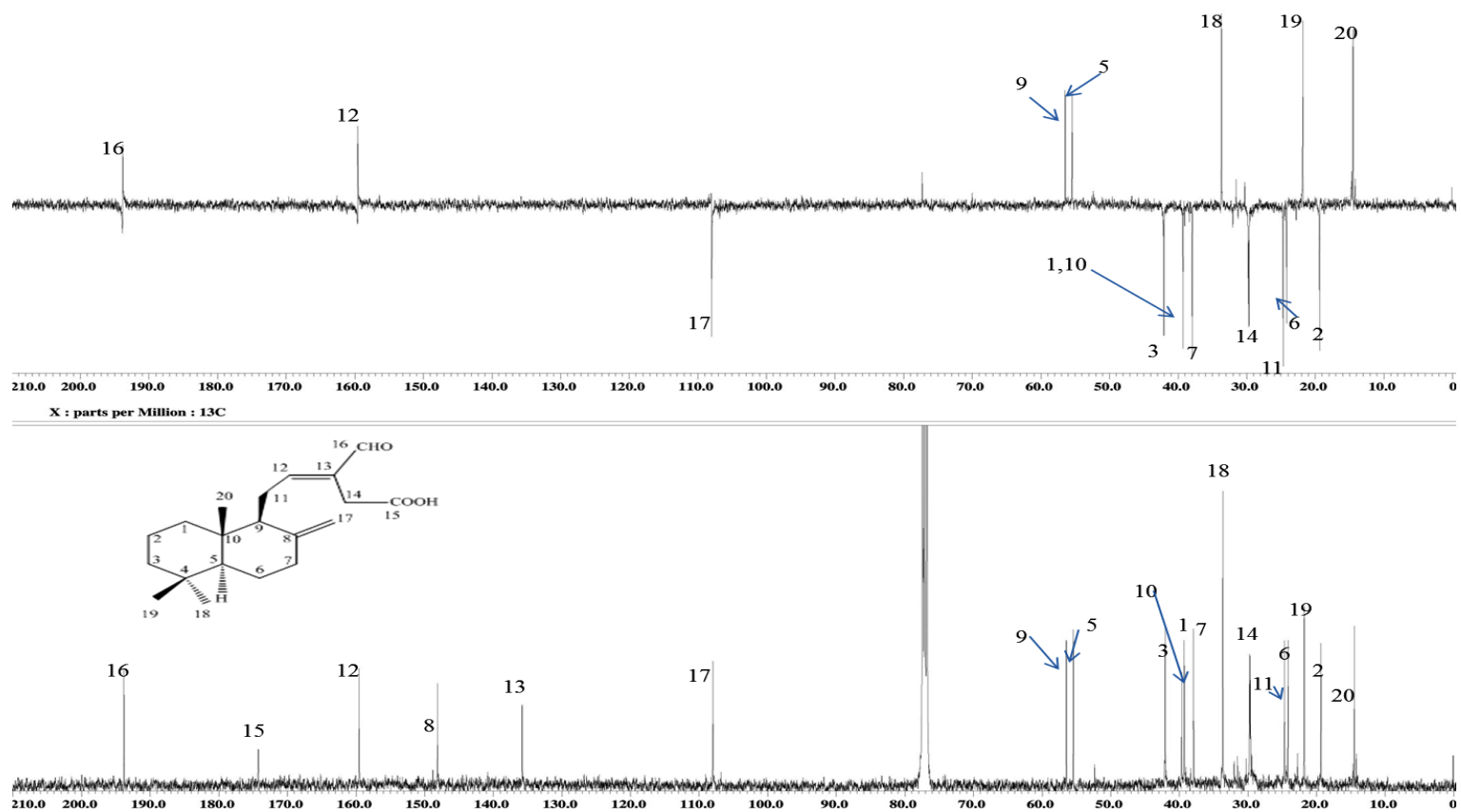


Figure 3.85: ^{13}C NMR and DEPT spectra of zerumin A 129

3.1.2 Phytochemical investigation of *C. purpurascens* rhizomes

No phytochemical work has been reported so far on the rhizomes of *C. purpurascens* (Temu tis). Therefore, an attempt was done towards the phytochemical investigation of it on its essential oil, SFE extracts, and crude extracts obtained by cold maceration with *n*-hex, DCM and MeOH.

The investigation resulted in the isolation of two major types of compounds:

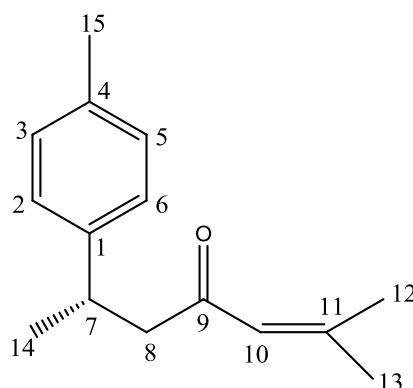
- (i) Bisabolane sesquiterpenoids were isolated from the *n*-hex extract.
- (ii) Curcuminoids and one guaiane sesquiterpene were isolated from DCM extract.

Table 3.23: Compounds isolated from *C. purpurascens*

No.	Compound	Skeleton
23	<i>ar</i> -Turmerone 74	Bisabolane
24	Curcumin 138	Diaryhepatanoid
26	Bisdemthoxymethycurcumin 139	Diaryhepatanoid
25	Demethoxycurcumin 140	Diaryhepatanoid
27	Zedoalactone B 60	Quaiane

3.1.2.1 Bisabolane type sesquiterpenoids

ar-Turmerone **74**



ar-Turmerone **74** was obtained as a pale yellow oil with $[\alpha]_D^{25} + 60$ (c 0.5, MeOH). The EI-MS spectrum showed a molecular ion peak (M^+) at m/z 216 corresponding to the molecular formula of $C_{15}H_{20}O$. The UV(MeOH) absorption λ_{max} at 240 nm indicating the presence of the benzene ring, the carbonyl, and the double bonds. The IR spectrum exhibited absorptions at 1700 cm^{-1} (carbonyl) and aromatic (1516 and 1618 cm^{-1}) groups.

The ^1H NMR spectrum (**Figure 3.87, Table 3.24**) showed obvious separation of proton signals into aliphatic and aromatic parts of the molecule. The spectrum displayed three methyl singlets, two of which were typical of allylic protons at δ 2.09 (H_3 -12), and 1.84 (H_3 -13), where the methyl protons attached to the benzene ring resonated further in the downfield region compared to a regular aliphatic methyl group due to the effect of aromatic deshielded to the methyl protons and resonated at 2.29 (H_3 -15). In addition to one methyl protons appeared as doublet ($J=7.36\text{ Hz}$) at δ 1.22 (H_3 -14). The proton spectrum also showed symmetrical four protons aromatic at δ 7.09 which can be easily assigned for the protons 3, 5, 2, and 6.

The ^{13}C NMR and DEPT-135 spectra (**Figure 3.88, Table 3.24**) are also nicely divided with aromatic and an aliphatic part. The spectrum revealed a total of 15 carbon signals carbons due to one carbonyl, three sp^2 quaternary carbons, five sp^2 methines, one sp^3 methine, one sp^2 methylene, and four methyls, among them six carbons were for the symmetrical aromatic ring, both C-2, and C-6 resonated at 126.7, similarly C-3, and C5 at δ 129.2, in addition C-1 and C-4 appeared at δ 143.7, and 135.6, respectively.

Therefore, the structure was deduced as turmerone by the spectral data analysis and also by comparing with the reported values (Chai Hee Hong et al., 2001).

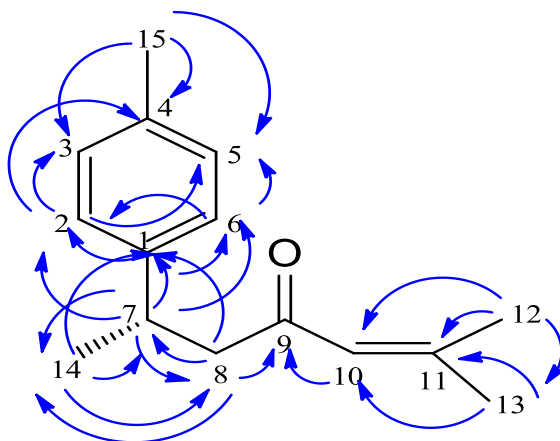


Figure 3.86: Selected HMBC Correlations H \rightarrow C of ar-turmerone A **101**

Table 3.24: ^1H NMR (400 MHz) and ^{13}C NMR (100 MHz) spectral data in CDCl_3 , of ar-turmerone **74**

Position	^1H δ_{H}	^{13}C δ_{C}
1	-	143.7
2	7.09, s	126.7
3	7.09, s	129.2
4	-	135.6
5	7.09, s	129.1
6	7.09, s	126.7
7	3.27, m	35.3
8	2.63, m	52.7
9	-	200
10	6.01, s	124.1
11	-	155.2
12	2.09, s	20.8
13	1.84, s	27.7
14	1.22, d (7.36)	22.1
15	2.29, s	21.1

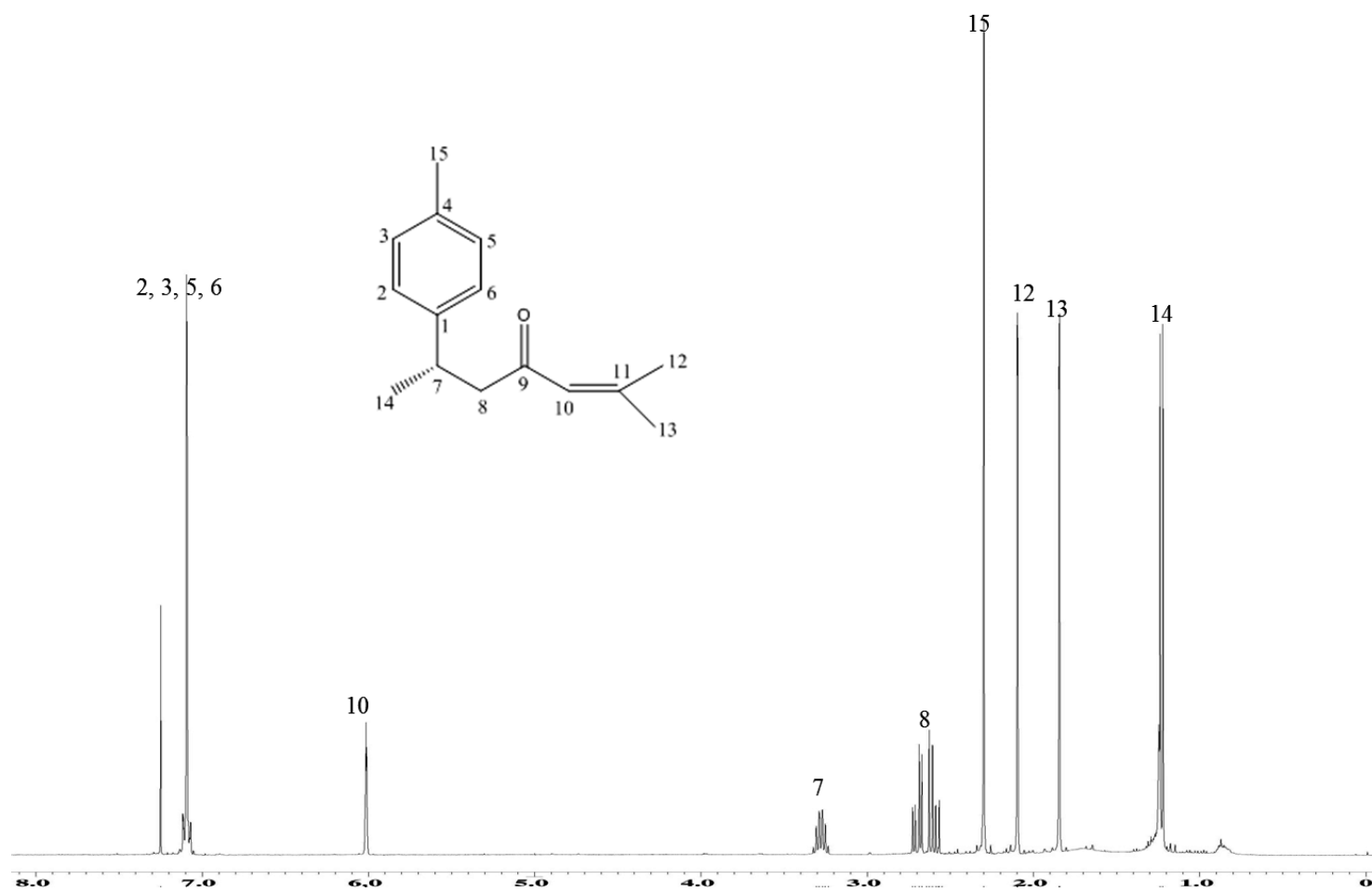


Figure 3.87: ¹H-NMR spectrum of ar-turmerone **74**

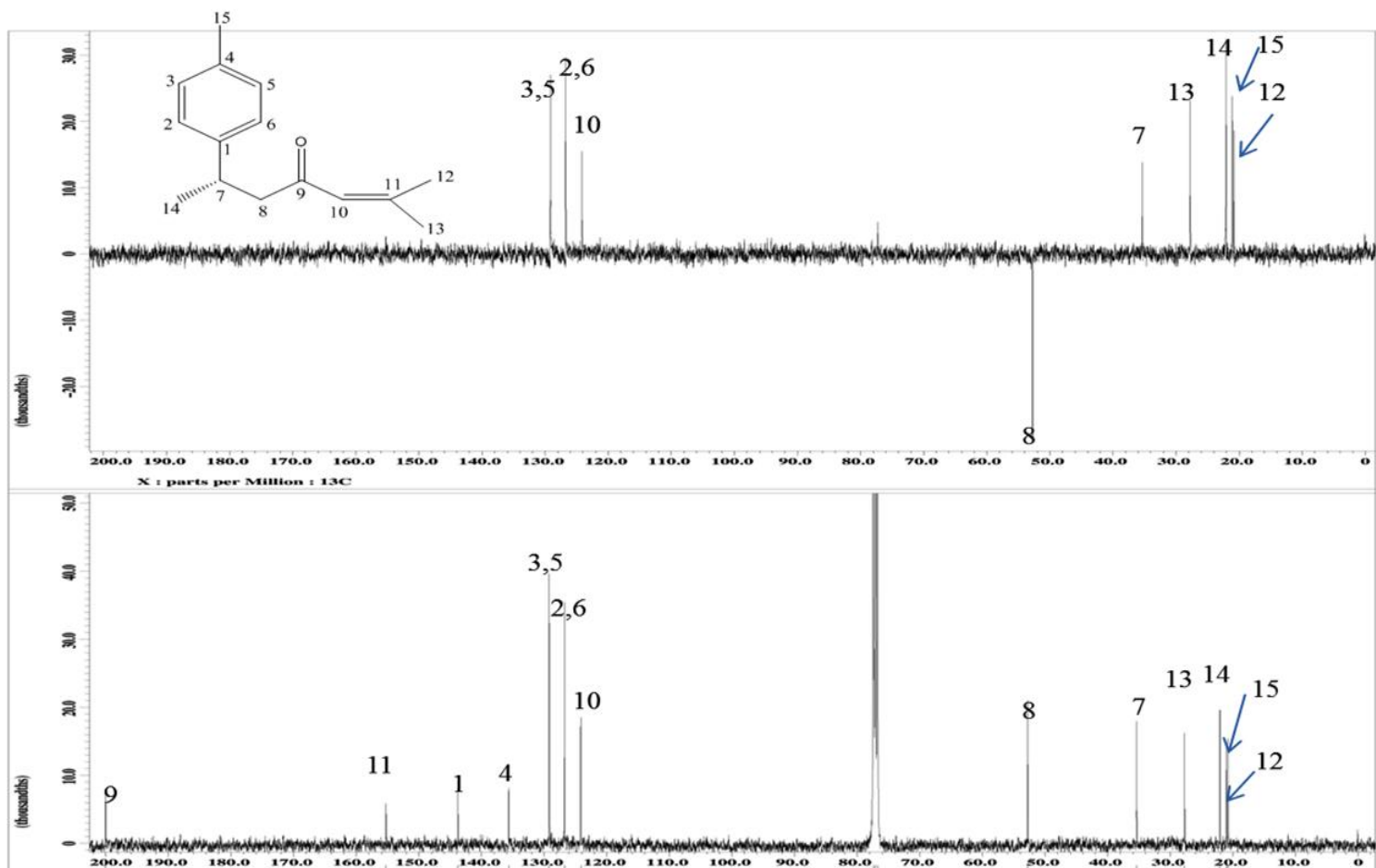


Figure 3.88: ^{13}C -NMR and DEPT-135 spectra of ar-turmerone 74

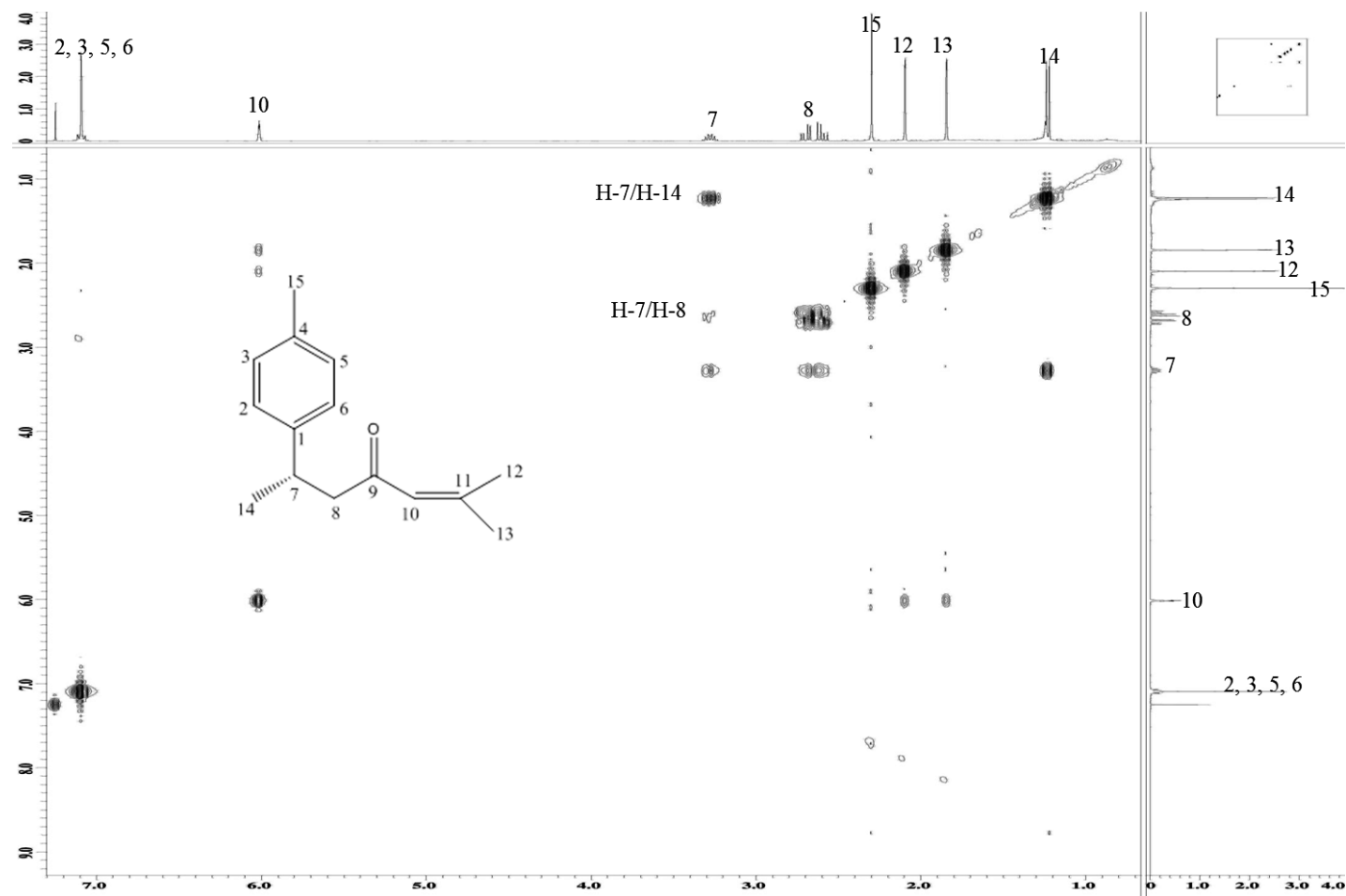


Figure 3.89: COSY spectrum of ar-turmerone **74**

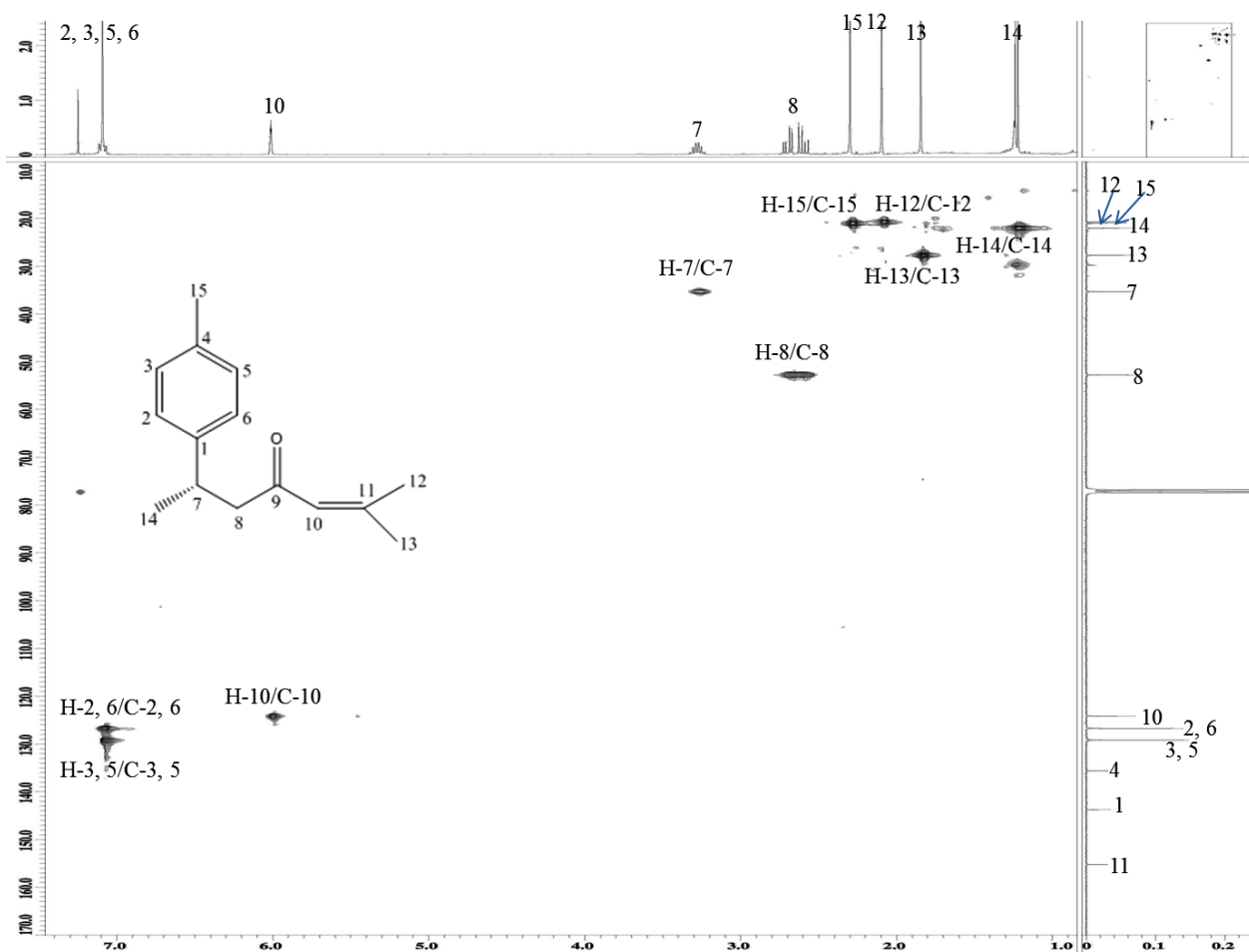


Figure 3.90: HSQC spectrum of ar-turmerone **74**

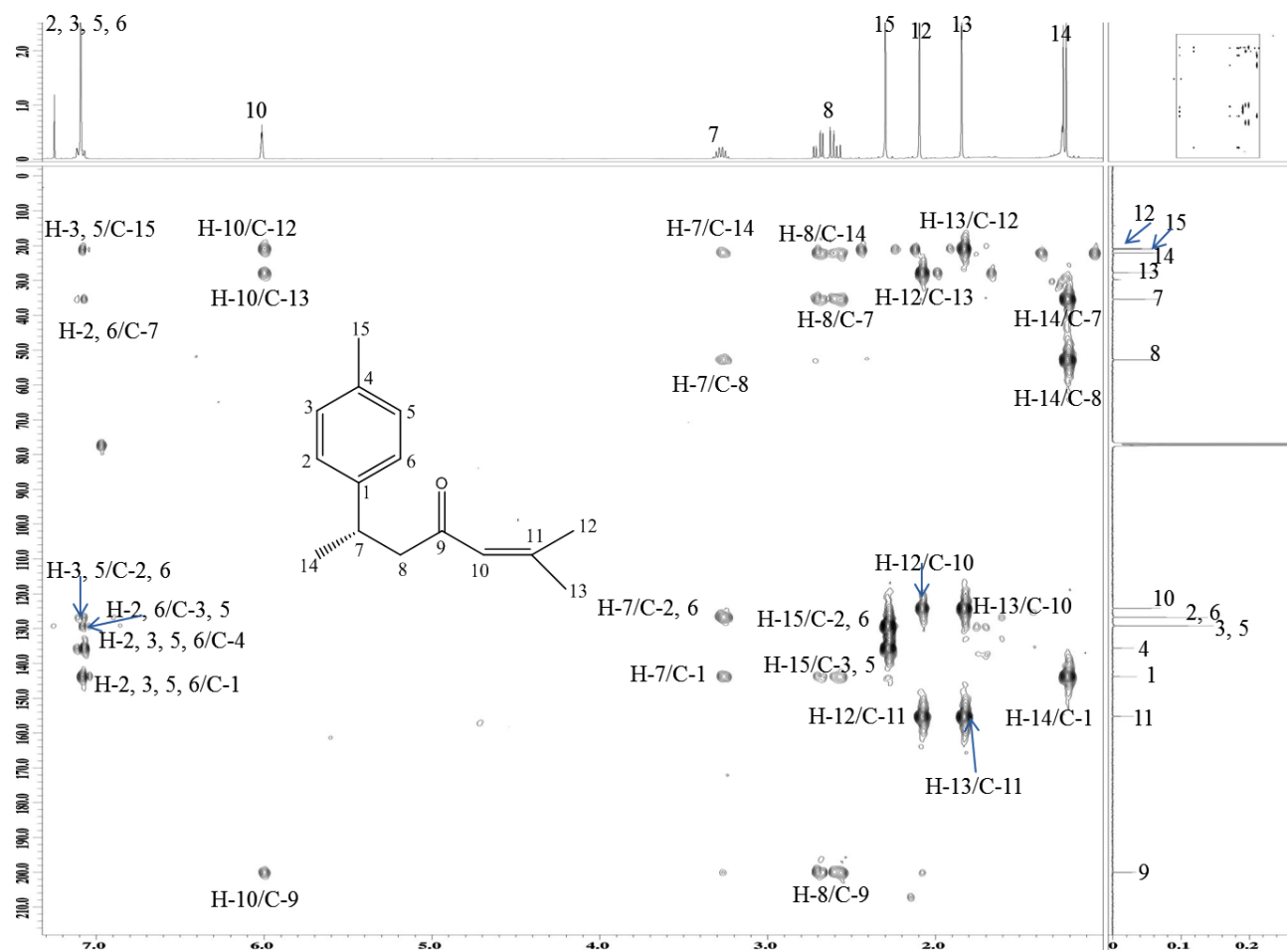
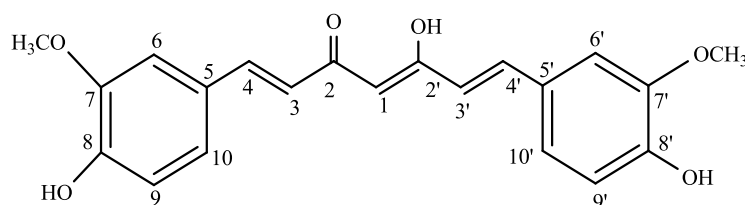


Figure 3.91: : HMBC spectrum of ar-turmerone **74**

3.1.2.2 Diarylheptanoids (curcuminoids)

Three diarylheptanoids were isolated from the DCM extract of *C. purpurascens* including curcumin **138**, bisdemethoxycucumin **139** and demethoxycurcumin **140**. However, the presence of curcumin and its structural analogues, predominantly found in the plant studied in a high amount arise the attention of the plant as a new potential source of chemotherapeutic agents.

Curcumin 138



Curcumin **138** was obtained as an orange crystal (m.p. 184-186°C). The HRESI-MS showed a pseudo molecular ion peak $[M+H]^+$ at m/z 369 consistent with the molecular formula of $C_{21}H_{20}O_6$. The UV absorption at 430 nm indicating the presence of a typical conjugated system. The IR spectrum presented absorption bands for phenolic hydroxyl group (OH stretching) at 1625 cm^{-1} and 1600 cm^{-1} .

Judging from the ^1H NMR spectrum (**Figure 3.93**, **Table 3.25**), the compound was truly aromatic due to the resonances of the ring protons between 7 and 9 ppm. The proton spectrum revealed obviously the presence of the pair of methoxy group signals at δ 3.89. The singlet appeared at δ 5.95 was assigned to H-1 indicating the symmetric structure as shown in the enol form. The proton spectrum also showed an AX spin system at δ 6.69 and δ 7.58 with a spin coupling of 16 Hz which were assigned to the

protons H-3, 3' and H-4, 4', respectively of the trans olefinic bond. The protons H-6, 6' (δ 7.31) showed small meta coupling ($J=1.84$ Hz) with 7.16 (H-10, 10'). The proton H-10, 10' showed ortho coupling with H-9, 9' (δ 6.86) with coupling constant $J=8.24$ Hz.

The ^{13}C -NMR, DEPT, and HSQC spectra (Figure 3.94, 3.96, **Table 3.25**) presented a total number of 11 signals carbons for the half the symmetrical system of the compound. Also the two obviously assignable signals are from the two methoxy groups at δ 55.8 and the carbonyl atom in the enol form at δ 183 (C-2, 2'). Three quaternary carbon signals at δ 149.2, 147.9, and 127.3 which were assigned for C-8, 8', C-7, 7', and C-5, 5', respectively. In addition, three signals sp^2 at the benzene ring were observed at δ 110.7 (C-6, 6'), 115.4 (C-9, 9'), and δ 123.0 (C-10, 10'). The two sp^2 olefinic signals at δ 121.1 (C-3,3'), and δ 140.5. The most shielded carbon signals appeared at δ 100.8 is due to the keto-enol equilibrium.

The ^1H - ^1H -COSY spectrum (**Figure 3.95**) showed clear spin couplings between H-3/H-4, H-3'/H-4', H-9/H-10, and H-9'/H-10'

In the HMBC spectrum (**Figure 3.97**), the assignment of the centred of the compound C_1 (δ 100.8) was clarified due to the correlations of cross peaks of H-3,3' (δ 6.69) and H-4, 4' (δ 7.58) to C-2, 2'. Furthermore, HMBC spectrum also showed the cross peaks of H-6' (δ 7.31) and H-OMe (δ 3.89) to C-7, 7' (δ 110.7).

Based on the above extensive 2D-spectral analysis, the identity of the compound was confirmed as curcumin **138** and in agreement of the literature reported values (Péret-Almeida, Cherubino, Alves, Dufosse, et al., 2005).

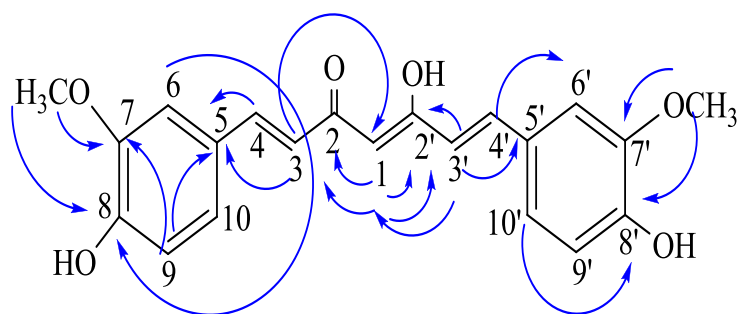


Figure 3.92: Selected HMBC Correlations H $\xrightarrow{\quad}$ C of *curcumin 138*

Table 3.25: ^1H NMR (400 MHz) and ^{13}C NMR (100 MHz) spectral data of curcumin **138** in acetone- D_6

Position	δ_{H}, J (Hz)	δ_{C}
1	5.95, s, 1H	100.8
2, 2'	-	183.7
3, 3'	6.69, d (16), 2H	121.1
4, 4'	7.58, d (16), 2H	140.5
5, 5'	-	127.3
6, 6'	7.31, d (1.84) 2H	110.7
7, 7'	-	147.9
8, 8'	-	149.2
9, 9'	6.86, d (8.24), 2H	115.4
10, 10'	7.16, , dd (8.24, 1.84) 2H	123.0
O-Me	3.89	55.8

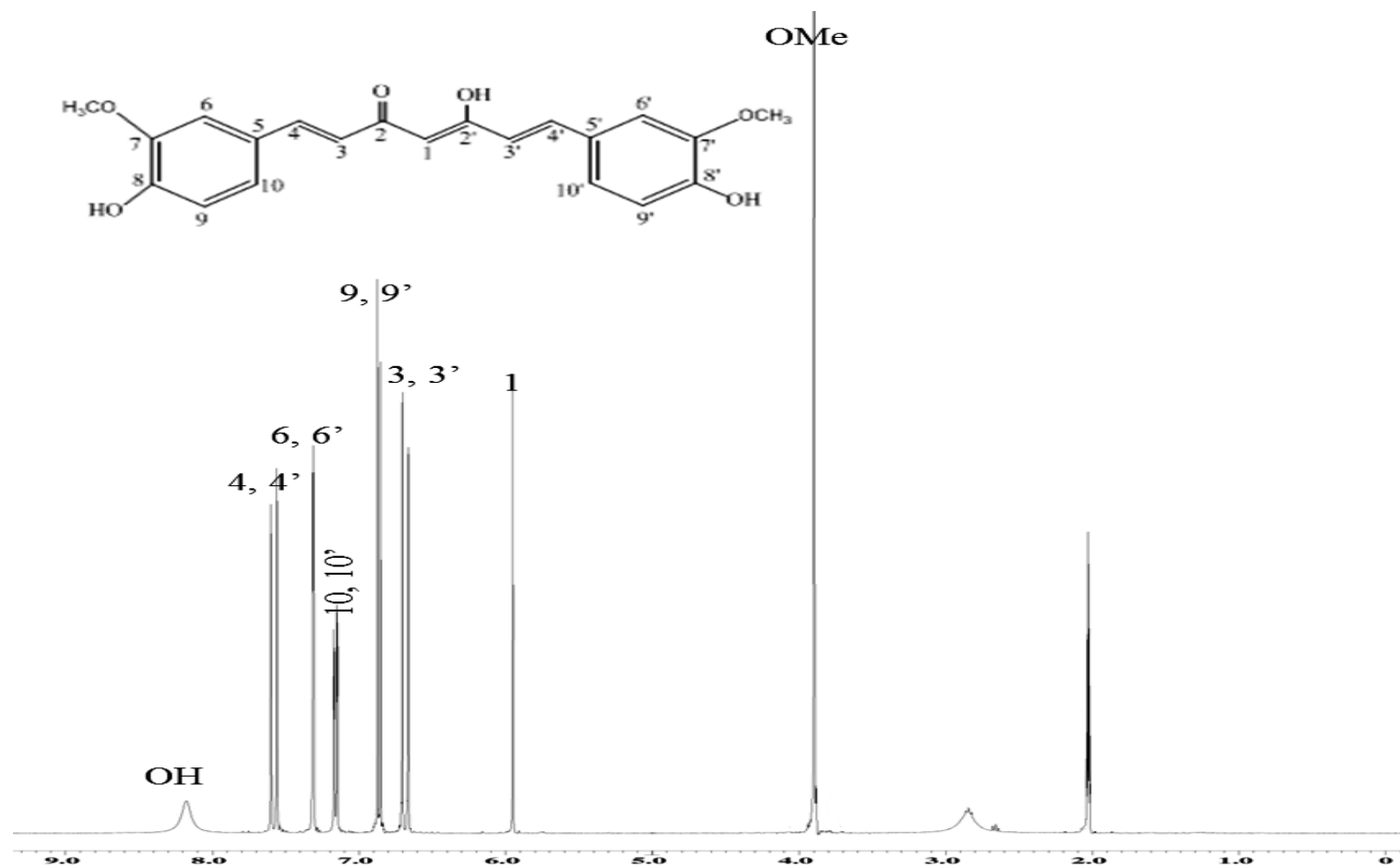


Figure 3.93: ^1H -NMR spectrum of curcumin 138

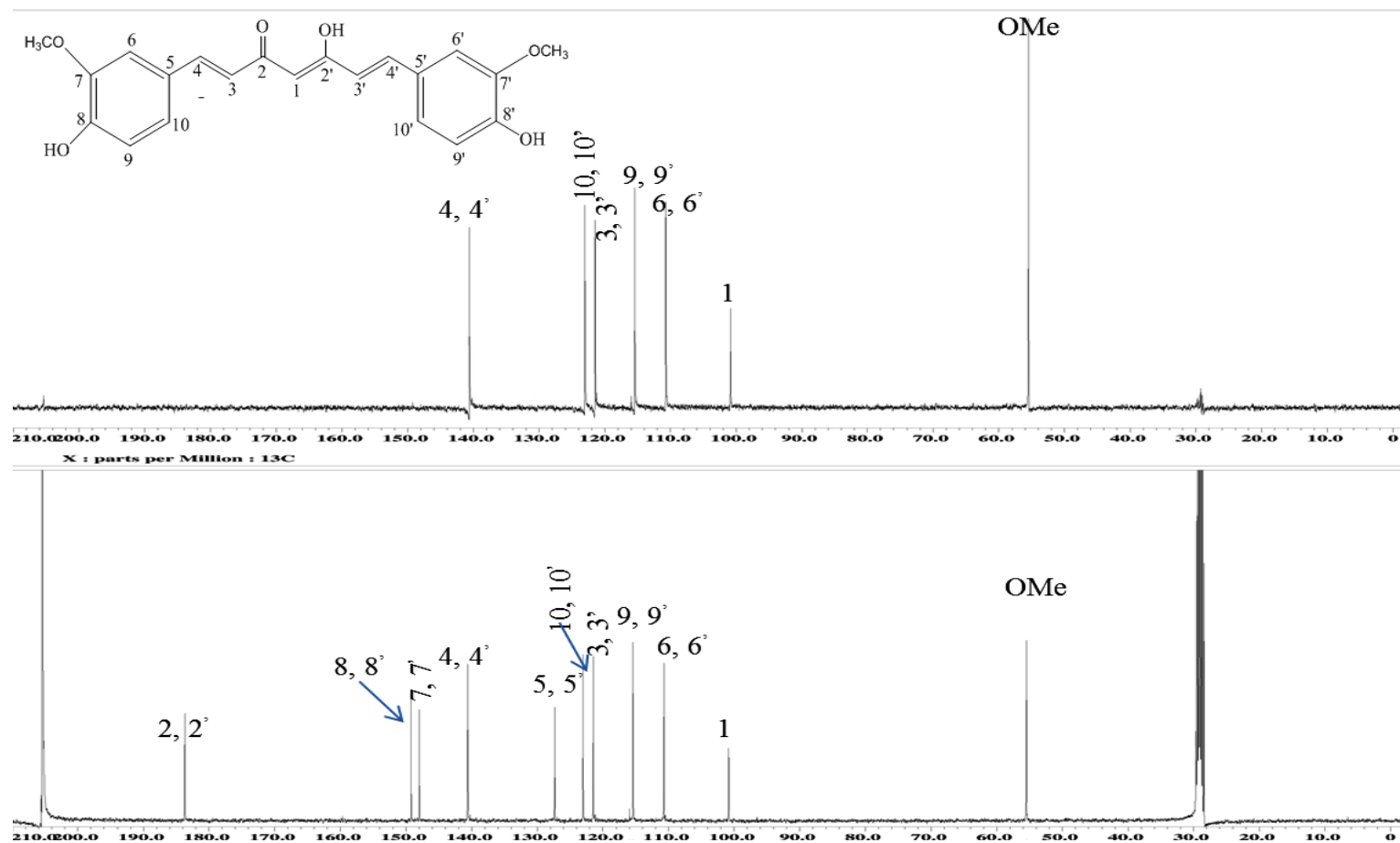


Figure 3.94: ¹³C-NMR and DEPT-135 spectra of curcumin 138

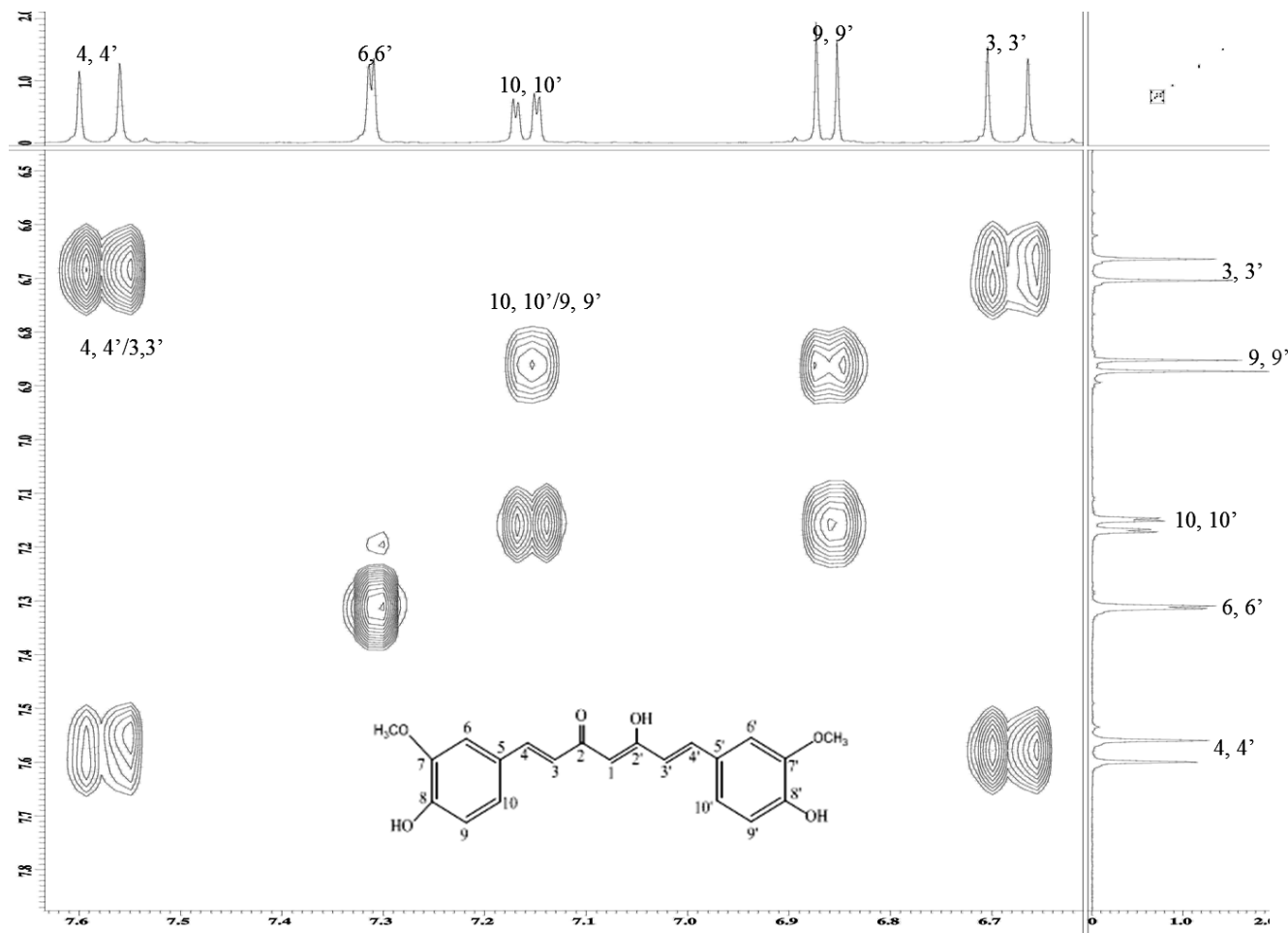


Figure 3.95: COSY spectrum of curcumin 138

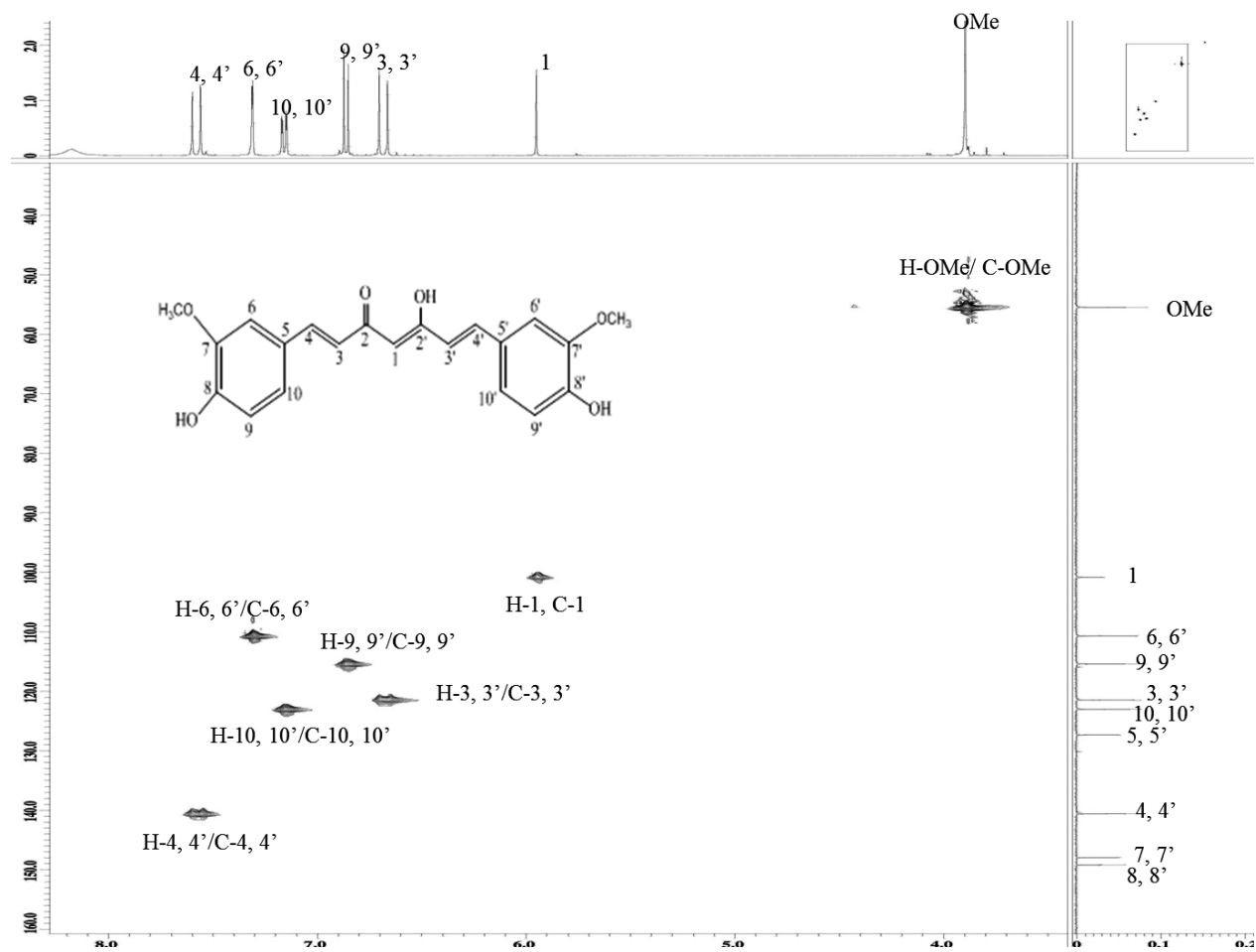


Figure 3.96: HSQC spectrum of curcumin 138

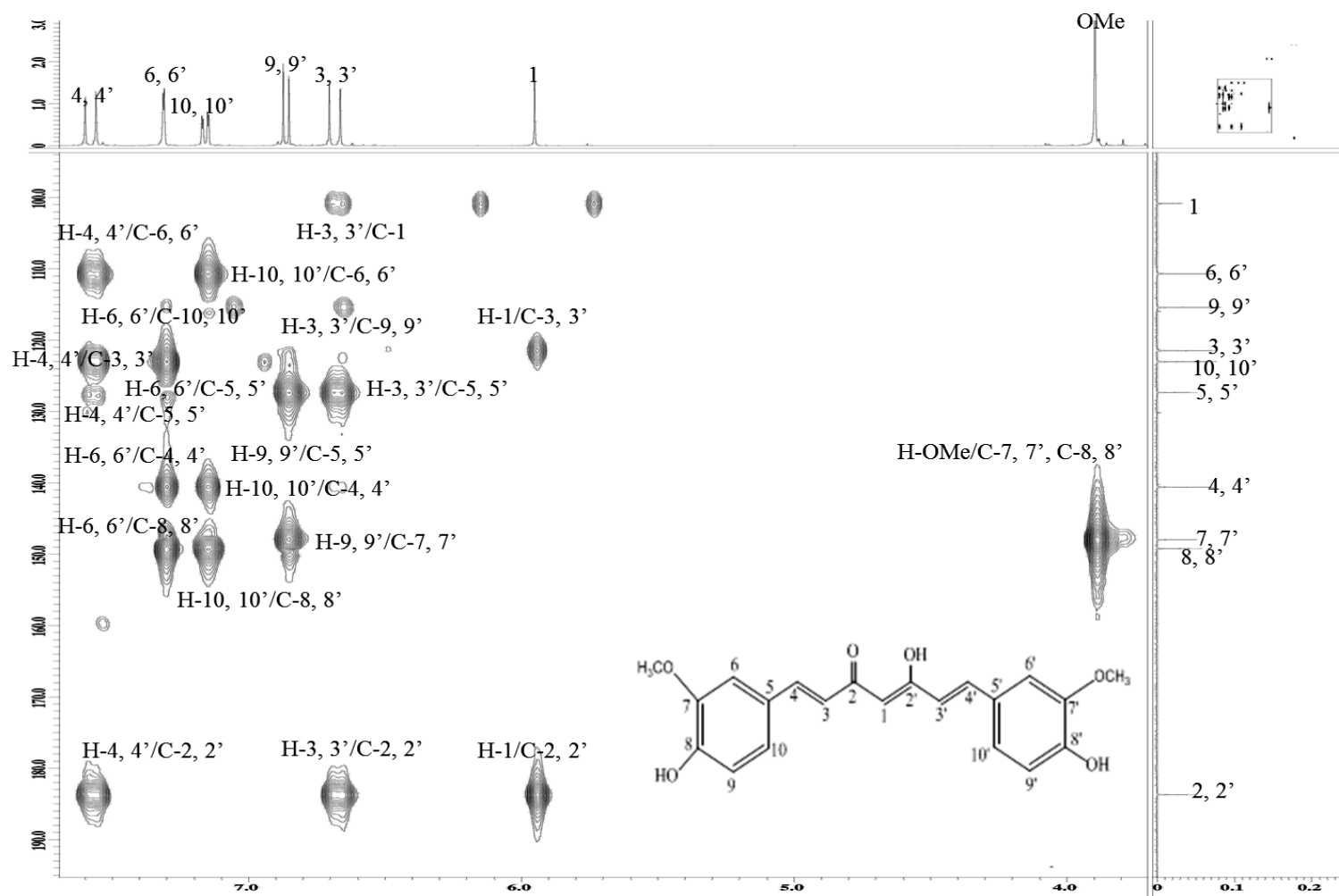
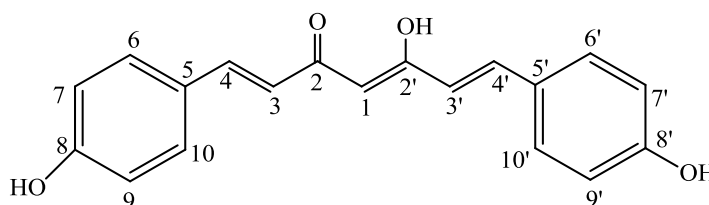


Figure 3.97: HMBC spectrum of curcumin 138

Bis-demethoxycurcumin 139



Bisdemethoxycurcumin **139** was afforded as a yellow powder (m.p. 312-314°C). The EI-MS of this compound showed a molecular ion at m/z 309 corresponding to the molecular formula $C_{19}H_{16}O_3$. The UV absorption maximum at 415 nm. The IR spectrum showed absorption peaks at 3440 (OH) and 1625 (C=O) cm^{-1} indicating the presence of the hydroxyl and carbonyl groups, respectively.

The 1H NMR spectrum (**Figure 3.98, Table 3.26**) displayed similar evidence for the presence of some signals common to diarylheptanid. the proton spectrum also showed some signals close to curcumin. Like the presence of aromatic pair of protons for H-6, H-6' at δ 7.57, H-7, and H-7' at δ 6.87. In addition, two sets of signals were observed at δ 6.87 and δ 7.55 attributed for the pairs H-9, H-9', and H-10, H-10'. The proton spectrum also exhibited the presence of two protons (trans, $J=16$ Hz) for the protons H-4, 4' at δ 7.60 and H-3, 3' at δ 6.64.

The ^{13}C NMR and DEPT-135 spectra (**Figure 3.99, Table 3.26**) exhibited the presence of eight signals due to two quaternary carbons; one carbonyl at δ 183.7 (C-2, 2') and sp^2 carbon at 126.8 (C-5, 5'). Four symmetrical aromatic sp^2 carbons at (C-7, 7') and similarly C-9, 9' at δ 115.9. In addition to C-6, 6' and C-10, 10' resonated similarly at δ 130.1. C-The enolic carbon appeared at 100.9 (C-1). Furthermore, two methines sp^2 appeared at δ 121.1 (C-3, 3'), and δ 140.2 (C-4, 4').

From the above spectral data and compared with the spectral data previously reported the structure of the compound was elucidated as bisdemethoxycurcumin **140** (Péret-Almeida, et al., 2005).

Table 3.26: ^1H NMR (400 MHz), and ^{13}C NMR (400 MHz) spectral data in acetone- d_6 of bisdemethoxycurcumin **139**

Position	$\delta_{\text{H}}, J \text{ (Hz)}$	δ_{C}
1	5.96, s	100.9
2, 2'	-	183.7
3, 3'	6.64, d (16)	121.1
4, 4'	7.60, d (16)	140.2
5, 5'	-	126.8
6, 6'	7.57, d (8.7)	130.1
7, 7'	6.87, d (8.7)	115.9
8, 8'	-	159.7
9, 9'	6.87, d (8.7)	115.9
10, 10'	7.55, d (8.7)	130.1

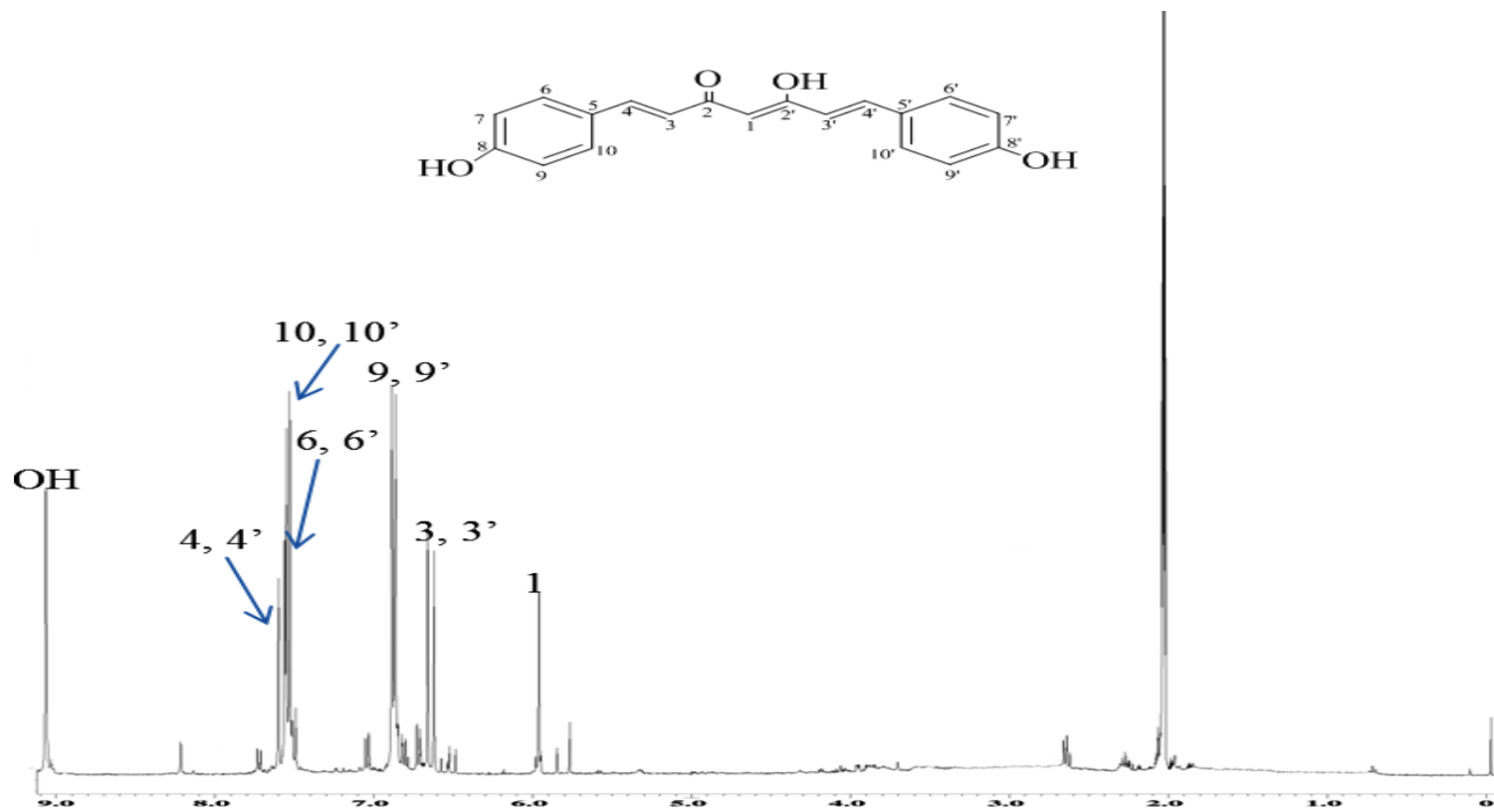


Figure 3.98: ^1H NMR spectrum of bisdemethoxycurcumin **139**

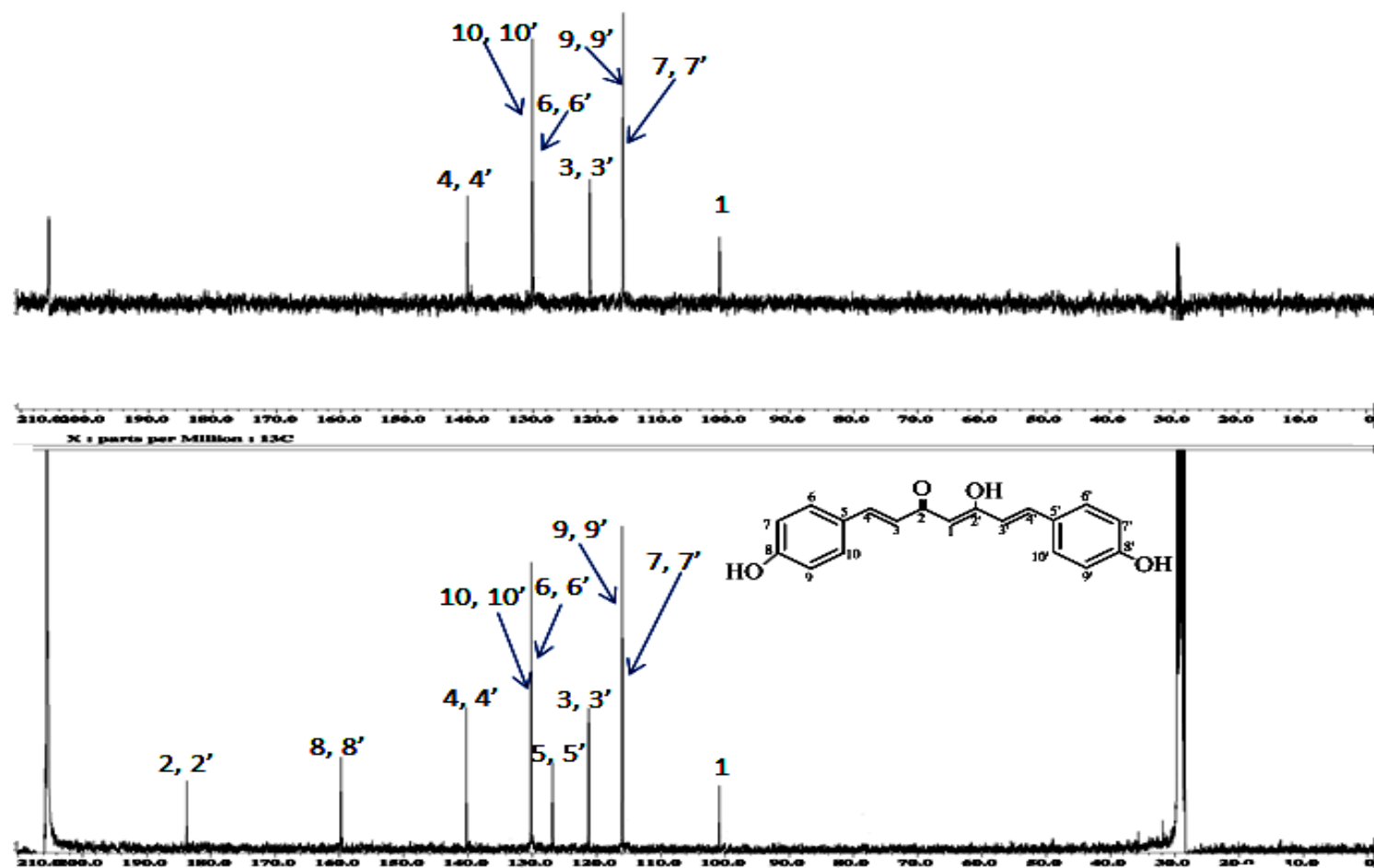
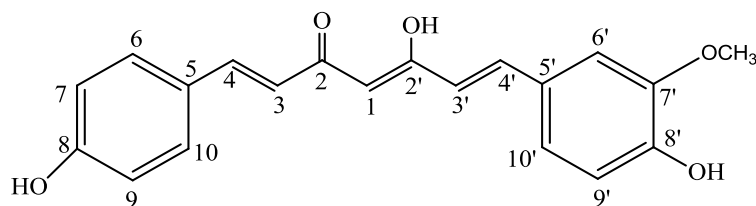


Figure 3.99: ^{13}C NMR and DEPT spectra of bisdemethoxycurcumin 139

Demethoxycurcumin **140**



Demethoxycurcumin **140** was obtained as an orange powder. The IR absorptions at 3400 cm^{-1} (OH^-), and 1624 cm^{-1} ($\text{C}=\text{O}$). The UV spectrum showed absorption maximum at 416 nm. The compound has a molecular formula of $\text{C}_{20}\text{H}_{18}\text{O}_3$ (MW 338).

The ^1H NMR and ^{13}C -NMR spectra (**Figure 3.100, 101, Table 3.27**) exhibited similar features as curcumin and were in evident that compound **140** was belong to curcuminds. Spectral analysis data for compound **140** is very close structural relationship to curcumin **138** except the presence of one methoxy group at δ 3.82 compared to two methoxy groups in curcumin. The carbons signals observed were observed in pairs in **140** with very close chemical shift values. Similarly as curcumin the the central carbon (C-1) had an enolic proton signal appeared as a singlet at δ 6.02 (H-1). Two sets of doublets with coupling constant 15.8 Hz resonated at 6.67 and 7.53 indicated the presence of two olefinic protons; 2H (3, 3') and 2H (4, 4'), respectively. Similarly two signals appeared as doublet with $J=8.3$ Hz at δ 6.81 and 7.13 assigned for H-9 and H-10, respectively.

The ^{13}C -NMR and DEPT-135 spectra (**Figure 3.101, Table 3.27**) showed a total of 16 carbon signals comprising of one methoxy, two carbonyls, one centered carbon, and 9 pairs of carbons signals were observed almost each pair appeared at close chemical shifts. The chemicals shift values of these carbon observed are presented in Table 3.26. Extensive

analysis of all spectroscopic data and with comparison to the literature values confirmed the identity of compound **140** as demethoxycurcumin (Péret-Almeida, Cherubino, Alves, Dufossé, et al., 2005).

Table 3.27: ^1H NMR (400 MHz) and ^{13}C NMR (400 MHz) spectral data of demethoxycurcumin **140** in acetone- d_6

Position	δ_{H}, J (Hz)	δ_{C}
1	6.02, s	100.9
2, 2'	-	183.2/183.1
3, 3'	6.67, d (15.8)	121.1/120.8
4, 4'	7.53, d (15.8)	140.7/140.4
5, 5'	-	126.4/125.8
6, 6'	7.31, d (1.6)	111.2/130.4
7, 7'	-	148.0/115.7
8, 8'	-	149.8/159.8
9, 9'	6.81, d (8.3)	115.9/115.7
10, 10'	7.13, dd (8.3, 1.6)	123.2/123.1
O-Me	3.82, s	55.7

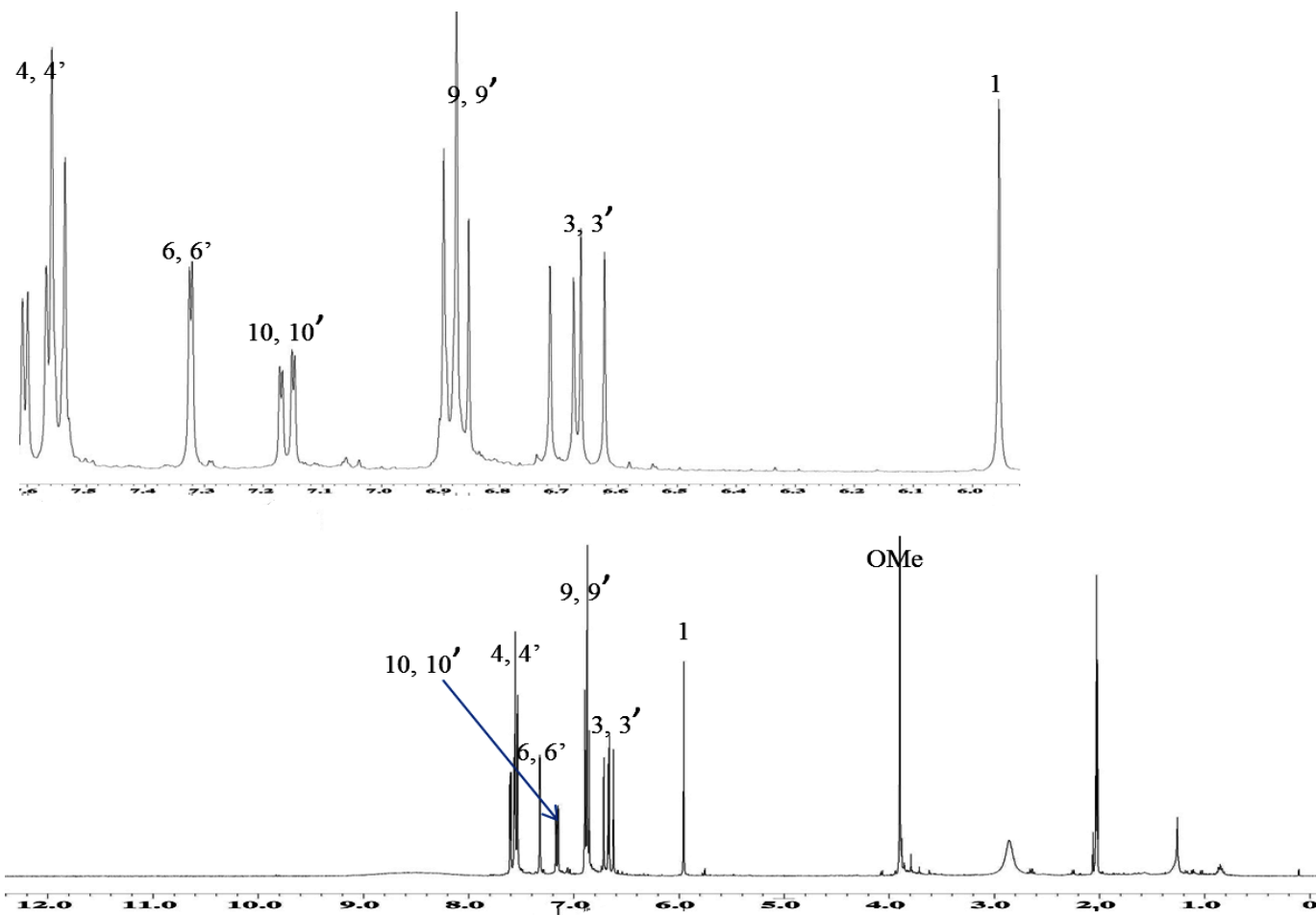


Figure 3.100: ^1H NMR spectrum of demethoxycurcumin **140**

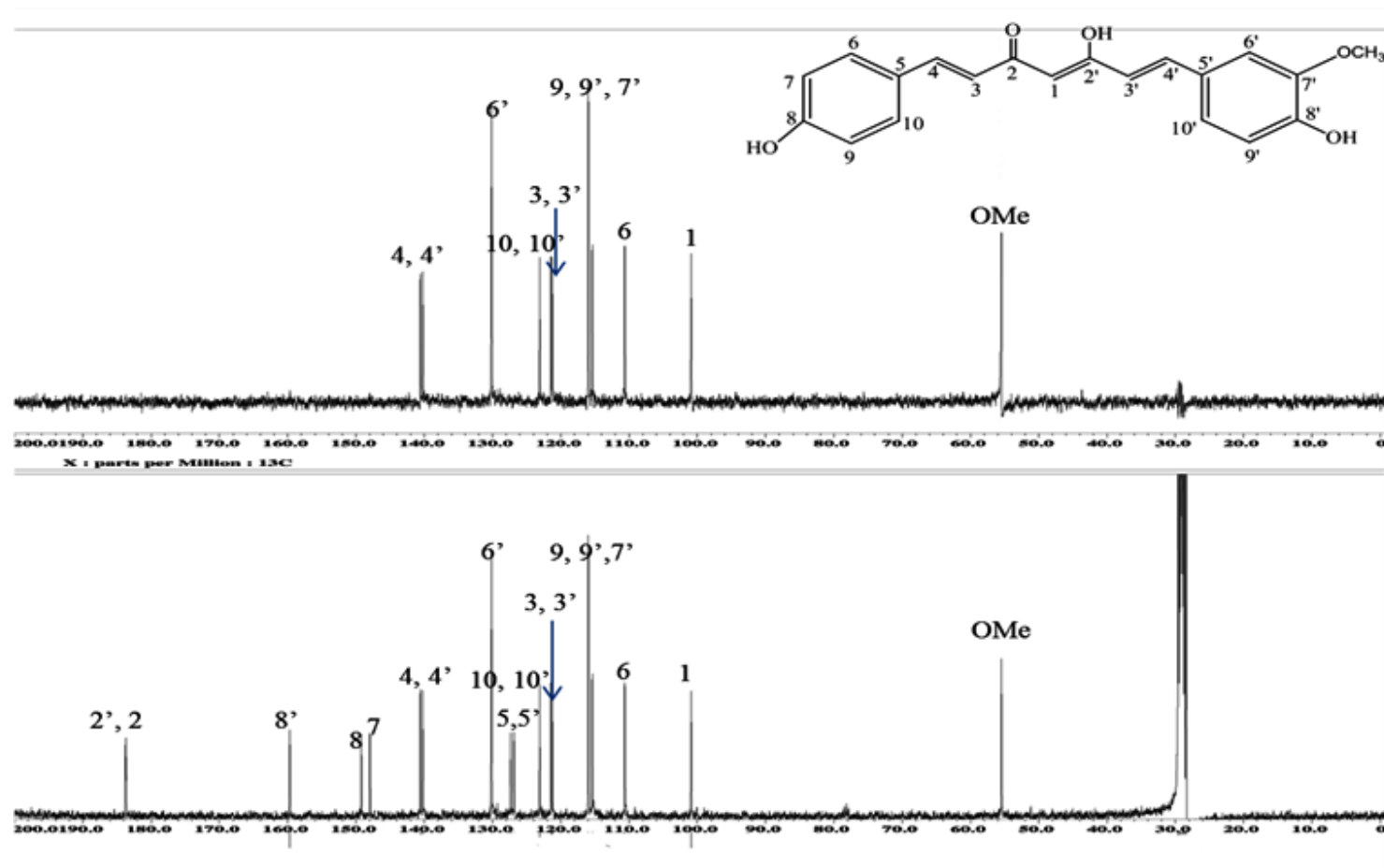
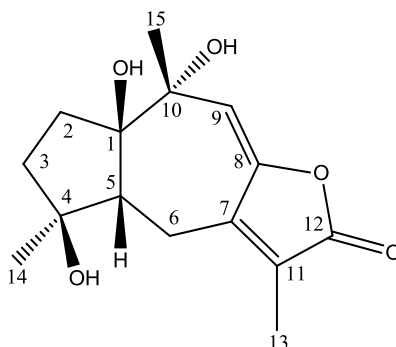


Figure 3.101: ¹³C NMR and DEPT-135 spectra of demethoxycurcumin 140

Guaiane type sesquiterpenoid

Zedoalactone B 60



Zedoalactone B **60** was isolated as a colourless oil. The HRESI-MS showed a quasi molecular ion peak at m/z 281 ($M+H$)⁺ corresponding to the molecular formula of C₁₅H₂₀O₅. The IR spectrum showed absorptions at 3441 cm⁻¹, 1732 cm⁻¹ presented for hydroxyl group α , β -unsaturated carbonyl, respectively. The UV spectrum displayed absorption band maximum at 262 nm implying the presence of a double bond conjugated with the lactone ring.

The ¹H NMR spectrum (**Figure 3.102, Table 3.28**) showed some proton signals similar to those observed for guaiane-lactone type sesquiterpene. Three methyl singlets were detected at δ 1.84, 1.44, and 1.26 attributed for H₃-15 and H₃-14 H₃-13, respectively. Further, one proton signal observed at δ 6.48 assigned for H-9. Multiple proton signals observed at δ 2.03, 2.53, 2.72 assignable for H-2, H-3, H-6, respectively. The proton spectrum also showed protons signal resonated at δ 3.40 appeared as dd with $J=2.8, 11.9$ Hz presented for H-5.

The ¹³C NMR and DEPT-135 (**Figure 3.103, Table 3.28**) exhibited a total of 15 carbon signals due to the presence of three sp³ methyls at δ 24.8 (C-15), 22.5 (C-14), and δ 7.8 (C-13). One sp² olefinic carbon was observed at δ 117.1 (C-9). Furthermore, three methylenes were detected at δ 34.6 (C-2), 40.4 (C-3), and 21.0 (C-6). In addition to six quaternary carbons, three of the six were sp² carbons at δ 150.3 (C-7), 148.1 (C-

8), and 125.4 (C-11) while two were sp^3 at δ 74.4 (C-1), and 79.0 (C-4). In addition, one carbonyl at δ 169.5 (C-12).

From the analysis of the above spectral evidence in combination with other 2D spectra, including HMBC, HSQC, NOESY confirmed the structure as zedoalactone B **60** and was in agreement with those published previously (Takano et al., 1995b).

Table 3.28: ^1H NMR (400 MHz), and ^{13}C NMR (100 MHz) spectral data in acetone- d_6 of zedoalactone **60**

Position	δ_{H}, J (Hz)	δ_{C}
1	-	74.4
2	2.03, m	34.6
3	2.53, m	40.4
4	-	79.0
5	3.40, dd (2.8, 11.9)	49.3
6	2.72, m	21.0
7	-	150.3
8	-	148.1
9	6.48, s	117.1
10	-	82.2
11	-	125.4
12	-	169.5
13	1.26, s	7.8
14	1.44, s	22.5
15	1.84, s	24.8

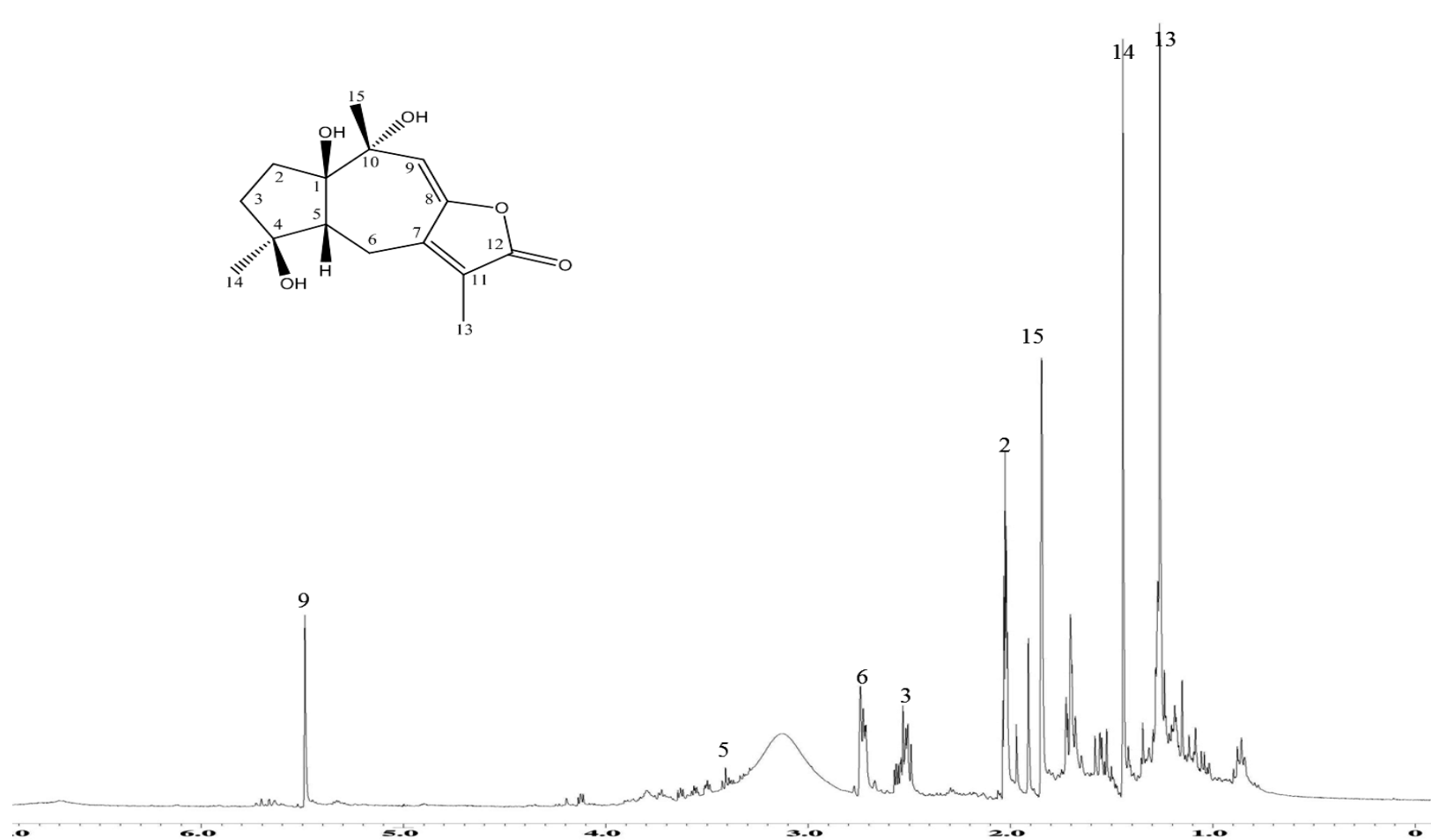


Figure 3.102: ^1H NMR spectrum of zedoalactone B 60

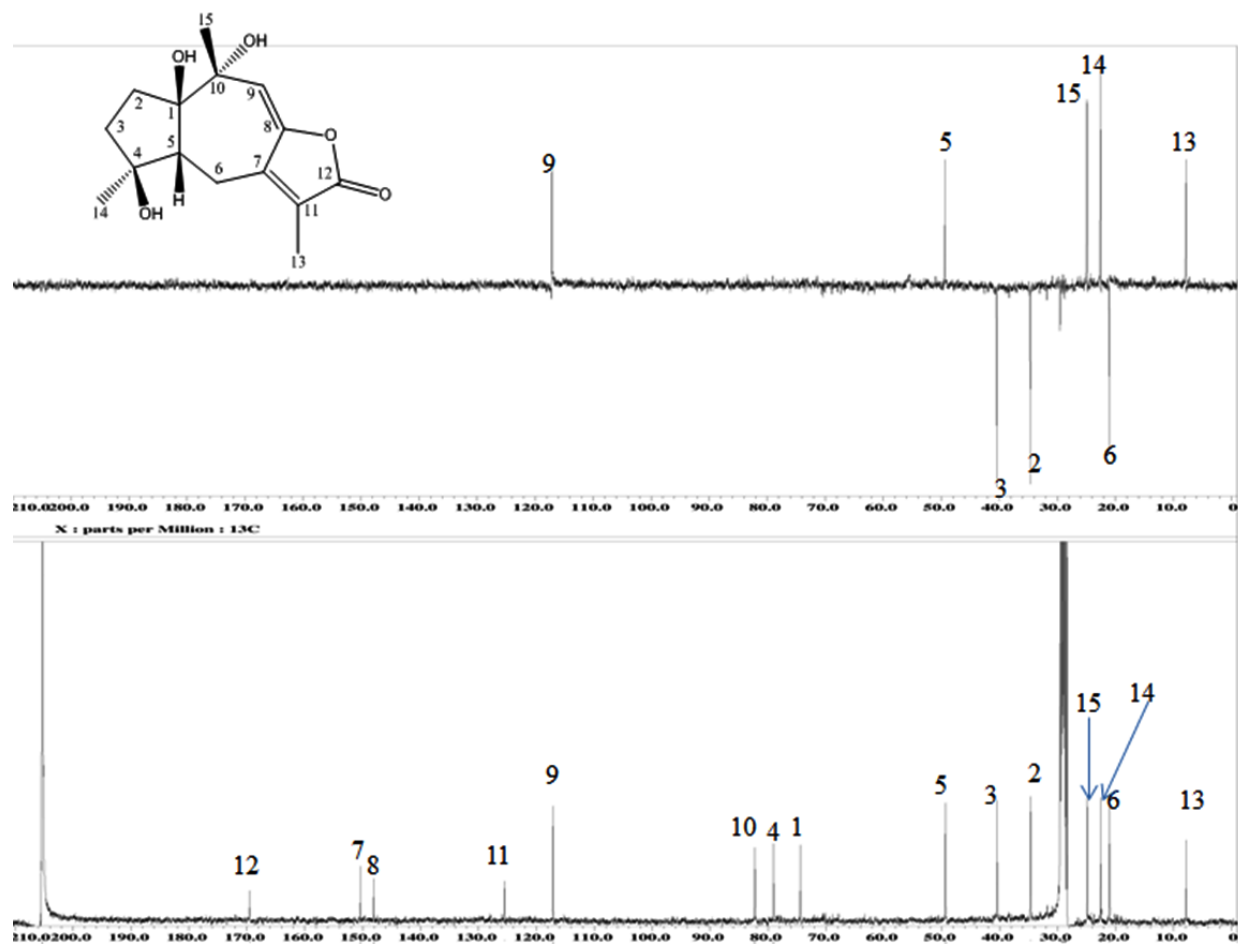


Figure 3.103: ^{13}C NMR and DEPT-135 spectra of zedoalactone B 60

3.1.2.3 Analysis of *C. purpurascens* essential oil

Two different techniques were introduced for oil extraction, with the aim of identifying the chemical constituents obtained by hydrodistillation with a view to determine the optimum parameters (temperature and pressure) for supercritical fluid extraction (SFE) for *C. purpurascens*. Thus attempts were made employing liquid CO₂ as a solvent with varying temperature and pressure to achieve higher yield and selectivity of the components in the extract.

(a) Chemical composition of hydrodistilled essential oil from *C. purpurascens*

The yield was 2.2 g from 300 g of sample. Therefore the percentage yield of the Essential oil extracted from *C. purpurascens* was 0.7% (w/w). The oil extracted by hydrodistillation was analysed by a combination of GC and GC-MS.

A total of 34 compounds accounting for 88.1% of the total oil were identified (**Figure 3.104**). Among these, eight were monoterpenoids, fifteen sesquiterpenes, and eleven sesquiterpenoids. The oil was especially rich in sesquiterpenoids (51.2%), of which the major components were found to be turmerone, followed by germacrone, ar-turmerone, germacrene-B, and curlone (**Table 3.29**). The identification of the compounds was performed by matching their mass spectra and arithmetic indices with references libraries.

Table 3.29: Chemical composition of the essential oil of *C. purpurascens* rhizomes

No.	Compounds	Arithmetic Indices (AI)		RT	Peak Area%	Methods of identification
		Calculated	Literature			
1	1,8-Cineole	1031	1026	16.87	3.3	MS, AI
2	Camphor	1144	1141	23.29	4.0	MS, AI
3	Borneol	1166	1165	24.45	0.3	MS, AI
4	Terpinen-4-ol	1178	1174	25.06	0.3	MS, AI
5	<i>p</i> -Cymen-8-ol	1184	1179	25.38	0.2	MS, AI
6	α -Terpinenol	1191	1186	25.75	0.8	MS, AI
7	Thymol	1293	1289	30.68	0.1	MS, AI
8	δ -Elemene	1339	1335	32.70	0.2	MS, AI
9	Piperitenone	1342	1340	32.87	0.7	MS, AI
10	β -Elemene	1393	1389	35.08	1.2	MS, AI
11	<i>cis</i> - α - Bergamotene	1416	1411	36.06	0.1	MS, AI
12	<i>trans</i> - Caryophyllene	1421	1417	36.24	1.8	MS, AI
13	γ -Elemene	1435	1434	36.82	1.6	MS, AI
14	Aromadendrene	1441	1439	37.05	0.1	MS, AI
15	α -Humulene	1455	1452	37.64	0.1	MS, AI
16	<i>trans</i> - β -Farnesene	1458	1454	37.75	0.2	MS, AI
17	γ -Muurolene	1478	1478	38.56	0.5	MS, AI
18	ar-Curcumene	1484	1479	38.82	2.6	MS, AI
19	α -Selinene	1488	-	39.98	1.3	MS ³
20	Curzerene	1500	1499	39.44	5.8	MS, AI
21	β -Bisabolene	1510	1505	39.85	0.4	MS, AI
22	Sesquiphellandrene	1526	1521	40.45	2.7	MS, AI
23	Selina-3,7(11)- diene	1544	1545	41.78	0.6	MS, AI
24	Germacrene-B	1561	1559	41.78	8.8	MS, AI
25	ar-Turmerol	1580	1580	42.50	3.3	MS ³ , AI
26	Guaiol	1595	1600	43.10	0.3	MS ³ , AI
27	<i>trans</i> - β - Elemenone	1607	1602	43.54	2.5	MS, AI
28	γ -Eudesmol	1633	1630	44.46	0.7	MS, AI
29	β -Eudesmol	1637	-	44.62	0.7	MS ³
30	Atractylone	1654	1657	45.21	0.6	MS ³ , AI
31	ar-Turmerone	1671	1668	45.83	9.4	MS, AI
32	Turmerone	1675	-	45.98	13.5	MS
33	Germacrone	1702	-	46.94	13.2	MS
34	Curlone	1705	-	47.07	6.2	MS

88.

Total rhizome oil =

1%

Remarks: MS = Mass Spectroscopy; AI = Arithmetic Indices; MS = Mass Spectroscopy. RT: Retention time

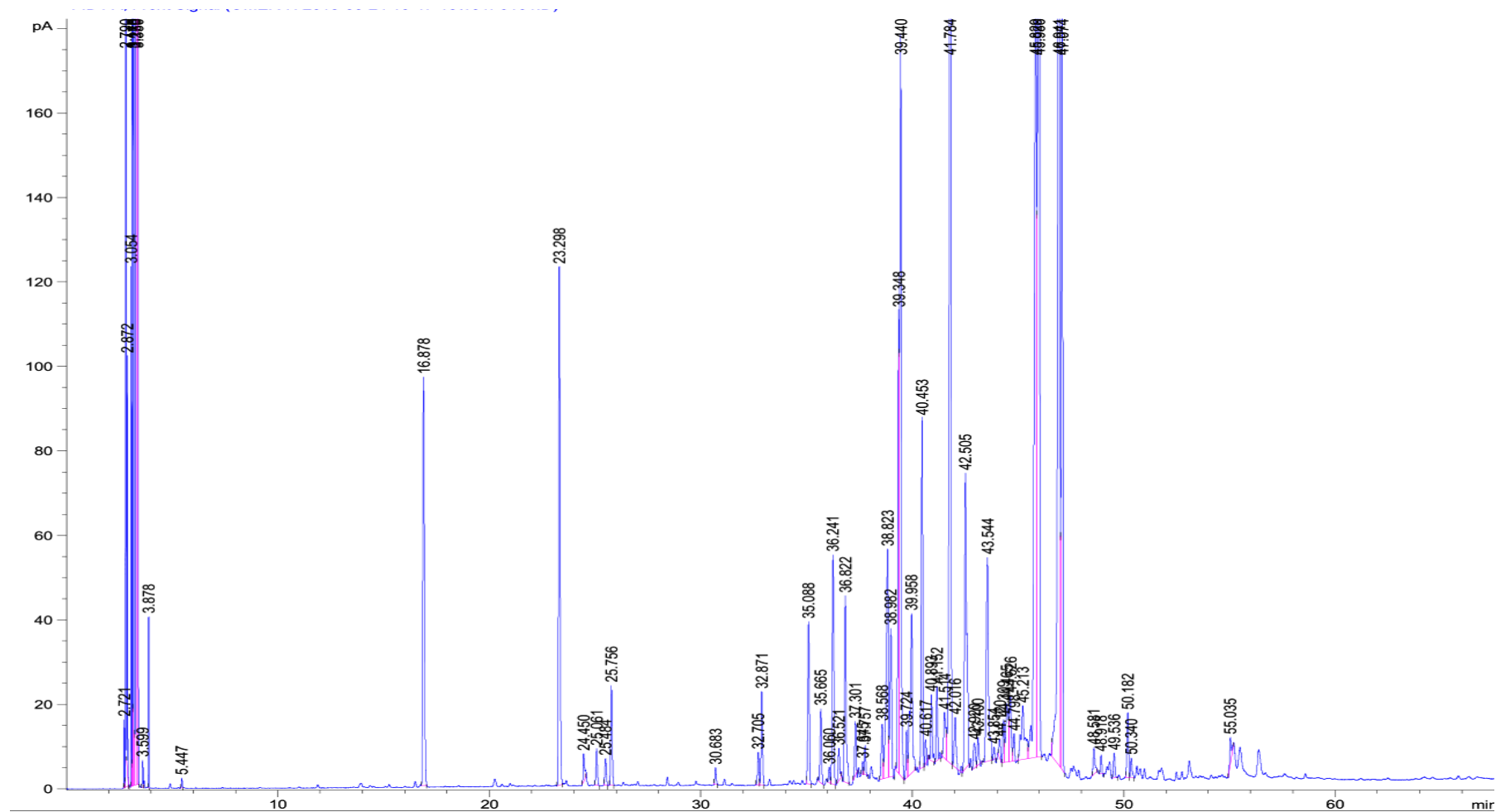


Figure 3.104: The GC-FID profile of the essential oil of *C.purpurascens* rhizomes

3.1.2.4 Supercritical carbon dioxide extraction of *C. purpurascens*

(a) General introduction

Supercritical fluid extraction (SFE) is an attractive alternative extraction technique to conventional solvent extraction due to the use of environmentally compatible fluids. It also offers the added advantage of oxygen free extraction environment, reduced solvent consumption, and shorter extraction time.

Use of liquid carbon dioxide (CO₂) as a solvent in SFE has the superiority over organic solvents since it is non flammable, nontoxic, and leaves no residue. It also has a low critical temperature compared to other solvents. Currently, SFE has been implemented in various applications on industrial scales.

(b) Supercritical carbon dioxide extraction of *C. purpurascens*

Supercritical carbon dioxide (SC-CO₂) was employed to extract oils from *C. purpurascens* rhizomes at temperatures of 313, 333, and 353 K and at pressures of 10.34 MPa (1500 Psi), 20.68 MPa (3000 Psi), and 34.47 MPa (5000 psi) at a constant flow rate of CO₂ liquid 12 ml/min. The process of variable pressure, temperature was studied for optimization of total oil yield.

The extraction rate was measured as a function of pressure and temperature. The extraction rate increased with an increase of pressure and decrease of temperature. The chemical components of SFE extracted oils were analysed by a combination of gas chromatography (GC) and gas chromatography-mass spectrometry (GC-MS) and the major components were identified as α -turmerone, turmerone, germacrone, and curlone. The composition *C. purpurascens* extract obtained by SFE was not different from the extract obtained by hydrodistillation. However, the components obtained in the extract were dependent on the pressure and temperature applied. Therefore, SFE is

much more specific in terms of selectivity as compared to conventional extraction methods. In all cases, the yield was more when extracted by SFE.

Table 3.30: The yields of the extracts obtained from *C. purpurascens* by SFE using variable temperatures and pressures

Exp. no.	Temperature (K)	Pressure (MPa)	Yield (g)
1	313	10.34	2.3024
2	313	20.68	0.1248
3	313	34.47	0.0434
4	333	10.34	2.2278
5	333	20.68	0.2421
6	333	34.47	0.4924
7	353	10.34	1.9486
8	353	20.68	0.5856
9	353	34.47	0.0498

K: Kelevin, MPa: mega Pascal

The extractions were performed in successive steps at increasing pressures to obtain the fractional extraction of the soluble compounds contained in the organic matrix.

The extraction rate increased with a decrease in temperature. The effect of pressure and temperature on the extracted oil suggested the optimum pressure 10.34 MPa (1500 Psi) and temperature of 313 K (40°C) for higher yield.

Initially, temperature was set to 313 K and maintained constant while varying the pressure, i.e., 10.34, 20.68 and 34.47 MPa for the same sample. The process was repeated for the same plant extract but at two different temperature levels (333 and 353 K).

The main goal of the present study was to investigate the effects of three different pressures starting from 10.34 MPa, increased to 20.68 MPa, followed by 34.47 MPa, in comparison to one step successive extraction using hex, DCM, and MeOH.

i SFE at 313 K and pressures of 10.34, 20.68, and 34.47 MPa

Interestingly, only ar-turmerone, turmerone, germacrone and curlone (rt: 45.7-47.0 min) can be extracted as the major soluble constituents at the pressure 10.34 MPa. It is therefore, saturated with these aforementioned constituents, and unable to extract other components of the plant material having similar polarity. A second extraction at a higher pressure allowed the extraction β -sesquiphellandrene (rt: 40.9 min) as the major component (peak range 99.9%). A further increase in the pressure to 34.47 MPa resulted in the extraction of 1H-3a, 7-methanoazulene as the major component (99.9%) along with other four minor components. Thus the pressure played the key role in the solubility of CO₂ offering a selective extraction of compound(s) from the plant material under investigation.

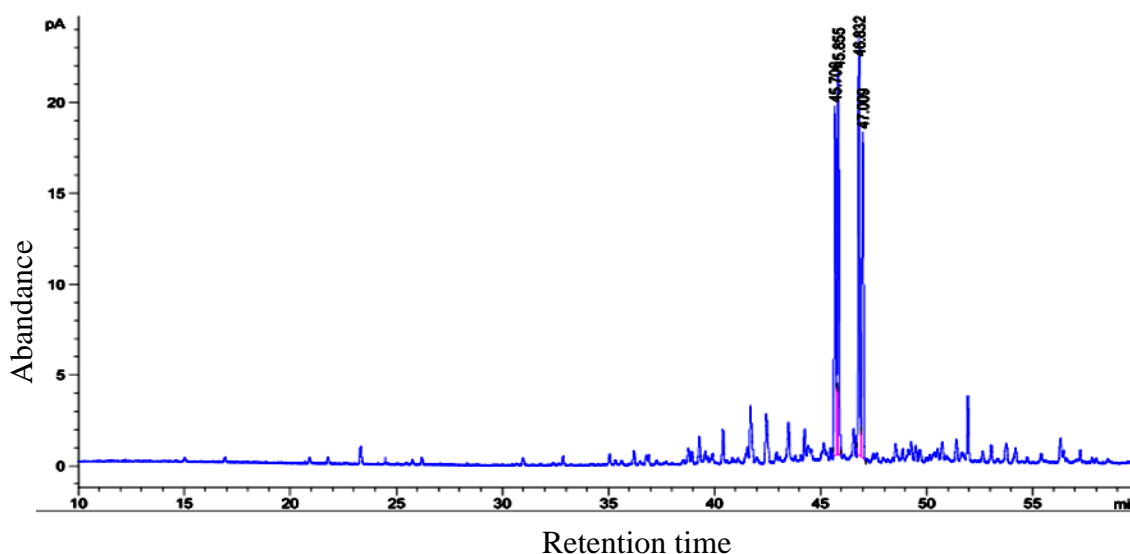


Figure 3.105: Gas chromatogram of SFE extract at 313K and 10.34 MPa

Table 3.31: Major components of SFE oil extracted at 313 K and 10.34 MPa

No	Retention time	Peak area %	Compound
1	45.70	20.96	Ar-turmerone
2	45.85	30.61	Turmerone
3	46.83	23.67	Germacrone
4	47.00	20.74	Curlone

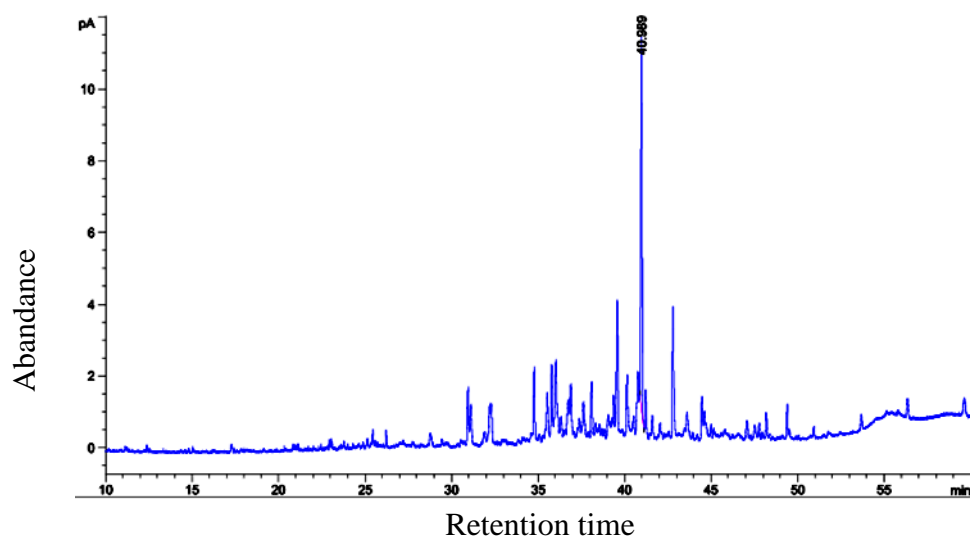


Figure 3.106: Gas chromatogram of SFE extracted oil at 313 K and 20.68 MPa

Table 3.32: Major component of SFE oil extracted at 313 K and 20.68 MPa

No	Retention time	Peak area %	Compound
1	40.99	93.9	β -sesquiphellandrene

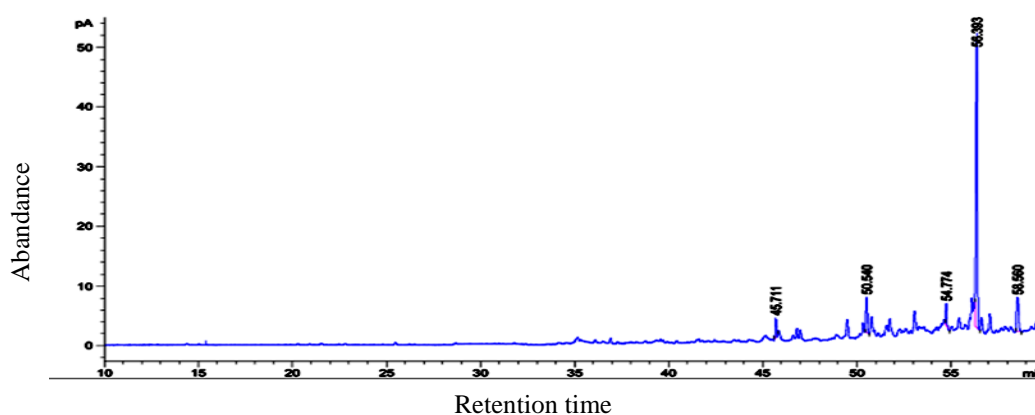


Figure 3.107: Gas chromatography profile of SFE extracted oil at 313 K and 34.47 MPa

Table 3.33: Major components of SFE oil extracted at 313 K and 34.47 MPa

no	Retention time	Peak area %	Compound
1	45.71	0.018	ar-Turnernone
2	50.54	0.038	Humulene
4	56.39	92.66	1H-3a, 7-Methanoazulene

ii SFE at 333 K and pressures of 10.34, 20.68, and 34.47 MPa

At 333 K, the four compounds observed in 40C, 1500psi also appeared as the major components of the extract but with a relatively lesser yield. It also resulted in the extraction of GC-MS detectable components in the same polarity region.

An increase in the pressure (3000psi) at the same temperature extracted more of the four major components, indicating that the extraction of these four compounds were not complete at the combination of 60C and 1500 psi in contrast to 40C 1500 psi where a complete extraction of these four compounds were observed. Further increase in the pressure to 5000 psi failed to render any GC-MS detectable component.

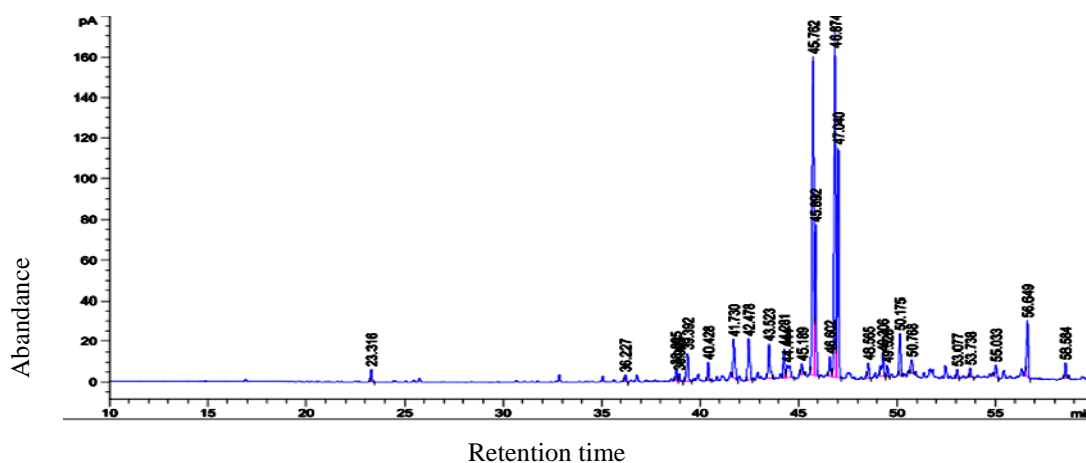


Figure 3.108: Gas Chromatogram of SFE extracted oil at 333 K and 10.34 MPa

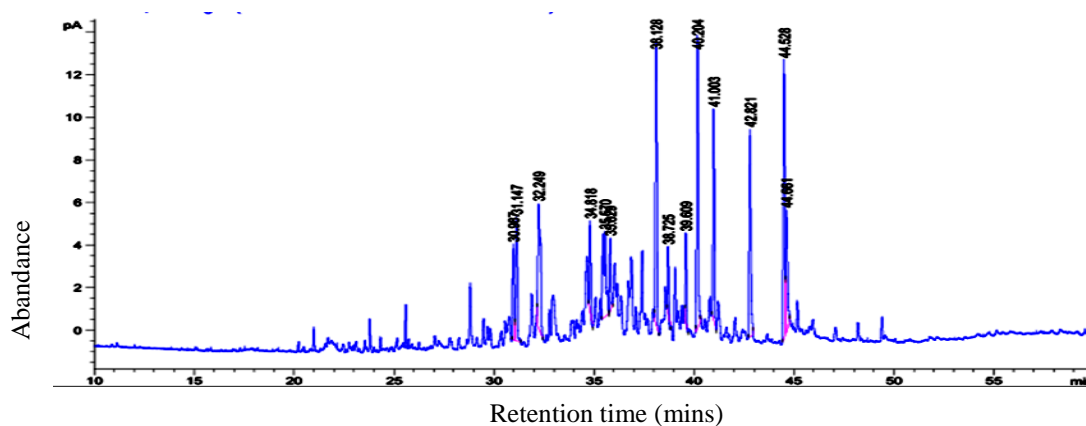
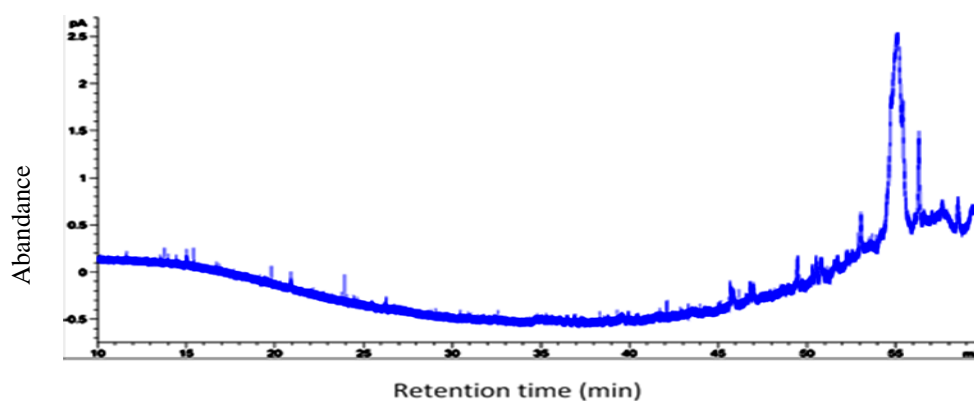


Figure 3.109: Gas Chromatogram of SFE extracted oil at 333 K and 20.68 MPa

Table 3.34: Major components of SFE extracted oil at 333 K and 10.34 MPa

no	Retention time	Peak area %	Compound
1	23.30	0.62	Camplor
2	32.87	0.29	Piperitenone
3	35.07	0.34	β -elemene
4	36.22	0.56	<i>cis</i> - α -Bergamotene
5	36.80	0.61	γ -elemene
1	45.70	19.20	ar-turmernone
2	45.85	10.90	Turmernone
3	46.83	20.08	Germacrone
4	47.00	12.90	Curlone

**Figure 3.110:** Gas chromatography profile of SFE extracted oil at 333 K and 34.47 MPa

iii SFE at 353 K and pressures of 10.34, 20.68, and 34.47 MPa

The extraction at 353 K with 10.34 psi followed a same pattern as that of 60C 1500psi, but with an additional major component which was identified as bisabolene

Increase in the pressure (3000 psi) was similar to extraction commenced at 1500 psi but with a greater variety of compounds (no of peaks, RT range) and the extraction was complete for these compounds as they were not observed for an increase in the pressure to 500psi.

The major indicated that the solvent CO₂ was fully saturated with the four compounds and unable to extract more compounds, it also confirming the powerful selective extraction by SFE. In addition, programming temperature at 313 K yielded

(2.3024 g, 6.97%) higher compared to 333 K (0.1248 g, 0.37%) and 353 K (0.0434, 0.13%) successive extraction for the same sample.

At pressure 20.68 MPa, ar-turmernone appeared with less quantity in comparison with 10.34 MPa.

At pressure 34.47 MPa, non-volatile constituents were observed at temperature 333 K and 353 k except one major compound observed at 40°C and it was identified as β -sesquiphellandrene.

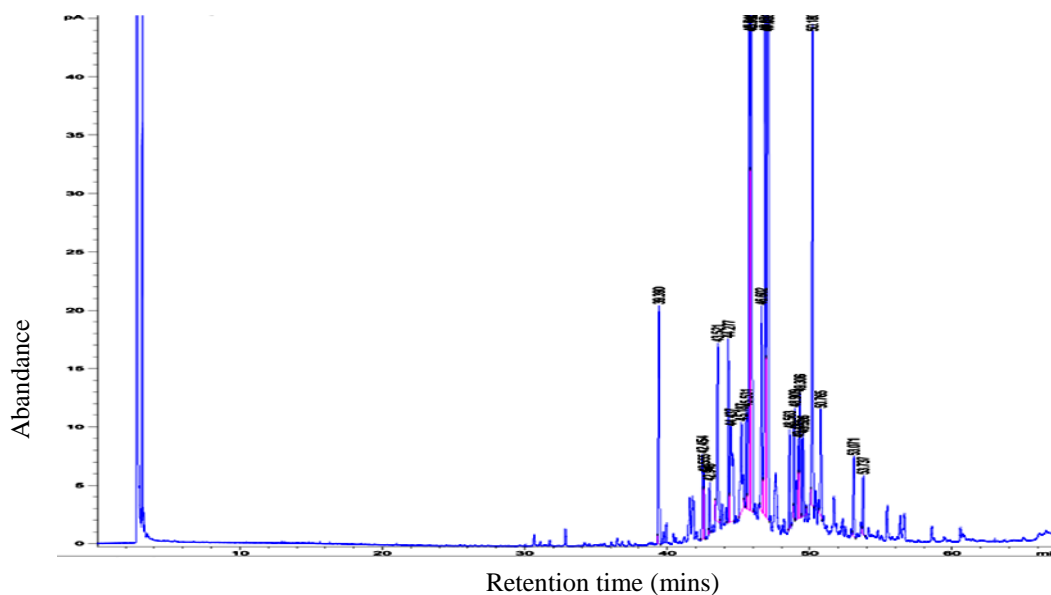


Figure 3.111: Gas Chromatogram of SFE extracted oil of at 353 K and 10.34 MPa

Table 3.35: Major components of SFE extracted oil of at 353 K and 10.34 MPa

No	Retention time	Peak area %	Compound
1	45.70	18.84	ar-Turmernone
2	45.85	13.42	Turmernone
3	46.83	19.14	Germacrone
4	47.00	12.22	Curlone

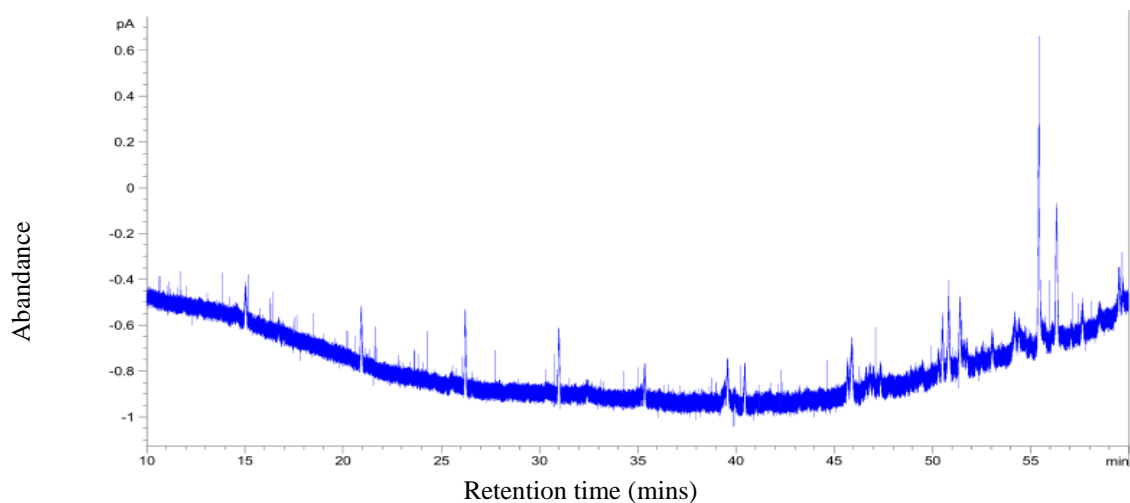


Figure 3.112: Gas Chromatography profile SFE extracted oil at 353 K and 20.68 MPa

Table 3.36: Major components of SFE extracted oil of at 353 K and 20.68 MPa

No	Retention time	Peak area %	Compound
1	45.70	13.56	Ar-turmernone
2	45.85	27.36	Turmernone
3	46.83	18.56	Germacrone
4	47.00	14.82	Curlone

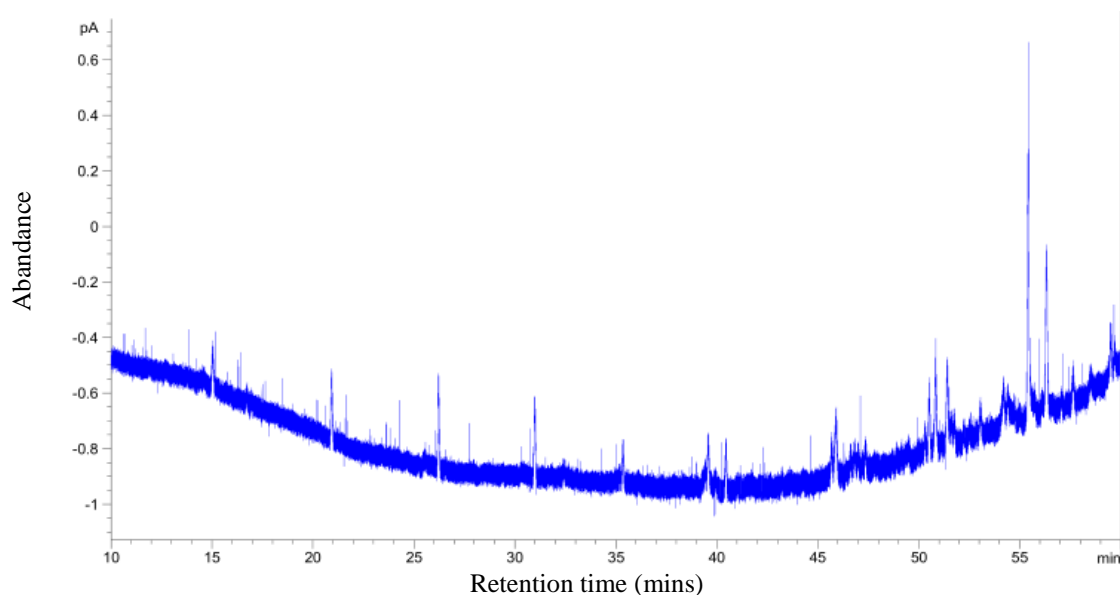


Figure 3.113: Gas chromatography profile of SFE extracted oil at 353 K and 34.47 MPa

Collectively, based on the above results, the optimum parameters to obtain higher yield and selective components were at temperature 313 K, pressure at 10.34 MPa and flow rate of liquid CO₂ at 12 ml/ min.

Further more, the yields decreased with the increase of temperature (313, 333, and 353 K) considering using the same pressure at 10.34 MPa. In addition,, the results also implied the powerful SFE technique as high selectively and high yields extractions method, it can be an effient way to extract ar- turmernone in a good quantity. Indeed, SFE showed immediate advantage over traditional extraction techniques.

3.2 Cytotoxicity

The cytotoxic effects of the crude extracts and the pure compounds isolated from the rhizomes of *C. zedoaria* and *C. purpurascens* were assessed against a range of cancer cell lines and non-cancerous cell lines.

3.2.1 Cytotoxic activity of the crude extracts and the pure compounds from the rhizomes of *C. zedoaria*

Initially, two human cancer cell lines (MCF-7 and Ca Ski), and non-cancerous cell lines (MRC-5 and HUVEC) were used in the MTT assay to test the cytotoxic activity of *C. zedoaria* extracts. The experiments were conducted in triplicate and presented as the mean (**Table 3.37**). The hexane (hex) extract showed strong inhibition against the two human cancer cell lines MCF-7 and CaSki with the IC₅₀ values of 18.4 and 19.0 µg/ml respectively whilst the dichloromethane extract (DCM) showed moderate cytotoxicity against MCF-7 (IC₅₀: 40.6 µg/ml) and weak cytotoxicity against Ca Ski (IC₅₀: 83.5 µg/ml). The extracts were non-toxic towards the non-cancer cell lines HUVEC and MRC-5 even at the highest concentration tested (100 µg/ml).

Table 3.37: Cytotoxic activity of *C. zedoaria* extracts against human cancer cells and

non-cancer cell lines (MRC-5 and HUVEC)

Extract	IC ₅₀ (µg/ml)*			
	Cancer cells		Non-cancer cells	
	MCF-7	Ca Ski	HUVEC	MRC-5
Hexane (Hex)	18.4 ± 1.6	19.0 ± 1.5	>100.0	>100.0
Dichloromethane (DCM)	40.6±2.3	83.5±2.7	>100.0	>100.0
Ethyl acetate (EA)	>100.0	>100.0	>100.0	>100.0
Methanol (MeOH)	>100.0	>100.0	>100.0	>100.0
Methanol(Soxhlet extraction) (MeOH S)	>100.0	>100.0	>100.0	
Doxorubicin	0.1±0.0	0.2±1.0	1.4±0.0	na

*Experiments were done in triplicate and presented as mean ± SD.

The pure compounds isolated from the active extracts (hex and DCM) of *C. zedoaria* were further evaluated on eight selected cancer cell lines (MCF-7, Ca Ski, HT-29, PC-3, WEHI-3, HL60, A549, and AS-SK-LU1) and non-cancerous cell HUVEC (human umbilical vein endothelial cell). The cytotoxic activity of the compounds is presented in Table 3.38. Collectively the compounds showed moderate cytotoxic effect against the human carcinoma cells. Interestingly two sesquiterpenoids, namely curcumenol **42** and curcumenone **65** demonstrated strong cytotoxic activity against MCF-7. Nevertheless, there is no report found on the cytotoxicity of compounds **42**, **65** and zerumbone epoxide **150** against human MCF-7, Ca Ski and PC-3 cell lines. Hence, it is the first time to document the selective activity of compounds **42** and **65** isolated from *C. zedoaria* against MCF-7 cell line. The results were also in agreement with previous study on procurcumenol **44** and zerumbone epoxide **151** where the compounds exhibited good cytotoxic effect against PC-3 and HT-29 cell lines. In another study, curcumenone **65** isolated from the rhizomes of *C. zedoaria* showed protective effect on alcohol-treated mice, accelerated the liver alcohol dehydrogenase activity, and suppressed D-galactosamine/lipopolysaccharide-induced acute liver injury (Hisashi Matsuda et al., 1998b). Among the compounds tested, **19**, **21**, **23**, **43**, **44**, **65**, **104**, **127**, **150** and **151** displayed appreciable cytotoxic activity against Ca Ski (IC₅₀ values ranging from 14.5 to 100.0 µg/ml). The rest of the compounds (**19**, **23**, **44**, **101**, **127** and

128) also exhibited moderate inhibitory effect against PC-3 and HT-29 cell lines. Although the pure compounds were not as effective as doxorubicin in inhibiting the proliferation of the cancer cells, they inflicted less damage to the non-cancerous cells. In this study, zerumin A **128**, isolated from the hexane extract displayed moderate cytotoxic effect on MCF-7, Ca Ski and PC-3 cell lines. This is in agreement with previous report where zerumin A **128** isolated from *C. mangga* exhibited anti-proliferative effect on Ca Ski and MCF-7 cells with IC₅₀ values of 8.7 and 14.2 µg/ml, respectively (S. N. A. Malek et al., 2011). The cytotoxicity test reported in the present study provided important preliminary data to help select from these compounds with potential anticancer properties for advanced studies.

An attempt to search for new anticancer agents that are safe as well as being effective, five isolated sesquiterpenoids were subjected to the MTT based cytotoxicity test using mouse myelomonocytic leukemia cells (WEHI-3), and promyelocytic human leukemia cells (HL-60). Procurecumenol **44** showed the strongest effect on WEHI-3 and HL-60 cells with IC₅₀ values of 6 and 25 µg, respectively. The results are presented in the Table.3.37.

In addition, nine sesquiterpenoids and two labdane diterpenoids were evaluated against two lungs cancer cell lines; human alveolar adenocarcinomic cells A549, and human lung adenocarcinomic SK-LU, and an immortal human keratinocyte line HaCaT. Three of these compounds demonstrated mild cytotoxic activity which includes hydrocurdione **19**, calcaratarin A **129**, and zerumbone epoxide **151** (Table.3.37).

Table 3.38: Cytotoxic activity of pure compounds isolated from *C. zedoaria* against various cell lines

Compounds	IC ₅₀ (µg/ml)								
	MCF-7	Ca Ski	PC-3	HT-29	WEHI-3	HL60	A549	AS-SK-LU1	HUVEC
Labda-8(17), 12 diene-15, 16 dial 127	16.3±0.2	14.5±0.1	26.3±2.4	21.5±3.1	-	-	-		45.3±1.9
Dehydrocurdione 19	33.0±1.1	21.7±1.1	19.1±2.8	22.7±2.4	-	-	17.4±2.3	20.96±1.61	24.0±2.1
Curcumenone 65	8.3±1.0	>100.0	39.8±4.2	43.3±6.2	35	99	na	na	50.0±8.6
Comosone II 104	>100.0	76.0±1.2	na	na	-	-	-	-	na
Curcumenol 42	9.3±0.3	18.5±1.0	17.3±1.2	24.8±2.7	66	39	na	na	25.9±1.4
Procurcumenol 44	16.1±2.2	62.4±0.3	13.3±1.7	15.5±2.3	6	25	na	na	16.3±1.0
Germacrone 23	59.1±2.9	39.3±1.2	55.2±4.9	42.9±4.1	-	-	na	na	73.7±0.3
Zerumbone epoxide 151	24.1±0.1	34.5±0.6	10.8±1.9	13.7±2.7	-	-	14.0±0.78	20.0±1.09	14.2±1.1
Zederone 26	>100.0	>100.0	27.0±1.9	19.1±2.5	> 100	> 100	na	na	42.1±2.7
Second monoclinic curcumenol 151	>100.0	>100.0	na	na	-	-	-	-	71.7±6.1
Furanodiene 21	36.5±2.6	na	39.5±4.5	47.2±4.4	-	-	na	na	40.9±2.6
Germacrone-4, 5-epoxide 24	37.2±4.0	na	43.9±7.2	39.6±4.6	-	-	-	-	48.4±4.7
Calcaratarin A 129	62.5±4.8	na	41.7±3.4	48.3±5.1	-	-	31.6±1.55	24.16±2.20	47.3±4.2
Isoprocucumenol 43	58.8±4.2	na	37.4±4.5	51.6±3.9	81	-	-	-	45.1±3.0
Germacrone-1, 10- epoxide 25	61.2±5.8	na	53.2±4.9	72.8±8.3	-	-	-	-	55.5±1.6
Zerumin A 128	22.3±1.1	na	21.9±1.6	17.4±2.0	-	-	na	na	25.8±1.9
Curcumanolide A 101	29.8±3.1	na	18.8±2.4	21.3±3.2	-	-	-	-	21.7±7.0
Curcuzedoalide 62	49.8±3.6	na	62.1±8.1	58.2±3.5	-	-	-	-	45.3±7.8
Gweicurculactone 41	31.2±3.2	na	38.3±2.2	35.7±5.8	-	-	-	-	71.7±6.1
Furanodione 22	32	32.5	na	na	-	-	-	-	-
Curdione 20	>100.0	>100.0	na	na	-	-	-	-	-
Curzerenone 111	56.5	60	na	na	-	-]-	-	-
Doxorubicin	0.1±0.0	0.2±1.0	na	na	na	na	na	na	1.4±0.0

*Experiments were done in triplicate and presented as mean ± SD.

3.2.2 Cytotoxic activity of crude extracts, essential oil, supercritical fluid extracts, and pure compounds from *C. purpurascens* rhizomes

Initially, the cytotoxicity activity of the *C. purpurascens* extracts (Hex, DCM, and MeOH) were examined against various human cancer cell lines (CEMSS, COAV, HEPG-2, SKOV3, MDA-MB-231 and MCF-7). DCM and MeOH extracts showed potent inhibitory effect against SKOV3 with the IC₅₀ values of 4.7 and 5.12 µg/ml (**Table 3.39**). The hexane extract showed activity ranging from weak to moderate levels against various cancer cell lines (**Table 3.39**).

In addition, the hydrodistilled oil of dried ground rhizomes was investigated against selected carcinoma cell lines (MCF-7, Ca Ski, A549, HT29, and HCT116) and normal human lung fibroblast cell line (MRC-5). Results from the MTT assay revealed strong cytotoxicity against HT29 cells (IC₅₀ value of 4.9 µg/ml), weak cytotoxicity against A549, Ca Ski, and HCT116 cells with IC₅₀ values of 46.3, 32.5, and 35.0 µg/ml, respectively (**Table 3.39**).

Furthermore, nine extracts obtained by SFE were evaluated for cytotoxicity by the MTT assay on SKOV and CAOV3 cells. The extracts obtained at 313 K, 34.46 MPa demonstrated stronger cytotoxic activity compared to the other extracts (IC₅₀:15 µg/ml). The other extracts obtained at 313 K, 10.34 MPa and 313 K, 34.46 MPa exhibited moderate cytotoxic activity against the CAOV3 with IC₅₀ values of 34 and 36 µg/ml, respectively (**Table 3.39**).

Table 3.39: Cytotoxic activity of crude extracts, hydrodistillation oil, and SFE extracts of the rhizomes of *C. purpurascens*

Extracts	IC ₅₀ (µg/ml)													
	CEMSS	COAV	HEPG-2	SKOV3	HT29	MDA-MB-231	MCF-7	WRL-68	WEH3	HL60	Ca Ski	A549	HT116	MRC-5
Hex.	200	147.78	80.1	138.7	68.1	56.24	121.9	100	79	24	-	-	-	-
DCM	22.13	22.42	31.11	4.7	32.58	21.91	21.03	21.63	32	11	-	-	-	-
MeOH	25	21.85	83.37	5.12	55.67	50	41.09	23.9	48	20	-	-	-	-
Hydrodistillation oil	-	-	-	-	4.9	-	>100	-	-	-	32.5	46.3	35.0	25.2
SFE, 313 K, 10.34 MPa	-	34	-	44	-	-	-	-	-	-	-	-	-	-
SFE, 313 K, 20.68 MPa	-	50	-	33	-	-	-	-	-	-	-	-	-	-
SFE, 313 K, 34.47 MPa	-	36	-	57	-	-	-	-	-	-	-	-	-	-
SFE, 333 K, 10.34 MPa	-	67	-	79	-	-	-	-	-	-	-	-	-	-
SFE, 333 K, 20.68 MPa	-	>100	-	76	-	-	-	-	-	-	-	-	-	-
SFE, 333 K, 34.47 MPa	-	>100	-	15	-	-	-	-	-	-	-	-	-	-
SFE, 353 K, 10.34 MPa	-	>100	-	>100	-	-	-	-	-	-	-	-	-	-
SFE, 353 K, 20.68 MPa	-	>100	-	>100	-	-	-	-	-	-	-	-	-	-
SFE, 353 K, 34.47 MPa	-	-	-	>100	-	-	-	-	-	-	-	-	-	-

The pure compounds isolated from *C. purpurascens* were subjected to the MTT based cytotoxicity assay using mouse myelomonocytic leukemia cells (WEHI-3), promyelocytic human leukemia cells (HL-60), ovarian cancer cell SKOV3, and ovarian carcinoma cells CAOV3. Curcumin **139** showed the strongest effect on WEHI-3 and HL-60 cells with IC₅₀ values of 25 and 23 µg/ml, respectively. Whereas, demethoxycurcumin **140** displayed cytotoxic activity against WEHI-3 and HL-60 with IC₅₀ values of 50 and 36 µg/ml, respectively. The results were presented in the **Table 3.40**

Table 3.40: Cytotoxic activity of compounds isolated from *C. purpurascens*

Compound	IC ₅₀ (µg/ml)				
	WRL)	WEH3	HL60	SKOV3	CAOV
Curcumin 139	23	25	23	> 100	> 100
Demethoxycurcumin 140	> 100	50	36	> 100	>100
Bisdemethoxycurcumin 141	> 100	> 100	80	> 100	>100
ar-Turmerone 74	-	> 100	> 100		
Zedoalactone B 60	-	84	78		

3.3 QSAR studies

Quantum chemical methods can be successfully applied to express molecular interactions between substrate and receptor in terms of molecular electronic properties of the substrates. In recent years, quantitative structure-activity relationships studies (QSAR) have been proven a powerful tool in the determination of the relationships between the observed biological activities of natural and synthesized compounds and their structural, electronic properties (descriptors). Various qualitative and quantitative analyses relationship studies can be found in the literature using quantum chemical and statistical methods to achieve correlations between calculated and biological activities of natural and synthetic substrates.

This study aimed at elucidating the structure-cytotoxic activity relationships of a series of 21 compounds isolated from *C. zedoaria* against four human cancer cells namely, breast carcinoma cells (MCF-7), cervical carcinoma cells (Ca Ski), human prostate cancer cells (PC-3), human colon adenocarcinoma cells (HT-29), and a normal cell line, human umbilical vein endothelial cells (HUVEC). Density functional theory (DFT) was adopted at the level of B3LYP/6-31+G (d, p) in order to calculate electronic and steric molecular descriptors of the isolated compounds, followed by the application of statistical methods including simple and multiple linear regressions (SLR, MLR), principal component analysis (PCA) and hierarchical cluster analysis (HCA) to determine the main descriptors responsible for the cytotoxic activity of the compounds under investigation.

In a view from the studies previously have done, Ishihara *et al.* employed semiempirical PM5 method to delineate the relationship between the cytotoxic activity and eleven chemical descriptors of a series of tropolone compounds and were able to show that the observed cytotoxic activity correlated well with compounds of structural

similarities and governed mainly by dipole moment (μ), hydrophobicity ($\log P$), hardness (η), electrophilicity (ω) and electronegativity (χ) (Ishihara et al., 2010). In another study, Stanchev *et al.* showed that the cytotoxic activity of a series of 4-hydroxycoumarins was well correlated with $\log P$, μ , volume (V) and molecular orbital energies (E_{HOMO} and E_{LUMO}) (Stanchev et al., 2008). In addition, Yang *et al.* used semiempirical method AM1 to determine the molecular descriptors of a series of ganoderic acids with cytotoxicity against tumour cells; they showed that E_{HOMO} , electronegativity, electronic energy, $\log P$ and molecular area (A) are the variables that best discriminate between highly and less active ganoderic acids (Yang et al., 2005).

In an effort to find lead compounds at lower cost and greater speed, techniques in computational chemistry offers fast and highly efficient ways for virtual screening. In recent years progress has been made in developing algorithms that predict molecular geometry and its effect at the binding site. Computational techniques are used to search databases of small molecules to find suitable compounds that can serve as drug leads. Such predictions are not meant to replace experimental affinity determination, but virtual screening methods can complement the experimental methods by producing an enriched subset of a large chemical database. On the other hand, these methods help to evaluate the strength of bonds between the compounds and their cellular interface. Possible enzymatic, physical and chemical degradation of the compound cores as the compounds will gain access to circulation through blood and lymphatic channels. Such efforts could give meaningful guidance to choose the potential compounds, combined with the experimental data, and could be involved in analysing the compound's metabolism *in vitro* and *in vivo*. Scoring function the calculation of pair-wise atomic terms includes evaluations for different secondary interactions, dispersion/repulsion, hydrogen bonding, electrostatics, and desolvation. Structure-based virtual screening typically employs quantum technique that is designed to explore the possible molecule

physical properties within a compound of interest. Thus, compounds from the subset that pass the initial virtual screening are found to be pharmaceutically interesting and to meet the criteria such as to (i) be reproducible, (ii) maintain the size of the compounds complex to a minimum, (iii) maintain the biological properties, (iv) provide chemical stability of the complex, and (v) be reliable.

Quantum chemistry has been applied recently to selectively recognize molecules, proteins, and cells of interest. It has revolutionized the processes of introducing molecules within research settings and improves their identification. As the unique physical and chemical properties of these molecules are being unravelled, new potential methods of therapeutic management are emerging. Additionally, quantum chemistry has shown the capability of specifically and effectively label molecular targets and been used as a diagnostic tool for cancer at cellular level. Through this technique, covalent conjugation of functional groups with a variety of biological molecules can be achieved. Once a biological interface has been provided, compounds can effectively and specifically target different cellular, tissue, and organ levels. The sampling and evaluating methods will be discussed in more detail in the next paragraphs.

To determine the structure-cytotoxicity activity relationship of a series of 21 compounds isolated from *C. zedoaria* a large number of electronic, steric and hydrophobicity descriptors were calculated using quantum calculations methods (density functional theory DFT). The following steps were followed:

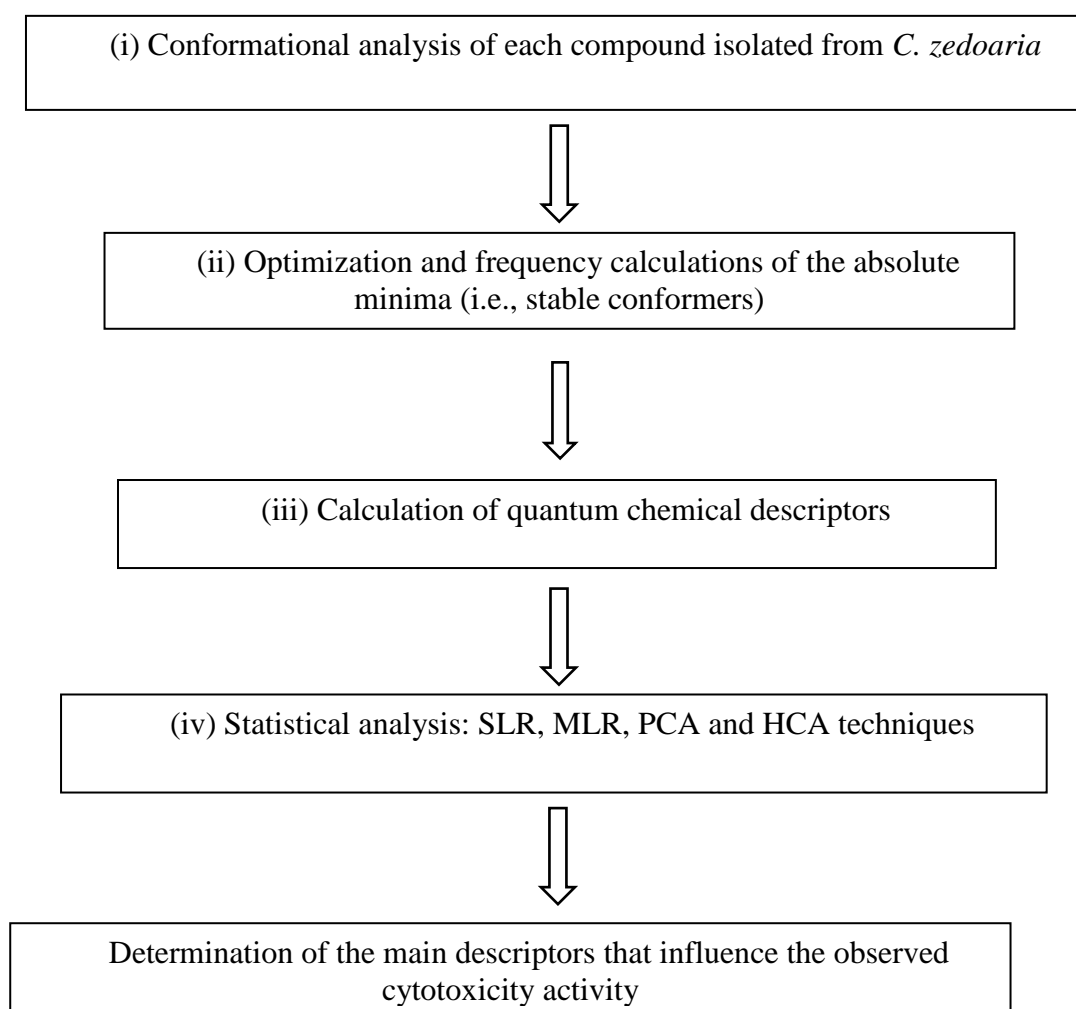
(i) Conformational analysis: For each compound, the stable conformer was obtained using molecular mechanics force field as implemented in Spartan Software.

(ii) The stable conformers of different compounds were optimized using B3LYP hybrid function. The absolute minima were confirmed by the absence of imaginary frequencies (i.e, all frequencies are positive).

(iii) The electronic descriptors were calculated from the HOMO and LUMO energies ($IP = -E_{HOMO}$ and $EA = -E_{LUMO}$).

(iv) SLR, MLR, PCA and HCA statistical techniques were used to determine the main descriptors that influence the cytotoxic activity of the isolated compounds.

The scheme for the QSAR study is presented as follows:



Scheme 3.1: QSAR studies framework

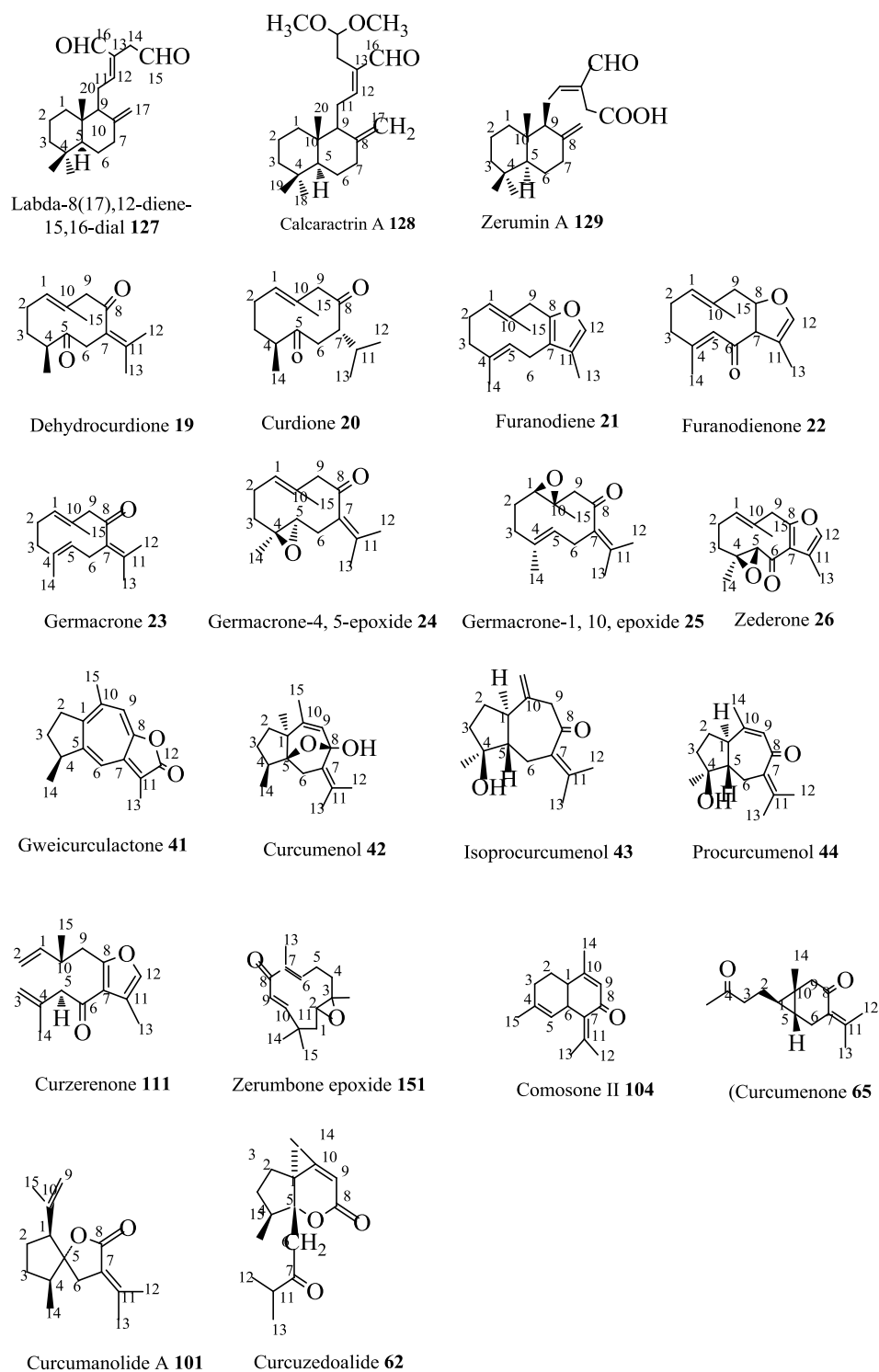


Figure 3.114: Structures of compounds isolated from *C. zedoaria*.

In the present study, QSAR study has been carried out on 21 terpenoids (**Figure 3.114**), for which the cytotoxic activity has been investigated. QSAR study was carried out using simple and multiple linear regressions (SLR and MLR), principal component

analysis (PCA) and hierarchical cluster analysis (HCA) analyses. Quantum-chemical calculations have been performed using density functional theory at the B3LYP/6-31+G (d, p) level of theory. The optimized structures were confirmed by the absence of imaginary frequencies. This methodology employed to calculate a set of molecular descriptors for the 21 compounds.

3.3.1 Simple linear regression (SLR) analysis

The values of the electronic, steric and hydrophobic descriptors of the studied compounds (**19-26**, **41-44**, **62**, **65**, **104**, **111**, **127-129** and **151**), as well as their cytotoxic activities (IC_{50} in μM) against MCF-7, Ca Ski, PC3, HT-29 and HUVEC cell lines are presented in **Table 3.41**. As can be observed from **Table 3.41**, the cytotoxic activity of the isolated compounds varied with the cell type. Thus a simple linear regression analysis was performed to determine the effect of each of the descriptors separately on the cytotoxicity of the isolated compounds. **Figure 3.115** displays simple linear regression curves obtained with each descriptor for the cytotoxicity of the test compounds against MCF-7 cells, while the statistical parameters (correlation coefficient (R^2), adjusted correlation coefficient (R^2_{adj}) and standard deviation (SD)) for SLR curves between each descriptor and each tested cell line is presented in **Table 3.42**.

Table 3.41: Cytotoxicity IC₅₀ (μM) and molecular descriptors obtained at B3P86/6-311+G (d, p) and B3P86/6-311+G (d, p) level for the compounds under investigation

Compound	IP	EA	χ	η	ω	α	μ	A	V	$\log P$	M	IC ₅₀ (μM)				
												MCF-7	Ca Ski	PC3	HT-29	HUVEC
127	6.87	2.15	4.51	4.71	2.16	324	6.13	400	470	3.45	302.46	53.9 ± 0.7	47.9 ± 0.3	87.0 ± 7.9	71.1 ± 10.2	149.8 ± 6.3
129	6.86	2.09	4.48	4.77	2.10	328	5.62	408	481	3.86	318.46	70.0 ± 3.3	NA	68.8 ± 5.0	54.6 ± 6.3	81.0 ± 6.0
128	6.85	2.00	4.43	4.85	2.02	363	5.63	457	541	4.20	348.53	14.3 ± 0.6	NA	119.6 ± 9.8	138.6 ± 14.6	135.7 ± 12.1
19	6.56	1.69	4.12	4.87	1.74	244	2.99	323	368	3.63	234.34	140.8 ± 4.7	92.6 ± 4.7	81.5 ± 11.9	96.9 ± 10.2	102.4 ± 9.0
20	6.52	1.26	3.89	5.26	1.44	238	1.40	331	377	4.01	236.35	NA	-	-	-	-
23	6.40	1.39	3.89	5.01	1.51	248	4.06	321	355	3.81	218.34	NA	180.0 ± 5.5	252.8 ± 22.4	196.5 ± 18.8	337.5 ± 1.4
21	5.96	0.29	3.12	5.67	0.86	238	1.88	304	341	1.84	216.32	271.9 ± 12.0	NA	182.6 ± 20.8	218.2 ± 20.3	189.1 ± 12.0
26	6.58	1.80	4.19	4.78	1.84	241	6.35	313	353	0.84	246.31	NA	NA	109.6 ± 7.7	77.5 ± 10.1	170.9 ± 11.0
24	6.54	1.39	3.96	5.14	1.53	241	5.59	318	364	2.71	234.34	218.8 ± 17.1	NA	187.3 ± 30.7	169.0 ± 19.6	206.5 ± 20.1
25	6.49	1.66	4.08	4.83	1.72	243	3.67	320	364	2.85	243.34	251.7 ± 23.9	NA	218.6 ± 20.1	299.2 ± 34.1	228.1 ± 6.6
22	6.07	1.46	3.76	4.61	1.54	240	4.37	320	356	2.60	232.32	137.7 ± 6.5	-	-	-	-
43	6.50	0.37	3.43	6.13	0.96	254	2.61	342	389	3.80	236.4	154.5 ± 17.8	NA	158.2 ± 19.0	218.3 ± 16.5	190.8 ± 12.7
44	6.54	1.77	4.16	4.78	1.81	252	7.48	327	362	2.71	234.34	127.2 ± 9.4	266.3 ± 1.3	56.8 ± 7.3	66.1 ± 9.8	69.6 ± 4.3
42	6.21	0.57	3.39	5.64	1.02	260	3.86	333	376	3.58	248.37	37.4 ± 37.4	74.5 ± 4.0	69.7 ± 4.8	99.9 ± 10.9	104.3 ± 5.6
41	5.71	2.26	3.99	3.45	2.30	290	11.67	305	330	3.46	228.29	136.8 ± 14.1	NA	167.8 ± 9.6	156.4 ± 25.4	314.1 ± 26.7
111	6.47	1.55	4.01	4.92	1.63	245	3.76	350	371	2.23	232.32	243.2 ± 13.8	-	-	-	-
151	7.09	2.12	4.61	4.97	2.14	227	4.90	298	339	3.43	220.31	109.4 ± 0.5	156.6 ± 2.7	49.0 ± 8.6	62.2 ± 12.3	64.5 ± 5.0
104	6.51	1.80	4.15	4.71	1.83	247	6.66	310	340	3.51	216.32	NA	351.3 ± 5.5	NA	NA	NA
65	6.77	1.64	4.21	5.13	1.72	256	0.71	362	394	3.5	248.37	32.2 ± 4.0	NA	160.2 ± 16.9	174.3 ± 25.0	201.3 ± 34.6
101	6.94	1.48	4.21	5.47	1.62	243	6.39	330	365	2.98	234.34	212.4 ± 13.2	80.2 ± 10.2	90.9 ± 13.7	92.6 ± 29.9	-
62	7.24	2.03	4.63	5.21	2.06	259	4.88	332	386	3.86	262.35	238.0 ± 13.8	236.7 ± 30.9	221.8 ± 13.3	172.7 ± 29.7	-

IP, EA, χ , ω , are in eV; α in Bohr³; μ in Debye; A in Å²; V in Å³ and M in g.mol⁻¹.

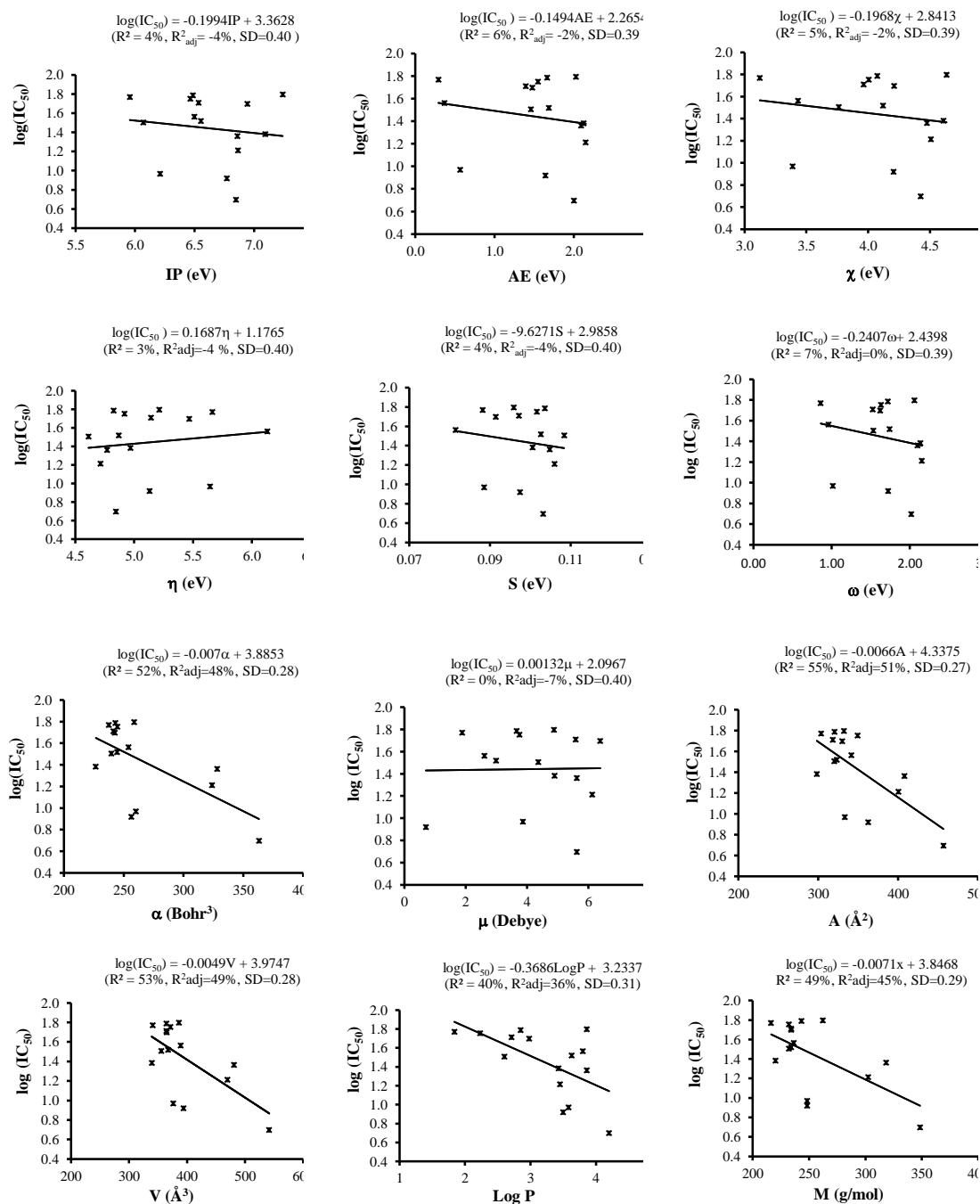


Figure 3.115: Simple linear regression correlation (SLR) curves between the cytotoxic activity on MCF-7 cells and each descriptor of test compounds from *C. zedoaria*.

Table 3.42: Correlation coefficients (R^2), adjusted correlation coefficients (R^2_{adj}) and standard deviations (SD) of simple linear regression curves (SLR) between each descriptor and cell lines assays

<i>Descriptor/s/SLR on cells</i>	MCF-7				Ca Ski			PC-3			HT-29			HUVEC		
	% R^2	% R^2_{adj}	SD		% R^2_{adj}	% R^2	SD	% R^2_{adj}	% R^2	SD	% R^2_{adj}	% R^2	SD	% R^2_{adj}	% R^2	SD
IP	4	-4	0.40		0	-14	0.31	8	2	0.22	14	8	0.22	30	4	0.19
EA	6	-2	0.39		6	-8	0.30	5	-2	0.23	19	14	0.21	3	4	0.23
χ	5	-2	0.39		2	-11	0.31	8	2	0.22	23	18	0.20	13		0.21
η	3	-4	0.40		11	-2	0.30	0	-6	0.23	5	-2	0.23	2	6	0.23
S	4	-4	0.40		10	-3	0.30	0	-7	0.23	2	-5	0.23	5	3	0.23
ω	7	0	0.39		4	-10	0.31	5	-1	0.23	14	19	0.21	3	4	0.23
α	52	48	0.28		28	18	0.27	2	-5	0.23	5	-1	0.23	1	7	0.23
DM	0	-7	0.40		9	-4	0.30	4	-3	0.23	13	7	0.22	0	8	0.23
A	55	51	0.27		42	33	0.24	2	-4	0.23	4	-2	0.23	3	4	0.23
V	53	49	0.28		43	34	0.24	3	-4	0.23	5	-1	0.23	5	2	0.22
Log P	40	36	0.31		0	-14	0.31	-7	0	0.23	0	-6	0.23	1	7	0.23
M	49	45	0.29		36	26	0.25	4	-3	0.23	8	2	0.22	-1	6	0.22

3.3.1.1 Cytotoxicity against MCF-7 cells and SLR analysis

Based on the IC_{50} values (**Table 3.41**), the compounds were sorted into two groups: inactive group ($IC_{50} > 400 \mu M$) and active group ($IC_{50} < 400 \mu M$). To avoid the large discrepancies in the IC_{50} values, active group was further subdivided into three subgroups: group A ($200 < IC_{50} < 300 \mu M$); group B ($100 < IC_{50} < 200 \mu M$) and group C ($IC_{50} < 100 \mu M$). The SLR analysis shows that the influence of a given descriptor on cytotoxic activity is dependent on the nature of the descriptor itself. For instance, the electronic descriptors IP, AE, χ , η , S, ω and μ have no significant influence ($R^2 \approx 0-7\%$), while modest correlations were observed for descriptors α , A, V, LogP and M ($R^2 \approx 40-55\%$) (Figure 3.129). These results are consistent with those obtained by Ishihara *et al.*, who showed that cytotoxic activity of twenty synthesized tropolones was poorly correlated with the eleven chosen descriptors (Ishihara *et al.*, 2010; Ishihara *et al.*, 2006). The ionization potentials (IP) and electronic affinities (AE) of the isolated compounds were obtained from the highest occupied molecular orbital (HOMO) and the lowest occupied molecular orbital (LUMO) energies (IP=-EHOMO and AE=-ELUMO). The low correlation obtained for IP and AE may be related to the weak electronic delocalization in HOMO and LUMO orbitals. For instance, HOMO and LUMO orbitals for **127** (labdane), **19** (germacrane) and **104** (cadinane) compounds showed weak charge distribution (Figure 3.130). As can be seen from HOMO and LUMO orbitals, electronic transition from HOMO to LUMO orbital induce a charge transfer from one side to another side of the molecular system (**Figure 3.116**).

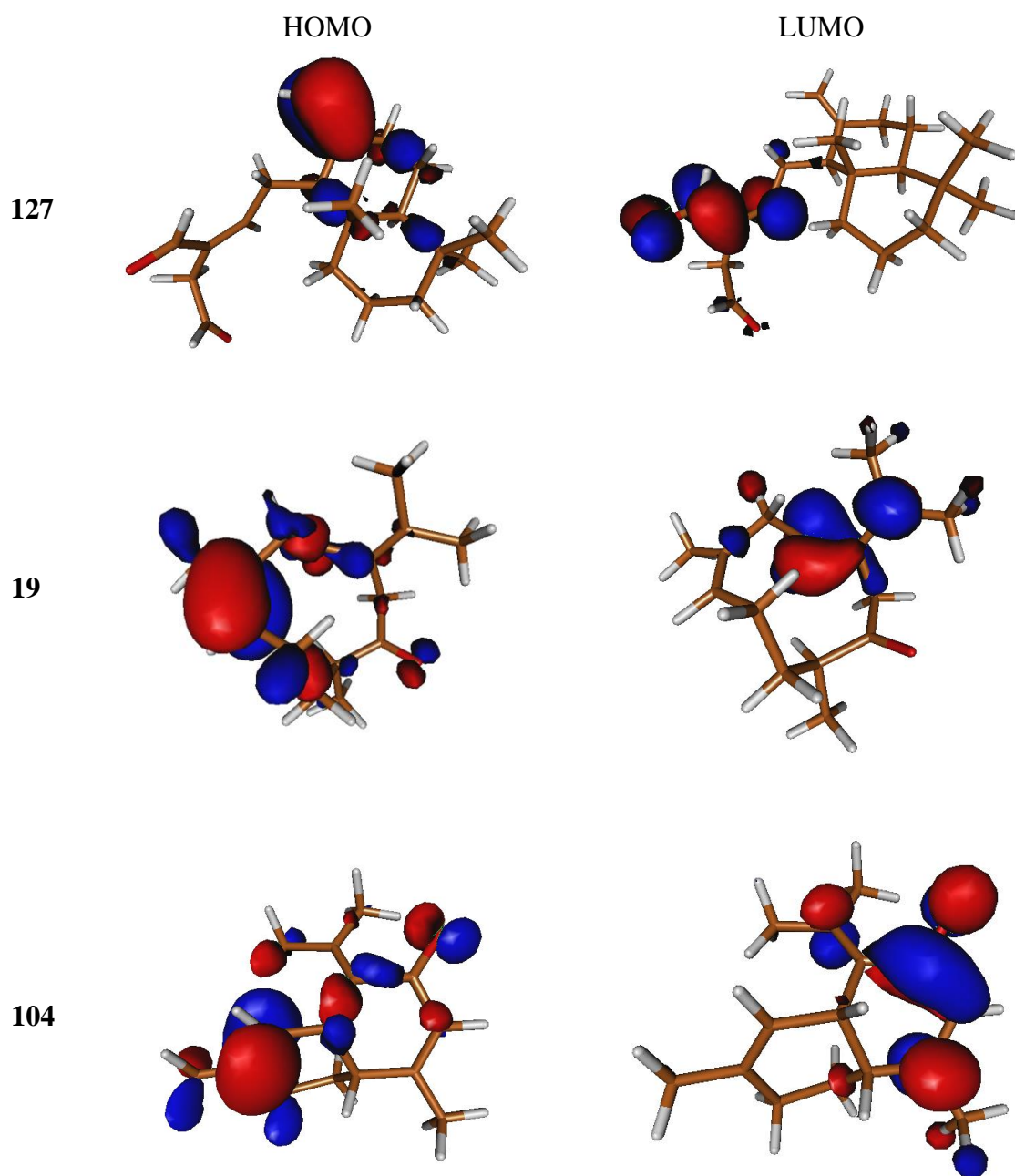


Figure 3.116: HOMO and LUMO orbitals of compounds **127**, **19** and **104**.

3.3.2 Cytotoxicity against PC-3 cells and SLR analysis

The compounds were classified into groups on the basis of their activity against PC-3 cells in the same fashion as discussed earlier. All chosen descriptors showed negligible effect on cytotoxic activity ($R^2 \approx 0-8\%$) (**Table 3.42**)

3.3.2.1 Cytotoxicity against HT-29 cells and SLR analysis

In case of cytotoxicity of the isolated compounds against HT-29 cells, moderate effects were obtained with the electronic descriptors namely IP, EA, χ , ω and μ with 14, 19, 23, 14 and 13% correlation coefficients, respectively. In contrast to the results obtained for MCF-7 and Ca Ski cells, the steric descriptors did not show significant effects ($R^2 \leq 8\%$) (**Table 3.42**).

3.3.2.2 Cytotoxicity against HUVEC cells and SLR analysis

For HUVEC cells, all descriptors showed no significant effect on the cytotoxic activity ($R^2 \leq 5\%$), except IP and χ , which showed moderate effects (30 and 13% correlation coefficients, respectively) (**Table 3.42**).

From the above assays, it was obvious that the cytotoxic activity of the isolated compounds depended both on molecular descriptor and type of the cancer cell line. The differences in the observed and the calculated results might be more related to different types of interactions between the isolated compounds and cell line enzymes.

3.3.3 Multiple linear regression (MLR) analysis

In an attempt to further investigate the correlations between the calculated descriptors and the cytotoxic activity of the isolated compounds against each cell line, the MLR analysis was performed, the MLR analysis was conducted only for the compounds of the active group.

3.3.3.1 Cytotoxicity against MCF-7 cells and MLR analysis

Among the 17 compounds, for which the IC_{50} were observed against MCF-7 cell line were subjected to the MLR analysis. Gweicurculactone **41** was used as the model compound, and therefore excluded from MLR analysis. The MLR model as given in equation 1 was obtained from the correlation observed between $\log(IC_{50})$ and the descriptors. The corresponding curve is presented in Figure 3.116.

$$\begin{aligned} \log(IC_{50})_{Pred.} = & -(60.85 \pm 73.65) + (2.91 \pm 3.91)IP - (0.70 \pm 2.22)EA + (1.10 \pm \\ & 2.62)\chi + (3.62 \pm 3.60)\eta + (314.17 \pm 359.28)S - (3.38 \pm 9.43)\omega - (0.01 \pm 0.06)\alpha \\ & - (0.05 \pm 0.16)\mu - (0.02 \pm 0.03)A + (0.01 \pm 0.04)V - (0.63 \pm 0.38)LogP + (0.01 \\ & \pm 0.03)M \end{aligned} \quad (1)$$

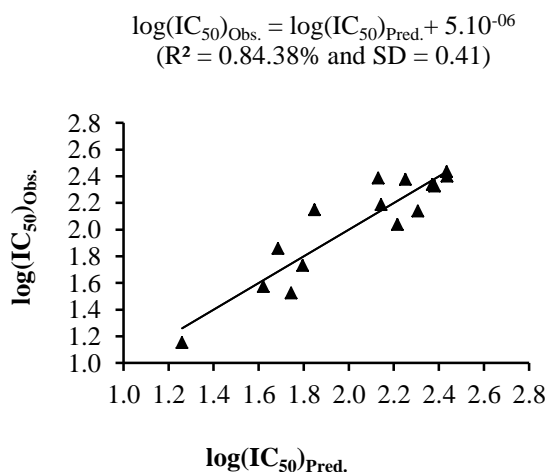


Figure 3.117: The predicted $\log(IC_{50})_{Pred.}$ and residuals to experimental $\log(IC_{50})_{Obs.}$ for the active compounds are given in Table 3.43.

Table 3.43: Experimental and predicted log(IC₅₀) for the active compounds.

Compound	Equation 1		Equation 2		Equation 3		Equation 5		Equation 6	
	log(IC ₅₀)		log(IC ₅₀)		log(IC ₅₀)		log(IC ₅₀)		log(IC ₅₀)	
	Pred.	Resid.	Pred.	Resid.	Pred.	Resid.	Pred.	Resid.	Pred.	Resid.
127	1.79	0.06	1.73	1.69	1.68	0.00	1.86	-0.08	2.02	2.18
129	1.69	-0.17	1.86	1.82	-	-	1.96	0.12	2.06	1.91
128	1.26	0.11	1.15	1.20	-	-	2.03	-0.05	2.13	2.13
19	1.85	0.30	2.15	2.13	-	-	2.39	-0.02	-	-
20	-	-	-	-	-	-	2.26	0.00	-	-
23	-	-	-	-	2.26	0.00	2.06	0.02	2.48	2.53
21	2.43	0.00	2.43	2.41	-	-	2.28	0.00	2.28	2.28
26	-	-	-	-	-	-	2.34	0.00	2.27	2.23
24	2.37	0.03	2.34	2.39	-	-	-	-	2.30	2.32
25	2.44	0.04	2.40	2.43	-	-	-	-	2.38	2.36
22	2.31	0.17	-	-	-	-	-	-	-	-
44	2.14	-0.05	-	-	-	-	-	-	-	-
43	-	-	-	-	2.43	-0.01	-	-	-	-
42	1.62	0.05	-	-	1.87	-0.01	-	-	-	-
41	-	-	-	-	-	-	-	-	-	-
111	2.13	-0.26	-	-	-	-	-	-	-	-
151	2.22	0.18	-	-	2.19	0.00	-	-	-	-
104	-	-	-	-	2.55	0.01	-	-	-	-
65	1.74	0.22	-	-	-	-	-	-	-	-
101	2.38	0.05	-	-	1.90	0.01	-	-	-	-
62	2.25	-0.13	-	-	2.37	0.00	-	-	-	-

The correlation between all descriptors and cytotoxicity was relatively weak, with a standard deviation of SD=0.41 and $R^2=84\%$. The predicted $\log(\text{IC}_{50})_{\text{Pred.}}$ for the model compound tested (**41**) is relatively high with a residual value of 2.34. While the predicted IC_{50} value suggested compound **41** to be categorised in the inactive group, observed IC_{50} indicates it as an active compound. Consequently, this model (eq. 1) was considered not suitable for cytotoxicity prediction. To obtain a better model, first eleven compounds (**127**, **129**, **128**, **19**, **20**, **23**, **21**, **26**, **24**, **25**, and **22**) with similar skeleton were chosen for MLR analysis. For better consistency in the analysis, they were further subdivided into labdane diterpenes (Compounds **127**, **129**, **128**) and germacrane sesquiterpenes (**19**, **20**, **23**, **21**, **26**, **24**, **25**, and **22**). Only the active compounds were subjected to MLR as shown in the equation 2 (eq.2). While compound **22** was selected as a test model in this study.

$$\log(\text{IC}_{50})_{\text{Pred.}} = (7.77 \pm 4.74) - (0.18 \pm 0.52)\text{IP} - (0.06 \pm 0.05)\text{A} + (0.03 \pm 0.04)\text{V} - (0.07 \pm 0.15)\text{LogP} + (0.02 \pm 0.01)\text{M} \quad (2)$$

The model of equation. 2 was found to be superior to the previous model (eq. 1) with a correlation coefficient of 99.37% and a SD of 0.09. For the purpose of validation, this model (eq. 2) was applied for compound **22**. The predicted $\log(\text{IC}_{50})_{\text{Pred.}}$ was 2.10, with a difference of only 0.04 from the experimental value. The difference between the predicted and observed cytotoxicity was 13 μM . The MLR model of equation. 2 demonstrated the importance of IP, steric parameters (area and volume), hydrophobicity (logP) and molecular weight (M) on the cytotoxic activity of the test compounds. These results were in good agreement where steric parameters and hydrophobicity were found to be the most important descriptors to classify compounds into high and low activities (Ishihara et al., 2010; H.-l. Yang et al., 2005). Thus the MLR of eq. 2 subdivided the test compounds into high and low cytotoxicity (**Figure 3.118**).

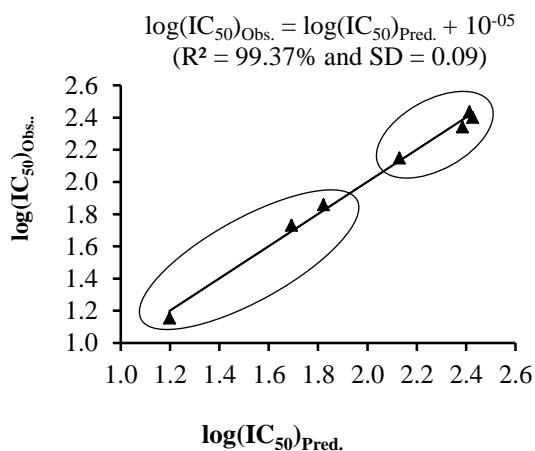


Figure 3.118: Multiple linear regression (MLR) correlation for cytotoxicity against MCF-7 of the active compounds with similar skeleton (**127-129**, **21**, **24-25**) and the most potent descriptors (see eq. 2).

3.3.3.2 Cytotoxicity Ca Ski cells and the MLR analysis

Nine compounds showing cytotoxic activity against Ca Ski cells were selected for this study. Compound **19** (dehydrocurdione) was chosen as model compound and thus excluded from the MLR analysis. The MLR model obtained between $\log(\text{IC}_{50})$ and six best descriptors is given in equation 3 and its corresponding regression curve is shown in **Figure 3.119**.

$$\begin{aligned} \log(\text{IC}_{50})_{\text{Pred.}} = & (122.80 \pm 7.42) - (11.88 \pm 0.73)\eta - (608.30 \pm 38.85)S + 0.03\alpha \\ & + 0.02A - 0.06V + 0.03M \end{aligned} \quad (3)$$

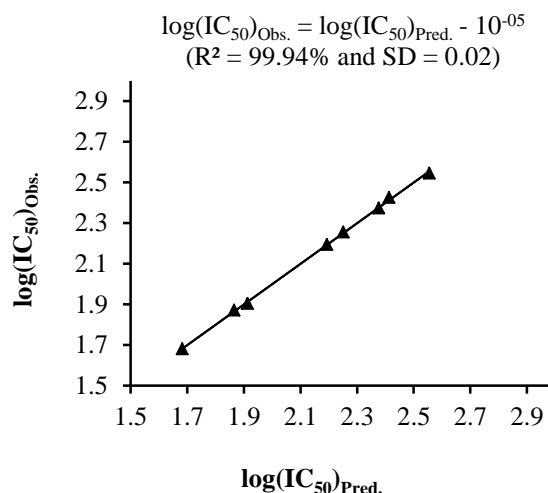


Figure 3.119: Multiple linear regression (MLR) correlation for cytotoxicity against Ca Ski of the active compounds and the most potent descriptors (see eq. 3).

The predicted $\log(\text{IC}_{50})$ and residuals with respect to experimental values of active isolated compounds are presented in **Table 3.43**. The model was found to correlate the descriptors to the observed $\log(\text{IC}_{50})$ with good accuracy (R^2 99.94% and SD 0.02). For the model compound (**19**) the predicted $\log(\text{IC}_{50})_{\text{pred.}}$ is 1.93, with a difference of 0.04 from the experimental value. The difference between the predicted and observed cytotoxicity was 8 μM . Equation. 3 shows the function of steric parameters (area and volume), molecular weight (M), hardness, softness and the polarizability of the isolated compounds towards the cytotoxicity against Ca Ski cells.

Cytotoxicity against PC3 cells and MLR analysis

Seventeen compounds showing cytotoxicity against PC3 cells were included in the MLR analysis while compound **19** (dehydrocurdione) was excluded as the model compound. The MLR model (equation. 4) obtained between $\log(\text{IC}_{50})$ and all descriptors gives a correlation of 88% (SD 0.17).

$$\log(\text{IC}_{50})_{\text{Pred.}} = -(42.62 \pm 12.74) + (3.48 \pm 0.94)\text{IP} + (217.76 \pm 58.86)\text{EA} - \quad (4)$$

$$(11.07 \pm 2.96)\chi - (0.20 \pm 0.05)\eta + (2.98 \pm 0.82)S - (0.23 \pm 0.11)\omega - (0.04 \pm 0.01)\alpha + (0.04 \pm 0.02)\mu + (0.02 \pm 0.01)A - (0.01 \pm 0.01)V + (0.98 \pm 0.48)\text{LogP} + (2.49 \pm 0.75)M$$

The predicted IC_{50} ($> 400 \mu\text{M}$) of the compound (**19**) suggested it as an inactive compound which is contradictory to the observed IC_{50} ($81.5 \mu\text{M}$) against PC3 cells. In attempt to derive a better model, the number of descriptors was reduced and the analysis was confined to compounds (**19-26**) with a similar basic skeleton. Compound **19** was excluded from MLR analysis. The best correlation was obtained with the electronic descriptors IP, EA, ω and μ (eq. 5 and **Figure 3.120**). The predicted $\log(\text{IC}_{50})$ and residuals to experimental results are presented in **Table 3.43**.

$$\text{Log}(\text{IC}_{50})_{\text{Pred.}} = (2.52 \pm 3.16) + (0.36 \pm 0.61)\text{IP} + (2.09 \pm 0.54)\text{EA} + - (3.30 \pm 0.92)\omega - (0.08 \pm 0.05)\mu \quad (5)$$

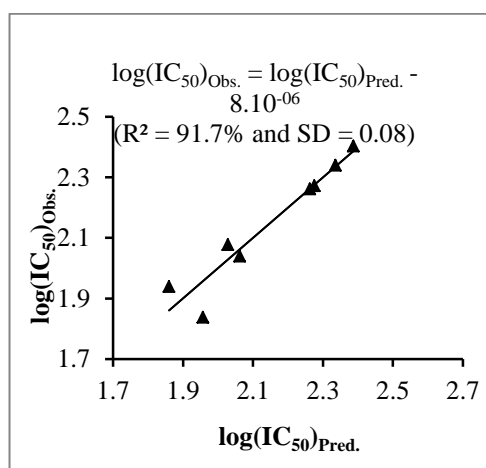


Figure 3.120: Multiple linear regression (MLR) correlation for cytotoxicity against PC3 cells of the active compounds with similar skeleton (**127-129**, **21**, **24-25**) and the most potent descriptors (see eq. 5).

The predicted $\log(\text{IC}_{50})_{\text{Pred.}}$ for the test compound **19** was 1.91, with a difference of 0.48 from the experimental value. Although the difference between predicted (160 μM) and experimental IC_{50} values, the predicted value (82 μM) was relatively high. The MLR analysis categorised it in the active group which was consistent with the observed result against PC-3 cells.

3.3.3.3 Cytotoxicity against HT-29 cells and MLR analysis

Seventeen compounds showing cytotoxicity against HT-29 cells (**Table 3.43**) were chosen for this study while compound **19** (dehydrocurdione) was excluded from MLR analysis. The MLR model obtained between $\log(\text{IC}_{50})$ and all descriptors derived a correlation of 81% (SD 0.22). The predicted value for the test compound **19** (IC_{50} = 283 μM) suggested it as an active compound (experimental IC_{50} = 97 μM). In terms of activity, compound **19** falls in group A as per predicted IC_{50} , which is quite different from its group (C) determined from the experimental IC_{50} . In an attempt to obtain a better model, the number of descriptors were reduced and the analysis was performed for first eleven compounds (**19-26**) with similar basic skeleton and compound **19** was excluded from MLR analysis as a model compound. However, in every case, the difference between experimental and predicted IC_{50} was more than 100 μM , and therefore not presented here.

(a) Cytotoxicity against HUVEC cells and MLR analysis

Fifteen compounds that showed activity against HUVEC were included in this study and compound **19** (dehydrocurdione) was excluded from MLR analysis. The correlation between $\log(\text{IC}_{50})$ and all descriptors gave an R^2 of 96% (SD 0.16). The predicted IC_{50} for compound **19** from this model was 142 μM , which is higher than the experimental. The best correlation was obtained with IP, χ , S and V descriptors (eq. 6) and **Figure 3.120**

$$\text{Log(IC}_{50}\text{)}_{\text{Pred.}} = (72.92 \pm 37.80) - (14.02 \pm 7.48)\text{IP} + (13.07 \pm 7.14)\chi + - (13.07 \pm 7.14)\text{S} - (0.0004 \pm 0.0016)\text{V} \quad (6)$$

A SD of 0.13 and R^2 of 77% were obtained using equation 6. The predicted $\log(\text{IC}_{50})$ and residuals to experimental values are reported in **Table 3.43** The predicted IC_{50} of tested compound showed that it is an active compound with a difference of 48 μM to the experimental IC_{50} value.

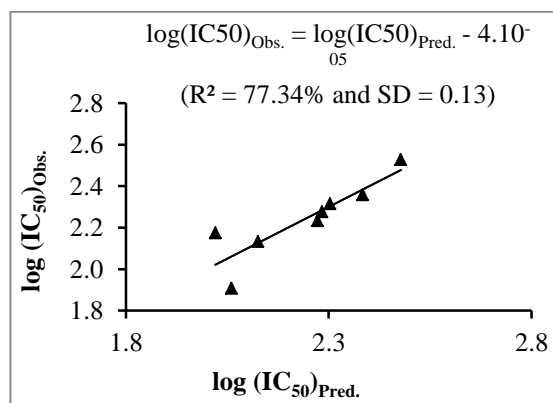


Figure 3.120 Multiple linear regression (MLR) correlation for cytotoxicity against HUVEC cells of the active compounds and the most potent descriptors (see eq. 6).

3.3.4 Principal component analysis (PCA)

Principal component analysis (PCA) allows the reduction of the number of variables used in a statistical analysis and to create a new set of variables (PCs) expressed in a linear combination of the original data set (Johnson et al., 2002). The first new variable (PC1) contains the largest variance; while the second contains the second largest variance, and so on. Before applying the PCA method, each variable was standardized for ease of comparison between each other on the same scale. PCA

analysis was performed only for MCF-7 assay. After several attempts to obtain a good classification of the isolated compounds, the best result was achieved with five variables, namely IP, A, V, logP and M. The first three components of PCA (PC1=90.50%, PC2=7.12, and PC3=2.27%) conceded 99.89% of the overall variance of the data set (**Table 3.44**), while the sole combination of PC1 and PC2 described 97.62% of that variance. The loading vectors for PC1, PC2, and PC3 are given in **Table 3.44**. The plot of the score vectors of the two principal components (PC1 \times PC2) is shown in **Figure 3.121**

As can be seen in **Figure 3.121**, the compounds under investigation are divided into two groups based on PCA analysis: compounds with high activity (**127**, **129**, and **128**) and low activity (**19**, **20**, **23**, **21**, **26**, **24**, and **25**).

Table 3.44: Variances (eigenvalues) obtained for the first three principal components

Component	Eigenvalue	Variance (%)	Cumulated variance (%)
PC1	4.525	90.50	90.50
PC2	0.3560	7.12	97.62
PC3	0.1134	2.27	99.89

Table 3.45: Loading vectors for the first three principal components

Variable	PC1	PC2	PC3
IP	0.43	0.61	0.66
A	0.46	-0.38	-0.04
V	0.46	-0.34	0.04
logP	0.43	0.51	-0.74
M	0.46	-0.32	0.08

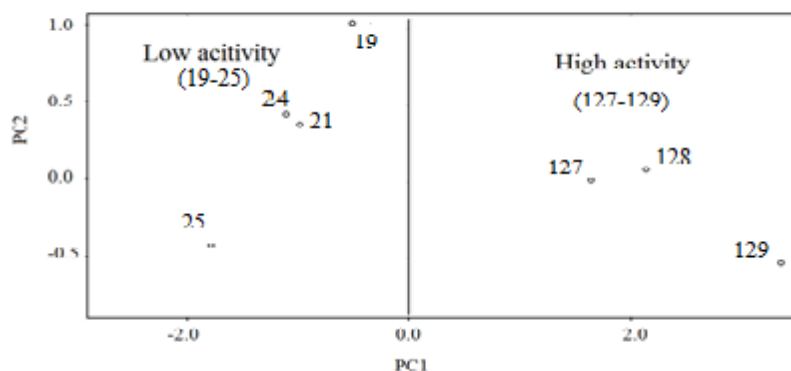


Figure 3.121: Plot of the score vectors of first principal components for cytotoxicity of compounds from *C. zedoaria* against MCF-7 cells.

The principal component PC1 presented in **Table 3.45** can be expressed through the following equation:

$$PC1 = 0.34IP + 0.46EA + 0.46V + 0.43\log P + 0.46M \quad (7)$$

Thus, a compound can be considered active if its IP, A, V, log P, and M values are similar to those described in equation 7. When compared with published literature, the results obtained from the present investigation found to follow same trend of some agreement and disagreement in the involvement of descriptors for the activity of a series of compounds for example, Yang *et al.* showed that cytotoxic ganoderic acids can be obtained when higher values for the variables E_{HOMO} , V, E_{el} , and logP is coupled with a smaller values for M (H.-l. Yang et al., 2005). Souza *et al.* found that for a given flavone to be active (anti-HIV activity), it must have smaller values for log P and V while EA must have a larger values (Souza Jr et al., 2003). In the present study, the results obtained from MLR or PCA methods are in coordination to show that the cytotoxicity of the compounds under investigation is dependent on the same descriptors (IP, A, V, logP and M) and afforded same classification of the isolated compounds. Considering the interactions between active isolated compounds and the biological

receptors, we can say that the more active isolated compounds present five main descriptors (IP, A, V, logP and M).

3.3.4.1 Hierarchical cluster analysis (HCA)

In case of preliminary data analysis, HCA is a powerful tool for examining data sets for expected or unexpected clusters, including the presence of outliers. It examines the distances between the samples in a data set and represents them in a dendrogram which provides similar information as that of PCA results (Kowalski et al., 1972). In HCA, each point forms only one cluster and then the similarity matrix is analysed. The most similar points are assembled forming one cluster and the process is repeated until all the points belong to only one group (Kowalski & Bender, 1972). The results obtained for MCF-7 assay are presented in the dendrogram **Figure 3.122**

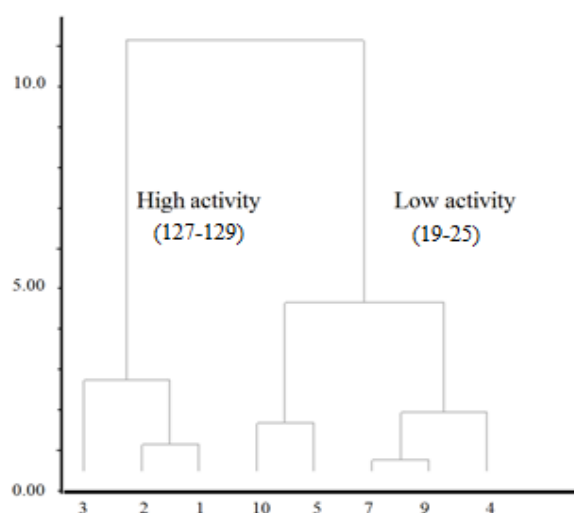


Figure 3.122: Dendrogram obtained with HCA for compounds with cytotoxic activity of compounds from *C. zedoaria*.

Vertical lines in the dendrogram represent the compounds while the horizontal lines represent the distances between compounds within the same group or of compounds

between groups. According to the distances, the compounds are subdivided into highly and weakly active groups and this classification is similar to those obtained from PCA, MLR analysis.

In summary, QSAR study showed that the influence of each descriptor separately on the cytotoxic activity of the isolated compounds is not significant with an R^2 less than 50% and a standard deviation higher than 0.20. The results showed that the cytotoxic activity of the isolated compounds depend both on the descriptors and cell types. MLR, PCA and HCA allowed us to classify the active isolated compounds into high, moderate, low active compounds. For instance, in the MCF-7 assay and based on specific chosen descriptors (ionization potential, steric parameters, hydrophobicity and molecular weight), the active compounds are classified into high (labdane diterpenes) and low active compounds (sesquiterpenes).

3.4 Neuroprotective and antioxidant activity

Parkinson's disease (PD) and Alzheimer's disease (AD) are two most common neurodegenerative diseases greatly affecting the health care system both in developing and underdeveloped countries. Present therapy only deals with the symptomatic relief of the above two diseases. Recent research shows that natural products represent a potential source for the development of drugs for the treatment of neurodegenerative disorders including Parkinson's disease and Alzheimer's disease. Thus selected compounds isolated through the phytochemical investigation of *C. zedoaria* were subjected to neuroprotective activity investigation. The compounds were also tested for antioxidant activity test to find their role in oxidative stress, which is a major cause of neurodegeneration.

3.4.1 Effect of test compounds on H₂O₂-induced cell death in NG108-15 cells

As summarized in **Table 3.47**, all the ten compounds tested, protected the NG108-15 cells from H₂O₂ induced oxidative stress at various degrees. Exposure to H₂O₂ (400 μ M) reduced the viability of NG108-15 cells to 67.6% after a period of 24 h. Pretreatment of the cells with curcumenol **42** showed the maximum protection (103%) at the concentration of 4 μ M. This effect varied from compound to compound as well as the concentration. For instance, effect of curcumenol **42** reduced to 97.7% as the concentration increased to 30 μ M. Dehydrocurdione **19** also showed strong activity (100% protection) at the concentration of 10 μ M, and the activity showed a decrease in the activity both for an increase or a decrease in the concentration. Germacrone **23**, zerumin A **128**, isoprocurcumenol **43**, procurcumenol **44**, and zerumbone epoxide **151** showed moderate activity (80-90% viability) as compared to the control.

Table 3.46: Neuroprotective evaluation of compounds against H₂O₂-induced cell death in NG108-15 cells.

Compound	Cell viability (%)					
	1 μ M	4 μ M	8 μ M	10 μ M	15 μ M	30 μ M
Control				100		
H ₂ O ₂				67.63 \pm 0.86		
Germacrone (23)	79.29 \pm 1.05*	77.80 \pm 1.15*	81.25 \pm 1.72*	79.61 \pm 2.38*	89.99 \pm 2.01*	78.68 \pm 1.39*
Dehydrocurdione (19)	82.90 \pm 1.77*	90.76 \pm 1.45*	98.05 \pm 2.33*	100.60 \pm 1.72*	99.98 \pm 2.60*	88.59 \pm 1.75*
Curcumenol (42)	78.03 \pm 1.23*	103.04 \pm 2.17*	100.73 \pm 2.63*	100.60 \pm 1.72*	99.98 \pm 2.60*	97.79 \pm 2.41*
ZeruminA (129)	77.89 \pm 1.95*	77.98 \pm 1.09*	82.69 \pm 1.12*	86.84 \pm 1.76*	91.14 \pm 1.42*	74.41 \pm 1.45
Isoprocurcumenol (43)	76.72 \pm 0.88*	79.51 \pm 0.91*	76.42 \pm 1.61*	77.08 \pm 1.07*	80.96 \pm 0.91*	75.94 \pm 1.01*
Curcumenone (65)	66.25 \pm 1.50	59.74 \pm 1.86	66.93 \pm 1.66	73.86 \pm 1.18	70.58 \pm 1.13	79.18 \pm 1.43*
Procurcumenol (44)	77.75 \pm 0.95*	79.08 \pm 1.289*	77.00 \pm 1.25*	75.73 \pm 2.22*	80.00 \pm 0.71*	72.87 \pm 0.71
Zerumbone epoxide (151)	75.66 \pm 0.68*	71.29 \pm 1.24	78.15 \pm 0.98*	73.66 \pm 1.70	74.63 \pm 1.27	84.32 \pm 1.09*
Zederone (26)	62.50 \pm 1.41	61.47 \pm 1.53	72.41 \pm 0.97	76.33 \pm 1.19*	70.79 \pm 2.88	74.51 \pm 0.85
Gweicurculactone (41)	59.84 \pm 2.	64.24 \pm 1.	59.44 \pm 0.	67.54 \pm 0.	75.45 \pm 1	75.21 \pm 1
	19	32	78	89	.04	.47

All experiments done in triplicate and results expressed as mean \pm S.E.

* P <0.05 vs H₂O₂ treated cells, One way ANOVA followed by Dunnett's test

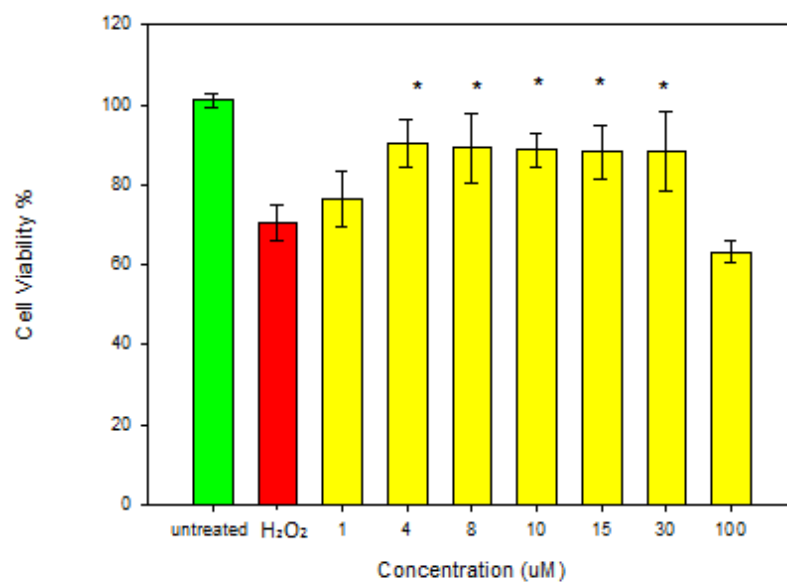


Figure 3.123: Neuroprotective effect of curcumenol **42** on the viability of NG108-15 cells

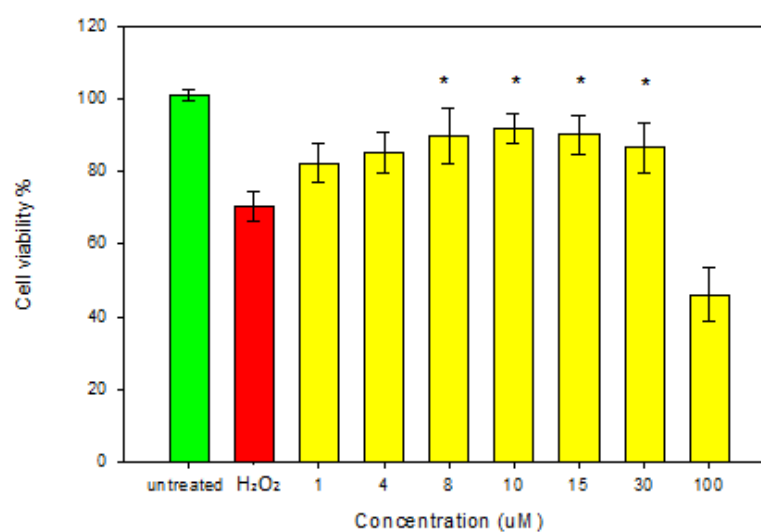


Figure 3.124: Neuroprotective effect of dehydrocurdione **19** on the viability of NG108-15 cells

3.4.2 ORAC assay

In the ORAC assay, zerumbone epoxide **151** showed the highest antioxidant activity with a Trolox equivalent (TE) of 35.41 μM per 100 μg of sample. Isoprocucumenol **43**, zederone **26**, dehydrocurdione **19**, germacrone **23** showed higher antioxidant capacity (26.43, 27.78, 26.18, and 24.86 TE/100 μg sample, respectively) than that of quercetin (21.73 TE/100 μg sample), used as standard in this assay. While the antioxidant activity of zerumin A **128**, gweicurculactone **41**, curcumenone **65**, procucumenol **44** were close to that of quercetin, curcumenol **42** showed a lesser extent of activity (Table 3.47).

Table 3.47: Antioxidant capacity of the compounds by ORAC method.

Compound	μM of Trolox per 100 $\mu\text{g}/\text{ml}$
Curcumenol	12.62 ± 2.67
Zerumin A	19.86 ± 3.92
Isoprocucumenol	26.43 ± 1.88
Zerumbone epoxide	35.41 ± 2.25
Gweicurculactone	18.26 ± 1.66
Zederone	27.78 ± 2.53
Curcuzedoalide	23.38 ± 1.50
Furanodiene	19.17 ± 2.90
Curcumenone	21.16 ± 2.12
Germacrone-4,5-epoxide	23.99 ± 2.14
Germacrone-1, 10-epoxide	11.86 ± 2.53
Curcumanolide A	12.87 ± 2.29
Dehydrocurdione	26.18 ± 2.59
Labd-8(17), 12-diene-15, 16-dial	30.19 ± 1.77
Germacrone	24.86 ± 2.33
Calcaratarin A	22.23 ± 2.82
Procucumenol	20.46 ± 1.88
Quercetin	21.73 ± 2.87

3.4.3 Activity correlations

In normal physiologic condition, small amount of H_2O_2 is produced during aerobic metabolism in the cell and is neutralised by redox systems of our body. This does not pose significant threat at young age due to the presence of strong antioxidant defence mechanism. However, in aged person, an increased production of ROS and functional decline of neutralising systems creates an imbalance, leading to detectable

level of oxidative damages. As a result of cumulative deposition of the pathogenesis, the effects get more noticeable which includes lack of coordination, imbalance, cognitive dysfunction and reduced muscle tone (Giacalone *et al.*, 2011).

Use of external H₂O₂ to create oxidative stress in NG108-15 cell is a popular method of studying neuroprotective effect of natural products (Ahlemeyer *et al.*, 2001, Weecharangsan *et al.*, 2006). Due to the neuronal glial properties, NG108-15, a mouse neuroblastoma-rat glioma hybridoma cell line is used extensively as a neuronal model in electrophysiological and pharmacological research (Wong *et al.*, 2012). Application of H₂O₂ to NG108-15 cells mimics the condition that takes place during the oxidative stress in the body.

Superoxide dismutase (SD), is an important enzyme of the antioxidant system to convert superoxide into H₂O₂ in the human body which further scavenged by catalase or glutathione redox pathway (Yanpallewar *et al.*, 2004). When there is an increased level of H₂O₂, the neutralization by catalase or tissue thiols fail, giving rise to various reactive oxygen species. Application of exogenous H₂O₂ creates oxidative stress that is beyond the manageable level of the endogenous antioxidant system (Wong *et al.*, 2012). Cell death may happen through two major mechanisms, apoptosis and necrosis. Apoptosis is the most noticeable programmed cell death mechanism and is associated with distinct morphological changes, such as membrane blebbing, cell shrinkage and DNA fragmentation. On the other hand, necrosis is the premature death of cells associated with the loss in cell membrane integrity followed by uncontrolled release of cell products into the extracellular space (Kanduc *et al.*, 2002).

In the present investigation, nine sesquiterpenes and one labdane diterpene were isolated from the rhizomes of *C. zedoaria* and further tested for their possible

neuroprotective role in H₂O₂-induced oxidative stress of NG108-15 cells. Among these, the guaiane type sesquiterpene, curcumenol **42** showed 100% protection of the cells at 4 μ M concentration. The compound showed very little change in its activity even at the concentration of 30 μ M, indicating that the compound might not be toxic to the cell within a wide concentration range. Dehydrocurdione **19**, a germacrane type sesquiterpene showed maximum protection at concentrations of 10 and 15 μ M, reduced by 10% at 30 μ M concentration. Curcumenol **42** and dehydrocurdione **19** are the two major phytoconstituents of *C. zedoaria* and their content in the rhizomes is more than that of any other part of the plant. However, seasonal variation can change the ratio of these two constituents in the plant (Pamplona *et al.*, 2005). In the above study by Pamplona *et al.* (2005), curcumenol **42** was found to be more potent than dehydrocurdione **19** in the inhibition of pain in experimental mice. Biogenetically, these two compounds are closely related compounds which is justified by the biomimetic transformation to convert dehydrocurdione **19** into curcumenol **42** in a highly selective manner (Shiobara *et al.*, 1985).

Curcumenol **42** is one of the well-studied compounds and contributed to hepatic cells protection from D-GalN-induced cytotoxicity and inhibition of the LPS (lipopolysaccharide)-induced nitric oxide (NO) production in mouse macrophage (Matsuda *et al.*, 1998). Although inducible NO synthase (iNOS) is not expressed in normal brain, it is expressed in microglia and astrocytes in the presence of cytokines and LPS. Cytokines release and neuroinflammation can trigger the infiltration of T cells and macrophage at the inflammatory site. These cells release immunomodulatory molecules including NO, promoting the immunresponse and leading to a more widespread CNS-injury (Akiyama *et al.*, 2000, Deleidi and Gasser, 2013, Jackson-Lewis *et al.*, 2002). A low level of NO is present in brain for cellular signalling, but a

high level of NO can be observed in neurodegenerative disorders causing neuronal cell death by inhibiting mitochondrial cytochrome oxidase (Brown and Cooper, 1994). Thus, the inhibition of NO production by curcumenol **42** can also contribute towards the neuroprotective activity of this compound.

In another study, curcumenol **42** was isolated as the major anti-inflammatory agent from *Curcuma phaeocaulis* using COX-2 inhibitory assay (Tanaka *et al.*, 2008). There is a strong evidence that COX-2 level increases significantly in neurodegenerative disease conditions. In AD, a direct correlation has been found with the COX-2 level with that of amyloid plaque and neuronal atrophy (Akiyama *et al.*, 2000). While in PD, injection of LPS in brain resulted in the increased level of inflammatory factors including COX-2 and iNOS prior to the death of dopaminergic neurons (Khandelwal *et al.*, 2011). Therefore, the neuroprotective effect of the curcumenol **42** may be due to its anti-inflammatory action stemming through the inhibition of COX-2 enzyme (Chung *et al.*, 2009).

To correlate the antioxidant activity of the compounds under investigation toward their neuroprotective activity, ORAC assay was performed. ORAC assay is considered as a complementary antioxidant test for neuroprotective assay (Giacalone *et al.*, 2011). It is a reliable method of testing antioxidant activity of biological samples including natural products due to its sensitivity towards broader class of compounds (Cao and Prior, 1998). Moreover, it is the only assay which involves the use of peroxy radical and quantifies the antioxidant capacity via area under curve (AUC) technique (Cao *et al.*, 1993, Cao *et al.*, 1995). The results obtained from this assay is from the direct quenching of free radicals, which is related to the antioxidant capacity of the molecule itself (Cao *et al.*, 1995). In the present experiment, quercetin was used as the standard for the comparison of antioxidant activity. All the compounds (**1-10**) tested

showed strong to moderate antioxidant activity, while zerumbone epoxide **151**, a humulane type sesquiterpene, showed the highest antioxidant capacity (35.41 TE/100 μg sample), and the activity was stronger than that of quercetin (21.16 TE/100 μg sample). In the neuroprotective assay, this compound showed a maximum of 84.32% protection of the cells at the highest concentration tested (30 μM). Interestingly, curcumenol **42**, which showed the strongest neuroprotective activity (100%) among all the compounds tested, exhibited a moderate antioxidant activity (12.62 TE/100 μg sample) in ORAC assay. This suggests that the neuroprotective activity of this compound is not a sole contribution from its antioxidant activity, rather a combined effect of its anti-inflammatory, antioxidant and NO-production inhibitory activity. Dehydrocurdione **19**, the other compound with strong neuroprotective activity (100%), showed an antioxidant capacity of 26.18 TE/100 μg sample.

Curcumenol **42** has been under use for the treatment of various diseases including tumor, inflammation and viral diseases. Sometimes it is given in combination with commonly available drugs. To investigate possible chance of drug interaction for its use with other drugs, curcumenol **42** was tested against seven isoforms of human liver microsomes. Curcumenol **42** was found to competitively inhibit CYP3A4 while the effect on others was negligible, indicating that it can be used safely without affecting the metabolism of most of the drugs (Sun *et al.*, 2010).

3.5 Spectrofluorometric and molecular docking studies on the binding of curcumenol 42 and curcumenone 65 to Human Serum Albumin (HSA)

Curcumenol **42** and curcumenone **65** are two major constituents of the plants of the genus *Curcuma*, and often govern the pharmacological effect of these plant extracts. Curcumenol **42** and curcumenone **65** are two of the most important sesquiterpenes possessing a number of beneficial biological activities. Curcumenol **42**, a guaiane type

sesquiterpene is known to exhibit analgesic (De Fátima Navarro et al., 2002), cytotoxic (O. A. Ahmed Hamdi et al., 2014; M. Aspollah Sukari et al., 2010), hepatoprotective (Matsuda et al., 1998) and antimicrobial (Sukari et al., 2007) properties, while curcumenone **65**, a carabrane type sesquiterpene has been reported to be a vasorelaxant (Hisashi Matsuda, Toshio Morikawa, et al., 2001a), hepatoprotective (Matsuda et al., 1998) and an effective inhibitor of intoxication (Kimura et al., 2013). These two compounds isolated from *C. zedoaria* rhizomes, were studied for their binding to human serum albumin (HSA) using the fluorescence quench titration method. Molecular docking was also performed to get a more detailed insight into their interaction with HSA at the binding site.

Human serum albumin (HSA) serves as the primary transport protein in the human circulation capable of binding reversibly both endogenous and exogenous ligands such as fatty acids, hormones and drugs. It consists of 585 amino acids in a single polypeptide chain (Peters Jr, 1995). Crystallographic data have shown the presence of three homologous domains (I, II, and III), each comprised subdomains A and B. The two high affinity ligand binding sites on HSA, known as Sudlow's site I and II, are located in subdomains IIA and IIIA, respectively (Carter et al., 1994).

The interaction of a compound with serum albumin is known to influence its bioavailability, distribution, metabolism and elimination from the body. In particular, the affinity between a protein and a ligand affects the concentrations of the free and bound forms of the ligand as well as the duration of its half-life, which consequently determine its efficacy (Peters Jr, 1995). Therefore, investigations on the interaction of serum albumin with bioactive ligands may provide valuable information concerning their therapeutic efficacies (Yang et al., 2014).

Being the major and active constituents of *C. zedoaria*, curcumenol **42** and curcumenone **65** play important roles in exerting pharmacological activities after

consumption of the herb. As the key components of a widely used natural product, curcumenol **42** and curcumenone **65** require the determination of pharmacokinetic parameters to establish their safety and efficacy. Furthermore, binding studies to HSA provide valuable parameters toward the establishment of the pharmacokinetic profile of such agents. In light of the above, the present study describes the binding properties of curcumenol **42** and curcumenone **65** to HSA based on fluorescence spectroscopic and molecular docking results.

3.5.1 Analysis of the binding data

In order to reveal the quenching mechanism of HSA fluorescence, the binding data were analyzed according to the Stern-Volmer equation (Lackowicz, 1983):

$$F_0/F = K_{SV}[Q] + 1 = k_q\tau_0[Q] + 1 \quad (8)$$

where F_0 and F are the fluorescence intensities of HSA in the absence and the presence of the quencher, respectively, K_{SV} is the Stern-Volmer constant, $[Q]$ is the quencher concentration, k_q is the bimolecular quenching constant and τ_0 is the fluorescence lifetime of free HSA. A value of 6.38×10^{-9} s was used for τ_0 (Abou-Zied et al., 2008).

The binding constant, K_b and the number of binding sites, n for ligand–HSA interactions were determined by treating the fluorescence data according to the following equation (Ahmad et al., 2011):

$$\log (F_0 - F)/F = n \log [Q] + \log K_b \quad (9)$$

3.5.2 Molecular modelling

The structures of curcumenol **42** and curcumenone **65** were drawn using ACD/ChemSketch Freeware (Advanced Chemistry Development Inc. Ontario, Canada), 3-D optimized and exported as a mol file. The geometric optimization of the structures was refined with the VegaZZ 2.08 (Pedretti et al., 2002) batch processing MOPAC script (mopac.r; keywords: MMOK, PRECISE, GEO-OK) using AM1 semiempirical theory (Dewar et al., 1985) and converted and stored as a mol2 file. Molecular docking, visualization and rendering simulation were performed using AutoDock 4.2 (Goodsell et al., 1996) and AutoDockTools 1.5.4 (Sanner, 1999) at the Academic Grid Malaysia Infrastructure. For the docking study, the non-polar hydrogens in the structures were merged and the rotatable bonds were defined. The crystal structure of HSA (PDB code 1BM0, res. 2.5 Å) was downloaded from the Protein Data Bank (PDB) (Berman et al., 2000). Its water molecules were removed and the atomic coordinates of chain A were stored in a separate file and used as input for AutoDockTools, where polar hydrogens, Kollman charges and solvation parameters were added. The two binding sites (site I and site II) were defined using two grids of 70×70×70 points each with a grid space of 0.375 Å centered at coordinates x=35.26 y=32.41 z=36.46 for site I and x=14.42 y=23.55 z=23.31 for site II. Lamarckian genetic algorithm with local search (GA-LS) was used as the search engine, with a total of 100 runs for each binding site. In each run, a population of 150 individuals with 27000 generations and 250000 energy evaluations were employed. Operator weights for crossover, mutation and elitism were set to 0.8, 0.02 and 1, respectively. For local search default parameters were used. Cluster analysis was performed on docked results using RMS tolerance of 2.0 Å. The protein-ligand complexes were visualized and analyzed using AutoDockTools.

3.5.3 Results of spectrofluorometric analysis

Interactions between small ligands and macromolecules such as proteins have been widely investigated using fluorescence spectroscopy. Quenching of the protein fluorescence as well as shift in the emission maximum in the presence of a ligand can indicate a number of phenomena including complex formation, random collisions, energy transfer and excited state reactions (Ahmad et al., 2011; Belatik et al., 2012; Varlan et al., 2010). **Figure 3.125** shows intrinsic fluorescence spectra of HSA in the wavelength range, 300–400 nm upon excitation at 280 nm, obtained in the absence and the presence of increasing curcumenol **42** and curcumenone **65** concentrations. Addition of increasing concentrations of these ligands to HSA produced progressive decrease in the fluorescence intensity and significant blue shift in the emission maximum, suggesting interactions between these compounds and HSA. About 40% decrease in the fluorescence intensity at 338 nm and 2 nm blue shift were observed at the highest curcumenol **42** concentration (60 μ M), used in this study. On the other hand, curcumenone **65** produced ~50% quenching in HSA fluorescence intensity, which was accompanied by a 6 nm blue shift in the emission maximum at the same ligand concentration. The shift in the emission maximum of HSA towards shorter wavelength suggested increased hydrophobicity in the microenvironment of the protein fluorophores upon interaction with these compounds (Lackowicz, 1983). The increased hydrophobicity can be ascribed to the burial of water-accessible surface area of the protein around the fluorophore(s). Since the major contributor of HSA fluorescence, Trp-214 is located in the vicinity of Sudlow's site I, the observed blue shifts suggested the involvement of Sudlow's site I in the binding of both curcumenol **42** and curcumenone **65** to HSA.

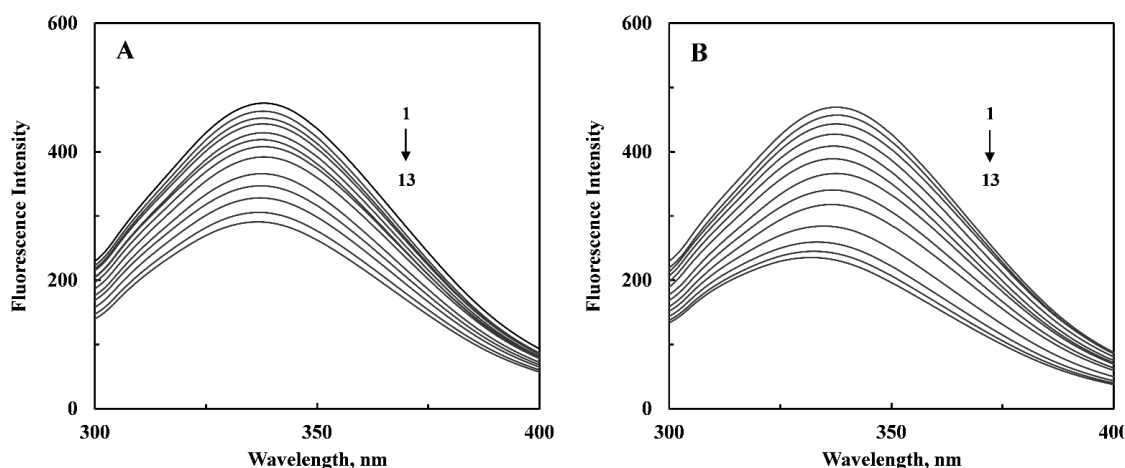


Figure 3.125: Emission spectra of HSA in the absence and the presence of increasing curcumenol (A) and curcumenone (B) concentrations, obtained in 20 mM sodium phosphate buffer, pH 7.4 upon excitation at 280 nm. [HSA] = 3 μ M, [Ligand] = (1-13): 0, 3, 6, 9, 12, 15, 18, 24, 30, 37.5, 45, 52.5 and 60 μ M. T = 25 $^{\circ}$ C.

Although quenching of protein fluorescence can be regarded as an indication of binding between a compound and the protein, it is equally probable that the quenching phenomenon was due to collisions between the quencher molecule and the protein (Lackowicz, 1983). These two mechanisms of fluorescence quenching are known as static and collisional quenching, respectively, and can be differentiated by the bimolecular quenching constant, k_q value, associated with the quenching process (Lackowicz, 1983). As a general rule, the k_q value for a diffusion-controlled phenomenon typically falls in the region of $10^{10} \text{ M}^{-1} \text{ s}^{-1}$, while higher k_q value indicates a binding reaction (Lackowicz, 1983). **Figure 3.126** displays Stern-Volmer plots of the ligand–HSA systems, obtained after analyzing the quenching data using Eq. 8. The resulting K_{SV} and k_q values for the interaction of both curcumenol **42** and curcumenone **65** with HSA are listed in **Table 3.48**. As can be seen, the k_q values obtained were two orders of magnitude higher than the value expected for a process following the collisional quenching mechanism. This suggested that the quenching of HSA by curcumenol **42** and curcumenone **65** were governed by the static quenching mechanism, which involved the formation of a ground state complex between the ligands and HSA.

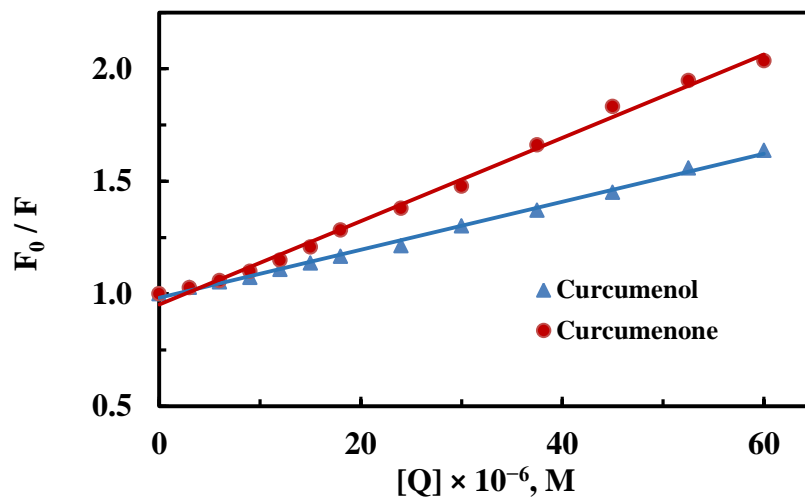


Figure 3.126: Stern-Volmer plots for the quenching of HSA fluorescence by curcumenol **42** and curcumenone **65**.

Table 3.48: Quenching and binding parameters for curcumenol-/ curcumenone-HSA interactions, as obtained in 20 mM sodium phosphate buffer, pH 7.4 at 25°C.

Parameter	Curcumenol 42	Curcumenone 65
K_{SV}, M^{-1}	1.07×10^4	1.85×10^4
$k_q, M^{-1} s^{-1}$	1.67×10^{12}	2.90×10^{12}
K_b, M^{-1}	1.97×10^4	2.46×10^5
n	1.07	1.26

The binding constant (K_b) for the ligand–HSA interaction and the number of binding sites (n) on the protein for these ligands were determined from the double logarithmic plots of $\log (F_0 - F)/F$ versus $\log [Q]$ (**Figure 3.127**). The values of n and K_b were obtained from the slope and the y-intercept of these plots, respectively, and are listed in

Table 3.48. The values of K_b , obtained for the interaction of curcumenol and curcumenone with HSA revealed intermediate affinity between these ligands and the protein. This was comparable to other ligand binding studies involving HSA (Feroz et al., 2012; Freitas et al., 2012; H. Matsuda et al., 1998; Varlan & Hillebrand, 2010). It is worth noting that higher extent of quenching of HSA fluorescence by curcumenone **65** was also reflected by its higher K_b ($2.46 \times 10^5 \text{ M}^{-1}$) value in comparison to that obtained for the curcumenol–HSA system ($1.97 \times 10^4 \text{ M}^{-1}$). Interestingly, the value of n for the interaction of curcumenone **65** with HSA was noticeably larger compared to that of curcumenol **42**. This may suggest the binding of curcumenone **65** to other site(s) on the protein molecule in addition to its primary binding site. On the other hand, the smaller n value observed for curcumenol **42** indicated the less likelihood of the compound binding to more than one site on HSA.

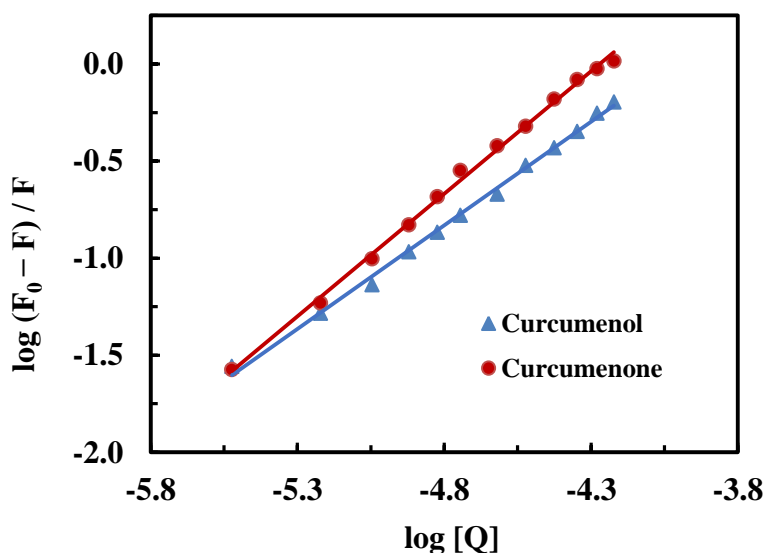


Figure 3.127: Double logarithmic plots for the interaction of HSA with curcumenol **42** and curcumenone **65**.

3.5.4 Results of molecular docking studies

In order to predict the binding modes of curcumenol **42** and curcumenone **65** to the two main ligand binding sites of HSA (site I and site II), docking simulations of the interaction between these ligands and HSA were carried out. For each binding site, 100 docking simulations and clustering analysis at a root-mean-square deviation tolerance of 2.0 Å were performed. The docking analysis of 1BM0-curcumenol complex at the binding site I revealed a total of eight (8) multimember conformation clusters (**Figure 3.128**) with the mean binding energy of $-6.40 \text{ kcal mol}^{-1}$. The highest populated cluster had 29 out of 100 conformations. However, the configuration with the lowest binding energy ($-6.77 \text{ kcal mol}^{-1}$) was not a member of the highest populated cluster. At the binding site II (**Figure 3.129**), six (6) multimember conformation clusters, possessing mean binding energy of $-5.53 \text{ kcal mol}^{-1}$ were identified, with the highest populated cluster having 72 members out of 100 conformations. Although the lowest binding energy configuration ($-5.72 \text{ kcal mol}^{-1}$) was a member of the highest populated cluster, its binding energy was higher compared to the lowest binding energy configuration at site I ($-6.77 \text{ kcal mol}^{-1}$). Thus, it was predicted that site I of HSA would be the preferable binding site of curcumenol to HSA (1BM0).

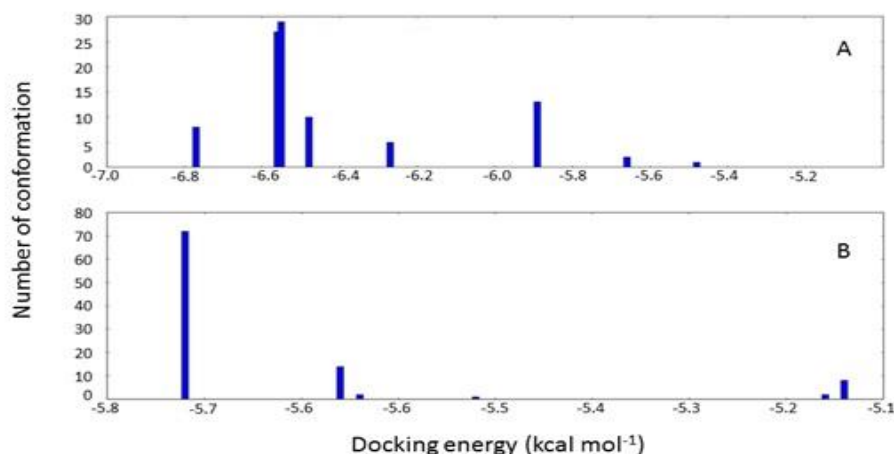


Figure 3.128: Cluster analyses of the AutoDock docking runs of curcumenol **42** in the drug binding site I (A) and site II (B) of HSA (1BM0).

Cluster analysis of the 1BM0-curcumenone complex (**Figure 3.129**) revealed similar clustering pattern for both binding sites, as observed with the 1BM0-curcumenol system. The lowest binding energy conformation for site I of 1BM0-curcumenone was -6.77 kcal mol⁻¹, while that for site II was -5.74 kcal mol⁻¹. These observations also suggested the preference of site I for curcumenone binding to HSA.

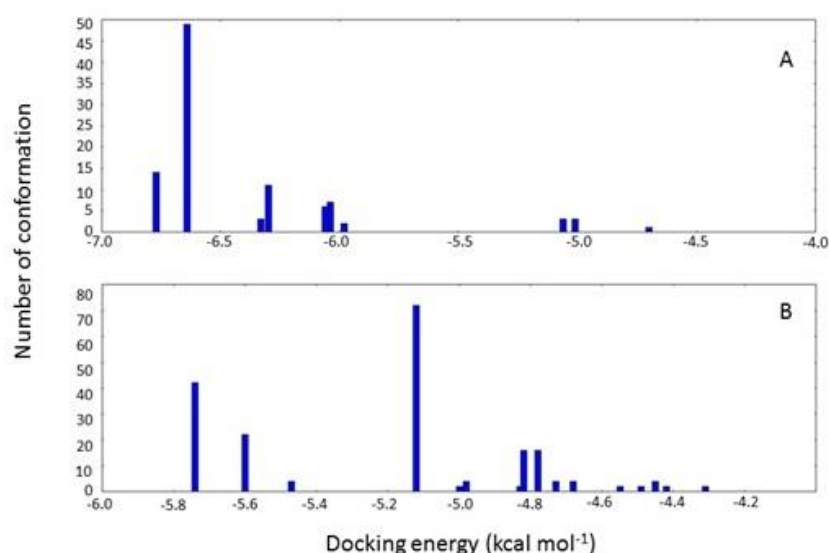


Figure 3.129: Cluster analyses of the AutoDock docking runs of curcumenone **65** in the drug binding site I (A) and site II (B) of HSA (1BM0).

The predicted binding models of curcumenol **42** and curcumenone **65** with the lowest docking energy (-6.77 kcal mol⁻¹) at site I of HSA were used for binding orientation

analysis (**Figure 3.130**). Since the cluster analysis also supported the binding of curcumenol and curcumenone at site II of HSA, the lowest docking energy complex for curcumenol ($-5.72 \text{ kcal mol}^{-1}$) and curcumenone ($-5.74 \text{ kcal mol}^{-1}$) at site II of HSA were also analysed (**Figure 3.131**). The ligand binding sites were defined as amino acid residues within 5 \AA distance of the ligand. In the 1BM0-curcumenol complex at site I, the binding site was found to be located deep within the protein structure in a hydrophobic cleft walled by 18 amino acids: Tyr-150, Lys-195, Gln-196, Lys-199, Leu-219, Arg-222, Asp-237, Leu-238, Val-241, His-242, Arg-257, Leu-260, Ala-261, Lys-286, Ser-287, His-288, Ile-290 and Ala-291. However, in the 1BM0-curcumenone complex at the same site, the binding site was surrounded by 16 amino acids: Tyr-150, Lys-195, Gln-196, Lys-199, Leu-219, Arg-222, Phe-223, Leu-234, Leu-238, His-242, Arg-257, Leu-260, Ile-264, Ser-287, Ile-290 and Ala-291. The 1BM0-curcumenol complex formation at site II involved 14 amino acid residues, namely Leu-394, Leu-398, Lys-402, Phe-403, Asn-405, Ala-406, Val-409, Arg-410, Lys-413, Thr-540, Lys-541, Glu-542, Leu-544 and Lys-545. On the other hand, 1BM0-curcumenone complex at site II was associated with 13 amino acid residues: Leu-398, Lys-402, Phe-403, Asn-405, Ala-406, Leu-407, Val-409, Arg-410, Lys-413, Thr-540, Lys-541, Glu-542, and Lys-545.

Presence of hydrophobic amino acid residues at the binding sites of HSA might have contributed towards the stability of the ligand-HSA complex through hydrophobic interactions. However, the presence of several polar amino acid residues within the proximity of the bound ligands indicated that the interactions between these ligands and HSA at both site I and site II cannot be presumed to be exclusively hydrophobic. Furthermore, in the 1BM0-curcumenol complex docking conformation, one hydrogen bond was predicted involving the hydrogen atom of Arg-257 and the ethereal oxygen atom of curcumenol (**Table 3.49**). For the 1BM0-curcumenone complex docking

conformation, 4 hydrogen bonds were predicted involving hydrogen atoms from 3 different amino acid residues of HSA (Tyr-150, Arg-222 and Arg-257) and the oxygen atoms of the acetyl and ketone groups of curcumenone. On the contrary, there was only one hydrogen bond in the 1BM0-curcumenone complex at site II, formed by the oxygen atom of curcumenone and the hydrogen atom of Lys-413 (**Table 3.49**). Both ligands showed one hydrogen bonding at the binding site. For 1BM0-curcumenol complex at site II, the hydrogen bond formed between the hydrogen atom of Lys-545 and the oxygen atom of hydroxyl group while for 1BM0-curcumenone complex, the hydrogen bond was associated with the hydrogen atom of Lys-413 and oxygen of the ketone group (**Table 3.49**).

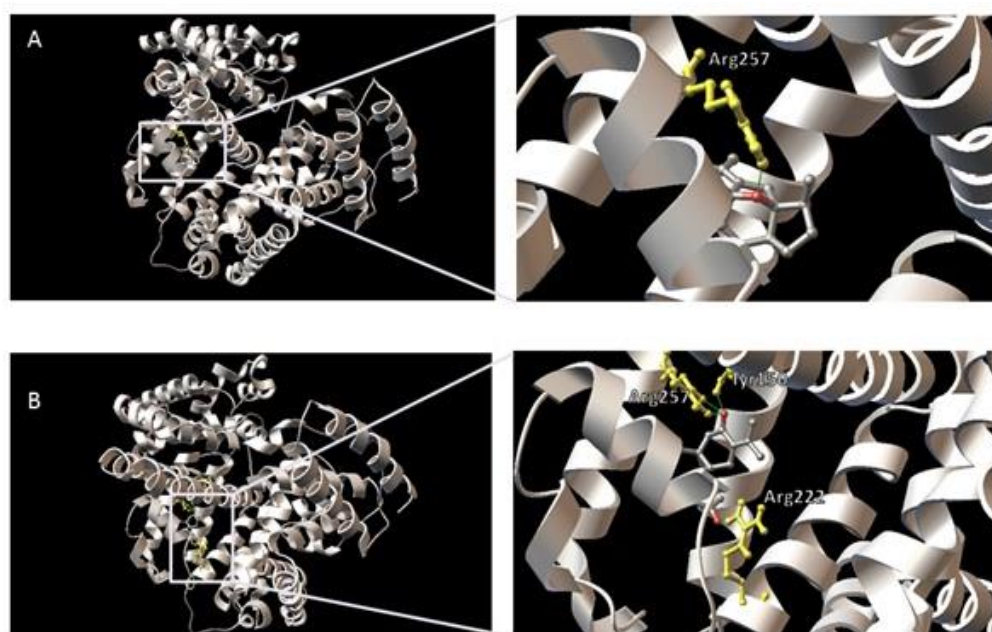


Figure 3.130: Predicted orientations of the lowest docking energy conformations of 1BM0-ligand complexes. The binding sites were enlarged to show hydrogen bonding (green lines) between amino acid residues and the ligands. Amino acid residues that form hydrogen bonds with the ligands are rendered in ball and stick and coloured yellow. (A) Curcumenol in the binding site I of HSA (1BM0). (B) Curcumenone in the binding site I of HSA (1BM0).

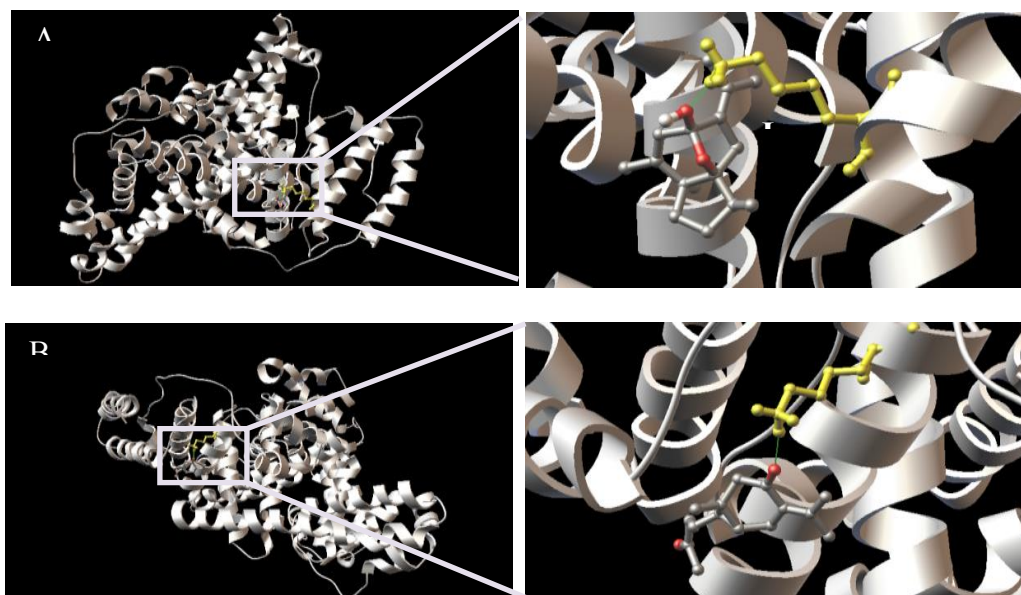


Figure 3.131: Predicted orientations of the lowest docking energy conformations of 1BM0-ligand complexes. The binding sites were enlarged to show hydrogen bonding (green lines) between amino acid residues and the ligands. Amino acid residues that form hydrogen bonds with the ligands are rendered in ball and stick and coloured yellow. (A) Curcumenol in the binding site II of HSA (1BM0). (B) Curcumenone in the binding site II of HSA (1BM0).

Table 3.49: Predicted hydrogen bonds between interacting atoms of the amino acid residues of HSA (1BM0) and the ligands at site I and site II.

Compound	HSA binding site	Protein atom	Ligand atom	Distance (Å)
Curcumenol	Site I	Arg257:HH22	O (etheral)	1.907
	Site II	Lys545:HZ3	O (hydroxyl)	1.684
Curcumenone	Site I	Tyr150:HH	O (ketone)	1.907
		Arg222:HH11	O (acetyl)	1.930
		Arg257:HE	O (ketone)	1.969
		Arg257:HH22	O (ketone)	2.236
	Site II	Lys413:HZ3	O (ketone)	2.025

These results suggested that although curcumenol **42** and curcumenone **65** can bind to both sites I and II of HSA, the binding is more preferable at site I, facilitated by hydrophobic forces and hydrogen bonds. Although, the lowest binding energies for both ligands at site I were the same ($-6.77 \text{ kcal mol}^{-1}$) in molecular docking study, the 1BM0-curcumenone complex involved a greater number of hydrogen bonding (four)

than that of 1BM0-curcumenol complex (one). This is reflected in the fluorescence quenching assay where curcumenone showed a higher extent of fluorescence quenching compared to curcumenol. Thus it can be inferred that both curcumenol and curcumenone showed similar HSA binding properties, with curcumenone having a slightly higher affinity towards HSA.

CHAPTER 4: MATERIALS AND METHODS

4.1 Phytochemical analysis

4.1.1 Plant Samples

4.1.1.1 *C. zedoaria* rhizomes

The rhizomes of *C. zedoaria* were collected from Tawamangu, Indonesia and a voucher specimen (KL 5764) was deposited at the herbarium of the Department of Chemistry, Faculty of Science, University of Malaya, Kuala Lumpur, Malaysia.

4.1.1.2 *C. purpurascens* rhizomes

The rhizomes of *C. purpurascens* were collected from Yogyakarta, Indonesia, and a voucher specimen (KL 5793) was deposited at the herbarium of the Department of Chemistry, Faculty of Science, University of Malaya, Kuala Lumpur, Malaysia.

4.1.2 Solvents

The industrial grade solvents (hexane, dichloromethane, ethyl acetate, and methanol) were used for bulk extractions, these solvents were distilled twice before use. The HPLC and analytical grade solvents (hexane, dichloromethane, ethyl acetate, acetone, petroleum ether, and methanol) were used for the final chromatographic separation of the pure compounds.

4.1.3 Instrumentation

- ^1H NMR spectra were obtained using JEOL LA 400 FT-NMR. Spectra were recorded in deuterated solvents including chloroform, methanol, and acetone. Chemical shifts were expressed in ppm and coupling constants were in Hertz (Hz).
- Mass spectra were carried out for the non-volatile compounds on Agilent

Technologies 6530 Accurate-Mass QTOF LC/MS, coupled with ZORBAX Eclipse XDB-C18 Rapid Resolution HT (4.6 mm i.d. \times 50 mm \times 1.8 μ m) column.

- The EI MS spectra were obtained for the volatile constituents on Shimadzu GC-MS QP2000A spectrometer, high-resolution ESI MS were measured on a LTQ Orbitrap XL (Thermo Scientific).
- UV spectra were recorded on a Shimadzu UV-Visible spectrophotometer using HPLC grade ethanol as solvent with mirror UV cell.
- The infrared (IR) spectra were obtained through Perkin Elmer FT-IR spectrometer Spectrum RX1 using chloroform as solvent.
- Melting points were taken on hot stage Gallen Kamp melting point apparatus and were uncorrected.
- Optical rotations were determined on JASCO (Japan) P1000 automatic digital polarimeter.

4.1.4 Chromatography

4.1.4.1 Thin Layer Chromatography (TLC)

Aluminium supported silica gel 60 F₂₅₄ plates were used to check the spots of the isolated compounds. UV Light Model UVGL-58 Mineralight Lamp 230V, 50/60 Hz was used to examine spots or bands on the TLC after spraying with the required reagents.

4.1.4.2 Column chromatography (CC)

Distilled industrial grade of the solvents (hex., DCM, EtOAc, and MeOH) were used to run column chromatography. Silica gel F₆₀, 230-400 mesh ASTM (Merck 9385) was used for column chromatography. A slurry of silica gel 60 (approximately 30:1 silica gel to sample ratio) in hex solvent system was poured into a glass column of

appropriate size with gentle tapping to remove trapped air bubbles. The crude extract was initially dissolved in minimum amount of solvent and loaded on top the packed column. The extract was eluted with an appropriate solvent system at a certain flow rate. Fractions were collected in conical flasks and evaporated for the next step. Fractions with similar spots were then combined by TLC monitoring.

4.1.4.3 Preparative Thin Layer Chromatography (PTLC)

PTLC silica gel 60 F₂₅₄ glass plates of size 20 cm × 20 cm (Merck 1.05715.0001) were used for the separation of compounds. UV Light Model UVGL-58 Mineralight Lamp 230V-50/60 Hz was used to examine bands on the PTLC.

4.1.4.4 High Performance Liquid Chromatography (HPLC)

Waters HPLC System was used for HPLC separation, equipped with Binary Gradient Module, System Fluidics Organizer and UV detector set at the range from 200-400 nm. Chromatographic analysis and separations were performed on a ZORBAX Eclipse Plus C18 (9.6 mm i.d. × 250 mm × 3.5 µm) HPLC columns. HPLC grade methanol, HPLC grade acetonitrile and deionized water were used as mobile phase solvents with HPLC grade formic acid as buffer. All solvents and samples were filtered with 0.45 µm nylon membrane filter (Waters) prior to HPLC analysis. The data were collected and analysed by using MassLynx software.

4.1.5 Visualisation

4.1.5.1 Vanillin-sulphuric acid vapour

Vanillin (1.0g) in 10 ml of concentrated H₂SO₄ was added upon cooling to 90 ml of ethanol before spraying onto the TLC plate. The TLC plate was then heated at 50°C until full development of colours had been observed. The

occurrence of blue, purple, dark green, grey or brown indicated the presence of terpenes and steroids.

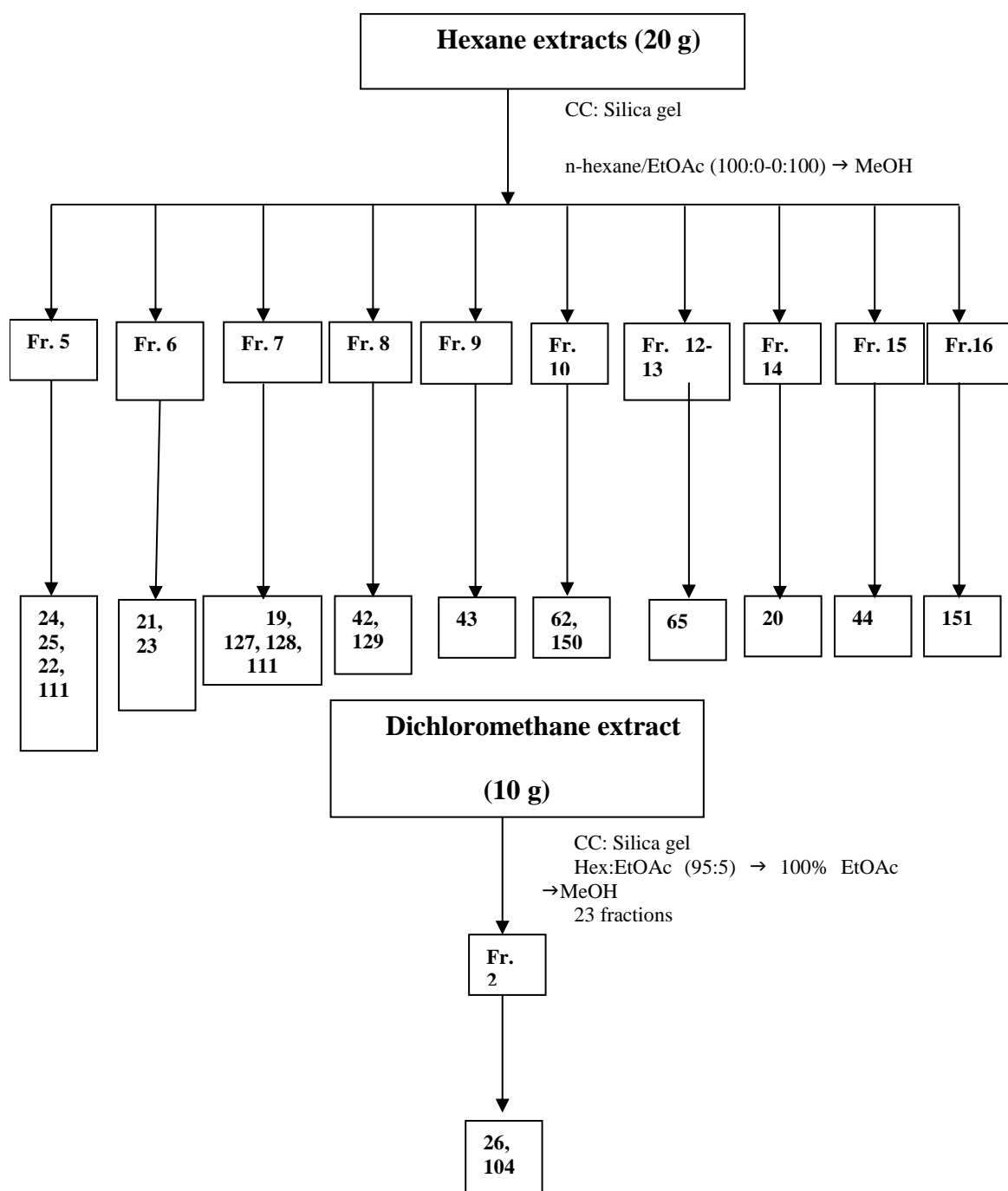
4.1.5.2 Anisaldehyde-sulphuric acid

An aliquot of 0.5 ml of anisaldehyde was mixed with 10 ml glacial acetic acid followed by 85 ml methanol and 5 ml of concentrated sulphuric acid.

4.1.6 Isolation of the pure compounds from *C. zedoaria*

The air dried, powdered rhizomes (1.0 kg) of *C. zedoaria* were successively extracted by maceration with *n*-hexane, dichloromethane (DCM), ethyl acetate (EtOAc) and methanol (MeOH). The *n*-hexane extract (20.2 g, yield 2.4%) was chromatographed on a silica gel column (0.063-0.200 mm) with a gradient elution system using *n*-hexane and ethyl acetate (100:0-0:100). Based on the TLC pattern, fractions were pooled together to get a total of 21 fractions. F5 by through further CC and preparative thin layer chromatography (PTLC), yielded four compounds, namely germacrone-4,5-epoxide (**24**, 12.4mg), germacrone-1,10-epoxide (**25**, 8.0 mg), curcuzerenone (**111**, 3.1 mg), and furanodienone (**22**, 8.0 mg). Fraction 6 was chromatographed on a silica gel column (0.043-0.063 mm) using a gradient elution system (*n*-hexane:EtOAc 100:0-0:100), followed by purification on preparative thin layer chromatography (*n*-hex:EtOAc 90:10, 3 times run) to get germacrone (**23**, 21.6 and furanodiene (**21**, 8.8 mg). Fraction 7 was subjected to size exclusion chromatography using MeOH and DCM in a 1:1 ratio, followed by PTLC (Hex:EtOAc 90:10) and HPTLC (Hex:EtOAc:MeOH 96:3:1) to afford dehydrocurdione (**19**, 34.5), two labdanes, namely labda-8(17),12-diene-15,16-dial (**127**, 16.2 mg) and labda-8(17),12-diene-15, 15-dimethoxy-16-al, also named calcaratarin A (**128**, 22.6 mg), and *curcumanolide* A (**101**, 4.9 mg). Fraction 8 was chromatographed by PTLC using petroleum ether (40-60°C) (PE) and EtOAc in a ratio of 85:15 for the first run and 82:18 for the second run to get curcumenol (**42**, 15.5 mg),

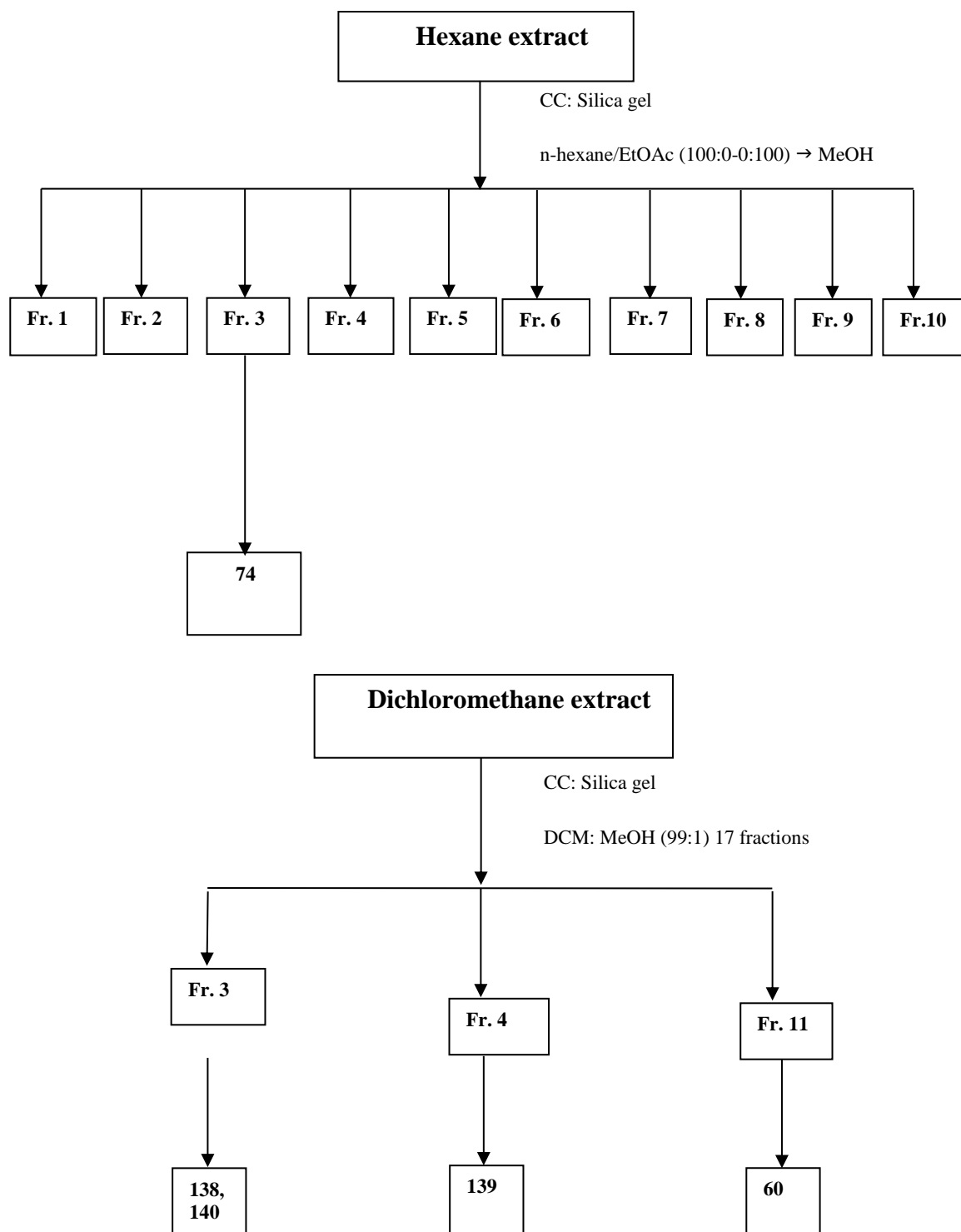
and zerumin A (**129**, 9.8 mg). Fraction 10 was chromatographed by CC followed by further purification by HPTLC to afford a second monoclinic modification of curcumenol as a crystallized dimer elucidated by single crystal X-ray diffraction analysis or known as 9-isopropylidene-2, 6-dimethyl-11-oxatricyclo [6.2.1.0^{1,5}] undec-6-en-8-ol (**150**, 5.4 mg) Isoprocurcumenol (**43**, 10.2 mg) was isolated from fraction 9 by successive development on PTLC using PE:EtOAc in the ratio of 90:10 and 85:15, respectively. Curcumenone (**65**, 16.4 mg) was purified from fraction 12 by PTLC using three times run with PE:EtOAc:MeOH in a ratio of 85:14:1. Curdione (**20**, 13.1mg) was obtained using CC, followed by PTLC using solvent system in first run (PE: EA: MeOH+formic acid 85%:14%:1%), second run using (PE:EA 80%:20%). Procurcumenol (**44**, 8.9 mg) was isolated from fraction 15 as a colourless oil by PTLC (PE:EtOAc:formic acid 85:14.5:0.5). Zerumbone epoxide (**151**, 11.9 mg) was isolated from silica gel (0.043-0.063 mm) column of fraction 16 using a gradient elution system of *n*-hexane and EtOAc (100:0-0:100), followed by three times run on HPTLC (Hex:EtOAc:1,4-dioxane(85:14:1). The DCM extract (10 g) was fractionated on a silica gel column (Hex:EtOAc 95:5-0:100) to give 23 fractions. Fraction 2 was subjected to micro silica gel column (0.043-0.063 mm) with a gradient elution system of Hex and EtOAc (100:0-0:100) followed by RP-HPLC (H₂O:MeOH 40:60, run time 80 min, flow rate 2.5 ml/min) which afforded zederone (**23**, 24.4 mg) and gweicurculactone (**41**, 3.6 mg) at the retention time of 15.26 and 20.16 min, respectively. Fraction 2 was also subjected to micro CC followed by two times run on PTLC (Hex:EtOAc 80:20) afforded comosone II (**104**, 6.6 mg).



Scheme 4.1: Isolation and purification of the compounds from hexane and DCM crudes of *C. zedoaria*

4.1.7 Isolation of the pure compounds from *C. purpurascens*

One kg of the powdered *C. purpurascens* rhizomes was successively extracted by maceration with *n*-hexane, DCM, and MeOH. The hexane extract (51.1 g) was chromatographed on a silica gel column (0.063-0.200 mm) with a gradient elution system using *n*-hexane and ethyl acetate (100:0-0:100). Based on TLC pattern, fractions were combined together to get a total of 16 fractions. Fraction 3 was subjected to CC and preparative thin layer chromatography (PTLC) using a combination of a solvent system, run twice: (petroleum ether PE: EA-95%: 5%) which afforded ar-turmerone (**74**, 20.2 mg). The DCM extract (10 g) was fractionated on a silica gel column (0.043-0.063 mm) with an isocratic elution system of DCM and MeOH in the ration of DCM 99%:MeOM 1%) to give 17 fractions. Fraction 3 was subjected to PTLC using a solvent system (DCM: MeOH-99%:1%), to get curcumin (**138**, 15.2 mg) and demethoxycurcumin (**140**, 12.5 mg). Bisdemethoxycurcumin (**139**, 11.2 mg) was isolated from fraction 4 by using DCM: MeOH in the ratio of 99:1. Zedoalactone B (**60**, 6.5 mg) was obtained from fraction 11 using the solvent system DCM:MeOH:acetone 97:2:1.



Scheme 4.2: Isolation and purification of the compounds from hexane and DCM crudes of *C. purpurascens*

4.1.8 Isolation of the essential oils from *C. purpurascens*

The dried rhizomes (300 g) were cut into small pieces, ground and immediately soaked in distilled (1.00 L) in a round-bottomed flask. The soaked sample was distilled in a Cleveger-type apparatus for 5 hours. The yield of the oil (2.16 g, 0.72%) was calculated based on the weight of the dried plant material.

The GC analysis of the oil was done on an Agilent Technologies 7890A GC system equipped with a FID detector using fused capillary column HP-5 (5% diphenyl and 95% dimethyl-polysiloxane, 30.00 M \times 0.32 mm ID, 0.25 μ m film thickness) with helium as a carrier gas at a flow rate of 1 ml per min. The column temperature was initially programmed from 60°C and kept isothermally for 10.0 minutes, then increased at 3.0°C per minute to 230°C, and held for 1.0 min. The temperature of the injector port and detector were set at 230°C and 250°C respectively, with a split ratio 1:20.

GC-MS analysis was performed on an Agilent Technologies 6890N GC System equipped with 5975 inert mass selective detector (70 eV direct inlet) on HP-5 ms capillary column (30.0 m \times 0.25 mm 1D, 0.25 μ m film thickness). The column temperature was programmed from 60°C for 10 minutes, then increased to 230°C at 3 °C per minute and was held for 1 minute at 230°C. The helium was used as the carrier gas at a flow rate of 1 ml per minutes with split ratio 1:20. The injector port temperature was set at 230°C and detector at 250°C. The total ion chromatogram obtained was auto integrated by ChemStation and the components were identified by comparison with an accompanying mass spectral database. Arithmetic index (A1) was experimentally measured from the programmed temperature GC-FID by arithmetic interpolation between bracketing alkane using a homologous series of n-alkanes as standard (Adams, 2012; Van den Dool et al., 1963).

4.1.9 Supercritical fluid extraction of *C. purpurascens*

In the present study, about 33 grams of the dried of *C. purpurascens* rhizomes was placed in 100 ml extraction vessel of an analytical-scale SFT 100 XW SFE system supported with a cylinder of liquid CO₂ (purity 99.8%, SFE grade). The system conditions studied were at 313 K and 10.34 MPa. One-step extractions were performed by feeding CO₂ into the system until the pressure 10.34 MPa was attained and the system temperature was set to 313 K. After 30 min of static extraction (no liquid flow), the sample material was subjected to dynamic extraction by flowing liquid CO₂ at a rate of 12 ml/min. During the extraction, 2 to 5 crude fractions were collected in the vials. Each fraction was collected after every 5-10 min from the previous collection. The extraction of the crude was terminated when no extract was visually observed in the collection vial, then continued by increasing the pressure to 20.68 MPa. Similarly the extraction was collected in the collection vials until the extraction was visually observed to be finished. Above steps were followed for extraction by setting the pressure to 30.34 MPa. Similar steps followed for temperatures set at 323 K and 333 K in separate run with pressures 20.68 and 30.34 MPa for each cases. The extracts obtained were subjected to GC and GC-MS for chemical analysis.

4.2 Cytotoxicity assessment

4.2.1 Cell Culture

The cancer cell lines MCF-7 (breast cancer), Ca Ski (cervical cancer) and HT-29 (colon cancer) were cultured as monolayer in RPMI 1640 growth media. HUVEC (human umbilical vein endothelial cells) and PC-3 (prostate cancer) cells were cultured in DMEM. All cells were purchased from the American Type Culture Collection (ATCC, USA) except for human umbilical vein endothelial cells (HUVEC) cells was obtained from ScienCell Research Laboratories (Carlsbad, CA). All the media were supplemented with 10% v/v foetal bovine serum (FBS), 100 µg/ml penicillin/streptomycin and 50 µg/ml amphotericin B. The cells were cultured in a 5% CO₂ incubator at 37°C.

4.2.2 MTT based cytotoxicity assay

Cell viability was investigated using 3-(4,5-dimethylthiazol-2-yl)-2,5-diphenyltetrazolium bromide (MTT) assay. Cells were detached from the 25cm³ tissue culture flask when it achieved 80% confluency. The detached cells were pelleted by centrifugation (1,000 rpm; 5 minutes). Cells (3.0×10^4 cells / ml) were seeded onto a 96-well microtiter plate (Nunc). The cells were incubated at 37°C, and 5% CO₂ incubator for 24 h to give adherent cells. The test compounds (1-100 µg/ml) were added onto the 96-well microtiter plate containing adherent cells. The untreated cells were incubated in 10% media containing 0.5% DMSO (without addition of any test compounds/extracts). This mixture was regarded as the negative control whereas doxorubicin as the positive control. The plates were incubated for 72 h at 37°C in a 5% CO₂ incubator. After 72 h, the media was removed and 100 µl of fresh medium and 20 µl of MTT (Sigma, filter sterile, 5 mg/ml) was added to each well and further incubated for 4 hours (37°C) after which the media was substituted with 150 µl DMSO. The 96-well microtiter plates were

then agitated at room temperature onto an incubator shaker to dissolve the formazan crystals. The absorbance (A) of the content of the plates was measured at 540 nm using a micro plate reader. The percentage of inhibition of each test sample was calculated according to the following formula: Percentage of inhibition (%) = $(A_{\text{control}} - A_{\text{sample}}) / A_{\text{control}} \times 100\%$. The average of three replicates was then obtained. The IC_{50} for each extract was extrapolated from the graphs of the percentage inhibition versus concentration of test agents. Cytotoxicity of each test agent is expressed as IC_{50} value. The IC_{50} value is the concentration of test agents that cause 50% inhibition or cell death, averaged from the three experiments.

4.3 QSAR studies of cytotoxic compounds

The geometry optimizations to final minimum energy structures of the 21 isolated compounds were performed by using the popular Becke three parameter Lee-Yang-Parr (B3LYP) exchange-correlation hybrid functional combined with a double- ξ Pople-type basis set 6-31+G (d,p), in which polarized and diffuse functions are taken into consideration (Becke, 1993). B3LYP hybrid functional includes a mixture of Hartree-Fock exchange (20% of HF) with DFT exchange-correlation functional. The frequency analyses were carried out at the same level of theory. The absence of imaginary frequencies confirmed that the structures are true minima on the potential energy surface. The choice of the hybrid functional B3LYP is based on previous QSAR studies (Mendes et al., 2012; Sarkar et al., 2012). The chemical descriptors that were chosen to be correlated with cytotoxicity activity are: (i) electronic descriptors: frontier molecular orbital energies (E_{HOMO} , E_{LUMO} , which are well accepted as molecular descriptors in medicinal chemistry, since they are related to the capacity of a molecule to form a charge transfer complex with its biological receptor), ionization potential (IP), electron affinity (EA), electronegativity (χ), hardness (η), softness (S), electrophilicity index

(ω), dipole moment (μ), molecular polarizability (α), (ii) steric descriptors: surface area of molecule (A), volume (V) and its molecular weights (M); and (iii) hydrophobicity descriptor: $\log P$, where P stands for the octanol-water partition coefficient. The calculations of $\log P$ were carried out using Hyperchem Molecular package (HyperChem, 2002) by means of the atomic parameters derived by Ghose, Pritchett and Crippen and later extended by Ghose and co-workers (Ghose et al., 1988; Viswanadhan et al., 1989). The other descriptors were calculated using the DFT method and obtained in two different ways: (i) Orbital consideration, which is based on Koopman's theorem where $IP = -E_{HOMO}$ and $EA = -E_{LUMO}$ (Koopmans, 1934); and (ii) energy consideration, which is based on the use of the classical finite difference approximation, where the change of one electron is usually involved $\Delta N = \pm 1$ (Parr et al., 1989). In this method, $IP = E_{+1} - E_0$ and $EA = E_0 - E_{-1}$ where E_0 , E_{-1} and E_{+1} are the electronic energies of neutral molecule, when adding and removing an electron to the neutral molecule, respectively. . In addition to the (i) and (ii) methods, the electronic descriptors (e.g. hardness) can be calculated using internally resolved hardness tensor (IRHT) approach (Grigorov et al., 1997; Mineva et al., 1998; Neshev et al., 1996), and it dealing with fractional occupation numbers based on the Janak's extension of DFT (Janak, 1978). This approach is also based on orbital energies and it dealing with fractional occupation numbers based on the Janak's extension of DFT (Janak, 1978). De Luca et al. (2002) used the above approaches to investigate the solvent effects on the hardness values of a series of neutral and charged molecules, and they found that the three methods gave similar results in the presence of solvent.

The solvent effects were taken into account implicitly by using the polarizable continuum model (PCM) as implemented in the Gaussian 09 package (M. J. Frisch et al., 2009). In PCM, the solute is embedded into a cavity surrounded by solvent

described by its dielectric constant ϵ (e.g., for methanol $\epsilon = 32.6$) (Tomasi et al., 2005). The use of an explicit solvent has been investigated notably by Guerra et al., who concluded to a better description of the electronic properties using PCM compared to the explicit solvent (Guerra et al., 2004). A hybrid model was tested by Trouillas et al. (Kozłowski et al., 2007). The authors showed that only slight differences were obtained compared to PCM. All theoretical calculations including ground state geometry optimization and frequency analysis calculations were performed with Gaussian 09 package (M. J. Frisch et al., 2009).

Simple and multiple linear regression (SLR and MLR, respectively) analyses were used to determine regression equations, correlation coefficients R^2 , adjusted R^2 and standard deviations (SD). PCA and HCA were employed to reduce dimensionality and investigate the subset of descriptors that could be more effective for classifying the isolated compounds according to their degree of cytotoxicity against tumour cells.

The regression models and statistical analyses of obtained results were carried out by using DataLab package (http://www.lohninger.com/datalab/en_home.html).

4.4 Neuroprotective and antioxidant activity investigation

NG108-15 hybridoma cell line was obtained from American Type Culture Collection (ATCC). Dulbecco's Modified Eagle's Medium (DMEM), phosphate buffered saline (PBS), sodium bicarbonate, HEPES sodium salt and 3-(4,5-dimethylthiazol-2-yl)-2,5-diphenyltetrazolium bromide (MTT) were purchased from Sigma-Aldrich; foetal bovine serum (FBS), penicillin/streptomycin and amphotericin B were purchased from PAA Laboratories, Austria; accutase was purchased from Innovative Cell Technologies, Inc.; hydrogen peroxide (H_2O_2) was purchased from System[®].

4.4.1 Assessment of neuroprotective activity

The neuroprotective effects of the test compounds against H₂O₂-induced cell death in NG108-15 cells were evaluated by MTT [3-(4,5-dimethylthiazol-2-yl)-2,5-diphenyltetrazolium bromide] assay. Cells were plated at a total density of 5×10^3 cells/well in a 96-well plate. The cells were left to adhere for 48 h and treated with LA (2 h) prior to H₂O₂ (400 μ M) exposure for 24 h. 20 μ L MTT solution (Sigma Aldrich) was added into each well and incubated at 37°C for another 4 h. The absorbance was measured by using a microplate reader (ASYS UVM340) at 570 nm (reference wavelength: 650 nm).

$$\% \text{ Cell viability} = \frac{\text{Absorbance of treated cells}}{\text{Absorbance of control cells}} \times 100\%$$

NG108-15 cells were rinsed with PBS, harvested with accutase and plated on 96-well microtitre plate such that each well contains 5×10^3 cells. It was kept for 48 h for the cells to adhere. Cells preincubated for 2 h with various compounds at different concentration (1-30 μ M) were exposed to H₂O₂ (400 μ M) for subsequent 24 h. After the incubation period is over, 20 μ l of MTT solution (5 mg/ml) was added to each well and incubated at 37°C for another 4 h. The medium was removed subsequently and DMSO was added to dissolve the formazan crystals. The eluted samples were measured directly in a microplate reader (ASYS UVM340) at 570 nm (with a reference wavelength of 650 nm) (Wong et al., 2012). Cell viability was calculated using the following formula:

$$\% \text{ Cell viability} = \frac{\text{Absorbance of treated cells (As)}}{\text{Absorbance of control cells (Ac)}} \times 100\%$$

4.4.2 Antioxidant activity test by ORAC assay

Oxygen radical antioxidant capacity (ORAC) assay was done as described by G. Cao et al. (1997) with slight modification. The assay was performed in a 96-well black microtitre plate, with 25 µl of sample, standard (Trolox), blank (solvent/PBS) or positive control (quercetin) in each well. Subsequently, 150 µl of working fluorescein solution was added to each well of the assay plate. The plate was incubated at 37°C for 5 min. Aliquot of (25 µl) AAPH working solution was then added to each well, making up a total volume of 200 µl. Fluorescence was recorded at an excitation wavelength of 485 nm and emission wavelength of 538 nm. Data were collected every 2 min during an observation period of 2 h, and were analysed by calculating the differences of area under fluorescence decay curve (AUC) of samples, standard or positive control against blank. The antioxidant capacity was expressed as Trolox equivalent (TE).

4.5 Binding and docking studies

4.5.1 Binding studies

Essentially fatty acid free human serum albumin (HSA) was obtained from Sigma-Aldrich Inc., USA. All other chemicals were of analytical grade purity.

The stock solution of HSA was prepared in 20 mM sodium phosphate buffer, pH 7.4 and its concentration was determined spectrophotometrically using a specific extinction coefficient value of 5.3 at 280 nm. Stock solutions of curcumenol **44** and curcumenone **65** were prepared by dissolving the desired quantity in 5 ml of ethanol and diluting it to the desired volume with 20 ml of sodium phosphate buffer, pH 7.4.

The interaction of curcumenol **44** and curcumenone **65** to HSA were studied by fluorescence quench titration method. A constant amount of protein was titrated with increasing concentrations of the ligands. The concentration of HSA was maintained at 3

μM , while the ligand concentrations ranged from 0–60 μM . The final volume of the reaction mixture was made up to 3 ml with the above sodium phosphate buffer. The samples were allowed to equilibrate for 30 min prior to fluorescence measurements. The fluorescence spectra of these samples were recorded on a Jasco FP-6500 spectrofluorometer with a 1 cm path length quartz cuvette. Both excitation and emission slits were set at 10 nm, while the scan speed was maintained at 500 nm/min. The samples were excited at 280 nm, and the emission spectra were recorded in the wavelength range, 300–400 nm.

4.5.2 Molecular docking

The structure of curcumenol **44** and curcumenone **65** were drawn using ACD/ChemSketch Freeware (Advanced Chemistry Development Inc. Ontario, Canada), 3-D optimized and exported as a mol file. The geometry optimization of these structures was refined with the VegaZZ 2.08 (Pedretti et al., 2002) batch processing MOPAC script (mopac.r; keywords: MMOK, PRECISE, GEO-OK) using AM1 semiempirical theory (Dewar et al., 1985) and converted and stored as a mol2 file. Molecular docking, visualization and rendering simulation were performed using AutoDock 4.2 (Goodsell et al., 1996) and AutoDockTools 1.5.4 (Sanner, 1999) at the Academic Grid Malaysia Infrastructure. For the docking study, the curcumenol and curcumenone non-polar hydrogens were merged and the rotatable bonds were defined. The crystal structure of HSA (PDB code 1BM0, res. 2.5 Å) was downloaded from the Protein Data Bank (PDB) (Berman et al., 2000). Its water molecules were removed and the atomic coordinates of chain A were stored in a separate file and used as input for AutoDockTools, where polar hydrogens, Kollman charges and solvation parameters were added. The two binding sites (site I and site II) were defined using two grids of 70x70x70 points each with a grid space of 0.375 Å centered at coordinates x=35.26

y=32.41 z=36.46 for site I and x=14.42 y=23.55 z=23.31 for site II. Lamarckian genetic algorithm with local search (GA-LS) was used as the search engine, with a total of 100 runs for each binding site. In each run, a population of 150 individuals with 27000 generations and 250000 energy evaluations were employed. Operator weights for crossover, mutation and elitism were set to 0.8, 0.02 and 1, respectively. For local search default parameters were used. Cluster analysis was performed on docked results using RMS tolerance of 2.0 Å. The protein-ligand complexes were visualized and analyzed using AutoDockTools.

4.6 Physical and spectral data of isolated compounds from *C. zedoaria*

4.6.1 Germacrane type sesquiterpenes

Dehydrocurdione 19	: Pale yellow oil
Molecular formula	: C ₁₅ H ₂₂ O ₂
$[\alpha]_D^{20}$: + 280° (c 0.3, MeOH)
IR (CHCl ₃) ν_{\max} cm ⁻¹	: 1680, 1742
UV MeOH) λ_{\max} nm (log ε)	: 207 (1.16)
¹ H NMR (CDCl ₃) δ ppm	: Refer Table 3.2
¹³ C NMR (CDCl ₃) δ ppm	: Refer Table 3.2
GC-MS	: RT 27.86 min, 234 (M ⁺ , 10), 178(27), 164(53), 152(49), 121(37), 96(53), 68(100), 41(59).

Curdione 20	: White amorphous powder
Molecular formula	: C ₁₅ H ₂₄ O ₂
$[\alpha]_D^{20}$: + 26° (c=1 in MeOH)
IR (CHCl ₃) ν_{\max} cm ⁻¹	: 3584, 2961, 2927, 2873, 1702
UV(MeOH) λ_{\max} nm (log ε)	: 204 (0.97)
¹ H NMR (CDCl ₃) δ ppm	: Refer Table 3.3
¹³ C NMR (CDCl ₃) δ ppm	: Refer Table 3.3

GC-MS : RT= 15.42 min, 180 (82), 167 (75), 69 (100), 55 (53), 41(57)

Furanodiene 21 : white amorphous powder

Molecular formula : C₁₅H₂₀O

IR (CHCl₃) ν_{\max} cm⁻¹ : 3429, 2928, 1740, 1448.

UV(MeOH) λ_{\max} nm (log ϵ) : 217 (1.385)

¹H NMR (CDCl₃) δ ppm : Refer Table 3.5

¹³C NMR (CDCl₃) δ ppm : Refer Table 3.5

GC-MS : 216, RT: 21.28 min., 216(M⁺, 48), 201(12), 159(23), 148(8), 145(2), 108(100), 91(28), 77(26), 65(12), 53(16), 41(31).

Furanodienone 22 : Colourless crystal

Molecular formula C₁₅H₁₈O₂

IR (CHCl₃) ν_{\max} cm⁻¹ : 2926, 1653, 1376

UV(MeOH) λ_{\max} nm (log ϵ) : 217 (1.38)

¹H NMR (CDCl₃) δ ppm : Refer Table 3.9

¹³C NMR (CDCl₃) δ ppm : Refer Table 3.9

GC-MS : GC-MS: 230 (32), 215 (15), 122 (100), 94(51), 77 (15), 66 (26), 65 (25), 41(13).

Germacrone 23 : White amorphous solid

Molecular formula : C₁₅H₂₂O

IR (CHCl₃) ν_{\max} cm⁻¹ : 1677

UV(MeOH) λ_{\max} nm (log ϵ) : 206 (1.47)

¹H NMR (CDCl₃) δ ppm : Refer Table 3.4

¹³C NMR (CDCl₃) δ ppm : Refer Table 3.4

GC-MS : RT: 25.90 min, 218(M⁺, 13), 175(27), 136(61), 135(85), 121(30), 107(100), 105(20), 91(31), 67(42).

Germacrone-4, 5-epoxide 24	: White solid
Molecular formula	: C ₁₅ H ₂₂ O ₂
IR (CHCl ₃) ν_{\max} cm ⁻¹	: 1702
UV(MeOH) λ_{\max} nm (log ϵ)	: 205 (1.17)
¹ H NMR (CDCl ₃) δ ppm	: Refer Table 3.7
¹³ C NMR (CDCl ₃) δ ppm	: Refer Table 3.7
GC-MS	: 31.8 min., 234 (100), 163 (33), 136 (47), 121 (68), 107 (40), 41 (31).

Germacrone 1, 10-epoxide 25	: white solid
Molecular formula	: C ₁₅ H ₂₂ O ₂
IR (CHCl ₃) ν_{\max} cm ⁻¹	: 1710
UV(MeOH) λ_{\max} nm (log ϵ)	: 218 (1.11)
¹ H NMR (CDCl ₃) δ ppm	: Refer Table 3.8
¹³ C NMR (CDCl ₃) δ ppm	: Refer Table 3.8
GC-MS	: 30.0 min., 97.15 (17.0), 84.1 (12.2), 81.10 (17.3), 44.05 (7.07), 43.05 (100), 41 (34.1).

Zederone 26	: Colourless crystal
Molecular formula	C ₁₅ H ₁₈ O ₃
$[\alpha]_D^{20}$: + 260° (c 0.5, MeOH)
IR (CHCl ₃) ν_{\max} cm ⁻¹	: 2929, 1664, 1527, 1404
UV (MeOH) λ_{\max} nm (log ϵ)	: 239 (2.08)
¹ H NMR (CDCl ₃) δ ppm	: Refer Table 3.6
¹³ C NMR (CDCl ₃) δ ppm	: Refer Table 3.6
GC-MS	: 32.09 min, 246 (33), 188(35), 176(35), 175(100), 161 (55), 119 (90), 91 (55), 43 (55).

4.6.2 Guaiane type sesquiterpenes

Gweicurculactone 41

	: Reddish crystal
Molecular formula	$C_{15}H_{16}O_2$
$[\alpha]_D^{20}$: + 15.2 (<i>c</i> 0.1, MeOH)
IR (CHCl ₃) ν_{\max} cm ⁻¹	: 1726 cm ⁻¹
UV(MeOH) λ_{\max} nm (log ϵ)	: 2.18 (1.02)
¹ H NMR (CDCl ₃) δ ppm	: Refer Table 3.10
¹³ C NMR (CDCl ₃) δ ppm	: Refer Table 3.10
GC-MS	: 228 (100), 199.1 (89.24), 157.1 (22.34), 142.1 (16.96), 115.10 (16), 51 (5.6).

Curcumenol 42

	: Colourless oil
Molecular formula	$C_{15}H_{22}O_2$
IR (CHCl ₃) ν_{\max} cm ⁻¹	: 3432 (OH), 2934 (C=C), 1457 (C-O)
UV(MeOH) λ_{\max} nm (log ϵ)	: 224.0(3.047)
¹ H NMR (CDCl ₃) δ ppm	: Refer Table 3.13
¹³ C NMR (CDCl ₃) δ ppm	: Refer Table 3.13

GC-MS	: 26.70 min, 234 [M ⁺ , 26], 189(53), 147(52), 145(30), 133 (53), 121(39), 119(35), 105(100), 91(37), 55(18), 41(25).
-------	--

Isoprocucumenol 43

	: Colourless oil
Molecular formula	$C_{15}H_{22}O_2$
IR (CHCl ₃) ν_{\max} cm ⁻¹	: 3450, 1674, 1610.
UV(MeOH) λ_{\max} nm (log ϵ)	: 205 (1.83)
¹ H NMR (CDCl ₃) δ ppm	: Refer Table 3.11
¹³ C NMR (CDCl ₃) δ ppm	: Refer Table 3.11
GC-MS	: 234, RT: 29.36 min, 158 (35), 121 (84), 105 (100), 93 (60), 43 (79)

Curcumenol second monoclinic 150

: Colourless crystal

Crystal data:

: $C_{15}H_{22}O_2$ M_r

: 234.33, Monoclinic

P2

: $a=9.3495 \text{ \AA}$, $b=12.535 \text{ \AA}$, $c=11.7727$ A°, β

: 96.532

 A°, V

: 1370.76 (18)

 A^{o3}, Z

: 4

Mo $K\alpha$ radiation, μ : 0.07 mm^{-1}

T

: 100 K, $0.4 \times 0.05 \times 0.05 \text{ mm}$ **Procucumenol 44**

: Colourless oil

Molecular formula

 $C_{15}H_{22}O_2$ IR ($CHCl_3$) $\nu_{\max} \text{ cm}^{-1}$

: 3409, 1712

UV(MeOH) $\lambda_{\max} \text{ nm (log } \epsilon)$

: 204.0 (1.16)

 $^1\text{H NMR (CDCl}_3)$ $\delta \text{ ppm}$

: Refer Table 3.12

 $^{13}\text{C NMR (CDCl}_3)$ $\delta \text{ ppm}$

: Refer Table 3.12

GC-MS

: 216 (79), 123 (75), 105 (55), 91 (41),
43 (100), 41 (40).**4.6.3 *Seco-guaiane* type sesquiterpene****Curcuzedoalide 62**

: White amorphous powder

Molecular formula

: $C_{15}H_{20}O_3$ IR ($CHCl_3$) $\nu_{\max} \text{ cm}^{-1}$

: 1717

UV(MeOH) $\lambda_{\max} \text{ nm (log } \epsilon)$

: 224.0 (3.047)

 $^1\text{H NMR (CDCl}_3)$ $\delta \text{ ppm}$

: Refer Table 3.14

 $^{13}\text{C NMR (CDCl}_3)$ $\delta \text{ ppm}$

: Refer Table 3.14

GC-MS

: 248 (M^+), 164 (57), 136 (49), 109
(35), 69 (100), 41 (95)

4.6.4 Elemene type sesquiterpene

Curzerenone 111	: Colourless oil
Molecular formula	: C ₁₅ H ₁₈ O
IR (CHCl ₃) ν_{\max} cm ⁻¹	: 1717
UV(MeOH) λ_{\max} nm (log ϵ)	: 224.0 (3.047)
¹ H NMR (CDCl ₃) δ ppm	: Refer Table 3.15
¹³ C NMR (CDCl ₃) δ ppm	: Refer Table 3.15
GC-MS	: 230 (M ⁺), 122 (100)

4.6.5 Humulane type sesquiterpene

Zerumbone epoxide 151	: Pale yellow
Molecular formula	: C ₁₅ H ₂₂ O ₂
IR (CHCl ₃) ν_{\max} cm ⁻¹	: 1717
UV(MeOH) λ_{\max} nm (log ϵ)	: 216 (2.6)
¹ H NMR (CDCl ₃) δ ppm	: Refer Table 3.16
¹³ C NMR (CDCl ₃) δ ppm	: Refer Table 3.16
GC-MS	: 234, RT: 16.88., 135 (89), 121 (44), 107 (99), 43 (100)

4.6.6 Cadinane type sesquiterpene

Comosone II 104	: Colourless oil
Molecular formula	: C ₁₅ H ₂₀ O
$[\alpha]_D^{20}$: + 10.1° (c, MeOH)
IR (CHCl ₃) ν_{\max} cm ⁻¹	: 1717
UV(MeOH) λ_{\max} nm (log ϵ)	: 220 (1.24).
¹ H NMR (CDCl ₃) δ ppm	: Refer Table 3.17

^{13}C NMR (CDCl_3) δ ppm	: Refer Table 3.17
GC-MS	: 216 ,RT: 18.8 min, 201 (90), 159 (95) 77 (100), 41 (100).

4.6.7 Carabrane-type sesquiterpene

Curcumenone 65	Colourless oil
Molecular formula	$\text{C}_{15}\text{H}_{22}\text{O}_2$
$[\alpha]_D^{20}$	-12.7°, c 1.0, CHCl_3).
IR (CHCl_3) ν_{max} cm^{-1}	1679, 1715
UV(MeOH) λ_{max} nm (log ϵ)	205 (1.28)
^1H NMR (CDCl_3) δ ppm	Refer Table 3.18
^{13}C NMR (CDCl_3) δ ppm	Refer Table 3.18
GC-MS	234, RT: 28.9, 176(78), 163(29), 161(48), 149 (43), 133(37), 107(32), 91(29), 68(91), 67(75), 43(100).

4.6.8 Spirolactone type sesquiterpene

Curcumanolide A 101	: colourless oil
Molecular formula	$\text{C}_{15}\text{H}_{22}\text{O}_2$
$[\alpha]_D^{20}$: -23°, c 1.0, CHCl_3)
IR (CHCl_3) ν_{max} cm^{-1}	: 1717
UV(MeOH) λ_{max} nm (log ϵ)	: 218 (1.019)
^1H NMR (CDCl_3) δ ppm	: Refer Table 3.19
^{13}C NMR (CDCl_3) δ ppm	: Refer Table 3.19
GC-MS	: 234 [M^+ , 7], 219(7), 191(20), 178(56), 165(78), 164(100), 152(72), 121(28), 109(26), 96(30), 69(45), 68(44), 67(45).

4.6.9 Labdane type diterpenoids

labda-8(17),12 diene-15,16 dial 127	: Colourless oil
Molecular formula	: $C_{20}H_{30}O_2$
IR ($CHCl_3$) ν_{max} cm^{-1}	: 889, 1643, 1683
UV(MeOH) λ_{max} nm (log ϵ)	: 226 (1.969), 208 (2.77)
1H NMR ($CDCl_3$) δ ppm	: Refer Table 3.20
^{13}C NMR ($CDCl_3$) δ ppm	: Refer Table 3.20
GC-MS	: 302, RT: 38.48 min, 137 (79), 123 (55), 109 (39), 95 (88), 81 (100), 69 (73).

Calcaratarin A 128	: Colourless oil
Molecular formula	: $C_{22}H_{44}O_3$
IR ($CHCl_3$) ν_{max} cm^{-1}	: 2929, 1708, 1688
UV(MeOH) λ_{max} nm (log ϵ)	: 200 (2.237)
1H NMR ($CDCl_3$) δ ppm	: Refer Table 3.21
^{13}C NMR ($CDCl_3$) δ ppm	: Refer Table 3.21
GC-MS	: 328, RT: 28.20 min, 300 (38), 137 (73), 123 (68), 109 (87), 81 (100), 41 (89).

Zerumin A 129	: Pale yellow oil
Molecular formula	: $C_{20}H_{30}O_2$
IR ($CHCl_3$) ν_{max} cm^{-1}	: 3080, 1646, 890, 1686
UV(MeOH) λ_{max} nm (log ϵ)	: 210 (1.37)
1H NMR ($CDCl_3$) δ ppm	: Refer Table 3.22
^{13}C NMR ($CDCl_3$) δ ppm	: Refer Table 3.22

GC-MS	: 318, RT= 24.32 min, 164 (100), 137 (81), 95 (60), 81 (70), 41 (55).
-------	---

4.7 Physical and spectral data of isolated compounds from *C. purpurascens*

4.7.1 Bisabolane type sesquiterpene

ar-Turmerone 74	: Pale yellow oil
Molecular formula	$C_{15}H_{20}O$
$[\alpha]_D^{20}$: + 60 (<i>c</i> 0.5, MeOH)
IR (CHCl ₃) ν_{\max} cm ⁻¹	: 1516, 1618, 1700
UV(MeOH) λ_{\max} nm (log ϵ)	: 240 (2.42)
¹ H NMR (CDCl ₃) δ ppm	: Refer Table 3.24
¹³ C NMR (CDCl ₃) δ ppm	: Refer Table 3.24
GC-MS	: 216 (M ⁺), 119 (100)

4.7.2 Diarylhepatoids

Curcumin 138	: Orange crystal
Molecular formula	: $C_{21}H_{20}O_6$
IR (CHCl ₃) ν_{\max} cm ⁻¹	: 1600, 1625
UV(MeOH) λ_{\max} nm (log ϵ)	: 430 (3.5)
¹ H NMR (CDCl ₃) δ ppm	: Refer Table 3.25
¹³ C NMR (CDCl ₃) δ ppm	: Refer Table 3.25
HRESI-MS	: [M+H] ⁺ at <i>m/z</i> 369

Bisdemethoxycurcumin 139	: Yellow powder
Molecular formula	: C ₁₉ H ₁₆ O ₃
IR (CHCl ₃) ν_{\max} cm ⁻¹	: 1625, 3440
UV(MeOH) λ_{\max} nm (log ϵ)	: 415 (2.5)
¹ H NMR (CDCl ₃) δ ppm	: Refer Table 3.26
¹³ C NMR (CDCl ₃) δ ppm	: Refer Table 3.26
HRESI-MS	: [M+H] ⁺ at m/z 309

Demethoxycurcumin 140	: Orange powder
Molecular formula	: C ₂₀ H ₁₈ O ₃
IR (CHCl ₃) ν_{\max} cm ⁻¹	: 1624, 3400
UV(MeOH) λ_{\max} nm (log ϵ)	: 416 (2.8)
¹ H NMR (CDCl ₃) δ ppm	: Refer Table 3.25
¹³ C NMR (CDCl ₃) δ ppm	: Refer Table 3.25
HRESI-MS	: [M+H] ⁺ at m/z 338

4.7.3 Quaiane type sesquiterpene

Zedoalactone B 60	: Colourless oil
Molecular formula	: C ₁₅ H ₂₀ O ₅
IR (CHCl ₃) ν_{\max} cm ⁻¹	: 1732, 3441
UV(MeOH) λ_{\max} nm (log ϵ)	: 262 (3.9)
¹ H NMR (CDCl ₃) δ ppm	: Refer Table 3.27
¹³ C NMR (CDCl ₃) δ ppm	: Refer Table 3.27
HRESI-MS	: m/z 281 (M+H) ⁺

CHAPTER 5: CONCLUSIONS

The phytochemical investigation of *C. zedoaria* and *C. purpurascens* led to the isolation of 27 compounds, majority of them were sesquiterpenes, while the rest were diterpenoids and curcuminoids. The proposed biosynthetic relationships of three sesquiterpenes types isolated from *C. zedoaria* in the present study is given in **scheme 5.1**.

The GC and GC-MS analysis of the essential oil isolated from *C. purpurascens* by hydrodistillation indicated the presence of 34 compounds, with turmerone, a bisabolane type sesquiterpene as the major component. The oil exhibited strong cytotoxicity against HT29 cells, but mild cytotoxicity against the non-cancerous human lung fibroblast cell line (MRC5).

Supercritical fluid extraction was performed with a view to find an optimum extraction parameter using a green technology that avoids the use of organic solvents. The investigation revealed that an increase in the pressure and decrease in the temperature could offer higher yield. A comparison of extract obtained from maceration as well as supercritical fluid extraction showed that both extracts had turmerone and ar-turmerone as the major constituents. However, the latter extract contained higher percentage of the above compounds suggesting it a more efficient extraction method for the isolation of these two compounds from *C. purpurascens*.

The isolated pure compounds were subjected to a number of bioactivity investigations to find potential lead towards the development of chemotherapeutic agent against some of the most problematic diseases including cancer and neurodegeneration. Complementary investigations were also carried out to support the observed biological activity. These include structure activity relationship study of the cytotoxic compounds, antioxidant activity study of neuroprotective compounds. Two compounds were also subjected to pharmacodynamic studies to investigate their binding modes with HSA.

In the biological studies, the *n*-hexane extract of *C. zedoaria* exhibited good anti-proliferative effect against MCF-7 and Ca Ski cells, supporting the ethnomedical application of *C. zedoaria* in the treatment of breast cancer. Several of the isolated compounds showed antiproliferative effect against four cancer cell lines (MCF-7, Ca Ski, PC-3 and HT-29). Among the compounds tested, curcumenol **42** and curcumenone **65** showed potent *in vitro* cytotoxicity towards the MCF-7 cells.

From the present investigation, as well as previous pharmacological reports, it could be proposed that curcumenol **42** could be considered as a promising candidate for advanced studies of anticancer drug development. However, further studies are necessary to determine its mode of action. It is noteworthy that the *n*-hexane extract of *C. zedoaria* and the two of its active compounds, curcumenol **42** and curcumenone **65** did not show toxicity towards the non-cancer cell line (HUVEC). Although *C. zedoaria* enjoys extensive use in traditional medicine, it is used cautiously since it shows toxicity at higher doses. As our investigation revealed, some of the sesquiterpenes of this plant had strong cytotoxic activity and might be responsible for its unwanted effects.

Quantum chemical analysis of the 21 cytotoxic compounds established the correlation between a set of electronic, steric and hydrophobicity descriptors that governs their cytotoxic activity against MCF7, Ca Ski, PC3 and HT-29 cancer cell lines, and HUVEC normal cell line. MLR, PCA and HCA allowed us to further categorize the active compounds according to their activity level into high, moderate, and low potential.

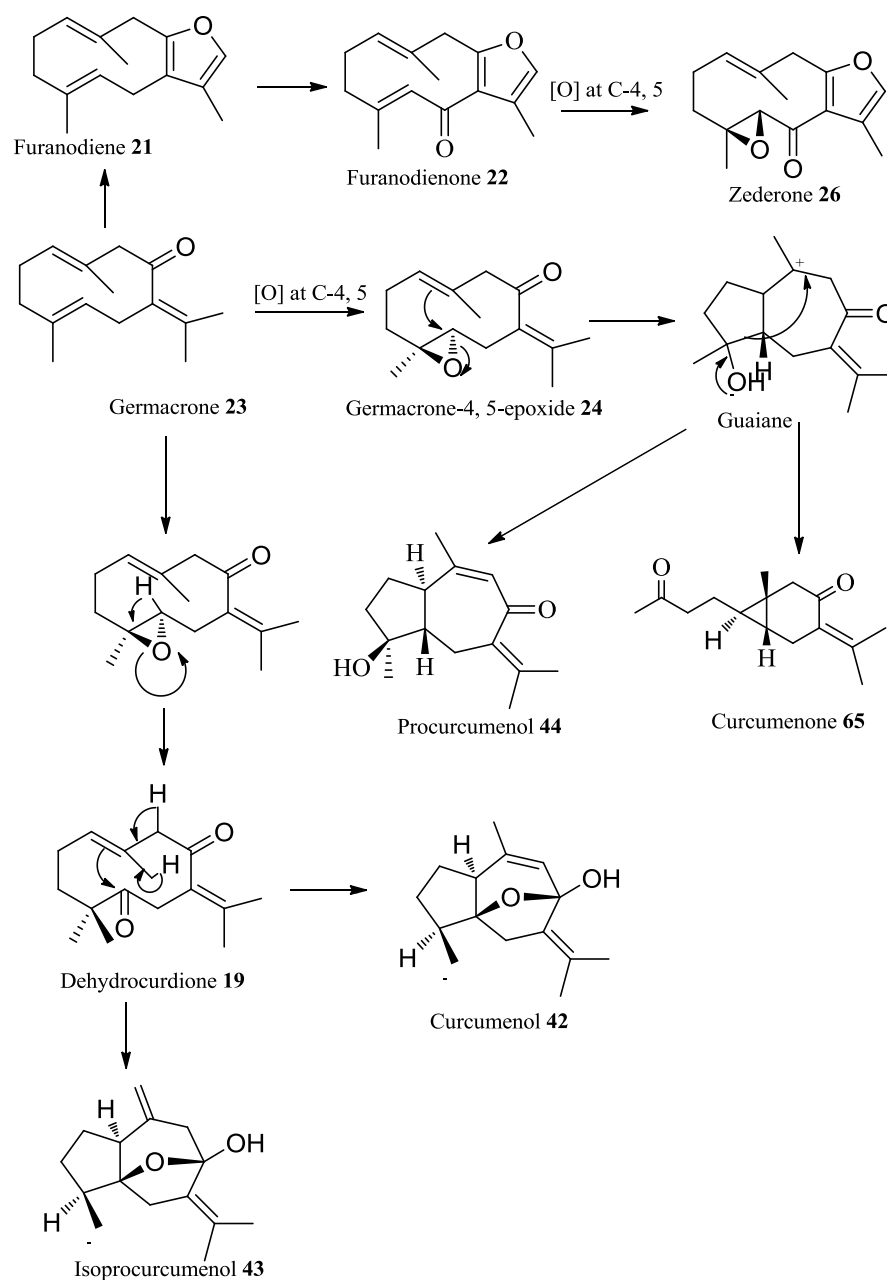
Among the nine sesquiterpenes and one labdane diterpene, tested for neuroprotective activity, dehydrocurdione **19** and curcumenol **42** were found to be the most promising providing 100% protection against hydrogen peroxide induced oxidative stress in NG108-15 cells. In the oxygen radical antioxidant capacity (ORAC) assay, zerumbone epoxide **151** showed the highest antioxidant activity. To date, no true

neuroprotective drug has been discovered, and curcumenol **42** holds a promising result to be considered as a template for the development of new drug for the treatment of neurodegenerative disorders.

The two most active compounds, curcumenol **42** and curcumenone **65** were further investigated for their binding properties to HSA which revealed that both compounds can bind to site I and site II, while site I is the preferred binding site.

The humulane type sesquiterpene zerumbone epoxide **151**, and three labdane diterpenes, namely labda-8(17),12 diene-15,16 dial **127**, calcaractrin A **128**, and zerumin A **129** are the first report from *C. zedoaria*.

The findings of the present study support the common practice of ethnopharmacological uses of the rhizomes of *C. zedoaria* in the treatment of breast cancer and this plant has the potential to be developed further as a nutraceutical for the treatment of cancer.



Scheme 5.1: The proposed biosynthetic relationships of three sesquiterpenes types isolated from *C. zedoaria*

REFERENCES

- Abas, F., Lajis, N. H., Shaari, K., Israf, D. A., Stanslas, J., Yusuf, U. K., & Raof, S. M. (2005). A Labdane Diterpene Glucoside from the Rhizomes of *Curcuma mangga*. *Journal of natural products*, 68(7), 1090-1093.
- Abou-Zied, O. K., & Al-Shihi, O. I. K. (2008). Characterization of Subdomain IIA Binding Site of Human Serum Albumin in its Native, Unfolded, and Refolded States Using Small Molecular Probes. *Journal of the American Chemical Society*, 130(32), 10793-10801.
- Adams, R. P. (2012). *Identification of essential oils by ion trap mass spectroscopy*: Academic Press.
- Aggarwal, B. B., Kumar, A., & Bharti, A. C. (2003). Anticancer potential of curcumin: preclinical and clinical studies. *Anticancer res*, 23(1A), 363-398.
- Ahmad, E., Rabbani, G., Zaidi, N., Singh, S., Rehan, M., Khan, M. M., . . . Khan, R. H. (2011). Stereo-selectivity of human serum albumin to enantiomeric and isoelectronic pollutants dissected by spectroscopy, calorimetry and bioinformatics. *PLoS ONE*, 6(11).
- Ahmed Hamdi, O., Awang, K., Hadi, A., Syamsir, D. R., & Ng, S. W. (2010). Curcumenol from *Curcuma zedoaria*: a second monoclinic modification. *Acta Crystallographica Section E: Structure Reports Online*, 66(11), o2844-o2844.
- Ahmed Hamdi, O. A., Syed Abdul Rahman, S. N., Awang, K., Abdul Wahab, N., Looi, C. Y., Thomas, N. F., & Abd Malek, S. N. (2014). Cytotoxic Constituents from the Rhizomes of *Curcuma zedoaria*. *The Scientific World Journal*, 2014, 11
- Alan Sheeja, D. B., & Nair, M. S. (2012). Phytochemical constituents of *Curcuma amada*. *Biochemical Systematics and Ecology*, 44(0), 264-266
- Angel, G. R., Menon, N., Vimala, B., & Nambisan, B. (2014). Essential oil composition of eight starchy *Curcuma* species. *Industrial Crops and Products*, 60(0), 233-238.
- Aspollah Sukari, M., Wah, T. S., Saad, S. M., Rashid, N. Y., Rahmani, M., Lajis, N. H., & Hin, T.-Y. Y. (2010). Bioactive sesquiterpenes from *Curcuma ochrorhiza* and *Curcuma heyneana*. *Natural product research*, 24(9), 838-845.
- Bakkali, F., Averbeck, S., Averbeck, D., & Idaomar, M. (2008). Biological effects of essential oils—a review. *Food and chemical toxicology*, 46(2), 446-475.
- Balunas, M. J., & Kinghorn, A. D. (2005). Drug discovery from medicinal plants. *Life sciences*, 78(5), 431-441.
- Bamba, Y., Yun, Y. S., Kunugi, A., & Inoue, H. (2011). Compounds isolated from *Curcuma aromatica* Salisb. inhibit human P450 enzymes. *J. Nat. Med.*, 65(3-4), 583-587.

- Banthorpe, D., Charlwood, B., & Francis, M. (1972). Biosynthesis of monoterpenes. *Chemical reviews*, 72(2), 115-155.
- Becke, A. D. (1993). A new mixing of Hartree-Fock and local-density-functional theories. *Journal of Chemical Physics*, 98(2), 1372-1377.
- Belatik, A., Hotchandani, S., Bariyanga, J., & Tajmir-Riahi, H. A. (2012). Binding sites of retinol and retinoic acid with serum albumins. *European journal of medicinal chemistry*, 48(0), 114-123
- Berman, H. M., Westbrook, J., Feng, Z., Gilliland, G., Bhat, T. N., Weissig, H., . . . Bourne, P. E. (2000). The Protein Data Bank. *Nucleic Acids Res*, 28(1), 235-242.
- Bordoloi, A. K., Sperkova, J., & Leclercq, P. A. (1999). Essential Oils of *Curcuma aromatica* Salisb. from Northeast India. *Journal of Essential Oil Research*, 11(5), 537-540.
- Brouk, B. (1975). *Plants consumed by man*: Academic Press Inc.(London) Ltd.
- Bugno, A., Nicoletti, M. A., Almodóvar, A. A., Pereira, T. C., & Auricchio, M. T. (2007). Antimicrobial efficacy of *Curcuma zedoaria* extract as assessed by linear regression compared with commercial mouthrinses. *Brazilian Journal of Microbiology*, 38(3), 440-445.
- Bülow, N., & König, W. A. (2000). The role of germacrene D as a precursor in sesquiterpene biosynthesis: investigations of acid catalyzed, photochemically and thermally induced rearrangements. *Phytochemistry*, 55(2), 141-168.
- Burkill, I. H. (1966). A dictionary of the economic products of the Malay Peninsula. *A Dictionary of the Economic Products of the Malay Peninsula.*, 2(2nd edition).
- Cao, G., Sofic, E., & Prior, R. L. (1997). Antioxidant and prooxidant behavior of flavonoids: structure-activity relationships. *Free Radical Biology and Medicine*, 22(5), 749-760.
- Cao, J., Qi, M., Zhang, Y., Zhou, S., Shao, Q., & Fu, R. (2006). Analysis of volatile compounds in *Curcuma wenyujin* YH Chen et C. Ling by headspace solvent microextraction–gas chromatography–mass spectrometry. *Analytica chimica acta*, 561(1), 88-95.
- Carson, C., Hammer, K., & Riley, T. (1995). Broth micro-dilution method for determining the susceptibility of *Escherichia coli* and *Staphylococcus aureus* to the essential oil of *Melaleuca alternifolia* (tea tree oil). *Microbios*, 82(332), 181-185.
- Carter, D. C., & Ho, J. X. (1994). Structure of serum albumin. *Adv Protein Chem*, 45, 153-203.
- Catalan, C., Bardon, A., Retamar, J., Gros, E., Verghese, J., & Joy, M. (1989). The essential oil of *Curcuma aromatica* Salisb. *Flavour and fragrance journal*, 4(1), 25-30.

- Chatterjee, S., Variyar, P. S., Gholap, A. S., Padwal-Desai, S., & Bongirwar, D. (2000). Effect of γ -irradiation on the volatile oil constituents of turmeric *Curcuma longa*. *Food research international*, 33(2), 103-106.
- Chaturvedi, D., Goswami, A., Saikia, P. P., Barua, N. C., & Rao, P. G. (2010). Artemisinin and its derivatives: a novel class of anti-malarial and anti-cancer agents. *Chemical Society Reviews*, 39(2), 435-454.
- Chen, P., & Lu, T. (2006). [Study on the chemical constituents of *Curcuma phaeocaulis*. *Zhong yao cai= Zhongyaocai= Journal of Chinese medicinal materials*, 29(7), 675-677.
- Chern, L. Y. (2014). Monoterpenes in Plants-a mini review. *Asian journal of plant biology (e-ISSN 2289-5868)*, 1(1), 15-19.
- Choudhury, S., Ghosh, A. C., Saikia, M., Choudhury, M., & Leclercq, P. A. (1996). Volatile constituents of the aerial and underground parts of *Curcuma aromatica* Salisb. from India. *Journal of Essential Oil Research*, 8(6), 633-638.
- De Fátima Navarro, D., De Souza, M. M., Neto, R. A., Golin, V., Niero, R., Yunes, R. A., . . . Cechinel Filho, V. (2002). Phytochemical analysis and analgesic properties of *Curcuma zedoaria* grown in Brazil. *Phytomedicine*, 9(5), 427-432.
- De Luca, G., Sicilia, E., Russo, N., & Mineva, T. (2002). On the hardness evaluation in solvent for neutral and charged systems. *Journal of the American Chemical Society*, 124(7), 1494-1499.
- Dekebo, A., Dagne, E., Hansen, L. K., Gautun, O. R., & Aasen, A. J. (2000). Crystal structures of two furanosesquiterpenes from *Commiphora sphaerocarpa*. *Tetrahedron Letters*, 41(50), 9875-9878.
- Dewar, M. J. S., Zebisch, E. G., Healy, E. F., & Stewart, J. J. P. (1985). Development and use of quantum mechanical molecular models. 76. AM1: a new general purpose quantum mechanical molecular model. *Journal of the American Chemical Society*, 107(13), 3902-3909.
- Dickschat, J. S. (2011). Isoprenoids in three-dimensional space: the stereochemistry of terpene biosynthesis. *Natural product reports*, 28(12), 1917-1936.
- Dong, J.-Y., Ma, X.-Y., Cai, X.-Q., Yan, P.-C., Yue, L., Lin, C., & Shao, W.-W. (2013). Sesquiterpenoids from *Curcuma wenyujin* with anti-influenza viral activities. *Phytochemistry*, 85(0), 122-128.
- Etoh, H., Kondoh, T., Yoshioka, N., Sugiyama, K., Ishikawa, H., & Tanaka, H. (2003). 9-Oxo-neoprocucumenol from *Curcuma aromatica* (Zingiberaceae) as an Attachment Inhibitor against the Blue Mussel, *Mytilus edulis galloprovincialis*. *Bioscience, biotechnology, and biochemistry*, 67(4), 911-913.
- Eun, S., Choi, I., & Shim, S. H. (2010). A New Sesquiterpenoid from the Rhizome of *Curcuma zedoaria*. *Bull Korean Chem Soc*, 31, 1387-1388.

- Faiz Hossain, C., Al-Amin, M., MahabuburRahman, K. M., Sarker, A., Mahamudul Alam, M., Hasan Chowdhury, M., . . . Nahar Sultana, G. N. Analgesic principle from *Curcuma amada*. *Journal of Ethnopharmacology*(0).
- Feroz, S. R., Mohamad, S. B., Bujang, N., Malek, S. N. A., & Tayyab, S. (2012). Multispectroscopic and Molecular Modeling Approach To Investigate the Interaction of Flavokawain B with Human Serum Albumin. *Journal of Agricultural and Food Chemistry*, 60(23), 5899-5908.
- Ficker, C. E., Smith, M. L., Susiarti, S., Leaman, D. J., Irawati, C., & Arnason, J. T. (2003). Inhibition of human pathogenic fungi by members of Zingiberaceae used by the Kenyah (Indonesian Borneo). *Journal of Ethnopharmacology*, 85(2), 289-293.
- Firman, K., Kinoshita, T., Itai, A., & Sankawa, U. (1988a). Terpenoids from *Curcuma heyneana*. *Phytochemistry*, 27(12), 3887-3891.
- Firman, K., Kinoshita, T., Itai, A., & Sankawa, U. (1988b). Terpenoids from *Curcuma heyneana*. *Phytochemistry*, 27(12), 3887-3891.
- Freitas, P. G., Barbosa, A. F., Saraiva, L. A., Camps, I., da Silveira, N. J. F., Veloso, M. P., . . . Schneedorf, J. M. (2012). Mangiferin binding to serum albumin is non-saturable and induces conformational changes at high concentrations. *Journal of Luminescence*, 132(11), 3027-3034.
- Garg, S., Naquvi, A., Bansal, R., Bahl, J., & Kumar, S. (2005). Chemical composition of the essential oil from the leaves of *Curcuma zedoaria* Rosc. of Indian origin. *Journal of Essential Oil Research*, 17(1), 29-31.
- Ghose, A. K., Pritchett, A., & Crippen, G. M. (1988). Atomic physicochemical parameters for three dimensional structure directed quantitative structure-activity relationships III: Modeling hydrophobic interactions. *Journal of Computational Chemistry*, 9(1), 80-90.
- Giang, P. M. (2003). Structure of humulene-8-hydroperoxide, a new humulane-type sesquiterpenoid from Vietnamese *Curcuma zedoaria*. *Tap Chi Hoa Hoc*, 41(3), 109-110.
- Giang, P. M., & Son, P. T. (2000). Isolation of Sesquiterpenoids from the Rhizomes of Vietnamese *Curcuma Aromatica* Salisb. *Tap Chi Hoa Hoc*, 38(4), 96-99.
- Goodsell, D. S., Morris, G. M., & Olson, A. J. (1996). Automated docking of flexible ligands: Applications of autodock. *Journal of Molecular Recognition*, 9(1), 1-5.
- Grigorov, M., Weber, J., Chermette, H., & Tronchet, J. M. (1997). Numerical evaluation of the internal orbitally resolved chemical hardness tensor in density functional theory. *International Journal of Quantum Chemistry*, 61(3), 551-562.
- Guerra, M., Amorati, R., & Pedulli, G. F. (2004). Water Effect on the O-H Dissociation Enthalpy of Para-Substituted Phenols: a DFT Study. *The Journal of Organic Chemistry*, 69(16), 5460-5467.

- Gupta, A., Gupta, M., & Kumar, S. (1999). Simultaneous determination of curcuminoids in *Curcuma* samples using high performance thin layer chromatography. *Journal of liquid chromatography & related technologies*, 22(10), 1561-1569.
- Gupta, P., Ali, M. M., Eranna, D., & Setty, S. R. (2003). Evaluation of anti-ulcer effect of root of *Curcuma zedoaria* in rats.
- Harimaya, K., Gao, J. F., Ohkura, T., Kawamata, T., Iitaka, Y., Guo, Y. T., & Inayama, S. (1991). A series of sesquiterpenes with a 7 α -isopropyl side chain and related compounds isolated from *Curcuma wenyujin*. *Chem. Pharm. Bull.*, 39(4), 843-853. doi: 10.1248/cpb.39.843
- Hatcher, H., Planalp, R., Cho, J., Torti, F., & Torti, S. (2008). Curcumin: from ancient medicine to current clinical trials. *Cellular and Molecular Life Sciences*, 65(11), 1631-1652.
- Heinig, U., & Jennewein, S. (2009). Taxol: A complex diterpenoid natural product with an evolutionarily obscure origin. *African Journal of Biotechnology*, 8(8).
- Hikino, H., Takahashi, S., Sakurai, Y., Takemoto, T., & Bhacca, N. (1968). Structure of zederone. *Chemical & pharmaceutical bulletin*, 16(6), 1081-1087.
- Hong, C. H., Hur, S. K., Oh, O.-J., Kim, S. S., Nam, K., & Lee, S. K. (2002). Evaluation of natural products on inhibition of inducible cyclooxygenase (COX-2) and nitric oxide synthase (iNOS) in cultured mouse macrophage cells. *Journal of Ethnopharmacology*, 83(1), 153-159.
- Hong, C. H., Kim, Y., & Lee, S. K. (2001). Sesquiterpenoids from the rhizome of *Curcuma zedoaria*. *Archives of pharmacal research*, 24(5), 424-426.
- HyperChem. (2002). Release 7.52 for Windows. Canada.
- Inoue, K., Nomura, C., Ito, S., Nagatsu, A., Hino, T., & Oka, H. (2008). Purification of curcumin, demethoxycurcumin, and bisdemethoxycurcumin by high-speed countercurrent chromatography. *Journal of agricultural and food chemistry*, 56(20), 9328-9336.
- Ishihara, M., Wakabayashi, H., Motohashi, N., & Sakagami, H. (2010). Quantitative Structure-Cytotoxicity Relationship of Newly Synthesized Tropolones Determined by a Semiempirical Molecular-orbital Method (PM5). *Anticancer research*, 30(1), 129-133.
- Ishihara, M., Yokote, Y., & Sakagami, H. (2006). Quantitative structure-cytotoxicity relationship analysis of coumarin and its derivatives by semiempirical molecular orbital method. *Anticancer research*, 26(4B), 2883-2886.
- Ishii, T., Matsuura, H., Kaya, K., & Vairappan, C. S. (2011). A new bisabolane-type sesquiterpenoid from *Curcuma domestica*. *Biochemical Systematics and Ecology*, 39(4-6), 864-867.

- Janak, J. (1978). Proof that $\partial E/\partial n_i = \epsilon$ in density-functional theory. *Physical Review B*, 18, 7165-7168.
- Ji, M., Choi, J., Lee, J., & Lee, Y. (2004). Induction of apoptosis by ar-turmerone on various cell lines. *International journal of molecular medicine*, 14(2), 253-256.
- Johnson, R. A., & Wichern, D. W. (2002). *Applied multivariate statistical analysis* (Vol. 5): Prentice hall Upper Saddle River, NJ.
- Khan, M. G., Nahar, K., Rahman, M. S., Hasan, C. M., & Rashid, M. A. (2010). Phytochemical and biological investigations of *Curcuma longa*. *Dhaka University Journal of Pharmaceutical Sciences*, 8(1), 39-45.
- Kimura, Y., Sumiyoshi, M., & Tamaki, T. (2013). Effects of the extracts and an active compound curcumenone isolated from *Curcuma zedoaria* rhizomes on alcohol-induced drunkenness in mice. *Fitoterapia*, 84(0), 163-169.
- Kitagawa, I. (1987). A reinvestigation of the structure of zederone, a furanogermacrane-type sesquiterpene from zedoary. *Chem. Pharm. Bull.*, 35(2), 924-927.
- Koller, E. (2009). *Javanese medical plants used in rural communities*. unwien.
- Koopmans, T. (1934). Über die Zuordnung von Wellenfunktionen und Eigenwerten zu den einzelnen Elektronen eines Atoms. *Physica*, 1(1), 104-113.
- Kowalski, B., & Bender, C. (1972). Pattern recognition. Powerful approach to interpreting chemical data. *Journal of the American Chemical Society*, 94(16), 5632-5639.
- Kozłowski, D., Trouillas, P., Calliste, C., Marsal, P., Lazzaroni, R., & Duroux, J.-L. (2007). Density Functional Theory Study of the Conformational, Electronic, and Antioxidant Properties of Natural Chalcones. *Journal of Physical Chemistry A*, 111(6), 1138-1145.
- Kuroyanagi, M., Ueno, A., Koyama, K., & Natori, S. (1990). Structures of sesquiterpenes of *Curcuma aromatica* Salisb. II. Studies on minor sesquiterpenes. *Chem. Pharm. Bull.*, 38(1), 55-58.
- Kuroyanagi, M., Ueno, A., Ujiie, K., & Sato, S. (1987). Structures of sesquiterpenes from *Curcuma aromatica* Salisb. *Chemical and pharmaceutical bulletin*, 35(1), 53-59.
- Kuttan, R., Bhanumathy, P., Nirmala, K., & George, M. (1985). Potential anticancer activity of turmeric (*Curcuma longa*). *Cancer Letters*, 29(2), 197-202.
- Lackowicz, J. R. (1983). Principles of fluorescence spectroscopy. *Plenum Press*, (New York, 1983) Chapter, 5, 111-150.
- Lai, E. Y., Chyau, C.-C., Mau, J.-L., Chen, C.-C., Lai, Y.-J., Shih, C.-F., & Lin, L.-L. (2004). Antimicrobial activity and cytotoxicity of the essential oil of *Curcuma zedoaria*. *The American journal of Chinese medicine*, 32(02), 281-290.

- Lai, P., & Roy, J. (2004). Antimicrobial and chemopreventive properties of herbs and spices. *Current medicinal chemistry*, 11(11), 1451-1460.
- Lakshmi, S., Padmaja, G., & Remani, P. (2011a). Antitumour effects of isocurcumenol isolated from *Curcuma zedoaria* rhizomes on human and murine cancer cells. *International Journal of Medicinal Chemistry*, Volume 2011(Article ID 253962), 13 pages.
- Lakshmi, S., Padmaja, G., & Remani, P. (2011b). Antitumour effects of isocurcumenol isolated from *Curcuma zedoaria* rhizomes on human and murine cancer cells. *International Journal of Medicinal Chemistry*, 2011.
- Lanzotti, V. (2013). Diterpenes for Therapeutic Use *Natural Products* (pp. 3173-3191): Springer.
- Larsen, K., Ibrahim, H., Khaw, S., & Saw, L. (1999). *Gingers of Peninsular Malaysia and Singapore*: Natural History Publications (Borneo).
- Lee, H., & Lin, J. (1988). Antimutagenic activity of extracts from anticancer drugs in Chinese medicine. *Mutation research*, 204(2), 229.
- Leite, J., De Lourdes V Seabra, M., Maluf, E., Assolant, K., Suchecki, D., Tufik, S., . . . Carlini, E. (1986). Pharmacology of lemongrass *Cymbopogon citratus* Stapf). III. Assessment of eventual toxic, hypnotic and anxiolytic effects on humans. *Journal of Ethnopharmacology*, 17(1), 75-83.
- Li, W., Wang, S., Feng, J., Xiao, Y., Xue, X., Zhang, H., . . . Liang, X. (2009). Structure elucidation and NMR assignments for curcuminoids from the rhizomes of *Curcuma longa*. *Magnetic Resonance in Chemistry*, 47(10), 902-908.
- Liu, X.-y., Lou, Y., Hu, D., Chen, L.-x., Bu, G.-m., & Qiu, F. (2007). Chemical constituents of essential oil from *Curcuma wenyujin*. *Shenyang Yaoke Daxue Xuebao*, 24(11), 682-686.
- Liu, Y., & Nair, M. G. (2011). Labdane diterpenes in *Curcuma mangga* rhizomes inhibit lipid peroxidation, cyclooxygenase enzymes and human tumour cell proliferation. *Food Chemistry*, 124(2), 527-532.
- Lobo, R., Prabhu, K. S., Shirwaikar, A., & Shirwaikar, A. (2009). *Curcuma zedoaria* Rosc.(white turmeric): a review of its chemical, pharmacological and ethnomedicinal properties. *Journal of Pharmacy and Pharmacology*, 61(1), 13-21.
- Lou, Y., Zhang, H., He, H., Peng, K., Kang, N., Wei, X., . . . Qiu, F. (2010). Isolation and identification of phase I metabolites of curcumol in rats. *Drug Metabolism and Disposition*, 38(11), 2014-2022.
- M. J. Frisch, G. W. T., H. B. Schlegel, G. E. Scuseria, M. A. Robb, J. R. Cheeseman, G.... and D. J. Fox,. (2009). *Gaussian 09, Revision A.02*.

- Maciel, N., & Criley, R. A. (2002). *Morphology, growth and flowering behavior of Curcuma zedoaria*. Paper presented at the XXVI International Horticultural Congress: Elegant Science in Floriculture 624.
- Maheshwari, R. K., Singh, A. K., Gaddipati, J., & Srimal, R. C. (2006). Multiple biological activities of curcumin: a short review. *Life sciences*, 78(18), 2081-2087.
- Makabe, H., Maru, N., Kuwabara, A., Kamo, T., & Hirota, M. (2006). Anti-inflammatory sesquiterpenes from *Curcuma zedoaria*. *Natural product research*, 20(7), 680-685.
- Malek, S. N., Seng, C. K., Zakaria, Z., Ali, N. A., Ibrahim, H., & Jalil, M. N. (2006). The essential oil of *Curcuma inodora* aff. Blatter from Malaysia. *Journal of Essential Oil Research*, 18(3), 281-283.
- Malek, S. N. A., Lee, G. S., Hong, S. L., Yaacob, H., Wahab, N. A., Faizal Weber, J.-F., & Shah, S. A. A. (2011). Phytochemical and cytotoxic investigations of *Curcuma mangga* rhizomes. *Molecules*, 16(6), 4539-4548.
- Masuda, T., Jitoe, A., Isobe, J., Nakatani, N., & Yonemori, S. (1993). Anti-oxidative and anti-inflammatory curcumin-related phenolics from rhizomes of *Curcuma domestica*. *Phytochemistry*, 32(6), 1557-1560.
- Matsuda, H., Morikawa, T., Ninomiya, K., & Yoshikawa, M. (2001a). Absolute stereostructure of carabrane-type sesquiterpene and vasorelaxant-active sesquiterpenes from Zedoariae Rhizoma. *Tetrahedron*, 57(40), 8443-8453.
- Matsuda, H., Morikawa, T., Ninomiya, K., & Yoshikawa, M. (2001b). Hepatoprotective constituents from zedoariae rhizoma: absolute stereostructures of three new carabrane-type sesquiterpenes, curcumenolactones A, B, and C. *Bioorganic & Medicinal Chemistry*, 9(4), 909-916.
- Matsuda, H., Morikawa, T., Toguchida, I., Ninomiya, K., & Yoshikawa, M. (2001). Medicinal foodstuffs. XXVIII. Inhibitors of nitric oxide production and new sesquiterpenes, zedoarofuran, 4-epicurcumenol, neocurcumenol, gajutsulactones A and B, and zedoarolides A and B, from Zedoariae Rhizoma. *Chem. Pharm. Bull.*, 49(12), 1558-1566.
- Matsuda, H., Ninomiya, K., Morikawa, T., & Yoshikawa, M. (1998b). Inhibitory effect and action mechanism of sesquiterpenes from Zedoariae Rhizoma on D-galactosamine/lipopolysaccharide-induced liver injury. *Bioorganic & Medicinal Chemistry Letters*, 8(4), 339-344.
- Matthes, H., Luu, B., & Ourisson, G. (1980). Cytotoxic components of Zingiber zerumbet, *Curcuma zedoaria* and *C. domestica*. *Phytochemistry*, 19(12), 2643-2650.
- Matthes, H., Luu, B., & Ourisson, G. (1982). Transannular cyclizations of zerumbone epoxide. *Tetrahedron*, 38(21), 3129-3135.

- Mau, J.-L., Lai, E. Y., Wang, N.-P., Chen, C.-C., Chang, C.-H., & Chyau, C.-C. (2003a). Composition and antioxidant activity of the essential oil from *Curcuma zedoaria*. *Food Chemistry*, 82(4), 583-591.
- Mau, J.-L., Lai, E. Y., Wang, N.-P., Chen, C.-C., Chang, C.-H., & Chyau, C.-C. (2003b). Composition and antioxidant activity of the essential oil from *Curcuma zedoaria*. *Food Chemistry*, 82(4), 583-591.
- Mendes, A. P., Borges, R. S., Neto, A. M. C., de Macedo, L. G., & da Silva, A. B. (2012). The basic antioxidant structure for flavonoid derivatives. *Journal of molecular modeling*, 18(9), 4073-4080.
- Mineva, T., Sicilia, E., & Russo, N. (1998). Density-functional approach to hardness evaluation and its use in the study of the maximum hardness principle. *Journal of the American Chemical Society*, 120(35), 9053-9058.
- Morikawa, T. (2007). Search for bioactive constituents from several medicinal foods: hepatoprotective, antidiabetic, and antiallergic activities. *Journal of Natural Medicines*, 61(2), 112-126.
- Morikawa, T., Matsuda, H., Ninomiya, K., & Yoshikawa, M. (2002). Medicinal Foodstuffs. XXIX. Potent Protective Effects of Sesquiterpenes and Curcumin from Zedoariae Rhizoma on Liver Injury Induced by D-Galactosamine/Lipopolysaccharide or Tumor Necrosis Factor-. ALPHA. *Biological and Pharmaceutical Bulletin*, 25(5), 627-631.
- Navarro, D. F., de Souza, M., Neto, R., Golin, V., Niero, R., Yunes, R., . . . Cechinel, F. V. (2002). Phytochemical analysis and analgesic properties of *Curcuma zedoaria* grown in Brazil. *Phytomedicine: international journal of phytotherapy and phytopharmacology*, 9(5), 427-432.
- Nerio, L. S., Olivero-Verbel, J., & Stashenko, E. (2010). Repellent activity of essential oils: a review. *Bioresource Technology*, 101(1), 372-378.
- Neshev, N., & Mineva, T. (1996). The Role of Interelectronic Interaction in Transition Metal Oxide Catalysts *Metal-Ligand Interactions* (pp. 361-405): Springer.
- Noorafshan, A., & Ashkani-Esfahani, S. (2013). A review of therapeutic effects of curcumin. *Current pharmaceutical design*, 19(11), 2032-2046.
- Oh, O.-J., Min, H.-Y., & Lee, S. K. (2007). Inhibition of inducible prostaglandin E2 production and cyclooxygenase-2 expression by curdione from *Curcuma zedoaria*. *Archives of pharmacal research*, 30(10), 1236-1239.
- Ohshiro, M., Kuroyanagi, M., & Ueno, A. (1990a). Structures of sesquiterpenes from *Curcuma longa*. *Phytochemistry*, 29(7), 2201-2205.
- Ohshiro, M., Kuroyanagi, M., & Ueno, A. (1990b). Structures of sesquiterpenes from *Curcuma longa*. *Phytochemistry*, 29(7), 2201-2205.
- Organization, W. H. (2002). WHO traditional medicine strategy 2002-2005.

- Organization, W. H. (2013). *WHO traditional medicine strategy: 2014-2023*: World Health Organization.
- Pamplona, C. R., de Souza, M. M., da Silva Machado, M., Filho, V., Navarro, D., Yunes, R., . . . Niero, R. (2006). Seasonal variation and analgesic properties of different parts from *Curcuma zedoaria* Roscoe (Zingiberaceae) grown in Brazil. *Zeitschrift fur Naturforschung C-Journal of Biosciences*, 61(1-2), 6-10.
- Pancharoen, O., Prawat, U., & Tuntiwachwuttikul, P. (2000). Phytochemistry of the zingiberaceae. *Studies in Natural Products Chemistry*, 23, 797-865.
- Pandey, A. K., & Chowdhury, A. R. (2003). Volatile constituents of the rhizome oil of *Curcuma caesia* Roxb. from central India. *Flavour and fragrance journal*, 18(5), 463-465.
- Pant, N., Jain, D., Bhakuni, R., Prajapati, V., Tripathi, A., & Kumar, S. (2001). Zederone: a sesquiterpenic keto-dioxide from *Curcuma aromatica*. *INDIAN JOURNAL OF CHEMISTRY SECTION B*, 40(1), 87-87.
- Park, G.-g., Eun, S., & Shim, S. H. (2012a). Chemical constituents from *Curcuma zedoaria*. *Biochemical Systematics and Ecology*, 40, 65-68.
- Park, G.-g., Eun, S., & Shim, S. H. (2012b). Chemical constituents from *Curcuma zedoaria*. *Biochemical Systematics and Ecology*, 40(0), 65-68.
- Parr, R. G., & Yang, W. (1989). *Density-functional theory of atoms and molecules* (Vol. 16): Oxford university press.
- Pedretti, A., Villa, L., & Vistoli, G. (2002). VEGA: a versatile program to convert, handle and visualize molecular structure on Windows-based PCs. *Journal of Molecular Graphics and Modelling*, 21(1), 47-49.
- Péret-Almeida, L., Cherubino, A., Alves, R., Dufosse, L., & Gloria, M. (2005). Separation and determination of the physico-chemical characteristics of curcumin, demethoxycurcumin and bisdemethoxycurcumin. *Food research international*, 38(8), 1039-1044.
- Péret-Almeida, L., Cherubino, A., Alves, R., Dufossé, L., & Gloria, M. (2005). Separation and determination of the physico-chemical characteristics of curcumin, demethoxycurcumin and bisdemethoxycurcumin. *Food research international*, 38(8), 1039-1044.
- Peters Jr, T. (1995). *All about albumin: biochemistry, genetics, and medical applications*: Academic press.
- Phan, M. G., Tran, T. T. N., Phan, T. S., Matsunami, K., & Otsuka, H. (2014). Guaianolides from *Curcuma kwangsiensis*. *Phytochemistry Letters*, 9(0), 137-140. doi: <http://dx.doi.org/10.1016/j.phytol.2014.05.009>
- Purkayastha, J., Nath, S. C., & Klinkby, N. (2006). Essential Oil of the Rhizome of *Curcuma zedoaria* (Christm.) Rose. Native to Northeast India. *Journal of Essential Oil Research*, 18(2), 154-155.

- Qiu, G., Yan, P., Shao, W., Zhou, J., Lin, W., Fang, L., . . . Dong, J. (2013). Two New Sesquiterpenoids Including a Sesquiterpenoid Lactam from *Curcuma wenyujin*. *Chemical and pharmaceutical bulletin*, 61(9), 983-986.
- Qu, Y., Xu, F., Nakamura, S., Matsuda, H., Pongpiriyadacha, Y., Wu, L., & Yoshikawa, M. (2009a). Sesquiterpenes from *Curcuma comosa*. *Journal of Natural Medicines*, 63(1), 102-104.
- Qu, Y., Xu, F., Nakamura, S., Matsuda, H., Pongpiriyadacha, Y., Wu, L., & Yoshikawa, M. (2009b). Sesquiterpenes from *Curcuma comosa*. *J. Nat. Med.*, 63(1), 102-104. doi: 10.1007/s11418-008-0282-8
- Raj, G., Baby, S., Dan, M., Thaha, A. R. M., Sethuraman, M. G., & George, V. (2008). Volatile constituents from the rhizomes of *Curcuma haritha* Mangaly and Sabu from southern India. *Flavour and fragrance journal*, 23(5), 348-352.
- Raut, J. S., & Karuppayil, S. M. (2014). A status review on the medicinal properties of essential oils. *Industrial Crops and Products*, 62(0), 250-264.
- Ravdin, P. M., Burris, H., Cook, G., Eisenberg, P., Kane, M., Bierman, W. A., . . . Bellet, R. E. (1995). Phase II trial of docetaxel in advanced anthracycline-resistant or anthracenedione-resistant breast cancer. *Journal of clinical oncology*, 13(12), 2879-2885.
- Ravindran, P., Babu, K. N., & Sivaraman, K. (2007). *Turmeric: the genus Curcuma*: CRC Press.
- Retnowati, R., Rahman, M. F., & Yulia, D. (2014). Chemical Constituents of the Essential Oils of White Turmeric (*Curcuma zedoaria* (Christm.) Roscoe) from Indonesia and its Toxicity toward *Artemia salina* Leach. *Journal of Essential Oil Bearing Plants*, 17(3), 393-396.
- Romero, M. R., Efferth, T., Serrano, M. A., Castaño, B., Macias, R. I., Briz, O., & Marin, J. J. (2005). Effect of artemisinin/artesunate as inhibitors of hepatitis B virus production in an “in vitro” replicative system. *Antiviral research*, 68(2), 75-83.
- Roth, G. N., Chandra, A., & Nair, M. G. (1998). Novel bioactivities of *Curcuma longa* constituents. *Journal of natural products*, 61(4), 542-545.
- Sadhu, S. K., Tamaki, M., Ohtsuki, T., Toume, K., Koyano, T., Kowithayakorn, T., & Ishibashi, M. (2009). Cadinane sesquiterpenes from *Curcuma parviflora*. *Journal of natural products*, 72(4), 782-783.
- Sakui, N., Kuroyanagi, M., Ishitobi, Y., Sato, M., & Ueno, A. (1992). Biotransformation of sesquiterpenes by cultured cells of *Curcuma zedoaria*. *Phytochemistry*, 31(1), 143-147.
- Sandur, S. K., Pandey, M. K., Sung, B., Ahn, K. S., Murakami, A., Sethi, G., . . . Aggarwal, B. B. (2007). Curcumin, demethoxycurcumin, bisdemethoxycurcumin, tetrahydrocurcumin and turmerones differentially

regulate anti-inflammatory and anti-proliferative responses through a ROS-independent mechanism. *Carcinogenesis*, 28(8), 1765-1773.

- Sanner, M. F. (1999). Python: a programming language for software integration and development. *J Mol Graph Model*, 17(1), 57-61.
- Sarkar, A., Middy, T. R., & Jana, A. D. (2012). A QSAR study of radical scavenging antioxidant activity of a series of flavonoids using DFT based quantum chemical descriptors—the importance of group frontier electron density. *Journal of molecular modeling*, 18(6), 2621-2631.
- Schramm, A., Ebrahimi, S. N., Raith, M., Zaugg, J., Rueda, D. C., Hering, S., & Hamburger, M. (2013). Phytochemical profiling of *Curcuma kwangsiensis* rhizome extract, and identification of labdane diterpenoids as positive GABAA receptor modulators. *Phytochemistry*, 96(0), 318-329.
- Seo, W.-G., Hwang, J.-C., Kang, S.-K., Jin, U.-H., Suh, S.-J., Moon, S.-K., & Kim, C.-H. (2005). Suppressive effect of *Zedoariae rhizoma* on pulmonary metastasis of B16 melanoma cells. *Journal of Ethnopharmacology*, 101(1-3), 249-257.
- Sessou, P., Farougou, S., & Sohounhloué, D. (2012). Major component and potential applications of plant essential oils as natural food preservatives: a short review research results. *Int. J. Biosci*, 2(8), 45-57.
- Sharma, R. K., Misra, B. P., Sarma, T. C., Bordoloi, A. K., Pathak, M. G., & Leclercq, P. A. (1997). Essential oils of *Curcuma longa* L. from Bhutan. *Journal of Essential Oil Research*, 9(5), 589-592.
- Shibuya, H., Yoshihara, M., Kitano, E., Nagasawa, M., & Kitagawa, I. (1986). [Qualitative and quantitative analysis of essential oil constituents in various *Zedoariae rhizoma* (gajutsu) by means of gas liquid chromatography-mass spectrometry]. *Yakugaku zasshi: Journal of the Pharmaceutical Society of Japan*, 106(3), 212-216.
- Shiobara, Y., Asakawa, Y., Kodama, M., & Takemoto, T. (1986). Zedoarol, 13-hydroxygermacrone and curzeone, three sesquiterpenoids from *Curcuma zedoaria*. *Phytochemistry*, 25(6), 1351-1353.
- Shiobara, Y., Asakawa, Y., Kodama, M., Yasuda, K., & Takemoto, T. (1985a). Curcumenone, curcumanolide A and curcumanolide B, three sesquiterpenoids from *curcuma zedoaria*. *Phytochemistry*, 24(11), 2629-2633.
- Singh, G., Kapoor, I. P. S., Singh, P., de Heluani, C. S., de Lampasona, M. P., & Catalan, C. A. N. (2010). Comparative study of chemical composition and antioxidant activity of fresh and dry rhizomes of turmeric (*Curcuma longa* Linn.). *Food and chemical toxicology*, 48(4), 1026-1031.
- Singh, G., Singh, O. P., & Maurya, S. (2002). Chemical and biocidal investigations on essential oils of some Indian *Curcuma* species. *Progress in Crystal growth and Characterization of Materials*, 45(1), 75-81.

- Singh, G., Singh, O. P., Prasad, Y., Lampasona, M., & Catalan, C. (2003). Chemical and biocidal investigations on rhizome volatile oil of *Curcuma zedoaria* Rosc Part 32. *Indian journal of chemical technology*, 10(5), 462-465.
- Singh, N. P., & Lai, H. C. (2004). Artemisinin induces apoptosis in human cancer cells. *Anticancer Research*, 24(4), 2277-2280.
- Singh, P., Singh, S., Kapoor, I., Singh, G., Isidorov, V., & Szczepaniak, L. (2013). Chemical composition and antioxidant activities of essential oil and oleoresins from *Curcuma zedoaria* rhizomes, part-74. *Food Bioscience*, 3, 42-48.
- Sirat, H. M., Jamil, S., & Hussain, J. (1998). Essential oil of *Curcuma aeruginosa* Roxb. from Malaysia. *Journal of Essential Oil Research*, 10(4), 453-458.
- Sirat, H. M., & LeeLay, M. (2009). Chemical components of the rhizome oil of *Curcuma heyneana* Val. *Malaysian Journal of Science*, 28(3), 323-328.
- Souza Jr, J., de Almeida Santos, R. H., Ferreira, M. M. C., Molfetta, F. A., Camargo, A. J., Maria Honório, K., & da Silva, A. B. F. (2003). A quantum chemical and statistical study of flavonoid compounds (flavones) with anti-HIV activity. *European Journal of Medicinal Chemistry*, 38(11), 929-938.
- Stanchev, S., Momekov, G., Jensen, F., & Manolov, I. (2008). Synthesis, computational study and cytotoxic activity of new 4-hydroxycoumarin derivatives. *European Journal of Medicinal Chemistry*, 43(4), 694-706.
- Sukari, M. A. H., Saad, S. M., Lajis, N. H., Rahmani, M., Muse, R., Yusuf, U. K., & Riyanto, S. (2007). Chemical constituents and bioactivity of *Curcuma aeruginosa* Roxb. *Natural Product Sciences*, 13(3), 175-179.
- Sun, X.-Y., Zheng, Y.-P., Lin, D.-H., Zhang, H., Zhao, F., & Yuan, C.-S. (2009). Potential anti-cancer activities of furanodiene, a sesquiterpene from *Curcuma wenyujin*. *The American journal of Chinese medicine*, 37(03), 589-596.
- Sun, X.-y., Zheng, Y.-p., Liu, Z.-f., Xu, L.-l., & Li, S.-h. (2006). Studies on the chemical constituents of sesquiterpenoids from *Curcuma wenyujin*. *Journal of Instrumental Analysis*, 25(6), 27.
- Suphrom, N., Pumthong, G., Khorana, N., Waranuch, N., Limpeanchob, N., & Ingkaninan, K. (2012a). Anti-androgenic effect of sesquiterpenes isolated from the rhizomes of *Curcuma aeruginosa* Roxb. *Fitoterapia*, 83(5), 864-871.
- Suphrom, N., Pumthong, G., Khorana, N., Waranuch, N., Limpeanchob, N., & Ingkaninan, K. (2012b). Anti-androgenic effect of sesquiterpenes isolated from the rhizomes of *Curcuma aeruginosa* Roxb. *Fitoterapia*, 83(5), 864-871.
- Syu, W.-J., Shen, C.-C., Don, M.-J., Ou, J.-C., Lee, G.-H., & Sun, C.-M. (1998). Cytotoxicity of curcuminoids and some novel compounds from *Curcuma zedoaria*. *Journal of natural products*, 61(12), 1531-1534.
- Takahashi, M., Koyano, T., Kowithayakorn, T., Hayashi, M., Komiyama, K., & Ishibashi, M. (2003). Parviflorene A, a novel cytotoxic unsymmetrical

sesquiterpene–dimer constituent from *Curcuma parviflora*. *Tetrahedron Letters*, 44(11), 2327-2329.

- Takano, I., Yasuda, I., Takeya, K., & Itokawa, H. (1995a). Guaiane sesquiterpene lactones from *Curcuma aeruginosa*. *Phytochemistry*, 40(4), 1197-1200.
- Takano, I., Yasuda, I., Takeya, K., & Itokawa, H. (1995b). Guaiane sesquiterpene lactones from *Curcuma aeruginosa*. *Phytochemistry*, 40(4), 1197-1200.
- TAKEYA, K. (1985). Studies on the antitumor bisabolane sesquiterpenoids isolated from *Curcuma xanthorrhiza*. *Studies*, 33(8), 3488-3492.
- Tavares, W. d. S., de Sousa Freitas, S., Graziotti, G. H., Parente, L. M. L., Lião, L. M., & Zanuncio, J. C. (2013). Ar-turmerone from *Curcuma longa* (Zingiberaceae) rhizomes and effects on *Sitophilus zeamais* (Coleoptera: Curculionidae) and *Spodoptera frugiperda* (Lepidoptera: Noctuidae). *Industrial Crops and Products*, 46(0), 158-164.
- Tohda, C., Nakayama, N., Hatanaka, F., & Komatsu, K. (2006). Comparison of anti-inflammatory activities of six *Curcuma* rhizomes: a possible curcuminoid-independent pathway mediated by *Curcuma phaeocaulis* extract. *Evidence-Based Complementary and Alternative Medicine*, 3(2), 255-260.
- Tomasi, J., Mennucci, B., & Cammi, R. (2005). Quantum Mechanical Continuum Solvation Models. *Chem. Rev. (Washington, DC, U. S.)*, 105(8), 2999-3093.
- Tsai, S.-Y., Huang, S.-J., Chyau, C.-C., Tsai, C.-H., Weng, C.-C., & Mau, J.-L. (2011). Composition and antioxidant properties of essential oils from *curcuma* rhizome. *Asian J Arts Sciences*, 2(1), 57-66.
- Tzortzakis, N. G., & Economakis, C. D. (2007). Antifungal activity of lemongrass *Cymbopogon citratus* L. essential oil against key postharvest pathogens. *Innovative Food Science & Emerging Technologies*, 8(2), 253-258.
- Uechi, S., Ishimine, Y., & Hongo, F. (2000). Antibacterial activity of essential oil derived from *Curcuma* sp.(Zingiberaceae) against foodborne pathogenic bacteria and its heat-stability. *Science Bulletin of the College of Agriculture-University of the Ryukyus*.
- Uehara, S., Yasuda, I., Takeya, K., & Itokawa, H. (1989). New bisabolane sesquiterpenoids from the rhizomes of *Curcuma xanthorrhiza* (Zingiberaceae). *Chem. Pharm. Bull.*, 37(1), 237-240. doi: 10.1248/cpb.37.237
- Uehara, S., Yasuda, I., Takeya, K., & Itokawa, H. (1992). [Terpenoids and curcuminoids of the rhizoma of *Curcuma xanthorrhiza* Roxb]. *Yakugaku zasshi: Journal of the Pharmaceutical Society of Japan*, 112(11), 817-823.
- Uehara, S., Yasuda, I., Takeya, K., Itokawa, H., & Itaka, Y. (1990). New bisabolane sesquiterpenoids from the rhizomes of *Curcuma xanthorrhiza* (Zingiberaceae) II. *Chem. Pharm. Bull.*, 38(1), 261-263.

- Usman, L., Hamid, A., George, O., Ameen, O., Muhammad, N., Zubair, M., & Lawal, A. (2009). Chemical composition of rhizome essential oil of *Curcuma longa* L. growing in North Central Nigeria. *World J. Chem*, 4(2), 178-181.
- Vairappan, C. S., Elias, U. M., Ramachandram, T. R., & Kamada, T. (2013a). Secondary metabolites from rhizome of *Curcuma caesia* Roxb. (Zingiberaceae). *Biochemical Systematics and Ecology*, 48(0), 107-110.
- Vairappan, C. S., Elias, U. M., Ramachandram, T. R., & Kamada, T. (2013b). Secondary metabolites from rhizome of *Curcuma caesia* Roxb. (Zingiberaceae). *Biochemical Systematics and Ecology*, 48, 107-110.
- Van den Dool, H., & Dec Kratz, P. (1963). A generalization of the retention index system including linear temperature programmed gas—liquid partition chromatography. *Journal of Chromatography A*, 11, 463-471.
- Varlan, A., & Hillebrand, M. (2010). Bovine and Human Serum Albumin Interactions with 3-Carboxyphenoxathiin Studied by Fluorescence and Circular Dichroism Spectroscopy. *Molecules*, 15(6), 3905-3919.
- Viswanadhan, V. N., Ghose, A. K., Revankar, G. R., & Robins, R. K. (1989). Atomic physicochemical parameters for three dimensional structure directed quantitative structure-activity relationships. 4. Additional parameters for hydrophobic and dispersive interactions and their application for an automated superposition of certain naturally occurring nucleoside antibiotics. *Journal of Chemical Information and Computer Sciences*, 29(3), 163-172.
- Wilson, B., Abraham, G., Manju, V., Mathew, M., Vimala, B., Sundaresan, S., & Nambisan, B. (2005). Antimicrobial activity of *Curcuma zedoaria* and *Curcuma malabarica* tubers. *Journal of Ethnopharmacology*, 99(1), 147-151.
- Wong, D., Kadir, H., & Ling, S. (2012). Bioassay-guided isolation of neuroprotective compounds from *Loranthus parasiticus* against H₂O₂-induced oxidative damage in NG108-15 cells. *Journal of Ethnopharmacology*, 139(1), 256.
- Xia, Q., Wang, X., Xu, D.-J., Chen, X.-H., & Chen, F.-H. (2012). Inhibition of platelet aggregation by curdione from *Curcuma wenyujin* essential Oil. *Thrombosis Research*, 130(3), 409-414.
- Xu, F., Nakamura, S., Qu, Y., Matsuda, H., Pongpiriyadacha, Y., Wu, L., & Yoshikawa, M. (2008). Structures of new sesquiterpenes from *Curcuma comosa*. *Chemical and pharmaceutical bulletin*, 56(12), 1710-1716.
- Xu, H.-X., Dong, H., & Sim, K.-Y. (1996). Labdane diterpenes from *Alpinia zerumbet*. *Phytochemistry*, 42(1), 149-151.
- Yan, J., Chen, G., Tong, S., Feng, Y., Sheng, L., & Lou, J. (2005). Preparative isolation and purification of germacrone and curdione from the essential oil of the rhizomes of *Curcuma wenyujin* by high-speed counter-current chromatography. *Journal of Chromatography A*, 1070(1-2), 207-210.

- Yang, F., Wang, H., Chen, H., Chen, J., & Xia, Z. (2011). Fractionation of volatile constituents from *curcuma* rhizome by preparative gas chromatography. *Journal of Analytical Methods in Chemistry*, 2011.
- Yang, F., Zhang, Y., & Liang, H. (2014). Interactive association of drugs binding to human serum albumin. *International Journal of Molecular Sciences*, 15(3), 3580-3595.
- Yang, H.-l., Chen, G.-h., & Li, Y.-q. (2005). A quantum chemical and statistical study of ganoderic acids with cytotoxicity against tumor cell. *European Journal of Medicinal Chemistry*, 40(10), 972-976.
- Yin, G.-P., An, Y.-W., Hu, G., Zhu, J.-J., Chen, L.-M., Li, L.-C., & Wang*, Z.-M. (2013). Three new guaiane sesquiterpene lactones from rhizomes of *Curcuma wenyujin*. *Journal of Asian natural products research*, 15(7), 723-730.
- Yoshioka, T., Fujii, E., Endo, M., Wada, K., Tokunaga, Y., Shiba, N., . . . Muraki, T. (1998). Antiinflammatory potency of dehydrocurdione, a *zedoary*-derived sesquiterpene. *Inflammation research*, 47(12), 476-481.
- Zeng, J. H., Xu, G. B., & Chen, X. (2009). Application of the chromatographic fingerprint for quality control of essential oil from GuangXi *Curcuma kwangsiensis*. *Medicinal chemistry research*, 18(2), 158-165.
- Zhou, X., Li, Z., Liang, G., Zhu, J., Wang, D., & Cai, Z. (2007a). Analysis of volatile components of *Curcuma sichuanensis* XX Chen by gas chromatography–mass spectrometry. *Journal of pharmaceutical and biomedical analysis*, 43(2), 440-444.
- Zhou, X., Li, Z., Liang, G., Zhu, J., Wang, D., & Cai, Z. (2007b). Analysis of volatile components of *Curcuma sichuanensis* XX Chen by gas chromatography–mass spectrometry. *Journal of pharmaceutical and biomedical analysis*, 43(2), 440-444.
- ZHU, K., LI, J., LUO, H., LI, J.-q., & QIU, F. (2009). Chemical constituents from the rhizome of *Curcuma kwangsiensis*. *Journal of Shenyang Pharmaceutical University*, 1, 008.

APPENDICES

Neuroprotective and Antioxidant Constituents from *Curcuma zedoaria* Rhizomes

Omer Abdalla Ahmed Hamdi¹, Lo Jia Ye², Muhamad Noor Alfarizal Kamarudin², Hazrina Hazni^{1,3}, Mohammadjavad Paydar⁴, Chung Yeng Looi⁴, Jamil A. Shilpi³, Habsah Abdul Kadir^{2,3} and Khalijah Awang^{1,3*}

¹Department of Chemistry, Faculty of Science, University of Malaya, 50603 Kuala Lumpur, Malaysia

²Biomolecular Research Group, Biochemistry Program, Institute of Biological Sciences, Faculty of Science, University of Malaya, 50603 Kuala Lumpur, Malaysia

³Centre for Natural Products and Drug Discovery (CENAR), University of Malaya, 50603 Kuala Lumpur, Malaysia

⁴Department of Pharmacology, Faculty of Medicine, University of Malaya, 50603 Kuala Lumpur, Malaysia

(Received July 15, 2014; Revised November 5, 2014; Accepted November 09, 2014)

Abstract: This study investigates the effect of phytochemical constituents from medicinally important plant *Curcuma zedoaria* (Christm.) Rosc., on hydrogen peroxide induced oxidative stress in mouse neuroblastoma-rat glioma hybridoma cells NG108-15. Phytochemical investigation of *C. zedoaria* rhizomes resulted in the isolation of nine sesquiterpenes (germacrone **1**, dehydrocurdione **2**, curcumenol **3**, isoprocucumenol **5**, curcumenone **6**, procucumenol **7**, zerumbone epoxide **8**, zederone **9** and gweicurculactone **10**) and one labdane diterpene (zerumin A **4**). Curcumenol (**3**) and dehydrocurdione (**2**) showed 100% protection of the NG108-15 cells at the concentrations of 4 and 10 μ M, respectively. Procucumenol (**7**), isoprocucumenol (**5**), zerumbone epoxide (**8**), zerumin A (**4**) and germacrone (**1**) showed moderate activity (80-90% protection). In the oxygen radical antioxidant capacity (ORAC) assay, all the test compounds showed strong antioxidant activity except curcumenol (**3**) which showed moderate antioxidant activity, as compared to the reference standard quercetin.

Keywords: Curcumenol; dehydrocurdion; zerumbone epoxide; ORAC assay; NG108-15 cells. © 2015 ACG Publications. All rights reserved.

1. Introduction

Increased prevalence of neurodegenerative disorders in the aged population is affecting both economically and the quality of life of the patient and carer. The most prevalent neurodegenerative disorders include Alzheimer's disease (AD) and Parkinson's disease (PD). Scientists have predicted that by the year 2050, 1 in 85 people will be affected by AD, which is characterised by neurofibrillary tangles and senile plaques [1]. Parkinson's disease (PD) is another common neurological disease, in which the dopaminergic neurons in the substantia nigra of midbrain and their terminals in the striatum undergo cell death [2]. It leads to movement-related problems in the early stages, and thinking and behavioural symptoms in the later stages. Both AD and PD are multi-factorial which involve different etiopathogenic mechanisms implicating various genetic and environmental factors [3, 4]. Oxidative

* Corresponding author: E-Mail: khalijah@um.edu.my; Phone: +60379674064; Fax: +60379674193

stress, which is the result of mitochondrial dysfunction, has long been considered to be one of the major causes of neurodegeneration. Being the most energy intensive organ (20% of whole body's need), the brain is highly dependent on mitochondrial aerobic oxidative phosphorylation (OXPHOS) to produce ATP. During OXPHOS, electrons leak from the electron transport chain (ETC) as superoxide ($O_2^{\cdot-}$) and give rise to various reactive oxygen species (ROS) including diatomic oxygen, hydrogen peroxide and hydroxyl radical [5]. In normal physiological condition, 1-2% of our consumed oxygen is converted into ROS, which is neutralised by the body's redox systems. As a second messenger system, the highly diffusible gaseous nitric oxide (NO) plays a vital role in the physiological functions in the CNS. The half-life of NO is very short and can convert into various reactive nitrogen species (RNS), including nitric oxide (NO^{\cdot}) by neuronal nitric oxide synthase (nNOS) and nitric oxide (NO^{\cdot}) derived free radicals, including peroxynitrite ($ONOO^{\cdot}$), nitrate (NO_3^{\cdot}) and nitrogen dioxide (NO_2^{\cdot}). Large amount of various ROS and RNS are produced in pathological conditions where the redox homeostasis is insufficient for the neutralisation of excess oxidative radicals [6]. This will then lead to catastrophic events, which include modifications of biomolecules, *e.g.*, lipid peroxidation, DNA mutations, and structural, functional alteration or fragmentation of proteins, leading to protein denaturation and neurodegeneration [7].

Plant extracts, including those rich in antioxidants are of great interest for their therapeutic and preventive role in neurodegenerative disorders. Numerous studies have been done on plant extracts and plant derived natural products for their neuroprotective activity. Some of the most highly studied plants include curcuma, ginger, ginkgo biloba, cinnamon, saffron, coffee, green tea and berries [8]. Phytochemical constituents including monoterpenes, sesquiterpenes, triterpenes, alkaloids, flavonoids and lignans were found to be the active component for the observed biological activity [9].

Curcuma zedoaria (Christm.) Rosc. (Zingiberaceae), locally known as "temu putih" in Malaysia, is a perennial herb largely found in tropical countries including Malaysia, Indonesia, India, Japan and Thailand. It is one of the medicinally important species from the genus *Curcuma*. Also known as 'Ezhu' in Chinese and 'Krachura' in Sanskrit, *C. zedoaria* is used alone or in combination in the herbal remedies of Malaysia, Indian Ayurveda and Chinese medicine [10]. In traditional medicine, the rhizomes of *C. zedoaria* is used for the treatment of menstrual disorders, dyspepsia, stomachic, vomiting and cancer [11]. The plant is reported to have antimicrobial [12], antiulcer [13], analgesic [14], anti-inflammatory [15], hepatoprotective [16], and cytotoxic [17] activity. The isolated bioactive compounds from *C. zedoaria* include curcumenol, dihydrocurdione, curcumin, dihydrocurcumin, tetrahydromethoxycurcumin, tetrahydrobismethoxycurcumin as the analgesic principles [14], curcumin, demethoxycurcumin, bisdemethoxycurcumin, curcumenol (**3**) as cytotoxic against various cancer cell lines [18, 19], furanodiene, germacrone (**1**), curdione, neocurdione, curcumenol (**3**), isocurcumenol, aerugidiol, zedoarondiol, curcumenone (**6**), curcumin as hepatoprotective [16], curzenone and dehydrocurdione (**2**) as anti-inflammatory agents [20].

Despite numerous studies on *C. zedoaria*, it has never been investigated for neuroprotective activity. In our continuous effort to study the bioactive compounds in medicinal plants used in Malaysia and South East Asian region [21-23], we have attempted the isolation of natural compounds from *C. zedoaria* and evaluated them for neuroprotective activity against H_2O_2 -induced oxidative stress in NG108-15 cells. Antioxidant activity of the compounds under investigation was further carried out to correlate their antioxidant ability towards the neuroprotective activity.

2. Materials and Methods

2.1. Plant material

The rhizomes of *Curcuma zedoaria* (Christm.) Rosc. were collected from Tawamangu, Indonesia and a voucher specimen (KL 5764) was deposited at the Herbarium, Department of Chemistry, University of Malaya.

2.2. Extraction and isolation

The air dried, powdered rhizomes (1.0 kg) of *C. zedoaria* was successively extracted by maceration with *n*-hexane (Hex) and dichloromethane (DCM). The *n*-hexane extract (20.2 g, yield

2.4%) was chromatographed on a silica gel column (0.063-0.200 mm) with a gradient elution system using *n*-hexane and ethyl acetate (EtOAc) (100:0-0:100). Based on the TLC pattern, fractions were pooled together to get a total of 21 fractions. Fraction 6 was chromatographed on a silica gel column (0.043-0.063 mm) using a gradient elution system (Hex:EtOAc 100:0-0:100), followed by purification through PTLC (Hex:EtOAc 90:10, 3 times run) to get germacrone (**1**, 21.6 mg). Fraction 7 was subjected to size exclusion chromatography using methanol (MeOH) and DCM in a 1:1 ratio, followed by PTLC (Hex:EtOAc 90:10) and HPTLC (Hex:EtOAc:MeOH 96:3:1) to afford dehydrocurdione (**2**, 34.5 mg). Fraction 8 was separated by PTLC using petroleum ether (40-60°C) (PE) and EtOAc in a ratio of 85:15 for the first run and 82:18 for the second run to get curcumenol (**3**, 15.5 mg), and zerumin A (**4**, 9.8 mg). Isoprocucumenol (**5**, 10.2 mg) was isolated from fraction 9 by successive development on PTLC using PE:EtOAc in the ratio of 90:10 and 85:15, respectively. Curcumenone (**6**, 16.4 mg) was purified from fraction 12 by PTLC using three times run with PE:EtOAc:MeOH in a ratio of 85:14:1. Procucumenol (**7**, 8.9 mg) was isolated from fraction 15 as a colourless oil by PTLC (PE:EtOAc:formic acid 85:14.5:0.5). Zerumbone epoxide (**8**, 11.9 mg) was isolated from silica gel (0.043-0.063 mm) column of fraction 16 using a gradient elution system of Hex and EtOAc (100:0-0:100), followed by three times run on HPTLC (Hex:EtOAc:1,4-dioxane (85:14:1). The DCM extract (10 g) was fractionated on a silica gel column (Hex:EtOAc 95:5-0:100) to give 23 fractions. Fraction 2 was subjected to silica gel column (0.043-0.063 mm) with a gradient elution system of Hex and EtOAc (100:0-0:100) followed by RP-HPLC (H₂O:MeOH 40:60, run time 80 min, flow rate 2.5 mL/min) which afforded zederone (**9**, 24.4 mg) and gweicurculactone (**10**, 3.6 mg) at the retention time of 15.26 and 20.16 min, respectively. The spectral data of the isolated compounds (**Fig. 1**) were in agreement with the literature [24-27].

2.3. Cell culture

NG108-15 was obtained from the American Type Culture Collection (ATCC) and cultured in DMEM (Sigma Aldrich) composed of 10% (v/v) heat inactivated FBS, 2% penicillin/streptomycin, 1% amphotericin B (all from PAA, Austria) and HAT (Sigma Aldrich). NG108-15 cells were cultured and conditioned at 5% CO₂ moist atmosphere at 37°C and checked routinely under inverted microscope (Motic) for any contamination. Cells with confluency of 70-80% were selected for the neuroprotective experiment. Cells exposed to vehicle alone (10% FBS DMEM, DMSO ≤ 0.5% v/v) was used as the control group.

2.4. Assessment of neuroprotective activity

The neuroprotective effect of the isolated compounds against H₂O₂-induced apoptosis in NG108-15 cells was evaluated by MTT [3-(4,5-dimethylthiazol-2-yl)-2,5-diphenyltetrazolium bromide] assay [28]. Cells were plated at a total density of 5×10^3 cells/well in a 96-well plate. The cells were left to adhere for 48 h and treated with test compounds (2 h) prior to H₂O₂ (400 μM) exposure for 24 h. Aliquots of MTT solution (20 μL) was added into each well and incubated at 37°C for another 4 h. The absorbance was measured on a microplate reader (ASYS UVM340) at 570 nm (reference wavelength: 650 nm).

$$\% \text{ Cell viability} = \frac{\text{Absorbance of treated cells}}{\text{Absorbance of control cells}} \times 100\%$$

2.5. ORAC assay

Oxygen radical antioxidant capacity (ORAC) assay was done as described by Cao et al. with slight modification [29]. The assay was performed on a 96-well black microtitre plate, with 25 μL of the samples, standard (Trolox), blank (solvent/PBS) or positive control (quercetin) in each well. Subsequently, 150 μL of working fluorescein solution was added to each well of the assay plate. The plate was incubated at 37°C for 5 min. Aliquot of (25 μL) AAPH working solution was added to each well, making up a total volume of 200 μL. Fluorescence was recorded at an excitation wavelength of 485 nm and emission wavelength of 538 nm. Data were collected every 2 min during an observation period of 2 h, and were analysed by calculating the differences of area under fluorescence decay curve

(AUC) of samples, standard or positive control against blank. The antioxidant capacity was expressed as Trolox equivalent (TE)/100 μg sample.

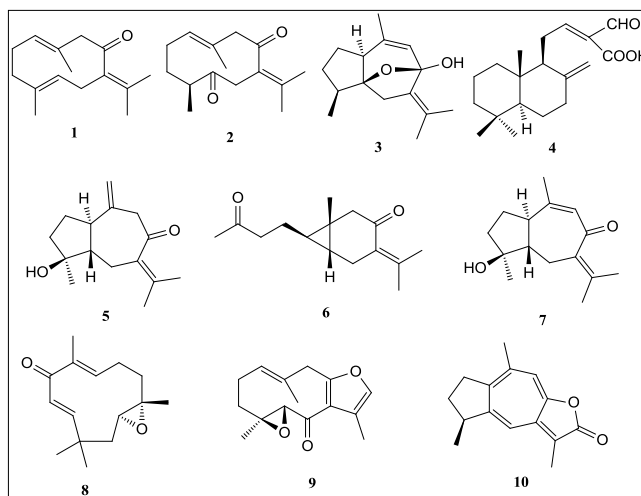


Figure 1. Structures of the isolated compounds from *C. zedoaria* rhizomes.

3. Results and Discussion

As summarized in **Table 1**, all the ten compounds tested, protected the NG108-15 cells from H_2O_2 induced oxidative stress at various degrees. Exposure to H_2O_2 (400 μM) reduced the viability of NG108-15 cells to 67.6% after a period of 24 h. Pretreatment of the cells with curcumenol (**3**) showed the maximum protection (100%) of the cells at the concentration of 4 μM but the effect reduced to 97.7% as the concentration increased to 30 μM . Dehydrocurdione (**2**) also showed strong activity (100% protection) at the concentration of 10 μM , and the activity reduced by either an increase or decrease in the concentration. Germacrone (**1**), zerumin A (**4**), isoprocucumenol (**5**), procucumenol (**7**), and zerumbone epoxide (**8**) showed moderate activity (80-90% viability) as compared to the control.

In the ORAC assay, zerumbone epoxide (**8**) showed the highest antioxidant activity with a TE of 35.41 $\mu\text{M}/100 \mu\text{g}$ of sample. Isoprocucumenol (**5**), zederone (**9**), dehydrocurdione (**2**), germacrone (**1**) showed higher antioxidant capacity than quercetin, used as standard in this assay. While the antioxidant activity of zerumin A (**4**), gweicurculactone (**10**), curcumenone (**6**), procucumenol (**7**) were close to that of quercetin, curcumenol (**3**) showed a lesser extent of activity (Table 2).

Table 1. Neuroprotective evaluation of compounds against H_2O_2 -induced cell death in NG108-15 cells.

Compound	Cell viability (%)					
	1 μM	4 μM	8 μM	10 μM	15 μM	30 μM
Control				100		
H_2O_2				67.63 \pm 0.86		
Germacrone (1)	79.29 \pm 1.05*	77.80 \pm 1.15*	81.25 \pm 1.72*	79.61 \pm 2.38*	89.99 \pm 2.01*	78.68 \pm 1.39*
Dehydrocurdione (2)	82.90 \pm 1.77*	90.76 \pm 1.45*	98.05 \pm 2.33*	100.60 \pm 1.72*	99.98 \pm 2.60*	88.59 \pm 1.75*
Curcumenol (3)	78.03 \pm 1.23*	103.04 \pm 2.17*	100.73 \pm 2.63*	100.60 \pm 1.72*	99.98 \pm 2.60*	97.79 \pm 2.41*
Zerumin A (4)	77.89 \pm 1.95*	77.98 \pm 1.09*	82.69 \pm 1.12*	86.84 \pm 1.76*	91.14 \pm 1.42*	74.41 \pm 1.45
Isoprocucumenol (5)	76.72 \pm 0.88*	79.51 \pm 0.91*	76.42 \pm 1.61*	77.08 \pm 1.07*	80.96 \pm 0.91*	75.94 \pm 1.01*
Curcumenone (6)	66.25 \pm 1.50	59.74 \pm 1.86	66.93 \pm 1.66	73.86 \pm 1.18	70.58 \pm 1.13	79.18 \pm 1.43*
Procucumenol (7)	77.75 \pm 0.95*	79.08 \pm 1.289*	77.00 \pm 1.25*	75.73 \pm 2.22*	80.00 \pm 0.71*	72.87 \pm 0.71
Zerumbone epoxide (8)	75.66 \pm 0.68*	71.29 \pm 1.24	78.15 \pm 0.98*	73.66 \pm 1.70	74.63 \pm 1.27	84.32 \pm 1.09*
Zederone (9)	62.50 \pm 1.41	61.47 \pm 1.53	72.41 \pm 0.97	76.33 \pm 1.19*	70.79 \pm 2.88	74.51 \pm 0.85
Gweicurculactone (10)	59.84 \pm 2.19	64.24 \pm 1.32	59.44 \pm 0.78	67.54 \pm 0.89	75.45 \pm 1.04	75.21 \pm 1.47

All experiments were done in triplicate and results expressed as mean \pm S.E.

* $P < 0.05$ vs H_2O_2 treated cells, One way ANOVA followed by Dunnett's test

Table 2. Antioxidant capacity of the compounds in ORAC assay.

Compound	TE*	Compound	TE*
Germacrone (1)	24.86 ± 2.33	Procurcumenol (7)	20.46 ± 1.88
Dehydrocurdione (2)	26.18 ± 2.59	Zerumbone epoxide (8)	35.41 ± 2.25
Curcumenol (3)	12.62 ± 2.67	Zederone (9)	27.78 ± 2.53
Zerumin A (4)	19.86 ± 3.92	Gweicurculactone (10)	18.26 ± 1.66
Isoprocucumenol (5)	26.43 ± 1.88	Quercetin	21.73 ± 2.87
Curcumenone (6)	21.16 ± 2.12		

*TE: Trolox equivalent in μM per 100 μg of sample; Results expressed as mean \pm SE

In normal physiologic condition, small amount of H_2O_2 is produced during aerobic metabolism in the cell and is neutralised by redox systems of our body. This does not pose significant threat at young age due to the presence of strong antioxidant defence system. However, in aged person, an increased production of ROS and functional decline of neutralising systems creates an imbalance, leading to detectable level of oxidative damages. As a result of cumulative deposition of the pathogenesis, the effects get more noticeable which includes lack of coordination, imbalance, cognitive dysfunction and reduced muscle tone [30].

Use of external H_2O_2 to create oxidative stress in NG108-15 cell is a popular method of studying neuroprotective effect of natural products [31]. Due to the neuronal glial properties, NG108-15, a mouse neuroblastoma-rat glioma hybridoma cell line is used extensively as a neuronal model in electrophysiological and pharmacological research [32]. An excess application of H_2O_2 to NG108-15 cells mimic a similar condition as it takes place during the oxidative stress in the body. Superoxide dismutase (SD), an important enzyme of antioxidant system of the body converts superoxide into H_2O_2 which is further scavenged by catalase or glutathione redox pathway [33]. When there is an increased level of H_2O_2 , the neutralisation by catalase or tissue thiols fail, giving rise to various reactive oxygen species. Application of excess exogenous H_2O_2 creates oxidative stress that is beyond the manageable level of the endogenous antioxidant system [32]. Cell death may happen through two major mechanisms, necrosis and apoptosis. Apoptosis is the most noticeable programmed cell death mechanism and is associated with distinct morphological changes, such as membrane blebbing, cell shrinkage and DNA fragmentation. On the other hand, necrosis is the premature death of cells associated with the loss in cell membrane integrity followed by uncontrolled release of cell death products into the intracellular space [34].

In the present investigation, nine sesquiterpenes and one labdane diterpene isolated from the rhizomes of *C. zedoaria* were tested for their possible neuroprotective role in H_2O_2 -induced oxidative stress in NG108-15 cells. Among these, the guaiane type sesquiterpene, curcumenol (3) showed 100% protection of the cells at 4 μM concentration. The compound showed very little change in its activity even at the concentration of 30 μM , indicating that the compound might not be toxic to the cell within a wide concentration range. Dehydrocurdione (2), a germacrane type sesquiterpene also showed maximum protection of the cells at the concentrations of 10 and 15 μM , which reduced by 10% at 30 μM concentration. Curcumenol (3) and dehydrocurdione (2) are the two major phytoconstituents of *C. zedoaria* and their content in the rhizomes is more than that of any other part of the plant. However, seasonal variation can change the ratio of these two constituents in the plant [14]. Biogenetically, these two compounds are also closely related which is evident from a biomimetic transformation study where dehydrocurdione (2) was converted into curcumenol (3) in a highly selective manner [35].

In a previous study, curcumenol (3) protected hepatic cells from D-GalN-induced cytotoxicity and inhibited LPS (lipopolysaccharide)-induced nitric oxide (NO) production in mouse macrophage [16]. Although inducible NO synthase (iNOS) is not expressed in normal brain, presence of cytokines and LPS can result in its expression in microglia and astrocytes. Neuroinflammations trigger immunoresponses resulting in the infiltration of T cells and macrophage at the inflammatory site. These cells release immunomodulatory molecules including NO which leads to a more widespread CNS-injury [36, 37]. A low level of NO is present in brain for cellular signalling, but a high level of NO can be observed in neurodegenerative disorders causing neuronal cell death by inhibiting mitochondrial cytochrome oxidase [38]. Thus, the inhibition of NO production by curcumenol (3) can also contribute towards the neuroprotective activity of this compound.

In another study, curcumenol (**3**) was isolated as the major anti-inflammatory agent from *Curcuma phaeocaulis* using COX-2 inhibitory assay [39]. There is strong evidence that COX-2 level increases significantly in neurodegenerative disease conditions. In AD, a direct correlation has been found with the COX-2 level with that of amyloid plaque and neuronal atrophy [36]. While in PD, injection of LPS in brain resulted in the increased level of inflammatory factors including COX-2 and iNOS prior to the death of dopaminergic neurons [40]. Therefore, the neuroprotective effect of the curcumenol (**3**) may be partly due to its anti-inflammatory action stemming through the inhibition of COX-2 enzyme [41].

To correlate the antioxidant activity of the compounds under investigation toward their neuroprotective activity, ORAC assay was performed. ORAC assay is considered as a complementary antioxidant test for neuroprotective assay [30]. It is a reliable method of testing antioxidant activity of biological samples including natural products due to its sensitivity towards broader class of compounds [42]. Moreover, it is the only assay which involves the use of peroxy radical and quantifies the antioxidant capacity via area under curve (AUC) technique [43]. The result obtained from this assay is from the direct quenching of free radicals, which is related to the antioxidant capacity of the molecule itself [43]. All the compounds (**1-10**) tested, showed strong to moderate antioxidant activity in the order of zerumbone epoxide (**8**) > zederone (**9**) > isoprocucumenol (**5**) > dehydrocurdione (**2**) > germacrone (**1**) > curcumenone (**6**) > procucumenol (**7**) > zerumin A (**4**) > gweicurculactone (**10**) > curcumenol (**3**). While zerumbone epoxide (**8**), a humulane type sesquiterpene, showed the highest antioxidant capacity (35.41 TE/100 µg sample), and the activity was stronger than that of quercetin (21.16 TE/100 µg sample); in the neuroprotective assay, this compound showed a maximum of 84.32% protection of the cells at the highest concentration tested (30 µM). Interestingly, curcumenol (**3**), which showed the strongest neuroprotective activity (100%) among all the compounds tested, exhibited a moderate antioxidant activity (12.62 TE/100 µg sample). This suggests that the neuroprotective activity of this compound is not the sole contributor from its antioxidant activity, rather a combined effect of its anti-inflammatory, antioxidant and NO-production inhibitory activity. In case of zerumbone epoxide (**8**), the effect might be chiefly due to its antioxidant property. Dehydrocurdione (**2**), the other compound with strong neuroprotective activity, showed an antioxidant capacity of 26.18 TE/100 µg sample, higher than the standard, quercetin.

This is the first report of neuroprotective activity of the constituents from *C. zedoaria* rhizomes. Curcumenol (**3**) and dehydrocurdione (**2**), two major constituent of 'Zedoary turmeric oil' were the most active compounds providing protection of NG108-15 cells. These two compounds have been the attention of researchers for their various pharmacological actions [14]. Present investigation dictates further investigation of curcumenol (**3**), dehydrocurdione (**2**) and other active constituents of *C. zedoaria* rhizomes for *in vitro* and *in vivo* studies to explore their usefulness in the development of potential drug or drug lead for the treatment of neurodegenerative disorders.

Acknowledgments

The authors wish to acknowledge the Ministry of Higher Education of Malaysia and the University of Malaya for financial assistance received through the following grants; University of Malaya High Impact Research (UMC/625/1/HIR/MOHE/SC/37 and J-21010-73848), RG015-09BIO, PS344/2009B, PV036/2011B and University of Malaya Research Program (RP001/2012).

Supporting Information

Supporting Information accompanies this paper on <http://www.acgpubs.org/RNP>

References

- [1] R. Brookmeyer, E. Johnson, K. Ziegler-Graham and H.M. Arrighi (2007). Forecasting the global burden of Alzheimer's disease, *Alzheimers Dement.* **3**, 186-191.
- [2] G.M. Cole, B. Teter, and S.A. Frautschy (2007). In: The molecular targets and therapeutic uses of curcumin in health and disease. Vol. 595. Advances in experimental medicine and biology *ed.* B.B. Aggarwal, Y.J. Surh and S. Shishodia, Springer, New York, pp. 197-212.

- [3] R. Brookmeyer, S. Gray and C. Kawas (1998). Projections of Alzheimer's disease in the United States and the public health impact of delaying disease onset, *Am. J. Public Health*. **88**, 1337-1342.
- [4] J.A. Obeso, M.C. Rodriguez-Oroz, C.G. Goetz, C. Marin, J.H. Kordower, M. Rodriguez, E.C. Hirsch, M. Farrer, A.H. Schapira and G. Halliday (2010). Missing pieces in the Parkinson's disease puzzle, *Nat. Med.* **16**, 653-661.
- [5] M.H. Yan, X. Wang and X. Zhu (2013). Mitochondrial defects and oxidative stress in Alzheimer disease and Parkinson disease, *Free Radic. Biol. Med.* **62**, 90-101.
- [6] J. Emerit, M. Edeas and F. Bricaire (2004). Neurodegenerative diseases and oxidative stress, *Biomed. Pharmacother.* **58**, 39-46.
- [7] B. Halliwell (2006). Oxidative stress and neurodegeneration: where are we now? *J. Neurochem.* **97**, 1634-1658.
- [8] M.M. Essa, R.K. Vijayan, G. Castellano-Gonzalez, M.A. Memon, N. Braidy and G.J. Guillemin (2012). Neuroprotective effect of natural products against Alzheimer's disease, *Neurochem. Res.* **37**, 1829-1842.
- [9] M. Adams, F. Gmünder and M. Hamburger (2007). Plants traditionally used in age related brain disorders— A survey of ethnobotanical literature, *J. Ethnopharmacol.* **113**, 363-381.
- [10] S. Lakshmi, G. Padmaja and P. Remani (2011). Antitumour effects of isocurcumenol isolated from *Curcuma zedoaria* rhizomes on human and murine cancer cells, *Int. J. Med. Chem.* **2011**, article ID 253962.
- [11] N. Saikia and S.C. Nath (2003). Ethnobotanical observations of some species of the genus *Curcuma* L. growing in Assam, *Journal of Economic & Taxonomic Botany* **27**, 430-433.
- [12] A. Bugno, M.A. Nicoletti, A.A. Almodóvar, T.C. Pereira, and M.T. Auricchio (2007). Antimicrobial efficacy of *Curcuma zedoaria* extract as assessed by linear regression compared with commercial mouthrinses, *Braz. J. Microbiol.* **38**, 440-445.
- [13] P. Gupta, M.M. Ali, D. Eranna and S.R. Setty (2003). Evaluation of anti-ulcer effect of root of *Curcuma zedoaria* in rats, *Indian J. Trad. Know.* **2**, 375-377.
- [14] C.R. Pamplona, M.M. de Souza, S. Machado Mda, V. Cechinel Filho, D. Navarro, R.A. Yunes, F. Delle Monache and R. Niero (2006). Seasonal variation and analgesic properties of different parts from *Curcuma zedoaria* Roscoe (Zingiberaceae) grown in Brazil, *Z. Naturforsch. C* **61**, 6-10.
- [15] C. Tohda, N. Nakayama, F. Hatanaka and K. Komatsu (2006). Comparison of anti-inflammatory activities of six *Curcuma* rhizomes: a possible curcuminoid-independent pathway mediated by *Curcuma phaeocaulis* extract, *Evid. Based Complement. Alternat. Med.* **3**, 255-260.
- [16] H. Matsuda, K. Ninomiya, T. Morikawa and M. Yoshikawa (1998). Inhibitory effect and action mechanism of sesquiterpenes from *Zedoariae Rhizoma* on D-galactosamine/lipopolysaccharide-induced liver injury, *Bioorg. Med. Chem. Lett.* **8**, 339-344.
- [17] W.G. Seo, J.C. Hwang, S.K. Kang, U.H. Jin, S.J. Suh, S.K. Moon and C.H. Kim (2005). Suppressive effect of *Zedoariae rhizoma* on pulmonary metastasis of B16 melanoma cells, *J. Ethnopharmacol.* **101**, 249-257.
- [18] W.J. Syu, C.C. Shen, M.J. Don, J.C. Ou, G.H. Lee and C.M. Sun (1998). Cytotoxicity of curcuminoids and some novel compounds from *Curcuma zedoaria*, *J. Nat. Prod.* **61**, 1531-1534.
- [19] O.A.A. Hamdi, S.N.S.A. Rahman, K. Awang, N.A. Wahab, C.Y. Looi, N. Thomas and S.N.A. Malek (2014). Cytotoxic constituents from the rhizomes of *Curcuma zedoaria*, *Sci. World J.* **2014**, article ID 321943.
- [20] H. Makabe, N. Maru, A. Kuwabara, T. Kamo and M. Hirota (2006). Anti-inflammatory sesquiterpenes from *Curcuma zedoaria*, *Nat. Prod. Res.* **20**, 680-685.
- [21] Y. Sivasothy, S.F. Sulaiman, K.L. Ooi, H. Ibrahim and K. Awang (2013). Antioxidant and antibacterial activities of flavonoids and curcuminoids from *Zingiber spectabile* Griff, *Food Control.* **30**, 714-720.
- [22] K. Awang, N.H. Abdullah, A.H.A. Hadi and Y. Su Fong (2012). Cardiovascular activity of labdane diterpenes from *Andrographis paniculata* in isolated rat hearts, *J. Biomed. Biotechnol.* **2012**, article ID 876458.
- [23] R. Othman, H. Ibrahim, M.A. Mohd, M.R. Mustafa and K. Awang (2006). Bioassay-guided isolation of a vasorelaxant active compound from *Kaempferia galanga* L., *Phytomedicine* **13**, 61-66.
- [24] K. Firman, T. Kinoshita, A. Itai and U. Sankawa (1988). Terpenoids from *Curcuma heyneana*, *Phytochemistry* **27**, 3887-3891.
- [25] P.M. Giang and P.T. Son (2000). Isolation of sequiterpenoids from the rhiromes of Vietnames *Curcuma aromatica* Salisb, *E-J. Chemistry.* **38**, 96-99.
- [26] M. Kuroyanagi, A. Ueno, K. Koyama and S. Natori (1990). Structures of sesquiterpenes of *Curcuma aromatica* Salisb. II. Studies on minor sesquiterpenes, *Chem. Pharm. Bull.* **38**, 55-58.
- [27] F. Xu, S. Nakamura, Y. Qu, H. Matsuda, Y. Pongpiriyadacha, L. Wu and M. Yoshikawa (2008). Structures of new sesquiterpenes from *Curcuma comosa*, *Chem. Pharm. Bull.* **56**, 1710-1716.

- [28] C.Y. Looi, B. Moharram, M. Paydar, Y.L. Wong, K.H. Leong, K. Mohamad, A. Arya, WF Wong and M.R. Mustafa (2013). Induction of apoptosis in melanoma A375 cells by a chloroform fraction of *Centrathrum anthelminticum* (L.) seeds involves NF-kappaB, p53 and Bcl-2-controlled mitochondrial signaling pathways, *BMC Complement. Altern. Med.* **13**, 166.
- [29] G. Cao, E. Sofic and R.L. Prior (1997). Antioxidant and prooxidant behavior of flavonoids: structure-activity relationships, *Free Radic. Biol. Med.* **22**, 749-760.
- [30] M. Giacalone, F. Di Sacco, I. Traupe, R. Topini, F. Forfori and F. Giunta (2011). Antioxidant and neuroprotective properties of blueberry polyphenols: a critical review, *Nutr. Neurosci.* **14**, 119-125.
- [31] B. Ahlemeyer, V. Junker, R. Hühne and J. Krieglstein (2001). Neuroprotective effects of NV-31, a bilobalide-derived compound: evidence for an antioxidative mechanism, *Brain Res.* **890**, 338-342.
- [32] D.Z.H. Wong, H.A. Kadir, C.L. Lee and B.H. Goh (2012). Neuroprotective properties of *Loranthus parasiticus* aqueous fraction against oxidative stress-induced damage in NG108-15 cells, *J. Nat. Med.* **66**, 544-551.
- [33] S. Yanpallewar, S. Rai, M. Kumar and S. Acharya (2004). Evaluation of antioxidant and neuroprotective effect of *Ocimum sanctum* on transient cerebral ischemia and long-term cerebral hypoperfusion, *Pharmacol. Biochem. Be.* **79**, 155-164.
- [34] D. Kanduc, A. Mittelman, R. Serpico, E. Sinigaglia, A.A. Sinha, C. Natale, R. Santacroce, M.G. Di Corcia, A. Lucchese, L. Dini, P. Pani, S. Santacroce, S. Simone, R. Bucci and E. Farber (2002). Cell death: apoptosis versus necrosis (review), *Int. J. Oncol.* **21**, 165-170.
- [35] Y. Shiobara, T. Iwata, M. Kodama, Y. Asakawa, T. Takemoto and Y. Fukazawa (1985). Biomimetic transformation of dehydrocurdione into curcumenol and isocurcumenol and their stereochemistries, *Tetrahedron Lett.* **26**, 913-916.
- [36] H. Akiyama, S. Barger, S. Barnum, B. Bradt, J. Bauer, G.M. Cole and N.R. Cooper et al (2000). Inflammation and Alzheimer's disease, *Neurobiol. Aging.* **21**, 383-421.
- [37] M. Deleidi and T. Gasser (2013). The role of inflammation in sporadic and familial Parkinson's disease, *Cell Mol. Life Sci.* **70**, 4259-4273.
- [38] G.C. Brown and C.E. Cooper (1994). Nanomolar concentrations of nitric oxide reversibly inhibit synaptosomal respiration by competing with oxygen at cytochrome oxidase, *FEBS Lett.* **356**, 295-298.
- [39] K. Tanaka, Y. Kuba, A. Ina, H. Watanabe and K. Komatsu (2008). Prediction of cyclooxygenase inhibitory activity of curcuma rhizome from chromatograms by multivariate analysis, *Chem. Pharm. Bull.* **56**, 936-940.
- [40] P.J. Khandelwal, A.M. Herman and C.E.H. Moussa (2011). Inflammation in the early stages of neurodegenerative pathology, *J. Neuroimmunol.* **238**, 1-11.
- [41] C.Y. Chung, J.B. Koprach, H. Siddiqi and O. Isacson (2009). Dynamic changes in presynaptic and axonal transport proteins combined with striatal neuroinflammation precede dopaminergic neuronal loss in a rat model of AAV α -synucleinopathy, *J. Neurosci.* **29**, 3365-3373.
- [42] G. Cao and R.L. Prior (1998). Comparison of different analytical methods for assessing total antioxidant capacity of human serum, *Clin. Chem.* **44**, 1309-1315.
- [43] G. Cao, C.P. Verdon, A. Wu, H. Wang and R.L. Prior (1995). Automated assay of oxygen radical absorbance capacity with the COBAS FARA II, *Clin. Chem.* **41**, 1738-1744.

Article

A Quantum Chemical and Statistical Study of Cytotoxic Activity of Compounds Isolated from *Curcuma zedoaria*

Omer Abdalla Ahmed Hamdi ¹, El Hassane Anouar ^{2,3,*}, Jamil A. Shilpi ⁴,
Zuhra Bashir Khalifa Al Trabolsy ³, Sharifuddin Bin Md Zain ¹,
Nur Shahidatul Shida Zakaria ³, Mohd Zulkefeli ³, Jean-Frédéric F. Weber ³,
Sri Nurestri A. Malek ⁵, Syarifah Nur Syed Abdul Rahman ⁵ and Khalijah Awang ^{1,4,*}

¹ Department of Chemistry, Faculty of Science, University of Malaya, Kuala Lumpur 50603, Malaysia; E-Mails: omerhamdi2001@hotmail.com (O.A.A.H.); smzain@um.edu.my (S.B.M.Z.)

² Department of Chemistry, College of Science, King Saud University, P.O. Box 2455, Riyadh 11451, Saudi Arabia

³ Atta-ur-Rahman Institute for Natural Product Discovery, Universiti Teknologi MARA Kampus Puncak Alam, Bandar Puncak Alam 42300, Malaysia; E-Mails: zuhrabasher@yahoo.com (Z.B.K.A.T.); nursha8760@puncakalam.uitm.edu.my (N.S.S.Z.); mzmj@salam.uitm.edu.my (M.Z.); jffweber@puncakalam.uitm.edu.my (J.-F.F.W.)

⁴ Centre for Natural Products and Drug Discovery (CENAR), University of Malaya, Kuala Lumpur 50603, Malaysia; E-Mail: jamilshilpi@yahoo.com

⁵ Institute of Biological Sciences, Faculty of Science, University of Malaya, Kuala Lumpur 50603, Malaysia; E-Mails: srimalak@um.edu.my (S.N.A.M.); snsar_attas@yahoo.com (S.N.S.A.R.)

* Authors to whom correspondence should be addressed;
E-Mails: anouarelhassane@yahoo.fr (E.H.A.); Khalijah@um.edu.my (K.A.);
Tel.: +603-3258-4771 (E.H.A.); +603-7967-4064 (K.A.);
Fax: +603-3258-4770 (E.H.A.); +603-7967-4193 (K.A.).

Academic Editor: Marie-Christine Bacchus

Received: 19 November 2014 / Accepted: 17 February 2015 / Published: 27 April 2015

Abstract: A series of 21 compounds isolated from *Curcuma zedoaria* was subjected to cytotoxicity test against MCF7; Ca Ski; PC3 and HT-29 cancer cell lines; and a normal HUVEC cell line. To rationalize the structure–activity relationships of the isolated compounds; a set of electronic; steric and hydrophobic descriptors were calculated using density functional theory (DFT) method. Statistical analyses were carried out using simple and multiple linear regressions (SLR; MLR); principal component analysis (PCA);

and hierarchical cluster analysis (HCA). SLR analyses showed that the cytotoxicity of the isolated compounds against a given cell line depend on certain descriptors; and the corresponding correlation coefficients (R^2) vary from 0%–55%. MLR results revealed that the best models can be achieved with a limited number of specific descriptors applicable for compounds having a similar basic skeleton. Based on PCA; HCA and MLR analyses; active compounds were classified into subgroups; which was in agreement with the cell based cytotoxicity assay.

Keywords: *Curcuma zedoaria*; diterpenes; sesquiterpenes; cytotoxicity; DFT; QSAR

1. Introduction

Curcuma zedoaria (Christm.) Rosc. (Zingiberaceae) is a medicinal herb largely found in tropical Asian countries, including Malaysia, Indonesia, India, Japan and Thailand [1]. Also known as *temu putih* in Malaysia and Indonesia, *C. zedoaria* is widely consumed as spice, a flavouring agent in native dishes and is frequently used in food preparations for women during post-partum confinement [2,3]. It has long been used as a folk medicine in different Asian countries for the treatment of menstrual disorders, dyspepsia, vomiting, cancer, stomachic, blood stagnation, hepato-protection and for promoting menstruation [1,4,5]. The rhizomes of *C. zedoaria* is considered as a rich source of terpenoids [6].

Quantum chemical methods can be successfully applied to express molecular interactions between substrate and receptor in terms of molecular electronic properties of the substrates. Various qualitative and quantitative analyses and relationship studies can be found in the literature that used quantum chemical and statistical methods to achieve correlations between calculated variables and biological activities of natural and synthetic substrates [7–13]. Ishihara *et al.* employed semi-empirical PM5 method to delineate the relationship between the cytotoxic activity and 11 chemical descriptors of a series of tropolone compounds and were able to show that the observed cytotoxic activity correlated well with compounds of structural similarities and was governed mainly by dipole moment (μ), hydrophobicity (logP), hardness (η), electrophilicity (ω) and electronegativity (χ) [14]. In another study, Stanchev *et al.* showed that the cytotoxic activity of a series of 4-hydroxycoumarins was well correlated with logP, μ , volume (V) and molecular orbital energies (E_{HOMO} and E_{LUMO}) [15]. Yang *et al.* used a semi-empirical method AM1 to determine the molecular descriptors of a series of ganoderic acids with cytotoxicity against tumour cells; they showed that E_{HOMO} , electronegativity, electronic energy, logP and molecular area (A) are the variables that best discriminate between highly and less active ganoderic acids [16].

The present study aimed at elucidating the structure–cytotoxic activity relationships of a series of 21 compounds isolated from *C. zedoaria* (Figure 1) against four human cancer cells and a normal cell, namely as hormone-dependent breast carcinoma cells (MCF-7), cervical carcinoma cells (Ca Ski), human prostate cancer cells (PC-3), human colon adenocarcinoma cells (HT-29), and human umbilical vein endothelial cells (HUVEC). Density functional theory was adopted at the level of B3LYP/6-31+G (d, p) in order to calculate electronic and steric molecular descriptors of the isolated compounds,

followed by the application of statistical methods (SLR, MLR, PCA and HCA) to determine the main descriptors responsible for the cytotoxic activity of the compounds under investigation.

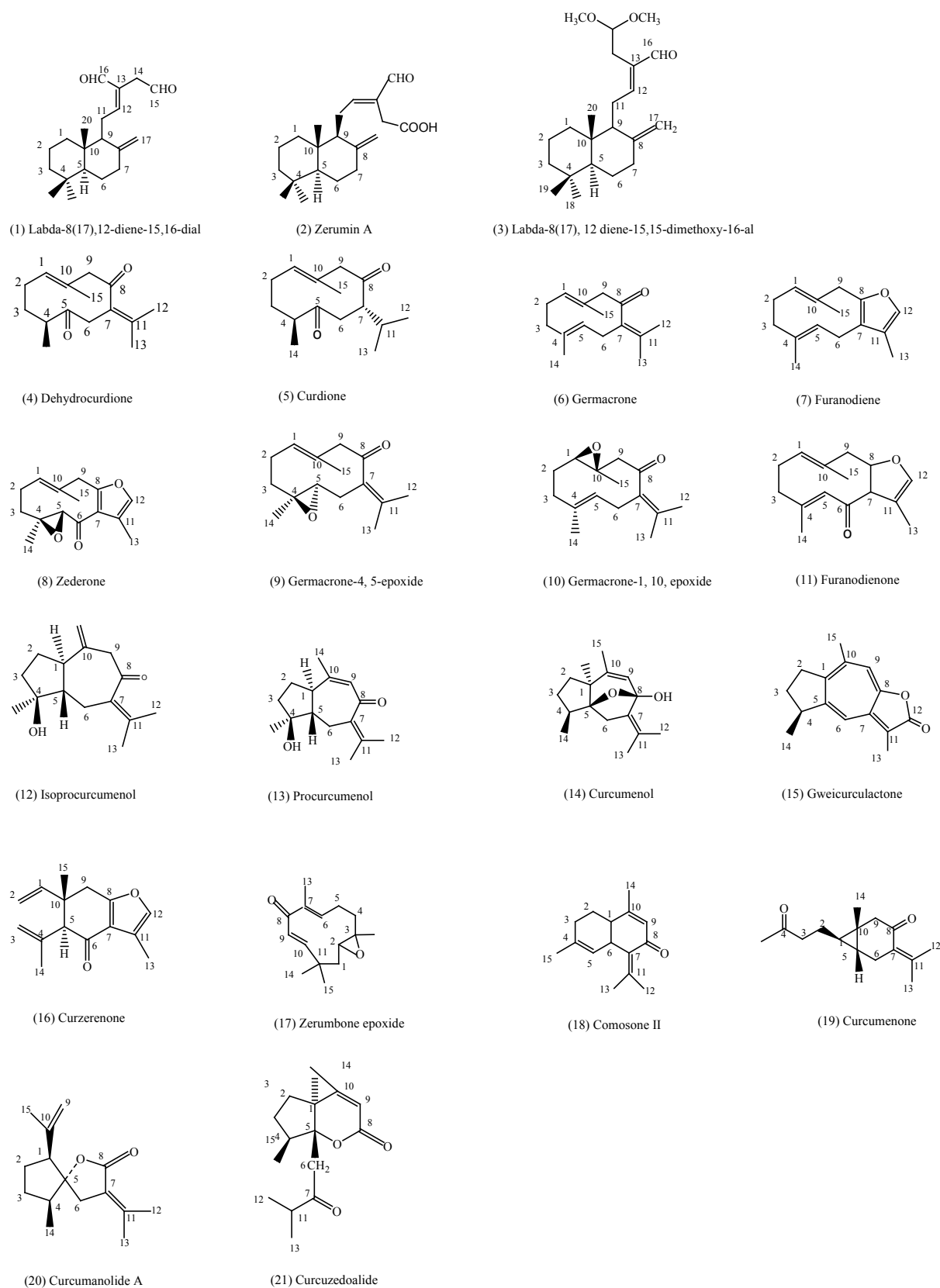


Figure 1. Structure of compounds isolated from *C. zedoaria*.

2. Results and Discussion

2.1. Simple Linear Regression (SLR) Analysis

The values of the electronic, steric and hydrophobic descriptors of compounds **1–21**, as well as their cytotoxic activities (IC_{50} in μM) against MCF-7, Ca Ski, PC-3, HT-29 and HUVEC cells are presented in Table 1. As observed, the cytotoxic activity of compounds (**1–21**) varied with the cell type. Thus, a simple linear regression analyses was done to determine the effect of each of the descriptors separately on the cytotoxicity of the isolated compounds. Figure 2 displays simple linear regression curves obtained with each descriptor for the cytotoxicity of the test compounds against MCF-7 cells, while the statistical parameters (correlation coefficient (R^2), adjusted correlation coefficient (R^2 adj) and standard deviation (SD)) for SLR curves between each descriptor and each tested cell line is presented in Table 2.

2.1.1. Cytotoxicity against MCF-7 Cells and SLR Analysis

Based on the IC_{50} values (Table 2), the compounds were sorted into an inactive group ($IC_{50} > 400 \mu M$) and an active group ($IC_{50} < 400 \mu M$). To avoid the large discrepancies in the IC_{50} values, the active group was further subdivided into group A ($200 < IC_{50} < 300 \mu M$); group B ($100 < IC_{50} < 200 \mu M$) and group C ($IC_{50} < 100 \mu M$). The SLR analysis shows that the influence of a given descriptor on cytotoxic activity is dependent on the nature of the descriptor itself. For instance, the electronic descriptors IP, AE, χ , η , S, ω and μ have no significant influence ($R^2 \approx 0\%–7\%$), while modest correlations were observed for descriptors α , A, V, LogP and M ($R^2 \approx 40\%–55\%$) (Figure 2). These results are consistent with those obtained by Ishihara *et al.*, who showed that cytotoxic activity of 20 synthesized tropolones was poorly correlated with each of 11 chosen descriptors [14,17].

2.1.2. Cytotoxicity against Ca Ski Cells and SLR Analysis

Following the same pattern as that of Section 2.1.1, the compounds were divided into inactive and active groups, while the active group was further subdivided into group A, group B, and group C based on their IC_{50} values against Ca Ski cells. Table 2 represents the SLR parameters between each descriptor and $\log(IC_{50})$. As it can be seen, the effects of electronic descriptors IP, AE, χ , η , S and ω are negligible ($R^2 \leq 10\%$), while α , A, V and M descriptors showed a moderate effect ($R^2 \approx 28\%–43\%$). Surprisingly, hydrophobicity played no role on the cytotoxicity of the compounds ($R^2 \approx 0$) (Table 2).

Table 1. Cytotoxicity IC₅₀ (μM) and molecular descriptors obtained at B3P86/6-311+G (d, p) level for the isolated compounds.

NO.	IP	EA	χ	η	ω	α	μ	A	V	Log P	M	IC ₅₀ (μM) ^a				
												MCF-7	Ca Ski	PC-3	HT-29	HUVEC
1	6.87	2.15	4.51	4.71	2.16	324	6.13	400	470	3.45	302.46	53.9 ± 0.7	47.9 ± 0.3	87.0 ± 7.9	71.1 ± 10.2	149.8 ± 6.3
2	6.86	2.09	4.48	4.77	2.10	328	5.62	408	481	3.86	318.46	70.0 ± 3.3	NA ^b	68.8 ± 5.0	54.6 ± 6.3	81.0 ± 6.0
3	6.85	2.00	4.43	4.85	2.02	363	5.63	457	541	4.20	348.53	14.3 ± 0.6	NA ^b	119.6 ± 9.8	138.6 ± 14.6	135.7 ± 12.1
4	6.56	1.69	4.12	4.87	1.74	244	2.99	323	368	3.63	234.34	140.8 ± 4.7	92.6 ± 4.7	81.5 ± 11.9	96.9 ± 10.2	102.4 ± 9.0
5	6.52	1.26	3.89	5.26	1.44	238	1.40	331	377	4.01	236.35	NA ^b	—	—	—	—
6	6.40	1.39	3.89	5.01	1.51	248	4.06	321	355	3.81	218.34	NA ^b	180.0 ± 5.5	252.8 ± 22.4	196.5 ± 18.8	337.5 ± 1.4
7	5.96	0.29	3.12	5.67	0.86	238	1.88	304	341	1.84	216.32	271.9 ± 12.0	NA ^b	182.6 ± 20.8	218.2 ± 20.3	189.1 ± 12.0
8	6.58	1.80	4.19	4.78	1.84	241	6.35	313	353	0.84	246.31	NA ^b	NA ^b	109.6 ± 7.7	77.5 ± 10.1	170.9 ± 11.0
9	6.54	1.39	3.96	5.14	1.53	241	5.59	318	364	2.71	234.34	218.8 ± 17.1	NA ^b	187.3 ± 30.7	169.0 ± 19.6	206.5 ± 20.1
10	6.49	1.66	4.08	4.83	1.72	243	3.67	320	364	2.85	243.34	251.7 ± 23.9	NA ^b	218.6 ± 20.1	299.2 ± 34.1	228.1 ± 6.6
11	6.07	1.46	3.76	4.61	1.54	240	4.37	320	356	2.60	232.32	137.7 ± 6.5	—	—	—	—
12	6.50	0.37	3.43	6.13	0.96	254	2.61	342	389	3.80	236.4	154.5 ± 17.8	NA ^b	158.2 ± 19.0	218.3 ± 16.5	190.8 ± 12.7
13	6.54	1.77	4.16	4.78	1.81	252	7.48	327	362	2.71	234.34	127.2 ± 9.4	266.3 ± 1.3	56.8 ± 7.3	66.1 ± 9.8	69.6 ± 4.3
14	6.21	0.57	3.39	5.64	1.02	260	3.86	333	376	3.58	248.37	37.4 ± 37.4	74.5 ± 4.0	69.7 ± 4.8	99.9 ± 10.9	104.3 ± 5.6
15	5.71	2.26	3.99	3.45	2.30	290	11.67	305	330	3.46	228.29	136.8 ± 14.1	NA ^b	167.8 ± 9.6	156.4 ± 25.4	314.1 ± 26.7
16	6.47	1.55	4.01	4.92	1.63	245	3.76	350	371	2.23	232.32	243.2 ± 13.8	—	—	—	—
17	7.09	2.12	4.61	4.97	2.14	227	4.90	298	339	3.43	220.31	109.4 ± 0.5	156.6 ± 2.7	49.0 ± 8.6	62.2 ± 12.3	64.5 ± 5.0
18	6.51	1.80	4.15	4.71	1.83	247	6.66	310	340	3.51	216.32	NA ^b	351.3 ± 5.5	NA ^b	NA ^b	NA ^b
19	6.77	1.64	4.21	5.13	1.72	256	0.71	362	394	3.5	248.37	32.2 ± 4.0	NA ^b	160.2 ± 16.9	174.3 ± 25.0	201.3 ± 34.6
20	6.94	1.48	4.21	5.47	1.62	243	6.39	330	365	2.98	234.34	212.4 ± 13.2	80.2 ± 10.2	90.9 ± 13.7	92.6 ± 29.9	—
21	7.24	2.03	4.63	5.21	2.06	259	4.88	332	386	3.86	262.35	238.0 ± 13.8	236.7 ± 30.9	221.8 ± 13.3	172.7 ± 29.7	—

^a The cytotoxicity results as reported by [18]; ^b NA = Not active.

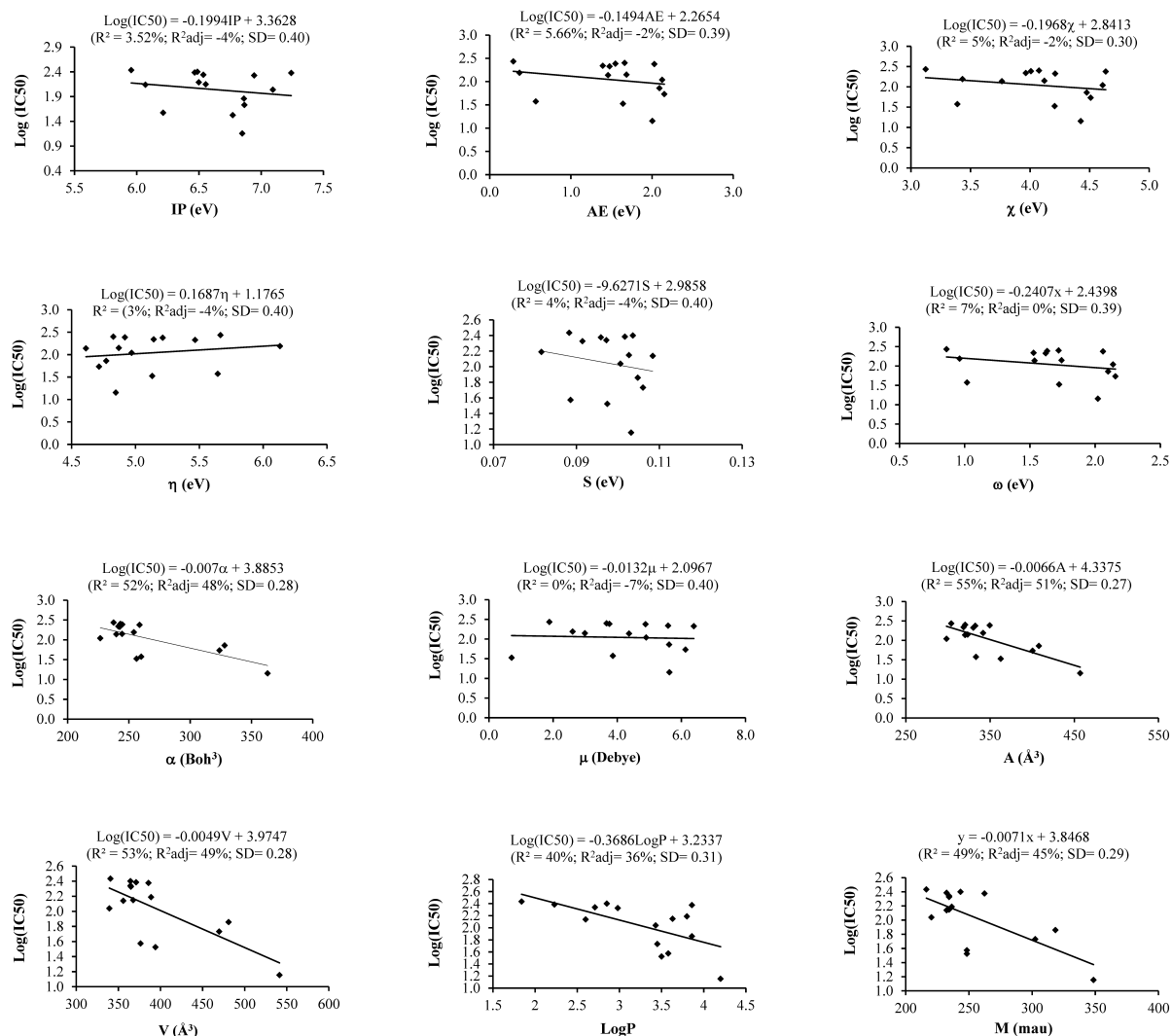


Figure 2. Simple linear regression correlation (SLR) curves between the cytotoxic activity on MCF-7 cells and each descriptor of isolated compounds from *C. zedoaria*.

Table 2. Correlation coefficients (R^2), adjusted correlation coefficients (R^2_{adj}) and standard deviations (SD) of simple linear regression curves (SLR) between each descriptor and the tested cell lines.

Descriptor/s/ SLR on Cells	MCF-7			Ca Ski			PC-3			HT-29			HUVEC		
	% R^2	% R^2_{adj}	SD	% R^2	% R^2_{adj}	SD	% R^2	% R^2_{adj}	SD	% R^2	% R^2_{adj}	SD	% R^2	% R^2_{adj}	SD
IP	4	−4	0.40	0	−14	0.31	8	2	0.22	14	8	0.22	30	24	0.19
EA	6	−2	0.39	6	−8	0.30	5	−2	0.23	19	14	0.21	3	−4	0.23
χ	5	−2	0.39	2	−11	0.31	8	2	0.22	23	18	0.20	13	7	0.21
η	3	−4	0.40	11	−2	0.30	0	−6	0.23	5	−2	0.23	2	−6	0.23
S	4	−4	0.40	10	−3	0.30	0	−7	0.23	2	−5	0.23	5	−3	0.23
ω	7	0	0.39	4	−10	0.31	5	−1	0.23	14	19	0.21	3	−4	0.23
α	52	48	0.28	28	18	0.27	2	−5	0.23	5	−1	0.23	1	−7	0.23
DM	0	−7	0.40	9	−4	0.30	4	−3	0.23	13	7	0.22	0	−8	0.23
A	55	51	0.27	42	33	0.24	2	−4	0.23	4	−2	0.23	3	−4	0.23
V	53	49	0.28	43	34	0.24	3	−4	0.23	5	−1	0.23	5	−2	0.22
Log P	40	36	0.31	0	−14	0.31	−7	0	0.23	0	−6	0.23	1	−7	0.23
M	49	45	0.29	36	26	0.25	4	−3	0.23	8	2	0.22	−1	6	0.22

2.1.3. Cytotoxicity against PC-3 Cells and SLR Analysis

The compounds were classified into groups on the basis of their activity against PC-3 cells in the same fashion as discussed earlier. All chosen descriptors showed negligible effect on cytotoxic activity ($R^2 \approx 0\%–8\%$) (Table 2).

2.1.4. Cytotoxicity against HT-29 Cells and SLR Analysis

In case of cytotoxicity of the isolated compounds against HT-29 cells, moderate effects were obtained with the electronic descriptors namely IP, EA, χ , ω and μ with 14%, 19%, 23%, 14% and 13% correlation coefficients, respectively. In contrast to the results obtained for MCF-7 and Ca Ski cells, the steric descriptors did not show significant effects ($R^2 \leq 8\%$) (Table 2).

2.1.5. Cytotoxicity against HUVEC Cells and SLR Analysis

For HUVEC cells, all descriptors showed no significant effect on the cytotoxic activity ($R^2 \leq 5\%$), except IP and χ , which showed moderate effects (30% and 13% correlation coefficients, respectively) (Table 2).

2.2. Multiple Linear Regression (MLR) Analysis

In an attempt to further investigate the correlations between the calculated descriptors and the cytotoxic activity of the isolated compounds against each cell line, MLR analysis was performed. MLR analysis was conducted only for the compounds of the active group.

2.2.1. Cytotoxicity against MCF-7 Cells and MLR Analysis

Among the 17 compounds for which the IC_{50} values were observed against MCF-7 cells, compound **15** (gweicurculactone) was used as the model compound, and therefore excluded from MLR analysis. The MLR model as given in Equation (1) was obtained from the correlation observed between $\log(IC_{50})$ and the descriptors. The corresponding curve is presented in Figure 3a.

$$\begin{aligned} \log(IC_{50})_{Pred.} = & -(60.85 \pm 73.65) + (2.91 \pm 3.91)IP - (0.70 \pm 2.22)EA + (1.10 \pm 2.62)\chi + \\ & (3.62 \pm 3.60)\eta + (314.17 \pm 359.28)S - (3.38 \pm 9.43)\omega - (0.01 \pm 0.06)\alpha - (0.05 \pm 0.16)\mu \\ & - (0.02 \pm 0.03)A + (0.01 \pm 0.04)V - (0.63 \pm 0.38)\log P + (0.01 \pm 0.03)M \end{aligned} \quad (1)$$

The predicted $\log(IC_{50})_{Pred.}$ and residuals to experimental $\log(IC_{50})_{Obs.}$ for the active compounds are given in Table 3. The correlation between all descriptors and cytotoxicity is relatively weak, with a standard deviation of $SD = 0.41$ and $R^2 = 84\%$. The predicted $\log(IC_{50})_{Pred.}$ for the model compound tested (compound **15**) is relatively high (4.48) with a residual value of 2.34. While the predicted IC_{50} value suggested compound **15** is categorised in the inactive group, the observed IC_{50} dictates it to be an active compound. Consequently, this model (Equation (1)) was considered not suitable for cytotoxicity prediction. To obtain a better model, the first 11 compounds (**1–11**) with similar skeletons were chosen for MLR analysis. For better consistency in the analysis, they were further subdivided into labdane diterpenes (compounds **1–3**) and germacrane sesquiterpenes (compounds **4–11**). Only the active

compounds were subjected to MLR as shown in Equation (2) while compound **11** was selected as a test model in this study.

$$\log(\text{IC}_{50})_{\text{Pred.}} = (7.77 \pm 4.74) - (0.18 \pm 0.52)\text{IP} - (0.06 \pm 0.05)\text{A} + (0.03 \pm 0.04)\text{V} - (0.07 \pm 0.15)\text{LogP} + (0.02 \pm 0.01)\text{M} \quad (2)$$

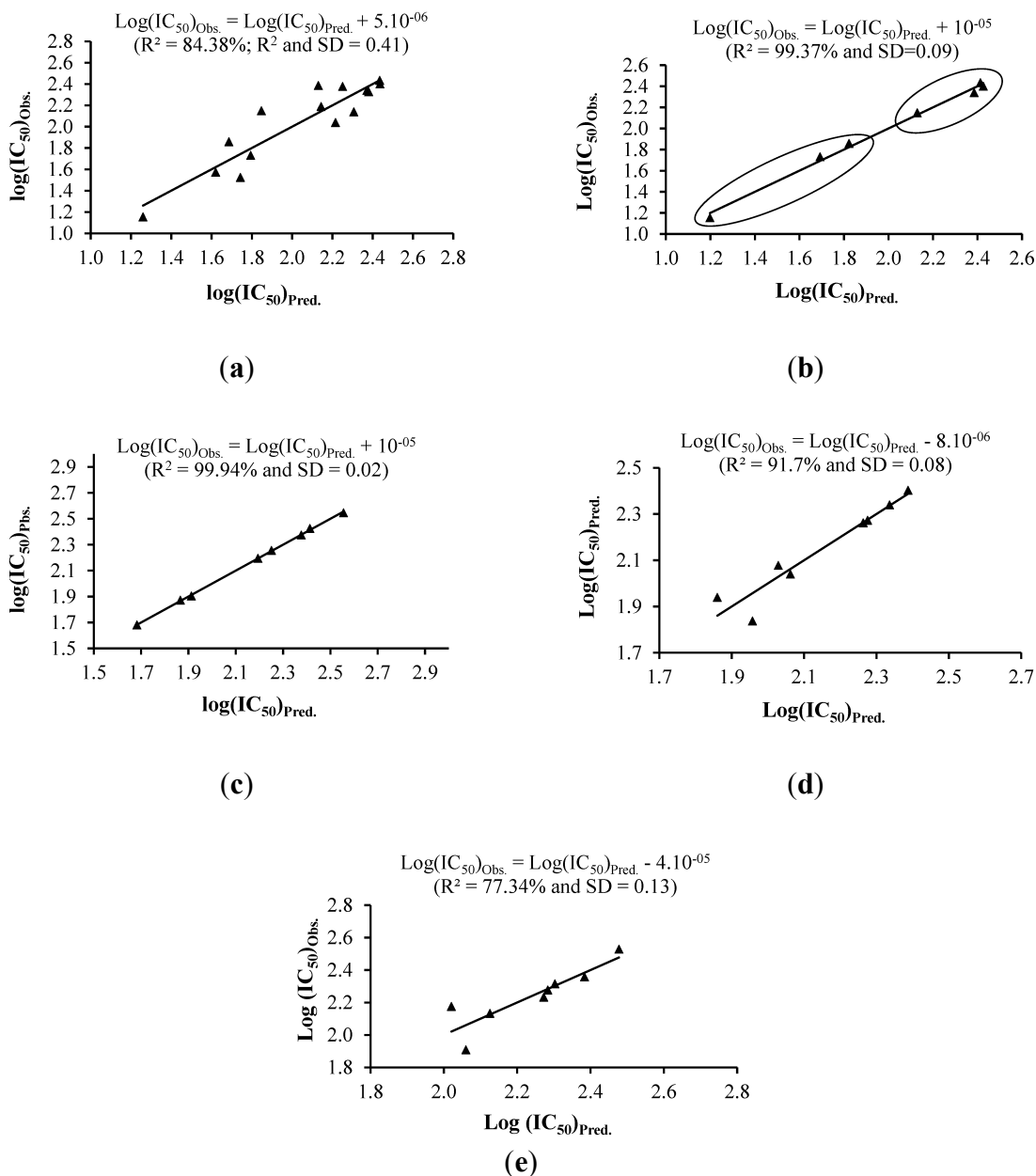


Figure 3. Multiple linear regression (MLR) correlations between most important descriptors and the cytotoxic activity of the active compounds isolated from *C. zedoaria*. (a) MLR analysis for cytotoxicity against MCF-7; (b) Modified MLR analysis of compounds **1–11** for cytotoxicity against MCF-7; (c) MLR analysis for cytotoxicity against Ca Ski; (d) MLR analysis for cytotoxicity against PC-3; (e) MLR analysis for cytotoxicity against HUVEC.

The model of Equation (2) was found to be superior to the previous model (Equation (1)) with a correlation coefficient of 99.37% and a SD of 0.09. For purpose of validation, this model (Equation (2)), was applied for compound **11**. The predicted $\log(\text{IC}_{50})_{\text{Pred.}}$ was found to be 2.10, with a difference of only 0.04 from the experimental value. The difference between the predicted and observed cytotoxicity is 13 μM . The MLR model of Equation (2) demonstrated the importance of IP, steric parameters (area and volume), hydrophobicity ($\log P$) and molecular weight (M) on the cytotoxic activity of the test compounds. These results are in good agreement with previous studies where steric parameters and hydrophobicity were found to be the most important descriptors to classify compounds into high and low activities [14,16]. Thus, the MLR of Equation (2) subdivided the test compounds into high and low cytotoxicity (Figure 3b).

2.2.2. Cytotoxicity against Ca Ski Cells and MLR Analysis

Nine compounds showing cytotoxic activity against Ca Ski cells were selected for this study. Compound **4** (dehydrocurdione) was chosen as model compound and thus excluded from MLR analysis. The MLR model obtained between $\log(\text{IC}_{50})$ and six best descriptors is given in Equation (3) and the corresponding regression curve is shown in Figure 3c.

$$\log(\text{IC}_{50})_{\text{Pred.}} = (122.80 \pm 7.42) - (11.88 \pm 0.73)\eta - (608.30 \pm 38.85)S + 0.03\alpha + 0.02A - 0.06V + 0.03M \quad (3)$$

The predicted $\log(\text{IC}_{50})$ and residuals with respect to experimental values of active isolated compounds are presented in Table 3. The model was found to correlate the descriptors to the observed $\log(\text{IC}_{50})$ with good accuracy (R^2 99.94% and SD 0.02). For the model compound (**4**), the predicted $\log(\text{IC}_{50})_{\text{pred.}}$ is 1.93, with a difference of 0.04 from the experimental value. The difference between the predicted and observed cytotoxicity is 8 μM . Equation (3) shows the function of steric parameters (area and volume), molecular weight (M), hardness, softness and the polarizability of the isolated compounds towards the cytotoxicity against Ca Ski cells.

2.2.3. Cytotoxicity against PC-3 Cells and MLR Analysis

Seventeen compounds showing cytotoxicity against PC-3 cells were included in MLR analysis while compound **4** (dehydrocurdione) was excluded as the model compound. The MLR model (Equation (4)) obtained between $\log(\text{IC}_{50})$ and all descriptors gives a correlation of 88% (SD 0.17).

$$\begin{aligned} \log(\text{IC}_{50})_{\text{Pred.}} = & -(42.62 \pm 12.74) + (3.48 \pm 0.94)\text{IP} + (217.76 \pm 58.86)\text{EA} - \\ & (11.07 \pm 2.96)\chi - (0.20 \pm 0.05)\eta + (2.98 \pm 0.82)S - (0.23 \pm 0.11)\omega - (0.04 \pm 0.01)\alpha + \\ & (0.04 \pm 0.02)\mu + (0.02 \pm 0.01)A - (0.01 \pm 0.01)V + (0.98 \pm 0.48)\log P + (2.49 \pm 0.75)M \end{aligned} \quad (4)$$

Table 3. Predicted $\log(\text{IC}_{50})_{\text{Pred.}}$ and residuals of the active compounds obtained using MLR Equations (1)–(6).

NO.	Equation (1)		Equation (2)		Equation (3)		Equation (5)		Equation (6)	
	$\log(\text{IC}_{50})_{\text{Pred.}}$	Resid.	$\log(\text{IC}_{50})_{\text{Pred.}}$	Resid.	$\log(\text{IC}_{50})_{\text{Pred.}}$	Resid.	$\log(\text{IC}_{50})_{\text{Pred.}}$	Resid.	$\log(\text{IC}_{50})_{\text{Pred.}}$	Resid.
1	1.79	0.06	1.73	1.69	1.68	0.00	1.86	−0.08	2.02	2.18
2	1.69	−0.17	1.86	1.82	—	—	1.96	0.12	2.06	1.91
3	1.26	0.11	1.15	1.20	—	—	2.03	−0.05	2.13	2.13
4	1.85	−0.30	2.15	2.13	—	—	2.39	−0.02	—	—
5	—	—	—	—	—	—	2.26	0.00	—	—
6	—	—	—	—	2.26	0.00	2.06	0.02	2.48	2.53
7	2.43	0.00	2.43	2.41	—	—	2.28	0.00	2.28	2.28
8	—	—	—	—	—	—	2.34	0.00	2.27	2.23
9	2.37	0.03	2.34	2.39	—	—	—	—	2.30	2.32
10	2.44	0.04	2.40	2.43	—	—	—	—	2.38	2.36
11	2.31	0.17	—	—	—	—	—	—	—	—
12	2.14	−0.05	—	—	—	—	—	—	—	—
13	—	—	—	—	2.43	−0.01	—	—	—	—
14	1.62	0.05	—	—	1.87	−0.01	—	—	—	—
15	—	—	—	—	—	—	—	—	—	—
16	2.13	−0.26	—	—	—	—	—	—	—	—
17	2.22	0.18	—	—	2.19	0.00	—	—	—	—
18	—	—	—	—	2.55	0.01	—	—	—	—
19	1.74	0.22	—	—	—	—	—	—	—	—
20	2.38	0.05	—	—	1.90	0.01	—	—	—	—
21	2.25	−0.13	—	—	2.37	0.00	—	—	—	—

The predicted IC_{50} ($>400 \mu M$) of compound (**4**) suggested it is an inactive compound, which is contradictory to the observed IC_{50} ($81.5 \mu M$) against PC-3 cells. In an attempt to derive a better model, the number of descriptors was reduced and the analysis was confined to compounds (**1–11**) with a similar basic skeleton. Compound **4** was excluded from MLR analysis. The best correlation was obtained with the electronic descriptors of IP, EA, ω and μ (Equation (5) and Figure 3d). The predicted $\log(IC_{50})$ and residuals to experimental results are presented in Table 3.

$$\text{Log}(IC_{50})_{\text{Pred.}} = (2.52 \pm 3.16) + (0.36 \pm 0.61)IP + (2.09 \pm 0.54)EA - (3.30 \pm 0.92)\omega - (0.08 \pm 0.05)\mu \quad (5)$$

The predicted $\log(IC_{50})_{\text{Pred.}}$ for the test compound **4** is 1.91, with a difference of 0.48 from the experimental value. Although the difference between the predicted ($244 \mu M$) and experimental IC_{50} value ($82 \mu M$) is relatively high ($162 \mu M$), MLR analysis categorised it in the active group which is consistent with the observed results against PC-3 cells.

2.2.4. Cytotoxicity against HT-29 Cells and MLR Analysis

Seventeen compounds showing cytotoxicity against HT-29 cells (Table 1) were chosen for this study while compound **4** (dehydrocurdione) was excluded from MLR analysis. The MLR model obtained between $\log(IC_{50})$ and all descriptors derived a correlation of 81% (SD 0.22). The predicted value for the test compound **4** ($IC_{50} = 283 \mu M$) suggested it as an active compound (experimental $IC_{50} = 97 \mu M$). In terms of activity, compound **4** falls in group A as per predicted IC_{50} , which is quite different from its group (C) determined from the experimental IC_{50} . In an attempt to obtain a better model, the number of descriptors was reduced and the analysis was performed for the first 11 compounds (**1–11**) with similar basic skeleton and compound **4** was excluded from MLR analysis. However, in every case, the difference between experimental and predicted IC_{50} was more than $100 \mu M$, and therefore not presented herein.

2.2.5. Cytotoxicity against HUVEC Cells and MLR Analysis

Fifteen compounds that showed activity against HUVEC cells were included in this study and compound **4** (dehydrocurdione) was excluded from MLR analysis. The correlation between $\log(IC_{50})$ and all descriptors gave an R^2 of 96% (SD 0.16). The predicted IC_{50} for compound **4** from this model was $142 \mu M$ higher than the experimental IC_{50} . The best correlation was obtained when three descriptors, namely IP, χ , S and V were taken into consideration (R^2 77%, SD 0.13) (Equation (6)). Predicted IC_{50} of compound **4** classified it as an active compound with a difference of $48 \mu M$ from the experimental IC_{50} value.

$$\text{Log}(IC_{50})_{\text{Pred.}} = (72.92 \pm 37.80) - (14.02 \pm 7.48)IP + (13.07 \pm 7.14)\chi + (13.07 \pm 7.14)S - (0.0004 \pm 0.0016)V \quad (6)$$

2.3. Principal Component Analysis (PCA)

Principal component analysis (PCA) allows the reduction of the number of variables used in a statistical analysis to create a new set of variables (PCs) expressed in a linear combination of the

original data set [19]. The first new variable (PC1) contains the largest variance; while the second contains the second largest variance, and so on. Before applying the PCA method, each variable was standardized for ease of comparison between each other on the same scale. PCA analysis was performed only on MCF-7 cells. After several attempts to obtain a good classification of the isolated compounds, the best result was achieved with five variables, namely IP, A, V, logP and M. The first three components of PCA (PC1 = 90.50%, PC2 = 7.12%, and PC3 = 2.27%) conceded 99.89% of the overall variance of the data set (Table 4), while the sole combination of PC1 and PC2 described 97.62% of variance (Table 4). The loading vectors for PC1, PC2, and PC3 are given in Table 5 and the plot of the score vectors of the two principal components (PC1 × PC2) is shown in Figure 4.

Table 4. Variances (eigenvalues) obtained for the first three principal components.

Component	Eigenvalue	Variance (%)	Cumulated Variance (%)
PC1	4.525	90.50	90.50
PC2	0.3560	7.12	97.62
PC3	0.1134	2.27	99.89

Table 5. Loading vectors for the first three principal components.

Variable	PC1	PC2	PC3
IP	0.43	0.61	0.66
A	0.46	−0.38	−0.04
V	0.46	−0.34	0.04
logP	0.43	0.51	−0.74
M	0.46	−0.32	0.08

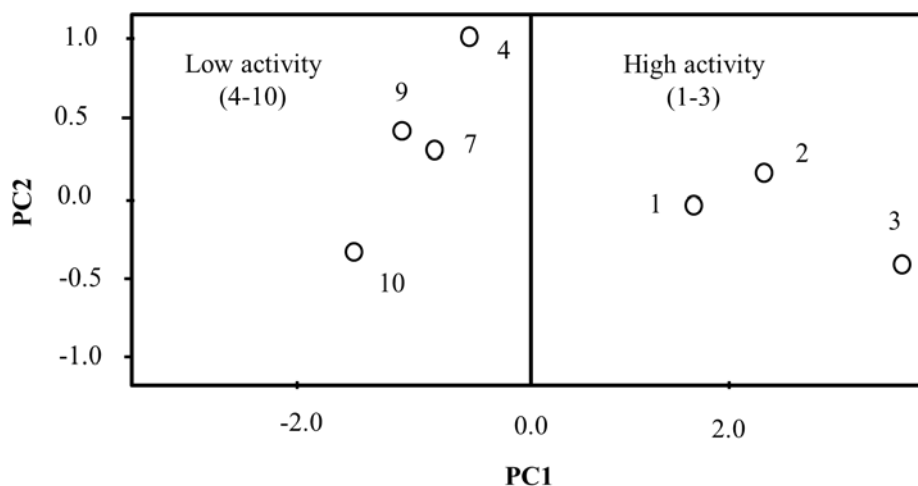


Figure 4. Plot of the score vectors of first principal components for cytotoxicity of compounds from *C. zedoaria* against MCF-7 cells.

As can be seen in Figure 4, the compounds under investigation are divided into two groups based on PCA analysis: compounds with high activity (1–3) and low activity (4–10). The principal component PC1 presented in Table 5 can be expressed through the following equation:

$$\text{PC1} = 0.34\text{IP} + 0.46\text{EA} + 0.46\text{V} + 0.43\text{logP} + 0.46\text{M} \quad (7)$$

Thus, a compound can be considered active if its IP, A, V, log P, and M values are similar to those described in the above Equation (7). When compared with published literature, the results of our present investigation followed the same trend with some agreement and disagreement in the involvement of descriptors for the activity of a series of compounds. For example, Yang *et al.* showed that cytotoxic ganoderic acids can be attained when higher values for the variables E_{HOMO} , V, E_{el} , and logP are coupled with a smaller value for M [16]. Sauza *et al.* found that for a given flavone to be active against HIV, it must have smaller values for log P and V while EA must have a larger value [7]. In the present study, the results obtained from MLR or PCA are in coordination to show that the cytotoxicity of the compounds under investigation is dependent on the same descriptors (IP, A, V, logP and M) and afforded the same classification of the compounds (Figures 3b and 4).

2.4. Hierarchical Cluster Analysis (HCA)

In case of preliminary data analysis, HCA is a powerful tool for examining data sets for expected or unexpected clusters, including the presence of outliers. It examines the distances between the samples in a data set and represents them in a dendrogram which provides similar information as that of PCA results [20]. In HCA, each point forms only one cluster, and then the similarity matrix is analysed. The most similar points are assembled forming one cluster and the process is repeated until all the points belong to only one group [20]. The results obtained from MCF-7 cells are presented in the dendrogram (Figure 5). Vertical lines in the dendrogram represent the compounds while the horizontal lines represent the distances between compounds within the same group or from compounds of other groups. According to the distances, the compounds are subdivided into highly and weakly active groups and this classification is similar to those obtained from PCA and MLR analysis.

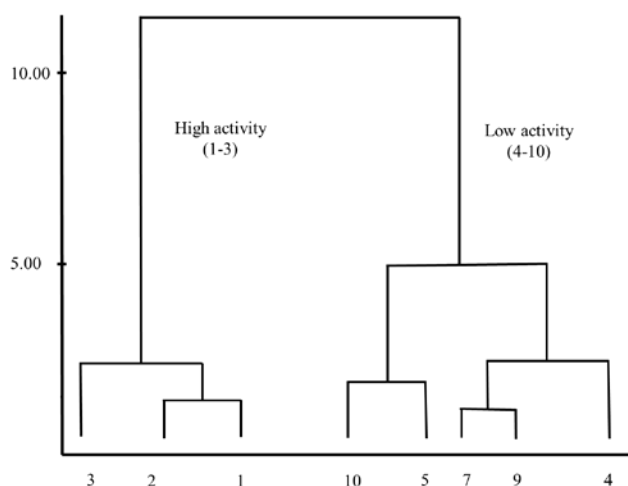


Figure 5. Dendrogram obtained from HCA of cytotoxicity of compounds from *C. zedoaria*.

3. Experimental Section

3.1. Extraction and Isolation of Compounds from *C. zedoaria*

Characterization of the isolated compounds (Figure 1) from *C. zedoaria* was performed by extensive spectroscopic studies including 1D, 2D NMR spectroscopy, GC, GC-MS analysis, and

compared with those reported in literature [21–24]. ^1H and ^{13}C NMR spectra of the isolated compounds (Figure 1) can be found in the supplementary data file. These compounds can be classified as labdane type diterpenes (**1–3**), germacrane type sesquiterpenes (**4–11**), guaiane type sesquiterpenes (**12–15**), elemene type sesquiterpenes (**16**), humulane type sesquiterpenes (**17**), cadinane type sesquiterpenes (**18**), carabran type sesquiterpenes (**19**), spiro lactone type sesquiterpenes (**20**), and a *seco*-guaiane type sesquiterpene (**21**).

3.2. Theoretical Calculations

Energy minimization and 3D structure optimization of the compounds were done by popular Becke three parameter Lee-Yang-Parr (B3LYP) exchange-correlation hybrid functional combined with a double- ζ Pople-type basis set 6-31+G (d,p), in which polarized and diffuse functions are taken into consideration [25]. B3LYP hybrid functional includes a mixture of Hartree-Fock exchange (20% of HF) with DFT exchange-correlation functional. The frequency analyses were carried out at the same level of theory. The absence of imaginary frequencies confirmed that the structures are true minima on the potential energy surface. The choice of the hybrid functional B3LYP is based on previous QSAR studies [26,27]. Recently, we successfully applied the hybrid functional B3P86 to calculate the electronic and structural descriptors for a series of phenolic Schiff bases [28].

The chemical descriptors selected to correlate with cytotoxic activity are: (i) electronic descriptors: frontier molecular orbital energies (E_{HOMO} , E_{LUMO} , which are well accepted as molecular descriptors in medicinal chemistry, since they are linked to the capacity of a molecule to form charge transfer complex with its biological receptor), ionization potential (IP), electronic affinity (EA), electronegativity (χ), hardness (η), softness (S), electrophilicity index (ω), dipole moment (μ), molecular polarizability (α); (ii) steric descriptors: surface area of a molecule (A), volume (V) and its molecular weight (M); and (iii) hydrophobicity descriptor: $\log P$, where P stands for the octanol-water partition coefficient. The calculations of $\log P$ were carried out using Hyperchem Molecular package [29] by means of the atomic parameters derived by Ghose, Pritchett and Crippen and later extended by Ghose and co-workers [30,31]. The other descriptors were calculated using the DFT method and obtained in two different ways: (i) Orbital consideration, which is based on Koopman's theorem where $\text{IP} = -E_{\text{HOMO}}$ and $\text{EA} = -E_{\text{LUMO}}$ [32]; and (ii) energy consideration, which is based on the use of the classical finite difference approximation, where the change of one electron is usually involved $\Delta N = \pm 1$ [33]. In this method, $\text{IP} = E_{+1} - E_0$ and $\text{EA} = E_0 - E_{-1}$ where E_0 , E_{-1} and E_{+1} are the electronic energies of neutral molecule, when adding and removing an electron to the neutral molecule, respectively. In addition to methods (i) and (ii), the electronic descriptors (e.g., hardness) can be calculated using internally resolved hardness tensor (IRHT) approach [34–36], which deals with the fractional occupation numbers based on Janak's extension of DFT [37]. This approach is also based on orbital energies and takes into account the fractional occupation numbers based on Janak's extension of DFT [37]. De Luca *et al.* used the above approaches to investigate the solvent effects on the hardness values of a series of neutral and charged molecules, and found that these three methods can give similar results in the presence of solvent [38].

The solvent effects were taken into account implicitly by using the polarizable continuum model (PCM) as implemented in the Gaussian 09 package [39]. In PCM, the solute is embedded into a cavity

surrounded by solvent described by its dielectric constant ϵ (e.g., for methanol $\epsilon = 32.6$) [40]. The use of an explicit solvent has been investigated notably by Guerra *et al.*, who obtained a better description of the electronic properties using PCM compared to the explicit solvent [41]. A hybrid model was tested by Trouillas *et al.* [42]. The authors showed that only slight differences can be observed as compared to PCM. All theoretical calculations including ground state geometry optimization and frequency analysis calculations were performed with Gaussian 09 package [39].

Simple and multiple linear regression (SLR and MLR, respectively) analyses were used to determine regression equations, correlation coefficients R^2 , adjusted R^2 and standard deviations (SD). PCA and HCA were employed to reduce dimensionality and investigate the subset of descriptors that could be more effective for classifying the isolated compounds according to their degree of cytotoxicity against tumour cells.

The regression models and statistical analyses of obtained results were carried out by using DataLab package [43].

4. Conclusions

In the present study, a set of electronic, steric and hydrophobicity descriptors were analysed using DFT quantum chemical calculations for a series of 21 compounds from *C. zedoaria* to determine the effect of the descriptors towards their cytotoxic activity against four different types of cancer cells (MCF-7, Ca Ski, PC-3 and HT-29), as well as a normal cell line (HUVEC). The statistical analyses showed that the influence of individual descriptor on the cytotoxicity of these compounds is not significant with an R^2 less than 50% and a standard deviation higher than 0.20. The results also showed that the cytotoxicity of the compounds towards a given cell line rather depends on a set of certain descriptors. MLR, PCA and HCA allowed us to define the cytotoxicity of the compounds as high, moderate, and low based on their cytotoxicity.

Acknowledgments

Authors thank (i) Mohamad Safwan bin Jusof for help to give access to supercomputer (PTMLXSMP, University of Malaya) (ii) and Federico Gago (Departamento de Farmacología, Universidad de Alcalá, 28871 Alcalá de Henares, Madrid, Spain) for his help to improve this paper. The authors thank University of Malaya for financial support through grant numbers UMRP (CRP001-1012A), UM-MOHE UM.C/625/1/HIR/MOHE/SC/02 and UM-MOHE UM.C/625/1/HIR/MOHE/SC/09. The authors thank French National Center for Scientific Research CNRS for financial support through grant numbers grant (57-02-03-1007).

Supplementary Materials

Supplementary materials can be found at <http://www.mdpi.com/1422-0067/16/05/9450/s1>.

Author Contributions

Khalijah Awang, El Hassane Anouar and Omer Abdalla Ahmed Hamdi designed the research. The isolation and identification of the compounds were performed by Omer Abdalla Ahmed Hamdi and

Khalijah Awang. The cytotoxicity tests were performed by Omer Abdalla Ahmed, Sri Nurestri A. Malek and Syarifah Nur Syed Abdul Rahman. The quantum chemical calculations and QSAR studies were performed by El Hassane Anouar, Zuhra Bashir Khalifa Al Trabolsy and Nur Shahidatul Shida Zakaria. The statistical analyses were performed by El Hassane Anouar and Sharifuddin Bin Md Zain. Mohd Zulkefeli, Jean-Frédéric F. Weber, Jamil A. Shilpi analyzed the data. The manuscript wrote by El Hassane Anouar, Omer Abdalla Ahmed Hamdi, Khalijah Awang and Jamil A. Shilpi. All authors read and approved the final manuscript.

Conflicts of Interest

The authors declare no conflict of interest.

References

1. Lobo, R.; Prabhu, K.S.; Shirwaikar, A.; Shirwaikar, A. *Curcuma zedoaria* Rosc. (white turmeric): A review of its chemical, pharmacological and ethnomedicinal properties. *J. Pharm. Pharmacol.* **2009**, *61*, 13–21.
2. Wilson, B.; Abraham, G.; Manju, V.; Mathew, M.; Vimala, B.; Sundaresan, S.; Nambisan, B. Antimicrobial activity of *Curcuma zedoaria* and *Curcuma malabarica* tubers. *J. Ethnopharmacol.* **2005**, *99*, 147–151.
3. Nadkarni, K.M. *Indian Materia Medica*; Popular Prakashan: Mumbai, India, 1996; Volume 1.
4. Etoh, H.; Kondoh, T.; Yoshioka, N.; Sugiyama, K.; Ishikawa, H.; Tanaka, H. 9-Oxo-neoprocucumenol from *Curcuma aromatica* (Zingiberaceae) as an attachment inhibitor against the blue mussel, *Mytilus edulis galloprovincialis*. *Biosci. Biotechnol. Biochem.* **2003**, *67*, 911–913.
5. Yoshioka, T.; Fujii, E.; Endo, M.; Wada, K.; Tokunaga, Y.; Shiba, N.; Hohsho, H.; Shibuya, H.; Muraki, T. Antiinflammatory potency of dehydrocurdione, a zedoary-derived sesquiterpene. *Inflamm. Res.* **1998**, *47*, 476–481.
6. Larsen, K.; Ibrahim, H.; Khaw, S.; Saw, L. *Gingers of Peninsular Malaysia and Singapore*; Natural History Publications: Borneo, Malaysia, 1999.
7. Souza, J., Jr.; de Almeida Santos, R.H.; Ferreira, M.M.C.; Molfetta, F.A.; Camargo, A.J.; Maria Honório, K.; da Silva, A.B.F. A quantum chemical and statistical study of flavonoid compounds (flavones) with anti-HIV activity. *Eur. J. Med. Chem.* **2003**, *38*, 929–938.
8. Kikuchi, O. Systematic QSAR procedures with quantum chemical descriptors. *Quant. Struct. Act. Relatsh.* **1987**, *6*, 179–184.
9. Dugas, A.J., Jr.; Castaneda-Acosta, J.; Bonin, G.C.; Price, K.L.; Fischer, N.H.; Winston, G.W. Evaluation of the total peroxy radical-scavenging capacity of flavonoids: Structure-activity relationships. *J. Nat. Prod.* **2000**, *63*, 327–331.
10. Camargo, A.; Mercadante, R.; Honório, K.; Alves, C.; Da Silva, A. A structure-activity relationship (SAR) study of synthetic neolignans and related compounds with biological activity against *Escherichia coli*. *Comp. Theor. Chem.* **2002**, *583*, 105–116.
11. Alves, C.N.; Macedo, L.G.D.; Honório, K.M.; Camargo, A.J.; Santos, L.S.; Jardim, I.N.; Barata, L.E.; Silva, A.B.D. A structure-activity relationship (SAR) study of neolignan compounds with anti-schistosomiasis activity. *J. Braz. Chem. Soc.* **2002**, *13*, 300–307.

12. Lameira, J.; Medeiros, I.; Reis, M.; Santos, A.; Alves, C. Structure–activity relationship study of flavone compounds with anti-HIV-1 integrase activity: A density functional theory study. *Bioorg. Med. Chem.* **2006**, *14*, 7105–7112.
13. Yang, H.-L.; Huang, F.-R. Quantum chemical and statistical study of hypocrellin dyes with phototoxicity against tumor cells. *Dyes Pigment.* **2007**, *74*, 416–423.
14. Ishihara, M.; Wakabayashi, H.; Motohashi, N.; Sakagami, H. Quantitative structure-cytotoxicity relationship of newly synthesized tropolones determined by a semiempirical molecular-orbital method (PM5). *Anticancer Res.* **2010**, *30*, 129–133.
15. Stanchev, S.; Momekov, G.; Jensen, F.; Manolov, I. Synthesis, computational study and cytotoxic activity of new 4-hydroxycoumarin derivatives. *Eur. J. Med. Chem.* **2008**, *43*, 694–706.
16. Yang, H.L.; Chen, G.H.; Li, Y.Q. A quantum chemical and statistical study of ganoderic acids with cytotoxicity against tumor cell. *Eur. J. Med. Chem.* **2005**, *40*, 972–976.
17. Ishihara, M.; Yokote, Y.; Sakagami, H. Quantitative structure-cytotoxicity relationship analysis of coumarin and its derivatives by semiempirical molecular orbital method. *Anticancer Res.* **2006**, *26*, 2883–2886.
18. Hamdi, O.A.A.; Syed Abdul Rahman, S.N.; Awang, K.; Abdul Wahab, N.; Looi, C.Y.; Thomas, N.F.; Abd Malek, S.N. Cytotoxic constituents from the rhizomes of *Curcuma zedoaria*. *Sci. World J.* **2014**, *2014*, 1–11.
19. Johnson, R.A.; Wichern, D.W. *Applied Multivariate Statistical Analysis*; Prentice Hall: Upper Saddle River, NJ, USA, 2002; Volume 5.
20. Kowalski, B.; Bender, C. Pattern recognition. Powerful approach to interpreting chemical data. *J. Am. Chem. Soc.* **1972**, *94*, 5632–5639.
21. Xu, F.; Nakamura, S.; Qu, Y.; Matsuda, H.; Pongpiriyadacha, Y.; Wu, L.; Yoshikawa, M. Structures of new sesquiterpenes from *Curcuma comosa*. *Chem. Pharm. Bull.* **2008**, *56*, 1710–1716.
22. Firman, K.; Kinoshita, T.; Itai, A.; Sankawa, U. Terpenoids from *Curcuma heyneana*. *Phytochemistry* **1988**, *27*, 3887–3891.
23. Giang, P.M.; Son, P.T. Isolation of sesquiterpenoids from the rhizomes of Vietnamese *Curcuma aromatica* Salisb. *Tap. Chi. Hoa. Hoc.* **2000**, *38*, 96–99.
24. Kuroyanagi, M.; Ueno, A.; Koyama, K.; Natori, S. Structures of sesquiterpenes of *Curcuma aromatica* Salisb. II. Studies on minor sesquiterpenes. *Chem. Pharm. Bull.* **1990**, *38*, 55–58.
25. Becke, A.D. A new mixing of Hartree-Fock and local-density-functional theories. *J. Chem. Phys.* **1993**, *98*, 1372–1377.
26. Mendes, A.P.; Borges, R.S.; Neto, A.M.C.; de Macedo, L.G.; da Silva, A.B. The basic antioxidant structure for flavonoid derivatives. *J. Mol. Model.* **2012**, *18*, 4073–4080.
27. Sarkar, A.; Middya, T.R.; Jana, A.D. A QSAR study of radical scavenging antioxidant activity of a series of flavonoids using DFT based quantum chemical descriptors—The importance of group frontier electron density. *J. Mol. Model.* **2012**, *18*, 2621–2631.
28. Anouar, E.H. A quantum chemical and statistical study of phenolic Schiff bases with antioxidant activity against DPPH free radical. *Antioxidants* **2014**, *3*, 309–322.
29. *HyperChem: Release 7.52 for Windows*; Hypercube Inc.: Gainesville, FL, USA, 2002.

30. Ghose, A.K.; Pritchett, A.; Crippen, G.M. Atomic physicochemical parameters for three dimensional structure directed quantitative structure-activity relationships III: Modeling hydrophobic interactions. *J. Comput. Chem.* **1988**, *9*, 80–90.
31. Viswanadhan, V.N.; Ghose, A.K.; Revankar, G.R.; Robins, R.K. Atomic physicochemical parameters for three dimensional structure directed quantitative structure-activity relationships. 4. Additional parameters for hydrophobic and dispersive interactions and their application for an automated superposition of certain naturally occurring nucleoside antibiotics. *J. Chem. Inf. Comput. Sci.* **1989**, *29*, 163–172.
32. Koopmans, T. Über die Zuordnung von Wellenfunktionen und Eigenwerten zu den einzelnen Elektronen eines Atoms. *Physica* **1934**, *1*, 104–113.
33. Parr, R.G.; Yang, W. *Density-Functional Theory of Atoms and Molecules*; Oxford University Press: New York, NY, USA, 1989; Volume 16.
34. Neshev, N.; Mineva, T. The role of interelectronic interaction in transition metal oxide catalysts. In *Metal-Ligand Interactions*; Springer: Dordrecht, The Netherlands, 1996; pp. 361–405.
35. Grigorov, M.; Weber, J.; Chermette, H.; Tronchet, J.M. Numerical evaluation of the internal orbitally resolved chemical hardness tensor in density functional theory. *Int. J. Quantum Chem.* **1997**, *61*, 551–562.
36. Mineva, T.; Sicilia, E.; Russo, N. Density-functional approach to hardness evaluation and its use in the study of the maximum hardness principle. *J. Am. Chem. Soc.* **1998**, *120*, 9053–9058.
37. Janak, J. Proof that $\partial E / \partial n_i = \epsilon$ in density-functional theory. *Phys. Rev. B* **1978**, *18*, 7165–7168.
38. De Luca, G.; Sicilia, E.; Russo, N.; Mineva, T. On the hardness evaluation in solvent for neutral and charged systems. *J. Am. Chem. Soc.* **2002**, *124*, 1494–1499.
39. Frisch, M.J.; Trucks, G.W.; Schlegel, H.B.; Scuseria, G.E.; Robb, M.A.; Cheeseman, J.R.; Scalmani, G.; Barone, V.; Mennucci, B.; Petersson, G.A.; *et al.* *Gaussian 09, Revision A.02*; Gaussian, Inc.: Wallingford, CT, USA, 2009.
40. Tomasi, J.; Mennucci, B.; Cammi, R. Quantum mechanical continuum solvation models. *Chem. Rev.* **2005**, *105*, 2999–3093.
41. Guerra, M.; Amorati, R.; Pedulli, G.F. Water effect on the O–H Dissociation enthalpy of para-substituted phenols: A DFT Study. *J. Org. Chem.* **2004**, *69*, 5460–5467.
42. Kozłowski, D.; Trouillas, P.; Calliste, C.; Marsal, P.; Lazzaroni, R.; Duroux, J.L. Density functional theory study of the conformational, electronic, and antioxidant properties of natural chalcones. *J. Phys. Chem. A* **2007**, *111*, 1138–1145.
43. DataLab-Version 2.701. Available online: http://www.lohninger.com/datalab/en_home.html (accessed on 18 November 2013).

Article

Spectrofluorometric and Molecular Docking Studies on the Binding of Curcumenol and Curcumenone to Human Serum Albumin

Omer Abdalla Ahmed Hamdi ¹, Shevin Rizal Feroz ², Jamil A. Shilpi ³, El Hassane Anouar ⁴, Abdul Kadir Mukarram ², Saharuddin B. Mohamad ², Saad Tayyab ² and Khalijah Awang ^{1,3,*}

¹ Department of Chemistry, Faculty of Science, University of Malaya, 50603 Kuala Lumpur, Malaysia; E-Mail: omerhamdi2001@hotmail.com

² Institute of Biological Sciences, Faculty of Science, University of Malaya, 50603 Kuala Lumpur, Malaysia; E-Mails: shevrzl@gmail.com (S.R.F.); ak.mukarram@yahoo.com (A.K.M.); saharuddin@um.edu.my (S.B.M.); saadtayyab2004@um.edu.my (S.T.)

³ Center of Natural products and Drug Discovery (CENAR), University of Malaya, 50603 Kuala Lumpur, Malaysia; E-Mail: jamilshilpi@yahoo.com

⁴ Atta-ur-Rahman Institute for Natural Product Discovery, Universiti Teknologi MARA, Kampus Puncak Alam, 42300 Bandar Puncak Alam, Malaysia; E-Mail: anouarelhassane@yahoo.fr

* Author to whom correspondence should be addressed; E-Mail: Khalijah@um.edu.my; Tel.: +603-7967-4064; Fax: +603-7967-4193.

Academic Editor: Jesus De Julián Ortiz

Received: 6 November 2014 / Accepted: 9 January 2015 / Published: 6 March 2015

Abstract: Curcumenol and curcumenone are two major constituents of the plants of medicinally important genus of *Curcuma*, and often govern the pharmacological effect of these plant extracts. These two compounds, isolated from *C. zedoaria* rhizomes were studied for their binding to human serum albumin (HSA) using the fluorescence quench titration method. Molecular docking was also performed to get a more detailed insight into their interaction with HSA at the binding site. Additions of these sesquiterpenes to HSA produced significant fluorescence quenching and blue shifts in the emission spectra of HSA. Analysis of the fluorescence data pointed toward moderate binding affinity between the ligands and HSA, with curcumenone showing a relatively higher binding constant ($2.46 \times 10^5 \text{ M}^{-1}$) in comparison to curcumenol ($1.97 \times 10^4 \text{ M}^{-1}$). Cluster analyses revealed that site I is the preferred binding site for both molecules with a minimum binding energy of $-6.77 \text{ kcal} \cdot \text{mol}^{-1}$. However, binding of these two molecules to site II cannot be ruled out

as the binding energies were found to be -5.72 and -5.74 kcal·mol⁻¹ for curcumenol and curcumenone, respectively. The interactions of both ligands with HSA involved hydrophobic interactions as well as hydrogen bonding.

Keywords: *Curcuma zedoaria*; sesquiterpene; human serum albumin; protein-ligand interaction; molecular docking; fluorescence spectroscopy

1. Introduction

Curcuma zedoaria (Christm.) Rosc. (Zingiberaceae), also known as “white turmeric” is a perennial herb, largely found in tropical countries including Malaysia, Indonesia, India and Thailand [1]. In Malaysia, it is known as “temu putih” and is widely consumed as spice, flavoring agent for native dishes and an additive in food preparations for women in confinement after child birth [2,3]. It is extensively used in folk medicine for the treatment of menstrual disorders, dyspepsia, vomiting, and blood stagnation [1,4,5]. The plant is also used in the practice of traditional Chinese medicine for the treatment of cervical cancer [6].

The rhizomes of *C. zedoaria* are considered as a rich source of bioactive sesquiterpenes [7]. Curcumenol (**A**) and curcumenone (**B**) (Figure 1) are two of the most important sesquiterpenes possessing a number of beneficial biological activities. Curcumenol, a guaiane type sesquiterpene is known to exhibit analgesic [8], cytotoxic [9,10], hepatoprotective [11] and antimicrobial [12] properties, while curcumenone, a caraborane type sesquiterpene has been reported to be a vasorelaxant [13], hepatoprotective [11] and an effective inhibitor of intoxication [14].

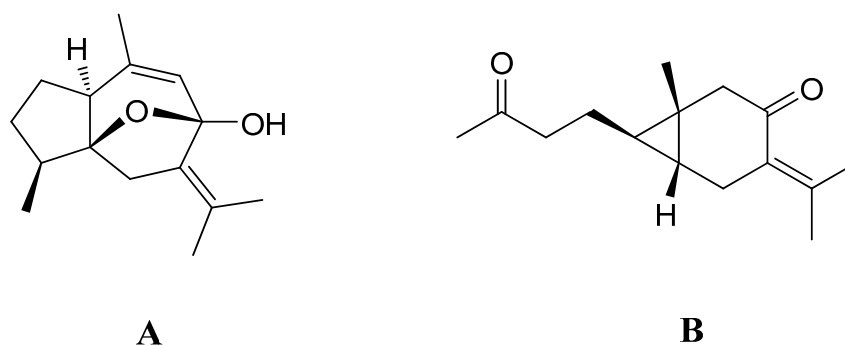


Figure 1. Chemical structures of curcumenol (**A**) and curcumenone (**B**).

Human serum albumin (HSA) serves as the primary transport protein in the human circulation capable of binding reversibly both endogenous and exogenous ligands such as fatty acids, hormones and drugs. It consists of 585 amino acids in a single polypeptide chain [15]. Crystallographic data has shown the presence of three homologous domains (I, II, and III), each comprised of subdomains A and B. The two high affinity ligand binding sites on HSA, known as Sudlow’s site I and II, are located in subdomains IIA and IIIA, respectively [16].

The interaction of a compound with serum albumin is known to influence its bioavailability, distribution, metabolism and elimination from the body. In particular, the affinity between a protein

and a ligand affects the concentrations of the free and bound forms of the ligand as well as the duration of its half-life, which consequently determine its efficacy [15]. Therefore, investigations on the interaction of serum albumin with bioactive ligands may provide valuable information concerning their therapeutic efficacies [17].

Being the major and active constituents of *C. zedoaria*, curcumenol and curcumenone play important roles in exerting pharmacological activities after consumption of the herb. As the key components of a widely used natural product, curcumenol and curcumenone require the determination of pharmacokinetic parameters to establish their safety and efficacy. Furthermore, binding studies to HSA provide valuable parameters toward the establishment of the pharmacokinetic profile of such agents. In light of the above, the present report describes the binding properties of curcumenol and curcumenone to HSA based on fluorescence spectroscopic and molecular docking results.

2. Results and Discussion

2.1. Quenching Mechanism

Interactions between small ligands and macromolecules such as proteins have been widely investigated using fluorescence spectroscopy. Quenching of the protein fluorescence as well as shift in the emission maximum in the presence of a ligand can indicate a number of phenomena including complex formation, random collisions, energy transfer and excited state reactions [18–20]. Figure 2 shows intrinsic fluorescence spectra of HSA in the wavelength range, 300–400 nm upon excitation at 280 nm, obtained in the absence and the presence of increasing curcumenol and curcumenone concentrations. Addition of increasing concentrations of these ligands to HSA produced progressive decrease in the fluorescence intensity and significant blue shift in the emission maximum, suggesting interactions between these compounds and HSA. About 40% decrease in the fluorescence intensity at 338 and 2 nm blue shift were observed at the highest curcumenol concentration (60 μ M), used in this study. On the other hand, curcumenone produced ~50% quenching in HSA fluorescence intensity, which was accompanied by a 6 nm blue shift in the emission maximum at the same ligand concentration. The shift in the emission maximum of HSA towards shorter wavelength suggested increased hydrophobicity in the microenvironment of the protein fluorophores upon interaction with these compounds [21]. It seems probable that ligand binding triggered the movement of hydrophobic residues in the vicinity of the fluorophores (Tyr and Trp), particularly around lone Trp-214, which is located in the vicinity of Sudlow's site I [15]. It is important to note that Trp fluorescence makes major contribution in the protein fluorescence due to the presence of the emission maximum around 338 nm [21]. This has been supported by our docking results in which about half of the residues lining the binding pocket are purely hydrophobic in nature. Furthermore, other lining residues such as Lys (4 CH₂ groups), Arg (3 CH₂ groups), Tyr (benzene ring), Gln (2 CH₂ groups) also contribute towards hydrophobicity of the binding pocket. Presence of hydrophobic milieu in the binding pocket makes favorable contribution in the ligand binding phenomenon as hydrogen bonds formed in the nonpolar environment seem to be much stronger.

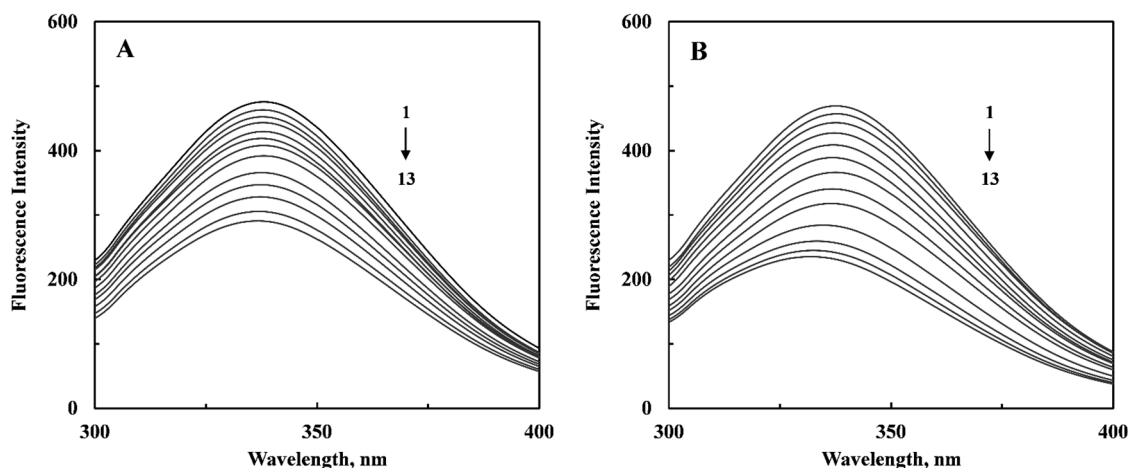


Figure 2. Emission spectra of human serum albumin (HSA) in the absence and the presence of increasing curcumenol (A) and curcumenone (B) concentrations, obtained in 20 mM sodium phosphate buffer, pH 7.4 upon excitation at 280 nm. [HSA] = 3 μ M, [Ligand] = (1–13): 0, 3, 6, 9, 12, 15, 18, 24, 30, 37.5, 45, 52.5 and 60 μ M. T = 25 $^{\circ}$ C.

Although quenching of protein fluorescence can be regarded as an indication of binding between a compound and the protein, it is equally probable that the quenching phenomenon was due to collisions between the quencher molecule and the protein [21]. These two mechanisms of fluorescence quenching are known as static and collisional quenching, respectively, and can be differentiated by the bimolecular quenching constant, k_q value, associated with the quenching process [21]. As a general rule, the k_q value for a diffusion-controlled phenomenon typically falls in the region of $10^{10} \text{ M}^{-1} \cdot \text{s}^{-1}$, while higher k_q value indicates a binding reaction [21]. Figure 3 displays Stern-Volmer plots of the ligand–HSA systems, obtained after analyzing the quenching data using Equation (1). The resulting K_{SV} and k_q values for the interaction of both curcumenol and curcumenone with HSA are listed in Table 1. As can be seen, the k_q values obtained were two orders of magnitude higher than the value expected for a process following the collisional quenching mechanism. This suggested that the quenching of HSA by curcumenol and curcumenone was governed by the static quenching mechanism, which involved the formation of a ground state complex between the ligands and HSA.

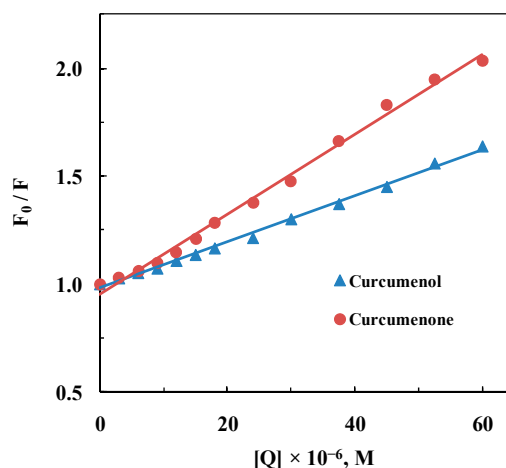


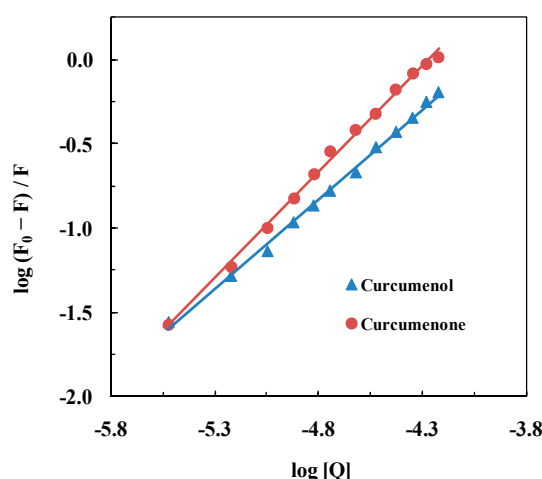
Figure 3. Stern-Volmer plots for the quenching of HSA fluorescence by curcumenol and curcumenone.

Table 1. Quenching and binding parameters for curcumenol-/curcumenone-HSA interactions, as obtained in 20 mM sodium phosphate buffer, pH 7.4 at 25 °C.

Parameter	Curcumenol	Curcumenone
K_{SV}, M^{-1}	1.07×10^4	1.85×10^4
$k_q, M^{-1} \cdot s^{-1}$	1.67×10^{12}	2.90×10^{12}
K_b, M^{-1}	1.97×10^4	2.46×10^5
n	1.07	1.26

2.2. Binding Parameters

The binding constant (K_b) for the ligand–HSA interaction and the number of binding sites (n) on the protein for these ligands were determined from the double logarithmic plots of $\log (F_0 - F)/F$ versus $\log [Q]$ (Figure 4). The values of n and K_b were obtained from the slope and the y-intercept of these plots, respectively, and are listed in Table 1. The values of K_b , obtained for the interaction of curcumenol and curcumenone with HSA revealed intermediate affinity between these ligands and the protein. This was comparable to other ligand binding studies involving HSA [11,20,22,23]. It is worth noting that higher extent of quenching of HSA fluorescence by curcumenone was also reflected by its higher K_b ($2.46 \times 10^5 M^{-1}$) value in comparison to that obtained for the curcumenol–HSA system ($1.97 \times 10^4 M^{-1}$). Interestingly, the value of n for the interaction of curcumenone with HSA was noticeably higher (1.26) compared to that (1.07) of curcumenol. There seems to be a higher likelihood of curcumenone to bind to other site(s) on the protein molecule in addition to its primary binding site. However, a slight difference in the value of “ n ” cannot be taken to clearly differentiate cooperative phenomenon with respect to curcumenone binding as double log Stern-Volmer equation suffers from several pitfalls.

**Figure 4.** Double logarithmic plots for the interaction of HSA with curcumenol and curcumenone.

2.3. Molecular Docking

In order to predict the binding modes of curcumenol and curcumenone to the two main ligand binding sites of HSA (site I and site II), docking simulations of the interaction between these ligands

and HSA were carried out. For each binding site, 100 docking simulations and clustering analysis at a root-mean-square deviation tolerance of 2.0 Å were performed. The docking analysis of 1BM0-curcumenol complex at the binding site I revealed a total of eight (8) multimember conformation clusters (Figure 5A) with the mean binding energy of $-6.40 \text{ kcal}\cdot\text{mol}^{-1}$. The highest populated cluster had 29 out of 100 conformations. However, the configuration with the lowest binding energy ($-6.77 \text{ kcal}\cdot\text{mol}^{-1}$) was not a member of the highest populated cluster. At the binding site II (Figure 5B), six (6) multimember conformation clusters, possessing mean binding energy of $-5.53 \text{ kcal}\cdot\text{mol}^{-1}$ were identified, with the highest populated cluster having 72 members out of 100 conformations. Although the lowest binding energy configuration ($-5.72 \text{ kcal}\cdot\text{mol}^{-1}$) was a member of the highest populated cluster, its binding energy was higher compared to the lowest binding energy configuration at site I ($-6.77 \text{ kcal}\cdot\text{mol}^{-1}$). Thus, we predict that site I of HSA would be the preferable binding site of curcumenol to HSA (1BM0).

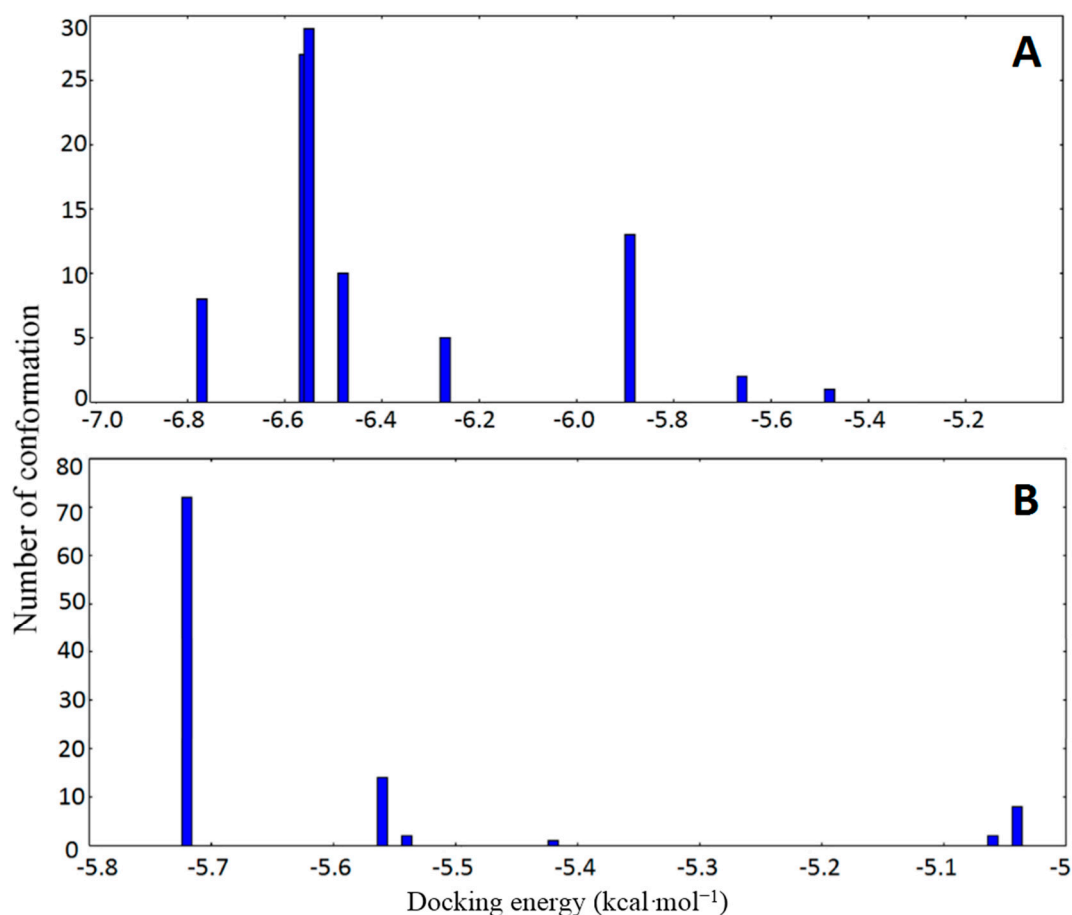


Figure 5. Cluster analyses of the AutoDock docking runs of curcumenol in the drug binding site I (A) and site II (B) of HSA (1BM0).

Clustering analysis of the 1BM0-curcumenone complex (Figure 6) revealed similar clustering pattern for both binding sites, as observed with the 1BM0-curcumenol system. The lowest binding energy conformation for site I of 1BM0-curcumenone was $-6.77 \text{ kcal}\cdot\text{mol}^{-1}$, while that for site II was $-5.74 \text{ kcal}\cdot\text{mol}^{-1}$. These observations also suggested the preference of site I for curcumenone binding to HSA.

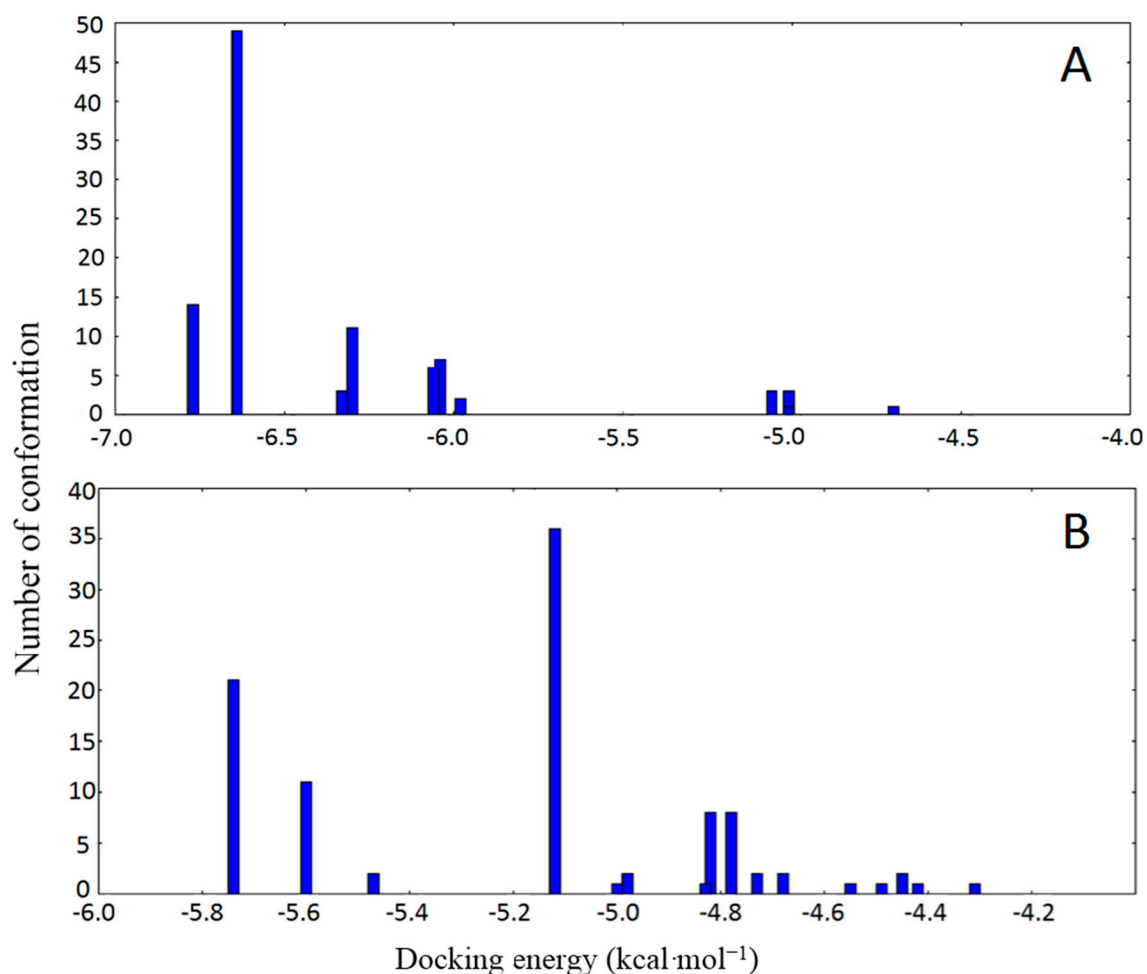


Figure 6. Cluster analyses of the AutoDock docking runs of curcumenone in the drug binding site I (A) and site II (B) of HSA (1BM0).

The predicted binding models of curcumenol and curcumenone with the lowest docking energy ($-6.77 \text{ kcal}\cdot\text{mol}^{-1}$) at site I of HSA were used for binding orientation analysis (Figure 7). Since the cluster analysis also supported the binding of curcumenol and curcumenone at site II of HSA, the lowest docking energy complex for curcumenol ($-5.72 \text{ kcal}\cdot\text{mol}^{-1}$) and curcumenone ($-5.74 \text{ kcal}\cdot\text{mol}^{-1}$) at site II of HSA were also analyzed (Figure 8). The ligand binding sites were defined as amino acid residues within 5 \AA distance of the ligand. In the 1BM0-curcumenol complex at site I, the binding site was found to be located deep within the protein structure in a hydrophobic cleft walled by 18 amino acids: Tyr-150, Lys-195, Gln-196, Lys-199, Leu-219, Arg-222, Asp-237, Leu-238, Val-241, His-242, Arg-257, Leu-260, Ala-261, Lys-286, Ser-287, His-288, Ile-290 and Ala-291. However, in the 1BM0-curcumenone complex at the same site, the binding site was surrounded by 16 amino acids: Tyr-150, Lys-195, Gln-196, Lys-199, Leu-219, Arg-222, Phe-223, Leu-234, Leu-238, His-242, Arg-257, Leu-260, Ile-264, Ser-287, Ile-290 and Ala-291. The 1BM0-curcumenol complex formation at site II involved 14 amino acid residues, namely Leu-394, Leu-398, Lys-402, Phe-403, Asn-405, Ala-406, Val-409, Arg-410, Lys-413, Thr-540, Lys-541, Glu-542, Leu-544 and Lys-545. On the other hand, 1BM0-curcumenone complex at site II was associated with 13 amino acid residues: Leu-398, Lys-402, Phe-403, Asn-405, Ala-406, Leu-407, Val-409, Arg-410, Lys-413, Thr-540, Lys-541, Glu-542, and Lys-545.

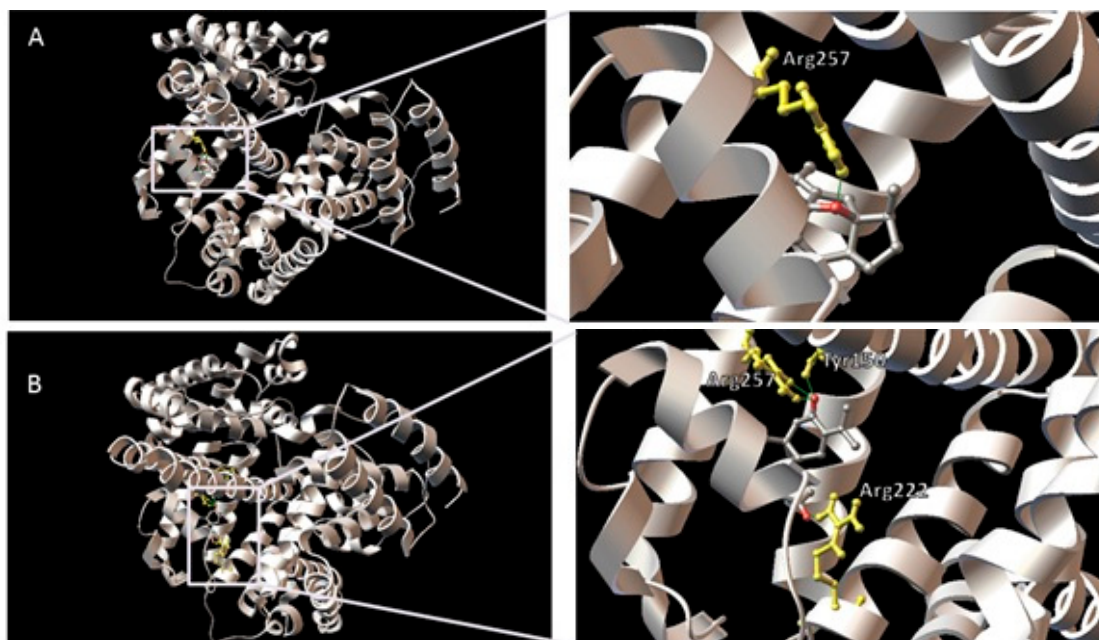


Figure 7. Predicted orientations of the lowest docking energy conformations of 1BM0-ligand complexes. The binding sites were enlarged to show hydrogen bonding (green lines) between amino acid residues and the ligands. Amino acid residues that form hydrogen bonds with the ligands are rendered in ball and stick and colored yellow. (A) Curcumenol in the binding site I of HSA (1BM0); (B) Curcumenone in the binding site I of HSA (1BM0).

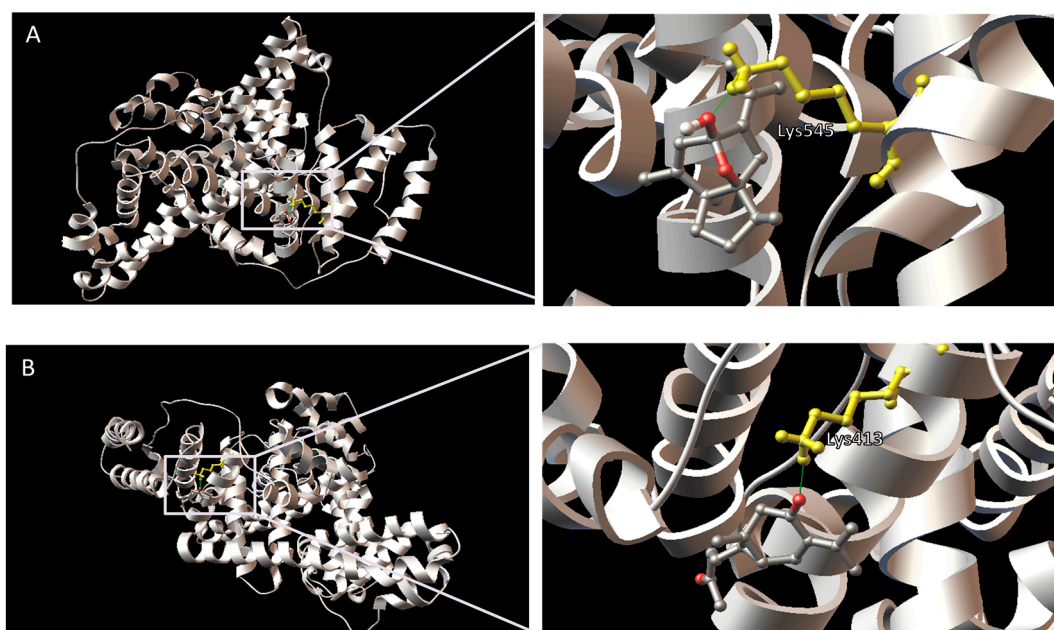


Figure 8. Predicted orientations of the lowest docking energy conformations of 1BM0-ligand complexes. The binding sites were enlarged to show hydrogen bonding (green lines) between amino acid residues and the ligands. Amino acid residues that form hydrogen bonds with the ligands are rendered in ball and stick and colored yellow. (A) Curcumenol in the binding site II of HSA (1BM0); (B) Curcumenone in the binding site II of HSA (1BM0).

Presence of hydrophobic amino acid residues at the binding sites of HSA might have contributed towards the stability of the ligand-HSA complex through hydrophobic interactions. However, the presence of several polar amino acid residues within the proximity of the bound ligands indicated that the interactions between these ligands and HSA at both site I and site II cannot be presumed to be exclusively hydrophobic. Furthermore, in the 1BM0-curcumenol complex docking conformation, one hydrogen bond was predicted involving the hydrogen atom of Arg-257 and the ethereal oxygen atom of curcumenol (Table 2). For the 1BM0-curcumenone complex docking conformation, 4 hydrogen bonds were predicted involving hydrogen atoms from three different amino acid residues of HSA (Tyr-150, Arg-222 and Arg-257) and the oxygen atoms of the acetyl and ketone groups of curcumenone. In contrast, there was only one hydrogen bond in the 1BM0-curcumenone complex at site II, formed by the oxygen atom of curcumenone and the hydrogen atom of Lys-413 (Table 2). Both ligands showed one hydrogen bonding at the binding site. For 1BM0-curcumenol complex at site II, the hydrogen bond formed between the hydrogen atom of Lys-545 and the oxygen atom of hydroxyl group while for 1BM0-curcumenone complex, the hydrogen bond was associated with the hydrogen atom of Lys-413 and oxygen of the ketone group (Table 2).

Table 2. Predicted hydrogen bonds between interacting atoms of the amino acid residues of HSA (1BM0) and the ligands at site I and site II.

Compound	HSA Binding Site	Protein Atom	Ligand Atom	Distance (Å)
Curcumenol	Site I	Arg257:HH22	O (ethereal)	1.907
	Site II	Lys545:HZ3	O (hydroxyl)	1.684
Curcumenone	Site I	Tyr150:HH	O (ketone)	1.907
		Arg222:HH11	O (acetyl)	1.930
		Arg257:HE	O (ketone)	1.969
		Arg257:HH22	O (ketone)	2.236
	Site II	Lys413:HZ3	O (ketone)	2.025

These results suggested that although curcumenol and curcumenone can bind to both sites I and II of HSA, the binding is more preferable at site I. Although, the lowest binding energies for both ligands at site I were the same ($-6.77 \text{ kcal}\cdot\text{mol}^{-1}$) in molecular docking study, the 1BM0-curcumenone complex involved a greater number of hydrogen bonding (four) than that of 1BM0-curcumenol complex (one). This is reflected in the fluorescence quenching assay where curcumenone showed a higher extent of fluorescence quenching compared to curcumenol. Thus, it can be inferred that both curcumenol and curcumenone showed similar HSA binding properties, with curcumenone having a slightly higher affinity towards HSA.

3. Experimental Section

3.1. Materials

Human serum albumin (HSA), essentially fatty acid free was obtained from Sigma-Aldrich Inc. (St. Louis, MO, USA). All other chemicals were of analytical grade purity.

3.2. Isolation and Purification of Curcumenol and Curcumenone

The rhizomes of *C. zedoaria* (1.0 kg) were finely powdered and macerated with *n*-hexane for three days at room temperature, followed by successive extractions with dichloromethane and ethyl acetate, and finally with Soxhlet extraction using methanol. The *n*-hexane extract yielded 24.2 g (2.4%), out of which 20.0 g were subjected to silica gel column chromatography. The elution was performed initially using *n*-hexane followed by *n*-hexane/ethyl acetate gradient. Fractions were then combined according to similarity of the TLC spots to give 21 fractions. Fraction 8 was further purified using preparative thin layer chromatography to give curcumenol (15.5 mg), whereas curcumenone (16.4 mg) was purified from fractions 12 and 13. The structures were established through extensive spectroscopic studies and were found consistent with previous reports [24,25].

3.3. Preparation of Protein and Ligand Solutions

The stock solution of HSA was prepared in 20 mM sodium phosphate buffer, pH 7.4 and its concentration was determined spectrophotometrically using a specific extinction coefficient value of 5.3 at 280 nm [26]. Stock solutions of curcumenol and curcumenone were prepared by dissolving desired quantities of their crystals in ethanol and diluting to the desired concentrations with 20 mM sodium phosphate buffer, pH 7.4.

3.4. Ligand Binding Studies

The interactions of curcumenol and curcumenone with HSA were studied using fluorescence quench titration method [23,27]. The concentration of HSA was maintained at 3 μ M, while the ligand concentrations ranged from 0–60 μ M. The final volume of the reaction mixture was made up to 3 mL with 20 mM sodium phosphate buffer, pH 7.4. The samples were allowed to equilibrate for 30 min prior to fluorescence measurements. The fluorescence spectra of these samples were recorded at 25 °C on a Jasco FP-6500 spectrofluorometer with a 1 cm path length quartz cuvette. Both excitation and emission slits were set at 10 nm, while the scan speed was maintained at 500 nm·min^{−1}. The samples were excited at 280 nm, and the emission spectra were recorded in the wavelength range, 300–400 nm.

3.5. Analysis of the Binding Data

In order to reveal the quenching mechanism of HSA fluorescence, the binding data were analyzed according to the Stern-Volmer equation [21]:

$$F_0/F = K_{SV}[Q] + 1 = k_q\tau_0[Q] + 1 \quad (1)$$

where F_0 and F are the fluorescence intensities of HSA in the absence and the presence of the quencher, respectively, K_{SV} is the Stern-Volmer constant, $[Q]$ is the quencher concentration, k_q is the bimolecular quenching constant and τ_0 is the fluorescence lifetime of free HSA. A value of 6.38×10^{-9} s was used for τ_0 [28].

The binding constant, K_b and the number of binding sites, n for ligand–HSA interactions were determined by treating the fluorescence data according to the following equation (Equation (2)) [18]:

$$\log (F_0 - F)/F = n \log [Q] + \log K_b \quad (2)$$

3.6. Molecular Modelling

The structures of curcumenol and curcumenone were drawn using ACD/ChemSketch Freeware (Advanced Chemistry Development Inc., Toronto, ON, Canada), 3-D optimized and exported as a mol file. The geometry optimization of these structures was refined with the VegaZZ 2.08 [29] batch processing MOPAC script (mopac.r; keywords: MMOK, PRECISE, GEO-OK) using AM1 semiempirical theory [30] and converted and stored as a mol2 file. Molecular docking, visualization and rendering simulation were performed using AutoDock 4.2 [31] and AutoDockTools 1.5.4 [32] at the Academic Grid Malaysia Infrastructure. For the docking study, the curcumenol and curcumenone non-polar hydrogens were merged and the rotatable bonds were defined. The crystal structure of HSA (PDB code 1BM0, res. 2.5 Å) was downloaded from the Protein Data Bank (PDB) [33]. Its water molecules were removed and the atomic coordinates of chain A were stored in a separate file and used as input for AutoDockTools, where polar hydrogens, Kollman charges and solvation parameters were added. The two binding sites (site I and site II) were defined using two grids of $70 \times 70 \times 70$ points each with a grid space of 0.375 Å centered at coordinates $x = 35.26$ $y = 32.41$ $z = 36.46$ for site I and $x = 14.42$ $y = 23.55$ $z = 23.31$ for site II. Lamarckian genetic algorithm with local search (GA-LS) was used as the search engine, with a total of 100 runs for each binding site. In each run, a population of 150 individuals with 27,000 generations and 250,000 energy evaluations were employed. Operator weights for crossover, mutation and elitism were set to 0.8, 0.02 and 1, respectively. For local search default parameters were used. Cluster analysis was performed on docked results using RMS tolerance of 2.0 Å. The protein-ligand complexes were visualized and analyzed using AutoDockTools (The Scripps Research Institute, La Jolla, CA, USA).

4. Conclusions

Curcumenol and curcumenone are well known as plant-derived natural products finding their use in therapeutic applications in recent years. The present investigation provides an insight into the HSA binding properties of these pharmacologically important molecules. Curcumenol and curcumenone showed similar binding characteristics, with the latter having a stronger affinity to HSA. Both compounds bind to site I and site II on HSA, facilitated by hydrophobic forces and hydrogen bonds. The data presented can be useful in the establishment of their pharmacokinetic profiles in the process of future drug development.

Acknowledgments

This work is supported by the University of Malaya Research Grant (UMRP) Malaysia, No. RP 001/2012A.

Author Contributions

Phytochemical work was done by Omer Abdalla Ahmed Hamdi under the supervision of Khalijah Awang, protein binding studies was investigated by Shevin Rizal Feroz under the supervision of Saad Tayyab. El Hassane Anouar and Abdul Kadir Mukarram performed molecular docking under the supervision of Saharuddin B. Mohamad. Omer Abdalla Ahmed Hamdi, Shevin Rizal Feroz

and Jamil A. Shilpi prepared the manuscript and the manuscript was checked by Saad Tayyab, Saharuddin B. Mohamad and Khalijah Awang.

Conflicts of Interest

The authors declare no conflict of interest.

References

1. Lobo, R.; Prabhu, K.S.; Shirwaikar, A.; Shirwaikar, A. *Curcuma zedoaria* Rosc. (white turmeric): A review of its chemical, pharmacological and ethnomedicinal properties. *J. Pharm. Pharmacol.* **2009**, *61*, 13–21.
2. Etoh, H.; Kondoh, T.; Yoshioka, N.; Sugiyama, K.; Ishikawa, H.; Tanaka, H. 9-Oxo-neoprocucumenol from *Curcuma aromatica* (Zingiberaceae) as an attachment inhibitor against the blue mussel, *Mytilus edulis galloprovincialis*. *Biosci. Biotechnol. Biochem.* **2003**, *67*, 911–913.
3. Yoshioka, T.; Fujii, E.; Endo, M.; Wada, K.; Tokunaga, Y.; Shiba, N.; Hohsho, H.; Shibuya, H.; Muraki, T. Antiinflammatory potency of dehydrocurdione, a zedoary-derived sesquiterpene. *Inflamm. Res.* **1998**, *47*, 476–481.
4. Makabe, H.; Maru, N.; Kuwabara, A.; Kamo, T.; Hirota, M. Anti-inflammatory sesquiterpenes from *Curcuma zedoaria*. *Nat. Prod. Res.* **2006**, *20*, 680–685.
5. Wilson, B.; Abraham, G.; Manju, V.S.; Mathew, M.; Vimala, B.; Sundaresan, S.; Nambisan, B. Antimicrobial activity of *Curcuma zedoaria* and *Curcuma malabarica* tubers. *J. Ethnopharmacol.* **2005**, *99*, 147–151.
6. Syu, W.J.; Shen, C.C.; Don, M.J.; Ou, J.C.; Lee, G.H.; Sun, C.M. Cytotoxicity of curcuminoids and some novel compounds from *Curcuma zedoaria*. *J. Nat. Prod.* **1998**, *61*, 1531–1534.
7. Larsen, K.; Ibrahim, H.; Khaw, S.; Saw, L. *Gingers of Peninsular Malaysia and Singapore*; Natural History Publications (Borneo): Kota Kinabalu, Malaysia, 1999.
8. De Fátima Navarro, D.; de Souza, M.M.; Neto, R.A.; Golin, V.; Niero, R.; Yunes, R.A.; Delle Monache, F.; Cechinel Filho, V. Phytochemical analysis and analgesic properties of *Curcuma zedoaria* grown in Brazil. *Phytomedicine* **2002**, *9*, 427–432.
9. Hamdi, O.A.A.; Rahman, S.N.S.A.; Awang, K.; Wahab, N.A.; Looi, C.Y.; Thomas, N.F.; Malek, S.N.A. Cytotoxic constituents from the rhizomes of *Curcuma zedoaria*. *Sci. World J.* **2014**, *2014*, 1–11.
10. Sukari, M.A.H.; Wah, T.S.; Saad, S.M.; Rashid, N.Y.; Rahmani, M.; Lajis, N.H.; Hin, T.Y. Bioactive sesquiterpenes from *Curcuma ochrorhiza* and *Curcuma heyneana*. *Nat. Prod. Res.* **2010**, *24*, 838–845.
11. Matsuda, H.; Ninomiya, K.; Morikawa, T.; Yoshikawa, M. Inhibitory effect and action mechanism of sesquiterpenes from Zedoariae Rhizoma on D-galactosamine/lipopolysaccharide-induced liver injury. *Bioorg. Med. Chem. Lett.* **1998**, *8*, 339–344.
12. Sukari, M.A.H.; Saad, S.M.; Lajis, N.H.; Rahmani, M.; Muse, R.; Yusuf, U.K.; Riyanto, S. Chemical constituents and bioactivity of *Curcuma aeruginosa* Roxb. *Nat. Prod. Sci.* **2007**, *13*, 175–179.

13. Matsuda, H.; Morikawa, T.; Ninomiya, K.; Yoshikawa, M. Absolute stereostructure of carabran-type sesquiterpene and vasorelaxant-active sesquiterpenes from Zedoariae Rhizoma. *Tetrahedron* **2001**, *57*, 8443–8453.
14. Kimura, Y.; Sumiyoshi, M.; Tamaki, T. Effects of the extracts and an active compound curcumenone isolated from *Curcuma zedoaria* rhizomes on alcohol-induced drunkenness in mice. *Fitoterapia* **2013**, *84*, 163–169.
15. Peters, T. *All about Albumin: Biochemistry, Genetics, and Medical Applications*; Academic Press: San Diego, CA, USA, 1996.
16. Carter, D.C.; Ho, J.X. Structure of serum albumin. *Adv. Protein Chem.* **1994**, *45*, 153–203.
17. Yang, F.; Zhang, Y.; Liang, H. Interactive association of drugs binding to human serum albumin. *Int. J. Mol. Sci.* **2014**, *15*, 3580–3595.
18. Ahmad, E.; Rabbani, G.; Zaidi, N.; Singh, S.; Rehan, M.; Khan, M.M.; Rahman, S.K.; Quadri, Z.; Shadab, M.; Ashraf, M.T.; *et al.* Stereo-selectivity of human serum albumin to enantiomeric and isoelectronic pollutants dissected by spectroscopy, calorimetry and bioinformatics. *PLoS One* **2011**, *6*, e26186.
19. Belatik, A.; Hotchandani, S.; Bariyanga, J.; Tajmir-Riahi, H.A. Binding sites of retinol and retinoic acid with serum albumins. *Eur. J. Med. Chem.* **2012**, *48*, 114–123.
20. Varlan, A.; Hillebrand, M. Bovine and human serum albumin interactions with 3-carboxyphenoxathiin studied by fluorescence and circular dichroism spectroscopy. *Molecules* **2010**, *15*, 3905–3919.
21. Lackowicz, J.R. *Principles of Fluorescence Spectroscopy*; Plenum Press: New York, NY, USA, 1983; pp. 111–150.
22. Freitas, P.G.; Barbosa, A.F.; Saraiva, L.A.; Camps, I.; da Silveira, N.J.F.; Veloso, M.P.; Santos, M.H.; Schneedorf, J.M. Mangiferin binding to serum albumin is non-saturable and induces conformational changes at high concentrations. *J. Lumin.* **2012**, *132*, 3027–3034.
23. Feroz, S.R.; Mohamad, S.B.; Bujang, N.; Malek, S.N.A.; Tayyab, S. Multispectroscopic and molecular modeling approach to investigate the interaction of flavokawain B with human serum albumin. *J. Agric. Food Chem.* **2012**, *60*, 5899–5908.
24. Xu, F.; Nakamura, S.; Qu, Y.; Matsuda, H.; Pongpiriyadacha, Y.; Wu, L.; Yoshikawa, M. Structures of new sesquiterpenes from *Curcuma comosa*. *Chem. Pharm. Bull.* **2008**, *56*, 1710–1716.
25. Firman, K.; Kinoshita, T.; Itai, A.; Sankawa, U. Terpenoids from *Curcuma heyneana*. *Phytochemistry* **1988**, *27*, 3887–3891.
26. Wallevik, K. Reversible Denaturation of human serum albumin by pH, temperature, and guanidine hydrochloride followed by optical rotation. *J. Biol. Chem.* **1973**, *248*, 2650–2655.
27. Song, M.; Liu, S.; Yin, J.; Wang, H. Interaction of human serum album and C60 aggregates in solution. *Int. J. Mol. Sci.* **2011**, *12*, 4964–4974.
28. Abou-Zied, O.K.; Al-Shihi, O.I.K. Characterization of subdomain iia binding site of human serum albumin in its native, unfolded, and refolded states using small molecular probes. *J. Am. Chem. Soc.* **2008**, *130*, 10793–10801.
29. Pedretti, A.; Villa, L.; Vistoli, G. VEGA: A versatile program to convert, handle and visualize molecular structure on Windows-based PCs. *J. Mol. Graph. Model.* **2002**, *21*, 47–49.

30. Dewar, M.J.S.; Zoebisch, E.G.; Healy, E.F.; Stewart, J.J.P. Development and use of quantum mechanical molecular models. 76. AM1: A new general purpose quantum mechanical molecular model. *J. Am. Chem. Soc.* **1985**, *107*, 3902–3909.
31. Goodsell, D.S.; Morris, G.M.; Olson, A.J. Automated docking of flexible ligands: Applications of autodock. *J. Mol. Recognit.* **1996**, *9*, 1–5.
32. Sanner, M.F. Python: A programming language for software integration and development. *J. Mol. Graph. Model.* **1999**, *17*, 57–61.
33. Berman, H.M.; Westbrook, J.; Feng, Z.; Gilliland, G.; Bhat, T.N.; Weissig, H.; Shindyalov, I.N.; Bourne, P.E. The protein data bank. *Nucleic Acids Res.* **2000**, *28*, 235–242.

© 2015 by the authors; licensee MDPI, Basel, Switzerland. This article is an open access article distributed under the terms and conditions of the Creative Commons Attribution license (<http://creativecommons.org/licenses/by/4.0/>).

Curcumenol from *Curcuma zedoaria*: a second monoclinic modification

Omer Abdalla Ahmed Hamdi, Khalijah Awang,
A. Hamid A. Hadi, Devi Rosmy Syamsir and Seik Weng Ng*

Department of Chemistry, University of Malaya, 50603 Kuala Lumpur, Malaysia
Correspondence e-mail: seikweng@um.edu.my

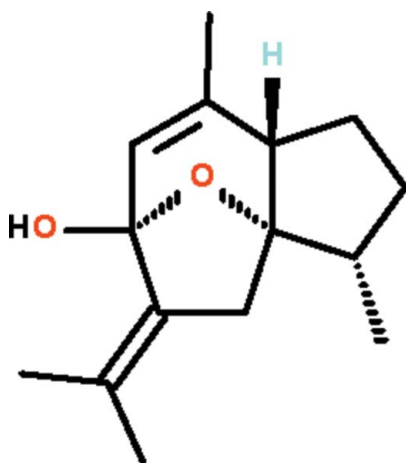
Received 7 October 2010; accepted 10 October 2010

Key indicators: single-crystal X-ray study; $T = 100$ K; mean $\sigma(\text{C}—\text{C}) = 0.003$ Å;
 R factor = 0.037; wR factor = 0.090; data-to-parameter ratio = 10.2.

The title compound, systematic name 9-isopropylidene-2,6-dimethyl-11-oxatricyclo[6.2.1.0^{1,5}]undec-6-en-8-ol, $\text{C}_{15}\text{H}_{22}\text{O}_2$, which crystallizes with two molecules of similar conformation in the asymmetric unit, features three fused rings, two of which are five-membered and the third six-membered. Of the two five-membered rings, the one with an O atom has a distinct envelope shape (with the O atom representing the flap). The six-membered ring is also envelope-shaped as it shares a common O atom with the five-membered ring. In the crystal, the two independent molecules are linked by a pair of $\text{O}—\text{H} \cdots \text{O}$ hydrogen bonds, generating a dimer.

Related literature

For the C2 modification isolated from *Globba malaccensis* Ridl, see: Muangsin *et al.* (2004).



Experimental

Crystal data

$\text{C}_{15}\text{H}_{22}\text{O}_2$
 $M_r = 234.33$
Monoclinic, $P2_1$
 $a = 9.3495$ (7) Å
 $b = 12.535$ (1) Å
 $c = 11.7727$ (9) Å
 $\beta = 96.532$ (1)°

$V = 1370.76$ (18) Å³
 $Z = 4$
Mo $K\alpha$ radiation
 $\mu = 0.07$ mm⁻¹
 $T = 100$ K
 $0.40 \times 0.05 \times 0.05$ mm

Data collection

Bruker SMART APEX
diffractometer
13257 measured reflections

3298 independent reflections
2882 reflections with $I > 2\sigma(I)$
 $R_{\text{int}} = 0.046$

Refinement

$R[F^2 > 2\sigma(F^2)] = 0.037$
 $wR(F^2) = 0.090$
 $S = 1.03$
3298 reflections
323 parameters
1 restraint

H atoms treated by a mixture of
independent and constrained
refinement
 $\Delta\rho_{\text{max}} = 0.21$ e Å⁻³
 $\Delta\rho_{\text{min}} = -0.18$ e Å⁻³

Table 1

Hydrogen-bond geometry (Å, °).

$D—H \cdots A$	$D—H$	$H \cdots A$	$D \cdots A$	$D—H \cdots A$
$\text{O1}—\text{H1} \cdots \text{O4}$	0.89 (3)	1.92 (3)	2.799 (2)	168 (3)
$\text{O3}—\text{H3} \cdots \text{O2}$	0.86 (3)	1.92 (3)	2.771 (2)	171 (3)

Data collection: *APEX2* (Bruker, 2009); cell refinement: *SAINT* (Bruker, 2009); data reduction: *SAINT*; program(s) used to solve structure: *SHELXS97* (Sheldrick, 2008); program(s) used to refine structure: *SHELXL97* (Sheldrick, 2008); molecular graphics: *X-SEED* (Barbour, 2001); software used to prepare material for publication: *pubCIF* (Westrip, 2010).

We thank the University of Malaya for supporting this study.

Supplementary data and figures for this paper are available from the IUCr electronic archives (Reference: HB5676).

References

- Barbour, L. J. (2001). *J. Supramol. Chem.* **1**, 189–191.
- Bruker (2009). *APEX2* and *SAINT*. Bruker AXS Inc., Madison, Wisconsin, USA.
- Muangsin, N., Ngamrojanavich, N., Onanong, S., Chaichit, N., Roengsumran, S. & Petsom, A. (2004). *J. Struct. Chem.* **45**, 293–297.
- Sheldrick, G. M. (2008). *Acta Cryst.* **A64**, 112–122.
- Westrip, S. P. (2010). *J. Appl. Cryst.* **43**, 920–925.

supplementary materials

Acta Cryst. (2010). E66, o2844 [doi:10.1107/S1600536810040559]

Curcumenol from *Curcuma zedoaria*: a second monoclinic modification

O. A. Ahmed Hamdi, K. Awang, A. H. A. Hadi, D. R. Syamsir and S. W. Ng

Comment

Zingerberaceae is a herbaceous plant found in tropical forests that comprises of 52 genera with 1500 species. Most species are found in the South East Asian region. *Curcuma zedoaria*, also known as white turmeric, is a species that is a rich source of terpenoids.

Curcumenol, isolated from *Globba malaccensis* Ridl, belongs to the monoclinic, space group $C2$, with a 16.8467 (4), b 7.6799 (2), c 11.8613 (10) Å and β 115.997 (1) °. This modification is less dense, as noted from its calculated density of 1.28 (Muangsin *et al.*, 2004). The present modification (I), (Fig. 1) shows nearly identical bond dimensions in the two independent molecules. The two molecules form a dimer in the crystal, being linked by two O—H \cdots O hydrogen bonds.

Experimental

The rhizome of *Curcuma zedoaria* was collected from Tawangmangu, Indonesia.

Dried rhizomes (1 kg) were powdered and extracted three times with *n*-hexane and after this, with dichloromethane, ethylacetate, and methanol. The extracts were concentrated under reduced pressure given several fractions.

The *n*-hexane crude extract (20 g) was subjected to column chromatography over silica gel 60(0.063–0.200 mm, 70–230 mesh ASTM) eluted with a mixture of *n*-hexane: ethyl acetate with increasing polarity. Separation by TLC gave 21 fractions.

Fraction 10 (1.41 g) was chromatographed over silica gel (0.040–0.063 mm, mesh 230–400 ASTM) eluted with a gradient solvent system of *n*-hexane: ethyl acetate to give 5 fractions. The second fraction was further purified by high performance thin layer chromatography and using petroleum ether: ethyl acetate: acidified methanol in a 85:14:1 ratio as the developing solvent. Slow evaporation of the solvent gave (I) as colorless prisms.

Refinement

Carbon-bound H-atoms were placed in calculated positions (C—H 0.95 to 0.98 Å) and were included in the refinement in the riding model approximation, with $U(\text{H})$ set to 1.2 to 1.5 $U(\text{C})$.

In the absence of heavy atoms, 2923 Friedel pairs were merged.

The hydroxy H-atoms were located in a difference Fourier map, and were refined without restraints; their U_{iso} values were freely refined.

The absolute configuration was assumed to be that of the $C2$ modification.

Figures

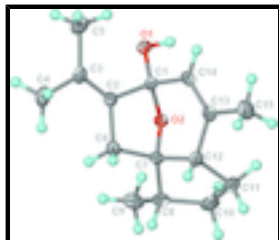


Fig. 1. View of the first molecule of (I) at the 70% probability level; hydrogen atoms are drawn as spheres of arbitrary radius.

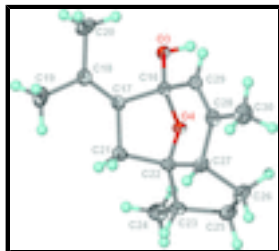


Fig. 2. View of the second molecule of (I) at the 70% probability level; hydrogen atoms are drawn as spheres of arbitrary radius.

9-isopropylidene-2,6-dimethyl-11-oxatricyclo[6.2.1.0^{1,5}]undec-6-en-8-ol

Crystal data

C₁₅H₂₂O₂

M_r = 234.33

Monoclinic, *P*2₁

Hall symbol: P 2yb

a = 9.3495 (7) Å

b = 12.535 (1) Å

c = 11.7727 (9) Å

β = 96.532 (1)°

V = 1370.76 (18) Å³

Z = 4

F(000) = 512

D_x = 1.135 Mg m^{−3}

Mo *K*α radiation, λ = 0.71073 Å

Cell parameters from 3511 reflections

θ = 2.4–27.4°

μ = 0.07 mm^{−1}

T = 100 K

Prism, colorless

0.40 × 0.05 × 0.05 mm

Data collection

Bruker SMART APEX
diffractometer

Radiation source: fine-focus sealed tube
graphite

ω scans

13257 measured reflections

3298 independent reflections

2882 reflections with *I* > 2σ(*I*)

*R*_{int} = 0.046

θ_{max} = 27.5°, θ_{min} = 2.2°

h = −12→12

k = −16→15

l = −15→15

Refinement

Refinement on *F*²

Least-squares matrix: full

Primary atom site location: structure-invariant direct
methods

Secondary atom site location: difference Fourier map

$$R[F^2 > 2\sigma(F^2)] = 0.037$$

$$wR(F^2) = 0.090$$

$$S = 1.03$$

3298 reflections

323 parameters

1 restraint

Hydrogen site location: inferred from neighbouring sites

H atoms treated by a mixture of independent and constrained refinement

$$w = 1/[\sigma^2(F_o^2) + (0.0535P)^2 + 0.0302P]$$

$$\text{where } P = (F_o^2 + 2F_c^2)/3$$

$$(\Delta/\sigma)_{\max} = 0.001$$

$$\Delta\rho_{\max} = 0.21 \text{ e } \text{\AA}^{-3}$$

$$\Delta\rho_{\min} = -0.18 \text{ e } \text{\AA}^{-3}$$

Fractional atomic coordinates and isotropic or equivalent isotropic displacement parameters (\AA^2)

	<i>x</i>	<i>y</i>	<i>z</i>	<i>U</i> _{iso} [*] / <i>U</i> _{eq}
O1	0.24626 (15)	0.50024 (12)	0.49296 (13)	0.0165 (3)
H1	0.268 (3)	0.497 (2)	0.569 (3)	0.033 (7)*
O2	0.06839 (14)	0.62132 (11)	0.52267 (11)	0.0136 (3)
O3	0.03989 (15)	0.49267 (12)	0.71017 (12)	0.0160 (3)
H3	0.045 (3)	0.538 (3)	0.656 (3)	0.043 (9)*
O4	0.28533 (14)	0.46600 (12)	0.72943 (11)	0.0137 (3)
C1	0.2006 (2)	0.60463 (17)	0.47181 (17)	0.0141 (4)
C2	0.1560 (2)	0.62872 (17)	0.34601 (17)	0.0153 (4)
C3	0.2186 (2)	0.59756 (17)	0.25570 (17)	0.0178 (4)
C4	0.1634 (3)	0.6348 (2)	0.13744 (18)	0.0266 (5)
H4A	0.0671	0.6656	0.1381	0.040*
H4B	0.1584	0.5741	0.0846	0.040*
H4C	0.2287	0.6890	0.1125	0.040*
C5	0.3508 (2)	0.52777 (19)	0.2618 (2)	0.0231 (5)
H5A	0.3878	0.5157	0.3421	0.035*
H5B	0.4248	0.5631	0.2226	0.035*
H5C	0.3257	0.4592	0.2248	0.035*
C6	0.0287 (2)	0.70366 (17)	0.34497 (17)	0.0171 (4)
H6A	−0.0595	0.6710	0.3051	0.020*
H6B	0.0476	0.7719	0.3070	0.020*
C7	0.0140 (2)	0.72101 (17)	0.47172 (17)	0.0144 (4)
C8	−0.1354 (2)	0.74213 (18)	0.50599 (18)	0.0188 (4)
H8	−0.1786	0.8026	0.4584	0.023*
C9	−0.2388 (2)	0.6479 (2)	0.4898 (2)	0.0252 (5)
H9A	−0.2524	0.6276	0.4089	0.038*
H9B	−0.3317	0.6681	0.5145	0.038*
H9C	−0.1987	0.5874	0.5356	0.038*
C10	−0.1057 (2)	0.7814 (2)	0.62979 (19)	0.0231 (5)
H10A	−0.0960	0.7204	0.6834	0.028*
H10B	−0.1851	0.8277	0.6495	0.028*
C11	0.0359 (2)	0.84454 (19)	0.63593 (19)	0.0232 (5)
H11A	0.1000	0.8254	0.7057	0.028*
H11B	0.0168	0.9222	0.6371	0.028*
C12	0.1062 (2)	0.81353 (17)	0.52712 (17)	0.0169 (4)
H12	0.0964	0.8756	0.4734	0.020*

supplementary materials

C13	0.2640 (2)	0.78423 (17)	0.54836 (17)	0.0165 (4)
C14	0.3074 (2)	0.68708 (17)	0.52234 (17)	0.0153 (4)
H14	0.4067	0.6693	0.5357	0.018*
C15	0.3668 (2)	0.86938 (19)	0.5957 (2)	0.0242 (5)
H15A	0.4647	0.8402	0.6069	0.036*
H15B	0.3395	0.8942	0.6692	0.036*
H15C	0.3634	0.9293	0.5420	0.036*
C16	0.1638 (2)	0.50276 (17)	0.78584 (16)	0.0139 (4)
C17	0.1685 (2)	0.42847 (17)	0.88859 (17)	0.0151 (4)
C18	0.0631 (2)	0.40510 (18)	0.95131 (17)	0.0185 (4)
C19	0.0876 (2)	0.3318 (2)	1.0536 (2)	0.0269 (5)
H19A	0.1859	0.3035	1.0596	0.040*
H19B	0.0187	0.2726	1.0443	0.040*
H19C	0.0740	0.3717	1.1232	0.040*
C20	−0.0861 (2)	0.4506 (2)	0.9308 (2)	0.0283 (6)
H20A	−0.0908	0.5024	0.8681	0.042*
H20B	−0.1099	0.4861	1.0004	0.042*
H20C	−0.1552	0.3930	0.9105	0.042*
C21	0.3243 (2)	0.39168 (18)	0.91067 (17)	0.0173 (4)
H21A	0.3322	0.3138	0.8986	0.021*
H21B	0.3659	0.4092	0.9895	0.021*
C22	0.3990 (2)	0.45412 (18)	0.82278 (17)	0.0154 (4)
C23	0.5286 (2)	0.40276 (19)	0.77721 (18)	0.0199 (5)
H23	0.5990	0.3832	0.8444	0.024*
C24	0.4981 (3)	0.3034 (2)	0.7059 (2)	0.0280 (5)
H24A	0.4503	0.2504	0.7499	0.042*
H24B	0.5888	0.2738	0.6855	0.042*
H24C	0.4354	0.3213	0.6361	0.042*
C25	0.5938 (2)	0.4943 (2)	0.71440 (19)	0.0229 (5)
H25A	0.5450	0.5011	0.6356	0.027*
H25B	0.6977	0.4818	0.7105	0.027*
C26	0.5709 (2)	0.5955 (2)	0.7840 (2)	0.0247 (5)
H26A	0.5388	0.6555	0.7327	0.030*
H26B	0.6613	0.6162	0.8310	0.030*
C27	0.4527 (2)	0.56609 (18)	0.86173 (17)	0.0172 (4)
H27	0.4996	0.5604	0.9422	0.021*
C28	0.3310 (2)	0.64559 (18)	0.85997 (17)	0.0176 (4)
C29	0.1969 (2)	0.61599 (17)	0.82481 (17)	0.0160 (4)
H29	0.1210	0.6664	0.8241	0.019*
C30	0.3704 (3)	0.75649 (19)	0.9014 (2)	0.0253 (5)
H30A	0.2833	0.8004	0.8977	0.038*
H30B	0.4378	0.7880	0.8529	0.038*
H30C	0.4158	0.7532	0.9806	0.038*

Atomic displacement parameters (\AA^2)

	U^{11}	U^{22}	U^{33}	U^{12}	U^{13}	U^{23}
O1	0.0223 (7)	0.0128 (7)	0.0142 (8)	0.0047 (6)	0.0011 (6)	0.0017 (6)

O2	0.0151 (6)	0.0123 (7)	0.0137 (7)	0.0011 (5)	0.0026 (5)	0.0029 (6)
O3	0.0140 (7)	0.0201 (8)	0.0134 (7)	−0.0019 (6)	−0.0002 (5)	0.0034 (6)
O4	0.0115 (6)	0.0172 (8)	0.0123 (7)	0.0015 (6)	0.0014 (5)	0.0005 (6)
C1	0.0155 (9)	0.0134 (10)	0.0136 (9)	0.0016 (8)	0.0027 (7)	0.0000 (8)
C2	0.0168 (9)	0.0130 (10)	0.0158 (10)	−0.0015 (8)	0.0002 (7)	0.0001 (8)
C3	0.0241 (10)	0.0146 (10)	0.0150 (10)	−0.0019 (9)	0.0029 (8)	0.0000 (8)
C4	0.0398 (13)	0.0256 (12)	0.0142 (10)	0.0004 (11)	0.0028 (9)	−0.0020 (9)
C5	0.0294 (12)	0.0206 (12)	0.0209 (11)	0.0032 (9)	0.0097 (9)	0.0001 (9)
C6	0.0192 (10)	0.0173 (11)	0.0144 (10)	−0.0004 (8)	0.0003 (8)	0.0017 (8)
C7	0.0150 (9)	0.0121 (10)	0.0157 (10)	0.0020 (8)	0.0006 (7)	0.0032 (8)
C8	0.0176 (10)	0.0192 (12)	0.0200 (10)	0.0042 (8)	0.0045 (8)	0.0044 (9)
C9	0.0153 (10)	0.0272 (13)	0.0333 (13)	0.0004 (9)	0.0043 (9)	0.0051 (10)
C10	0.0243 (11)	0.0230 (12)	0.0231 (11)	0.0077 (9)	0.0080 (9)	0.0025 (9)
C11	0.0266 (11)	0.0226 (13)	0.0201 (11)	0.0070 (10)	0.0012 (9)	−0.0038 (9)
C12	0.0229 (10)	0.0127 (10)	0.0147 (10)	0.0015 (8)	0.0012 (8)	0.0020 (8)
C13	0.0203 (10)	0.0153 (11)	0.0138 (10)	−0.0030 (8)	0.0011 (8)	0.0028 (8)
C14	0.0139 (9)	0.0190 (11)	0.0128 (10)	−0.0013 (8)	0.0011 (7)	0.0036 (8)
C15	0.0260 (11)	0.0192 (12)	0.0263 (12)	−0.0064 (9)	−0.0014 (9)	0.0006 (10)
C16	0.0130 (9)	0.0163 (10)	0.0122 (9)	0.0007 (8)	0.0016 (7)	0.0002 (8)
C17	0.0159 (9)	0.0152 (10)	0.0134 (9)	−0.0011 (8)	−0.0015 (8)	0.0002 (8)
C18	0.0192 (10)	0.0214 (12)	0.0144 (10)	−0.0023 (9)	−0.0003 (8)	0.0024 (9)
C19	0.0257 (12)	0.0342 (14)	0.0205 (11)	−0.0088 (10)	0.0016 (9)	0.0083 (10)
C20	0.0165 (11)	0.0448 (16)	0.0241 (12)	−0.0011 (11)	0.0049 (9)	0.0047 (11)
C21	0.0172 (10)	0.0199 (11)	0.0144 (10)	0.0026 (9)	0.0010 (8)	0.0033 (8)
C22	0.0123 (9)	0.0213 (11)	0.0119 (10)	0.0018 (8)	−0.0023 (7)	0.0017 (8)
C23	0.0155 (10)	0.0271 (13)	0.0173 (10)	0.0053 (9)	0.0021 (8)	0.0033 (9)
C24	0.0269 (11)	0.0262 (14)	0.0322 (13)	0.0075 (10)	0.0096 (10)	−0.0035 (10)
C25	0.0163 (10)	0.0322 (13)	0.0206 (11)	0.0011 (9)	0.0040 (8)	0.0044 (10)
C26	0.0169 (10)	0.0300 (13)	0.0272 (12)	−0.0034 (9)	0.0034 (9)	0.0039 (10)
C27	0.0158 (10)	0.0238 (12)	0.0114 (10)	−0.0031 (8)	−0.0008 (8)	−0.0002 (8)
C28	0.0228 (10)	0.0179 (11)	0.0128 (10)	−0.0004 (9)	0.0041 (8)	−0.0005 (8)
C29	0.0183 (9)	0.0151 (11)	0.0150 (10)	0.0018 (8)	0.0044 (8)	0.0014 (8)
C30	0.0295 (12)	0.0221 (12)	0.0240 (12)	−0.0065 (10)	0.0023 (9)	−0.0060 (10)

Geometric parameters (Å, °)

O1—C1	1.390 (3)	C14—H14	0.9500
O1—H1	0.89 (3)	C15—H15A	0.9800
O2—C1	1.449 (2)	C15—H15B	0.9800
O2—C7	1.453 (2)	C15—H15C	0.9800
O3—C16	1.385 (2)	C16—C29	1.513 (3)
O3—H3	0.86 (3)	C16—C17	1.523 (3)
O4—C22	1.447 (2)	C17—C18	1.329 (3)
O4—C16	1.455 (2)	C17—C21	1.522 (3)
C1—C14	1.511 (3)	C18—C20	1.501 (3)
C1—C2	1.523 (3)	C18—C19	1.512 (3)
C2—C3	1.329 (3)	C19—H19A	0.9800
C2—C6	1.515 (3)	C19—H19B	0.9800
C3—C4	1.503 (3)	C19—H19C	0.9800

supplementary materials

C3—C5	1.510 (3)	C20—H20A	0.9800
C4—H4A	0.9800	C20—H20B	0.9800
C4—H4B	0.9800	C20—H20C	0.9800
C4—H4C	0.9800	C21—C22	1.529 (3)
C5—H5A	0.9800	C21—H21A	0.9900
C5—H5B	0.9800	C21—H21B	0.9900
C5—H5C	0.9800	C22—C23	1.522 (3)
C6—C7	1.530 (3)	C22—C27	1.542 (3)
C6—H6A	0.9900	C23—C24	1.511 (3)
C6—H6B	0.9900	C23—C25	1.529 (3)
C7—C8	1.521 (3)	C23—H23	1.0000
C7—C12	1.545 (3)	C24—H24A	0.9800
C8—C9	1.524 (3)	C24—H24B	0.9800
C8—C10	1.534 (3)	C24—H24C	0.9800
C8—H8	1.0000	C25—C26	1.539 (3)
C9—H9A	0.9800	C25—H25A	0.9900
C9—H9B	0.9800	C25—H25B	0.9900
C9—H9C	0.9800	C26—C27	1.557 (3)
C10—C11	1.537 (3)	C26—H26A	0.9900
C10—H10A	0.9900	C26—H26B	0.9900
C10—H10B	0.9900	C27—C28	1.511 (3)
C11—C12	1.554 (3)	C27—H27	1.0000
C11—H11A	0.9900	C28—C29	1.328 (3)
C11—H11B	0.9900	C28—C30	1.505 (3)
C12—C13	1.514 (3)	C29—H29	0.9500
C12—H12	1.0000	C30—H30A	0.9800
C13—C14	1.330 (3)	C30—H30B	0.9800
C13—C15	1.500 (3)	C30—H30C	0.9800
C1—O1—H1	105 (2)	H15A—C15—H15C	109.5
C1—O2—C7	103.23 (13)	H15B—C15—H15C	109.5
C16—O3—H3	108 (2)	O3—C16—O4	108.49 (15)
C22—O4—C16	103.31 (13)	O3—C16—C29	114.09 (17)
O1—C1—O2	108.73 (15)	O4—C16—C29	106.99 (15)
O1—C1—C14	113.42 (17)	O3—C16—C17	113.64 (17)
O2—C1—C14	107.18 (16)	O4—C16—C17	102.46 (15)
O1—C1—C2	113.92 (17)	C29—C16—C17	110.27 (16)
O2—C1—C2	102.77 (15)	C18—C17—C21	126.42 (19)
C14—C1—C2	110.05 (16)	C18—C17—C16	128.31 (19)
C3—C2—C6	126.34 (18)	C21—C17—C16	105.13 (16)
C3—C2—C1	128.53 (19)	C17—C18—C20	124.1 (2)
C6—C2—C1	105.00 (16)	C17—C18—C19	121.5 (2)
C2—C3—C4	120.92 (19)	C20—C18—C19	114.39 (18)
C2—C3—C5	124.38 (19)	C18—C19—H19A	109.5
C4—C3—C5	114.66 (17)	C18—C19—H19B	109.5
C3—C4—H4A	109.5	H19A—C19—H19B	109.5
C3—C4—H4B	109.5	C18—C19—H19C	109.5
H4A—C4—H4B	109.5	H19A—C19—H19C	109.5
C3—C4—H4C	109.5	H19B—C19—H19C	109.5
H4A—C4—H4C	109.5	C18—C20—H20A	109.5

H4B—C4—H4C	109.5	C18—C20—H20B	109.5
C3—C5—H5A	109.5	H20A—C20—H20B	109.5
C3—C5—H5B	109.5	C18—C20—H20C	109.5
H5A—C5—H5B	109.5	H20A—C20—H20C	109.5
C3—C5—H5C	109.5	H20B—C20—H20C	109.5
H5A—C5—H5C	109.5	C17—C21—C22	103.41 (16)
H5B—C5—H5C	109.5	C17—C21—H21A	111.1
C2—C6—C7	103.77 (16)	C22—C21—H21A	111.1
C2—C6—H6A	111.0	C17—C21—H21B	111.1
C7—C6—H6A	111.0	C22—C21—H21B	111.1
C2—C6—H6B	111.0	H21A—C21—H21B	109.0
C7—C6—H6B	111.0	O4—C22—C23	108.73 (16)
H6A—C6—H6B	109.0	O4—C22—C21	102.34 (15)
O2—C7—C8	109.23 (15)	C23—C22—C21	117.75 (18)
O2—C7—C6	102.38 (16)	O4—C22—C27	108.54 (16)
C8—C7—C6	118.09 (17)	C23—C22—C27	104.17 (16)
O2—C7—C12	108.61 (15)	C21—C22—C27	115.02 (16)
C8—C7—C12	104.05 (16)	C24—C23—C22	115.91 (18)
C6—C7—C12	114.25 (16)	C24—C23—C25	114.24 (18)
C7—C8—C9	114.86 (18)	C22—C23—C25	103.31 (18)
C7—C8—C10	103.63 (17)	C24—C23—H23	107.7
C9—C8—C10	114.29 (18)	C22—C23—H23	107.7
C7—C8—H8	107.9	C25—C23—H23	107.7
C9—C8—H8	107.9	C23—C24—H24A	109.5
C10—C8—H8	107.9	C23—C24—H24B	109.5
C8—C9—H9A	109.5	H24A—C24—H24B	109.5
C8—C9—H9B	109.5	C23—C24—H24C	109.5
H9A—C9—H9B	109.5	H24A—C24—H24C	109.5
C8—C9—H9C	109.5	H24B—C24—H24C	109.5
H9A—C9—H9C	109.5	C23—C25—C26	105.89 (17)
H9B—C9—H9C	109.5	C23—C25—H25A	110.6
C8—C10—C11	105.77 (17)	C26—C25—H25A	110.6
C8—C10—H10A	110.6	C23—C25—H25B	110.6
C11—C10—H10A	110.6	C26—C25—H25B	110.6
C8—C10—H10B	110.6	H25A—C25—H25B	108.7
C11—C10—H10B	110.6	C25—C26—C27	105.59 (19)
H10A—C10—H10B	108.7	C25—C26—H26A	110.6
C10—C11—C12	105.99 (18)	C27—C26—H26A	110.6
C10—C11—H11A	110.5	C25—C26—H26B	110.6
C12—C11—H11A	110.5	C27—C26—H26B	110.6
C10—C11—H11B	110.5	H26A—C26—H26B	108.8
C12—C11—H11B	110.5	C28—C27—C22	112.18 (17)
H11A—C11—H11B	108.7	C28—C27—C26	114.80 (18)
C13—C12—C7	111.99 (17)	C22—C27—C26	105.62 (17)
C13—C12—C11	114.85 (17)	C28—C27—H27	108.0
C7—C12—C11	105.52 (17)	C22—C27—H27	108.0
C13—C12—H12	108.1	C26—C27—H27	108.0
C7—C12—H12	108.1	C29—C28—C30	123.2 (2)
C11—C12—H12	108.1	C29—C28—C27	120.2 (2)

supplementary materials

C14—C13—C15	122.5 (2)	C30—C28—C27	116.66 (18)
C14—C13—C12	120.07 (19)	C28—C29—C16	120.68 (18)
C15—C13—C12	117.38 (19)	C28—C29—H29	119.7
C13—C14—C1	120.76 (19)	C16—C29—H29	119.7
C13—C14—H14	119.6	C28—C30—H30A	109.5
C1—C14—H14	119.6	C28—C30—H30B	109.5
C13—C15—H15A	109.5	H30A—C30—H30B	109.5
C13—C15—H15B	109.5	C28—C30—H30C	109.5
H15A—C15—H15B	109.5	H30A—C30—H30C	109.5
C13—C15—H15C	109.5	H30B—C30—H30C	109.5
C7—O2—C1—O1	−166.41 (15)	C22—O4—C16—O3	−165.83 (16)
C7—O2—C1—C14	70.62 (18)	C22—O4—C16—C29	70.65 (18)
C7—O2—C1—C2	−45.36 (18)	C22—O4—C16—C17	−45.36 (18)
O1—C1—C2—C3	−41.0 (3)	O3—C16—C17—C18	−42.5 (3)
O2—C1—C2—C3	−158.4 (2)	O4—C16—C17—C18	−159.3 (2)
C14—C1—C2—C3	87.7 (3)	C29—C16—C17—C18	87.1 (3)
O1—C1—C2—C6	142.99 (17)	O3—C16—C17—C21	141.52 (17)
O2—C1—C2—C6	25.6 (2)	O4—C16—C17—C21	24.7 (2)
C14—C1—C2—C6	−88.34 (19)	C29—C16—C17—C21	−88.93 (19)
C6—C2—C3—C4	−1.1 (3)	C21—C17—C18—C20	175.0 (2)
C1—C2—C3—C4	−176.4 (2)	C16—C17—C18—C20	−0.2 (4)
C6—C2—C3—C5	176.2 (2)	C21—C17—C18—C19	−2.8 (4)
C1—C2—C3—C5	1.0 (4)	C16—C17—C18—C19	−178.0 (2)
C3—C2—C6—C7	−173.7 (2)	C18—C17—C21—C22	−172.6 (2)
C1—C2—C6—C7	2.5 (2)	C16—C17—C21—C22	3.6 (2)
C1—O2—C7—C8	172.96 (16)	C16—O4—C22—C23	173.18 (17)
C1—O2—C7—C6	47.00 (17)	C16—O4—C22—C21	47.91 (18)
C1—O2—C7—C12	−74.17 (17)	C16—O4—C22—C27	−74.09 (17)
C2—C6—C7—O2	−29.52 (19)	C17—C21—C22—O4	−30.8 (2)
C2—C6—C7—C8	−149.48 (18)	C17—C21—C22—C23	−149.86 (18)
C2—C6—C7—C12	87.7 (2)	C17—C21—C22—C27	86.7 (2)
O2—C7—C8—C9	−48.6 (2)	O4—C22—C23—C24	−49.5 (2)
C6—C7—C8—C9	67.7 (2)	C21—C22—C23—C24	66.2 (3)
C12—C7—C8—C9	−164.47 (18)	C27—C22—C23—C24	−165.10 (18)
O2—C7—C8—C10	76.7 (2)	O4—C22—C23—C25	76.2 (2)
C6—C7—C8—C10	−166.94 (19)	C21—C22—C23—C25	−168.10 (18)
C12—C7—C8—C10	−39.1 (2)	C27—C22—C23—C25	−39.4 (2)
C7—C8—C10—C11	34.1 (2)	C24—C23—C25—C26	162.08 (18)
C9—C8—C10—C11	159.84 (18)	C22—C23—C25—C26	35.3 (2)
C8—C10—C11—C12	−15.7 (2)	C23—C25—C26—C27	−17.4 (2)
O2—C7—C12—C13	38.7 (2)	O4—C22—C27—C28	38.7 (2)
C8—C7—C12—C13	155.00 (16)	C23—C22—C27—C28	154.41 (17)
C6—C7—C12—C13	−74.8 (2)	C21—C22—C27—C28	−75.2 (2)
O2—C7—C12—C11	−86.90 (18)	O4—C22—C27—C26	−87.07 (18)
C8—C7—C12—C11	29.4 (2)	C23—C22—C27—C26	28.7 (2)
C6—C7—C12—C11	159.54 (17)	C21—C22—C27—C26	159.03 (17)
C10—C11—C12—C13	−132.17 (19)	C25—C26—C27—C28	−131.0 (2)
C10—C11—C12—C7	−8.3 (2)	C25—C26—C27—C22	−6.9 (2)
C7—C12—C13—C14	−1.7 (3)	C22—C27—C28—C29	−1.6 (3)

C11—C12—C13—C14	118.7 (2)	C26—C27—C28—C29	119.0 (2)
C7—C12—C13—C15	176.55 (17)	C22—C27—C28—C30	177.41 (17)
C11—C12—C13—C15	−63.1 (2)	C26—C27—C28—C30	−62.0 (2)
C15—C13—C14—C1	−178.33 (18)	C30—C28—C29—C16	−179.05 (19)
C12—C13—C14—C1	−0.2 (3)	C27—C28—C29—C16	−0.1 (3)
O1—C1—C14—C13	−154.67 (18)	O3—C16—C29—C28	−154.60 (18)
O2—C1—C14—C13	−34.7 (2)	O4—C16—C29—C28	−34.6 (2)
C2—C1—C14—C13	76.4 (2)	C17—C16—C29—C28	76.1 (2)

Hydrogen-bond geometry (Å, °)

<i>D</i> —H \cdots <i>A</i>	<i>D</i> —H	H \cdots <i>A</i>	<i>D</i> \cdots <i>A</i>	<i>D</i> —H \cdots <i>A</i>
O1—H1 \cdots O4	0.89 (3)	1.92 (3)	2.799 (2)	168 (3)
O3—H3 \cdots O2	0.86 (3)	1.92 (3)	2.771 (2)	171 (3)

Fig. 1

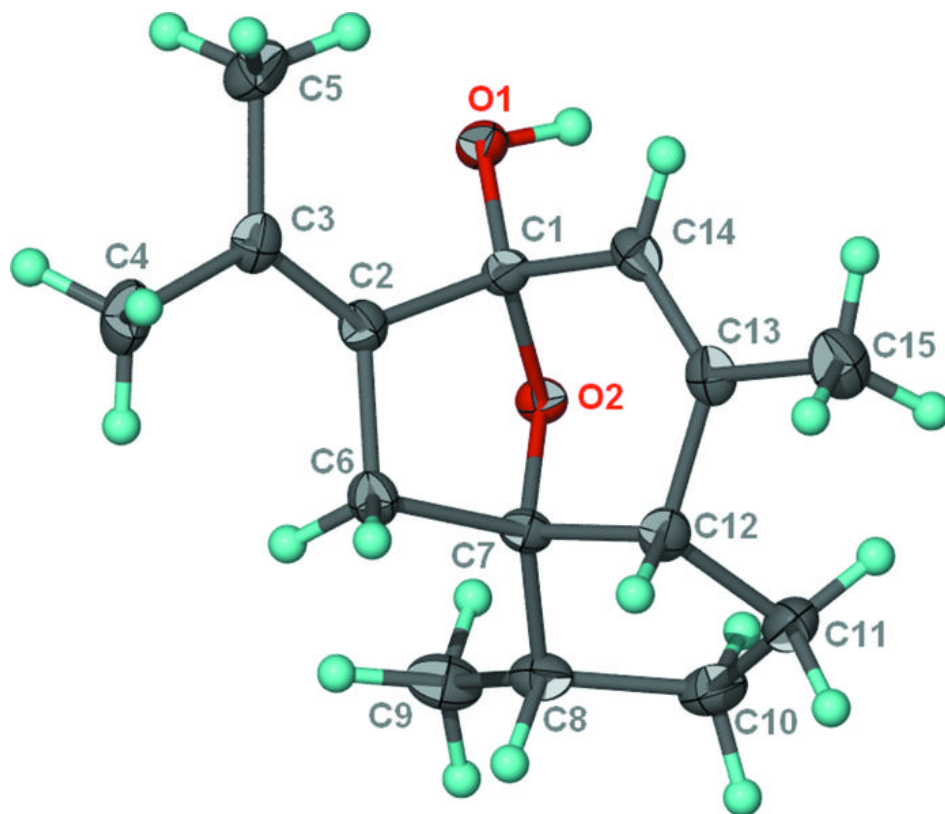
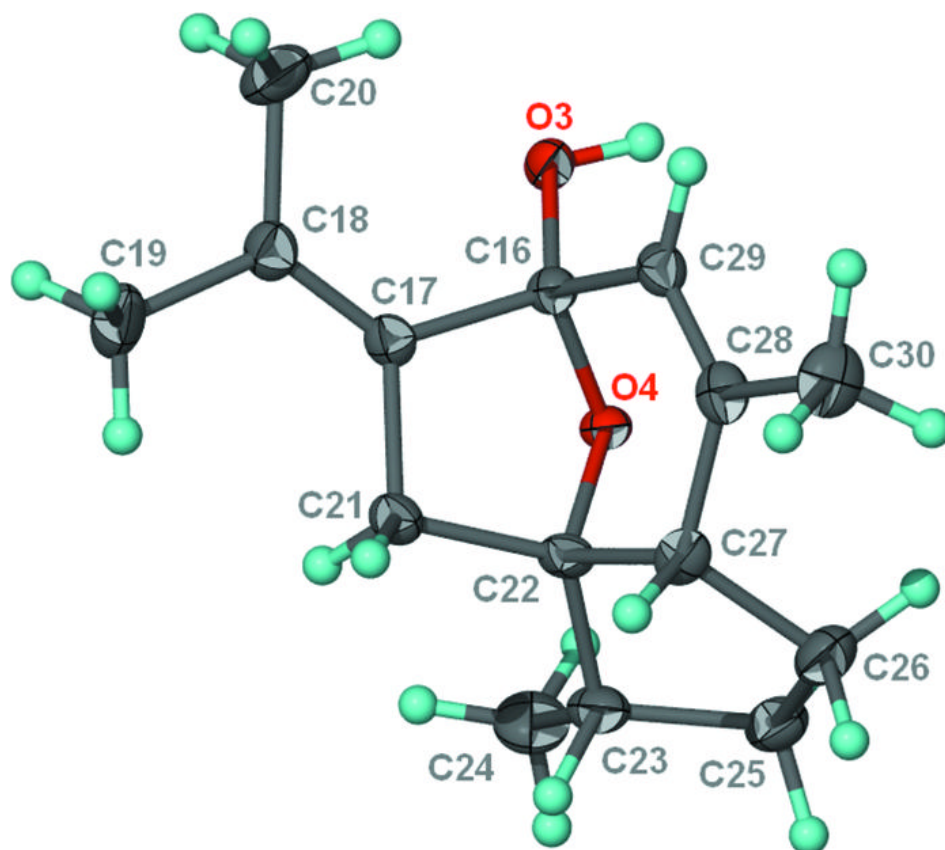


Fig. 2



Research Article

Cytotoxic Constituents from the Rhizomes of *Curcuma zedoaria*

Omer Abdalla Ahmed Hamdi,^{1,2} Syarifah Nur Syed Abdul Rahman,³
Khalijah Awang,^{1,2} Norhanom Abdul Wahab,^{1,4} Chung Yeng Looi,^{1,5}
Noel Francis Thomas,² and Sri Nurestri Abd Malek^{1,3}

¹ Center for Natural Products and Drugs Discovery (CENAR), University of Malaya, 50603 Kuala Lumpur, Malaysia

² Department of Chemistry, Faculty of Science, University of Malaya, 50603 Kuala Lumpur, Malaysia

³ Institute of Biological Sciences, Faculty of Science, University of Malaya, 50603 Kuala Lumpur, Malaysia

⁴ Biology Division, Center for Foundation Studies in Science, University of Malaya, 50603 Kuala Lumpur, Malaysia

⁵ Department of Pharmacology, Faculty of Medicine, University of Malaya, 50603 Kuala Lumpur, Malaysia

Correspondence should be addressed to Sri Nurestri Abd Malek; srimallek@um.edu.my

Received 14 February 2014; Accepted 8 June 2014; Published 13 July 2014

Academic Editor: Xin Ming

Copyright © 2014 Omer Abdalla Ahmed Hamdi et al. This is an open access article distributed under the Creative Commons Attribution License, which permits unrestricted use, distribution, and reproduction in any medium, provided the original work is properly cited.

Curcuma zedoaria also known as *Temu putih* is traditionally used in food preparations and treatment of various ailments including cancer. The cytotoxic activity of hexane, dichloromethane, ethyl acetate, methanol, and the methanol-soxhlet extracts of *Curcuma zedoaria* rhizomes was tested on two human cancer cell lines (Ca Ski and MCF-7) and a noncancer cell line (HUVEC) using MTT assay. Investigation on the chemical components in the hexane and dichloromethane fractions gave 19 compounds, namely, labda-8(17),12 diene-15,16 dial (1), dehydrocurdione (2), curcumenone (3), comosone II (4), curcumenol (5), procurcumenol (6), germacrone (7), zerumbone epoxide (8), zederone (9), 9-isopropylidene-2,6-dimethyl-11-oxatricyclo[6.2.1.0^{1,5}]undec-6-en-8-ol (10), furanodiene (11), germacrone-4,5-epoxide (12), calcaratarin A (13), isoprocucumenol (14), germacrone-1,10-epoxide (15), zerumin A (16), curcumanolide A (17), curcuzedoalide (18), and gweicurculactone (19). Compounds (1–19) were evaluated for their antiproliferative effect using MTT assay against four cancer cell lines (Ca Ski, MCF-7, PC-3, and HT-29). Curcumenone (3) and curcumenol (5) displayed strong antiproliferative activity ($IC_{50} = 8.3 \pm 1.0$ and $9.3 \pm 0.3 \mu\text{g/mL}$, resp.) and were found to induce apoptotic cell death on MCF-7 cells using phase contrast and Hoechst 33342/PI double-staining assay. Thus, the present study provides basis for the ethnomedical application of *Curcuma zedoaria* in the treatment of breast cancer.

1. Introduction

It is widely reported that more than 35,000 plant species are used for medicinal purposes worldwide. Of these, 1,200 and 2,000 plant species from Peninsular Malaysia and East Malaysia respectively, are used in folklore medicine [1]. One such plant is *Curcuma zedoaria* (Berg.) Rosc. belonging to the Zingiberaceae family and known by the locals as *Temu putih* or *Kunyit putih*. The leaf blades are 80 cm long, usually with a purple-brown flush running along the midrib on both surfaces of the leaf. In the young plants, the rhizomes of *Curcuma zedoaria* are easily confused with those of *Curcuma aeruginosa* and *Curcuma mangga* because both have almost similar yellow color. However, a cross-section of the rhizomes

of the mature plants of *Curcuma aeruginosa* is slightly dark purplish whilst *Curcuma mangga* have brighter yellow color [2]. *Temu putih* is used by the Malays in the preparation of traditional medicine—consumed either on their own or in mixtures with other plant species. They are also widely consumed as spices, as flavors in native dishes, and as food preparations in postpartum confinement [2–4]. *Curcuma zedoaria* also called *Er-chu* in Chinese is clinically used for the treatment of cervical cancer [5]. In Japan, it has also been used as an aromatic stomachic [6]. Whilst in the Ayurvedic medicine, it is used for the treatment of fevers (cooling), antiseptic, mild expectorant, and deodorizer [7]. In Indonesia, *Curcuma zedoaria* is widely consumed in the form of “jamu” for the treatment of breast and cervical

cancers [8]. Medicinal plants are used widely especially in Asia as an alternative medicine for cancer-related diseases because it is believed for having active natural occurring compounds in killing cancer [9, 10]. However, there are only limited studies on the efficacy on the use of medicinal plants [11]. It is therefore important to identify the components which are responsible for the chemotherapeutic effects and the molecular pathway by which these compounds affect cancer cell death. Up to date, there are numerous reported articles on the cytotoxic components of *Curcuma zedoaria* and the mechanism of cell death exerted by some of these compounds [5–8, 12–20]. In our continuous effort to study the bioactive and their mode of actions from medicinal plants of *Curcuma* species, this communication reports the isolation of 19 compounds and among these, two bioactive compounds (curcumenone and curcumenol) were identified as cytotoxic components and were able to induce apoptosis.

2. Materials and Methods

2.1. Plant Samples. *Curcuma zedoaria* rhizomes were collected from Tawamangu, Indonesia, and a voucher specimen (KL 5764) was deposited at the herbarium of the Department of Chemistry, Faculty of Science, University of Malaya, Kuala Lumpur, Malaysia.

2.2. Extraction of Plant Sample. Briefly, the washed and dried rhizomes of *Curcuma zedoaria* were finely ground. The fine powders of *Curcuma zedoaria* (1.0 kg) were soaked in n-hexane for 3 days. Then, the solvent containing extract was decanted and filtered (were repeated twice each time with five liters of n-hexane). All the filtrates were combined and evaporated using a rotary evaporator (Buchi, Switzerland) to give the n-hexane extract. The n-hexane-insoluble residue was further extracted with CH_2Cl_2 to give the CH_2Cl_2 -soluble extract and CH_2Cl_2 -insoluble residue. The CH_2Cl_2 -insoluble residue was further extracted with EtOAc to give the EtOAc-soluble and EtOAc-insoluble extract. The EtOAc-insoluble extract was then extracted with MeOH to give the MeOH extract. The insoluble residue obtained after MeOH extraction was further subjected to soxhlet extraction using methanol to give the MeOH SE extract after evaporation of excess solvent. All the extracts were weighed after solvent evaporation.

2.3. Cell Culture. The human cell lines MCF-7 (breast cancer), Ca Ski (cervical cancer), and HT-29 (colon cancer) were cultured as monolayer in RPMI 1640 growth media. HUVEC (human umbilical vein endothelial cells) and PC-3 (prostate cancer) cells were cultured in DMEM. All cells were purchased from the American Tissue Culture Collection (ATCC, USA) except for human umbilical vein endothelial cells (HUVEC) which were obtained from ScienCell Research Laboratories (Carlsbad, CA). All the media were supplemented with 10% v/v foetal bovine serum (FBS), 100 $\mu\text{g}/\text{mL}$ penicillin/streptomycin, and 50 $\mu\text{g}/\text{mL}$ amphotericin B. The cells were cultured in a 5% CO_2 incubator at 37°C.

2.4. MTT Cytotoxicity Assay. Cell viability was investigated using 3-(4, 5-dimethylthiazol-2-yl)-2, 5-diphenyltetrazolium bromide (MTT) assay. Cells were detached from the 25 cm^3 tissue culture flask when it achieved 80% confluency. The detached cells were pellet by centrifugation (1,000 rpm; 5 minutes). Cells (3.0×10^4 cells/mL) were seeded onto a 96-well microtiter plate (Nunc). The cells were incubated at 37°C CO_2 incubator for 24 h to give adherent cells. The test compounds (1–100 $\mu\text{g}/\text{mL}$) were added onto the 96-well microtiter plate containing adherent cells. The untreated cells were incubated in 10% media containing 0.5% DMSO (without addition of any test compounds/extracts). This mixture was regarded as the negative control whereas doxorubicin as the positive control. The plates were incubated for 72 h at 37°C in a 5% CO_2 incubator. After 72 h, the media were removed and 100 μL of fresh medium and 20 μL of MTT (Sigma, filter sterile, 5 mg/mL) were added to each well and further incubated for 4 hours (37°C) after which the media were substituted with 150 μL DMSO. The 96-well microtiter plates were then agitated at room temperature onto an incubator shaker to dissolve the formazan crystals. The absorbance (A) of the content of the plates was measured at 540 nm using a microplate reader. The percentage of inhibition of each test sample was calculated according to the following formula: Percentage of inhibition (%) = $(A_{\text{control}} - A_{\text{sample}})/A_{\text{control}} \times 100\%$. The average of three replicates was then obtained. The IC_{50} for each extract was extrapolated from the graphs of the percentage inhibition versus concentration of test agents. Cytotoxicity of each test agent is expressed as IC_{50} value. The IC_{50} value is the concentration of test agents that cause 50% inhibition or cell death, averaged from the three experiments [21–23]. The selectivity index (SI) was also calculated as described by [24, 25] using the ratio between IC_{50} of the extract or compounds on normal cell lines (HUVEC) and IC_{50} of the tested extract or compounds on cancerous cell lines. Selectivity index (SI) values equal or greater than three were considered to have a high selectivity towards cancerous cells. An SI value denotes the selectivity of the sample to the tested cell lines [24, 25].

2.5. General Methods on Characterization of the Active Principles. TLC techniques were used to monitor the purity of isolated compounds. Analytical TLC was performed on the precoated plates with silica gel 60 F₂₅₄ (Merck of 20.25 mm) (normal phase). HPTLC and PTLC were carried out on the precoated plates with silica gel 60 GF₂₅₄ (Merck, 20.25 mm). Spots were detected by UV (254, 360 nm) and by spraying of vanillin- H_2SO_4 or anisaldehyde- H_2SO_4 followed by gentle heating. CC was carried out on Kieselgel 60 (0.043–0.063 mm and 0.063–0.200 mm) (Merck) and Sephadex LH 20 (25–100 m) (Merck). HPLC was used to isolate and purify the compounds. HPLC was performed using Waters System equipped with Binary Gradient Module (Waters 2545), System Fluidics Organizer and Photodiode Array Detector (190–400 nm; Waters 2998), and Sample Manager (Waters 2767). The column used was Waters XBridge Prep C18 5 μM (10 \times 250 mm) column with Waters XBridge Prep C18 5 μM (10 \times 10 mm) column guard cartridge. The data were collected

and analyzed by MassLynx software. 1D NMR (^1H , ^{13}C , Dept 135) and 2D NMR (HSQC, HMBC, COSY, NOESY) spectra were recorded from a JEOL 400 MHz FT NMR spectrometer at 400 MHz for ^1H -NMR and at 100 MHz for ^{13}C -NMR. Chemical shifts in ppm were referenced to the internal standard TMS ($\delta = 0$ ppm) for use in ^1H -NMR and CDCl_3 (δ : 77.0 ppm), ^{13}C -NMR spectra, respectively. The GC-MS analyses were performed using Shimadzu QP2010 Series gas chromatography and operated in the split less mode at 275°C. The column used was DM 5MS (5% diphenyl/95% dimethyl polysiloxane) capillary column (30.0 m \times 0.25 mm \times 0.25 μm) with helium as carrier gas at a flow rate of 1 mL min $^{-1}$. The column temperature was programmed as follows: initially at 60°C, then increased to 250°C at 5°C per minute, and then held for 1 minute. The total ion chromatogram was obtained by autointegration using Chem Station and the components were identified by comparing their mass spectral data with the accompanying Spectral Database (NIST 05, Mass Spectral Library, USA) whenever possible. IR spectra were obtained on a Perkin Elmer 1600 Series FT-IR infrared spectrophotometer with chloroform as solvent. The wavelength is indicated in cm $^{-1}$. Mass spectra of LC-MS were recorded using Agilent Technologies 6530 Accurate-Mass Q-TOF LC-MS.

2.6. Extraction and Isolation of Pure Compounds. The powdered rhizomes (1.0 kg) were initially extracted with hexane to give the hexane extract (24.2 g, 2.4%). The hexane extract (20.0 g) was then subjected to silica gel column chromatography (CC) eluting initially with hexane followed by hexane enriched with increasing percentages of ethyl acetate (EtOAc). Fractions were then combined according to similarity of thin layer chromatography (TLC) spots to give 21 fractions (fractions 1–21). Germacrone-4, 5 epoxide (**12**, 12.4 mg) and germacrone-1, 10 epoxide (**15**, 8.0 mg) were isolated from fraction 5 through micro CC and preparative thin layer chromatography (PTLC). Fraction 6 afforded germacrone (**7**, 21.6 mg) and furanodiene (**11**, 8.8 mg) upon purification with CC and PTLC. Fraction 7 was further chromatographed using various isolation techniques such as Sephadex-LH20, PTLC, and high performance thin layer chromatography (HPTLC) to afford dehydrocurdione (**2**, 34.5 mg), curcumanolide A (**17**, 4.9 mg), and two labdanes, namely, labda-8 (**17**), 12 diene-15, 16 dial (**1**, 16.2 mg) and labda-8(**17**), 12 diene-15, 15-dimethoxy-16-al or calcaratarin A (**13**, 22.6 mg). Fraction 8 was further purified using PTLC to give curcumenol (**5**, 15.5 mg) and zerumin A (**16**, 9.8 mg). Isoprocucumenol (**14**, 10.2 mg) was isolated from fraction 9 using two successive PTLC. Fraction 10 was chromatographed and further purified by HPTLC to afford a second monoclinal modification of curcumenol as a crystallized dimer elucidated by single crystal X-ray diffraction analysis. This dimer is 9-isopropylidene-2, 6-dimethyl-11-oxatricyclo [6.2.1.0 1,5] undec-6-en-8-ol (**10**, 5.4 mg) as previously described [20], whilst curcuzedoalide (**18**, 13.4 mg) was isolated from fraction 10 using HPLC. Curcumenone (**3**, 16.4 mg) was purified from fractions 12 and 13. Procucumenol (**6**, 8.9 mg) and zerumbone epoxide (**8**, 11.9 mg) were isolated from fractions 15 and 16, respectively,

using micro CC and PTLC. The CH_2Cl_2 extract (10 g) was then subjected to silica gel CC with initial elution of 5% EtOAc-hexane and gradually increasing the polarity to 100% EtOAc and finally with MeOH. Fractions were then combined according to similarity of TLC spots to give 23 fractions (fractions 1–23). Fraction 2 was subjected to micro CC to afford comosone II (**4**, 6.6 mg), zederone (**9**, 24.4 mg), and gweicurculactone (**19**, 3.6 mg) upon purification with HPLC. All the isolated compounds were identified using NMR spectroscopy and other supportive data (MS, IR, and UV) and results obtained were consistent with reported data [14–18, 20, 23, 26–32]. The structures of isolated compounds are shown in Figure 1. The method of isolation is summarized in Figure 2.

2.7. Phase Contrast Microscopy. Briefly, MCF-7 cells (5×10^5) were grown in a tissue culture dishes (60 mm) for overnight. Then, the cells were treated with curcumenone (**3**) and curcumenol (**5**) at a concentration of 12.5 and 25 $\mu\text{g/mL}$, respectively. After 48 hours, cells were gently rinsed with PBS. The observation of morphological changes of apoptotic MCF-7 cells after treatment with the two bioactive compounds was viewed using an inverted phase contrast microscope (Leica DMI 3000B, Germany) at 400x magnification according to the method [33].

2.8. Fluorescence Microscopy. The morphological features of MCF-7 cells upon treatment by the test compounds also observed by double staining of Hoechst 33342/PI assay [33–37] using the inverted fluorescence microscope (Leica, DM16000B). Briefly, 5×10^5 cells were grown overnight and treated with 12.5 and 25 $\mu\text{g/mL}$ of curcumenone (**3**) and curcumenol (**5**). After treatment of cells with the test compounds for 48 hours, both floating and adherent cells were collected by centrifugation and washed once with cold PBS. Then, Hoechst 33342 solutions (10 $\mu\text{g/mL}$) were added and incubated at 37°C for 7 minutes. The cells were then stained with PI (2.5 $\mu\text{g/mL}$) and further incubated in the dark for 15 minutes. Cell suspension (100 μL) was mounted onto glass microscope slides and observed under fluorescence microscope using UV/488 dual excitation (460 nm emission of Hoechst 33342, 575 nm emission of PI). Approximately a total of 200 target cells were calculated and the morphological characteristics of the nuclei were analyzed for quantification of apoptosis and necrosis [37]. The percentage of apoptotic, necrotic, and dead cells was determined according to the formula described by [37].

2.9. Statistical Analysis. All data were presented as mean \pm standard deviation. All experiments were conducted in triplicates. The data were subjected to one-way analysis of variance (ANOVA) with the significant differences between groups determined by Duncan's multiple range tests (DMRT) at 95% significant difference ($P < 0.05$) using STATGRAPHICS Plus software (version 3.0, Statistical Graphics Corp., Princeton, NJ, USA).

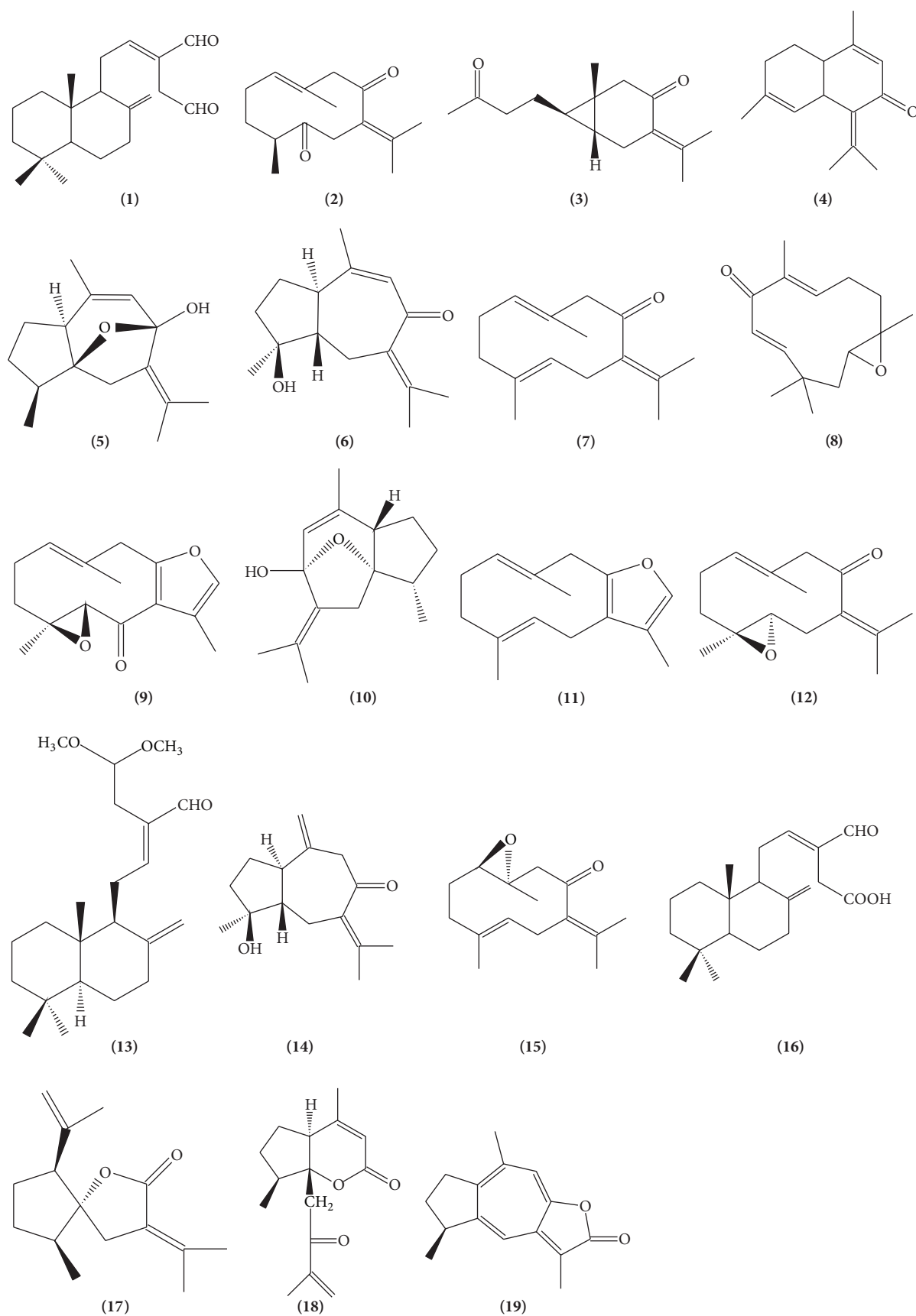


FIGURE 1: The structures of isolated compounds.

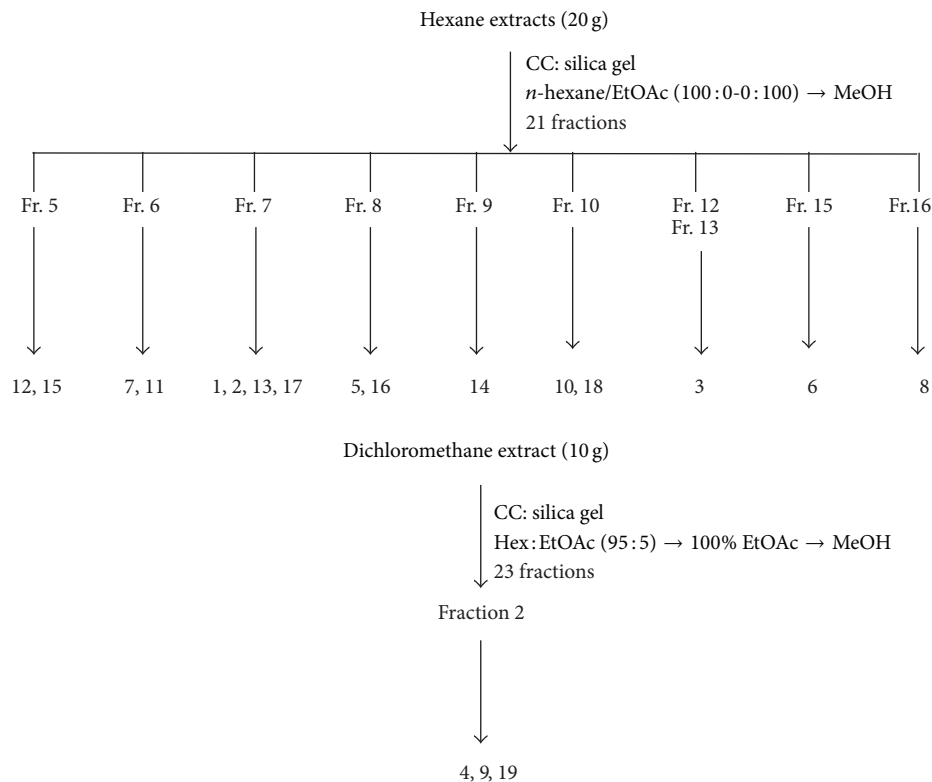


FIGURE 2: Schematic represents the isolation method of the bioactive compounds from *Curcuma zedoaria*.

TABLE 1: Antiproliferative activity [IC_{50} values ($\mu\text{g/mL}$)] and selectivity index of crude and fractionated extracts of *Curcuma zedoaria* against human cancer and noncancer (HUVEC) cell lines.

Extracts	IC_{50} ($\mu\text{g/mL}$) ^a				
	MCF-7	SI ^b	Ca Ski	SI ^b	HUVEC
Hexane	18.4 ± 1.6	5.4	19.0 ± 1.5	5.3	>100.0
Dichloromethane	40.6 ± 2.3	2.5	83.5 ± 2.7	1.2	>100.0
Ethyl acetate	>100.0	1.0	>100.0	1.0	>100.0
Methanol	>100.0	1.0	>100.0	1.0	>100.0
Methanol (soxhlet extraction)	>100.0	1.0	>100.0	1.0	>100.0

^aData are presented as mean ± standard deviation (SD) of three replicates.
^bSI is the selectivity index. SI values ≥ 3.0 denote high selectivity towards cancerous cells.

3. Results and Discussion

3.1. Detection of Cell Viability by MTT Assay. The antiproliferative activity of crude and extracts of *Curcuma zedoaria* was analysed using MTT assay. The IC_{50} values ($\mu\text{g/mL}$) were evaluated for these crude extracts averaged from three experiments against two human cancer cell lines (Ca Ski and MCF-7) and a noncancer cell (HUVEC) and the result is summarized in Table 1. A plant extract with $IC_{50} \leq 20 \mu\text{g/mL}$ is considered active [21–23]. The hexane extract showed high inhibitory activity against Ca Ski and MCF-7 cells, whilst, the dichloromethane (CH_2Cl_2) extract possessed mild cytotoxicity against MCF-7 and exhibited weak cytotoxicity against Ca Ski. The extracts of *Curcuma zedoaria* altogether showed to be essentially ineffective on the normal cells. Selectivity indexes (SI) of the antiproliferative activity of

Curcuma zedoaria extracts were evaluated by the ratio of the cytotoxic activity (IC_{50}) of each extracts against the cancer cells with the normal cells (HUVEC).
The SI with greater or equal value of three was considered to be highly selective towards cancer cells [24, 25, 38, 39]. As shown in Table 1, the hexane extract showed selective activity towards Ca Ski and MCF-7 cells with SI values of 5.3 and 5.4, respectively. Thus, the data have revealed that the hexane extracts exhibited antiproliferative effect and possessed selective activity towards Ca Ski and MCF-7 cells, in reference to normal cells (HUVEC).
3.2. Isolation of Active Principles. The isolation of the active principles (compounds 1–19) has been described extensively in section methodology. These chemical components were

TABLE 2: Antiproliferative activity [IC_{50} values ($\mu\text{g/mL}$)]^a and selectivity index of isolated compounds against selected human cancer cell lines and human umbilical vein endothelial cells (HUVEC).

Compounds	IC_{50} ($\mu\text{g/mL}$) SI ^b				
	MCF-7	Ca Ski	PC-3	HT-29	HUVEC
labda-8(17), 12 diene-15, 16 dial (1)	16.3 \pm 0.2 (2.8)	14.5 \pm 0.1 (3.1)	26.3 \pm 2.4 (1.7)	21.5 \pm 3.1 (2.1)	45.3 \pm 1.9
dehydrocurdione (2)	33.0 \pm 1.1 (0.7)	21.7 \pm 1.1 (1.1)	19.1 \pm 2.8 (1.3)	22.7 \pm 2.4 (1.1)	24.0 \pm 2.1
curcumenone (3)	8.3 \pm 1.0 (6.0)	>100.0 (0.5)	39.8 \pm 4.2 (1.3)	43.3 \pm 6.2 (1.2)	50.0 \pm 8.6
comosone II (4)	>100.0	76.0 \pm 1.2	na	na	na
curcumenol (5)	9.3 \pm 0.3 (2.8)	18.5 \pm 1.0 (1.4)	17.3 \pm 1.2 (1.5)	24.8 \pm 2.7 (1.0)	25.9 \pm 1.4
procurcumenol (6)	16.1 \pm 2.2 (1.0)	62.4 \pm 0.3 (0.3)	13.3 \pm 1.7 (1.2)	15.5 \pm 2.3 (1.1)	16.3 \pm 1.0
germacrone (7)	59.1 \pm 2.9 (1.2)	39.3 \pm 1.2 (1.9)	55.2 \pm 4.9 (1.3)	42.9 \pm 4.1 (1.7)	73.7 \pm 0.3
zerumbone epoxide (8)	24.1 \pm 0.1 (0.6)	34.5 \pm 0.6 (0.4)	10.8 \pm 1.9 (1.3)	13.7 \pm 2.7 (1.0)	14.2 \pm 1.1
zederone (9)	>100.0 (0.4)	>100.0 (0.4)	27.0 \pm 1.9 (1.6)	19.1 \pm 2.5 (2.2)	42.1 \pm 2.7
second monoclinic curcumenol (10)	>100.0 (0.7)	>100.0 (0.7)	na	na	71.7 \pm 6.1
furanodiene (11)	36.5 \pm 2.6 (1.1)	na	39.5 \pm 4.5 (1.0)	47.2 \pm 4.4 (0.9)	40.9 \pm 2.6
germacrone-4, 5-epoxide (12)	37.2 \pm 4.0 (1.3)	na	43.9 \pm 7.2 (1.1)	39.6 \pm 4.6 (1.2)	48.4 \pm 4.7
calcaratarin A (13)	62.5 \pm 4.8 (0.8)	na	41.7 \pm 3.4 (1.1)	48.3 \pm 5.1 (1.0)	47.3 \pm 4.2
isoprocucumenol (14)	58.8 \pm 4.2 (0.8)	na	37.4 \pm 4.5 (1.2)	51.6 \pm 3.9 (0.9)	45.1 \pm 3.0
germacrone-1, 10-epoxide (15)	61.2 \pm 5.8 (0.9)	na	53.2 \pm 4.9 (1.0)	72.8 \pm 8.3 (0.8)	55.5 \pm 1.6
zerumin A (16)	22.3 \pm 1.1 (1.2)	na	21.9 \pm 1.6 (1.2)	17.4 \pm 2.0 (1.5)	25.8 \pm 1.9
curcumanolide A (17)	29.8 \pm 3.1 (0.7)	na	18.8 \pm 2.4 (1.2)	21.3 \pm 3.2 (1.0)	21.7 \pm 7.0
curcuzedoalide (18)	49.8 \pm 3.6 (0.9)	na	62.1 \pm 8.1 (0.7)	58.2 \pm 3.5 (0.8)	45.3 \pm 7.8
gweicurculactone (19)	31.2 \pm 3.2 (2.3)	na	38.3 \pm 2.2 (1.9)	35.7 \pm 5.8	71.7 \pm 6.1 (2.0)
doxorubicin*	0.1 \pm 0.0 (4.0)	0.2 \pm 1.0 (2.0)	na	na	1.4 \pm 0.0

^aData are presented as mean \pm standard deviation (SD) of three replicates.

^bSI is the selectivity index. SI ≥ 3.0 denotes high selectivity towards cancerous cells.

*na-not available.

identified using spectroscopic (NMR, IR, and UV) and spectrometric studies (GS-MS, LC-MS, and MS) and were found to be in agreement with reported data [14–18, 20, 23, 26–32].

3.3. Antiproliferative Activity of Compounds (1–19). The compounds (1–19) isolated from the hexane and dichloromethane extracts were further evaluated on four selected cancer cell lines (MCF-7, Ca Ski, HT-29, and PC-3) and a normal human umbilical vein endothelial cell (HUVEC). Many researchers have utilized HUVEC cell lines in determining cytotoxicity of test samples against normal cells [40–44]. Similar approach has also widely employed in high-throughput screening in drug discovery [45]. Test samples showing mild or no toxicity towards normal cell lines (HUVEC) would be a potentially good candidate for drug development. The antiproliferative activity of the compounds (1–19) is presented in Table 2. The isolated terpenoids from *Curcuma zedoaria* were found to possess moderate antiproliferative effect against the four selected human carcinoma. In the present study, only curcumenone (3) and curcumenol (5) demonstrated strong antiproliferative activity against MCF-7. Curcumenone (3) was selectively toxic to MCF-7 cells whilst curcumenol (5) displayed appreciable selectivity towards MCF-7 in reference to HUVECs with SI values of 6.0 and 2.8, respectively.

It appeared therefore that compounds (3) and (5) have selective activity towards MCF-7 cell line. To the best of our knowledge, there is no report on the cytotoxicity of compounds (3), (5), and (10) against human MCF-7, Ca Ski, and PC-3 cell lines. In a study by [14], curcumenone isolated from the rhizomes of *Curcuma zedoaria* has been reported to have protective effect on alcohol-treated mice and acceleration of liver alcohol dehydrogenase activity. It is also been found as an effective protective effect on D-galactosamine/lipopolysaccharide-induced acute liver injury [5]. In a previous reported publication, [46] claimed that curcumenol is widely used to treat cancer and inflammation and also known as an antibiotic or anticancer drug. In their study, [46] found that curcumenol is not a mechanism-based inhibitor through time- and NADPH-dependent inhibitions and also suggested that curcumenol may be safely used without inducing metabolic drug-drug interaction through P450 inhibition. Labda-8(17), 12 diene-15, 16 dial (1) displayed high selective activity towards Ca Ski and appreciable selectivity to MCF-7 but only exhibited moderate cytotoxicity against the cancer cells. Procurcumenol (6) and zerumbone epoxide (8) exhibited good cytotoxic effect against PC-3 and HT-29 cell lines but were not selective on these tumor cells. Previously, [26] described that zerumbone epoxide isolated from the rhizomes of *Curcuma zedoaria* possessed cytotoxic effects. Thus, this is in a good agreement with our current

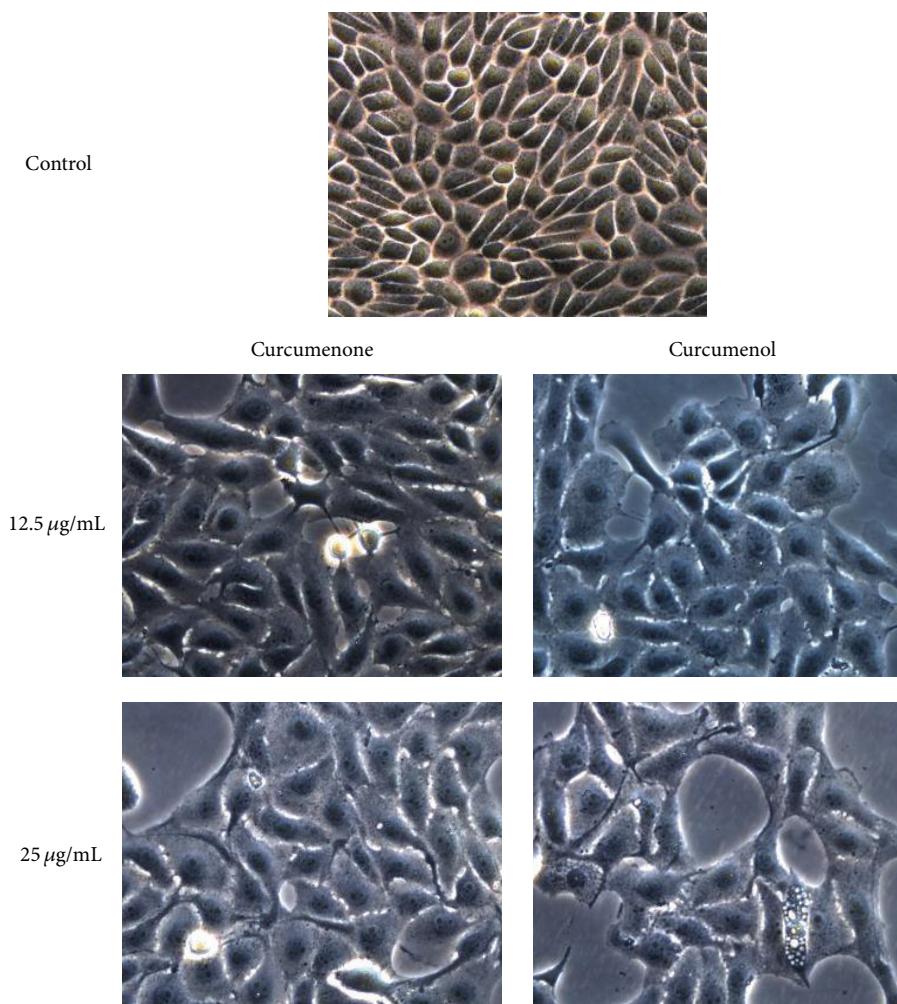


FIGURE 3: Morphological analysis of MCF-7 cells treated with curcumenone and curcumenol as observed under inverted phase contrast microscope (400x).

study. Compounds (**1–10**) displayed appreciable to weak cytotoxic activity against Ca Ski (IC_{50} values ranging from 14.5 ± 0.1 to $100.0 \mu\text{g/mL}$, respectively). Only curcumenone (**3**) did not show any antiproliferative activity against Ca Ski. Other compounds (**1, 2, 5, 9, 16, and 17**) also exhibited moderate inhibitory activity against the tested carcinoma PC-3 and HT-29 cell lines. All tested compounds showed mild cytotoxicity towards the normal cell lines (HUVEC). Curcumenone (**3**) and zerumbone epoxide (**8**) were found to have slight toxicity towards the normal cell. Although the pure compounds are not as effective as doxorubicin in inhibiting the proliferation of the cancer cells, they inflict less damage to the noncancerous cells. To the best of our knowledge, it is important to note that compounds (**1, 8, 12–13, and 19**) are reported here for the first time from *Curcuma zedoaria*. In this study, zerumin A (**16**) was isolated from the hexane fraction and displayed moderate cytotoxic effect on MCF-7, Ca Ski, and PC-3 cell lines. This is in agreement with that reported by [23] whereby zerumin A isolated from *Curcuma mangga* exhibited antiproliferative effect on Ca Ski and MCF-7 displaying IC_{50} of 8.7 ± 0.29 and $14.2 \pm 0.06 \mu\text{g/mL}$,

respectively. In our previous study [19], curzerenone and alismol were also reported present in *Curcuma zedoaria* which were not found in the present study. The reason for this difference is possibly due to the source of the plant samples. The plant sample in the present study was obtained from Tawamangu, Java, Indonesia, whilst those in the earlier report were collected from Jogjakarta, Indonesia. In addition, it is also important to note that diterpenoids (compounds **1, 13, and 16**) were not detected in the sample obtained from Jogjakarta, and the isolation of curzerenone and alismol were based on bioassay-guided procedure. The cytotoxicity assay used in the present study could only provide important preliminary data to help select isolated compounds with potential anticancer properties. Further studies on the effect of curcumenone (**3**) and curcumenol (**5**) on the mode of MCF-7 cell death were thus pursued.

3.4. Induction of Apoptosis. The result from the cytotoxicity assay provides important preliminary data that may help select compounds with promising anticancer effects for

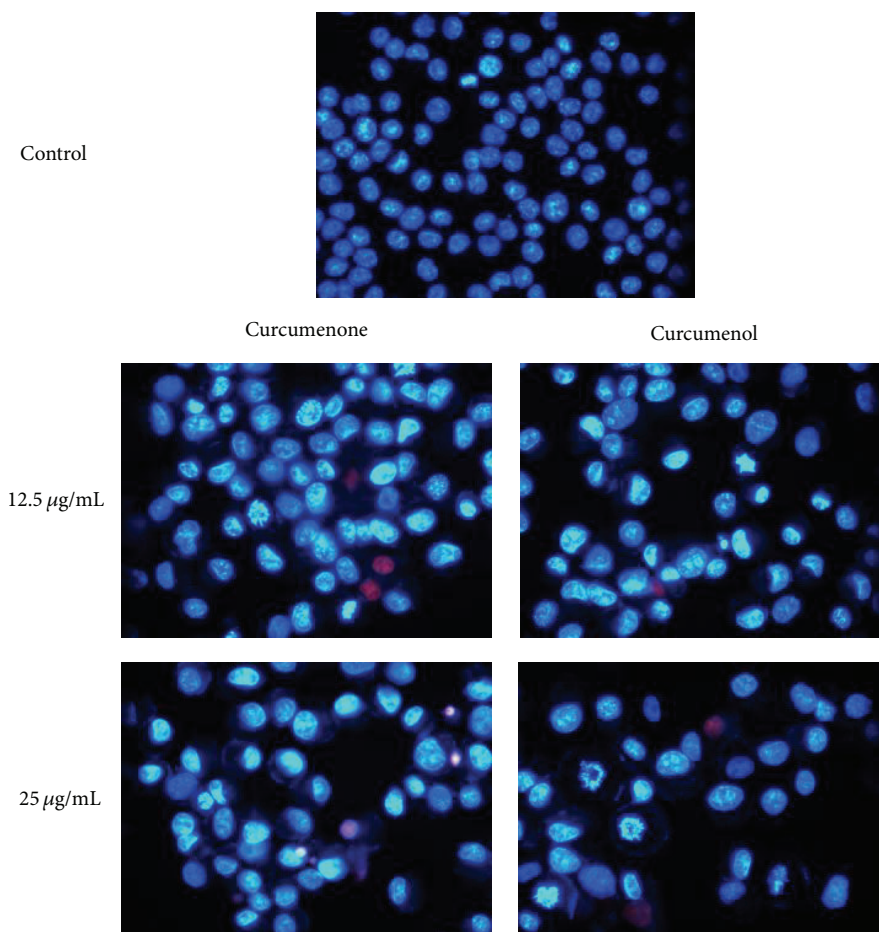


FIGURE 4: Apoptosis-inducing effect of curcumenone and curcumenol on MCF-7 cells by double staining using Hoechst 33342/PI and visualized under fluorescence microscope (630x).

further work. A detailed investigation on the underlying mechanism involved in cell death would provide a more convincing evidence of anticancer effect. Thus, apoptosis induction of the active compounds in the cancer cells was investigated. Apoptosis is described as programmed cell death. It is an essential process that enables the removal of cells from tissues thus maintaining the proper function of multicellular organisms. In the average human adult, about 50–70 billion cells die by apoptosis each day. However, diseases such as cancer resulted when cells fail to die. A series of events is involved in the process of apoptosis. The events start with cell dehydration which leads to cytoplasm condensation and alteration in cell shape and size. The next event is chromatin condensation which starts at the nuclear periphery and results in the concave shape of the nucleus, followed by nuclear membrane integration and nuclear fragmentation. Nuclear fragmentation and other organelles of the apoptotic cells are enveloped by fragments of cytoplasm and form apoptotic bodies which are phagocytosized by neighboring cells, thus preventing inflammatory reaction. These events can be observed in an inverted phase contrast and fluorescence microscope. Thus, apoptosis was first and is still best described morphologically [37]. Induction of apoptosis based on biochemical changes or flow cytometric

analyses should always be backed up with morphological studies [37].

3.5. Morphology of MCF-7 Cells Treated with Curcumenone and Curcumenol as Observed under Inverted Phase Contrast Microscope. In this study, the apoptosis inducing capacity of the two bioactive compounds, namely, curcumenone (3) and curcumenol (5), on MCF-7 cells was thus investigated using inverted phase contrast microscope. MCF-7 cells were incubated for 48 h with 12.5 and 25 $\mu\text{g/mL}$ of curcumenone (3) and curcumenol (5), respectively. Exposure of MCF-7 cells to the compounds led to cell shrinkage, loss of contact with adjacent cells, and decrease in cell numbers (Figure 3). In comparison, the untreated (control) cells were observed as intact and were cuboids or polygonal in shape. Floating cells detached from the surface of the tissue culture dishes (not shown) were also observed.

3.6. Hoechst 33342/PI Staining of MCF-7 Cells upon Treatment with Curcumenone and Curcumenol. Dual staining by Hoechst 33342/propidium iodide (PI) of MCF-7 and Ca Ski cells revealed that induction of apoptotic death occurred after 48 h incubation with curcumenone (3) and curcumenol (5).

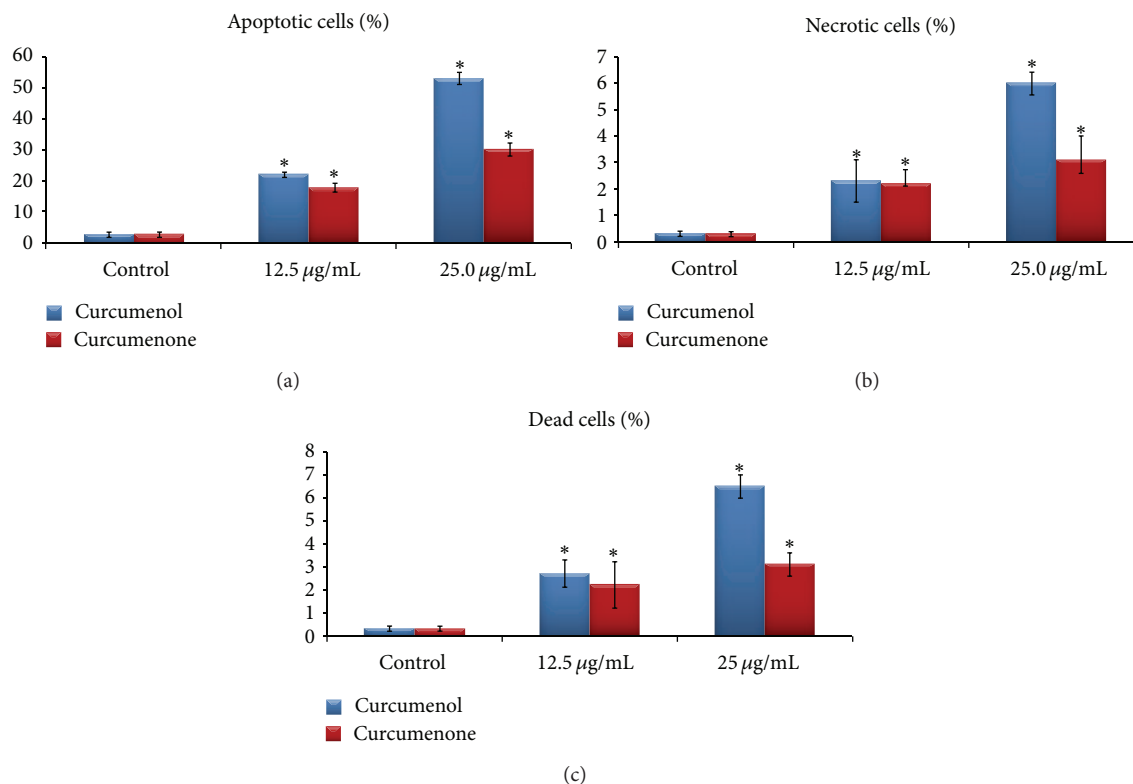


FIGURE 5: Apoptotic index and percentage of necrotic cells. Values expressed are means \pm standard deviation (s.d.) of triplicate measurements. The asterisks (*) denote significant differences between groups ($P < 0.05$).

The untreated cells displayed intact regular form and were homogeneously stained with a dimmer blue color. After the cells were treated (48 h) with 12.5 and 25 µg/mL of curcumenone (3) and curcumenol (5), respectively, apoptotic nuclei emitted much brighter blue fluorescence due to the highly condensed chromatin. As in Figure 4, crescents were observed around the periphery of the nucleus due to chromatin condensation. Cells that were in late apoptosis emitted pink fluorescence. The organized structure of pink chromatin denoted dead cells with normal nuclei. Dead cells with apoptotic nuclei showed highly condensed and fragmented bright pink chromatin. Necrotic cells were swollen with irregular membranes and fluorescence bright pink chromatin (due to PI). There was a significant increase in the percentage of apoptotic cells due to increasing dose of tested compounds. Curcumenol (5) revealed better inducing apoptosis capacity in comparison to curcumenone (3) as observed in Figure 5.

4. Conclusions

In this study, *Curcuma zedoaria* was shown to possess several compounds that have antiproliferative effect on four cancer cell lines (MCF-7, Ca Ski, PC-3, and HT-29). Amongst these, two compounds, namely, curcumenone (3) and curcumenol (5), present in the hexane extract were able to induce apoptosis in MCF-7 cells by inhibiting the proliferation of the cancer cells. However, further investigations are necessary

to determine their mode of action. It is noteworthy to mention that the hexane extract and the two compounds curcumenone and curcumenol showed low toxicity towards the normal cell line (HUVEC). If this also occurs *in vivo* then this plant has the potential to be developed as anticancer agent.

Conflict of Interests

The authors declare that there is no conflict of interests regarding the publication of this paper.

Acknowledgments

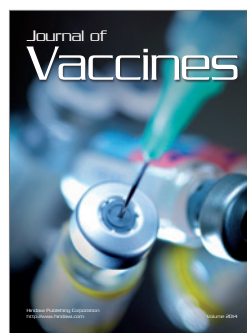
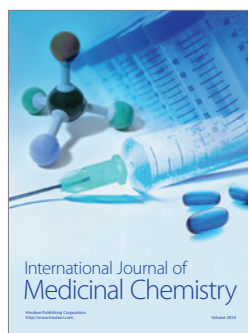
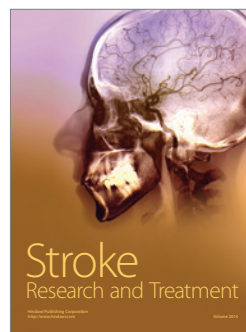
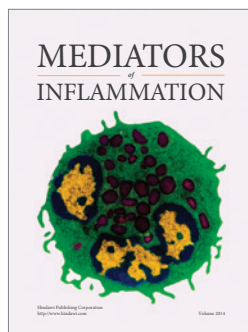
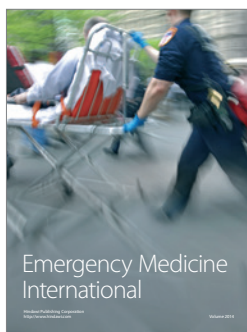
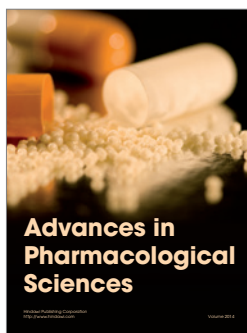
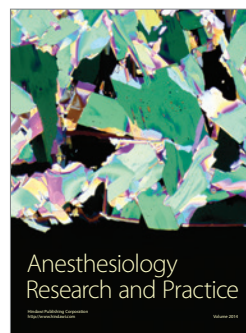
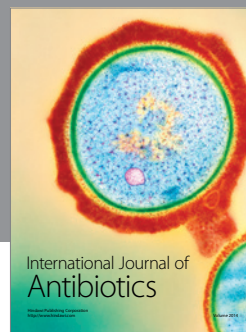
The authors wish to acknowledge the Ministry of Higher Education of Malaysia and the University of Malaya for financial assistance received through the following grants: UM High Impact Research Grant UM-MOHE UM.C/625/1/ HIR/MOHE/SC/02, RG015-09BIO, PS344/2009B, and PV036/2011B.

References

- [1] I. Jantan, "Conservation of medicinal plants and their traditional knowledge," in *Proceedings of the seminar UPM on Medicinal Plants: Cure for the 21st Century (Biodiversity, Conservation and Utilization of Medicinal Plants)*, M. N. B. Nair and G. Nathan, Eds., pp. 20–24, Serdang, Malaysia, October 1998.

- [2] S. N. Malek, F. Abdullah, N. M. Ali, H. Ibrahim, and M. N. Jalil, "Analysis of essential oil of *Curcuma zedoaria*," *Journal of Tropical Medicinal Plants*, vol. 5, no. 1, pp. 29–32, 2004.
- [3] H. Burkill, *A Dictionary of the Economic Products of the Malay Peninsula*, Ministry of Agriculture and Cooperative, 2nd edition, 1966.
- [4] K. Larsen, H. Ibrahim, S. H. Khaw, and L. G. Saw, *Gingers of Peninsular Malaysia and Singapore*, Natural History Publications Borneo Sdn Bhd, Borneo, Malaysia, 1999.
- [5] H. Matsuda, K. Ninomiya, T. Morikawa, and M. Yoshikawa, "Inhibitory effect and action mechanism of sesquiterpenes from *zedoariae* rhizoma on D-galactosamine/lipopolysaccharide-induced liver injury," *Bioorganic and Medicinal Chemistry Letters*, vol. 8, no. 4, pp. 339–344, 1998.
- [6] S. Park, J. Jung, H. Lee et al., "Zedoariae rhizoma and curcumin inhibits platelet-derived growth factor-induced proliferation of human hepatic myofibroblasts," *International Immunopharmacology*, vol. 5, no. 3, pp. 555–569, 2005.
- [7] S. Lakshmi, G. Padmaja, and P. Remani, "Antitumour effects of isocurcumenol isolated from *Curcuma zedoaria* rhizomes on human and murine cancer cells," vol. 2011, Article ID 253962, 13 pages, 2011.
- [8] W. Tuti and L. Andriani, "The use of *Curcuma zedoaria*, *Rosc.* meal to reduce abdominal fat and meat cholesterol in broiler," in *Proceedings of the International Symposium Modern Animal Husbandry-Food Safety and Socio-Economic Development*, vol. 53, pp. 126–129, Universitatea de Stiinte Agricole si Medicina Veterinara Ion Ionescu de la Brad, April 2010.
- [9] N. Hasima, L. I. L. Aun, M. N. Azmi et al., "1'S-1'-Acetoxyeugenol acetate: a new chemotherapeutic natural compound against MCF-7 human breast cancer cells," *Phytomedicine*, vol. 17, no. 12, pp. 935–939, 2010.
- [10] K. Awang, M. Nurul Azmi, L. I. Lian Aun, A. Nazif Aziz, H. Ibrahim, and N. Hasima Nagoor, "The apoptotic effect of 1'S-1'-Acetoxychavicol acetate from *Alpinia conchigera* on human cancer cells," *Molecules*, vol. 15, no. 11, pp. 8048–8059, 2010.
- [11] R. Othman, H. Ibrahim, M. A. Mohd, M. R. Mustafa, and K. Awang, "Bioassay-guided isolation of a vasorelaxant active compound from *Kaempferia galanga* L.," *Phytomedicine*, vol. 13, no. 1-2, pp. 61–66, 2006.
- [12] R. Lobo, K. S. Prabhu, and A. Shirwaikar, "*Curcuma zedoaria* Rosc. (white turmeric): a review of its chemical, pharmacological and ethnomedicinal properties," *Journal of Pharmacy and Pharmacology*, vol. 61, no. 1, pp. 13–21, 2009.
- [13] O.-J. Oh, H. Y. Min, and S. K. Lee, "Inhibition of inducible prostaglandin E₂ production and cyclooxygenase-2 expression by curdione from *Curcuma zedoaria*," *Archives of Pharmacological Research*, vol. 30, no. 10, pp. 1226–1239, 2007.
- [14] Y. Kimura, M. Sumiyoshi, and T. Tamaki, "Effects of the extracts and an active compound curcumenone isolated from *Curcuma zedoaria* rhizomes on alcohol-induced drunkenness in mice," *Fitoterapia*, vol. 84, no. 1, pp. 163–169, 2013.
- [15] J. Lu, Y. Dang, M. Huang, W. Xu, X. Chen, and Y. Wang, "Anti-cancer properties of terpenoids isolated from *Rhizoma Curcumae*—a review," *Journal of Ethnopharmacology*, vol. 143, no. 2, pp. 406–411, 2012.
- [16] M. K. Jang, H. J. Lee, J. S. Kim, and J. Ryu, "A curcuminoid and two sesquiterpenoids from *Curcuma zedoaria* as inhibitors of nitric oxide synthesis in activated macrophages," *Archives of Pharmacological Research*, vol. 27, no. 12, pp. 1220–1225, 2004.
- [17] H. W. D. Matthes, B. Luu, and G. Ourisson, "Cytotoxic components of *Zingiber zerumbet*, *Curcuma zedoaria* and *C. domestica*," *Phytochemistry*, vol. 19, no. 12, pp. 2643–2650, 1980.
- [18] Y. Shiobara, Y. Asakawa, M. Kodama, K. Yasuda, and T. Take-moto, "Curcumenone, curcumanolide A and curcumanolide B, three sesquiterpenoids from *Curcuma zedoaria*," *Phytochemistry*, vol. 24, no. 11, pp. 2629–2633, 1985.
- [19] S. N. Syed Abdul Rahman, N. Abdul Wahab, and S. N. Abd Malek, "In vitro morphological assessment of apoptosis induced by antiproliferative constituents from the rhizomes of *Curcuma zedoaria*," *Evidence-Based Complementary and Alternative Medicine*, vol. 2013, Article ID 257108, 14 pages, 2013.
- [20] O. A. Ahmed Hamdi, K. Awang, A. H. A. Hadi, D. R. Syamsir, and S. W. Ng, "Curcumenol from *Curcuma zedoaria*: a second monoclinic modification," *Acta Crystallographica E*, vol. 66, no. 11, p. o2844, 2010.
- [21] R. I. Geran, N. H. Greenberg, M. M. McDonald, A. M. Schumacher, and B. J. Abbott, "Protocols for screening chemical agents and natural products against animal tumor and other biological systems," *Cancer Chemotherapy Reports*, vol. 3, pp. 17–19, 1972.
- [22] E. Borenfreund and J. A. Puermer, "Toxicity determined in vitro by morphological alterations and neutral red absorption," *Toxicology Letters*, vol. 24, no. 2-3, pp. 119–124, 1985.
- [23] S. N. A. Malek, G. S. Lee, S. L. Hong et al., "Phytochemical and cytotoxic investigations of *Curcuma mangga* rhizomes," *Molecules*, vol. 16, no. 6, pp. 4539–4548, 2011.
- [24] P. M. Herst, T. Petersen, P. Jerram, J. Baty, and M. V. Berridge, "The antiproliferative effects of phenoxodiol are associated with inhibition of plasma membrane electron transport in tumour cell lines and primary immune cells," *Biochemical Pharmacology*, vol. 74, no. 11, pp. 1587–1595, 2007.
- [25] S. Ramasamy, N. A. Wahab, N. Z. Abidin, S. Manickam, and Z. Zakaria, "Growth inhibition of human gynecologic and colon cancer cells by *Phyllanthus watsonii* through apoptosis induction," *PLoS ONE*, vol. 7, no. 4, Article ID e34793, pp. 1–15, 2012.
- [26] F. Xu, S. Nakamura, Y. Qu et al., "Structures of new sesquiterpenes from *Curcuma comosa*," *Chemical and Pharmaceutical Bulletin*, vol. 56, no. 12, pp. 1710–1716, 2008.
- [27] P. M. Giang and P. T. Son, "Isolation of sesquiterpenoids from the rhizomes of Vietnamese *Curcuma aromatica salisb*," *Journal of Chemistry*, vol. 38, pp. 96–99, 2000.
- [28] K. Firman, T. Kinoshita, A. Itai, and U. Sankawa, "Terpenoids from *Curcuma heyneana*," *Phytochemistry*, vol. 27, no. 12, pp. 3887–3891, 1988.
- [29] M. Kuroyanagi, A. Ueno, K. Ujiie, and S. Sato, "Structures of sesquiterpenes from *Curcuma aromatica* SALISB," *Chemical and Pharmaceutical Bulletin*, vol. 35, no. 1, pp. 53–59, 1987.
- [30] D. Chávez, L. A. Acevedo, and R. Mata, "Jimenezin, a novel annonaceous acetogenin from the seeds of *Rollinia mucosa* containing adjacent tetrahydrofuran-tetrahydropyran ring systems," *Journal of Natural Products*, vol. 61, no. 4, pp. 419–421, 1998.
- [31] A. Dekebo, E. Dagne, and O. Sterner, "Furanosidesquiterpenes from *Commiphora sphaerocarpa* and related adulterants of true myrrh," *Fitoterapia*, vol. 73, no. 1, pp. 48–55, 2002.
- [32] M. Kuroyanagi, A. Ueno, K. Koyama, and S. Natori, "Structures of sesquiterpenes of *Curcuma aromatica* SALISB—II. Studies on minor sesquiterpenes," *Chemical and Pharmaceutical Bulletin*, vol. 38, no. 1, pp. 55–58, 1990.

- [33] P. Moongkarndi, N. Kosem, S. Kaslungka, O. Luanratana, N. Pongpan, and N. Neungton, "Antiproliferation, antioxidation and induction of apoptosis by *Garcinia mangostana* (mangosteen) on SKBR3 human breast cancer cell line," *Journal of Ethnopharmacology*, vol. 90, no. 1, pp. 161–166, 2004.
- [34] S. I. Abdel Wahab, A. B. Abdul, A. S. Alzubairi, M. M. Elhassan, and S. Mohan, "In vitro ultramorphological assessment of apoptosis induced by Zerumbone on (HeLa)," *Journal of Biomedicine and Biotechnology*, vol. 2009, Article ID 769568, 10 pages, 2009.
- [35] J. M. Brown and L. D. Attardi, "The role of apoptosis in cancer development and treatment response," *Nature Reviews Cancer*, vol. 5, no. 3, pp. 231–237, 2005.
- [36] G. Thuret, C. Chiquet, S. Herrag et al., "Mechanisms of staurosporine induced apoptosis in a human corneal endothelial cell line," *British Journal of Ophthalmology*, vol. 87, no. 3, pp. 346–352, 2003.
- [37] H. J. M. Brady, *Apoptosis Methods and Protocols*, Humana Press, Totowa, NJ, USA, 2004.
- [38] J. R. Dimmock, P. Kumar, A. J. Nazarali et al., "Cytotoxic 2,6-bis(arylidene)cyclohexanones and related compounds," *European Journal of Medicinal Chemistry*, vol. 35, no. 11, pp. 967–977, 2000.
- [39] W. Mahavorasirikul, V. Viyanant, W. Chaijaroenkul, A. Itharat, and K. Na-Bangchang, "Cytotoxic activity of Thai medicinal plants against human cholangiocarcinoma, laryngeal and hepatocarcinoma cells *in vitro*," *BMC Complementary and Alternative Medicine*, vol. 10, no. 55, pp. 1–8, 2010.
- [40] H. Xuan, Z. Li, H. Yan et al., "Antitumor activity of Chinese propolis in human breast cancer MCF-7 and MDA-MB-231 cells," *Evidence-Based Complementary and Alternative Medicine*, vol. 2014, Article ID 280120, 11 pages, 2014.
- [41] D. Su, Y. Cheng, M. Liu et al., "Comparison of piceid and resveratrol in antioxidation and antiproliferation activities *in vitro*," *PLoS ONE*, vol. 8, no. 1, Article ID e54505, 2013.
- [42] J. Parada-Turska, R. Paduch, M. Majdan, M. Kandefer-Szerszeń, and W. Rzeski, "Antiproliferative activity of parthenolide against three human cancer cell lines and human umbilical vein endothelial cells," *Pharmacological Reports*, vol. 59, no. 2, pp. 233–237, 2007.
- [43] Y. K. Yong, J. J. Tan, S. S. Teh et al., "Clinacanthus nutans extracts are antioxidant with antiproliferative effect on cultured human cancer cell lines," *Evidence-Based Complementary and Alternative Medicine*, vol. 2013, Article ID 462751, 8 pages, 2013.
- [44] T. R. L. Siekmann, K. M. Burgazli, M. A. Bobrich, G. Nöll, and A. Erdogan, "The antiproliferative effect of pinostrobin on human umbilical vein endothelial cells (HUVEC)," *European Review for Medical and Pharmacological Sciences*, vol. 17, no. 5, pp. 668–672, 2013.
- [45] The Native Antigen Company, 2088, <http://www.thenativeantigencompany.com/native-antigen-services-drug-testing.asp>.
- [46] D. Sun, Z. Fang, Y. Zhang, Y. Cao, L. Yang, and J. Yin, "Inhibitory effects of curcumenol on human liver cytochrome P450 enzymes," *Phytotherapy Research*, vol. 24, no. 8, pp. 1213–1216, 2010.



Research Article

Essential Oil Content of the Rhizome of *Curcuma purpurascens* Bl. (*Temu Tis*) and Its Antiproliferative Effect on Selected Human Carcinoma Cell Lines

Sok-Lai Hong,¹ Guan-Serm Lee,¹ Syarifah Nur Syed Abdul Rahman,¹
Omer Abdalla Ahmed Hamdi,² Khalijah Awang,²
Nurfina Aznam Nugroho,³ and Sri Nurestri Abd Malek¹

¹ Institute of Biological Sciences, Faculty of Science, University of Malaya, 50603 Kuala Lumpur, Malaysia

² Department of Chemistry, Faculty of Science, University of Malaya, 50603 Kuala Lumpur, Malaysia

³ Faculty of Mathematics and Sciences, Yogyakarta State University, Yogyakarta 55281, Indonesia

Correspondence should be addressed to Sri Nurestri Abd Malek; srimalek@um.edu.my

Received 14 February 2014; Revised 24 June 2014; Accepted 9 July 2014; Published 11 August 2014

Academic Editor: Valdir Cechinel Filho

Copyright © 2014 Sok-Lai Hong et al. This is an open access article distributed under the Creative Commons Attribution License, which permits unrestricted use, distribution, and reproduction in any medium, provided the original work is properly cited.

Curcuma purpurascens Bl., belonging to the Zingiberaceae family, is known as *temu tis* in Yogyakarta, Indonesia. In this study, the hydrodistilled dried ground rhizome oil was investigated for its chemical content and antiproliferative activity against selected human carcinoma cell lines (MCF7, Ca Ski, A549, HT29, and HCT116) and a normal human lung fibroblast cell line (MRC5). Results from GC-MS and GC-FID analysis of the rhizome oil of *temu tis* showed turmerone as the major component, followed by germacrone, *ar*-turmerone, germacrene-B, and curlone. The rhizome oil of *temu tis* exhibited strong cytotoxicity against HT29 cells (IC_{50} value of $4.9 \pm 0.4 \mu\text{g/mL}$), weak cytotoxicity against A549, Ca Ski, and HCT116 cells (with IC_{50} values of 46.3 ± 0.7 , 32.5 ± 1.1 , and $35.0 \pm 0.3 \mu\text{g/mL}$, resp.), and no inhibitory effect against MCF7 cells. It exhibited mild cytotoxicity against a noncancerous human lung fibroblast cell line (MRC5), with an IC_{50} value of $25.2 \pm 2.7 \mu\text{g/mL}$. This is the first report on the chemical composition of this rhizome's oil and its selective antiproliferative effect on HT29. The obtained data provided a basis for further investigation of the mode of cell death.

1. Introduction

Curcuma is a renowned genus in the family of Zingiberaceae due to the popularity of turmeric, *Curcuma longa* L. [1]. *Curcuma* species are native to several countries of Southeast Asia and extensively cultivated in Bangladesh, India, China, Taiwan, Sri Lanka, Indonesia, Peru, Australia, and the West Indies [2]. The name *Curcuma* was established by Linnaeus (1753), and its generic epithet is derived from the Arabic word “*kurkum*,” meaning yellow colour, which refers to the colour of the rhizomes [3, 4]. *Curcuma* has been circumscribed by its cone-like inflorescence of few-flowered, congested bracts and versatile, usually spurred anthers [5]. *Curcuma* is mostly grown for its foliage or rhizomes, which are widely used as a starch source, food seasoning or flavours in native dishes, coloured pigments (orange, yellow, citron,

amber, blue, greenish-blue, and violet-blue), and ingredients in traditional medicines to treat various ailments, including aches, pains, wounds, liver disorders, and cancers [4, 6, 7].

Curcuma purpurascens Bl. is one of the less known *Curcuma* species and is considered of minor importance [4]. *C. purpurascens*, locally known as *temu tis* in Yogyakarta, Indonesia, is also known as Solo's (east of Yogyakarta) *temu glenyeh* or *temu blenyeh*, whose scientific name is *Curcuma soloensis* Val. [8]. Villagers from the Kediri district of East Java plant *C. purpurascens* or *temu tis* at the base of Mount Wilis. The rhizomes are dried and ground before being sold to wholesalers as alternative medicine. The powdered rhizomes are usually taken together with other herbs to treat ailments, such as cough and skin infections [8, 9]. *Temu tis* can grow up to 1.75 m in height and usually flowers from October to February [9]. Morphologically, the rhizomes of

temu tis are similar to those of common turmeric (*Curcuma longa*). However, cross-sections of the rhizomes of *temu tis* are slightly bigger and paler in colour in comparison to common turmeric [8]. Hence, the dried ground rhizomes of *temu tis* are often used to adulterate dried ground rhizomes of common turmeric and *Curcuma xanthorrhiza* (locally known as *temulawak*) for higher profit margins [8].

Until now, the phytochemical and biological investigations reported on this plant have been very limited. The plantlet of *temu tis* was reported to be successfully transplanted to soil via propagation using *in vitro* tissue culture methods [9]. The essential oil content of the dried ground rhizomes of *temu tis* showed the presence of only four compounds, namely, turmerone and *ar*-turmerone (as the major components), as well as xanthorrhizol and isofuranogermacrene (also known as curzerene) [8]. Hexane and chloroform extracts of the rhizomes of *C. purpurascens* were reported to exhibit the strongest inhibition against *Candida albicans* [10]. Fractions C and G obtained from the hexane extract and fraction *a* obtained from the chloroform extract were found to have good antifungal activity, comparable to that of the reference standard, miconazole [10]. 1- α -Terpineol, β -eudesmol, farnesol, 1,6-dimethyl-9-(1-methylethylidene)-5,12-dioxatricyclo[9.1.0.0(4,6)]dodecan-8-one, and caryophyllene oxide were identified in these fractions via gas chromatography-mass spectrometry (GC-MS) [10].

Although *temu tis* is considered one of the less important *Curcuma* species, there is still a need to investigate the chemical constituents of its rhizome oil and its biological activity. Results from chemical investigation of the rhizome oil of *temu tis* can be utilised to authenticate *temu tis* and to determine the presence of adulteration in ground turmeric. Results from biological investigations on the rhizome oil or extracts of *temu tis* would provide more insight into the potential use of this plant for therapeutic purposes. Thus, in the present study, the essential oil obtained from hydrodistilled dried ground rhizome oil of *temu tis* was analysed for its chemical composition, and its antiproliferative activity against selected human carcinoma cell lines was also investigated. This is the first report on the chemical content of the hydrodistilled dried ground rhizome oil of *temu tis* and its antiproliferative activity against selected human cell lines.

2. Materials and Methods

2.1. Collection of Plant Materials and Extraction of Rhizome Oil. The dried rhizomes of *temu tis* were collected from Yogyakarta, Indonesia, in September 2012. A voucher specimen, KL 5793, was deposited at the herbarium of the Chemistry Department, Faculty of Science, University of Malaya, Kuala Lumpur, Malaysia. The rhizomes (300.00 g) were cut into small pieces, ground, and immediately soaked in distilled water (1.00 L) in a round-bottomed flask. The soaked sample was distilled in a Clevenger-type apparatus for 5 hours. The yield of the oil (2.16 g, 0.72%) was calculated based on the weight of the dried plant material.

2.2. GC-MS and GC-FID Analysis. The oil was analysed on an Agilent Technologies 7890A GC system equipped with an FID detector using a fused HP-5 silica capillary column (5% diphenyl- and 95% dimethyl-polysiloxane, 30.00 m \times 0.32 mm ID, 0.25 μ m film thickness) with helium as the carrier gas at a flow rate of 1.0 mL per minute. The column temperature was initially programmed to and kept at 60.0°C for 10.0 minutes, then increased at 3.0°C per minute to 230.0°C, and held for 1.0 minute. The temperatures of the injector port and detector were set to 230.0°C and 250.0°C, respectively, with a split ratio of 1:20. GC-MS analysis was performed on an Agilent Technologies 6890N GC System equipped with a 5975 inert mass selective detector (70 eV direct inlet) on an HP-5ms capillary column (30.0 m \times 0.25 mm ID, 0.25 μ m film thickness). The column temperature was programmed to 60.0°C for 10.0 minutes, then increased to 230.0°C at 3.0°C per minute, and held for 1.0 minute at 230.0°C. Helium was used as the carrier gas at a flow rate of 1.0 mL per minute with a split ratio of 1:20. The injector port temperature was set to 230.0°C and detector to 250.0°C. The obtained total ion chromatogram was autointegrated by ChemStation, and the components were identified by comparison with an accompanying mass spectral database [11]. The arithmetic index (AI) was experimentally measured from the programmed temperature GC-FID by arithmetic interpolation between bracketing alkanes, using a homologous series of n-alkanes as standards [12, 13].

2.3. Cell Propagation. Human breast carcinoma cells (MCF7), human cervical carcinoma cells (Ca Ski), human lung carcinoma cells (A549), human colon carcinoma cells (HCT116 and HT29), and noncancerous human lung fibroblast cells (MRC5) were purchased from the American Tissue Culture Collection (ATCC, USA). All the cells were cultured using protocols described earlier [14]. MCF7, Ca Ski, A549, and HT29 cells were cultured in supplemented RPMI 1640 medium, HCT116 cells in supplemented McCoy's 5A medium, and MRC5 in supplemented Eagle's minimum essential medium (EMEM). The RPMI 1640, McCoy's 5A, and EMEM media (Sigma-Aldrich, USA) were supplemented with 10.0% v/v foetal bovine serum (PAA Laboratories, Austria), 100.0 μ g/mL penicillin/streptomycin (PAA Laboratories, Austria), and 50.0 μ g/mL amphotericin B (PAA Laboratories, Austria). The EMEM medium was also supplemented with 11.0 mg/mL sodium pyruvate (Sigma-Aldrich, USA). Briefly, the cells were cultured in 25.0 cm³ tissue culture flasks (Nunc, Denmark) in 5.0% CO₂ in an air-jacketed incubator (ESCO, USA) kept at 37.0°C in a humidified atmosphere and routinely observed under inverted microscope (Carl Zeiss Axio Vert.A1, Germany) for any contamination. The medium was replaced every 2 or 3 days until cell confluence was achieved, and the cells were detached using Accutase (PAA Laboratories, Austria). The rhizome oil of *temu tis* was dissolved in molecular-biology-grade dimethyl sulfoxide (DMSO) from Sigma-Aldrich, USA.

2.4. Antiproliferative Assay. The antiproliferative assay was performed using an MTT assay according to the method of

TABLE 1: Chemical composition of the essential oil of *temu tis* rhizomes.

Number	Compounds	Arithmetic indices (AI)		Percentage of peak area	Methods of identification
		Calculated	Literature [13]		
1	1,8-Cineole	1031	1026	3.3	MS, AI
2	Camphor	1144	1141	4.0	MS, AI
3	Borneol	1166	1165	0.3	MS, AI
4	Terpinen-4-ol	1178	1174	0.3	MS, AI
5	<i>p</i> -Cymen-8-ol	1184	1179	0.2	MS, AI
6	α -Terpineol	1191	1186	0.8	MS, AI
7	Thymol	1293	1289	0.1	MS, AI
8	δ -Elemene	1339	1335	0.2	MS, AI
9	Piperitenone	1342	1340	0.7	MS, AI
10	β -Elemene	1393	1389	1.2	MS, AI
11	<i>cis</i> - α -Bergamotene	1416	1411	0.1	MS, AI
12	<i>trans</i> -Caryophyllene	1421	1417	1.8	MS, AI
13	γ -Elemene	1435	1434	1.6	MS, AI
14	Aromadendrene	1441	1439	0.1	MS, AI
15	α -Humulene	1455	1452	0.1	MS, AI
16	<i>trans</i> - β -Farnesene	1458	1454	0.2	MS, AI
17	γ -Murolene	1478	1478	0.5	MS, AI
18	<i>ar</i> -Curcumene	1484	1479	2.6	MS, AI
19	α -Selinene	1488	—	1.3	MS
20	Curzerene	1500	1499	5.8	MS, AI
21	β -Bisabolene	1510	1505	0.4	MS, AI
22	β -Sesquiphellandrene	1526	1521	2.7	MS, AI
23	Selina-3,7(11)-diene	1544	1545	0.6	MS, AI
24	Germacrene-B	1561	1559	8.8	MS, AI
25	<i>ar</i> -Turmerol	1580	1580	3.3	MS, AI
26	Guaiol	1595	1600	0.3	MS, AI
27	<i>trans</i> - β -Elemenone	1607	1602	2.5	MS, AI
28	γ -Eudesmol	1633	1630	0.7	MS, AI
29	β -Eudesmol	1637	—	0.7	MS
30	Atractylone	1654	1657	0.6	MS, AI
31	<i>ar</i> -Turmerone	1671	1668	9.4	MS, AI
32	Turmerone	1675	—	13.5	MS
33	Germacrone	1702	—	13.2	MS
34	Curlone	1705	—	6.2	MS
Total rhizome oil =				88.1%	

Remarks: MS: mass spectroscopy [11]; AI: arithmetic indices [13].

[15] with some modifications. Cells were plated into sterile 96-well culture plates at a density of 3.0×10^4 cells/mL. The 96-well plates were incubated in 5.0% CO₂ in an air-jacketed incubator at 37.0°C for 24 hours for the cells to adhere. The medium was removed after 24 hours of incubation, and 150.0 μ L of fresh medium containing various concentrations of the rhizome oil of *temu tis* was added. The plates were further incubated for 72 hours. Then, 20.0 μ L of MTT solution (Sigma-Aldrich, USA) was added to each well, and the plates were again incubated for 4 hours. Medium containing MTT was discarded, and 150.0 μ L of DMSO was added into each well to dissolve the formazan crystals. The absorbance of each well was measured at 570 nm using a microplate reader (Synergy H1 Hybrid Multi-Mode Microplate Reader, USA).

The IC₅₀ values were determined by the interpolation of the dose-response curve for each cell line.

3. Results and Discussion

3.1. Yield of Rhizome Oil Extraction. Hydrodistillation of the dried rhizomes of *temu tis* (300.0 g) yielded 2.2 g (0.7%) of oil. The identified constituents of the rhizome oil are listed in Table 1. The constituents were identified by matching their mass spectra and arithmetic indices with reference libraries [11–13]. Thirty-four (34) compounds consisting of eight (8) monoterpenoids (9.7%), fifteen (15) sesquiterpenes (22.2%), and eleven (11) sesquiterpenoids (56.2%) were identified from the rhizome oil of *temu tis*.

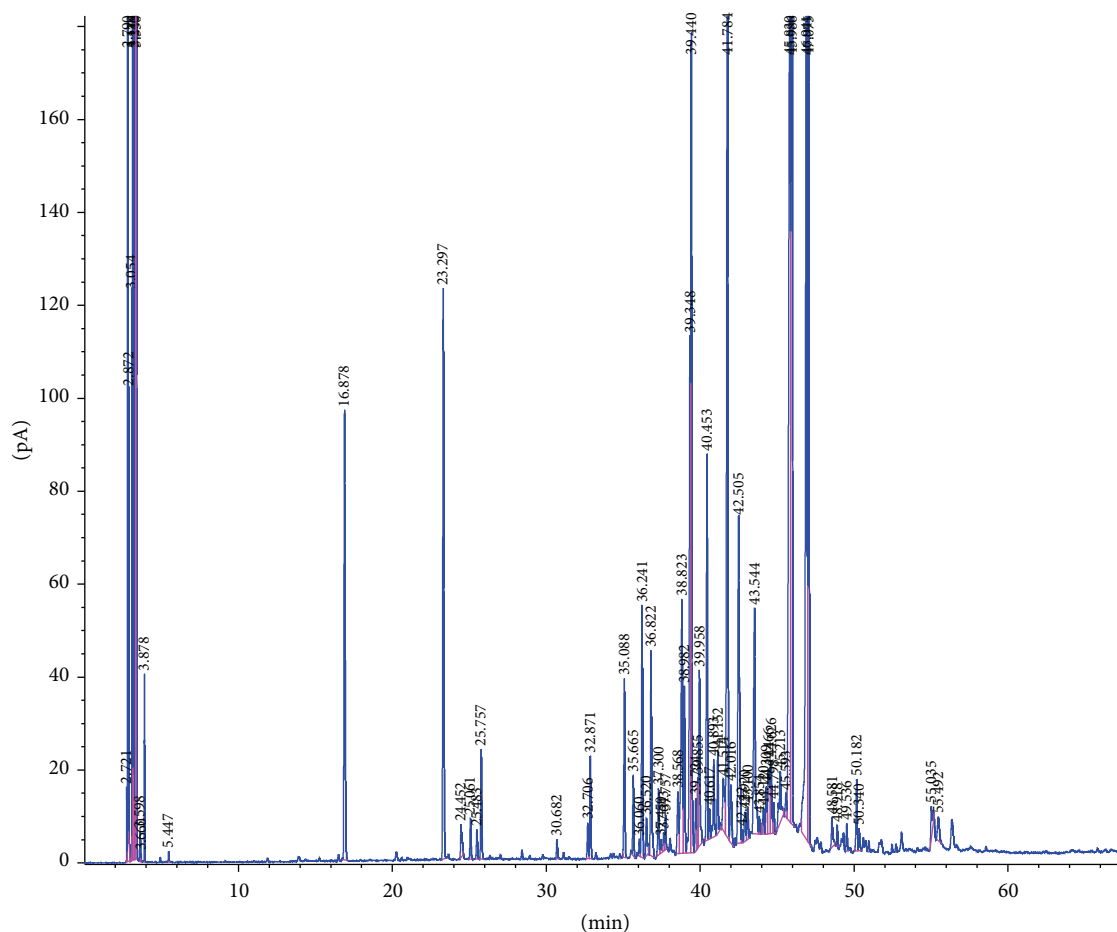


FIGURE 1: The GC-FID profile of the essential oil of rhizomes of *Curcuma purpurascens* Bl. (*temu tis*).

The monoterpenoids are 1,8-cineole, camphor, borneol, terpinen-4-ol, *p*-cymen-8-ol, α -terpineol, thymol, and piperitone, while the sesquiterpenes are δ -elemene, β -elemene, cis- α -bergamotene, trans-caryophyllene, γ -elemene, aromadendrene, α -humulene, trans- β -farnesene, γ -muurolene, *ar*-curcumene, α -selinene, β -bisabolene, β -sesquiphellandrene, selina-3,7(11)-diene, and germacrene-B. The identified sesquiterpenoids are curzerene, *ar*-turmerol, guaial, trans- β -elemenone, γ -eudesmol, atractylone, *ar*-turmerone, turmerone, germacrone, and curlone. These components made up 88.1% of the total components detected in the GC chromatogram of the oil (Figure 1). The major components identified were turmerone (13.5%), germacrone (13.2%), *ar*-turmerone (9.4%), germacrene-B (8.8%), and curlone (6.2%), which together amount to 51.1% of the total oil.

3.2. GC-MS and GC-FID Analysis. The findings of this study differ from a previous study on the rhizome oil of *temu tis*, which reported turmerol and *ar*-turmerone as the major components [8]. The current study also did not find xanthorrhizol in the rhizome oil of *temu tis*. This study identified thirty-four (34) compounds in the rhizome oil of *temu tis*, but the previous study identified only turmerone, *ar*-turmerone,

xanthorrhizol, and curzerene [8]. Ground rhizomes of *temu tis* have been used as adulterants in ground common turmeric and *C. xanthorrhiza* (*temulawak*) for higher profit margins [8]; thus, it is necessary to compare the chemical content of its rhizome oil with those of common turmeric and *temulawak*. Previous studies on the essential oil content of dried rhizomes of common turmeric reported *ar*-turmerone as the major component, ranging from 21.4% to 49.0% [16–18], while the essential oil content of fresh rhizomes showed *ar*-turmerone content ranging from 24.4% to 49.1% [16, 19, 20]. Others reported α -turmerone as the major component ranging from 21.4% to 44.1% [21, 22]. *Ar*-curcumene (40.0% to 65.0%) was reported to be the major compound identified from the rhizome oil of *temulawak* [23, 24], followed by xanthorrhizol (21.5%) [24]. A recent report identified xanthorrhizol as the major component (31.9% to 64.4%) in the rhizome oil of *temulawak* [25, 26]. Hence, the results of chemical investigations on the rhizome oil of *temu tis* in this study differ from those reported in the literature for both common turmeric and *temulawak*. The presence of *ar*-turmerone and xanthorrhizol found in the essential oil of *temu tis* by the Indonesian researchers in the previous study could possibly be due to adulteration by common turmeric and *temulawak* in the sample used [8].

TABLE 2: Cytotoxicity activity of the rhizome oil of *temu tis*.

	Cell lines					
	MCF7	Ca Ski	A549	HCT116	HT29	MRC5
IC ₅₀ values ($\mu\text{g/mL}$)	>100.0	32.5 \pm 1.1	46.3 \pm 0.7	35.0 \pm 0.3	4.9 \pm 0.4	25.2 \pm 2.7

Tabulated values are mean standard error (SE, SE < 5.00) of three replicates.

The yield of the rhizome oil of *temu tis* reported in the previous study was 4.6% [8], while that of the rhizome oil of *temu tis* obtained in this study is only approximately 0.7%. A previous study on the rhizome oil of *temulawak* showed that the yield of the rhizome oil from *temulawak* is approximately 4.5% [25], while the yield of essential oil from both fresh and dried rhizomes of common turmeric ranged from 0.7% to 1.1% [17, 19, 21, 22]. The similarity of the yield of the rhizome oil of *temu tis* obtained by the Indonesian researchers (4.6%) with that obtained by Jantan et al. [25] again indicated that the ground *temu tis* used in their study could have been adulterated with *temulawak*.

3.3. Antiproliferative Effect. The antiproliferative effects of the rhizome oil of *temu tis* against human breast carcinoma cells (MCF7), human cervical carcinoma cells (Ca Ski), human lung carcinoma cells (A549), human colon carcinoma cells (HCT116 and HT29), and noncancerous human lung fibroblast cells (MRC5) were investigated via an MTT assay, and the results are shown in Table 2. According to the US NCI's plant screening program, crude extracts with IC₅₀ values (concentration that inhibited 50% of cell proliferation) of less than 20.0 $\mu\text{g/mL}$ following incubation between 48 and 72 hours are considered to have *in vitro* cytotoxic activity [27]. The rhizome oil of *temu tis* exhibited very good cytotoxic effects against HT29 cells with an IC₅₀ value of 4.9 \pm 0.4 $\mu\text{g/mL}$. However, it exhibited no inhibitory effect against MCF7 cells and very mild cytotoxicity against A549, Ca Ski, and HCT116 cells with IC₅₀ values of 46.3 \pm 0.7, 32.5 \pm 1.1, and 35.0 \pm 0.3 $\mu\text{g/mL}$, respectively. The rhizome oil of *temu tis* also exhibited mild cytotoxicity against the noncancerous human lung fibroblast cell line, MRC5 (IC₅₀ value of 25.2 \pm 2.7 $\mu\text{g/mL}$).

There are few reports found in the scientific literature on the antiproliferative effect of the rhizome oil of *Curcuma* species. Two studies reported that the rhizome oil of *Curcuma zedoaria* exhibited an inhibitory effect on the growth of a human promyelocytic leukaemia cell line (HL-60) and nonsmall cell lung carcinoma cell lines (H1299, A549, and H23) with IC₅₀ values of 500.0, 80.0, 80.0, and 185.0 $\mu\text{g/mL}$, respectively [28, 29]. The rhizome oil of *Curcuma wenyujin* had an antiproliferative effect on the human hepatoma cell line, HepG2, with an IC₅₀ value of 70.0 $\mu\text{g/mL}$ [30]. However, the reported antiproliferative effects for the rhizome oil of both *Curcuma zedoaria* and *Curcuma wenyujin* did not meet the definition of *in vitro* cytotoxic activity defined by the US NCI's plant screening program [27] because their IC₅₀ values are greater than 20.0 $\mu\text{g/mL}$ following 72 hours of incubation. Thus, the rhizome oil of *temu tis* exhibited better antiproliferative effects against the investigated human carcinoma cell lines in comparison to those reported in the

literature [28–30], and the obtained IC₅₀ value against HT29 cells is less than 20.0 $\mu\text{g/mL}$ following 72 hours of incubation.

The good cytotoxic effect exerted by the rhizome oil of *temu tis* against HT29 cells may be due to the presence of an appreciable amount of *ar*-turmerone (9.4%) and germacrene-B (8.8%) in the rhizome oil. Germacrene-B was reported to exhibit good cytotoxicity against a human ovarian cell line, A2780, with an IC₅₀ value of 6.4 $\mu\text{g/mL}$; however, presently, there is no report on the molecular pathway of cancer cell death induced by germacrene-B [31]. *Ar*-turmerone was reported to have an inhibitory effect against several cell lines, namely, a human myelogenous leukaemia carcinoma cell line (K562), a human histiocytic lymphoma carcinoma cell line (U937), a mouse lymphocytic leukaemia carcinoma cell line (L1210), and a rat basophilic leukaemia carcinoma cell line (RBL-2H3), with IC₅₀ values between 20.0 and 50.0 $\mu\text{g/mL}$ [32]. *Ar*-turmerone was also reported to induce apoptosis in HepG2 cells (a human hepatocellular carcinoma cell line) via reactive oxygen species- (ROS-) mediated activation of extracellular signal-related (ERK) and c-Jun N-terminal (JNK) kinases, which then trigger both extrinsic and intrinsic caspase cascades, leading to apoptosis [33].

In this study, the rhizome oil of *temu tis* was found to exhibit a strong inhibitory effect against HT29 cells but very mild cytotoxicity against HCT116 cells, even though both cells are human colon carcinoma cell lines. HT29 cells express cyclooxygenase-2 (COX-2), while HCT116 cells do not [34]. The expression of COX-2 protein is elevated during colon carcinogenesis [35]. A recent study reported that *ar*-turmerone blocked the NF- κ B, PI3K/Akt, and ERK1/2 signalling pathways in human breast cancer cells, which led to suppression of 12-*O*-tetradecanoylphorbol-13-acetate-(TPA-) induced upregulation of matrix metalloproteinase-(MMP-) 9 and COX-2 expression [36]. *Ar*-turmerone (9.4%) in the rhizome oil of *temu tis* may have suppressed COX-2 expression by blocking the NF- κ B, PI3K/Akt, and ERK1/2 signalling pathways, and synergistic effects of other constituents, such as turmerone, germacrone, germacrene-B, and curlone, may have inhibited the proliferation of HT29 cells. However, the amount of *ar*-turmerone was insufficient to exert any inhibition against the proliferation of MCF7 cells. Further *in vivo* toxicity studies on animal models will be attempted to determine the toxicity of the rhizome oil of *temu tis*, as it showed a mild inhibitory effect against MRC5 cells, the noncancerous human lung fibroblast cell line (IC₅₀ value of 25.2 \pm 2.7 $\mu\text{g/mL}$).

4. Conclusion

In conclusion, GC-MS analysis of the rhizome oil of *temu tis* could be developed into a standard method to identify

and differentiate the rhizome of *temu tis* from the rhizomes of common turmeric and *temulawak*. The rhizome oil of *temu tis* exhibited selective cytotoxic effect towards HT29 cell lines. Its inhibitory effect against HT29 cells may be due to the augmentation of COX-2 expression levels by *ar*-turmerone and synergistic effects of other constituents, such as turmerone, germacrone, germacrene-B, and curlone. In addition, the data obtained from this study provide a scientific basis for the use of this rhizome oil in the treatment of cancer-related diseases.

Conflict of Interests

The authors declare that there is no conflict of interests regarding the publication of this paper.

Acknowledgments

This work was financially supported by UM High Impact Research Grant UM-MOHE UM.C/625/1/HIR/MOHE/SC/02 from Ministry of Higher Education Malaysia. The authors gratefully acknowledge the facilities provided by the Institute of Biological Sciences, Faculty of Science, University of Malaya.

References

- [1] J. L. Skornicková, O. Sída, V. Jarolímová et al., "Chromosome numbers and genome size variation in Indian species of *Curcuma* (Zingiberaceae)," *Annals of Botany*, vol. 100, no. 3, pp. 506–526, 2007.
- [2] L. Nahar and S. D. Sarker, "Phytochemistry of the genus *Curcuma*," in *Turmeric: The Genus Curcuma*, pp. 71–106, CRC Press, 2007.
- [3] P. N. Ravindran, K. N. Babu, and K. N. Shiva, "Botany and crop improvement of turmeric," in *Turmeric: The Genus Curcuma*, pp. 15–70, CRC Press, 2007.
- [4] K. N. Babu, K. N. Shiva, M. Sabu, M. Divakaran, and P. N. Ravindran, "Turmeric," in *Genetic Resources, Chromosome Engineering, and Crop Improvement: Medicinal Plants*, vol. 6, pp. 451–511, CRC Press, 2011.
- [5] W. John Kress, L. M. Prince, and K. J. Williams, "The phylogeny and a new classification of the gingers (Zingiberaceae): evidence from molecular data," *American Journal of Botany*, vol. 89, no. 10, pp. 1682–1696, 2002.
- [6] H. Burkill, *A Dictionary of the Economic Products of the Malay Peninsula*, Ministry of Agriculture and Cooperative, 2nd edition, 1966.
- [7] L. M. Perry, *Medicinal plants of South and South East Asia*, The MIT Press, Cambridge, Mass, USA, 1980.
- [8] M. H. Santoso, Suyanto, and W. Dyatmiko, "Analisa fitokimia minyak atsiri rimpang temu glenyeh dari Kecamatan Grogol-Kediri," in *Prosiding Simposium Nasional / Tumbuhan Obat dan Aromatik*, pp. 50–57, 1996.
- [9] D. S. H. Hoesen, Sumarnie, and G. Panggabean, "Kultur jaringan temu glenyeh (*Curcuma soloensis* Val.)," in *Prosiding Simposium Nasional/Tumbuhan Obat dan Aromatik*, pp. 272–277, 1996.
- [10] Y. Vibrianti, *Isolasi dan Identifikasi Fraksi Aktif Antijamur dalam Rimpang Temu Tis (Curcuma purpurascens Bl.)*, Fakultas Matematika dan Ilmu Pengetahuan Alam, Universitas Sebelas Maret, Surakarta, Indonesia, 2005, <http://digilib.uns.ac.id/pengguna.php?mn=showview&id=2389>.
- [11] Wiley 9th edition & NIST 11 Mass Spectral Library, Agilent Technologies, Palo, Calif, USA, 2011.
- [12] H. van Den Dool and P. Dec. Kratz, "A generalization of the retention index system including linear temperature programmed gas-liquid partition chromatography," *Journal of Chromatography A*, vol. 11, pp. 463–471, 1963.
- [13] R. P. Adams, *Identification of Essential Oil Components by Chromatography/Mass Spectrometry*, Allured Business Media, Carol Stream, Ill, USA, 4th edition, 2012.
- [14] S. N. S. Abdul Rahman, N. Abdul Wahab, and S. N. Abd Malek, "In vitro morphological assessment of apoptosis induced by antiproliferative constituents from the rhizomes of *Curcuma zedoaria*," *Evidence-Based Complementary and Alternative Medicine*, vol. 2013, Article ID 257108, 14 pages, 2013.
- [15] Y. F. Ho, S. A. Karsani, W. K. Yong, and S. N. Abd Malek, "Induction of apoptosis and cell cycle blockade by helichrysetin in A549 human lung adenocarcinoma cells," *Evidence-Based Complementary and Alternative Medicine*, vol. 2013, Article ID 857257, 10 pages, 2013.
- [16] G. Singh, I. P. S. Kapoor, P. Singh, C. S. de Heluani, M. P. de Lampasona, and C. A. N. Catalan, "Comparative study of chemical composition and antioxidant activity of fresh and dry rhizomes of turmeric (*Curcuma longa* Linn.)," *Food and Chemical Toxicology*, vol. 48, no. 4, pp. 1026–1031, 2010.
- [17] S. Tsai, S. J. Huang, C. C. Chyau, C. H. Tsuai, C. Weng, and J. Mau, "Composition and antioxidant properties of essential oils from *Curcuma* rhizome," *Asian Journal of Arts and Sciences*, vol. 2, no. 1, pp. 57–66, 2011.
- [18] N. K. Leela, A. Tava, P. M. Shafi, S. P. John, and B. Chempakam, "Chemical composition of essential oils of turmeric (*Curcuma longa* L.)," *Acta Pharmaceutica*, vol. 52, no. 2, pp. 137–141, 2002.
- [19] J. U. Chowdhury, N. C. Nandi, M. N. I. Bhuiyan, and M. H. Mobarak, "Essential oil constituents of the rhizomes of two types of *Curcuma longa* of Bangladesh," *Bangladesh Journal of Scientific and Industrial Research*, vol. 43, no. 2, pp. 259–266, 2008.
- [20] S. Singh, B. Sankar, S. Rajesh, K. Sahoo, E. Subudhi, and S. Nayak, "Chemical composition of turmeric oil (*Curcuma longa* L. cv. Roma) and its antimicrobial activity against eye infecting pathogens," *Journal of Essential Oil Research*, vol. 23, no. 6, pp. 11–18, 2011.
- [21] J. Chane-Ming, R. Vera, J. Chalchat, and P. Cabassu, "Chemical composition of essential oils from rhizomes, leaves and flowers of *Curcuma longa* L. from Reunion Island," *Journal of Essential Oil Research*, vol. 14, no. 4, pp. 249–251, 2002.
- [22] V. K. Raina, S. K. Srivastava, and K. V. Syamsundar, "Rhizome and leaf oil composition of *Curcuma longa* from the lower Himalayan region of northern India," *Journal of Essential Oil Research*, vol. 17, no. 5, pp. 556–559, 2005.
- [23] S. Yasni, K. Imaizumi, K. Sin, M. Sugano, and G. Nonaka, "Identification of an active principle in essential oils and hexane-soluble fractions of *Curcuma xanthorrhiza* Roxb. showing triglyceride-lowering action in rats," *Food and Chemical Toxicology*, vol. 32, no. 3, pp. 273–278, 1994.
- [24] J. H. Zwaving and R. Bos, "Analysis of the essential oils of five *Curcuma* species," *Flavour and Fragrance Journal*, vol. 7, no. 1, pp. 19–22, 1992.

- [25] I. Jantan, F. C. Saputri, M. N. Qaisar, and F. Buang, "Correlation between chemical composition of curcuma domestica and *Curcuma xanthorrhiza* and their antioxidant effect on human low-density lipoprotein oxidation," *Evidence-based Complementary and Alternative Medicine*, vol. 2012, Article ID 438356, 10 pages, 2012.
- [26] H. P. A. Mary, G. K. Susheela, S. Jayasree, A. M. Nizy, B. Rajagopal, and S. Jeeva, "Phytochemical characterization and antimicrobial activity of *Curcuma xanthorrhiza* Roxb," *Asian Pacific Journal of Tropical Biomedicine*, vol. 2, no. 2, pp. S637–S640, 2012.
- [27] C. C. Lee and P. Houghton, "Cytotoxicity of plants from Malaysia and Thailand used traditionally to treat cancer," *Journal of Ethnopharmacology*, vol. 100, no. 3, pp. 237–243, 2005.
- [28] E. Y. C. Lai, C. Chyau, J. Mau et al., "Antimicrobial activity and cytotoxicity of the essential oil of *Curcuma zedoaria*," *The American Journal of Chinese Medicine*, vol. 32, no. 2, pp. 281–290, 2004.
- [29] C. C. Chen, Y. Chen, Y. T. Hsi et al., "Chemical constituents and anticancer activity of *Curcuma zedoaria* roscoe essential oil against non-small cell lung carcinoma cells in vitro and in vivo," *Journal of Agricultural and Food Chemistry*, vol. 61, pp. 11418–11427, 2013.
- [30] Y. Xiao, F. Yang, S. Li, G. Hu, S. M. Lee, and Y. Wang, "Essential oil of *Curcuma wenyujin* induces apoptosis in human hepatoma cells," *World Journal of Gastroenterology*, vol. 14, no. 27, pp. 4309–4318, 2008.
- [31] V. S. P. Chaturvedula, J. K. Schilling, J. S. Miller, R. Andriantsiferana, V. E. Rasamison, and D. G. I. Kingston, "New cytotoxic terpenoids from the wood of *Vepris punctata* from the madagascar rainforest," *Journal of Natural Products*, vol. 67, no. 5, pp. 895–898, 2004.
- [32] M. Ji, J. Choi, J. Lee, and Y. Lee, "Induction of apoptosis by ar-turmerone on various cell lines," *International Journal of Molecular Medicine*, vol. 14, no. 2, pp. 253–256, 2004.
- [33] S. Cheng, L. Wu, Y. Hsieh et al., "Supercritical carbon dioxide extraction of aromatic turmerone from *Curcuma longa* Linn. Induces apoptosis through reactive oxygen species-triggered intrinsic and extrinsic pathways in human hepatocellular carcinoma HepG2 cells," *Journal of Agricultural and Food Chemistry*, vol. 60, no. 38, pp. 9620–9630, 2012.
- [34] B. Agarwal, P. Swaroop, P. Protiva, S. V. Raj, H. Shirin, and P. R. Holt, "Cox-2 is needed but not sufficient for apoptosis induced by Cox-2 selective inhibitors in colon cancer cells," *Apoptosis*, vol. 8, no. 6, pp. 649–654, 2003.
- [35] H. Sano, Y. Kawahito, R. L. Wilder et al., "Expression of cyclooxygenase-1 and -2 in human colorectal cancer," *Cancer Research*, vol. 55, no. 17, pp. 3785–3789, 1995.
- [36] S. Y. Park, Y. H. Kim, and S. Lee, "Aromatic-turmerone attenuates invasion and expression of MMP-9 and COX-2 through inhibition of NF- κ B activation in TPA-induced breast cancer cells," *Journal of Cellular Biochemistry*, vol. 113, no. 12, pp. 3653–3662, 2012.

